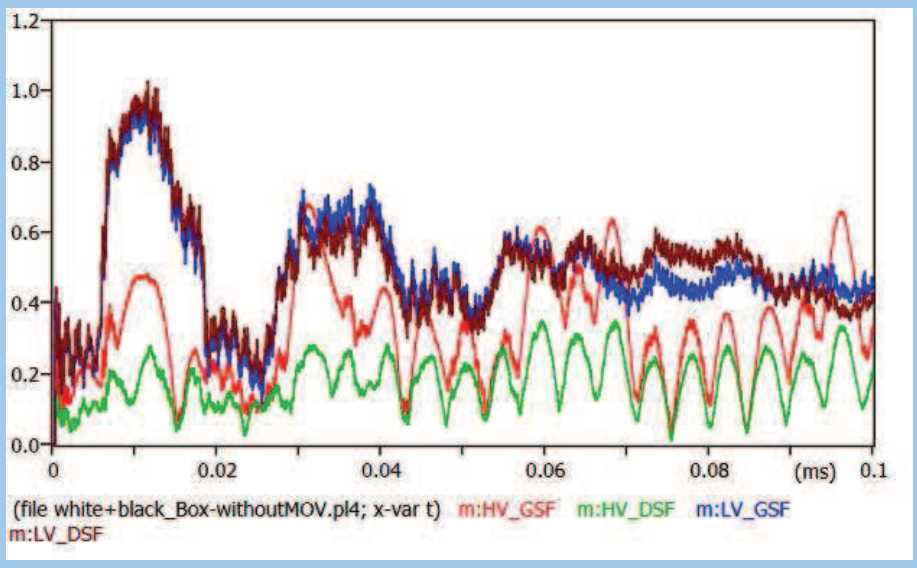


Figure 1. White+black box package: TDSF at HV and LV windings without protection (MOV).

A severity factor assesses the dielectric stress of a transformer winding considering the incoming transient overvoltage. It determines the safety margin regarding the standard acceptance tests either in the frequency or time domain.

In the case of the TDSF gives further detailed information in the time domain on the severity supported by the transformer windings due to the transient event coming from the power system, regarding the internal transient response due to dielectric tests in the time domain. The TDSF is formulated as:

$$TDSF(i) = \frac{\Delta V_{sw}(i)}{\Delta V_{env}(i)} \tag{2}$$

where $\Delta V_{sw}(i)$ is the maximum voltage drop along the ith dielectric path due to the transient events and $\Delta V_{env}(i)$ is the maximum voltage drop along the same ith dielectric path for all standards dielectric tests.

ISBN 978 - 84- 617 - 9183- 5

Published & Edited by
Xose M. López-Fernández

e-ARWtr 2016

Advanced Research Workshop on transformers

(2) 3- 5 October 2016. La Toja Island – Spain

Published &Edited by
Xose M. López-Fernández

Edited by: Xose M. López Fernández

Cover figures were obtained by Xose M. López-Fernandez & Casimiro Alvarez-Mariño.

All rights reserved.

The publisher makes no representation, expressed or implied, with regard to the accuracy of the information contained in this book and cannot accept any legal responsibility or liability for any error that may be made.

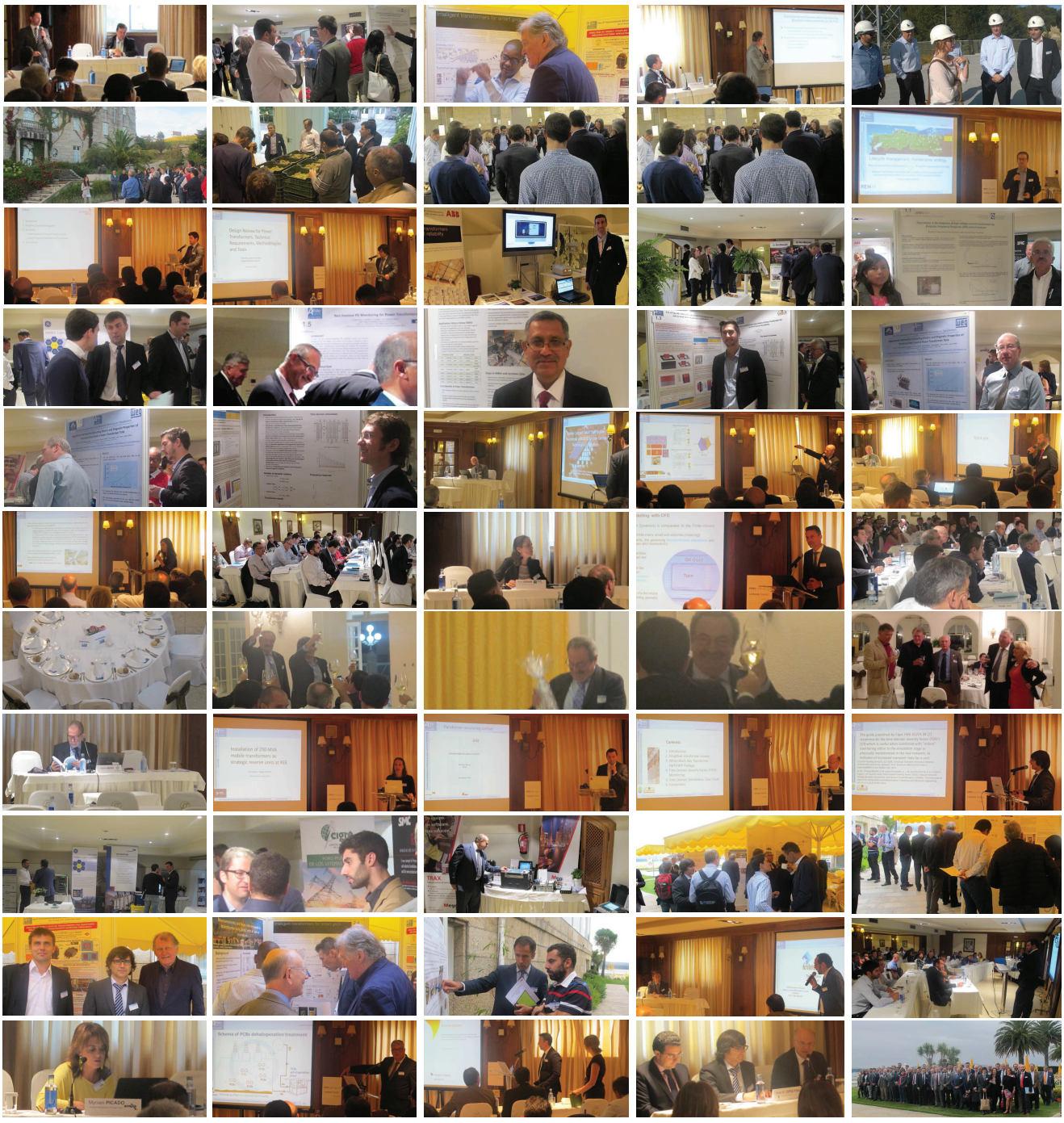
Address for correspondence:
Prof. Dr. Xose M. Lopez-Fernandez
Os Pereiriños- A Xunqueira, 20
36378 BORREIROS
Gondomar- SPAIN

ISBN: 978-84-617-9183-5

Nº REG.: 2017017061



This **e-ARWtr2016** Transformer book collects the material post-meeting in an electronic version with its own ISBN 978-84-617-4915-6. The material was updated according to suggestions made during the event days.



THE ARWtr 2016 **IS ORGANISED BY**

Dept of Electrical Engineering
University of Vigo
Spain
Spanish Association for Transformer Innovation

THE ARWtr 2016 **IS UNDER HONORARY PATRONAGE OF**

CIGRE Spanish National Committee
CIGRE Portuguese National Committee
CIGRE Study Committee A2 Transformers
IEEE PES Spanish Chapter

THE ARWtr 2016 **IS SUPPORTED BY**

Gas Natural Fenosa, Energetic Spanish Company, Spain

IBERDROLA, Group of Energetic Spanish Companies, Spain

NYNAS AB, UK - Nynas Petróleo S.A., Spain & Portugal

GE General Electric, Spain

REE, Spanish TSO (Transmission and System Operator), Spain

ABB, Asea Brown Boveri S.A., Spain

OMICRON Technologies España S.L., Spain

MR Reinhausen Luxembourg S.A., Luxembourg

Sea Marconi Technologies S.a.s., Italy

Megger Instruments S.L., Spain & Portugal

Arteche Instrument Transformers, Bizkaia, Spain

Krilinex Power Solutions, Spain

UNIVERSITY OF VIGO, Spain

ARWtr 2016 **INTERNATIONAL HONORARY COMMITTEE**

Januz Turowski
Retired from Technical University of Lodz, Poland

Emilio Palazuelos Berto
DICAT-TRATE IBERDROLA, Spain

Angel Gallego
Chairman of CIGRE Spanish National Committee

Victor Baptista
Chairman of CIGRE Portuguese National Committee

Luis Rouco Rodriguez
Chairman of IEEE PES Spanish Chapter

ARWtr 2016 **INTERNATIONAL ORGANISING COMMITTEE**

Xose M. López-Fernández
General ARWtr Chairman - *University of Vigo, Spain*

J. Turowski *(Honorary ARWtr2013Director)*
Retired from Technical University of Lodz, Poland

S. V. Kulkarni *(ARWtr2013 Advisory member)*
Indian Institute of Technology-Bombay, India

ARWtr 2016 **INTERNATIONAL TECHNICAL COMMITTEE**

Xose M. López-Fernández (Editorial Board Chairman)

J. C. Burgos – Carlos III University, Madrid, Spain
H. Cadavid – Elect Eng. Dept., Cali University, Colombia
B. Ertan – Middle East Tech. University, Ankara, Turkey
S. Gubanski – Chalmers University of Tech., Sweden
A. Kladas – National Tech. University of Athens, Greece
S. V. Kulkarni – Indian Inst. of Tech.-Mumbai, India
F. De León – Polytech. Inst. of New York University, USA
E. Lesniewska - Technical University of Lodz, Poland
M. Popov – University of Delf, Neitherland
R. Degeneff – Utility Systems Technologies, Inc., USA
P. Di Barba – University of Pavia, Italy
J. Sykulski – University of Southampton, UK
S. Wiak – Technical University of Lodz, Poland
S. Cabral –University of Blumenau (FURB), Brazil
D. Matveev – MPEI, Moscow, Russia

ARWtr 2016 **INTERNATIONAL SUPPORTING COMMITTEE**

E. Pérez Moreno
(*ARWtr2016 Supporting Committee Chairman*)
Gas Natural Fenosa, Technology Manager, Spain

H. Gago García
(*Spanish A2 CIGRE Regular Member)*
DICAT-TRATE IBERDROLA, Spain

P. Rodríguez Herrerías
(*Spanish CIGRE National Committee Secretary)*
Red Eléctrica de España (REE), Spain

O. Ribeiro
RIAC Secretary, Portugal

G. Anderson
Officer of IEEE Transformer Committee, USA

M. Picado Fernández
Nynas AB España & Portugal, Spain

C. Gonzalez-Patiño
Red Eléctrica de España (REE), Spain

M. Pérez Pérez
GE Grid Solutions, Spain

B. Batlle
OMICRON Technologies España S.L., Spain

M. Cuesto
ABB Asea Brown Boveri S.A., Cordoba, Spain

S. Hölzer
MR Reinhausen Luxembourg S.A., Luxembourg

V. Tumiatti
Sea Marconi Technologies S.a.s., Italy

M. Ohlen
Megger Instruments S.L., Spain & Portugal

A. Ibero
ARTECHE Instrument Transformers, Spain

R. Zaballa
Krilinex Power Solutions, Spain

M. Silvestre
Power Transformer Consultant, Porto, Portugal

ARWtr 2016 **LOCAL ORGANISING MEMBERS**

Casimiro Alvarez-Mariño

Hugo Rodríguez-Ignacio

Luis A. Alvarez-Gómez

IEEE PES Spanish Chapter

cigré

UNIVERSIDADE DE VIGO

ARWtr2016 PREFACE

The 5th Advanced Research Workshop on Transformers (ARWtr2016: http://webs.uvigo.es/arwtr2016) is organised by Department of Electrical Engineering-University of Vigo.

ARWtr conferences are held every three years and its aim is to provide a meeting of specialists from industrial, academic and research world engaged in an intense exchange of practical knowledge and the establishment of collaboration links on new trends and issues of transformers. It was initiated in **ARWtr**2004 in Vigo-Spain, following Baiona-Spain in **ARWtr** 2007, **ARWtr**2010 in Santiago de Compostela-Spain, **ARWtr**2013 in Baiona-Spain. This edition **ARWtr**2016 comes to La Toja Island-Spain.

The most important fact is that the **ARWtr** gathers a relatively small, but strongly connected and faithful group which is the best guarantee for further flourishing development of this specific Workshop, which first objective is the practical application in such sophisticated subject.

As it is usually the **Advanced Research Workshop on transformers (ARWtr 2016)** is held under honorary patronage of CIGRE Spanish and Portuguese National Committee, Study Committee of Transformer A2, and IEEE Power Engineering Society Spanish Chapter.

La Toja Island in the Ría de Arousa Estuar, placed between Santiago de Compostela and Vigo cities, is one of the most attractive coastal destinations in Galicia, into the green region in the north-west of Spain. Galicia is an autonomous community in Spain where its beauty, people, good environment, wine and cuisine, and its cultural heritage offer a specific atmosphere.

The collected works for presenting at the ARWtr2016 cover an interesting range of topics on transformers with emphasis in current practices, real case studies, interaction with the power system, complex phenomena inside transformer, available proposals on on-line monitoring and smart sensors as well as new trends on smart transformers. These works will be presented by the authors to be discussed during Poster Sessions and in the Oral Sessions by the Speakers. They are specialist in the transformer area and they are strongly involved either with leading transformer work factories or utilities, active electricity companies and research centers.

In addition to Oral and Poster technical Sessions, and the technical visits to Sanxenxo Substation and Tambre III a small hydro-power owned by GNF–Gas Natural Fenosa on Monday, a number of social events have been arranged: On Sunday evening a Welcome Spanish-Wine Reception at Gran Hotel; Dinner at *Pazo Baión* with tasting *albariño* white wine on Monday; The ARWtr2016 Dinner at Gran Hotel on Tuesday.

Thanks are given to all participants and sponsors for their interest on ARWtr2016, as well as committee members and institutions for their support, having actively contributed to organise the 5th edition of the Workshop.

The ARWtr2016 Directors hope you find the Workshop enriched technically and scientifically, and stimulating for making many fruitful personal contacts which permit you to establish interest links of collaboration.

TABLE OF CONTENTS

Pages

ARWtr 2016 LECTURES

1.- Online Condition Monitoring Becomes Standard Configuration of Transformers-Practical Application for Optimized Operation, Maintenance and to Avoid Failures 1 - 10

Bartlomiej DOLATA, Sebastian COENEN
Monitoring & Diagnostics, GE Grid Solutions
Moenchengladbach, D-41065, Germany

2.- High-Temperature Transformers: History, Standards and Applications 11 - 19

Richard P. MAREK
DuPont Energy Solutions
5401 Jefferson Davis Highway, Richmond, VA 23234 USA

3.- Innovative Solutions for Maintenance-Free Regulated Power Transformers 20 - 32

Rainer FROTSCHER
Maschinenfabrik Reinhausen GmbH
Falkensteinstr. 8, 93059 Regensburg, Germany

4.- Dynamic Resistance Measurements on Load Tap-Changers 33 - 42

Matz OHLEN
Megger Sweden AB
Rinkebyvagen 19, SE-182 17, Danderyd, Sweden

5.- Transformer on-Site Refurbishment Activities at REN (Red Eléctrica Nacional de Portugal) – Assessment of 15 Years' Experience as a Solution for Lifetime Extension 43 - 57

Mário A. SOARES and Jorge F. MARTINS
Department of Asset Engineering, REN
Rua Casal dos Mogos, Vermoim, Maia, Portugal

6.- Practical Case Study of Switching Transient Effects on Power Transformers 58 - 67

Marcos ARENILLAS GAY [(1)], Jaime PALOMO ÁLVAREZ [(1)], Ernesto PÉREZ MORENO [(1)]
Ricardo CASTRO LOPES [(2)]
[(1)]GNF Engineering
[(2)]EFACEC Transformers R&D

7.- Design Review for Power Transformers. Technical Requirements, Methodologies and Tools 68 - 81

Hugo RODRIGUEZ-IGNACIO[(1)] and Xose M. LOPEZ-FERNANDEZ[(1)(2)]
[(1)]Dept. of Electrical Engineering, Universidade de Vigo, Spain
[(2)]Spanish Association for Innovation in Transformers

8.- A New Compact Smart Distribution Transformer with OLTC for Low Carbon Technologies Integration 82 - 91

Luis DEL RÍO ETAYO[1)], Jon ALCORTA[1)], Asier SOTO[1)], Alena ULASENKA[2)]
Severo ARANAGA[1)], Pablo CIRUJANO[2)], Gonzalo PEREZ DE NANCLARES[2)]
[1)]ORMAZABAL Corporate Technology, Parque Empresarial Boroa, nº 24 – 48340 Amorebieta (Vizcaya) - Spain
[2)]ORMAZABAL COTRADIS - Polígono El Caballo - Parcela nº 56 – 28890 Loeches (Madrid) – Spain

Pages

9.- Smart Transformer based on Power Electronics: Current Developments and Future Trends 92 - 110

Alberto PIGAZO[(1)], Marco LISERRE[(2)], Tamás KEREKES[(3)] and Giampaolo BUTICCHI[(2)]
[(1)] Dept. of Computer Systems and Electronics, University of Cantabria, Santander, Spain
[(2)] Chair of Power Electronics, Christian-Albrechts University, Kiel, Germany
[(3)] Dept. of Energy Technology, Aalborg University, Aalborg, Denmark

10.- Power Voltage Transformers. Applications and Particularities 111 - 119

Adolfo IBERO[(1)] and Javier GARCIA[(1)], Xose M. LOPEZ-FERNANDEZ[(2)(3)] and Hugo RODRIGUEZ-IGNACIO[(2)]
[(1)] High Voltage Instruments Transformers Department, ARTECHE. Derio Bidea 28, 48100 Mungia, Spain
[(2)] Dept. of Electrical Engineering, Universidade de Vigo, Spain
[(3)] Spanish Association for Innovation in Transformers

11.- Toroidal Transformer for Full-Wave Rectifier Cooperation - Design and Properties 120 - 123

Boguslaw GRZESIK, Mariusz STEPIEN
Department of Power Electronics, Electrical Drives and Robotics, The Silesian University of Technology
2 Boleslawa Krzywoustego str., 44-100 Gliwice, Poland

12.- Environmental Protection for Larger Onshore and Offshore Wind Turbine Transformers 124 - 129

Lorena CEBRIÁN, Rafael MURILLO, Miguel CUESTO
Technology Center for Transformers, ABB
Ctra. de Madrid km 314, 50012 Zaragoza, Spain

13.- Cooling Ability of Insulation Liquids 130 - 138

B. PAHLAVANPOUR , J. WEESMAA and C.P. WOLMARANS
Nynas Naphthenics, Raffinaderivagen 21, 149 82, Nynashamn, Sweden

14.- Enhancing Transformer Liquid Insulation with Nanodielectric Fluids: State of the Art and Future Trends 139 -149

Víctor A. PRIMO[(1),] Belén GARCÍA[(1)], Juan Carlos BURGOS[(1)], Ricardo ALBARRACÍN[(2)]
[(1)]Department of Electrical Engineering, Universidad Carlos III de Madrid, Spain.
[(2)]Dept. of Electrical, Electronics and Automation Eng. and Applied Physics, Universidad Politécnica de Madrid, Spain

15.- Optical and Numerical Investigation of Oil Flow Velocities Inside a Zigzag Cooled Winding Model 150 - 156

S. TENBOHLEN[1], N. SCHMIDT[1], C. BREUER[2], S. KHANDAN[1], R. LEBRETON[3]
[1]University of Stuttgart, Germany
[2]GE Grid Solutions, Germany
[3]GE Grid Solutions, France

16.- Installation of 250 MVA Mobile Transformers as Strategic Reserve Units at REE (Red Eléctrica de España) 157 - 166

Ana AZNAR, Sergio QUINTÍN
Department of Substation Maintenance, REE (Red Eléctrica de España)
Paseo Conde de los Gaitanes 177, 28050 Alcobendas (Madrid), Spain

Pages

17.- Transformer Maintenance Planning through Continuous Insulation Condition Monitoring 167 - 174

Laurentiu-Viorel BADICU[1], Wojciech KOLTUNOWICZ[1], Victor Lozano SANCHEZ[2], Boris BATLLE[2]
[1]OMICRON Energy Solutions GmbH, 5 Lorenzweg, Berlin, Germany
[2]OMICRON Technologies, Calle la Caléndula, 93, Edificio L, 28109 Alcobendas, Madrid, Spain

18.- Fast Front Transients in Transformer Connected to Gas Insulated Substations: (White+Black) Box Models and TDSF Monitoring 175 - 183

Luis ROUCO[1], Xose M. LOPEZ-FERNANDEZ[2,3], Casimiro ALVAREZ-MARIÑO[3] and Hugo GAGO[4]
[1]Instituto de Investigación Tecnológica (IIT), E.T.S. de Ingeniería ICAI, Universidad Pontificia Comillas Alberto Aguilera, 23, 28015 Madrid, Spain
[2]Departamento de Ingeniería Eléctrica, Universidad de Vigo- Campus Lagoas-Marcosende, 36310 Vigo
[3]Spanish Association for Innovation in Transformer
[4]Iberdrola Distribución, Federico Salmón, 5, 28016 Madrid, Spain

19.- Equipment Condition Monitoring (ECM) Using Smart Sensors for Power Transformers with Special Focus on Real Time Asset Diagnosis and Prognosis 184 - 197

Marcos E. G. ALVES[1], Daniel P. SANTOS[2] and Gilberto A. MOURA[3]
[1]Department of R&D Electrical Engineering, RADICE, Praça Claudino Alves, 141 - Atibaia, Brasil
[2]Development Engineering, TREETECH, Praça Claudino Alves, 141 - Atibaia, Brasil
[3]Application Engineering, TREETECH, Praça Claudino Alves, 141 - Atibaia, Brasil

20.- Risk of Contamination of the Oil During the Different Processes after Testing a New Transformer. Detection and Analysis of this Contamination and Description of the Process to Remove it Successfully 198 - 205

Miguel MARTÍNEZ RONDEROS, Carlos VILA MONTAÑÉS, Diego LUMBRERAS BASAGOİTİ, Laura HERNÁNDEZ FERNÁNDEZ and Emilio SIERRA GÓMEZ
IBERDROLA DISTRIBUCION ELECTICA, Transformers Standardization and Maintenance Department

21.- BAT/BEP Diagnostics & Treatments for Smart Life Cycle Management of Oils & Transformers (Smart LCM-O&T): Case Histories of DBDS/Corrosion & PCBs 206 - 223

Vander TUMIATTI, M. TUMIATTI, C. ROGGERO, R. ACTIS and R. MAINA*
Sea Marconi Technologies S.a.s., Via Ungheria 20, 10093 Collegno (Turin) – Italy
*Founder and General Partner of Sea Marconi and Ass. Secretary IEC TC 10

22.- Partial Discharge Detection Method BlueBOX® Technology for Cable Boxes in Power Transformers 224 - 234

Cristina MEDEL OSUNA. Carlos DELGADO REDONDO. Ángel M. GONZALO CHICOTE
Regulated Electricity Business. Unión Fenosa Distribución. Gas Natural Fenosa

ARWtr 2016 PAPERS

23.- Experiences in the Diagnosis of High Voltage Current Transformers by Dielectric Frequency Response (DFR) and Oil Analysis 235 - 240

Roberto LIÑÁN GARCÍA, Arali GUZMÁN LÓPEZ, Daniel PÉREZ DORANTES.
Instituto Nacional de Electricidad y Energías Limpias (INEEL), Reforma No. 113, Col. Palmira, CP 62490, Cuernavaca, Morelos, México.

Pages

24.- Experimental Method for Evaluating Electric and Magnetic Properties of Structural Steel Used in Power Transformer Tank 241 - 246

Phamella R. T. PICCOLI [1], Sérgio H. L. CABRAL [2], Luiz F. de OLIVEIRA [3], Odirlan IARONKA [3], Diogo HARMEL [3], João E. SAPELI [2], João P. VIEIRA [3]
[1] Católica de Santa Catarina, Brazil
[2] Universidade de Blumenau, Brazil
[3] WEG Energía, Blumenau

25.- Use of Specific Finite Element Methods to Compute Load and no Load Losses in Power Transformers 247 - 252

Guillaume LAI, Vincent LECONTE
ALTAIR
38450 Meylan Cedex, France

26.- Implicit and Explicit State Space Models of Power Transformers for Fast Front Transient Simulations 253 -258

Luis ROUCO and Alfredo del RÍO
Instituto de Investigación Tecnológica (IIT), E.T.S. de Ingeniería ICAI,
Universidad Pontificia Comillas, Alberto Aguilera, 23, 28015 Madrid

27.- Non Invasive PD Monitoring for Power Transformers 259 - 263

Fernando GARNACHO (1), Javier ORTEGO (2), Fernando ÁLVAREZ (3), Miguel A. SÁNCHEZ-URÁN (3)
(1) LCOE- FFII; C/ Eric Kandel, nº1, Getafe, Madrid, Spain
(2) DIAEL S.L. C/ Peñuelas nº 38, 28005, Madrid, Spain
(3) Department of Electrical Engineering, Polytechnic University of Madrid, Spain

28.- Network Modelling on Dry-Type Transformer Cooling Systems 264 - 269

Andrea CREMASCO[1], Wei WU[2], Andreas BLASZCZYK[3], Bogdan CRANGANU-CRETU[4]
[1]ABB-Trasfor Development Center, Lugano, Switzerland
[2]ABB Inc., Raleigh, NC, USA
[3]ABB Corporate Research Center, Baden, Switzerland
[4]*ABB Transformers, Zürich, Switzerland*

29.- The Development of 400kV Transformers with Ester-based Dielectric Liquids 270 - 275

Mark LASHBROOK, Attila GYORE, Manjunath RAMAKRISHNA, Russell MARTIN
M&I Materials Ltd, Hibernia Way, Trafford Park, Manchester, M32 0ZD, UK

30.- Two-Dimensional Methodology for the Optimized Design of Power Transformer Insulation System 276 - 281

Hugo RODRIGUEZ-IGNACIO[1], Xose M. LOPEZ-FERNANDEZ[1,2], Casimiro ALVAREZ-MARIÑO[2]
[1]Departamento de Ingeniería Eléctrica, Universidad de Vigo- Campus Lagoas-Marcosende, 36310 Vigo
[2]Spanish Association for Innovation in Transformers

31.- Estimation of the Condition of Power Transformers and Shunt Reactors with Corrosive Sulphur 282 - 287

Arali GUZMÁN LÓPEZ, Roberto LIÑÁN GARCÍA, Horacio FLORES SANCHEZ
Instituto Nacional de Electricidad y Energías Limpias (INEEL), Reforma 113, Cuernavaca, Morelos, México

Pages

32.- Partial Discharge Monitoring of Power Transformers by UHF Sensors 288 - 293

S. TENBOHLEN[1], M. SIEGEL[2], M. BELTLE[2]
[1]Institute of Power Transmission and High Voltage Technology (IEH), University of Stuttgart, Pfaffenwaldring 47, D-70569 Stuttgart, Germany
[2]BSS Hochspannungstechnik GmbH, Hohenheimer Str. 9, D-70184 Stuttgart, Germany

33.- Analysis of Highly Coupled Transformers for Resistance Welding Systems Operated with Increased Frequency 294 - 299

Mariusz STEPIEN[1], Bogulaw GRZESIK[1], Zygmunt MIKNO[2]
[1]Silesian University of Technology, B. Krzywoustego 2, 44-100 Gliwice, Poland
[2]Institute of Welding, Blogoslawionego Czeslawa 66-68, 44-100 Gliwice, Poland

34.- Intelligent Transformers for Smart Grids 300 - 305

Goizeder PÁJARO, Oscar PICÓ, Miguel CUESTO
Regional Service Center for Transformers, ABB
Barrio Galindo s/n, 48510 Trapagaran, Vizcaya, Spain

35.- Measurements and Finite Element Model of Transformer Core Joints with DC and AC Excitation 306 - 311

Hilary K. CHISEPO[1], Leslie D. BORRILL[1, 2], C. Trevor GAUNT[1]
[1]Department of Electrical Engineering, University of Cape Town, South Africa, 7700
[2]Eskom Holdings, Cape Town, South Africa, 7441

36.- Use of the Hot-Spot Temperature in Determining Health Indices of Power Transformers 312 - 315

Félix ORTIZ, Fernando DELGADO, Agustín SANTISTEBAN, Cristina FERNÁNDEZ, Alfredo ORTIZ
Department of Electrical and Energy Engineering, University of Cantabria
Avenida Los Castros (ETSIIndustriales), 39005 Santander, Spain

37.- Determination of Three-Phase Three-Legged YNynd Transformer Zero-Sequence Impedance from Design Data 316 - 321

Elmer SORRENTINO[1], Juan Carlos BURGOS[2]
[1] Universidad Simón Bolívar, Caracas, Venezuela
[2] Electrical Engineering Department, Universidad Carlos III de Madrid, Madrid, Spain

38.- Experience on Short Circuit Design Conception and Validation of a 570 MVA, Single-Phase GSU-Transformer by SC-Withstand Tests on a Mock-up 322 - 329

Miguel CUESTO[1], Jose PORRERO[1], Marta MUÑOZ[1], Jorge CAMARA[1]
Patrice HURLET[2], Alain TANGUY[3], Mohammed RYADI[3]
[1]ABB s.a, Cordoba, Spain
[2]EDF – CNEPE, France
[3]EDF – R&D, France
e-mail: miguel.cuesto@es.abb.com

Online Condition Monitoring Becomes Standard Configuration of Transformers - Practical Application for Optimized Operation, Maintenance and to Avoid Failures

Bartlomiej DOLATA, Sebastian COENEN

Monitoring & Diagnostics, GE Grid Solutions
Moenchengladbach, D-41065, Germany
Phone: (+49) 2161944480, fax: (+49) 2161944594, e-mail: bartlomiej.dolata@ge.com

Abstract — **The recent CIGRE failure statistic confirms the necessity of continuous online monitoring of all major components of power transformer's. The application of various sensors and their integration into only one monitoring system as well as correlation of all measurements and analyzed data build a so called "comprehensive monitoring system" and allow obtaining significant information about the actual as well as predictive condition of the power transformer/reactor. In the course of the ongoing extension and optimization of power systems, more and more intelligent devices are applied in order to improve the utilization of power transformers and reactors, to detect early incipient faults and avoid unexpected outages, to support operators in accurately timed maintenance activities and to ensure higher availability and reliability from energy generation to transmission and distribution.**

The paper deals with operating experiences with comprehensive online condition monitoring systems for power transformers. Examples of practical cases of bushing and active part monitoring will be presented and an intelligent alarm management for effective user information is demonstrated. Additionally an overview will be given of various applications of comprehensive online monitoring systems including advanced bushing monitoring as well as trends and new developments, like monitoring of fast transient overvoltages, ultra-high frequency partial discharge monitoring.

Keywords — **Transformers, online monitoring, bushing monitoring, transient events**

I. INTRODUCTION

Today, utilities focus, on one hand, on improving or maintaining system security by preventing outages, and on the other, reducing operation and maintenance costs of their assets. Both objectives rely on information about asset conditions. As such, an increasing number of power transmission and power generation utilities are equipping their power transformers with continuous on-line monitoring systems. Step-by-step, this equipment becomes a standard configuration of power transformers.

The paper gives an introduction about new technology and trends in the field of continuous on-line condition monitoring of transformers. The trends are described and exemplarily discussed related to the following topics: The monitoring system itself; growing importance of the implementation of continuous on-line monitoring of transient overvoltages and new ultra-high frequency technology for partial discharge monitoring.

II. COMPREHENSIVE CONTINUOUS ON-LINE MONITORING SYSTEM

A power transformer consists of several components: transformer tank with active part and oil-paper insulation, conservator, cooling unit, on-load tap changer and bushings, to mention some. These components can be fitted with various sensors, which are integrated into one monitoring IED (Intelligent Electronic Device) by means of analogue or digital signals and different protocols, building a comprehensive condition monitoring and expert system, see Fig. 1.

Raw data acquired from a wide range of demand-specific selectable sensors are analysed by means of implemented models, and stored in the on-line condition monitoring and expert system. Data acquisition and processing alone, however accurate, are of limited value if operators cannot prioritize and exploit the masses of generated information. An expert system included in the monitoring device becomes a powerful tool to accomplish this. Configurable report generators automatically create user-friendly reports providing

ISBN 978-84-617–9183–5

information about the status of the transformer and its main components, upon request or to be sent periodically by email.

Expert systems also generate recommendations and information concerning transformer operation and service/maintenance. They also allow setting alarms according to data values and can be correlated to other data impacting the identified problem. Messages, including necessary actions, are displayed in a status overview window. The processed data is stored in the expert system, becoming a knowledgeable database.

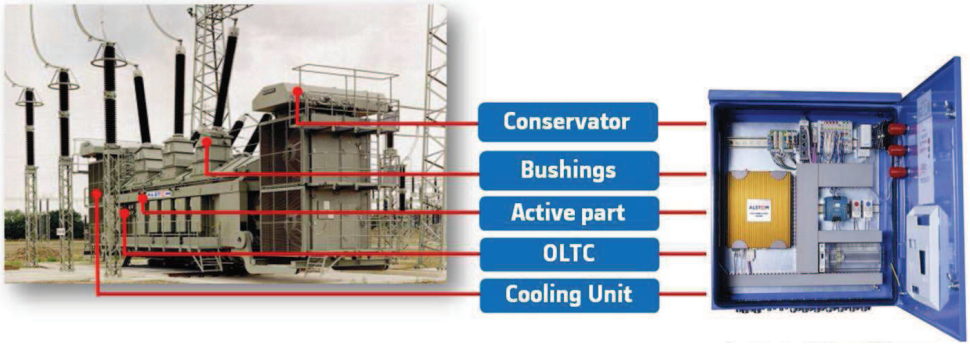


Figure 1. Example of MS 3000 (transformer continuous on-line monitoring system) module to collect and analyse data from various sensors placed at strategic points of the transformer.

III. ARCHITECTURE OF EXEMPLARY APPLICATION

The monitoring solution MS 3000 consists of a MS 3000 IED (intelligent electronic device) which is e.g. located in the so called Master Module on one transformer cubical. All signals of that transformer are measured with analogue input modules and are transferred and stored within the IED. To collect data of further transformers, a so called field-bus technology is used, here Profibus. Data from further transformers are collected via that fieldbus and are also transferred and stored at the IED within the Master Module, see Fig. 2.

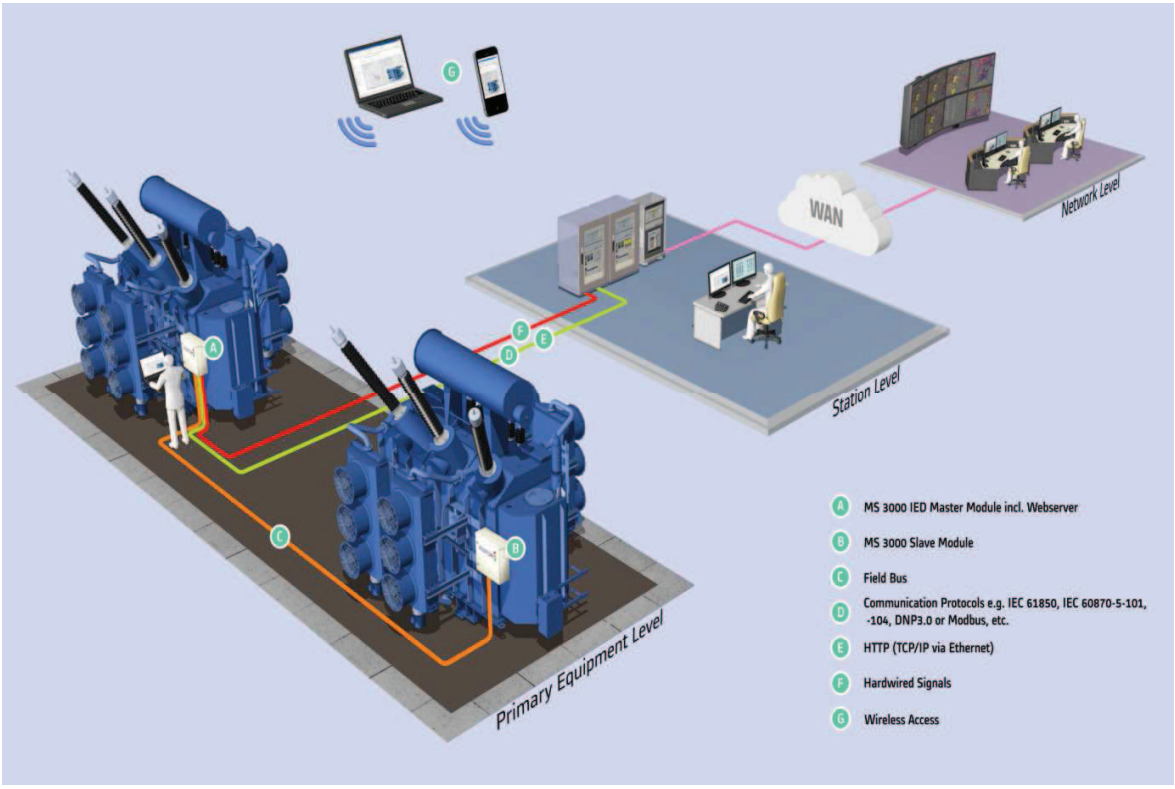


Figure 2. Exemplary architecture of transformer monitoring solution.

ISBN 978-84-617–9183–5

The Master Module collects data from various transformers in the field and transfers the data to the station level via communication protocols like IEC 61850 [1], IEC 60870-5-101 or -104, DNP3 or Modbus. From there the data might be transferred via wide area network (WAN) to control centres on network level to maintenance experts and operational staff of e.g. dispatch centres. According philosophy alarming of experts via e-mail or messages on mobile devices is possible and allows an effective asset management.

IV. CONTINUOUS BUSHING MONITORING

High voltage condenser bushings of power transformers, according to their construction and age, are amongst the most endangered components from all operating equipment used. In the past, off-line measurements like the measurement of bushing insulator capacitances and measurement of the dissipation factor were carried out successfully for determining the operational state. Today, modern microprocessor and computer technology makes it possible to carry out these procedures on-line with the help of a monitoring system.

The monitoring of the electrical measurement quantities is achieved by a voltage measurement consisting of a bushing adaptor, directly connected to the measurement tap of the bushing and the connected voltage sensor, see Fig. 3. The voltage sensor essentially consists of a capacitance C_M, which normally has values of 1...2 µF, see sketch in Fig. 4.

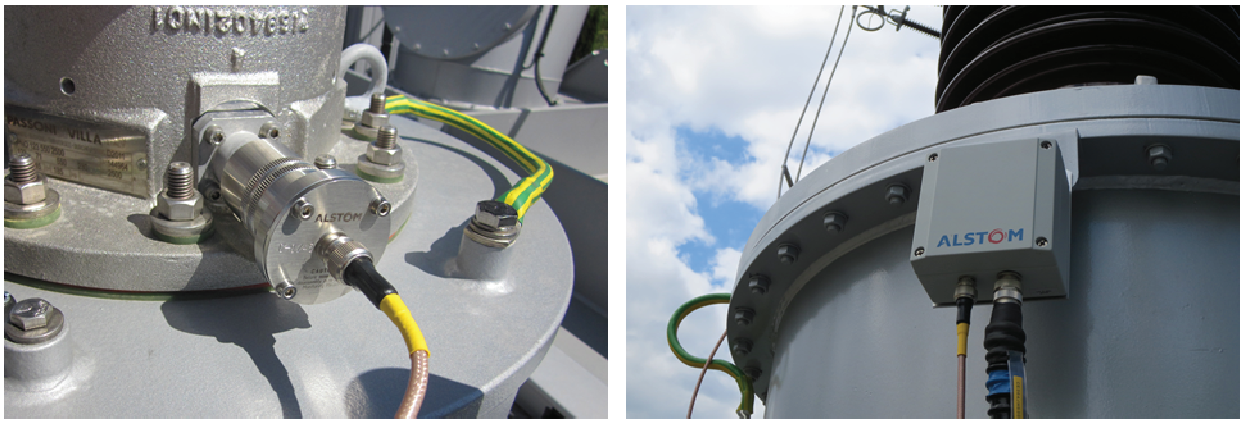


Figure 3. Bushing adaptor (left) and voltage sensor (right).

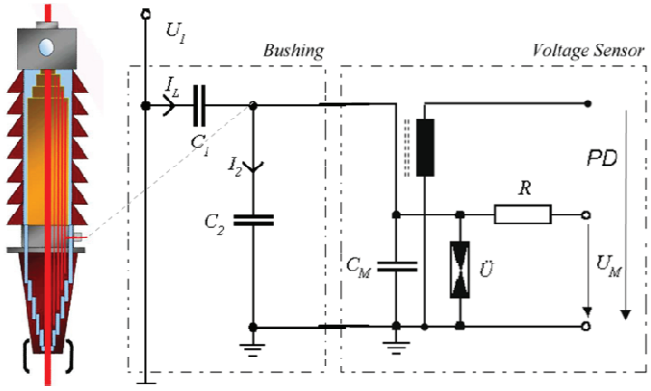


Figure 4. Sketch of bushing and equivalent circuit diagram of the bushing and the voltage sensor.

Since $C_M >> C_2$ (with $C_2 \approx 300$ pF), I_2 is practically 0. The resistance R terminates the connected coaxial cable with a surge impedance of 50 Ω. The potential divider ratio between C_1 and C_M is dimensioned that a measurement voltage U_M of 57 V AC is set. In addition, there is an overvoltage suppressor (Ü) installed, which protects the sensor and the cable from overvoltages, and as there are no electronic components used in the sensor at the bushing, this measurement procedure is not sensitive to electromagnetic emission. Another

ISBN 978-84-617–9183–5

advantage of the technology used is in the high signal-to-noise ratio owing to the transmission of a voltage signal of about 57 V AC.

The monitoring of the change in the bushing capacitances (Δ C) is achieved by means of a three-phase voltage measurement. Here, the output signal of the presented voltage sensor is compared with the two remaining phases. The result of the algorithm is based on an averaging in order to eliminate voltage fluctuations in the network in this manner. The influences of temperature can be compensated by the three-phase measurement principle. In consequence, the relative change in capacitance is used for determining the Δ C. This method has also proven itself over a prolonged time in the field [2] also impressing through its high signal-to-noise ratio.

V. CASE STUDIES

Comprehensive monitoring systems offer the advantage of collecting all important information about the condition of a transformer. Failures can be avoided by proactive maintenance measures e.g. replacing conspicuous components like e.g. bushings. In case of failures monitoring systems allow the decent investigation of failures to increase knowledge about failure modes. Very helpful for investigations is the possibility to correlate different information and various measurements to distinguish the root cause of failures which can exemplarily be shown in the following case studies.

a. 350 MVA, 420 kV Transformer

The effect of a partial flashover of 2 layers of a 420 kV bushing is depicted in Fig. 5. The 3-phase operating voltages (phase L1, L2, L3) together with overvoltages of the 350 MVA regulating transformer are shown.

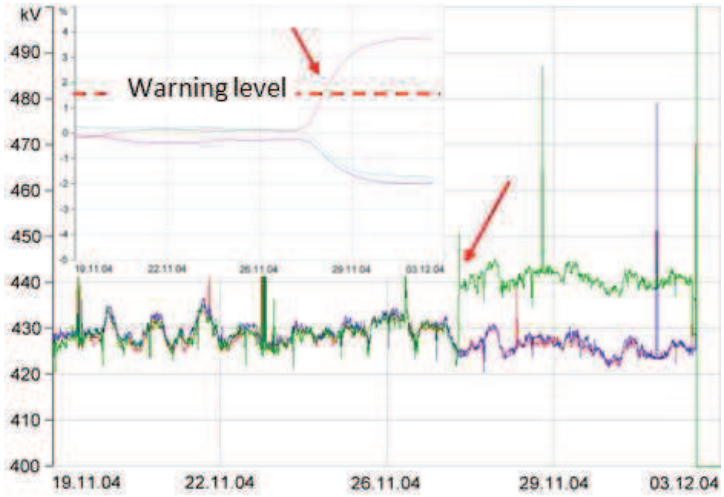


Figure 5. Detection of partial flashover of 420 kV bushing and avoidance of collateral damage of 350 MVA regulating transformer, 3-phase operating voltages (phase L1, L2, L3) with overvoltages (large figure), identified by change of capacitance Δ C (small figure).

On 27.11.2004 after only 1 ½ years of bushing operation a warning was generated automatically by the on-line monitoring system identified by a change in the bushing capacitance by 3.6 % (Fig. 5, small figure).

After switching off the transformer an off-line measurement was performed and proved the on-line determined value. The bushing was shipped to the manufacturer who also confirmed the result. Due to the installation of an on-line monitoring system a collateral damage could be prevented. In addition the system indicated that the transformer has been affected by overvoltages which could have been the most probable reason for the damage.

ISBN 978-84-617–9183–5

b. 850 MVA, 400 kV Transformer

In the evening of 28th of June 2013 a 850 MVA, 400/27kV transformer, manufactured in 2000, was tripped due to a catastrophic bushing failure of high voltage side in phase V. Analysing the measurement data of the monitoring system reveals that the catastrophic failure was detectable approximately 3 days in advance, see Fig. 6.

On 26th of June, the voltage measurement on phase V showed a voltage rise of approx. 2.5 % what correlates to one layer breakdown in the condenser bushing. Beginning approximately 6 hours in advance of the trip a cascade breakdown inside the bushing occurs and the voltage rose up to additional 15 % of nominal voltage. However, in this case the alarm management functionality of the on-line condition monitoring system was not implemented into the SCADA system. The active use of the bushing monitoring functionality would have avoided that major bushing failure and the unscheduled outage. Due to that experience the utility decided to implement from now on the bushing monitoring into the active alarm management.

In Fig. 6 it can be seen that overvoltages have been detected prior to the fault, which might have been a possible root cause for the bushing failure. Therefore comprehensive monitoring systems can be used to correlate transient overvoltages and capacity change of bushings for a deeper understanding of those additional dielectric stresses.

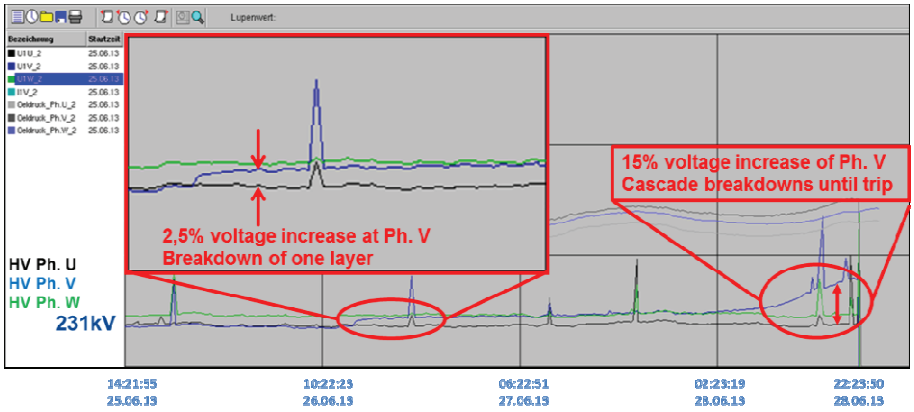


Figure 6. Increase of measured voltage (phase to ground voltage measurement on bushing test tap at high voltage side) on a failed bushing of a 850 MVA transformer.

In case the monitoring system would have been used to protect the bushing with appropriate thresholds, the system might have protected the transformer for that unscheduled tripping by raising a warning 3 days in advance and an alarm 6 hours in advance with a possible de-energization of the transformer.

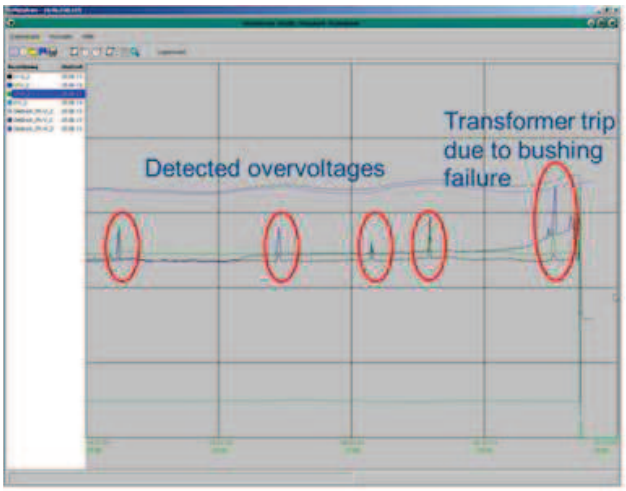


Figure 7. Detected overvoltages prior transformer trip.

ISBN 978-84-617–9183–5

c. 520 MVA, 238/21 kV Generator step-up transformer

A 520 MVA generator transformer was put in service in a power plant. The transformer has been equipped with a comprehensive monitoring solution incl. on-line DGA sensor. The historical data of the load factor, gas in oil content and top oil temperature are depicted for time range of approx. 1 year of operation in Fig. 8. Over one year of operation an increase of gas in oil content has been detected. The customer has decided to carry out the oil treatment. After drying and degassing of the transformer oil the unit was put back in operation. After approx. 4 months of operation a repeated increase of gas in oil content with higher gradient has been detected. The customer decided to take the transformer out of operation.

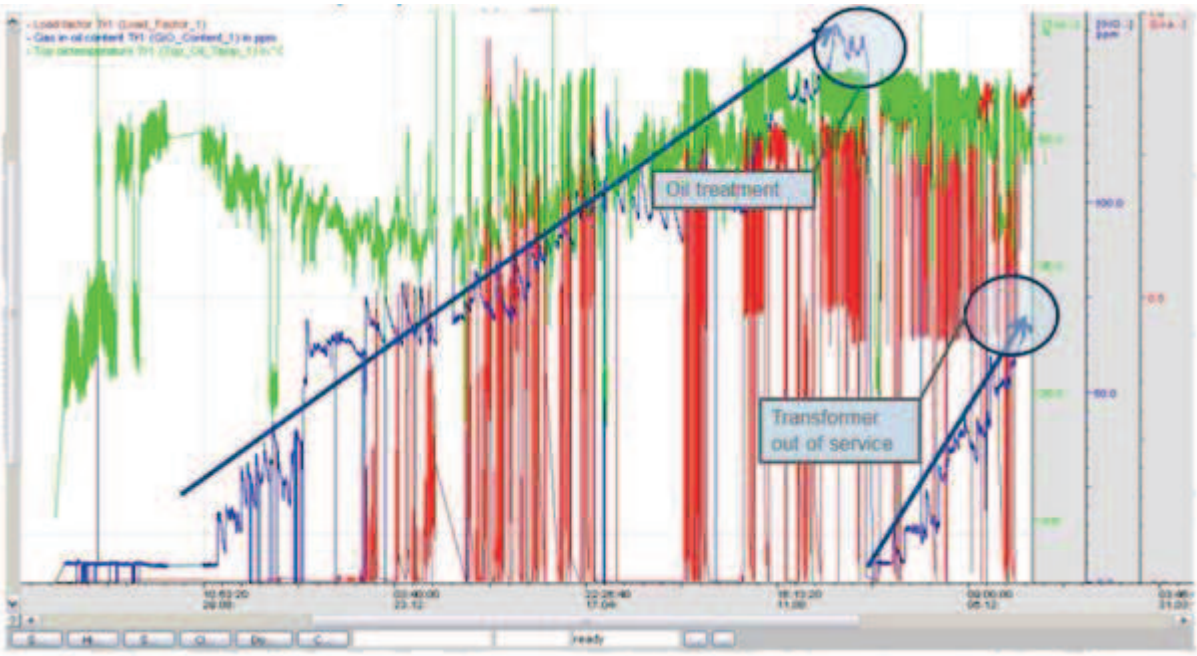


Figure 8. Historical data of load factor, gas in oil content and top oil temperature of the 520MVA generator transformer.

The root cause analysis has indicated reasonable suspicion on hot-spot issue. Fig. 9 shows evaluation of DGA values done by the GE monitoring system with indication of thermal issue.

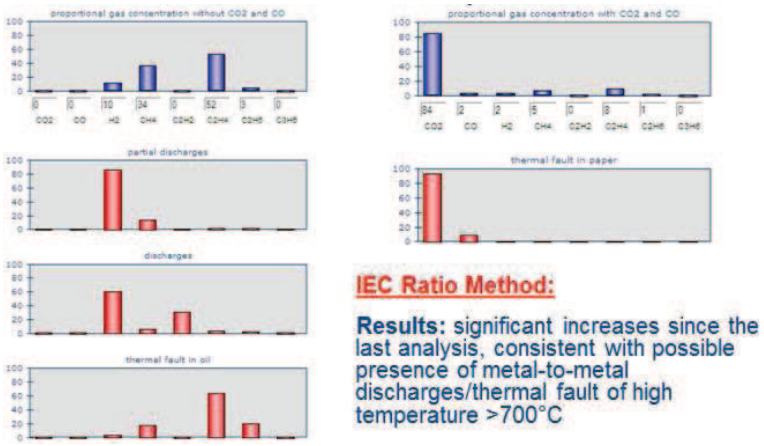


Figure 9. Evaluation of DGA values by the GE monitoring system.

After inspection of the transformer at the factory, traces on core lamination and PSP barriers has been found. The reason can be found out by detailed analysis of the monitoring data base. Fig. 10 shows detected overvoltages during operation of the transformer which probably caused local overheating of the transformer magnet circuit.

ISBN 978-84-617–9183–5

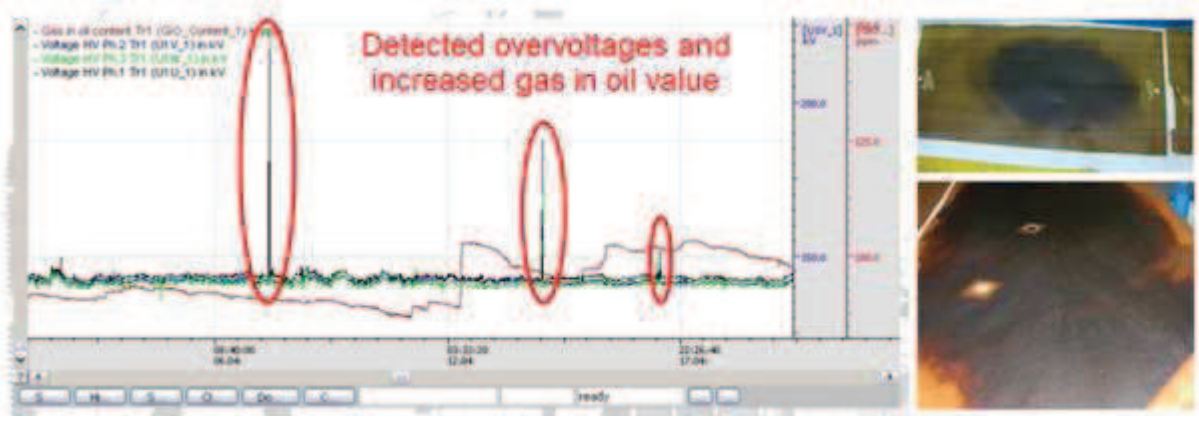


Figure 10. Detected overvoltages and traces on core laminations.

VI. MONITORING OF TRANSIENT OVERVOLTAGES

Transient overvoltages are a considerable risk for the insulation of transformer bushings and windings. Therefore, detection and evaluation of these transients is of great importance when it comes to reliability assessment of power transformers.

Transformers in service are exposed to different types of transient overvoltage events which impose high stresses on their insulation structure. Transient overvoltages, because of their high amplitudes and frequencies, can cause breakdowns either between turns or from coil to earth, resulting in extensive damage to the transformer. A significant number of transformer failures in literature are reported as dielectric failures [3, 4]. Such failures are not related to any system event at the time of their occurrence and may occur due to pre-damage induced by prior transient overvoltage events. The following different types of transient overvoltages may occur:

- Transient atmospheric overvoltages – full wave

These are transient overvoltages originating from atmospheric discharges, usually as lightning strikes, which act directly by striking one or more line conductors, or indirectly by striking a point near to the line such as a pylon or an earth wire. The standardized wave shape form consists of a wave front duration of 1.2 μs and a wave tail duration of 50 μs (1.2/50 μs).

- Transient atmospheric overvoltages – chopped wave

These transient overvoltages occur when the lightning strike voltage wave is modified and reduced after a flash over across spark gaps of insulators or by activation of a transient overvoltage protection device like a surge arrester. Higher frequency content than in the full wave transient atmospheric overvoltage cause higher stress to the insulation system of transformers by less homogeneous voltage distribution along the winding turns.

- Transient overvoltages due to switching operations

Circuit breakers and disconnectors cause transient overvoltages due to re- and prestrikes during operation. The standardized wave shape form is described by a wave front duration of 250 μs and a wave tail duration of 2000 μs (250/2000 μs). In gas insulated switchgear (GIS) transient overvoltage waves with higher frequency content are propagating through the system and get reflected and superimposed on each discontinuity of the line impedance, e.g. transformers.

- Transient overvoltages due to new network service conditions

Increasingly used new technology of power grid components like HVDC converters, capacitor bank switchings, reactor switching, cause in case of internal faults and trips transient overvoltages with wave shapes and frequency content which are not directly addressed by existing standard wave forms and tests.
The current factory proof tests [5, 6, 7, 8] contained in the standards do not completely address all types of transient events that occur in the field. The use of the standard lightning impulse wave shape is not appropriate in the case of the fast-front or oscillatory waveforms occurring in actual service conditions with reactor switching, HVDC converters, capacitor banks switching, and GIS switching. As network configurations

ISBN 978-84-617–9183–5

change, high frequency modelling is challenging as high frequency models of transformers and all attached equipment like power lines, GIS, circuit breakers and connectors are not always available. Therefore the continuous on-line measurement of transient overvoltages is often the only way to analyse interactions between the transformer and the power grid to analyse failures, adopt protection and improve transformer specifications. As transient overvoltages impose high stress for transformer insulation system, risk of transformer failures may increase by increased number and extend of experienced transient overvoltages. By identification of highly affected transformers in specific power network areas or constellations, on-line monitoring of transient overvoltages may help to reduce risks and failure rates.

VII. MS 3000 TRANSIENT MONITORING SOLUTION

Lightning impulses and chopped lightning impulses were generated and are captured simultaneously with an oscilloscope and the intelligent data acquisition unit (iDAU). Fig. 11 shows the captured chopped lightning impulse.

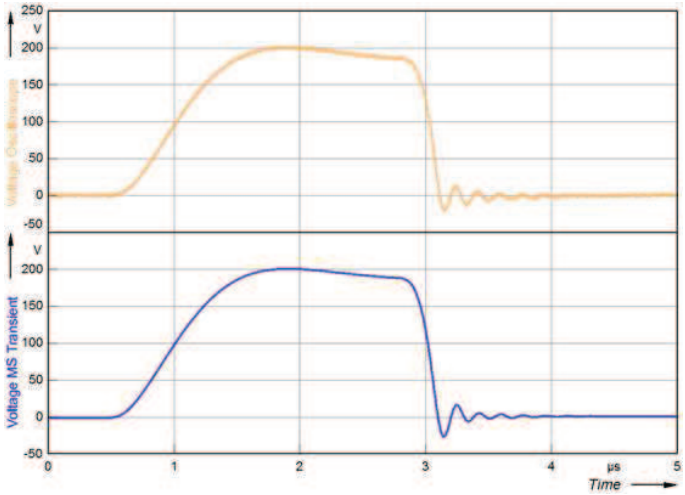


Figure 11. Chopped lightning impulse, yellow (top): reference measurement with 100 MHz broad-band oscilloscope, blue (bottom): DAU measurement result of transient monitoring solution.

The yellow (top) curve is the reference measurement performed with a 100 MHz broad-band oscilloscope and the blue (bottom) curve is the measurement reading of the transient monitoring solution. Both curves are obviously identical, i.e. the transient monitoring solution is able to measure chopped lightning impulses.

VIII. MONITORING OF UHF EVENTS

The reliability of electrical energy networks depends on quality and availability of the electrical equipment like power transformers. Local failures inside their insulation may lead to breakdowns and may cause high costs due to outages and penalties. To prevent these destroying events power transformers are e.g. tested on partial discharge (PD) activity before commissioning and are monitored on PD activity during service.

The conventional PD online monitoring measurements according to IEC 60270 are often affected by external noise like corona discharges on overhead lines. The new trend deals with the electromagnetic method, also known as UHF method [11]. The UHF method with a bandwidth from 300 MHz to 3 GHz based on the fact, that PD inside oil filled transformers emit electromagnetic waves measurable with oil valve sensors inside the transformer tank, see Fig. 12. The UHF PD module measures electromagnetic emission of internal PD pulses [12]. The UHF sensor uses the transformer tank as a “Faraday Cage” and allows the detection of PD activity from inside the transformer only.

The Phase Resolved Partial Discharge pattern (PRPD) evaluation provides typical characteristic PD pattern

ISBN 978-84-617–9183–5

which can be used for the interpretation of possible PD sources, see exemplary PRPD in Fig. 12 (right).

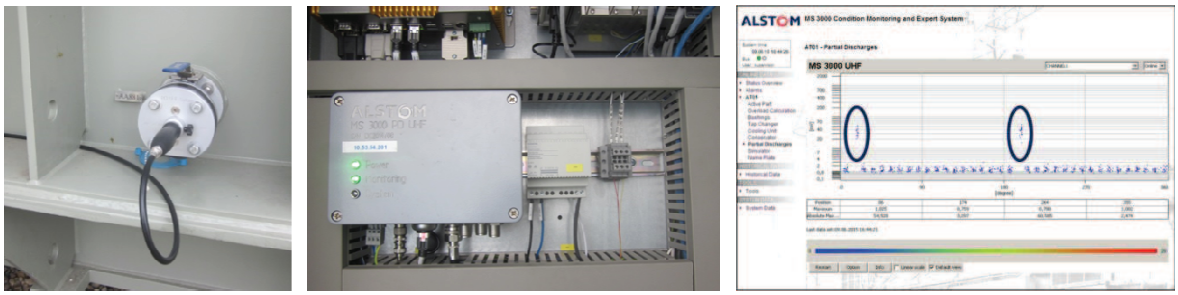


Figure 12. UHF PD Monitoring solution, left: At DN 50 standard valve installed UHF sensor middle: UHF PD monitoring module in monitoring cubicle, right: UHF PRPD with UHF impulses of a phase synchronized UHF signal generator.

The UHF PD data can be correlated to all measured and analysed values of the monitoring system on the transformer, including for instance, load condition, On-Load Tap Changer (OLTC) operation or DGA; and hence allows further condition and risk assessment of PD effects.

IX. CONCLUSIONS

The paper gives an introduction about new technology and trends in the field of continuous on-line condition monitoring of transformers. The trends are described and exemplarily discussed related to the following topics: The monitoring system itself; growing importance of the implementation of continuous on-line monitoring of transient overvoltages and new ultra-high frequency technology for partial discharge monitoring.

The focus in this paper was to demonstrate how capacitive controlled bushings can be protected by on-line monitoring devices. The underlying principle of the measurement technique is based on the use of a capacitive voltage sensor that is installed at the measurement tap of the bushing. In this manner, the operational voltages can be measured, and deriving therefrom, overvoltages and transient voltages can be detected.

The change in the bushing capacitance as the most important characteristic quantity for determining the operational state can be analyzed reliably on this basis. Hence the change of capacitance can be chosen as protection criteria and thresholds are clear distinguished by bushings internal design and number of layers.

Case studies demonstrated, that a critical damage of a 350 MVA grid coupling transformer could be avoided by a detection of a partial flashover of layers of a bushing indicated by a change in the bushing capacitance. Another collateral damage of an 850 MVA transformer bushing might have been prevented in case the bushing monitoring system based on capacitive voltage measurements would have been authorized to trip the transformer.

The current factory proof tests contained in the standards may not always completely address all types of transient events that occur in the field. As network configurations change, high frequency modelling is challenging as high frequency models of transformers and all attached equipment like power lines, GIS, circuit breakers and connectors are not always available. Therefore the continuous on-line measurement of fast transient overvoltages directly measured on the test tap is often the only way to analyse interactions between the transformer and the power grid to analyse failures, adopt protection and improve transformer specifications. The conventional PD online monitoring measurements according to IEC 60270 are often affected by external noise like corona discharges on overhead lines. The new solution monitors electromagnetic emission of internal PD pulses in the ultra-high frequency range (UHF). The UHF sensor uses the transformer tank as a “Faraday Cage” and allows the detection of PD activity from inside the transformer only.

ISBN 978-84-617–9183–5

REFERENCES

[1] *IEC 61850 Communication networks and systems in substations*, International Electrotechnical Commission, Edition 1, 2013.

[2] T. Stirl, R. Skrzypek, S. Tenbohlen, R. Vilaithong. *On-line condition monitoring and diagnosis for power transformers their bushings, tap changer and insulation system*, CMD Korea, 2006.

[3] A. da C.O. Rocha, et.al *Electrical transient interaction between transformers and the power system – Part 2: Case studies*, TB 577B, CIGRE, 2014.

[4] Power transformer – Part 3: *Insulation levels, dielectric tests and external clearances in air*, IEC Standard IEC 60076-3, 2013.

[5] Power transformers – Part 4: *Guide to lightning impulse and switching impulse testing – power transformers and reactors*, IEC Standard 60076-4, 2002.

[6] *Test code for liquid-immersed distribution, power and regulating transformers,* IEEE Standard C57.12 90, 2010.

[7] Guide for transformer impulse tests, IEEE Standard C57.98, 2011.

[8] D. Kind, H. Kärner *High voltage Insulation Technology*, Friedr. Vieweg & Sohn, Braunschweig, 1982.

[9] Working Group CIGRE 12.05 *An International Survey on Failures of Large Power Transformers in Service*, Electra number 88, 1983.

[10] K. Widmaier *Bushing – a very highly stressed component*, MICAFIL Symposium, Stuttgart, 2002.

[11] S. Coenen, *Measurements of Partial Discharge using Electromagnetic Signals*, Dissertation Universität Stuttgart, Books on Demand GmbH, ISBN 978-3-84821-936-0, 2012.

[12] B. Dolata, G. Luna and M. Siegel, *Condition Monitoring of Power Transformers by using of UHF PD Technology*, Cigre Colloquium, Zürich R, 2013.

ISBN 978-84-617–9183–5

High-Temperature Transformers: History, Standards and Applications

Richard P. MAREK

DuPont Energy Solutions
5401 Jefferson Davis Highway, Richmond, VA 23234 USA
Phone: (+1) 804 383 2376, fax: (+1) 804 383 2009, e-mail: richard.p.marek@dupont.com

Abstract — **By 2035, the global demand for energy is expected to increase by 36%, bringing with this expansion certain challenges. In 2014 in the United States alone, there were more than 7600 generating stations. Globally, transformers sit in the background of our everyday lives transferring this power to our businesses, our homes and to every modern convenience to which we have become accustomed. Along with growth, security issues have also grown over the last few years. An April 2014 report by the United States Department of Energy, explains that large power transformers "require a long lead time, and transporting them can be challenging. . . . If several [large power transformers] were to fail at the same time, it could be challenging to quickly replace them." In early April, 2012, the United States Department of Homeland Security announced that a successful emergency drill had been completed during five days in March to move, deploy and energize three single-phase, high-temperature, 200 MVA fast-recovery transformers that serve as prototypes for the utility industry, to dramatically reduce the recovery time associated with transformer-related outages. These power transformers were designed with a hybrid insulation system that helped to make these large capacity transformers light enough and small enough to transport by conventional low-boy trailers, within normal maximum shipping weights and height. Many obstacles lay in the path to seeking grid security and meeting growth needs. However, in this development, new materials and techniques certainly will become more important.**

Keywords — **high-temperature, grid security, thermal class, transformer insulation, hybrid insulation system**

I. INTRODUCTION

By 2035, the global demand for energy is expected to increase by 36%, bringing with this expansion certain challenges. Recently, Electricity of Viet Nam (EVN) spent nearly US$22.3 billion to build power plants and grids including 865 new transformer stations and transmission lines. This significant development is an example of only one developing country investing in their grid infrastructure. In 2014 in the United States alone, there were nearly 20 000 generators rated more than one megawatt, at more than 7 600 generating stations. Globally, transformers sit in the background of our everyday lives, transferring this power to our businesses, our homes and to every modern convenience to which we have become accustomed.

Along with growth, security issues have also grown over the last few years. Concerns over the security of the national electrical grid in the United States have led to the recent formation of a new company called Grid Assurance. As stated in their petition to the US Federal Energy Regulatory Commission, "Grid Assurance seeks to address a critical national security need – supporting the resiliency of the bulk power system in the event of a catastrophic event such as a natural disaster or an attack – by making critical replacement equipment for the transmission grid readily available." This organization is only in its infancy, but is certainly a sign of the times.

An April 2014 report by the United States Department of Energy, explains that large power transformers "require a long lead time, and transporting them can be challenging. . . . If several [large power transformers] were to fail at the same time, it could be challenging to quickly replace them." In early April, 2012, the United States Department of Homeland Security announced that a successful emergency drill had been completed during five days in March to move, deploy and energize three single-phase, high-temperature, 200 MVA fast-recovery transformers that serve as prototypes for the utility industry, to dramatically reduce the recovery time associated with transformer-related outages. These power transformers were designed with a hybrid insulation system that helped to make these large capacity transformers light enough and small enough to transport by conventional low-boy trailers, within normal maximum shipping weights.

Many obstacles lay in the path to seeking grid security and meeting growth needs. However, in this development, new materials and techniques certainly will become more important. Today, state-of-the-art

ISBN 978-84-617–9183–5

computer programs have extracted about as much cost as possible in pursuit of competitive designs for liquid immersed transformers, while still maintaining the highest global standards of quality and reliability. But conventional materials inherently limit size or weight reduction and life extension is limited to lowering the winding temperature rise and correspondingly increasing transformer size and weight.

High-temperature insulation offers a new avenue to explore the possibilities of matching an application with optimized cost and is now one of the few opportunities available for a true step-change in design strategy for life extension, increased capacity or smaller size. High-temperature design has been around for many years, but now global standards are also in place and available to help shape development in this important area.

II. HISTORY OF HIGH-TEMPERATURE LIQUID IMMERSED TRANSFORMERS

2017 will mark fifty years of commercial applications for DuPont Nomex® aramid high-temperature insulation papers. The early transformer applications were dry-type, varnish encapsulated units that are still quite popular today. The 1970's saw applications expand into much lighter weight, high-temperature traction transformers for European and Japanese high speed trains, using silicone liquid as a high-temperature dielectric and coolant.

In the early 1980's, the liquid of choice began to transition to synthetic esters, replacing silicone. Also, aramid board was developed, expanding the use of aramid in railway traction transformers and opening the way for high-temperature power transformers. At first, the primary applications were repair for increased capacity and mobile transformers and substations. The concept was simple. The aramid allowed higher temperature, which in turn allowed more capacity for the repaired units. The higher capacity was also an advantage for the mobile units. Maximizing weight reduction allowed more power while remaining within the highway load limits. All of the power applications used mineral oil as the dielectric coolant, due to the higher voltage requirements compared to the traction transformers.

Weight restricted applications expanded in the 1990's. In one example in Korea 150 kVA pole mounted transformers use aramid insulation and silicone liquid to provide the increased capacity needed with a 25% reduction in weight, thereby eliminating the need for an extra pole and platform. 40 and 60 MVA units were also developed to meet reduced bridge weight restrictions. Natural ester liquids were developed as a replacement for mineral oil during this period and although sensitive to oxidation, show promise for higher operating temperature capability. Although high-temperature transformers are rarely lower in cost compared to a conventional transformer, the overall installation can often be cost effective, when size, weight or overload issues are considered.

III. HIGH-TEMPERATURE STANDARDS

Standards development has played a major role in expanding high-temperature liquid immersed transformer applications. The early applications were specialized and mostly fell into categories of products that were not normally included in the standards. So the lack of a standard was not a significant obstacle. However, as applications expanded, so did the need for standards. While standards guide the products in an industry, they typically follow the technology development until it is decided that standards are needed to set the road map for future development. The transformer industry has been no different and in 1997, IEEE Std 1276, Guide for the Application of High-Temperature Insulation Materials in Liquid-Immersed Power Transformers [1] was published after this working group first published a thorough background paper in 1994, Background Information on High Temperature Insulation for Liquid-Immersed Power Transformers [2]. This informational paper summarized the state of the art at the time and is still a very useful document.

In the early 2000's it became apparent that a more definitive document than a guide was needed. Two editions of IEC 60076-14, Liquid-immersed power transformers using high-temperature insulation materials [3] were published as Technical Specifications. One was published in 2004 and the second one in 2009. In 2008, the development of a similar document was begun by IEEE. Since the standard ambient temperature is 20°C in IEC documents and 30°C in IEEE documents, it was decided to maintain different standards to avoid confusion. IEEE Std C57.154, Standard for the Design, Testing, and Application of Liquid-Immersed Distribution, Power, and Regulating Transformers Using High-Temperature Insulation Systems and Operating at Elevated

ISBN 978-84-617–9183–5

Temperatures [4] was published in 2012. The IEC International Standard version of IEC 60076-14 was then published a year later. Table I shows the temperature limits defined in the IEC document for hybrid insulation systems. Table II shows the temperature limits defined for high-temperature insulation systems. A number of papers and presentations have already described the IEC 60076-14 standard in detail, so only a short summary will be discussed in this paper [5][6][7].

One of the more important features of the standard was a number of terminology definitions. For example, conventional was defined as the commonly used insulation system composed of non-thermally upgraded kraft and mineral oil. The high-temperature insulation system was defined as any system where the liquid and the solid insulation are all high-temperature. Hybrid refers to a blend of these two systems where high-temperature solid is used in varying degrees, but the liquid temperature is limited to that of mineral oil. However, other liquids may be used as long as the temperature limit of mineral oil is not exceeded. Table I and Table II show the thermal limits for hybrid and high-temperature insulation systems respectively.

Table I. Hybrid Insulation Windings – Thermal Limits

	Conventional insulation system	Hybrid insulation systems				
		Semi-hybrid insulation winding	Mixed hybrid insulation winding	Full hybrid insulation winding		
Minimum required solid high-temperature insulation thermal class	105	120	130	130	140	155
Top liquid temperature rise (K)	60	60	60	60	60	60
Average winding temperature rise (K)	65	75	65	85	95	105
Hot-spot temperature rise for solid insulation (K)	78	90	100	100	110	125

Table II. High Temperature Insulation Windings – Thermal Limits

	Ester liquid				Silicone liquid			
Minimum required high-temperature solid insulation thermal class	130	140	155	180	130	140	155	180
Top liquid temperature rise (K)	90	90	90	90	115	115	115	115
Average winding temperature rise (K)	85	95	105	125	85	95	105	125
Hot-spot temperature rise (K)	100	110	125	150	100	110	125	150

Another important feature of this document and illustrated by these two tables is that the temperature limits are defined by thermal class. Previously, the temperature limits were related to the materials and basically, there was only one system. In developing the standard, it became apparent that the document needed to be more generic in order to allow future development and yet still set temperature limits and guidelines for overload. These thermal classes are similar to those that have been used in motors and dry type transformers for many years. Table III shows the thermal classes defined for liquid immersed transformers and the associated hot spot temperatures. Note that these thermal classes were taken from IEC 60085, Electrical insulation - Thermal evaluation and designation [8], with the exception of the 140 class. The working group felt that there was a large gap between the 130 and the 155 classes for the generally lower temperature rated liquid immersed transformers, so an intermediate temperature class was added.

ISBN 978-84-617–9183–5

Table III. Thermal Classes and Associated Hot Spot Temperatures

Thermal Class	Hot Spot Temperature
105	98
120	110
130	120
140	130
155	145
180	170
200	190

Note also that ester liquids are lumped together in this document as a generality with the same assigned temperature capability. In reality, this is not likely to be true and more recently, we see that the natural ester liquids are now being made from many different seeds. These liquids are also being used at high-temperature more frequently, while the ratings remain essentially estimates based on the manufacturer's recommendations and field experience. The reason is that there are no standards available to determine the thermal class of a liquid, and the standards organizations have been reluctant to address this question. The task has been shunted to CIGRE and there is a proposal to initiate a study group on this subject in August 2016.

IV. INSULATION SYSTEM THERMAL EVALUATION

Having defined insulation thermal classes, determining the thermal class of an insulation system becomes the next task. Both IEC and IEEE have documents defining the procedures for thermal evaluation. However, IEEE Std C57.100, Standard test procedure for thermal evaluation of insulation systems for liquid-immersed distribution and power transformers [9] is a full standard, while IEC/TS 62332-2, Electrical Insulation Systems (EIS) - Thermal evaluation of combined liquid and solid components - Part 2: Simplified Test [10] is a Technical Specification. Technical Specifications are temporary documents established for trial use before they are finalized as International Standards. Although the two documents are similar, there are fundamental differences that cause concern about the IEC version. For example, it targets 20 000 hours in establishing the Arrhenius curve and the comparative method references non-thermally upgraded kraft paper in mineral oil, for which there is no established Arrhenius curve. The IEEE version references the well-established curve for thermally upgraded paper in mineral oil and targets 180 000 hours. The document as it was revised in 2011 also fixed many issues with the previous document dated 1999, which was actually only really intended to be a quality check procedure. This old procedure is not suitable as a standalone procedure for determining an insulation system thermal class as it has been used to validate all of the ester/cellulose testing.

In the most comprehensive change to this document, the revised standard adopted the well-known RTI (relative thermal index) concept of evaluation, where the candidate system is compared to a known system. In this case, the known system, described as the "industry-proven system" by the standard, is thermally upgraded cellulose in mineral oil. This system has a widely accepted Arrhenius life curve, which projects the system life to 180 000 hours at a hot spot temperature of 110°C. Additional requirements include a stipulation that the aging temperatures must be at least 15 °C apart, and the test results, when complete, cannot be extrapolated by more than 40 °C, with a curve having at least a 95% confidence factor. Suggested candidate test temperatures and the required reference cell temperatures and corresponding test durations are shown in Table IV. As shown, at least three temperatures must be tested for the new candidate system. For the reference system, three cells must be tested for each of the three test temperatures indicated. At the end of the respective test period, the retained tensile strength is measured and the results of the nine cells are averaged. This average then becomes the target for the candidate test temperatures. Specific material ratios of solid to liquid are also required and there are separate ratios for distribution and power applications. See Table V for details. See Fig. 1 for photos of a typical cell with materials. A practical example of this testing can be found in a recent CIGRE paper by Marek, et al [11].

ISBN 978-84-617–9183–5

Table IV. Ageing times and temperatures for three-point test

Insulation System		Expected increase in thermal rating	Ageing time number 1	Ageing time number 2	Ageing time Number 3
Industry-proven system	Time duration		4434 h	1316 h	424 °C
	Temperature		150 °C	165°C	180 °C
Candidate system		10 °C	160 °C	175 °C	190 °C
		20 °C	170 °C	185 °C	200 °C
		30 °C	180 °C	195 °C	210 °C

Table V. Sealed tube material ratios

	Transformer type	
Material	Power	Distribution
Insulating liquid	200 cm^3	200 cm^3
0.05 to 0.10 mm conductor insulation	6.5 cm^3	
0.13 to 0.38 mm layer insulation		11.2 cm^3
1.00 to 3.00 mm low-density pressboard		1.2 cm^3
2.00 to 8.00 mm low-density pressboard	16.4 cm^3	
Ratio – liquid to solid	8.8 to 1	16.3 to 1

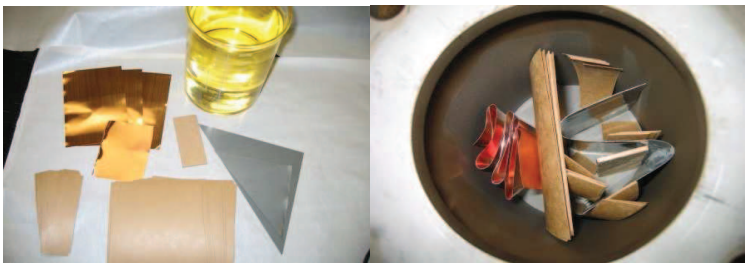


Figure 1. Sealed tube cells and materials.

V. HIGH-TEMPERATURE APPLICATIONS

As mentioned in the history, mobile transformers and substations have been some of the earliest and most enduring applications of high-temperature insulation in power transformers. Generally less than 100 MVA, these transformers are used for temporary or emergency application. While this type of equipment is popular around the world, many are conventional transformers. However, in the United States virtually all of these units are high-temperature due to restrictive road weight regulations. This is the classic application where maximum power is required for a given weight limit. Even after more than thirty years, a dozen or so units are produced every year. Fig. 2 shows a sampling of some of these units.



Figure 2. Mobile transformers and substations.

ISBN 978-84-617–9183–5

More than fifteen years ago, manufacturers began building high-temperature wind turbine transformers. These specialized transformers were first designed to a very narrow profile to allow them to fit through the doorway of the pedestal on the wind turbine towers. By using the same tower, increased turbine power was possible with much of the existing structure. These smaller more compact high-temperature units have losses competitive with conventional units and ranged up to 6 MVA. A photo collage of these unitscan be seen in Fig. 3.



Figure 3. Wind turbine transformers.

Recently, there was an interesting example for the use of the new aramid enhanced cellulose paper. Three generator step-up transformers were built for a refurbished and upgraded power plant in Egypt. The installation was in a hot climate area, and the units were expected to operate continuously close to their nameplate ratings. Although the rated temperatures were reduced to accommodate for the expected high average ambient temperatures during the year, the insulation thermal class was specified for at least 130 according to IEEE Std C57.154. The aramid enhanced cellulose paper with a thermal rating of 130 was selected for the conductor insulation in combination with high-temperature aramid board meeting the requirements of a hybrid insulation system. A photo of one of the 310 MVA units is shown in Fig. 4. A more detailed description of this unit may be found in a paper by Szewczyk, et al [12].



Figure 4. 310 MVA GSU Transformer Using Aramid Enhanced Cellulose Paper.

Grid security and grid resilience are increasingly becoming topics of interest worldwide by utilities critically evaluating their networks and their vulnerabilities. A project in Spain addressed this issue with a newly designed hybrid insulated high-temperature transformer. This 250 MVA, 400 kV autotransformer was designed and built as a shell type transformer, the largest of its kind ever built with a hybrid insulation system. The concept of this special transformer was to replace the 117 MVA fast deployable units that are currently used for emergency replacement. However, a bank of three of these single phase transformers only equates to 351 MVA while most of the network systems are rated at 600 MVA using three banked 200 MVA units. This shortfall has

ISBN 978-84-617–9183–5

now been remedied by using aramid in a hybrid insulation system to achieve 2.1 times the capacity and only 17% higher weight than the conventional fast deployable units. These units can be shipped by truck and can be installed and operating in just a few days. Critical to the project was hot spot monitoring and ongoing periodic dissolved gas analysis, which proved high hot spot temperatures can be achieved in the windings without exceeding the temperature capability of the mineral oil. Cuesto, et al [13] detail this project and present some of the test results. Fig. 5 shows a photo comparing the size of the 250 MVA hybrid transformer to two conventional 150 MVA units.

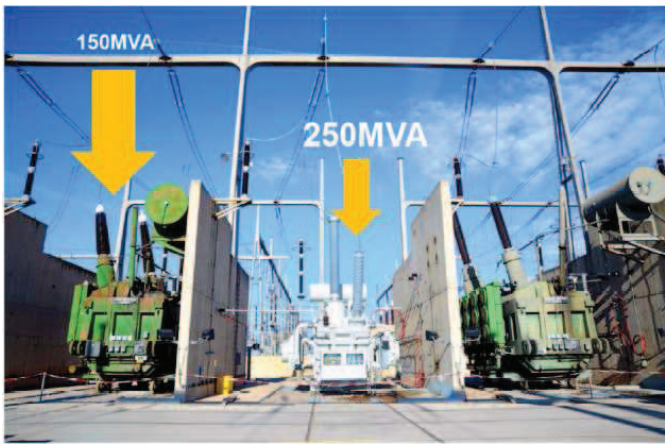


Figure 5. 250 MVA 400 kV fast deployable autotransformer.

About the same time that this fast deployable unit was developed in Spain, a similar project was developed in the United States. The United States Department of Homeland Security (HLS) had determined that the network system has a number of severe vulnerabilities. A consortium of HLS, ABB, Electric Power Research Institute (EPRI) and CenterPoint Energy joined forces to develop and produce a bank of three single-phase 200 MVA, 400 kV units, as emergency replacements for the normal 600 MVA units. These units were modular in construction and the concept was to store them dry, filled with nitrogen to reduce shipping weight. As a demonstration, the three units were shipped by normal truck from the factory to the site along with bushings, coolers and oil. Installation was complete and the units were energized in just five days. Fig. 6 shows photos of the shipment and installation. An interesting video [14] produced by HLS chronicles the demonstration project.



Figure 6. Rapid recovery transformer initiative (RecX).

ISBN 978-84-617–9183–5

In April, Siemens Transformers globally launched its resilience concept, Pretact™ at the 2016 Hannover Fair. It offers solutions to the many network transformer threats: network failures made worse by an aged fleet, physical and cyber-attacks and natural disasters such as hurricanes, tornados, flood and fires. At the same time they announced an order for six ultra-flexible units for a major utility in the United States. These 335 kV, single phase units, rated at 300 MVA in a three phase bank are extremely small and light-weight. They can be shipped by truck and can be installed and energized in just two to four days. These backup units are filled with synthetic ester liquid making them environmentally friendly, flame-retardant and suitable for densely populated areas.

VI. CONCLUSION

High-temperature insulation has been used in liquid immersed transformers for more than forty years. Over these years there have been many applications, but interest has grown with the advent of high-temperature transformer standards. These standards have legitimized these transformers and have opened the door to the development of new insulations and the development of new applications. Grid resiliency is just the latest in the series of applications that see great advantage in the size and weight reduction capabilities of using high-temperature insulation. Undoubtedly, the development of additional insulation materials, liquids and applications will continue into the future.

REFERENCES

[1] IEEE Std 1276™-1997, *Guide for the application of high-temperature insulation materials in liquid-immersed power transformers*.

[2] *Background information on high temperature insulation for liquid-immersed power transformers*, IEEE Transactions on Power Delivery, Vol. 9, No. 4, 1994.

[3] IEC 60076-14:2013, *Power transformers – Part 14: Liquid-immersed power transformers using high-temperature insulation materials.*

[4] IEEE Std C57.154™-2012, *IEEE Standard for the Design, Testing, and Application of Liquid-Immersed Distribution, Power, and Regulating Transformers Using High-Temperature Insulation Systems and Operating at Elevated Temperatures*.

[5] R. P. Marek, *Discussions on a New IEC Document for Liquid-Filled Transformers*, 10th Insucon International Conference, Birmingham, 75-81, 2006.

[6] R. P. Marek, *Standards for High-Temperature Insulation Systems,* Advanced Research Workshop on Transformers, AWRtr2010, Santiago de Compostela, Spain, 3-6 October, 2010.

[7] H. M. Wilhelm, L. langer, G. Dal Pont, P. O. Fernandes, L. G. Feitosa, R. P. Marek, L. Galhardo, E. Wang, *A study of liquid-immersed transformer reference insulation systems used to determine thermal class,* CIGRE Session 46, D1_29_2016, Paris, France, August 21 - 26, 2016.

[8] IEC 60085:2007, *Electrical insulation - Thermal evaluation and designation.*

[9] IEEE Std C57.100™-2011, *Standard test procedure for thermal evaluation of insulation systems for liquid-immersed distribution and power transformers*.

[10] IEC/TS 62332-2:2014, *Electrical insulation (EIS) - Thermal evaluation of combined liquid and solid components - Part 2: Simplified Test*.

[11] R. P. Marek, R. C. Wicks, L. Galhardo, R. Szewczyk, *New cellulose enhanced with aramid – practical example of material thermal evaluation acc. To IEEE Std C57.100-2011*, CIGRE SCD1 Colloquium, Rio de Janeiro, Brazil, September 13-18, 2015.

ISBN 978-84-617–9183–5

[12] R. Szewczyk, R. P. Marek, *Aramid Enhanced Cellulose paper for Extended Life of Transformer Insulation System*, 81st International Conference of Doble Clients, Boston, Massachusetts, USA, 2014.

[13] M. Cuesto, M. Oliva, A. Prieto, J. C. Sanchez, L. Navarro, *Fast-deployable HV network transformer with hybrid insulation: a solution against major events,* CIGRE, 54-PS3, Paris, 2013.

[14] https://www.dhs.gov/science-and-technology/recx-demo-video

ISBN 978-84-617–9183–5

Innovative Solutions for Maintenance-Free Regulated Power Transformers

Rainer FROTSCHER

Maschinenfabrik Reinhausen GmbH
Falkensteinstr. 8, 93059 Regensburg, Germany
Phone: (+49) 4090-4136, e-mail: r.frotscher@reinhausen.com

Abstract — **The use of vacuum type on-load tap-changers suggests innovations like the use of alternative insulating liquids, sealed applications, combined oil volumes and DGA. The paper meets all these challenges by theoretical considerations which are backed up by results from laboratory tests and field experience. Solutions for the protection of the tap-changer oil against contact with ambient air (sealing) are presented and answers on how to connect the oil households of transfomer and tap-changer without influencing transformer DGA by tap-changer gases are given. Furthermore, methods for successful tap-changer DGA are depicted and limit values for acetylene are set for network service.**

Keywords — **vacuum type on-load tap-changer, DGA, hermetically sealed, combined oil volumes**

I. INTRODUCTION

Regulated power transformers are equipped with a regulating winding with multiple taps which are connected to a tap-changer to adjust the transformer ratio. On-load tap-changers (OLTCs) are used if the ratio shall be changed while the transformer is under load. These tap-changers consist of a tap selector which connects to two adjacent taps of the regulating winding and a diverter switch which performs the load switching operation between the two selected taps without interrupting the load current. If both functions are combined in a single functional unit, the tap-changer is called selector switch. Diverter switches respectively selector switches feature an own oil compartment which separates the tap-changer oil from the transformer oil. In all modern tap-changers, these oil compartments are pressure tight and gas tight.

The arc-switching operations of conventional diverter switches deteriorate the oil in the tap-changer compartment severely and so produce huge amounts of carbon, soot and gases. For these OLTC models, regular maintenance is necessary to replace the oil, clean the oil compartment and replace worn contacts. They further require free-breathing oil conservators so that the switching gases can be released to the ambient air.

Modern OLTC models use vacuum interrupters for making and breaking the load current. These vacuum interrupters fully encapsulate the switching arcs so that the diverter switch oil is no longer carbonized. The benefits are:

- An extremely long contact life leads to maintenance intervals of 300’000 or 600’000 operations, depending on the respective OLTC model. For standard applications in power supply networks with 5’000 to 10’000 switching operations per year, this means that the tap-changer mechanism is free of maintenance for the whole transformer life of 30 to 60 years.
- A high quality of the tap-changer oil is maintained over the whole lifetime so that the tap-changer oil doesn’t have to be replaced regularly.
- Very low amounts of dissolved gases are produced during normal service. This enables DGA to be an appropriate method to monitor the “health” condition of the OLTC, in the same way as it is commonly applied to transformers.
- Persisting high oil quality and low amounts of dissolved gases enable the combination of tap-changer oil and transformer oil. A strict separation of the two oil volumes is no longer necessary.
- Vacuum type OLTCs don’t produce free gases during normal service. This enables sealed applications, as they are required if natural ester liquids shall be used.

ISBN 978-84-617–9183–5

These benefits pave the way for innovative developments concerning the interplay of transformer and tap-changer, as they will be discussed in the following.

II. DGA FOR VACUUM TYPE OLTCS

By encapsulating the switching arcs inside vacuum interrupters, the conditions for the tap-changer oil are comparable to the conditions for the transformer oil. Under normal operating conditions (including overload), no free gases are produced, and the ppm values of hydrocarbon gases dissolved in the oil are in many cases in the 1- or low 2-digit range. Over the working life of the tap-changer, they turn out to be fairly constant, which enables a proper evaluation and trend analysis.

II.1. GAS SOURCES

For a full understanding of the development of gases inside a vacuum type OLTC, it is advisable to first define the gas generating components and the determining parameters.

- The vacuum interrupters are sealed systems, which do not release or produce any gases in the surrounding oil. In case of an unlikely leakage, the vacuum inside the interrupter tube is lost, oil may intrude and the switching contacts act under oil with highly reduced switching capability. It may happen then that the tube breaks, due to enormous overpressure. In this case, huge amounts of arcing gases will be produced which can easily be detected as a fault.
- In some OLTC types, the main contact respectively by-pass contact commutates the load current from the continuous current path onto the main path, causing it to flow through the vacuum interrupter (MSV); see Fig. 1, positions 1 and 2 as an example. Because inductance and resistance of the main

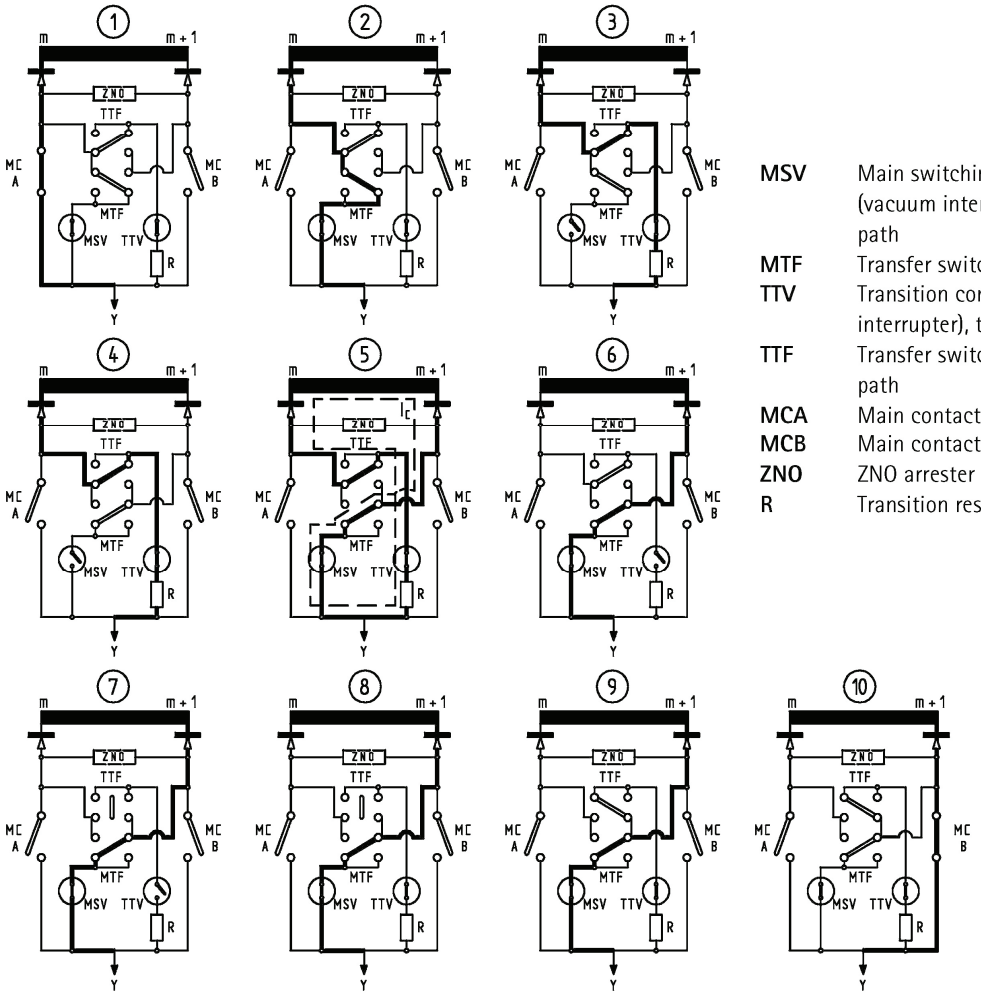


Figure 1. Switching sequence of VACUTAP® VR.

ISBN 978-84-617–9183–5

path are higher than in the continuous current path, some sparks or low-energy arcs are generated at the main contacts (MCA, MCB).

- The transition resistors are heated when the load current flows through the transition path; see Fig. 1, positions 3-5 as an example. For operation under nominal load, the design value has been set not to exceed a temperature rise of 190 K per operation. With the oil temperature added, the maximum surface temperature will be below 300 °C, which causes a certain heat gas pattern. Operations under overload, or multiple consecutive operations as they can occur in service, will cause higher temperatures, but because they are rare, they will not change the typical gas pattern significantly. On the other hand, when switching operations under no load or partial load are performed, the resistors heat up very moderately and so will produce none or only negligible amounts of hydrocarbon gases. At surface temperatures of less than 100 °C, only CO and CO_2 are produced due to incipient oil ageing which can be used as indicator for moderate thermal stress of the oil [1]. The use of CO and CO_2 as thermal indicators is possible here because tap-changers only contain negligible amounts of cellulose, whose degradation usually causes CO and CO_2.
- Transition reactances, as they are used in combination with reactor type OLTCs, show very low losses; therefore, they don't heat up significantly and so produce only negligible amounts of gases. Furthermore, they are located in the transformer tank and so cannot influence tap-changer DGA.
- The tap selector can be equipped with a change-over selector which doubles the regulating range of the transformer, either by reversing the regulating winding or by adding a coarse tap winding. When the change-over selector is operated, the potential of the regulating winding is only determined by the capacitances to the neighboured winding(s) and/or the transformer core or tank; see Fig. 2. This condition can cause significant potential drift of the regulating winding. Even if the change-over selector does not have to switch the load current, it must be able to break capacitive currents up to 500mA and withstand recovery voltages on the open contacts up to 50kV. It is obvious that such stress will cause switching sparks and arcs in the transformer oil which can be visible in the transformer DGA, in case the number of change-over selector operations is extraordinarily high. In the majority of cases, switching of the change-over selector will not disturb transformer DGA. It also does not influence tap-changer DGA. The only exception is the compartment type OLTC VACUTAP® RMV-II, which houses the change-over selector inside the tap-changer compartment.

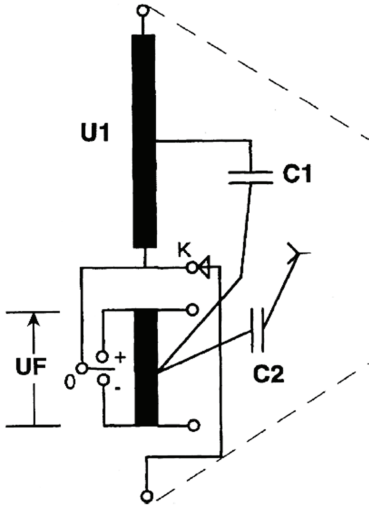


Figure 2. Capacitive coupling of the regulating winding during operation of the change-over selector (example: reversing switch).

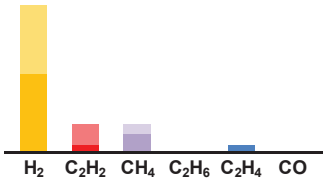
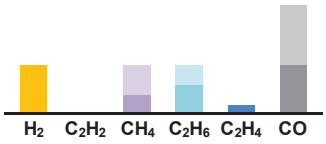
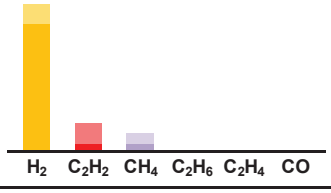
II.2. GAS PATTERNS

The typical gas patterns for each gas source are illustrated in Table I. The patterns originate from various laboratory and field test data and have been aligned with literature [2], [3]. As the intensity of commutation sparks, arcing of change-over selector and resistor heating strongly depend on the individual application, the absolute ppm amount of each gas and the composition of gases with them will differ significantly. CO_2 has not been visualized here, because, in free-breathing systems, it can also be introduced by ambient air in amounts up to 400 ppm. With this, CO_2 should only be used as indicator for the thermal stress of the oil in sealed systems, or by following the change over time (trend analysis).

Because the ppm gas values are usually very low during the normal service of any VACUTAP® OLTC, the gas patterns may be masked by "stray-gassing" processes, which is a self-gassing activity of strongly hydro-treated oils, preferably when they are in contact with certain metals [4]. Results of a test on the stray-gassing activity of the used transition resistor material are given in chapter III.1. With this, the gas pattern caused by the commutation processes (sparking) may be tampered. Depending on the applied oil brand, stray-gassing can suggest more commutation activity than actually present.

ISBN 978-84-617–9183–5

Table I. Typical Gas Patterns of Components of Vacuum Type OLTCs

Source	Gas Pattern		Determining Factors
commutation contacts, by-pass contacts	sparking / low energy arcing		▪ Inductance and resistance of main current path ▪ load current
transition resistors	heating <300°C		▪ design values of step voltage and through-current (application-specific) ▪ actual load, load profile ▪ oil temperature
change-over selector	low energy arcing / sparking		▪ capacitances of regulating winding to neighboured windings resp. core/tank ▪ voltage of regulating winding ▪ design (type-specific) ▪ operating speed

Inside the tap-changer oil compartment, the gas patterns superimpose, depending on the gas sources present. Concerning VACUTAP® VV and VR, this will lead to a mixture of sparking and heating gases. For VACUTAP® VM, only heating gases will be present, because there is no commutation contact. In contrast, the compartment type OLTC VACUTAP® RMV-II will only show sparking/arcing gases, due to current commutation and operation of the change-over selector in the OLTC tank. Because this OLTC type has a much higher oil volume than VACUTAP® VR, VV or VM, the absolute values will be lower. As a result, the typical gas patterns of oil-filled VACUTAP® OLTCs are shown in Fig. 3.

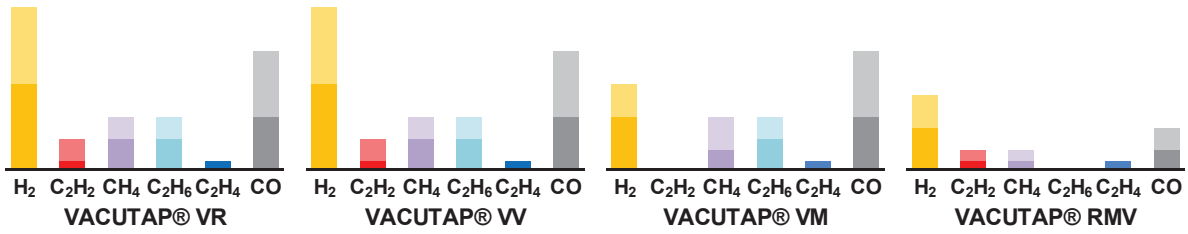


Figure 3. Typical gas patterns of VACUTAP® OLTCs (qualitative).

It can be seen that the usual ranges of gas levels (pale colors) will lead to significant variations of the gas patterns observed in practice. This is mainly due to the low absolute levels, which are influenced by the specific OLTC configuration (single-phase/three-phase, U_m, design of transition resistors), the operating mode (transformer load, total number of OLTC operations per day, switching profile), the breathing conditions (equilibrium between gas generation and gas loss via the breather) and also the oil brand (stray-gassing). With this, each application will show its individual fingerprint within the typical model-specific pattern.

III. Laboratory Researches

III.1. Gassing of Transition Resistors

Comprehensive investigations have been performed at IEH, University of Stuttgart, to determine the gassing behaviour of transition resistors with various surface temperatures in different insulating liquids. In a suitable, sufficiently sealed test setup, the resistor material was stressed with current impulses to generate temperature rises of 100, 200, 350 und 600K; see Fig. 4. This roughly corresponds to the actual heating which is generated

ISBN 978-84-617–9183–5

by the transition resistors inside an MR in-tank tap-changer when working under different loads. After 0, 250 (500) and 1000 (500) current impulses, oil samples were taken and the dissolved gases were determined by headspace chromatography. The maximum oil temperature was limited to 60°C by circulating the oil through a radiator. Possible free gases were collected in a glass cylinder which was mounted at the highest point of the system. The tests were performed with degassed, air-saturated and thermally aged mineral oil (SHELL Diala D) as well as with synthetic ester (MIDEL 7131) and natural ester liquid (ENVIROTEMP FR3).

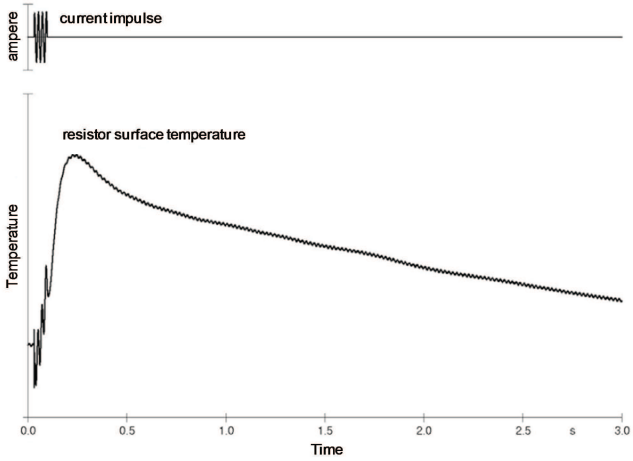


Figure 4. Measured resistor temperature curve caused by current impulse.

After 1000 impulses with 100K temperature rise, no significant amounts of dissolved heating gases could be detected. For 200 and 350K, low amounts of CH_4, C_2H_4 and C_3H_6 with 3 to 7 ppm per gas were detected in the mineral oils. 500 current impulses with 600K caused significant amounts of CH_4, C_2H_6, C_2H_4 und C_3H_6 (150-300 ppm, depending on the gas) in air-saturated unused oil and thermally aged oil. For degassed unused oil, the gas pattern was similar, but with much lower values (40 ppm per gas maximum). The ester liquids showed almost no gassing at 100 and 200K, but started at 350K with significantly higher values than the mineral oils, mainly producing C_2H_6. Such behavior has also been reported by Wang [5]. At 600K, all heating gases (C_2H_6, CH_4, C_2H_4, C_3H_8, C_3H_6) were present in much higher amounts than for the mineral oils. Overall, MIDEL7131 showed a more distinct gas production than FR3. No arcing gas C_2H_2 was detected in all tests.

Significant amounts of C_2H_4 and C_3H_6 plus low amounts of H_2 and C_2H_6 were found after an additional test with degassed mineral oil at room temperature (without resistor heating), see Fig. 5. This "stray-gassing" can be attributed to the transition resistor material, a nickel-chromium alloy.

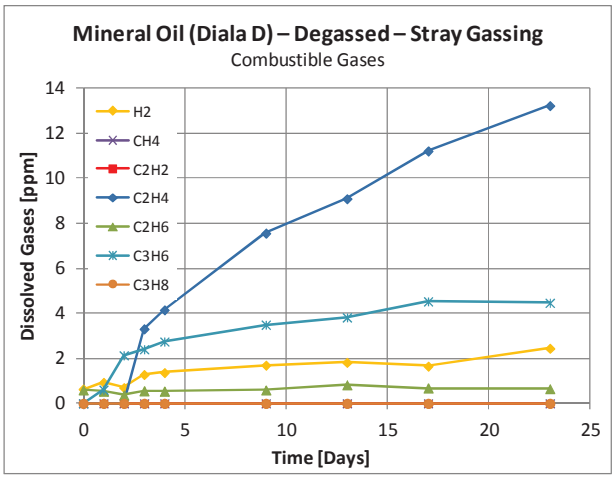


Figure 5. Stray-gassing of degassed unused mineral oil.

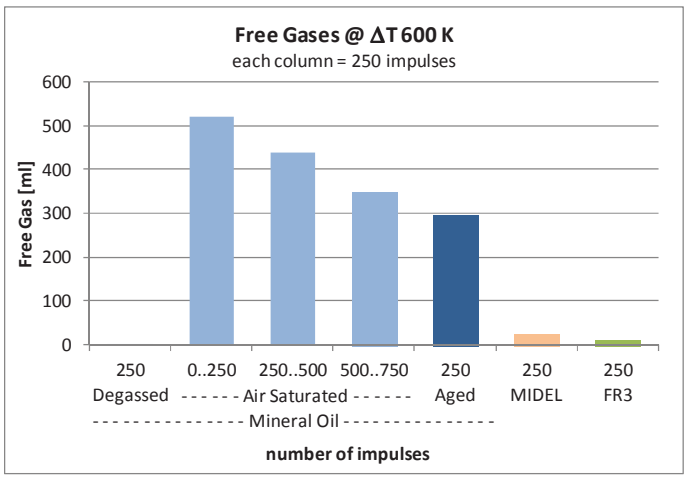


Figure 6. Free gases at ΔT = 600 K after 250 current impulses.

Remarkable amounts of free gases developed only in air-saturated unused oil and thermally aged oil for temperature rises of 350K and 600K (see Fig. 6). MIDEL7131 and FR3 showed free gases a magnitude less, and degassed mineral oil showed none, even at 600K. The decreasing amount of free gas produced from air-saturated mineral oil results from a partial degassing, caused by the heating impulses. The total amount of dissolved gases (TDG) has been measured to decrease with over 10'000 ppm during the test duration.

III.2. Gassing of Vacuum Type OLTCs under Nominal Load

Power switching tests with vacuum type OLTCs (VACUTAP® VV, VM, VR, RMV-II) have been performed to determine the gassing behaviour under different load conditions (partial load, nominal load, overload).

ISBN 978-84-617–9183–5

Table II. Typical Gas Generation Rates [ppm/1000 Operations] for VACUTAP® OLTCs under Nominal Load

	VV	VM	VR	RMV-II
H_2	0.4	2.1	3	0.8
CO	1.2	2.1	0.3	0.3
C_2H_2	<0.1	n.d.	0.3	<0.1
C_2H_4	<0.1	0.2	0.3	<0.1

30'000 to 60'000 switching operations have been performed within some weeks. The development of gases has been recorded with different online-DGA monitoring systems (hydrogen-, composite gas- and four gases- monitor) and was supported by additional regular laboratory analyses. The three online sensors have been mounted on a special test stand which provided the same amount of oil to stream along each sensor. In a closed circuit, a special pump with minimized turbulences transported the oil out of the OLTC oil compartment to the sensors and back. A sealed expansion tank with rubber bag was used to compensate for the thermal expansion of the oil without gas losses. Due to the extreme time-squeezing the amount of dissolved gases developed on a level which could reliably be measured by the online sensors. Free gases did not occur at any time. From the recorded data, gas generation rates (ppm per 1000 operations) could be derived; see Table II. H_2, C_2H_2 and C_2H_4 can be attributed to the commutation activity, but H_2 could (partially) also have been generated by stray-gassing processes. As described in chapter II.1., CO can be used as indicator for incipient thermal oil ageing, caused by the heat of the transition resistors. Unlisted gases in Table II were not reliably detectable.

During normal network operation, the actual gas generation rates will be lower, because a) gas loss will occur via the breathing system (if not sealed) and b) under partial load, commutation processes will be weaker and resistor heating will be lower than in the tests under nominal load.

It should be emphasized that the VACUTAP® VM is the only vacuum type OLTC which, due to its missing main contact, does not produce C_2H_2 in reliably measurable amounts (above the quantification limit, typically 10 times the detection limit) during normal service. This OLTC type leads the load current continuously through the vacuum interrupter(s) in the main path.

III.3. Gas Exchange through Combined Oil Volumes

A possible exchange of dissolved gases between tap-changer oil and transformer oil has been investigated using a model setup consisting of a small oil compartment (65 litres, "tap-changer") which was mounted inside a bigger tank (1185 litres, "transformer"). Both oil volumes were connected by a pipe elbow; see Fig. 7, and filled with degassed unused mineral oil (NYNAS Nytro Taurus). Via the sampling valve, the tap-changer oil was inoculated with C_2H_2. The resistor inside the small compartment was heated by current impulses controlled by an electronic AC power controller. The current impulses ("switching operation", similar to Fig. 4) generated temperature rises of 160K and 250K respectively, which represent the typical resistor heating of an MR tap-

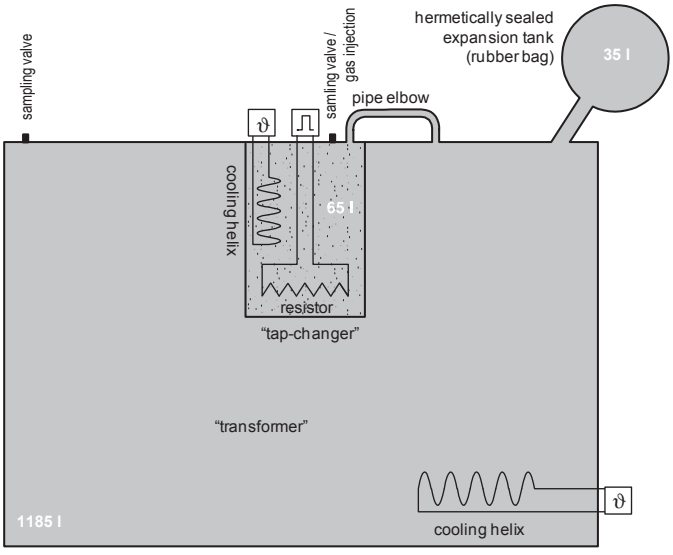


Figure 7. Test setup for gas exchange with combined oil volumes.

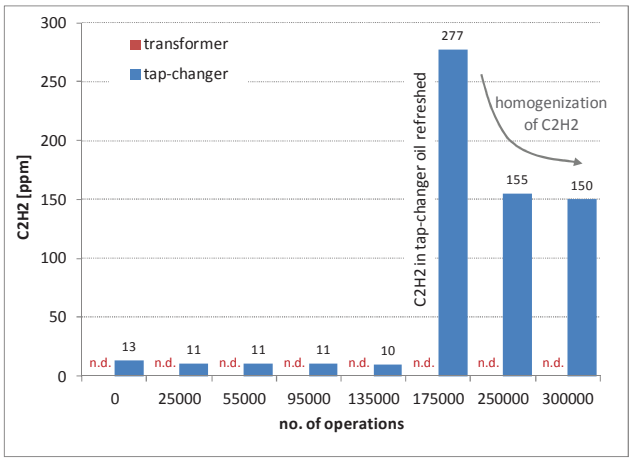


Figure 8. C_2H_2 content in "transformer" and "tap-changer".

ISBN 978-84-617–9183–5

changer under network load and under 1.5 times overload. 300'000 current impulses were applied in total. The maximum oil temperature in both oil compartments was limited to 50°C by appropriate cooling systems (cooling helixes) to minimize a potential self-gassing activity of the oil.
The heat energy introduced by the resistor heated the tap-changer oil and so caused a thermal expansion. With each impulse, the tap-changer oil volume expanded for approximately 1 ml. A temperature rise of 25K (difference between room temperature 25°C and maximum oil temperature 50°C) caused a volume increase of approximately 1.2 l. Less the volume inside the connecting pipe elbow (ca. 0.5 l), a total oil volume of 0.7 l was pumped into the transformer tank during the heating interval, and it was drawn back during the cooling period. In total, 17 heating/cooling periods within 1 month time were performed, causing a permanent oscillation of 1.2 l of oil.

In regular intervals, oil samples were taken from both oil compartments and DGAs were performed. At the end of the test, the tap-changer oil showed a slight increase of the heating gases CH_4, C_2H_4, C_3H_8 and C_3H_6 between 1 and 7 ppm for each gas. In the transformer oil, the increase of dissolved heating gases was below 1 ppm.
The inoculated C_2H_2 was not detectable in the transformer oil after the end of test, see Fig. 8.

IV. Field Studies

Vacuum type OLTCs in network service are considered as almost maintenance-free and are usually not conscientiously monitored. For the time being, only sparse field data are available, as they are the property of users all over the world. The tap-changer manufacturer is only contacted in isolated cases by users to give a statement on DGA. In the following, several instructive cases are described.

IV.1. Network Service

A two years field study has been performed on a free-breathing VACUTAP® VM OLTC, which is doing service in a 40MVA network transformer in Germany, 110kV/21kV, with 110kV ±16% regulating range. The step voltage is 1129 V, the maximum through-current 250 A. During a full load operation, the transition resistors were calculated to heat up for 60 K. After 2 years in service, the OLTC had performed approximately 4000 operations. The transformer oil temperature, which was recorded continuously, showed an average value of 27 °C, indicating a very moderate average load. Low amounts of H_2, CH_4 and CO were measured, with H_2 and CH_4 near the quantification limit. The CO content was significantly higher which gives an indication on light thermal oil ageing, caused by the transition resistor heating. Following Duval Triangle No. 4 (for stray-gassing and low temperature faults) [6], H_2 and CH_4 can be attributed to *"stray-gassing"*; see Fig. 9.

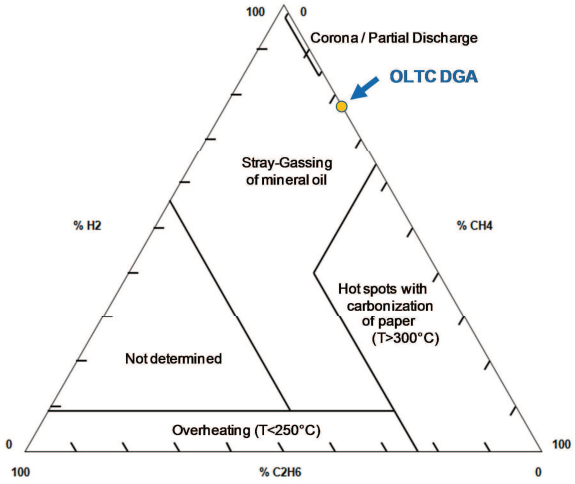


Figure 9. OLTC DGA using Duval Triangle No. 4 VACUTAP® VM, network service.

In another example, DGA was performed on two free-breathing VACUTAP® VRC OLTCs working in transformers sized 280MVA, 155kV ±13%, which are located in Germany at the landing station of an offshore North Sea wind park. After 3 years in service, only 440 operations have been performed. The DGAs showed significant values of H_2 (90 and 114 ppm) and low amounts of CH_4 (5 and 4 ppm), which is an indication for the sparking activity of the main contact, caused by current commutation (refer to chapter II.1.). Such pattern appears as *"corona/partial discharge"* in Duval Triangle No. 4; see Fig. 10.

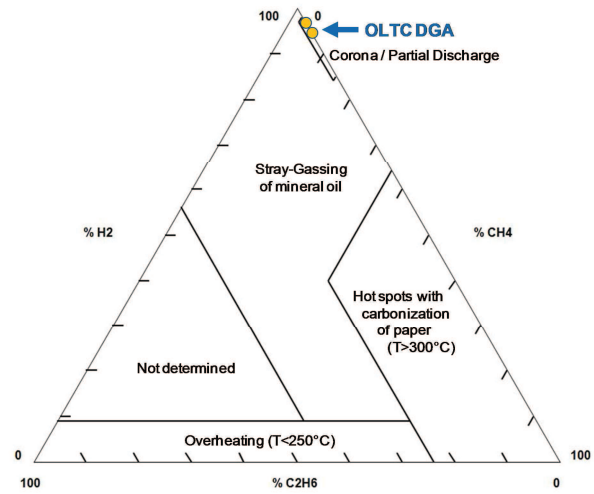


Figure 10. OLTC DGA using Duval Triangle No. 4 VACUTAP®VRC, network service.

ISBN 978-84-617–9183–5

Additionally, CO (95 and 76 ppm) and CO_2 (1020 and 736 ppm) were detected, which represent the thermal stress from the transition resistors. The oil was saturated with air.
As it is often the case, no "zero sample" from the date of commissioning was available. So one can only guess if all deterioration gases developed during the time in service.

IV.2. INDUSTRIAL SERVICE

In a steel mill in the U.S., a VACUTAP RMV-II 1500 is working for over 10 years on an arc furnace transformer and has performed over 1.5 million operations up to now. Regular maintenance was done to ensure the proper function of this heavy-loaded OLTC at any time. Nevertheless, the tap-changer shows exceptional amounts of C_2H_2 and a steady rise, while other gases (H_2 and heating gases) stay fairly constant. Inspections have verified that this unit is working properly, and that the formation of C_2H_2 must be fully attributed to the normal current commutation on the by-pass contacts (similar to the main contacts MCA, MCB in Fig. 1). No excessive contact erosion could be found on the by-pass contacts. Approximately 280'000 operations/year have been performed over the last years, causing a rise in C_2H_2 of approximately 50 ppm/year. The gas generation rate for C_2H_2 has been calculated to approximately 0.16 ppm per 1000 operations, which exceeds the values given in Table II, but appears to be reasonable for arc furnace applications. An equilibrium between gas production and gas loss via the breather could not be achieved so far, indicating that there are very low changes in oil temperature, which means low breathing activity. Because the operator is concerned about the high C_2H_2 values, the tap-changer oil is exchanged or degassed in regular intervals. Fig. 11 shows the latest DGA records of an operating interval between two inspections, Fig. 12 shows the graphic representation of data points in Duval Triangle No. 2 (LTC triangle).

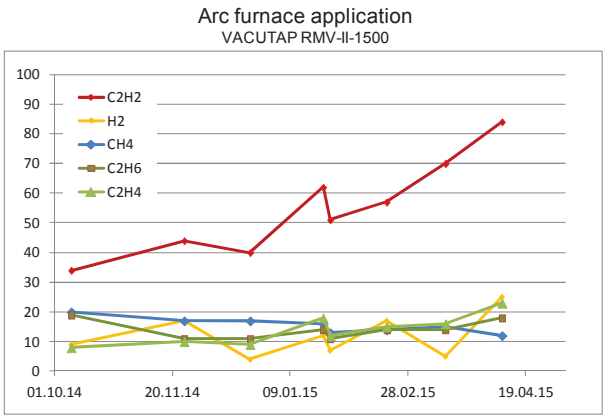


Figure 11. Development of dissolved gases between Oct 2014 and Apr 2015.

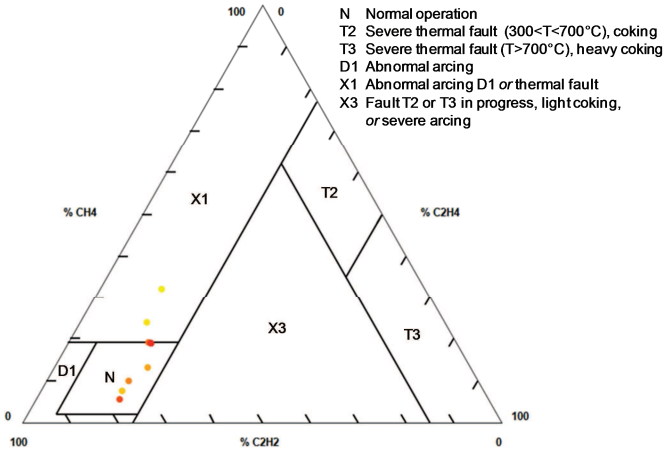


Figure 12. Data acc. to Fig. 11 in Duval Triangle No. 2.

It can be seen that all points are cumulated in or near the "N" zone. Even if the LTC triangle has been originally designed for reactive oil switching OLTC types (as typically for the U.S.), it is also applicable to reactive vacuum type LTCs [7].

V. SOLUTIONS AND FINDINGS

The tests described in chapter III.1. have revealed that the development of dissolved gases in mineral oil, which are generated by the transition resistors, considerably depends on the degree of thermal oil aging (oxidation). Air-saturated oil tends to produce free gases more easier than degassed oil. Ester liquids start gassing at higher temperatures than mineral oil, but then they produce more gases than mineral oil. The gas patterns are slightly different to the patterns observed with mineral oil.

The power switching tests (chapter III.2.) and the field studies (chapter IV.1.) have shown that the real gas development for vacuum type tap-changers in network applications is very moderate. The transition resistors

ISBN 978-84-617–9183–5

only produce low amounts of heating gases, even for occasional overload, and the commutation contacts produce only low amounts of sparking or arcing gases. In free-breathing systems, the hydrocarbon gases will be near the limit of quantification or will appear as low 1-digit numbers. This enables innovative solutions, such as sealed applications or the combination of the two oil volumes of transformer and tap-changer.

V.1. SEALING OF TAP-CHANGER OIL COMPARTMENT

If an on-load tap-changer is hermetically sealed, there is no definite way for free gases to escape. Free gases will cause a rise in system pressure which may reach inadmissible levels. The admissible pressure range for the tap-changer oil compartment goes from 0.7 to 1.8 bar absolute. To avoid free gases also under overload conditions, the design of the transition resistors can be adapted, if necessary, to limit surface temperatures to values below 300 °C. The generated heat depends on the individual configuration for a given application.
Sealing measures can only be applied to vacuum type OLTCs. Different methods have been developed, which use flexible rubber balloons, nitrogen cushions or flexible tank walls and radiators. Fig. 13 shows common solutions.

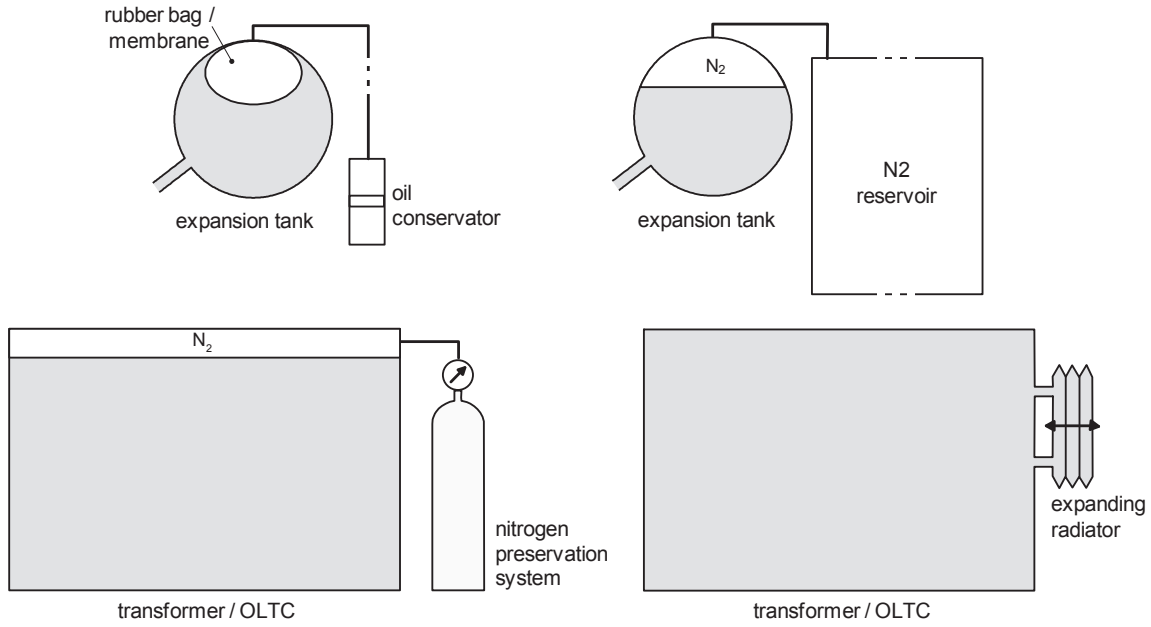


Figure 13. Common technical solutions for hermetical sealing of transformers and vacuum type OLTCs.

During commissioning, the oil is filled in under vacuum which ensures that the oil is (at least partially) degassed, leading to a further reduced tendency to produce free gases.

Sealing measures are required if natural ester liquids should be used. Such liquids are prone to oxidation, which causes polymerization and consequently an inadmissible increase in viscosity [8].

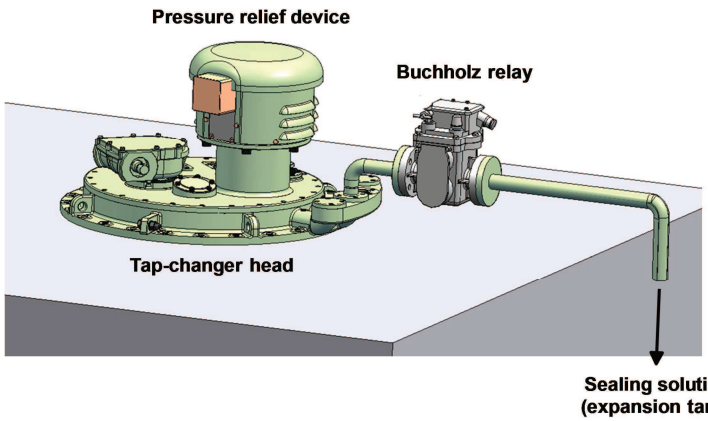


Figure 14: Protection concept for sealed tap-changers (in-tank type).

According to IEC 60214-1, the tap-changer must be equipped with a protective device in order to minimize the risk of fire or explosion which can result from an internal fault within the diverter or selector switch compartment. The protection concept is different for free-breathing and sealed applications. For free-breathing applications, an oil-flow relay acts as protective device and triggers the circuit breaker in case of a fault inside the tap-changer oil compartment. In sealed tap-changers, the reliable operation of the oil-flow relay cannot be guaranteed, because the

ISBN 978-84-617–9183–5

sealed expansion tank may impede the oil flow. Therefore, a pressure-relief device (PRD), mounted on the tap-changer head cover, acts as protective device (see Fig. 14). The PRD guarantees extremely responsive, effective protection of the OLTC which always triggers under the same, precisely defined conditions. This is the only way of implementing a protection concept that ensures reliable function under all operating conditions, regardless of the solution chosen for hermetic sealing and independently of the pipe geometries. Additionally, a Buchholz relay detects free gases which may accumulate in case of a beginning failure and then produces a warning signal.

V.2. CONNECTING THE OIL VOLUMES OF TRANSFORMER AND TAP-CHANGER

As verified in chapter III.3, transformer DGA is not influenced by the tap-changer oil even if it contains remarkable amounts of combustible gases. The field studies have shown that the actual amount of gases is much lower. So it is a logical step to combine the two oil households of tap-changer and transformer. This combination is available for free-breathing systems as well as for sealed systems. The first field study in chapter IV.1. features connected oil volumes in a free-breathing application. Practical experience on a sealed application is given in [9]. These and other network applications have proven that transformer DGA is not measurably influenced by tap-changer gases.

The connection of oil volumes of transformer and tap-changer offers several advantages and savings, such as a simplified piping construction and the omission of a second oil conservator. Fig. 15 shows a possible solution for free-breathing applications. The pipe from the tap-changer which normally leads to the OLTC expansion tank is connected directly to the pipe which leads from the transformer to the expansion tank. With this, the separate chamber in the expansion tank for the OLTC can be omitted, including its oil level indicator and oil conservator. It has to be considered that, in case of a malfunction, fault gases cannot be explicitly assigned to the transformer or the OLTC. If this is a problem, an alternative piping can be used which connects the OLTC pipe to the expansion tank *behind* the Buchholz relay; see Fig. 15. This also minimizes a possible gas exchange between the two oil volumes.

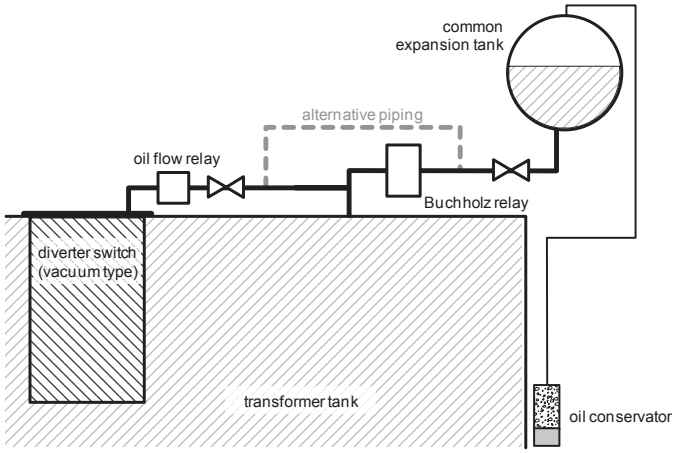


Figure 15: Connected oil volumes for free-breathing applications.

Concerning sealed applications, the sealing method applied is often unknown to the tap-changer manufacturer, so that the proper function of the oil-flow relay cannot be guaranteed. If the protection concept from chapter V.1. is applied in combination with the piping shown in Fig. 15, the solution acc. to Fig. 16 (left) is achieved. If

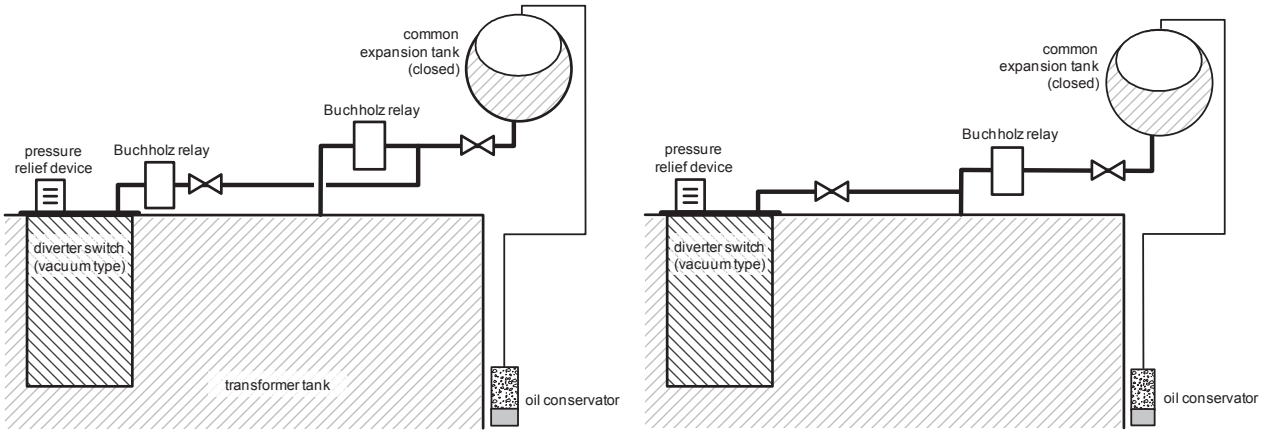


Figure 16. Connected oil volumes for sealed applications
left: principal schematic / right: optimized solution.

ISBN 978-84-617–9183–5

a separate tap-changer gas warning is not required, the Buchholz relay of the transformer can adopt this function (Fig. 16 (right), optimized solution). It has to be pointed out that, like in Fig. 15, the origin of possible free gases cannot be located. Anyhow, the OLTC protection concept for sealed applications is fully supported.

V.3. DGA

As explained in chapter II and in the field studies, DGA data from vacuum type OLTCs usually show very low ppm values. H_2 and CO, CO_2 however, are measured to greater amounts and have turned out to be indicative for the arcing/sparking behaviour (H_2) and the thermal load of the OLTC (CO, CO_2). For sealed applications, the values are supposed to be slightly higher, and tap-changers in industrial services with frequent overload and/or a high number of operations, such as arc-furnace applications, show DGA values one magnitude higher than in network service. This impedes the definition of universal admissible limit values. However, unexpected high amounts of dissolved gases or the formation of free gases usually indicate abnormality. Practical experience has shown that incipient failures developing slowly or single exceptional events (like non-destroying flashovers with low energy) could reliably be detected by unusual elevated amounts of dissolved gases.

Besides that, there are also cases with exceptional gassing behaviour without allocation to a definite root cause. The reasons for such behaviour can be manifold:

- data may be inconsistent or erroneous due to sampling or analyzing errors
- only a single DGA without any reference to the history is available
- important operational parameters are unknown, such as
  - temperature of oil sample / oil brand name
  - total no. of OLTC operations; average number of operations per day
  - actual load of the transformer; information on recent load changes
  - application data (network service, industrial application, …)
  - date of last OLTC maintenance
  - OLTC serial no.
- relevant information on specific features of the application is missing, like information on
  - additional equipment like oil filter units, coolers or heaters which can influence the gassing behaviour
  - breathing situation (sealed / free-breathing)
- unusual wave forms of load current or voltage
- exceptional combination of part tolerances
- pollution of the oil with gases from industrial environment

In such cases, the DGA values must be accepted “as they are”, and they suggest a more intensive observation by regular monitoring.

High C_2H_2 values inside a vacuum type OLTC represent distinct arcing activity. With this, C_2H_2 is the most significant gas to be monitored. Field experience has shown that, in case the absolute value of dissolved C_2H_2 exceeds 50 ppm, an inspection of the OLTC is recommendable.

With respect to exceptional cases of gassing without indication of a fault, the following maximum gas generation rates for C_2H_2 per 1000 operations are defined for normal operation in network service (Table III):

Table III. Maximum C_2H_2 Gas Generation Rates for VACUTAP® OLTCs in Network Service.

	ppm C_2H_2 / 1000 operations
VACUTAP® VV	<2
VACUTAP® VR	<4
VACUTAP® VM	0
VACUTAP® RMV-II	<3

ISBN 978-84-617–9183–5

These values should be used as guiding values which may occur between two consecutive DGA samples. They may not be used to define limit values for C_2H_2 for a defined number of switching operations. The number of operations between these two samples must be known.

Trend analysis of significant gases or TDCG (Total Dissolved Combustible Gases) is a powerful tool to evaluate the development of gases even at low ppm values or at low gas increasing rates. Intelligent algorithms like harmonic regression can suppress periodic variations due to daily load changes or other influences. Piecewise linear approximation methods can be used to differ between the normal gas increasing rate and unusual behaviour. To be successful, DGA data must be correlated with corresponding operational parameters, such as actual load, oil temperature and time stamps of OLTC operations. The determination of relevant correlation factors or equations (linear or non-linear) may be complicated, but for identifying correlations, statistical methods (data-mining techniques) can be applied on reference data bases containing faulty and non-non-faulty equipment. The correlation parameters can be tuned then on the specific application by learning algorithms.

These functions can be implemented as software in suitable online monitoring systems, such as TAPGUARD®. As a result of such intelligent evaluation, caution and warning limits can be individually set and so are specific to the individual application. More general limit values which are valid for a specific OLTC population or model family are also possible by combining data from several installations. The greater the data base, the more stable are correlations and the more reliable are the results. With increasing experience, limit values and interpretation results can be adjusted and refined.

If necessary, additional monitoring techniques like vibro-acoustic [10] and/or dynamic resistance measurement (DRM) [11] can support tap-changer DGA.

VI. CONCLUSION / OUTLOOK

Innovative solutions for on-load tap-changers are only applicable with vacuum switching technology. As long as no solid-state tap-changers are available for all voltage classes and transformer ratings, vacuum type OLTCs offer the best performance. In future, power transformers will be increasingly filled with natural esters, as the call for low flammability and environmental friendliness is getting louder. Due to the limited oxidation stability of natural ester liquids, they can be only used in sealed applications. The combination of a sealed transformer with sealed tap-changer with connected oil volumes and natural ester filling fulfils all needs and leads to a really environmentally friendly transformer.

In advancing the “connected oil volumes” technique, single-phase tap-changer units without dedicated oil compartment are imaginable, which are powered by intelligent direct drives, separate for tap selector and diverter switch. This offers an extremely high flexibility, because the tap-changer modules can be mounted at optimal positions inside the transformer tank, reducing its footprint and oil volume. Such considerations are part of various concepts for a “Smart Transformer”, which forcefully combine monitoring data of the transformer, tap-changer, bushings and other connected equipment as well as from the electrical network to achieve an optimized operation and optimized power flow. Out of the comprehensive monitoring data, a “Health Index” of the equipment can be generated which enables an effective fleet management and so increases the reliability and the lifetime of the equipment. Cross-linking of data and intelligent monitoring enables smart power supply systems for the future.

REFERENCES

[1] I. Höhlein-Atanasova, SIEMENS, R. Frotscher, MR: *Carbon Oxides in the Interpretation of Dissolved Gas Analysis in Transformers and Tap-Changers*, IEEE Electrical Insulation Magazine, Vol. 26, No. 6, pp. 22-26, Nov/Dec 2010.

[2] D. Dohnal, MR, *Classification of on-load tap-changers (LTCs) with regard to dissolved gas analysis (DGA)*, Tutorial Session, IEEE Transformers Committee Meeting, Vancouver, Spring 2002.

ISBN 978-84-617–9183–5

[3] M. Shirai, S. Shimoji, T. Ishii, Mitsubishi Electric Corp., *Thermodynamic Study on the Thermal Decomposition of Insulating Oil*, IEEE Transactions on Electrical Insulation, Vol EI-12 No 4, Aug 1977.

[4] I. Höhlein-Atanasova, SIEMENS: *Unusual Cases of Gassing in Transformers in Service*, IEEE Insulation Magazine, Vol. 22, No. 1, January/February 2006.

[5] Z. Wang, University of Manchester, J. Hinshaw, BPL Global, J. Noakhes, TjH2b, *Fault Gas Generation in Natural-Ester Fluid Under Localized Thermal Faults*, IEEE Electrical Insulation Magazine, Vol. 28, No. 6, pp. 45-56, Nov/Dec 2012.

[6] M. Duval, *The Duval Triangle for Load Tap Changers, Non-Mineral Oils and Low Temperature Faults in Transformers*, IEEE Electrical Insulation Magazine, Vol. 24, No. 6, pp. 22-29, Nov/Dec 2008.

[7] M. Duval, *Interpretation of Dissolved Gas Analysis in Electrical Equipment with Duval Triangles and Pentagons*, Technical Presentation at IEEE Transformer Committee, Atlanta (GA), Mar 2016.

[8] R. Frotscher, MR, *On-Load Tap-Changers with Vacuum Switching technology for increased fire safety, reliability and environmental performance*, ARWtr2010, Santiago de Compostela, Spain, Oct 2010

[9] T. Stirl, J. Harthun, ALSTOM, R. Frotscher, MR, *Offshore Use – A Challenge for the Transformer*, Stuttgarter Hochspannungssymposium, Germany, 2012.

[10] M. Foata, R. Beauchemin, K. Viereck, A. Saveliev, H. Hochmuth, MR: *New Vibro-Acoustic Tap-Changer Diagnostic Method: First results and Practical Experience*, paper A2-104, CIGRE Session Paris, 2016

[11] Raka Levi, ARCE, Budo Milovic, IBEKO Power, *OLTC Dynamic Testing*, TechCon North America, San Francisco (CA), 2011

ISBN 978-84-617–9183–5

Dynamic Resistance Measurements on Load Tap-Changers

Matz OHLEN

Megger Sweden AB
Rinkebyvagen 19, SE-182 17, Danderyd, Sweden
Phone: (+46) 708307787, fax: (+46) 851019595, e-mail: matz.ohlen@megger.com

Abstract — **Dynamic Resistance Measurement (DRM) has been used for circuit-breaker diagnostics for over 20 years. It is an interesting technique that can be used also to verify the switching operation of load tap changers (LTC). Existing methods and techniques for dynamic measurements on load tap-changers are based on measuring current and/or voltage on the primary side of the transformer and short-circuiting the secondary side to minimize the inductance in the circuit. Static resistance measurements per tap are performed in a separate test sequence with the secondary side open. A new technique is to combine current measurement with voltage measurements on both primary and secondary side of the transformer and then use the transformer modelling parameters to calculate inductive and resistive voltages to be able to calculate the dynamic resistance during a tap change.**

Keywords — **Transformer, Tap-changer, OLTC, DRM, measurement**

I. INTRODUCTION

The power transformer is an integral and expensive part of all electric power networks at all levels from generation and transmission down to distribution. The on-load tap changer is the only moving part connected to the transformer windings, and as such is the most susceptible to failure. The importance of its reliability cannot be overemphasised. Taking a transformer off the system to investigate an internal problem with a tap changer is an expensive exercise; therefore it is in every utility's interest to carry out condition assessments of their tap changers to help detect developing faults at an early stage.

II. TAP CHANGER TYPES

Tap changers can be divided into two main types; On-load (OLTC, On-load Tap Changer) and Off-load/de-energized (DETC, De-Energized Tap Changer). The OLTC allows selection of voltage change while the transformer is in service. In Europe and internationally, the most common configuration is to have the tap-changer on the HV side of the transformer. Fig. 1 depicts a typical on-load tap changer with tap selector and diverter switch with transition resistors. Fig. 2 a linear-type OLTC with diverter resistors.

The resistors in the diverter switch are typically a few ohms. Total operation time of an LTC is between 3 and 10 sec pending design. Contact switching time is usually in the order of 30-100 ms (resistor types).

Reactance type LTC's, common in US and mostly mounted on the LV side of the transformer, use a preventive auto transformer instead of the two resistors in the standard diverter switch which mean that the additional resistance in the diverter device is very low. Measurements on reactance type load tap-changers are not covered in this paper.

III. STATIC MEASUREMENTS ON TAP-CHANGERS

The most common diagnostics test for tap-changers is to perform winding resistance measurements [1]. WRM is normally performed for each tap in the same way as an individual winding without taps. A suitable test current is injected through the winding and the resistance for each tap is measured sequentially as the tap changer is stepped through its positions. Results are typically presented as a graph or table with resistance values for each tap. Resistance change per tap should be consistent throughout all positions, with only minor deviations. An example showing deviations between taps is shown in Fig. 3. Red phase – OK, Blue phase – "Questionable". Fig. 4 shows a linear selector switch design is good/as-new condition

ISBN 978-84-617–9183–5

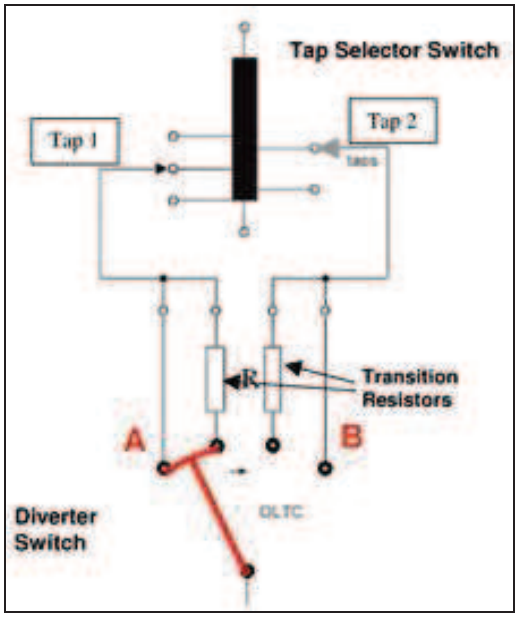


Figure 1. A typical diverter switch type OLTC showing both tap selector switch and diverter switch (MR).

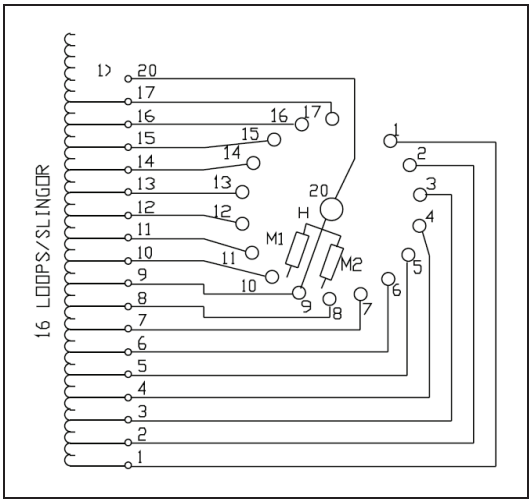


Figure 2. A typical OLTC with selector switch (17 taps linear) (ABB).

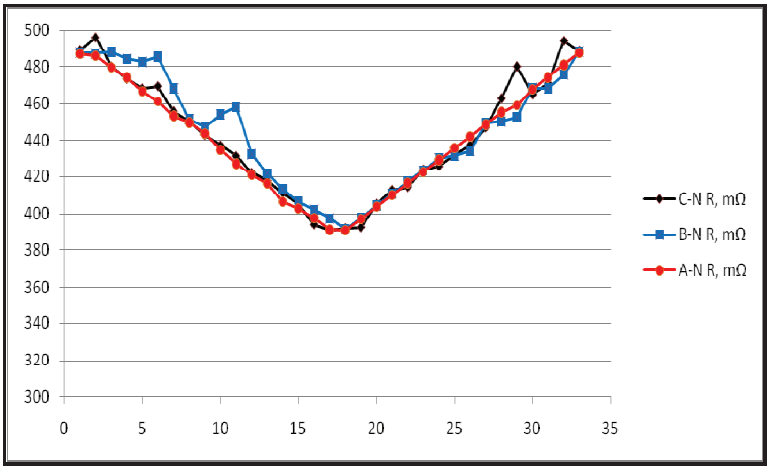


Figure 3. WRM/tap, diverter design – Old/aged condition.

ISBN 978-84-617–9183–5

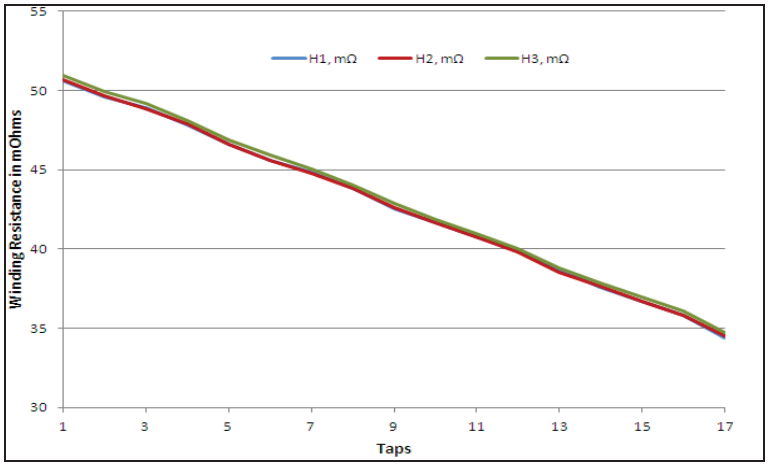


Figure 4. WRM/tap. Selector switch (linear type) tap changer in as-new condition.

IV. DYNAMIC MEASUREMENTS ON TAP-CHANGERS

There are several methods developed for dynamic testing of tap changers but common for all is that a current is injected in the tap changer and the current and/or the voltage is measured as a function of time during the operation of the tap changer. Test currents vary from about 0.1 A to standard test current for winding resistance measurements (typically 1% of rated current for the transformer winding). The measurements are sometimes performed at the same time as measuring winding resistance and sometimes as a separate test. The most common tests are;

- Continuity/make-before-break verification
  - Shut-off if current path is interrupted
- Dynamic measurements
  - Dynamic current/"ripple"
  - Dynamic voltage
  - Dynamic resistance, DRM

IV.1 CONTINUITY TESTING

This test should detect if there is a break-before-make condition in the tap changer by monitoring current change. The measurement is typically performed at the same time as winding resistance measurements and the instrument detects if the contact switching is continuous or if there is an interruption in the current path.

Open contact detection can be made by a variety of methods/detection principles but common for all of them is that if the current drop/change exceeds a certain value, the instrument identifies this state as "open circuit" and sets an alarm or stops test current injection.

IV.II DYNAMIC CURRENT MEASUREMENTS

Dynamic current measurements (DCM) assume that the power supply can be seen as a constant voltage source and the results are pending test current. If the test is performed at a current level below saturation level, the inductance in the transformer winding is high and smooths the current change. If the test is performed at a current level at or above saturation level, the inductance is low and current level change will be higher [1].

A method to reduce transformer inductance when performing DCM test is to short-circuit the not tested corresponding LV (or HV) windings. This action is principally "replacing" the inductance of the winding with the short-circuit impedance. Inductance is greatly reduced and changes in current can be measured more precisely. Fig. 5-8 below show dynamic current measurements on a 30 MVA, 130/46 kV, YNyn0 transformer using different test currents and with LV windings shorted and open respectively [2].

ISBN 978-84-617–9183–5

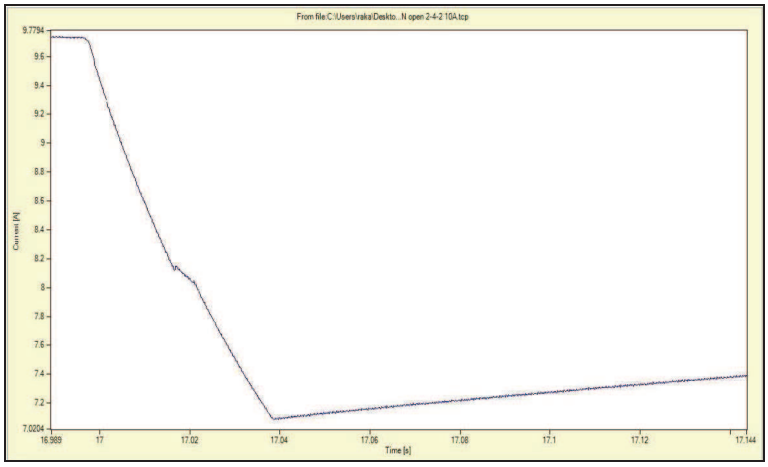


Figure 5. 10 A test current, shorted LV.

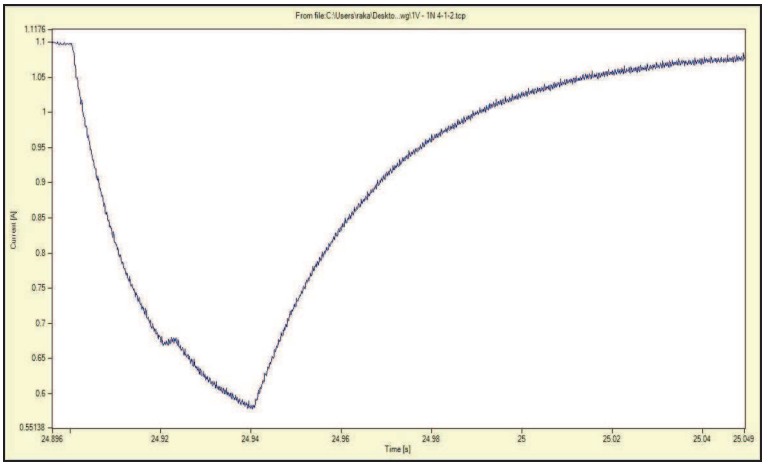


Figure 6. 1 A test current, shorted LV.

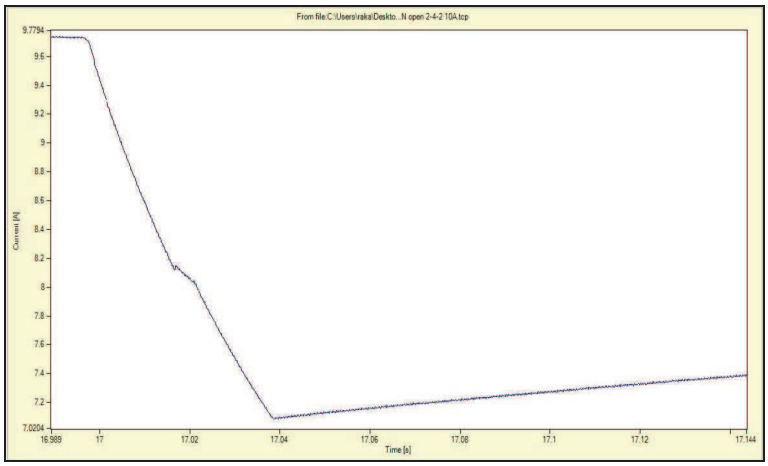


Figure 7. 10 A test current, open LV.

As seen in the fig, dynamic current measurements are pending the inductance of the circuit. If the test is performed at high current or with LV shorted (low inductance), timing of the tap switch can be identified and estimated. Resistor values cannot be estimated.

ISBN 978-84-617–9183–5

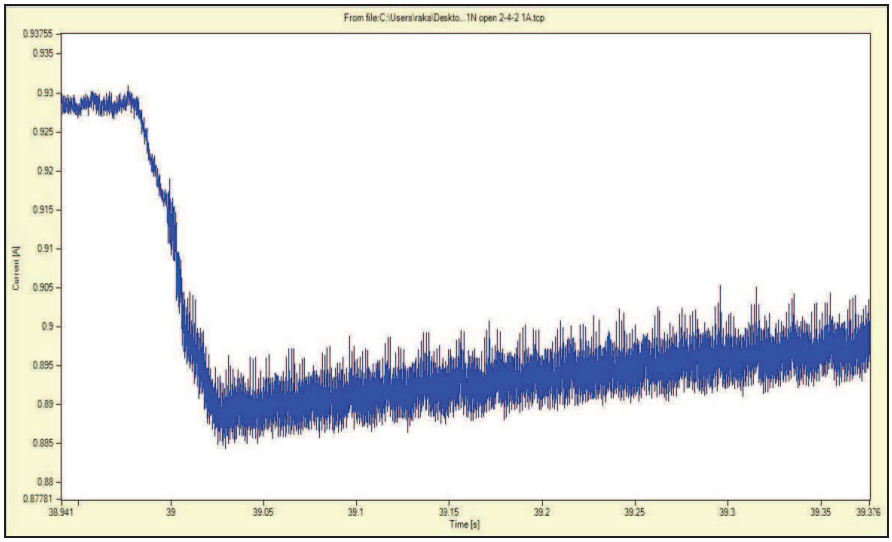


Figure 8. 1 A test current, open LV.

IV.III Dynamic Voltage Measurement

Dynamic voltage measurements on LV side of the transformer (assuming a resistive type OLTC on HV) can also be used for timing measurements. The advantage is simplicity; it is e.g. possible to use a single voltage measurement channel to perform a timing check of the tap-changer (not resistor values). A typical measurement result is shown in Fig. 9.

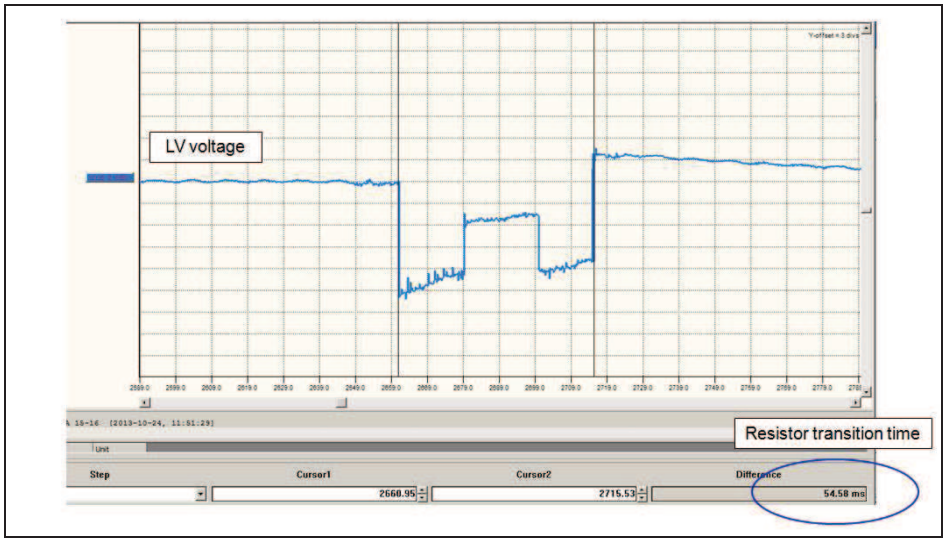


Figure 9. Dynamic voltage recording for an OLTC tap transition.

IV.IV Dynamic Resistance Measurement with Shorted LV

Dynamic resistance measurement (DRM) is a standard method for circuit-breaker testing and can also be applied to tap changer contacts [3]. A relatively small test current (0.1 to 1A) is injected through the tap changer using a high-impedance current source and the LV windings of the transformer are short-circuited. Contact timing as well as diverter resistor values can be measured. A test setup is described in Fig. 10.

As seen in Fig. 11, contact timing and resistance values are easily recognized. Fig. 12 provides a summary of measured switch times for this linear type tap-changer with 17 taps/16 transitions. No malfunctions detected.

ISBN 978-84-617–9183–5

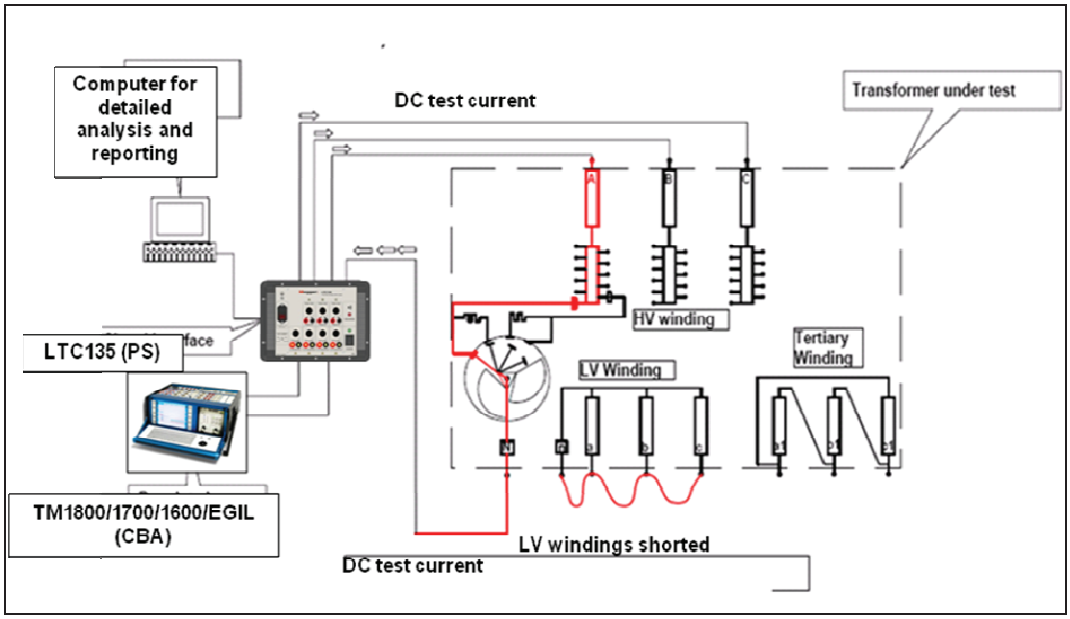


Figure 10. Dynamic Resistance Measurements on a load tap-changer (direct method).

An example from measurements on a 20MVA, 22/10 kV transformer is shown in Fig. 11 and 12.

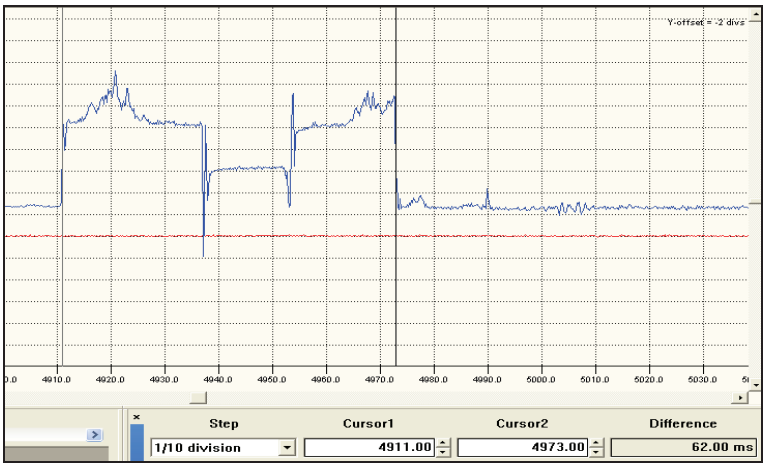


Figure 11. DRM on OLTC, 0.1 A test current, constant current source, shorted LV. Red; Current, Blue; Resistance.

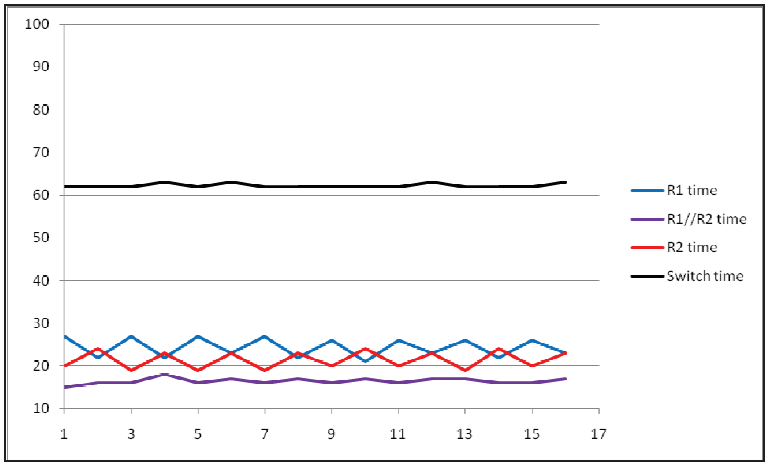


Figure 12. H1 OLTC transition times (ms). 1-2 to 16-17 tap change.

ISBN 978-84-617–9183–5

IV.V Dynamic Resistance Measurement with Open LV

A new method (patent pending) is to measure dynamic resistance in the tap-changer by simultaneously measuring the test current together with voltages on both HV and LV windings and combine the results with transformer modelling. The test setup is the same as in Fig. 10 but with the difference that the LV winding is left open.

An example of a measurement is shown in Fig. 13. The source impedance in this example is about 10 ohm and we can see a small current change during tap change. Due to the inductance in the circuit, the HV voltage change is rather high (open LV). This voltage is a sum of inductive and resistive voltage and cannot be used for directly calculating the resistance in the circuit. However the LV voltage is purely inductive and if we use transformer modelling parameters to calculate the inductive voltage on the primary, we can deduct this value from the measured HV voltage and calculate the resistance in the circuit.

The results are presented as OLTC switching times and diverter resistance as seen in Fig. 13.

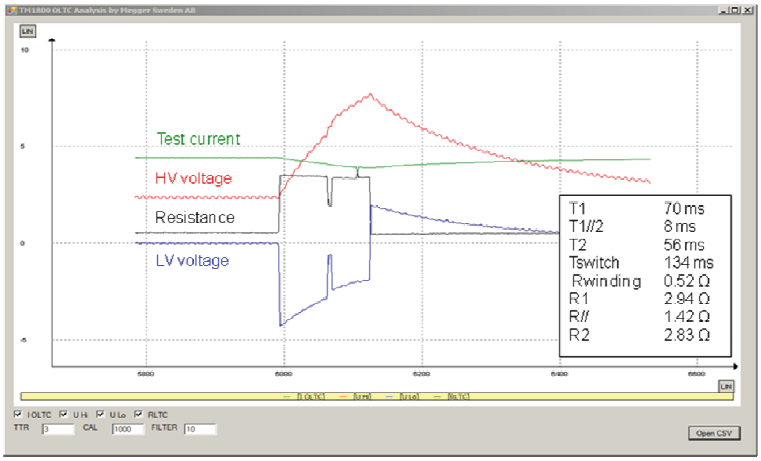


Figure 13. DRM on OLTC, 5 A test current, source impedance 10 Ω, Green; Test current, Red; HV voltage, Blue; LV voltage, Black; Resistance.

V. OLTC Measurements at TSV, Lyon, France

A mutual project between Megger and TSV (Transformer Service Venissieux) to study different test methods for DRM on tap-changers was performed at TSV, Lyon, France. Several tap-changers were measured with and without simulated faults, as separate units and mounted in transformers [4].

V.I Summary of Tests

In the initial tests, a separate (not mounted in a transformer) unit V-type OLTC was used as a test object for verifying the methodology. Test equipment was a constant current supply and a data recording device, test setup as in Fig. 10.

The initial measurement results for verifying the methodology on a tap-changer without any known defects are summarized in Fig. 14 and 15.

As seen in Fig. 14, contact timing is rather stable except for the very first two operations 17-16 and 16-15. The reason was that the unit had not been operated in a quite long time and this is an example of the importance to "exercise" a switching device before stable timing results can be achieved. Measured resistance values (Fig. 15) are as expected almost constant with R1 slightly higher than R2.

ISBN 978-84-617–9183–5

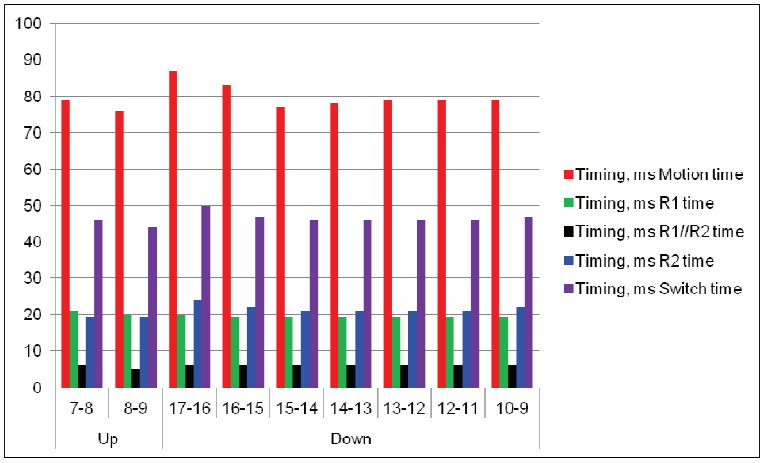


Figure 14. Contact timing for the load tap-changer.

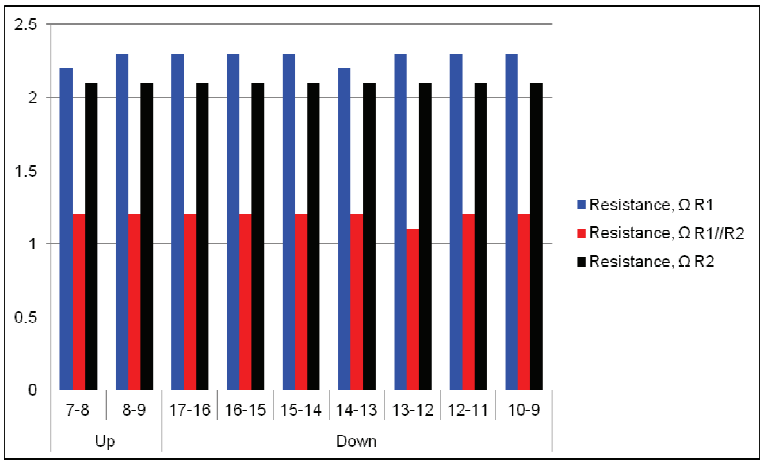


Figure 15. Resistance values during switching of the tap-changer.

V.II MEASUREMENT DETAILS

Several failures/defects have been simulated in attempt to characterize faults based on DRM results and determine the viability of this diagnostic method. The investigated tap-changer is an OLTC type VIII 350A 60kV 17/19 3W.
Two examples of individual DRM results are presented in Fig. 16 and 17. Nominal load resistor value is 1.9 Ω

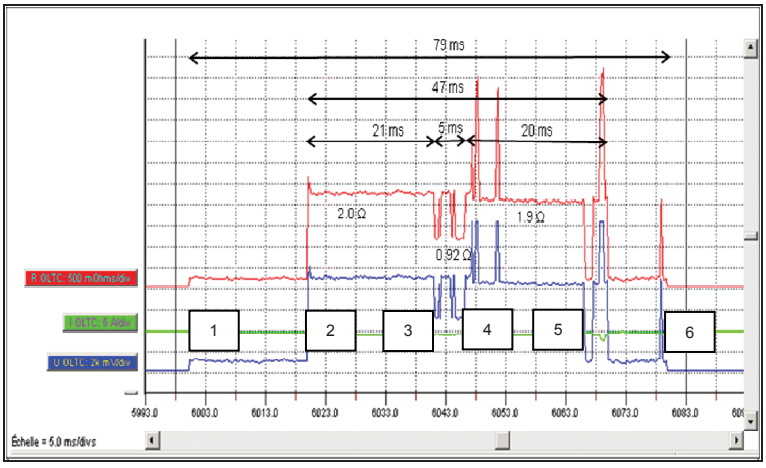


Figure 16. DRM on V-type OLTC, test current 5A, normal condition.

ISBN 978-84-617–9183–5

Note that this tap-changer type has 6 distinctive states for each tap switch. Each of them including the switching from load to non-load contacts is recognized in the DRM test.

1. Load contact releases
2. R1 inserted
3. R2 inserted in parallel with R1
4. R1 released
5. R2 released
6. Load contact makes

Contact bouncing can be seen, especially related to R2 making.
Fig. 17 presents results for a simulated fault. Spring damage, one of the two springs removed.

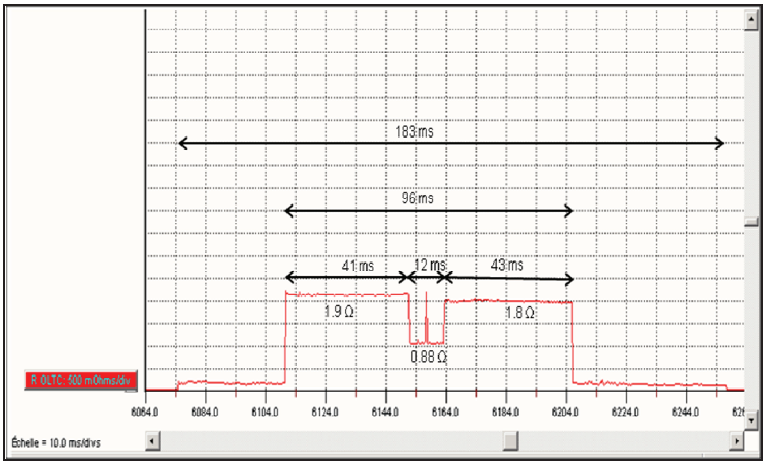


Figure 17. DRM on V-type OLTC, test current 5A, simulated spring defect (one spring removed).

With one spring removed, switching time is about twice as long as when two springs are engaged. Note that contact bouncing almost disappeared due to the lower contact speed.

VI. SUMMARY AND CONCLUSIONS

A recording device together with a suitable power supply is a good tool for performing various dynamic measurements e.g. on load tap-changers. To measure dynamic properties in a tap changer (in this paper assumed to be mounted on the HV side of the transformer), several methods are possible:

- Measure dynamic current/"ripple" on primary with a constant voltage source and secondary open
  - Current drop values are strongly dependent on test current/winding inductance and can only be used as fingerprint
  - Contact timing may be measured (difficult)
  - Diverter resistor values cannot be measured
  - Winding resistance/tap can be measured in the same sequence
- Measure dynamic current/"ripple" on primary with a constant voltage source and secondary short-circuited
  - Current drop values are slightly dependent on test current/winding inductance
  - Contact timing can be measured
  - Diverter resistor values cannot be measured
  - Winding resistance/tap cannot be measured in the same sequence (very long stabilization time)
- Measure dynamic resistance on primary with a constant current source and secondary short-circuited
  - Contact timing (including load-contacts) can be measured
  - Actual diverter resistor values can be measured (high impedance source)

ISBN 978-84-617–9183–5

    - Winding resistance/tap can be measured in the same sequence
- Measure dynamic voltage on secondary winding (secondary open), dynamic voltage on primary and test current
    - Contact timing (including load-contacts) can be measured
    - Diverter resistor values can be calculated
    - Winding resistance/tap can be measured in the same sequence

REFERENCES

[1] D. Chajer and Matz Ohlen, *Preventive Maintenance of Transformer Accessories - Bushings & Tap Changers*, 2011 Weidman conference, USA

[2] J. J. Erbrink et al, *Reproducibility of Dynamic Resistance Measurement Results of On-Load Tap Changers – Effect of Test Parameters*, Proceedings of the 2010 International Conference on Condition Monitoring and Diagnosis, September 6-11, 2010, Tokyo, Japan

[3] AM Forum, *Measurement results from OLTC WG* Workshop, Madrid, Spain, 2011

[4] N. Wacklen, *Timing of Tap Changers*, Programma Electric Application Guide, 1996

[5] P. Illuzzi, *Abstract about measures on V-type OLTC Model*, TSV Lyon-Megger Sweden internal report, 2012

[6] M. Ohlen, R. Yvrard, N. Wacklen, *A new technique for dynamic measurements on load tap-changers*, Proceedings of the 18th International Symposium on High Voltage Engineering, ISH 2013, August 25-30, 2013, Seoul, Korea

ISBN 978-84-617–9183–5

Transformer On-Site Refurbishment Activities at REN - Assessment of 15 Years' Experience as a Solution for Lifetıme Extension

Mário A. SOARES, Jorge F. MARTINS

Department of Asset Engineering, REN
Rua Casal dos Mogos, Vermoim, Maia, Portugal
Phone: (+351) 220011600, e-mail: mario.soares@ren.pt; jorgefilipe.martins@ren.pt

Abstract — **The lifecycle management of a fleet of power transformers requires the definition of an adequate maintenance strategy, which should include condition assessment activities, periodic preventive maintenance, and in some cases, a deeper intervention in order to restore the condition of some parts of the transformer and to allow an extension of the expected lifetime, that may be defined as *refurbishment*. This work presents the results of 15 years' experience of power transformer refurbishment activities at REN in terms of lifetime extension and transformer condition evolution. The assessment focuses on more than 30 transformers, installed in the Portuguese transmission grid, that were refurbished between 2001 and 2015, and includes oil tests, electrical tests, bushing tests, DP measurements, electrical test . The available accumulated data and experience, allowed to check that the medium-long term results desired were achieved, to identify the kind of problems that may appear, and to provide information for cost/benefit analysis that support this activity.**

Keywords — **Refurbishment - lifetime extension - oil tests - 2-FAL – DP – bushings.**

I. INTRODUCTION

Power transformers are critical and expensive assets of an electrical power transmission grid which play an important role in its reliability and availability. They are also critical in terms of safety, as a potential failure can result in catastrophic consequences, beyond the loss of the equipment and available energy. Being large electrical oil immersed machines, with many tonnes of mineral oil, the risk of occurring dangerous fires, explosions and oil spills is significant, and represent the worse-case scenario when exploring them.

The ultimate objective for their lifecycle management is to have the minimum total cost of ownership, which translates in having best performance and safe operation, minimizing operation and maintenance costs, and extending the service life as much as possible with adequate levels of reliability.

As transformers keep ageing, their condition will degrade inevitably, up to the point where important decisions have to be made, such as:

- Keep in operation (assuming the risk);
- Increase monitoring – more frequent analysis, further tests (advanced diagnosis), off-line tests;
- Perform maintenance operations – repairs, oil treatment, component replacement;
- Change operating conditions – reduce load, relocate, use only as back-up element;
- ***Perform full refurbishment*** – maintenance and lifetime extension operations;
- Schedule replacement (end of life criteria).

To have a proper support for these decisions it is important to have a wide source of information for condition assessment, including inspections, oil analysis, off-line diagnosis (on-site tests), on-line monitoring. Operation history and company experience also play a major role to tune the decisions for each particular case.

The decision for intrusive maintenance has consequences on the availability and high costs associated, due to the logistics involved and expertise needed. So, when the results of the condition assessment detect something that requires action, the first step should be to perform further investigation and diagnosis. For example, some faults detected by DGA may be kept under surveillance by further DGA analysis, and combined with off-line tests when possible. One also has to evaluate the urgency of the need for action, which may vary according to

ISBN 978-84-617–9183–5

the company policy. For instance, an oil leak, originated in a place that requires complete oil draining for proper repair, may keep on waiting to combine with other deeper maintenance action. It is also very important to always put each case in perspective, in comparison to the entire fleet of equipment (ranking), in relation to its particular role in the grid (critical node, n-1, etc.), and taking in account previous experience, as one can react with a better judgement to a situation that has happened before.

For the last 15 years, REN has been performing on-site refurbishment activities as part of the maintenance strategy to extend the service life of power transformers that present some ageing signs and maintenance needs but are still in good enough condition to endure the desired lifetime extension. This is typically a "midlife" operation that is planned to provide an estimated life extension of 10-20 years. The effects on the equipment are evaluated after each refurbishment, but the main goals can only be checked at medium / long term. During that period, this activity has been performed, under similar technical specifications, on approximately 50% of the population with more than 25 years in service. A significant number of these cases have now been in service after refurbishment for 10 or more years and allowed to perform a general assessment of this activity.

II. REFURBISHMENT METHODOLOGY

It is commonly accepted that transformer life time is directly related to the thermal ageing of the solid insulation, and its loss of mechanical resistance, that can be estimated by the degree of polymerization of the insulating paper (DP). The first ageing symptoms can be detected by oil analysis, and result from the thermal ageing process or contamination. To slow down the ageing rate, it is necessary to keep the oil in good condition and eliminate the moisture and contaminants, as much as possible. The service life extension achieved, for a typical end of life criteria based on DP (< 200), can be illustrated in a simple way by the graphic shown in Figure 1 [7].

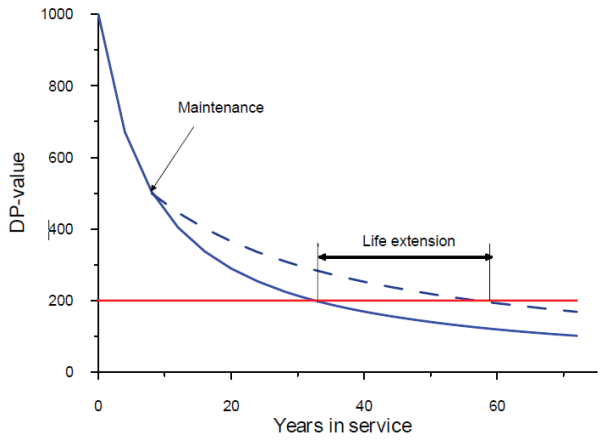


Figure 1. Estimated effect of the refurbishment in service life [7].

The refurbishment core operations are based on the main goal of moisture and contamination elimination. The activity also includes a complete and deep maintenance program. Since intrusive action has to be done, and a significant outage planned, it provides opportunity to perform such tasks. It can also be convenient to defer and some corrective maintenance tasks and include them in the refurbishment scope in order to benefit from the resources put available on site when the refurbishment takes place. For components that aren't expected to have a service life as long as the transformer, it should be considered their replacement. The transformer is also submitted to some modifications in order to comply with the more recent technical specifications concerning new accessories, piping configuration and circuit diagrams.

The complete refurbishment is expected to be performed only once in the lifetime of the transformer, typically as a midlife activity. Its main operations may be grouped as follows:

ISBN 978-84-617–9183–5

a. Oil & Paper – active part life extension

- Oil replacement by new uninhibited mineral oil;
- Moisture removal, through the application of active part drying with "hot oil spray" process;
- Oxidation reduction, by installing new sealed oil preservation system (rubber membrane);
- Complete gasket replacement, to avoid contamination and leaks.

b. Components – renovation and maintenance

- Tap changer complete inspection, including tap selector, diverter switch and all components;
- Bushing HV testing (laboratory) or replacement;
- Tank painting and anti-corrosive protection;
- Valve replacement;
- Accessories and protection devices replacement (pressure relief valve, buchholz relay, oil flow relay, thermometers, oil levels, air dryers);
- Cooling system refurbishment (fans, pumps, radiator cleaning);
- New control cabinet and complete wiring;
- Installation of online monitoring devices (on selected equipment).

c. Testing and documentation

- Condition assessment "fingerprint", based on oil tests, electrical field tests and functional tests.
- Update technical documentation – drawings, reports, manuals.

III. OVERVIEW OF REN POWER TRANSFORMER FLEET

The electrical energy transmission grid in Portugal has been submitted on the last decade to significant investments and expansion works, due to several factors such as the needs of integration of new power sources, interconnection reinforcements, and increase in supply security. These investments reflect strongly on the power transformer fleet managed by REN, which has increased almost 70% the number of elements in the last 15 years, and more than doubled the total installed MVA, and are responsible for the reduction on the average asset age from 21 years (in 2001) to 17 years (in 2016). Other relevant facts for this period were the introduction of new types of equipment, such as phase shifting autotransformers (in 2004) and oil immersed shunt reactors (in 2009). These elements also count for the power transformer fleet, which has reached 207 units (each unit being a three-phase equipment or a bank of three single-phase equipment). The fleet breakdown per age group is shown in Figure 2 below.

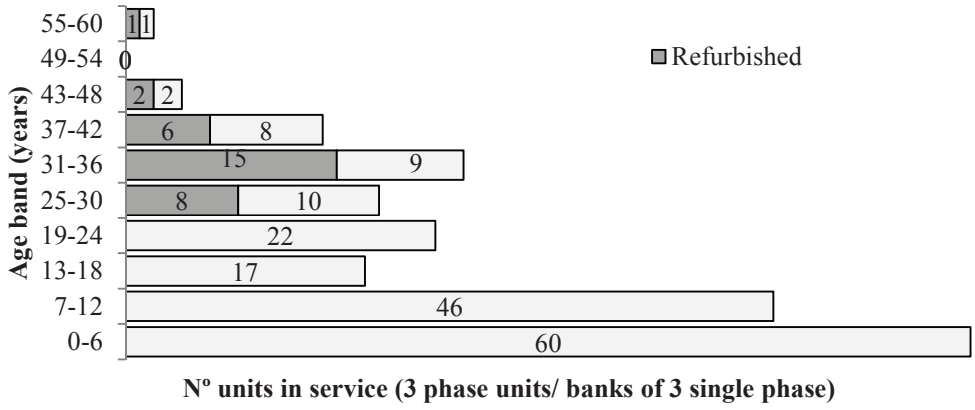


Figure 2. Age distribution of power transformers, autotransformers and oil immersed shunt reactors in service at REN.

For managing the maintenance and lifecycle of this fleet, two immediate concerns emerge by observation of this distribution:

ISBN 978-84-617–9183–5

- A very large number of units have fallen in the same age bands (the most recent), which may be a concern in the medium-long term, as they will all age "naturally" at the same time.
- A still considerably large group of units is in service with age over or equal to 25 years, which cannot be concealed by the very high number of "new" units, for which a more frequent condition monitoring and life extension measures should be considered.

We can analyse the evolution of the fleet since 2001, per voltage level, presented in Table I. This shows the highest growth for the 400 kV level (in %) and 220 kV (in number of units).

Table I. Power Transformer Population Evolution between 2001 and 2016 – Number of Units.

		Voltage Level			
Period	**Situation**	**150 kV**	**220 kV**	**400 kV**	**Total**
2001	Total in service	48	58 (20)	17 (4)	123 (24)
2001-2015	Decomissioned	16	16 (15)	0	32 (15)
	Awaiting recommissioning	2	1	0	3
	Kept in service	19	27 (3)	9	55 (3)
	Refurbished	**11**	**14 (2)**	**8 (4)**	**33 (6)**
	New - Transformers & AT	22	52 (1)	33 (2)	107 (3)
	New - SR	1	2 (2)	5	8 (2)
	New - PSA	0	0	4	4
2016	Total in service	53 (2)	95 (8)	59 (6)	207 (16)

*(*n*) - number of banks of three single-phase transformers / auto/ SR included

Most decommissioned transformers were 220 kV banks of single phase transformers and 150 kV three phase transformers. Most of these units were decommissioned as strategic options: to install units with higher and standardized rated power or to upgrade some 150 kV substations to 220 kV and 400 kV. The average end of service life age was 45 years. Most new units are three phase equipment, which became the standard solution by default.

There was a single case of recommissioning cancelled due to the remaining life assessment, which suggested an already advanced thermal ageing and derailed the investment in refurbishment and relocation. Only one unit (bank of three single phase 220/150 kV autotransformers) had an accelerated decommissioning due to inacceptable risk of operation (very high tan delta in oil and windings), but was already in a disinvestment stage, and didn't need replacement.

IV. REFURBISHED POPULATION ANALYSIS

IV.1 TRANSFORMER SELECTION OVERVIEW

For the present assessment, the group of the 33 refurbished transformers in the 2001-2015 period was evaluated. The available post-refurbishment amount of data can be illustrated by Figure 3, which shows for each unit the number of years that have already passed.

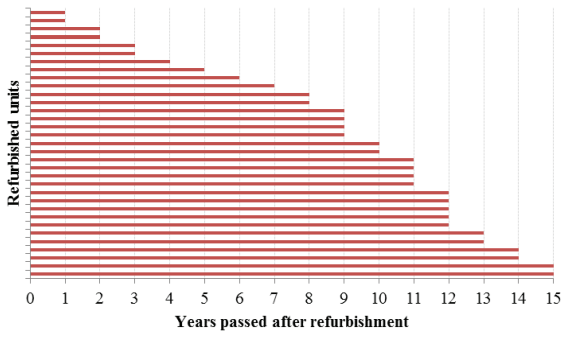


Figure 3. Post-refurbishment accumulated history.

ISBN 978-84-617–9183–5

The selection of these units for refurbishment was, in most cases, according to their condition assessment combined with their criticality to the grid, which allowed the definition of the priority list and planning of the refurbishment activity. It was also necessary to cross-check the needs identified by the maintenance and operations departments with the development planning of the transmission grid. When plans for decommissioning or recommissioning exist, the refurbishment decision is affected. Another basic condition is to check if the transformer complies with the grid and substation needs for the long term, to justify the lifetime extension investment. As an example, at REN, the rated power specification for transformers is minimum 126 MVA. This led to the decision of keeping the 63 MVA units out of the refurbishment plan.

From the group of the 33 transformers analyzed, there were 8 units refurbished due to relocation and recommissioning needs. The inclusion of refurbishment activities in the scope of the recommissioning program enable economies of scale and should be considered, whenever technical viable and justified. Exceptions are when:

- Relocating an "almost new" unit (too early for refurbishment). Although some cases don't raise any doubts, when the equipment is close to borderline (around 15 years, depending on the family, type) it may be wise to anticipate the refurbishment. This means that the condition assessment should take in account the previous condition shown in service, but also predict the effect of the transport, inactivity period, disassembled parts and risk of exposing insulation. Summing this up with the economies of scale mentioned above, the refurbishment is well justified. This was a "lesson learned", because our initial approach, for the condition assessment that defined the extension of operations to include in the recommissioning, was strict to present condition.
- The remaining life assessment indicates a reduced value (cases where the relocation is only for a temporary solution). This may result from the actual transformer age and devaluation as an asset, condition and reliability of installed components, advanced thermal ageing on paper diagnosed by oil analysis and eventually complemented by DP measurements. These activities are presented with more detail in section IV.3.
- Transformer has already been submitted to a full refurbishment before. As a general strategy, it is not supposed to refurbish more than once, due to technical (mainly the effect of repeated drying of the active part) and economic reasons, but should be studied case by case.

In some cases, operational performance was the trigger for the refurbishment. This may occur incidentally, following a major failure that requires deep intervention, or as a result of an accumulation of reported situations that recommend to program corrective actions.

The average age at the refurbishment time was 25,5 years, which reflects the "midlife" nature of this operation, as substation transformers are expected to last up to 50 years in service, with the appropriate life extension strategy. As shown in Table II, most of the units were refurbished in the period between 21-30 years of service age.

Table II. Refurbished Population Overview.

	Nº years in service at refurbishment time				
Type of Equipment	**11-20**	**21-30**	**31-40**	**41-50**	**Total nº units**
3 phase	**4**	**21**	**2**		**27**
Autotransformer		**4**			**4**
400 kV - 360 / 450 MVA		4			4
Transformer	**4**	**17**	**2**		**23**
220 kV / 150 kV - 120 / 126 MVA	3	14	1		18
220 kV / 150 kV - 63 MVA	1	3	1		5
Bank of 3 single phase		**5**	**1**	**1**	**6**
Autotransformer		**4**	**1**	**1**	**5**
220 kV - 120 MVA				1	1
400 kV - 450 MVA		3	1		4
Transformer		**1**			**1**
220 kV - 120 MVA		1			1
Total nº units	**4**	**25**	**3**	**1**	**33**

ISBN 978-84-617–9183–5

Three units from the less aged group (< 20 years) refer to recommissioned transformers, which accelerated the selection process. The 4th element had some operational issues related to the tap changer that contributed to the priority and anticipation given to it.

Only in one case it was not included the oil replacement within the refurbishment scope, because the oil was in relatively good condition, and it was intended to keep the budget bellow the defined limits. This was the case of the oldest refurbished transformer (45 years in service) that was recommissioned due to grid reconfiguration, to a location where lower loading was expected and medium term replacement programmed ("AT-SZR").

It is also important to notice the equipment constructive type. Most of the units of this population are shell-type (29), and only 4 are core-type.

IV.2 CONDITION ASSESSMENT

The bases for transformer condition monitoring are the oil tests performed yearly, including routine tests for physical properties, DGA analysis and HPLC for furan analysis. This allows to classify the units according to their condition, and give priority to the most critical. It also enables trend analysis and clustering data.

On Table III below, the evaluation for all refurbished transformers is showed for some "key properties" of oil condition assessment.

Table III. Transformer Oil Condition, Based on IEC 60422 Properties and Classification (Number of Units).

Key property	Good	Fair	Poor
Water content (at 20˚C)	0	4	29
Acidity	2	4	27
Interfacial tension	0	4	29
Dielectric dissipation factor at 90 ºC	27	5	1
Colour	1	7	25

Most of the units had shown "poor" condition for water content and acidity. This justifies the active part drying and oil replacement. On the other hand, the dielectric dissipation factor was found good in most units. Experience shows that oil with physical and chemical degradation can keep good insulating ability up to a certain point, but will have a negative effect on solid insulation and other materials, accelerating the ageing process.

For the transformer insulating paper condition assessment, the furan analysis, obtained from HPLC method, is a useful tool to detect situations where the ageing process has reached significant levels. The 2-FAL concentration gives a good estimative of the units that raise more concerns about the health of their insulating paper. They are performed at REN as complementary tests to check for paper degradation signs periodically.

Table IV. Transformer Insulating Paper Condition Assessment, Based on Furan Analysis.

Key pameter	< 0,5 ppm	0,51 - 1 ppm	1,01 to 2 ppm	> 2 ppm
[2-FAL]	19	3	5	6
Condition	Moderate signs of paper ageing	Relevant signs of paper ageing	High level of paper degradation	Advanced paper degradation

As shown on Table IV, one third (5+6) of the refurbished population had more serious paper degradation signs. Since the refurbishment process is not effective on restoring the paper condition, but can only reduce the ageing rate, when there are signs of advanced paper degradation, the condition assessment should be deepened to make sure that the refurbishment investment is economic viable for the remaining life expected. Some of such studies are described with more detailed in the next section.

ISBN 978-84-617–9183–5

IV.3 PAPER AGEING DIAGNOSIS

DP estimation

An end of life criteria based on thermal ageing is usually expressed in terms of DP as "DP < DPmin", where DPmin≈200. A lot of research has been carried to define good correlation models that adapt to each particular case in order to obtain more information about the actual paper degradation in terms of DP level without intrusive action. Some equations were developed experimentally in laboratory to establish the relation of DP with the 2-FAL concentration. In Portugal, experimental studies were conducted by the oil analysis chemical laboratory of reference, having determined specific equations for REN's power transformers with kraft paper insulation, one for shell-type (based on oil/paper weight ratio of 4) and another adapted to core-type transformers (based on oil/paper weight ratio of 8) [4]:

M. A. Martins' Equations:

(shell type)	$Log_{10}[2\text{-FAL}] = 2{,}25 - 0{,}0046\ DP$	(1)
(core type)	$Log_{10}[2\text{-FAL}] = 2{,}57 - 0{,}0046\ DP$	(2)

Other reference equations ([4],[6]) were also applied for DP estimation comparison, like:

De Pablo	$DP([2\text{-FAL}]+2{,}3) = 1850DP$	(3)
RTE	$DP = 500 - 333.Log_{10}[2\text{-FAL}]$	(4)

The DP value does is not uniform for all the transformer, so the bigger concern is with the minimum DP value, which in theory should be located by the winding hottest spot. The variation of the paper DP value inside the transformers, depend on several factors, like temperature and oxygen profiles, water content, oil type, and level of oil degradation. Moreover, the measured [2-FAL] in oil, depends not only on the production rate of 2-FAL, but also on its degradation rate (2-FAL stability) and on its partition coefficient, between oil and paper, introducing an additional uncertainty [3]. Maintenance actions that include oil circulation with degasification and drying can also introduce further shifts in the expected 2-FAL concentration.

DP measurement on samples

In order to get real direct DP values from the transformers with signs of more advanced paper degradation and get better assessment of the estimated remaining life, paper samples were taken out from selected accessible points of the transformers, in order to measure the DP of the cellulose, and compare it with the evaluation based on [2-FAL] in oil analysis.

The process of paper sampling involves disconnecting the transformer and draining off the oil. The sampling points should be accessible, allowing a re-insulation with kraft paper tape. The sampling requires some specific expertise, has high costs and some risks associated, so it is performed only for the most critical cases where [2-FAL] > 2 ppm.

During the studied period, 7 transformers were submitted to this process (in two cases, for two times). The chosen sampling points were the connecting leads of High Voltage (HV), Medium Voltage (MV) and regulating windings, located in the upper parts of the tank, which are submitted to the thermal stresses induced by the top oil temperature and load currents, and so give the best possible approximation of the thermal degradation of the hot spot insulation (the most stressed spot of the cellulose insulation).

The selected sampling points can be more or less representative of the thermal behavior inside the windings. The design needs are tailored to each particular type of transformer. Additionally the type of paper used in the leadings and inside the discs can also be different and introduce additional uncertainty.

At each point, 2 samples were taken: from the first outer layer, in direct contact with the transformer oil, and from the 3rd layer counting from the outside. Paper samples removed from the outer layers, had normally a slightly lower DP (about 10% lower), compared to samples from the 3rd outer layer of the same lead, which reveals the additional contribution of the oil degradation to the paper degradation.

ISBN 978-84-617–9183–5

[2-FAL] vs DP results

The results of DP calculations based on [2-FAL] and DP measurements from paper samples are presented in Table V, as well as the decisions that followed the assessment, supported by those results.

Table V. DP Results Measured in Selected Samples vs Calculated with Experimental Equations.

ID	Year	[2-FAL] (ppm)	Average DP measured from samples	Min. DP measured from samples	Remaining life estimative (for DPmin)	Calc. DP (1)	Calc. DP (2)	Calc. DP (3)	Outputs / decision supported
SCG1*	2002	2,6	551	332	20%	399	378	362	Refurbishment
SCG1*	2010	2,6	380	240	11%	398	375	360	Replacement plan
SPN1*	2004	1,9	561	347	21%	432	447	412	Refurbishment
SCG3*	2005	4,3	721	536	39%	352	281	289	Refurbishment
SPC1*	2007	3,2	367	301	17%	378	335	330	Decommissioning DP investigation
SPC1*	2008	-	324**	304**	-	-	-	-	DP mapping , case study
SFF2*	2008	3,3	439	323	19%	376	330	327	Refurbishment
SETM2*	2011	3,3	260	232	10%	377	332	328	Replacement plan
STN1#	2008	8,1	682	510	36%	291	177	197	2FAL investigation
STN1#	2015	6,1	669	543	39%	319	222	240	Refurbishment

(1) M.A. Martins equations
(2) De Pablo equation
(3) RTE equation

* Shell type
\# Core type
**56 sampling points from disc windings

Significant deviations were found between the calculated DP based on [2-FAL] and the minimum DP found on samples, mainly for cases of higher [2-FAL] values, as illustrated in Figure 4. This was somehow predictable, as many uncertainty factors are involved in the process.

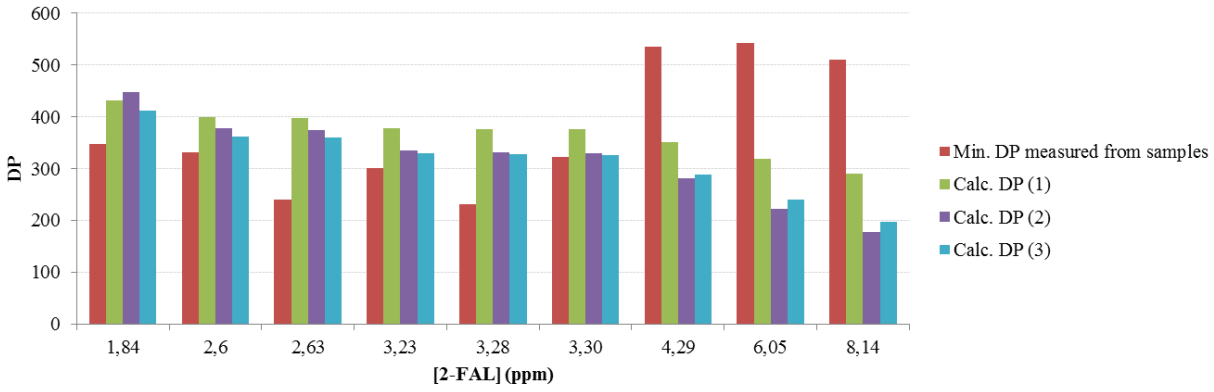


Figure 4. DP estimation / measurement for each case of [2-FAL].

Case study "SPC1"

In the case identified in Table V as "SPC1", the result of the DP tests supported the decision to cancel the eventual relocation and refurbishment after decommissioning forced by grid reconfiguration. This allowed performing a controlled scrapping in a transformer that didn't suffer from a failure, so paper condition reflected only thermal ageing and wasn't contaminated by internal faults. A detailed investigation of the DP values from paper sampled from 56 locations, distributed from different windings (disc type) was conducted involving REN, chemical laboratory and manufacturer ([3]) and, among other results and conclusions, it was confirmed that the DP minimum value found in the windings was similar to the minimum DP obtained from the paper samples taken from the leads. Further investigation should be performed on other decommissioned transformers to build up some patterns of relations between DP from different points and previously recorded data from oil test results.

ISBN 978-84-617–9183–5

Case study "STN1"

Another case study for paper ageing, due to the outlier values of [2-FAL] found over time was "STN1" transformer. The maximum [2-FAL] reached almost 2 times the maximum [2-FAL] ever recorded for REN transformers, and it was reached at a relatively early stage of service life (3,42 ppm at 10 years, 8,1 ppm at 17 years). For investigating this phenomenon, an early paper sampling was done in 2008, where acceptable DP values were measured. In 2015, due to its selection for refurbishment, new sampling was performed in order to check the evolution of the paper degradation. No DP value was found as low as the expected from the 2-FAL analysis. Therefore it was decided to check visually the insulation of other parts of the transformer – active part inspection – with untanking on-site. No specific signs or points of particular degradation were detected. The refurbishment was performed based on DP and inspection results and a specific reason for 2-FAL abnormal values was not found.

V. REFURBISHMENT MEDIUM/LONG-TERM RESULTS

The gathered data from oil tests of refurbished transformers, before and after this action, allow us to verify that in general there is a medium/long-term stability in most condition assessment properties monitored regularly, as shown in Figure 5 and Figure 6. These graphs show the oil properties evolution, with all the values referent to the condition before refurbishment, and the following results for every year passed (each series representing one refurbished transformer). The horizontal lines represent the classification limits according to [8], for oil properties. For the 2-FAL graph in Figure 7, the represented limits were defined according to the utility experience and chemical laboratory recommendations.

V.1 OIL CONDITION EVOLUTION

When replacing oil in an old transformer, previously impregnated with a different type of oil, it isn't expected to have the exact same behavior of new oil in a new transformer. Nevertheless, with the combined hot oil spray drying process, which has also a cleaning effect to the windings, we expected a good long term stability of the oil quality.

Figure 5 shows the plotting of some key properties for oil quality evaluation to reflect oxidation stability and contamination:

- Acidity – very low and stable values found, even for the units that have accumulated more service years after refurbishment.
- Interfacial tension (IFT) – this property has presented relatively stable values over the years, even though in some cases, it has already fallen in the "fair" condition category. From our experience, the signs of loss of IFT appear quite sooner than the rise of acidity, and some recent transformers also have reached "fair" condition within the first 10 service years. It was also noted that the starting value for this property for refurbished transformers (average of 30 mN/m, very close to the "yellow line") hasn't been as high as the registered for new transformers (40 mN/m in average).
- Dielectric dissipation factor at 90 ˚C (tgδ) – for this property it is important to separate one of the cases ("AT-SZR"), that as mentioned before in section IV, didn't suffer a complete oil replacement, and the tgδ kept on rising above the "red line" as shown in the graph. All others keep below the limit lines, mostly with stable values, but one case already shows a rising trend. This case had one of the highest tgδ values before refurbishment, and is one of those performed earlier in the analysis period, so the performance is satisfactory.
- Colour – all units are kept below the limit line and don't show significant variation in colour. The darkest index registered is "L3,0" but we could verify that the cases that show darkest colours, already had the darkest colours immediately after the refurbishment to start with.

ISBN 978-84-617–9183–5

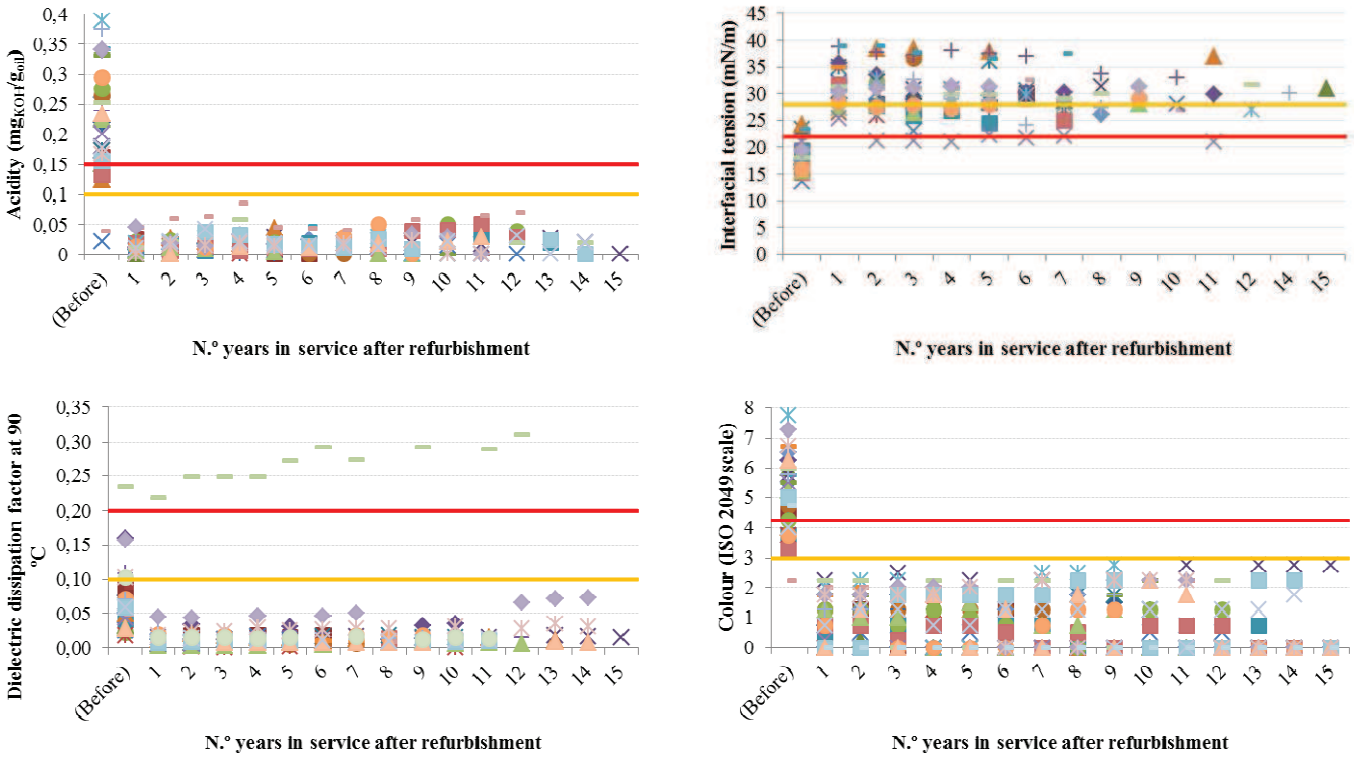


Figure 5. Oil condition evolution for refurbished transformers, described by key-properties: (i) acidity; (ii) interfacial tension; (iii) dielectric dissipation factor at 90°C; (iv) oil colour.

For some properties, it was noted that the long term performance depends highly on the initial values. The technical specification for refurbishment activities may benefit from the inclusion of more rigorous clauses regarding oil properties after works.

V.2 Moisture in Oil / Paper Evolution

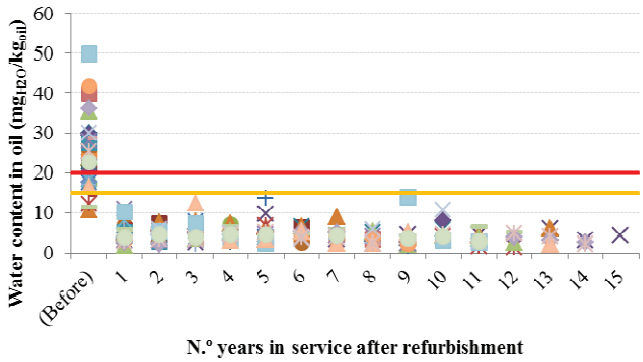


Figure 6. Water content evolution for refurbished transformers.

In this graph, we can observe that all the registered values after refurbishment fall in “good” condition category, according to changes introduced with the latest version of the IEC standard 60422. The limits that define “fair” and “poor” categories were changed to 15 and 20 ppm respectively, and the classification is based on measured (non-corrected) values of water content. The water content analysis in the oil/paper insulation system shouldn’t be based exclusively on water content in oil, but this gives us a good rule of thumb indication of the effectiveness of the drying process over the years.

ISBN 978-84-617–9183–5

V.3 PAPER AGEING SYMPTOMS

The furan analysis becomes less representative of the real paper condition because oil replacement resets the furan compounds level, as we can see on the graph of Figure 7, but the ageing level is maintained. The maximum value found after refurbishment was 0,3 ppm, and without visible increase over time (residual values after oil replacement).

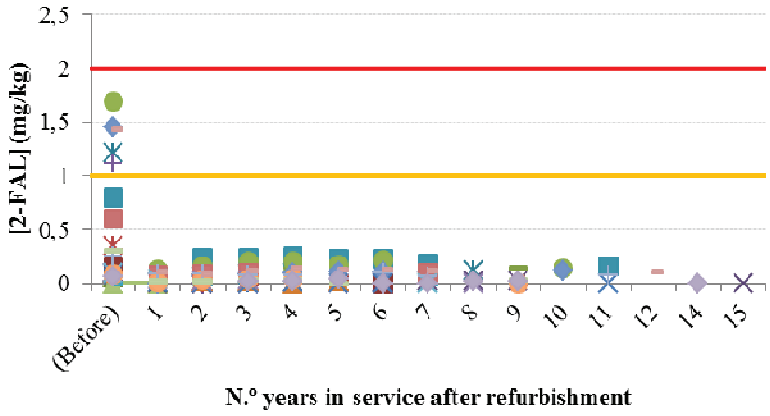


Figure 7. Paper ageing symptoms evolution after refurbishment.

After refurbishment it is important to keep record of the [2-FAL] level before oil replacement and check the appearance and rate of formation of new furan compounds dissolved in oil for future paper condition assessment analysis.

V.4 DGA OVERVIEW

Dissolved gas levels in service along the last 15 years were analyzed for the refurbished units, and are presented in Figure 8. Condition limits proposed by IEEE standard [9] were included in the graphs, to give a general overview of the performance. This limit-lines separate condition levels 1 to 4. In some cases, the higher levels (3 and 4) are not represented in the graph, because measured results never fell under those levels.

The cases of higher gas concentration and rates of gas increase are submitted to a deeper analysis, applying standard diagnosis methods (key gas, ratios, Duval triangles) and more frequent sampling in order to obtain more accurate diagnosis. This should be performed only when typical gas concentration (TGC) values and / or typical rate of gas increase (TRGI) values are exceeded.

The TGC for each gas is defined based on the 90th percentile of the collected data for a population, as recommended by IEC 60599 [10]. The TGC suffers influence from various parameters, like type of equipment, type of oil, age and operating conditions. Therefore, when sufficient data is available to be statistically significant, it should be calculated specifically for the population of transformers to be evaluated.

The TGC's were calculated for REN's population and also for specific sub-groups: refurbished units and new (1-15 years), which have the same oil type as the refilling oil of the refurbished units, to establish some comparison. As we can see in Table VI, all of the TCG values for REN groups fall in the IEC 60599 ranges, with exception of CH4 and C2H6 of refurbished units. Since almost all of these units are shell-type (88%), we collected information from Cigre WG32 work [10] where it was observed (with no particular explanation) that shell-type units produce markedly higher levels of hydrocarbons (except C2H2), as seen by the TCG included in Table VI.

ISBN 978-84-617–9183–5

Table VI. 90% Typical Gas Concentration Values (TGC) in ppm for Different Populations

Group	H2	CH4	C2H4	C2H6	C2H2	CO	CO2
IEC 60599 (ranges)	60-150	40-110	60-280	50-90	3-50	540-900	5100-13000
REN - all units	40	71	91	94	17,5	576	8260
REN - 1-15 years	45	37	5	49	0,4	255	2218
REN – refurbished population	62	196	211	116	4	387	4565
CIGRE TB 296 survey - shell type	51	169	241	1109	13	530	4579

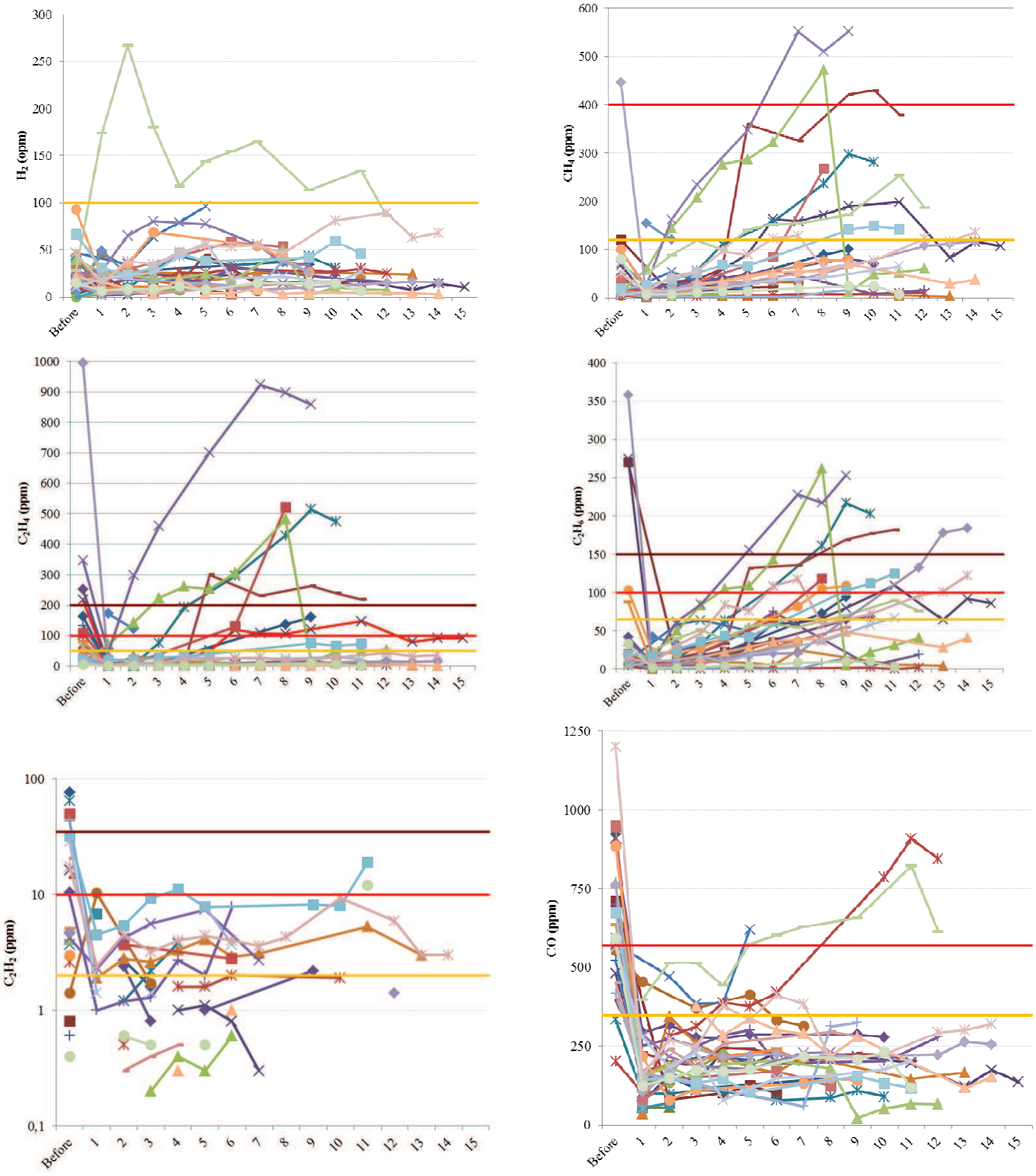


Figure 8. Key-gas levels in service before / after refurbishment and their evolution in a 15 year period.

ISBN 978-84-617–9183–5

By observation of the graphs, it is clear that some units have overpassed the indicative limits for some gases, and we can detect a gassing trend in some of the refurbished units, with values surpassing the TGC levels mainly for CH4, C2H4, C2H6 and CO. Yet, no serious failure-related event was registered, nor the diagnosis produced a confirmed fault indication, since no permanent gas generation was found.

Possible causes for gassing increase in some cases may not be related to an actual fault, but further investigation would be necessary. The following factors may have influenced the obtained results:

- The type of oil used in the last 15 years, which was applied on the refurbished population and on the filling of new transformers during that period. TGC calculated were lower for the "new" population, as seen in Table VI, so it seems that the oil reacts differently in terms of gassing for refurbished transformers, where materials are different and have been impregnated for many years with a different type of oil.
- The modification for a sealed type conservator (membrane) also has some impact, because the normal gas losses through the conservator will be limited [11].

In order to allow a better understanding of the gas concentration evolution, it has been considered the installation of some online monitoring systems during the refurbishment activities, but the implementation of such systems is still in an early stage at REN.

VI. Electrical and Dielectric Tests

VI.1 On-Site Testing

After the refurbishment, a set of electrical and dielectric tests should be performed, in addition to the functional tests, as listed in Table VII. If possible, they should be performed also before the refurbishment, or the previous results should be available for analyzing the effect of the refurbishment.

Some of these tests have a clear result of pass / fail, but others like insulation resistance, capacity and dielectric dissipation factor, may have different levels of results. Tests like SFRA allow to define a specific fingerprint for future reference, but also to detect some anomaly based on general typical curves expected.

Table VII. Electrical and Dielectric Tests Performed On-Site

Test	Before refurb.	After refurb.
Insulation resistance	Level ("lower")	Level ("higher")
Winding capacity / dielectric dissipation factor (C/DDF)	Pass / Level ("higher")	Pass / Level ("lower")
Bushing capacity and dielectric dissipation factor (C/DDF)	Pass / Level ("ok=pass")	Pass / Level ("ok"=pass)
Winding resistance	Pass	Pass
Turns ratio test	Pass	Pass
Leakage reactance/ short circuit impedance measurement	Pass	Pass
Frequency Response Analysis (SFRA)	Fingerprint	Fingerprint / compare to previous

For results that can be graded in different levels within the acceptable values, some statistics was made for a sample (25%) of the refurbished population in order to get a general view of the achieved improvements (the values presented concern to HV windings):

DDF: average value reduced from 0,43% to 0,38%, where the biggest reduction detected was from 0,68% to 0,42% in one case.

Insulation resistance: average value increased from 1070MΩ to 7710MΩ, where the biggest improvement detected was from 550MΩ to 10240MΩ. In a few cases the final insulation resistance was quite below average (2400 – 4200MΩ). This difference may be result from a worse condition of the insulation, a less effective refurbishment or testing uncertainty.

ISBN 978-84-617–9183–5

VI.2 BUSHING TESTS VS REPLACEMENT

Bushings are a critical component for transformer safe operation. Several publications have accounted bushing failures as a significant cause for power transformers failures. These pieces of equipment are highly stressed dielectrically, to assure the proper insulation to the grounded tank, mechanically, as they are submitted to traction forces from external connections, cantilever forces due to mounting position, and chemically, due to presence of oil inside (bushing oil) and outside (transformer oil).

During the refurbishment operations, it is convenient to remove the bushings, so they can be tested with full applied voltage at laboratory. The necessary manipulation of the bushings introduces some risks, and some cases of damages during removal and transport have occurred. For this reason, HV laboratory tests aren't performed on 400 kV bushings in general, only if the on-site condition assessment raises some suspicions about them.

The laboratory tests include cleaning and detailed visual inspection, applied voltage test with partial discharge measurement, dielectric dissipation factor and capacity measurements up to full voltage. The on-site tests are dielectric dissipation factor and capacity measurements at 2-10 kV for C1 and according to test tap voltage for C2.

In some cases, the transformer refurbishment included replacement of some bushings. The replacement strategy has suffered some evolution based on the experience and results.

At first, it was done only as a consequence of negative test results, taking advantage of a significant amount of spare units available.

For the bushings up to 73 kV, it was noted that the cost of new bushings, factory tested, could be competitive in comparison to the laboratory testing costs and related logistics. Testing costs are aggravated, in average, by a factor that depends on the test failure rate, which will demand new tests on a spare unit:

$$\text{“actual tests cost”} = \text{tests cost} * (n^{o}\ \text{failed bushings} + n^{o}\ \text{approved bushings}) / n^{o}\ \text{approved bushings} \quad (5)$$

The types of bushings installed in the generation of transformers that were refurbished during the analyzed period are OIP (oil impregnated paper) and RBP (resin bonded paper) with porcelain housing. Results of the tests performed on almost 200 bushings show the following statistics:

- Failed tests or present damages: OIP = 23%; RBP = 37 %; global failure rate = 29%.

The failure modes presented include high PD activity, high dielectric dissipation factor and physical damages (mainly oil leaks and cracks). RBP bushing failures are associated to PD activity (39% of cases), high DDF (30%) and physical damages (31%), while OIP failures are more related to physical damages (60%).

Other findings with the laboratory test experience are related to acceptance criteria for on-site tests. Typical maximum acceptable DDF values should take in account the type and age of bushing. But even when values are below the limits, if significant variation has occurred, further analysis should be undertaken (e.g. DGA or lab tests).

As result of our experience, bushing replacement has been considered as preventive measure to include in the scope of refurbishment activities when age and type of bushing suggest higher risk of failure, for all voltage levels. When replacement is not included, online bushing monitoring sensors are being installed, as a risk mitigation tool.

ISBN 978-84-617–9183–5

VII. CONCLUSIONS

This report gives an overview of the power transformer population at REN and its evolution along the last years and how the refurbishment activity has been implemented as a lifetime extension operation. The collected information also illustrates the importance of this activity in the long-term, due to the high concentration of new units in a recent period.

The results achieved allowed to validate the refurbishment activities as an effective measure for lifetime extension, as well as focus on some criteria for the transformer selection and condition assessment practices. Paper ageing diagnosis methods and practical cases studies were presented.

The medium/long-term analysis of oil properties show a good stability and contribute to the slowdown of the ageing process. Some gassing tendency was found in some units, but without proven related fault, so further investigation to determine gassing causes should be considered.

The analysis of a large set of data allowed to support decisions of changes in the scope of refurbishments, such as the replacement decision for HV bushings and installation of monitoring sensors / systems, and also to have more detailed acceptance criteria for desired test results after refurbishment (for oil and electrical tests).

REFERENCES

[1] J.F.Martins, *Techniques for Power Transformer Maintenance and Refurbishing*, ARWtr 2007.

[2] J.F.Martins and P. Monteiro, *Techniques for Power Transformer Life Cycle Extension*, ARWtr 2010.

[3] M. Augusta Martins, Mónica Fialho, Jorge Martins, Mário Soares, Maria Cristina, R. Castro Lopes, Hugo M.R. Campelo, *Power Transformer End-Of-Life Assessment - Pracana Case Study*, ARWtr 2010.

[4] CIGRE TB 445, *Guide for Transformer Maintenance*, 2011.

[5] M. Augusta Martins, *Envelhecimento térmico do papel isolante de transformadores. Investigação experimental. Modelos de degradação* – Ciência e Tecnologia dos Materiais. Vol.22, nº 1/2, p. 77- 86. Jan/Jun 2010.

[6] R. Blanc, et al, *Transformer refurbishment policy at RTE conditioned by the residual lifetime assessment* – CIGRE session, Paris, 2008.

[7] CIGRE TB 323, *Ageing of Cellulose in Mineral-Oil Insulated Transformers*, 2007.

[8] IEC 60422 Standard, *Mineral insulating oils in electrical equipment – Supervision and maintenance guide*. 4th Edition, 2013.

[9] IEEE C57.104 Standard, *Guide for the Interpretation of Gases Generated in Oil-Immersed Transformers*, 2008

[10] CIGRE TB 296, *Recent developments in DGAS interpretation*, 2011.

[11] CIGRE TB 443, *DGA in Non-Mineral Oils and Load Tap Changers and Improved DGA Diagnosis Criteria*, 2011.

ISBN 978-84-617–9183–5

Practical Case Study of Switching Transient Effects on Power Transformers

Marcos ARENILLAS-GAY[(1)], Jaime PALOMO-ALVAREZ[(1)], Ernesto PEREZ MORENO[(1)], Ricardo CASTRO-LOPES[(2)]

(1) GNF Engineering, e-mail: marenillas@gasnaturalfenosa.com, jpalomoa@gasnaturalfenosa.com, eperez@gasnaturalfenosa.com
(2) EFACEC Transformers R&D, e-mail: ricardol@efacec.com

Abstract — **During the energization work of a power transformer, the system tripped and registered an unusual fault. Following tests showed that, despite of the short duration and low magnitude of the fault, the transformer accounted some internal damages. The internal inspection revealed deformations in the conductors as well as relevant damages in the insulation. Simulation studies pointed out that an unintended phase-to-phase fault in the low-voltage winding during the energization work in the high-voltage side resulted in transient overcurrents and overvoltages that ended up affecting physically the high voltage winding of the power transformer. Although the occurrence of these kind of events is very infrequent, it is too risky to ignore them since they can result not only in major damages in the transformers but also in important power outages should they happen at some strategic point of the grid. Thus, it is essential to address this problem at the design stage and to acquire the know how necessary to ensure the transformer's security and integrity under such an event. This paper will therefore present the investigation's results concluded by Gas Natural Fenosa and EFACEC, which will enhance future design methodologies in order to avoid this kind of risks.**

Keywords — **Transformer modelling, Energization and De-energization, Fast Transient**

I. INTRODUCTION

The power transformer number C-0348B subject of this study was manufactured in 2009 by EFACEC and it is one of many similar 30 MVA transformers that have been in service for many years. This transformer has the following characteristics:

- Three-phase Power Transformer, three leg core type, 50 Hz, ONAN cooling;
- 30/30/10 MVA, 136 +/-10*1.2% - 21 – 10 kV, YNyn0+d11, 11% SC impedance;
- Basic Insulation Levels HV(L-N): 650-250/ MV:125/ Tertiary: 125 kVp

This particular unit (that had been subjected to and passed quality assurance protocols including design's review as well as all routine FAT dielectric tests [1], counting 1.2x50 uS full wave impulse). The routines performed prior to the energization work did not reveal any deficiency in the transformer nor in the insulation. For this reason, the unit was about to be put into service at an Unión Fenosa's substation. Afterwards, during the energization work at the substation, each MV terminal was connected to three parallel underground cables with an approximate length of seventy meters according to the standard procedure followed in these proceedings. However, just before the transformer's start-up, a pre-set short circuit between two phases (u and v) was provoked at the exit of the underground gallery. When the connection work finished, the transformer's start-up began through the HV side configured at tap position number four, with the MV switch opened and the tertiary winding grounded at one corner of the delta configuration.

Yet, 75 mS after the energization, the differential protection relay tripped out the transformer succeeding the detection of the pre-set short circuit and before any of the transformer's protection devices had the chance to react. The magnitudes of the recorded currents were within the maximum design short circuit magnitudes for this unit. Since there were no reasons to explain such an event, EFACEC decided to go beyond by carrying out an investigation to figure out the causes and implications of this episode.

Former investigations were developed onsite revealing that the HV winding of phase U could not withstand a single phase 10 kV, 50 Hz excitation current test, although the turns ratio measured for lower voltages was correct. An oil sample was sent to the EFACEC chemical lab but the test did not reveal proofs as there were no dissolved gases mixed with the sample.

ISBN 978-84-617–9183–5

Consequently, and based on the electrical test results, the decision made was to take the transformer back to the EFACEC Transformers facility in Porto to untank it in order to carry out more exhaustive tests to find out the origin of the failure and the most suitable solution.

As a consequence, the next stage was to disassemble every part of the transformer towards an internal inspection. One of the most important findings was that there was a localized darkened area between a pair of radial spacers at the middle height of the HV winding of phase U – between disks #36 and #37, as shown in Fig. 1. Moreover, a tilted [2] outer conductor belonging to disk number 40 was also visible.

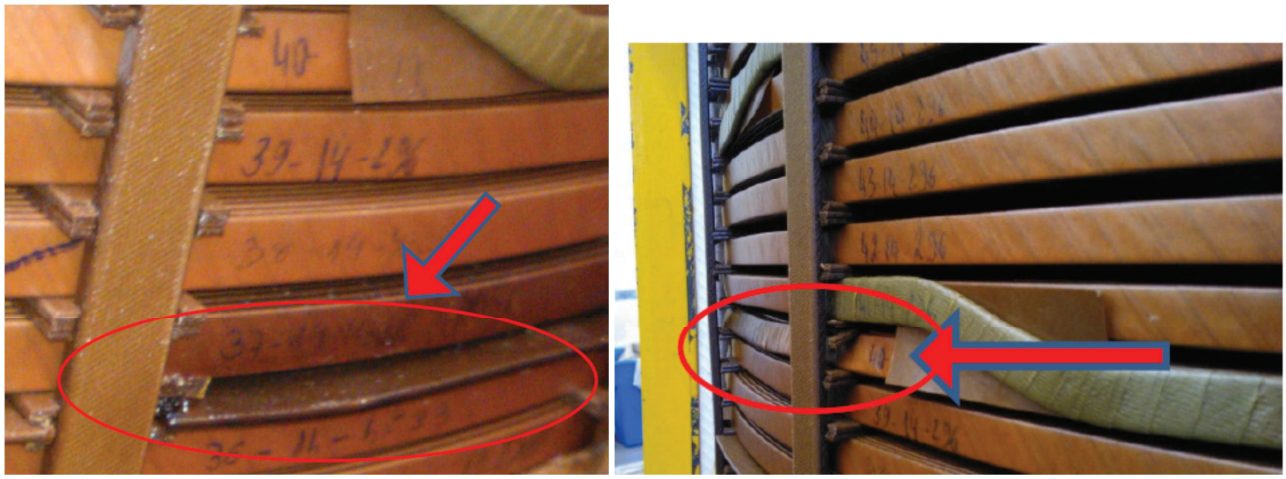


Figure 1. Fully interleaved HV winding with 72 disks and two parallel strands per turn from phase U with localized dark area between disks number 36 and 37 and with the outer conductor from disk number 40 tilted.

The inspection of phase U did not reveal further damages at the tertiary, MV nor regulation windings, including the vertical strips, radial spacers and insulation cylinders - with the exception of the aforementioned darkened area at the outer insulation cylinder of the HV winding, next to the failure point.

II. Switching Transient Effects Investigation

The substation features include SF6 circuit breakers with embedded current transformers, another twin unit connected in parallel and no surge arresters, according to Fig. 2.

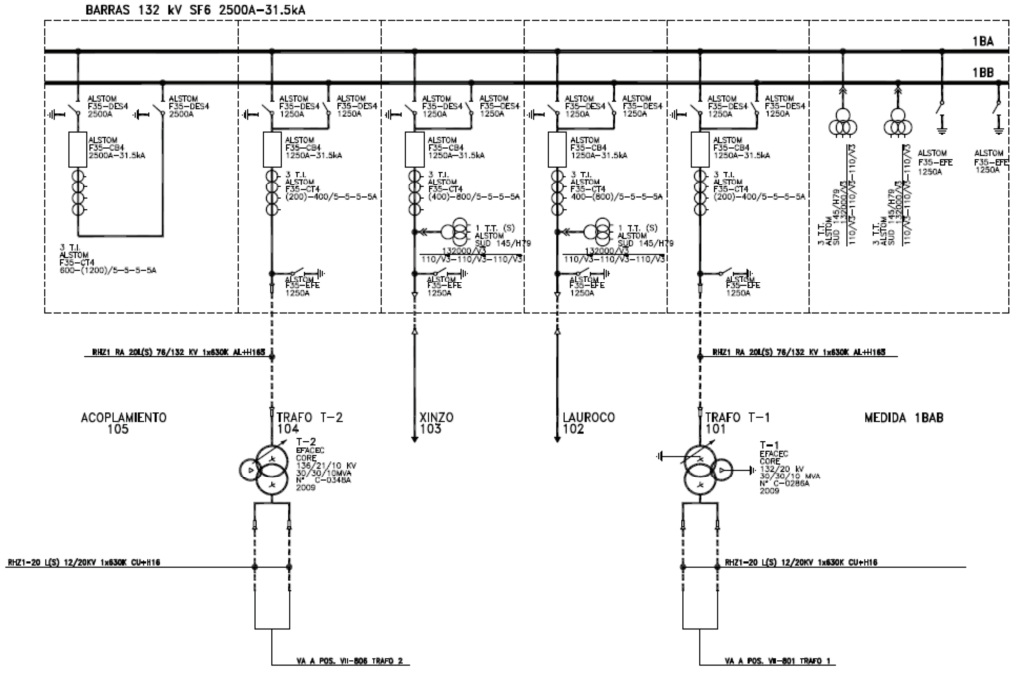


Figure 2. Single line diagram of the GNF substation.

ISBN 978-84-617–9183–5

The investigation included the analysis of the oscillograms of the event that registered the full transient sequence prior to the closing stage (energization) and until the extinction of the fault resulting from the opening of the circuit breaker (de-energization) as shown in Fig. 3.

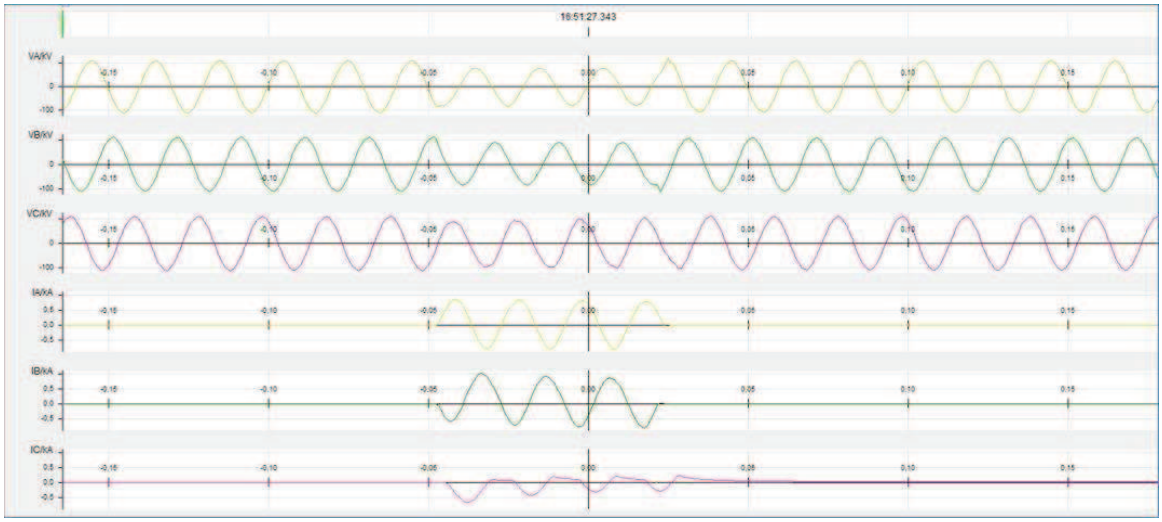


Figure 3. Oscillograms of the HV winding voltages and currents collected at the GNF Substation with a scanning frequency of 1600 Hz. The voltages were collected upstream of the circuit breaker and the currents are from the same branch of the circuit breaker.

III. Non-Linear Power Frequency Model Developed for the First Transient (Energization)

It is important to note that although the magnitudes of the recorded currents were within the maximum short circuit levels for this unit, owing to the fact that the power transformer was facing non-standard and out of design's practice inrush plus a short-circuit event with unbalanced ampere-turns in the windings, the evaluation of the dynamic short-circuit axial forces acting in the windings with a 3D electromechanical model was considered necessary.

Once this requirement was acknowledged, a first simulation model - that included the transformer, the closure moment of the circuit breaker and the system short-circuit impedance - was developed in a SPICE software model in order to calculate all the inrush plus short-circuit currents in relation to time in all the windings – Fig. 4.

The transformer's core was modeled with a non-linear magnetic model based on the Jiles-Atherton model that took into account the geometry of the transformer and was calibrated with the available no-load FAT test results. The short circuit FAT tests between all the windings were also considered in the model calibration.

On the other hand, the simulation of the energization process with this model permitted to calculate the currents throughout all the windings, including the windings where there were no oscillograms available.

The comparison between the three phase current oscillograms of the HV winding registered at the substation regarding to the simulated ones allowed to obtain an estimation of the several influencing parameters, including the switching time instant, the local grid short circuit impedance, the non-simultaneous phase switching delay, the residual magnetization in the transformer core, the voltage level and the magnitude of the DC current developed by the sympathetic inrush phenomenon [3] experienced by the operating next door transformer. It is important to take into account that the transformer and cable capacitances were not considered in this power frequency model.

Thereupon the previously calculated transient currents were to be introduced in the 3D electromechanical model in order to calculate the electromagnetic forces developed in the windings. As the early visual inspection

ISBN 978-84-617–9183–5

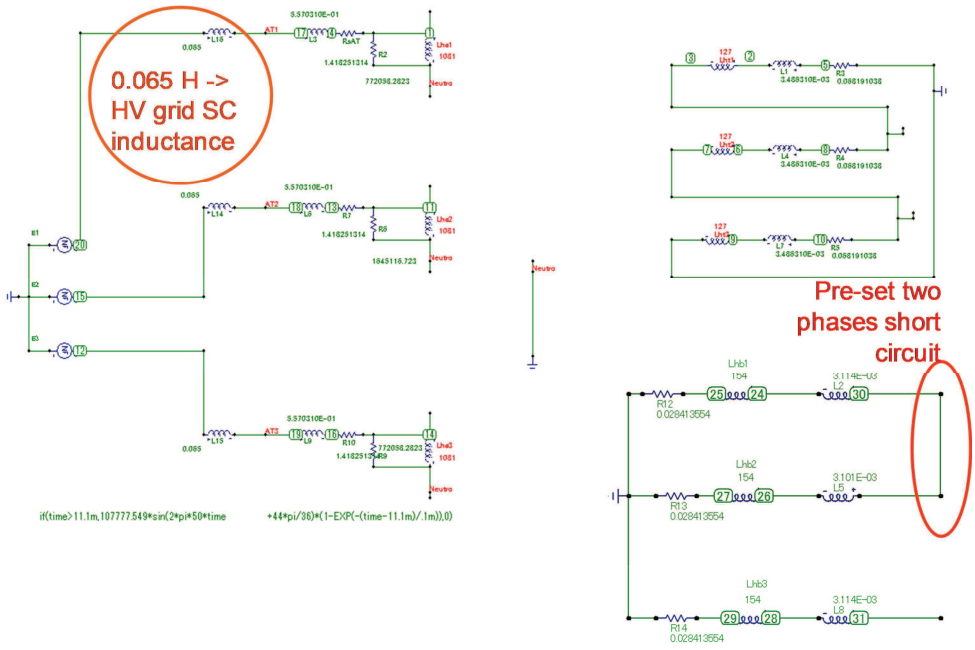


Figure 4. Three-phase schematic SPICE model representing the energization conditions of the transformer.

indicated, the HV conductors could have suffered a tilt force (Fig. 1). For this reason, this force was analyzed accounting several criteria such as axial pressure in the insulation, conductor bending between radial spacers, etc. [2].

On top of that, the tilting safety margin (i.e., the ratio between the critical force that triggers a collapse made because of conductor tilting and the maximum axial compression force acting on the winding) determined by the stresses resulting from the inrush currents alone (Fig. 5) was calculated to be 30. The same tilting safety margin determined using the stress thresholds resulting from the inrush plus short-circuit currents that matched the registered oscillograms was calculated to be equal to 6.3 – Fig. 6.

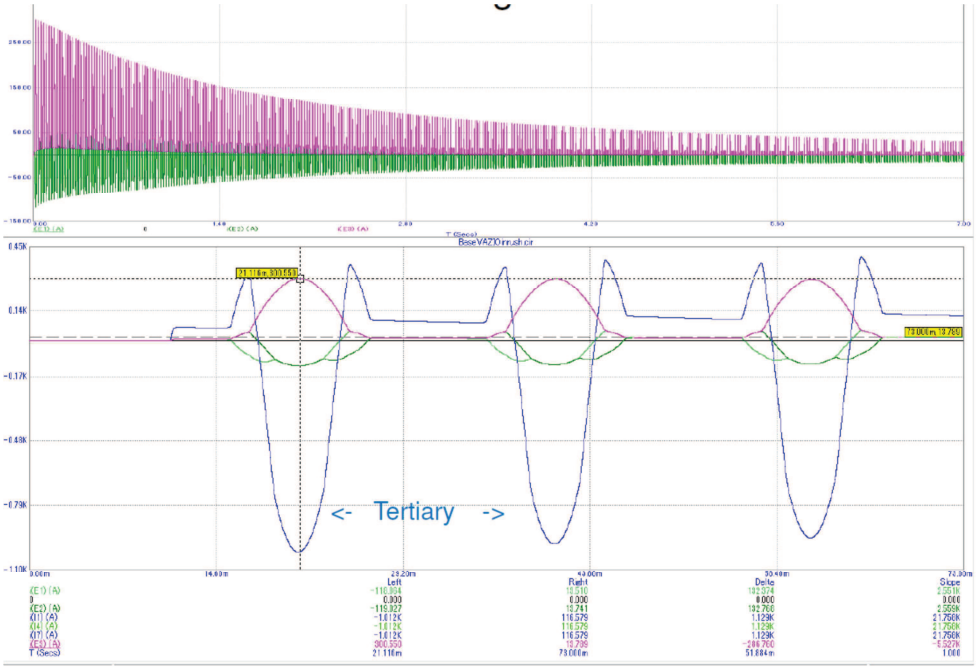


Figure 5. Simulated inrush currents at the HV and tertiary windings resulting from the energization of the transformer through the HV winding with the MV in open circuit condition.

ISBN 978-84-617–9183–5

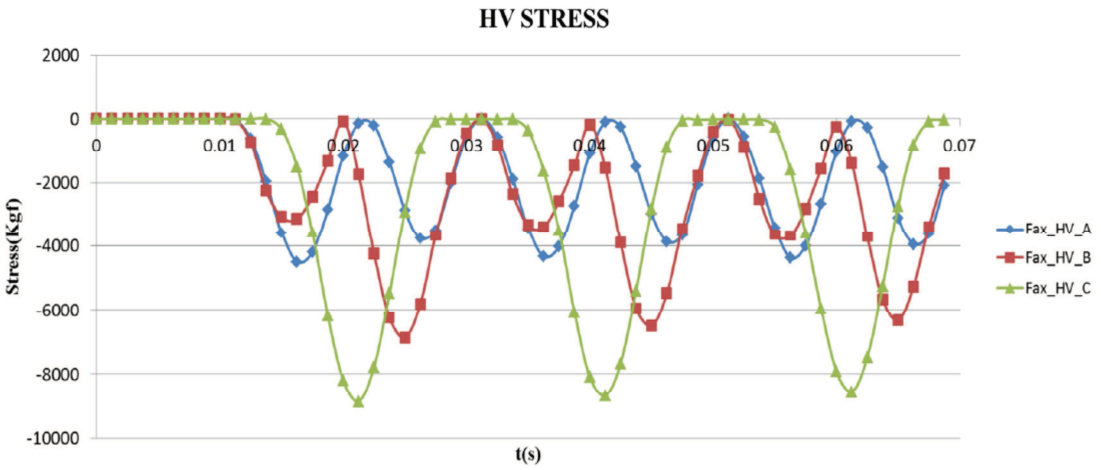


Figure 6. Transient electrodynamic analysis; cumulative electrodynamic axial force at the middle height of the HV winding over time for the two phases short-circuit plus inrush currents case. Calculated tilting safety margin equal to 6.3.

Further simulations were performed, with the purpose of evaluating the safety margins that could result from different switching time instants, considering 12 x 30-degree energization voltage angles for the inrush plus two-phase short-circuits case – Fig. 7. The correspondent tilting safety margin was calculated to be within fixed between 3.7 to 11.6 – Fig. 8.

Correntes AT [Amp-pico]	Amplitude	Correntes AT [Amp-pico]	Amplitude	Correntes AT [Amp-pico]	Amplitude	Correntes AT [Amp-pico]	Amplitude
IA	1018	IA	1367	IA	1718	IA	1819
IB	1063	IB	1464	IB	1721	IB	1820
IC	652	IC	592	IC	435	IC	226
Correntes AT [Amp-pico]	Amplitude	Correntes AT [Amp-pico]	Amplitude	Correntes AT [Amp-pico]	Amplitude	Correntes AT [Amp-pico]	Amplitude
IA	1688	IA	1354	IA	980	IA	1399
IB	1704	IB	1375	IB	987	IB	1405
IC	19	IC	57	IC	73	IC	66
Correntes AT [Amp-pico]	Amplitude	Correntes AT [Amp-pico]	Amplitude	Correntes AT [Amp-pico]	Amplitude	Correntes AT [Amp-pico]	Amplitude
IA	1707	IA	1815	IA	1715	IA	1449
IB	1712	IB	1825	IB	1702	IB	1320
IC	44	IC	241	IC	449	IC	600

Figure 7. HV winding three phase currents magnitudes [Amp-peak], resulting from the inrush plus two phase short-circuit at the LV winding, for different energizing voltage angles and for the same residual magnetization in the core.

ISBN 978-84-617–9183–5

Unbalanced vs balanced Ampere-turns (AT) influence on the axial forces in transformer windings:

In the previous calculation, two parameters that can significantly influence the tilting safety factor can be identified: the former is the magnitude of the different currents and the latter is the percentage of the balancing



Figure 8. Oscillograms of the cumulative electrodynamic axial force at the middle height of each phase of the HV winding over time and tilting safety factor, corresponding to the calculated currents presented in Fig. 7.

ampere-turns [3] between the windings. Seeking to evaluate the leverage of this last parameter, another exercise was done using the same transformer model but in this case removing the influence of the delta tertiary winding where some balancing Ampere-turns could circulate.
If the AT unbalance index is defined as:

$$\%ATunbalance = \frac{AT_HV + AT_MV}{AT_HV} \quad (1)$$

Taking as a reference the three phase short-circuit with full balancing ampere-turns between HV and MV – i.e., with *%ATunbalance* equal to zero, according to (1) - a parametric analysis was performed with the 3D electromechanical software, keeping fixed Ampere-turns in the HV winding and changing the MV Ampere-turns from fully balanced (*%ATunbalance=0*) to fully unbalanced (*%ATunbalance=1*). The resulting cumulative electrodynamic axial force at the middle height of the HV winding increased by a factor of 4.5 as shown in Fig. 9.

IV. Second Transient Wideband Nonlinear Model

Up to this point, the energization of the transformer was the main object of the study. The firstly developed SPICE simulation model that represented the first transient (energization of the transformer) allowed the calculation of all the currents that, afterwards, were introduced in the 3D electromechanical model. The resulting mechanical forces were much lower than the design forces and so not responsible for the winding damages revealed by the internal inspection.

ISBN 978-84-617–9183–5

The focus then turned to the second transient related with the opening process of the circuit breaker and to the de-energization of the transformer. The causes of insulation failure related with this switching operation could be the overvoltage at the HV winding terminals (since there were no surge arresters in the substation), the possible internal electrical resonances of the windings or a combination of both.

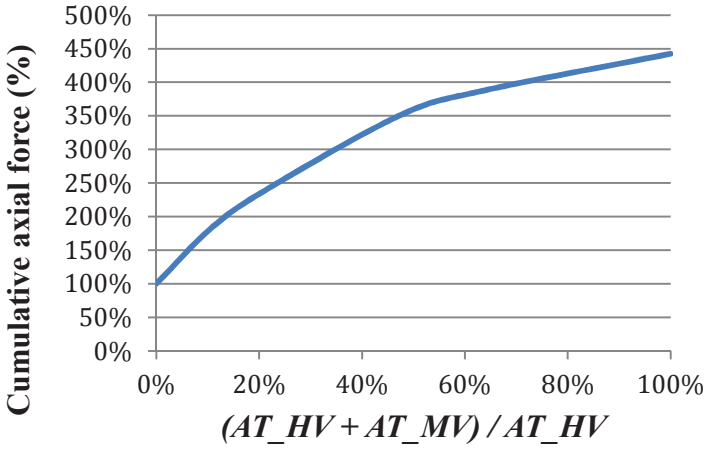
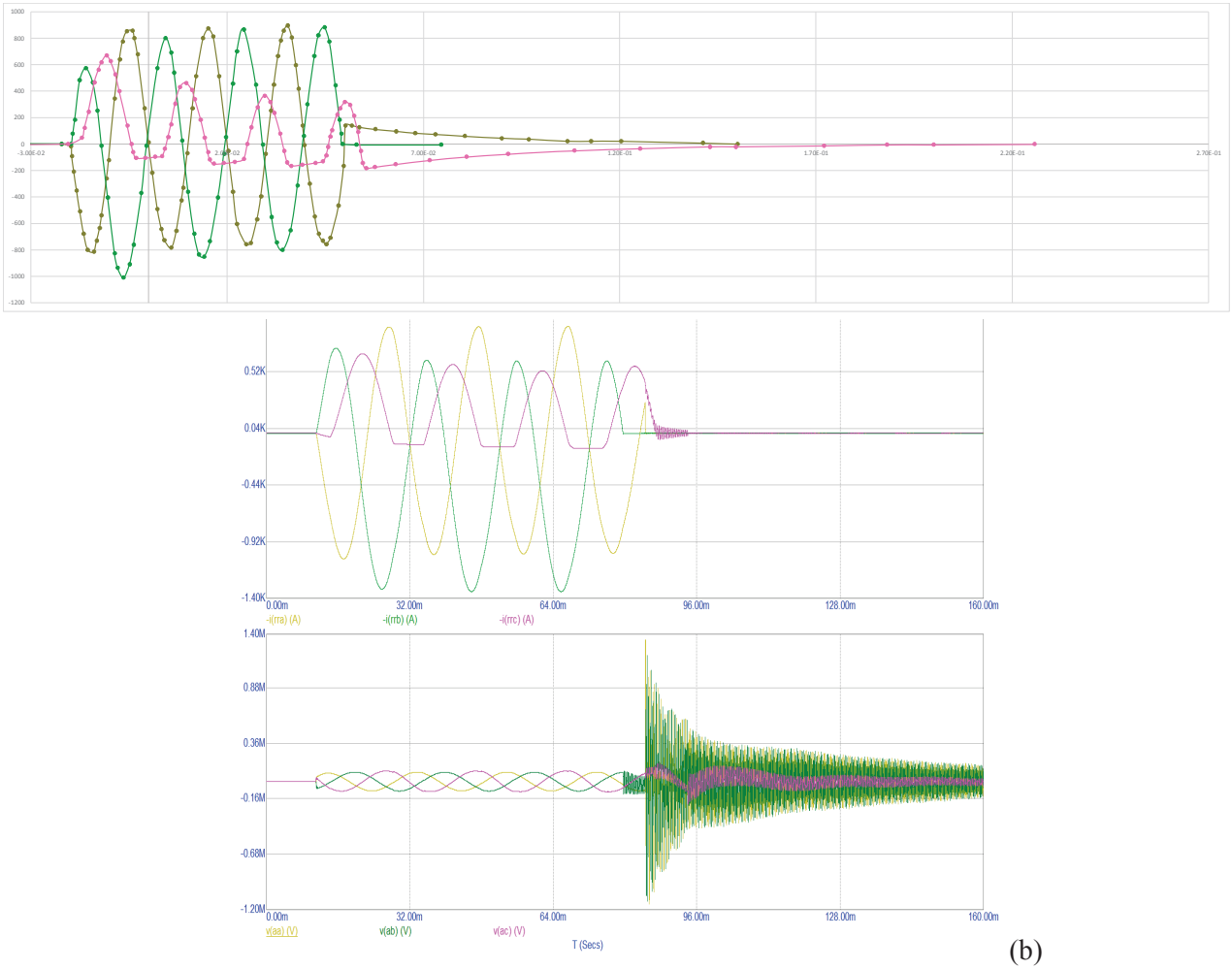


Figure 9. Cumulative electrodynamic axial force at the middle height of the HV winding variation with the ampere-turns unbalance calculated according to (1) and with the tertiary winding excluded for the simplicity of this analysis.



(a)

(b)

Figure 10. (a) Line currents oscillograms measured at the SF6 circuit breaker's embedded current transformers with a scanning frequency of 1600 Hz; The currents from phases A (light green) and C (pink) are being extinguished away from the ideal power-frequency current zero; (b) Simulated line currents (top) and voltages to ground at the transformer's terminals (bottom).

ISBN 978-84-617–9183–5

Consequently, a new SPICE simulation model was developed with more windings' subcategories in order to permit a higher frequency range of voltages that could result from the opening of the circuit breaker. The axial and radial capacitances of the windings as well as the estimated LV cable and circuit breaker capacitances were included to account for the highest frequency transient.

The following attempt to match the simulated currents with the registered oscillograms revealed an endless effort, due to the large amount of unknowns that needed to be estimated. Furthermore, the scanning frequency of the oscillograms was limited to 1600 Hz, overlooking higher frequency components that are crucial in the accuracy of the simulations. Nevertheless, the effort to match the simulated currents with the available current oscillograms was taken as far as possible with the results presented in Fig. 10:

As it can be seen in Fig. 10a, two of the phases (A and C) presented a deviation from the ideal switching characteristics where the current through each pole would be extinct at its power-frequency current zero. Instead, the oscillogram revealed two decaying exponential currents with the possible superimposed high frequency components being omitted due to the limited scanning frequency. As a consequence, the short circuited power transformer (which resembles a highly inductive load) released its magnetic energy (which was interchanged between the inductances and capacitances of the system) and a switching surge voltage stress occurred [4].

At this point, it is key to bear in mind that the magnitude of this overvoltage is very sensitive on how closely the currents are extinguished near the power frequency current zero. In the simulated case presented in Fig. 10b, the voltage magnitude at the transformer's terminal phase A reached a value of 1.4 MV, which is much higher than any dielectric design requirement for this unit. Additionally it is necessary to consider that this voltage could not be registered by the voltage transformers at the substation because such devices were located upstream to the circuit breaker (Fig. 2).

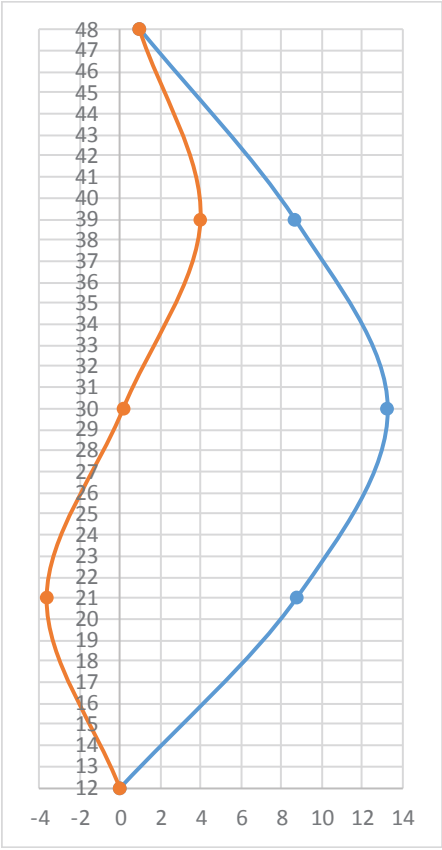


Figure 11. HV winding calculated internal disk coil voltages to ground for resonance frequencies of 9.6 kHz (blue) and 13.6 kHz (orange) with 1 p. u. at line terminal (top) and 0 p. u. at bottom terminal. The vertical axis represents the 36 sections of the HV winding model.

ISBN 978-84-617–9183–5

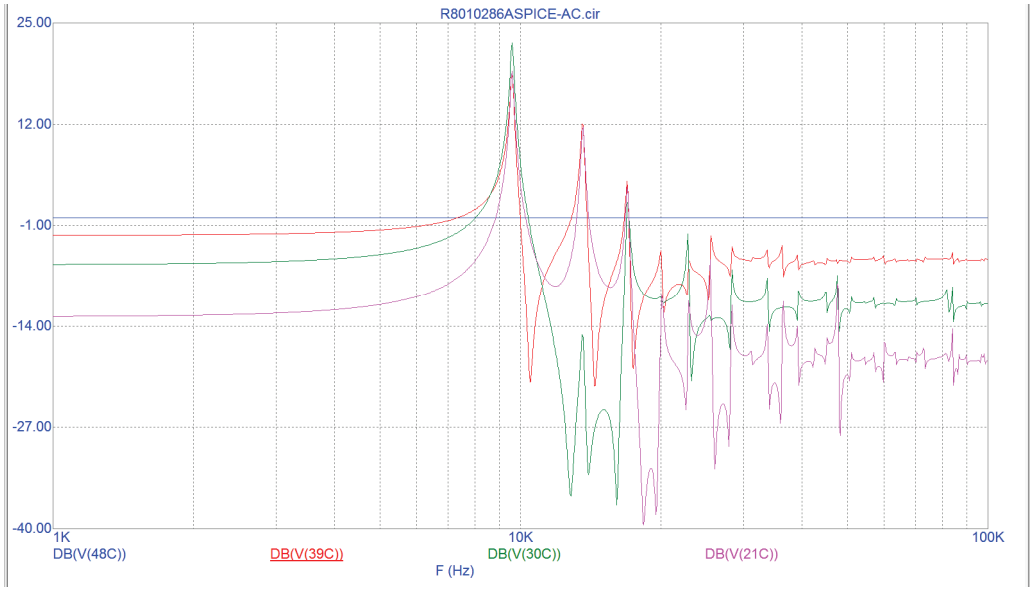


Figure 12. Calculated frequency spectrum representing the gain function 20*LOG$_{10}$ of per unit voltage at the nodes located at 25% (node 21c), 50% (node 30c), 75% (node 39c) and 100% (node 48c) of the height of the main HV winding, for the nominal tap position. HV winding modelled with 36 sections.

Besides voltage stresses' magnitude at the transformer's terminals, their frequency spectrum was also a point of concern. If some of the transformer's internal natural frequencies is excited, an internal overvoltage beyond the dielectric strength could result at some point of the winding. Fig. 11 and Fig. 12 show the internal nodes' location of the equivalent circuit that represents the HV winding modeled with 36 sections and the correspondent first two vibration modes [4], [5], [6].

INVESTIGATION ROAD MAP

The transients in power systems is an ongoing research topic. The investigation of this incident, focused on the shape of overvoltages and overcurrents that results from the analysis of the available data from the grid together with the pertinent modeling of the system's components To summarize, the road map followed to study this case was as shown in Fig. 13.

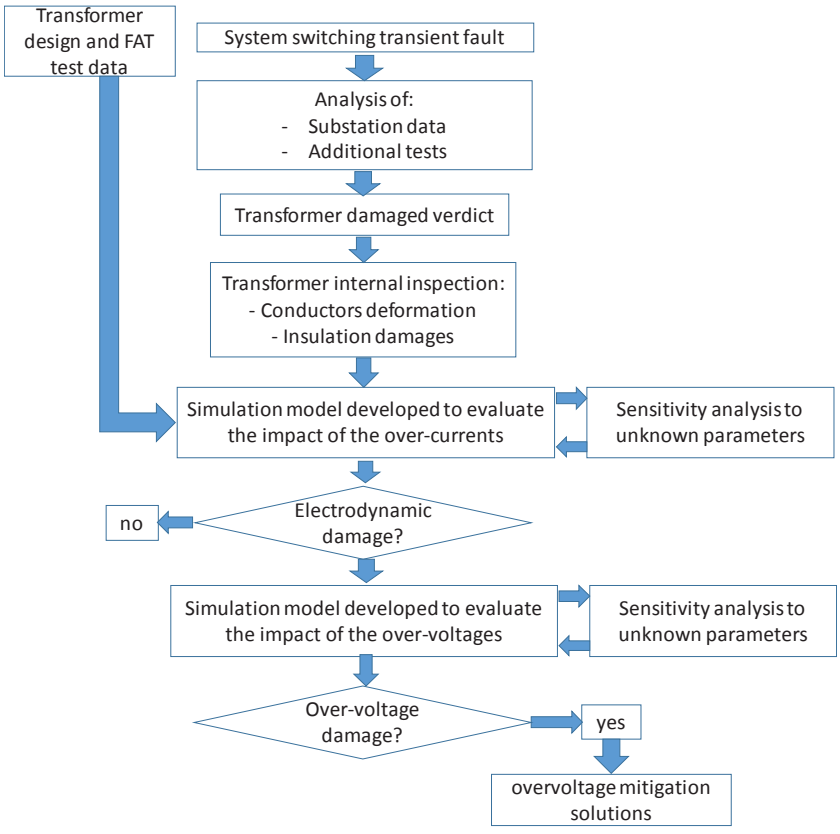


Figure 13. Investigation road map.

V. CONCLUSIONS

The issue presented along this paper reveals that incorrect phase-switching provokes severe consequences on power transformers despite of the low magnitude of the fault and the appropriate detection and intervention. The study showed the origination of important overvoltages with high frequency components.

ISBN 978-84-617–9183–5

After analyzing the aforementioned results, for the same current magnitudes, the Ampere-turns unbalances between the windings can increase the cumulative axial forces by a factor of 4.5. On top of that, the inrush phenomena with a pre-set short-circuit, lead to mechanical axial stresses about five times higher than those resulting from the inrush currents acting alone.

Furthermore, and based on the available information and considered parameters, the studies performed revealed that the HV winding electrodynamic stresses were below the design values for this unit.

Apart from the overvoltages originated by natural discharges, switching processes may also provoke overvoltages that result in major damages in the internal insulation of the transformer. Therefore, it is recommended the installation of surge arresters at the HV side to limit overvoltages next to the transformer's terminals to prevent from potential outages and irreversible harms in the power transformer.

On top of that, during the opening operation transient phenomena, even if the terminal voltage is kept within the design values, high internal voltages caused by the external oscillatory excitations at some of the transformers natural frequencies can result in internal insulation damages. Several mitigation devices [4] have been developed over the last years, including the use of RC snubbers (limited to medium voltage applications), switching devices equipped with pre-insertion resistors and the insertion of varistors connected across portions of the transformer's winding structure. This last measure can effectively address the concerns at one frequency and one location within the winding but shall not be considered as a complete solution for all natural frequencies.

Finally, according to the feedback received from this study, in order to avoid the risks involved during the energization work, all the commissioning protocols have been reviewed and this phenomenon is being considered from now on during the design review stage.

REFERENCES

[1] IEC 60076-3 - 2013 - *Power Transformers - Part 3 Insulation levels, dielectric tests and external clearances in air*.

[2] IEC 60076-5 - 2006 - *Power transformers - Part 5: Ability to withstand short circuit*.

[3] S.V. Kulkarni, S.A. Khaparde, *Transformer Engineering Design, Technology, and Diagnostics, Second Edition*, CRC Press 2013.

[4] IEEE Std C57.142-2010 - *Guide to Describe the Occurrence and Mitigation of Switching Transients Induced by Transformers, Switching Device, and System Interaction*.

[5] W. J. McNutt, T. J. Blalock and R. A. Hinton, *Response Of Transformer Windings To System Transient Voltages*, IEEE Transactions on Power Apparatus and Systems (Volume: PAS-93 , Issue: 2), March 1974.

[6] R. C. Degeneff, *A General Method For Determining Resonances In Transformer Windings*, IEEE Transactions on Power Apparatus and Systems, Vol. PAS-96, no. 2, March/April 1977

ISBN 978-84-617–9183–5

Design Review for Power Transformer: Technical Requirements, Methodologies and Tools

Hugo RODRÍGUEZ-IGNACIO[(1)] and Xose M. LOPEZ-FERNANDEZ[(1)(2)]

(1) Department of Electrical Engineering, University of Vigo
Campus Lagoas-Marcosende, E 36310 Vigo, Spain
Phone: (+34) 813478, fax: (+34) 814014, e-mail: xmlopez@uvigo.es
(2) Spanish Association for Innovation in Transformers

Abstract — **The aim of this paper is to identify the base guidelines for conducting the design review procedure during the power transformer procurement. The user specification, the design and the manufacturing procedures are addressed. Some of the main technical requirements, methodologies and tools of the dielectric, thermal and mechanical design are also remarked.**

Keywords — **Design Review, Manufacturing Review, Power Transformer, User Specification**

I. INTRODUCTION

Power transformer is one of the most critical and expensive devices of power systems. So, the acquisition of the transformers is a very important decision for utilities [1]. In this context, the design review has become a hedging technique for risk reduction and generating savings when purchasing power transformers [2]. The aim of the design review is to ensure the understanding between purchaser and manufacturer regarding to the user specification, as well as to examine that the design requirements are met, using the manufacturer's proved materials and methodology. However, the enormity of the transformer design subject demands deep expertise of constructional details, design and manufacturing procedures that sometimes hampers the effective participation in the design review procedure.
Therefore, the purpose of this paper is to provide base guidelines which could be considered during the design review to assure that:

1. The manufacturer understands the user specification.
2. The proposed design is supported by calculation principles based on sound data and successful prototype test experience.
3. The manufacturing process is established by consolidated practices, documented in terms of safety and quality aspects.

The main steps to review during the transformer procurement based on the user specification, the design and the manufacturing procedures are covered in the following sections, as shown in Fig. 1.

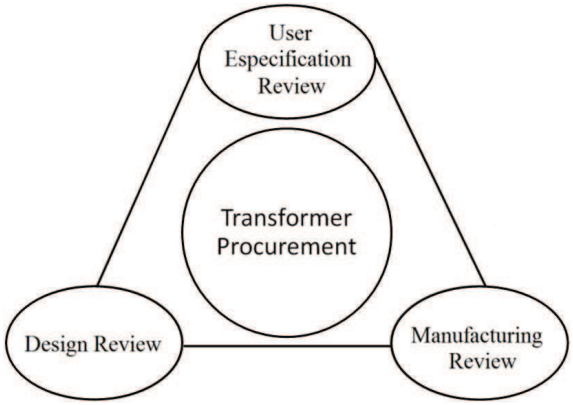


Figure 1. Stages of the transformer procurement.

ISBN 978-84-617–9183–5

II. DESIGN REVIEW OBJECTIVES

The main objectives of the design review for power transformer are:

- To ensure that the transformer technical requirements according to user specification and applicable industry standards are understood by both the purchaser and the manufacturer.
- To pay attention to the power system requirements, which can reveal aspects to be considered in the transformer design.
- To check if the proposed design fulfils the technical requirements imposed by the corresponding standards and the user specification.
- To identify any first full-scale application of a new design and evaluate its reliability and risks.
- To exchange useful practices between the purchaser and the manufacturer identifying improvements either in the design or in the specification.
- To ensure that the purchaser understands the technical capabilities of the manufacturer.
- To strengthen the technical relationship between purchaser and manufacturer.

These objectives are according to the Technical Brochure (TB) "*Guide for Conducting Design Reviews for Power Transformer*" elaborated by the CIGRE working group (WG) A2.36 [3]. This WG consists of worldwide technical experts whose experience and expertise are recognized.

III. USER SPECIFICATION REVIEW

User specification determines all of the operating characteristics of the transformer. Therefore, the review of the user specification is carried out to ensure they are understood by the manufacturer, and the purchaser could be aware of the technical capabilities of the manufacturer. The user specification requirements will condition the design criteria, the selection of components and materials, the manufacturing process, and the acceptance tests at the manufacturer's plant. According to the contract terms, transport, installation, commissioning and supply of spares components or maintenance equipment might be included in the requirements. Usually, the user specification relies on national and/or international standards. However, depending upon the operating environment of the power delivery, the user may include nonstandard operating requirements for the transformer. To help the purchasers and manufacturers when preparing transformer specifications, the CIGRE has available the TB "*Guide for Preparing Specifications for Power Transformers*" [4], which may be a document to be considered.

In the following subsections, aspects to be considered into the user specification review are listed.

III.1. SPECIFIED RATINGS

The design reviewers must ensure the transformer rating parameters, among others:

- Voltage, current and MVA ratings.
- Winding temperature rise.
- Cooling class.
- Insulation levels.
- Sound level.
- Special mechanical or physical arrangements.

III.2. UNUSUAL OPERATING CONDITIONS

A transformer might have to operate in conditions not covered in the applicable standards. The reviewers must verify that the proposed design is adjusted to special requirements, some of which are:

- Cooling design for different than standard ambient temperature and altitude conditions.
- Phase to phase, to ground and bushing clearances for BIL requirements at high altitudes.
- Bushing creepage distances for operation in a dusty, damp or corrosive atmosphere.

ISBN 978-84-617–9183–5

- Internal winding clamping design for operation under seismic conditions.
- Core induction levels for continuous overvoltage operation with saturation.
- Winding conductors temperature under frequent short-circuit applications at full load.
- Methods to mitigate winding resonance during switching operations.

IV. DESIGN REVIEW

Design review is conducted once the user specification review is completely finished, before the key materials are ordered and the manufacturing commences. Previously, the reviewer will have available the design information to properly prepare the design review meeting. The manufacturer might require to the purchaser the signature of an undisclosed contract before sending the information based on its design expertise. Usually, the reviewers follow their own checklist of topics to be reviewed [5]. In any case, the checkpoints given by the CIGRE WG A2.36 could be taken as a reference [3]. An overview of the checkpoints recommended to evaluate is related to the core, windings, active part drying, leads and cleats, leakage flux control, seismic and auxiliary equipment. In the following subsection, design aspects to evaluate these checkpoints are presented. Then, some technical requirements, methodologies and tools of key aspects of the transformer design, described by dielectric, thermal and mechanical (short-circuit, tank and sound level) design are outlined (Fig. 2).

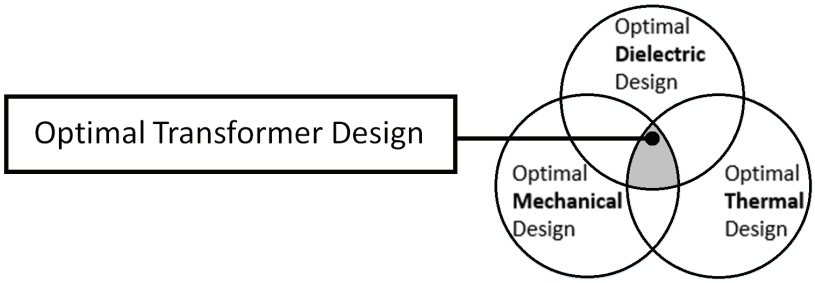


Figure 2. Optimal transformer design combining the dielectric, thermal and mechanical phenomena.

IV.1. GENERAL DESIGN REVIEW CHECKPOINTS

Core

The core is built from thin steel sheets that are electrically insulated between each other and stacked resulting in different cross-sectional.

The geometric description must be given in order to perform the core design review, which covers the maximum and minimum thickness, the type of insulation, weight and magnetic properties of the laminations. The number of wounded and unwounded yokes, its number of steps and the resulting cross-sectional areas should be available. Since legs and yokes are overlapped through mitred or non-mitred joints, the type of joint should be indicated as well as the dimensions of the core and the window.

The clamping elements and forces between core and the inner-most winding should be evaluated, as well as the clamping elements and core grounding. The bonding to earth and how it stays secure over the service life of the transformer should be inspected.

From magnetic point of view, magnetizing and inrush current characteristics, as well as the maximum flux densities both at rated and overexcitation conditions should be indicated. The stray losses magnitude and location, and the method for control the stray flux, i.e. the magnetic shield and shunts, non-magnetic flitch plate, frames and inserts should be reviewed.

ISBN 978-84-617–9183–5

Since magnetic steel can reach high temperatures, the cooling ducts between core sheets, the core surface and hottest-spot temperature should be analyzed. The cooling and dielectric properties of the oil surrounding the core should be specified.

Considering that the magnetic forces cause vibration and noise in the core, the sound level, the vibrations and anti-vibrations techniques could be examined.

If the transformer is three-phase three-legged core-type with star connection in the primary, the asymmetry of the core could be taken into account for evaluating the level of zero-sequence leakage flux.

The maximum temperature at the core surface and the hottest-spot temperature for no load, full load and over load should be provided.

The clamping elements of the tank intended to provide support to the core for handling and transportation of the transformer should be indicated.

In order to prevent undesired levels of vibrations and noise, the natural and resonant frequencies of the core could be checked.

Windings

In core-type transformers, windings are concentric cylinders placed around the core. Whilst in shell-type transformers, windings are composed of HV and LV pancake coils ordered in an alternative way. The conductors, made of copper (sometimes aluminum), usually are covered with insulating paper and between their sections there are pressboard pieces to provide dielectric and mechanical strength.

The general arrangement of each winding should be provided by the manufacturer for the design review.

The type of winding conductor (individual, grouped or CTC), its dimensions, arrangement, insulations and total number of turns in each phase should be supplied. The type of winding, its dimensions, the weight of its materials and the current density in windings should be indicated.

Since the windings determine the size of the core window and also the general size of the transformer, the sizing and pressing of the windings should be reviewed.

The clamping elements of the windings as well as the mechanical forces that it is subjected and withstands should be analyzed. The resulting safety margin and the error of its calculation should be given.

The tapping leads are placed either in the HV, or LV winding, therefore their arrangement should be checked.

The effects of the leakage field should be considered. Measures to control the eddy and circulating current losses such as sheets with lower thickness and the use of CTC should be inspected.

The additional loss factor that results from the harmonics of the leakage field should be specified.

The analysis of the winding temperature distribution and its dependence with load as well as the location of the hot-spot temperatures should be verified.

Special requirements for testing transformer windings could be provided.

Due to winding is one of the main root of heating, the arrangement and insulating materials of the axial and radial cooling ducts and spacers should be examined.

The layout of the insulation design including the principal insulation systems (major and minor insulation) should be supplied. For each insulation system, the test that imposes the worst condition and an outline of the

ISBN 978-84-617–9183–5

resulting stresses should be indicated. The choice of the selected materials should be explained and accompanied of its characteristics such as temperature capability and humidity, oxygen and acids resistances.

Core, winding assembly and drying

The core and winding are assembled to assure the safe support of all directions and to provide mechanical strength in short-circuit conditions. They are dried to increase the dielectric strength of the core and winding insulation.

Since there are structural elements that support stresses due to winding clamping, short-circuit and rising the core and winding assembly, the general assembly of the core and winding should be reviewed.

The core construction, drying and assembly should be indicated.

The winding clamping, its clamping pressure to increase short-circuit withstand capability and its compression during drying should be examined.

Moisture and particles reduces oil dielectric strength, so the methods to remove the moisture from the insulation should be available. The acceptance criteria could be provided.

The supply of the core and windings as a clean and dry setting should be reviewed.

The design, strength of materials, location, temperature resulting from stray flux and materials of the tie rods and tie plates should be analyzed.

Leads and cleats

The leads are taken out from the tank to connect the winding to the power system. Inside the tank, the leads are clamped with supporting cleats.

The arrangements and interconnections of the winding leads should be described. The brazed, crimped, bolted and spring connections should be reviewed.

The methods for joining interconnections and the draw of the rod connections taking into account the current densities could be indicated.

The contact resistant measurement between leads and cleats could be examined.

Leakage flux control

Load current is significantly higher than magnetizing current and so, magnetic flux leak out the core inducing eddy-currents in metallic parts of the transformer that cause diverse negative effects. Leakage flux and loss densities at full load and overload should be analyzed.

Stray losses in the structural elements can be reduced through the control of the leakage flux, so the design, materials and the grounding methods for the shields and shunts should be reviewed.

Seismic requirements

There are cases in which the transformer is going to operate in regions where earthquakes have to be taken into account. In this situation, special design considerations are required.

ISBN 978-84-617–9183–5

The structural analysis for seismic loading could be required. Seismic requirements involve a solid anchoring of the unit, so the anchoring capability of the provision to the foundation could be checked.

The conservator and some ancillaries such as the radiators and the bushings must withstand the earthquake forces and so it must be examined.

The welding design and loading could be indicated.

Accessories and auxiliary equipment:

Power transformers have a set of accessories and auxiliary equipment whose function is to contribute to the transformer's operation. It includes the bushings, tap changers, surge protection elements and control cabinet. The correct selection and maintenance of the auxiliary equipment is important for the proper performance of the transformer.

Regarding bushings, the type, construction, availability of spares, shed materials and shed profile should be reviewed

Wet and dry creep and flashover lengths, as well as the sensitivity of matching the shields and bushing should be evaluated.

Regarding tap changers, the type, ratings, tapping range, power factor, maintenance or any special requirement should be indicated.

The overload and dielectric capabilities, and the transient withstand capability of the tap changers should be available.

Some protection elements intended to avoid that surges voltages reach to the transformer are the rod gaps, the internal surge arresters and the internal tertiary reactors. Details and data of these items should be provided. The justification, location and the mounting arrangement of the internal surge arresters should be examined.

Cables of the control cabinet should meet the standard and be suitable for the environment and the climate. They should be inside a cabinet of an adequate size.

The auxiliary AC and DC voltage system and the cooling controls, heating and ventilation should be checked.

The blocking and deblocking functions to respectively avoid or allow reenergizing a transformer after a fault could be inspected.

Regarding the connection diagram, the presence of the winding endings and all the fixed components should be checked. In case there are current transformers, its location and polarity must be identified, as well as bushing and tap changers [6].

The type of coolers (plates or tubes) of the heat exchangers as well as their working pressure should be indicated. The valves, pumps and fans should to be reviewed.

IV.2. DIELECTRIC DESIGN REVIEW

The dielectric design is based on the evaluation of the safety margin (SM) in critical parts of the insulation system to assure that it is free from partial discharges (PD). To review the dielectric design of the power transformers the technical aspects that could be taken into account of the key insulation system structures are listed below.

ISBN 978-84-617–9183–5

- For the inter-turn insulation, it could be checked:
  - Inter-turn voltage calculated by the manufacturer for impulse and AC test voltage.
  - Inter-turn stresses assessment for AC and impulse voltage test conditions.
- Regarding winding to ground and winding to winding insulation, it could be considered:
  - The normal and creep stresses in the oil gaps, angles and barriers must be below the dielectric strength referenced to each medium.
  - Usually, the angle and barrier insulation system surrounding the line coil and the HV to LV space is the most stressed and should be evaluated under different standard tests.
  - Creepage stress along the spacer that separate the winding sections and the stress in the oil gaps.
  - Insulation design to limit the stress in the critical regions of the winding.
- For the insulations of the lead and bushing connections, it could be inspected:
  - Electrical stress during tests on paper insulated leads which links the windings and tap connections.
  - Creepage stress at the solid and oil interface.
  - Creepage stress at the conductor and paper tape insulation interface.
  - Creepage stress at the cable supports.
  - Dielectric design of winding to bushing connections.

The design review of an insulation system structure might follow the methodology shown in the flowchart in Fig. 3:

- For each standard test (lighting impulse, switching impulse, separated source AC, short and long duration induced AC) obtain their respective withstand voltage (basic insulation level (BIL), switching insulation level (SIL), separated source AC withstand voltage (AC applied), short and long duration induced AC withstand voltage (ACSD and ACLD)) correlated to the highest voltage for equipment, U_n, according to the selected standard (i.e. IEC 60076-3 [7]).
- Following, the design insulation level (DIL) factor approach, convert these withstand voltages in one equivalent voltage (U_{BIL}, U_{SIL}, $U_{Applied}$, U_{ACSD} and U_{ACLD}), respectively, and select the maximum of them as DIL voltage (U_{DIL}).
- With the DIL voltage, the electrical stress (E_{stress}) in each critical point inside the transformer must be calculated. Nowadays, numerical methods like Finite Element Method (FEM) are well established to compute the electrical stress distribution, as illustrated in Fig. 4.
- Then, the electrical stress (E_{stress}) has to be compared with the dielectric strength ($E_{strength}$). Dielectric strength is the maximum admissible design value of low probability of PD inception. Thus, a SM is derived and it has to be lower than the SM selected as reference by the insulation designer.

The dielectric design is finally corroborated by means of the insulation tests. These are based on the conditions that the transformer will experience during its life in service. Purchaser must detail in the specification any special requirement, and both the purchaser and manufacturer must agree on how each of the dielectric tests must be performed.

IV.3. THERMAL DESIGN REVIEW

Certain levels of temperature deteriorate electrical insulation, which reduces the service life of the transformer [8]. Therefore, the proper determination of hotspots is vital for the thermal design and to assure that the insulation is not over heated [9]. Technical aspects that could be considered during the review of the thermal design of power transformers are:

ISBN 978-84-617–9183–5

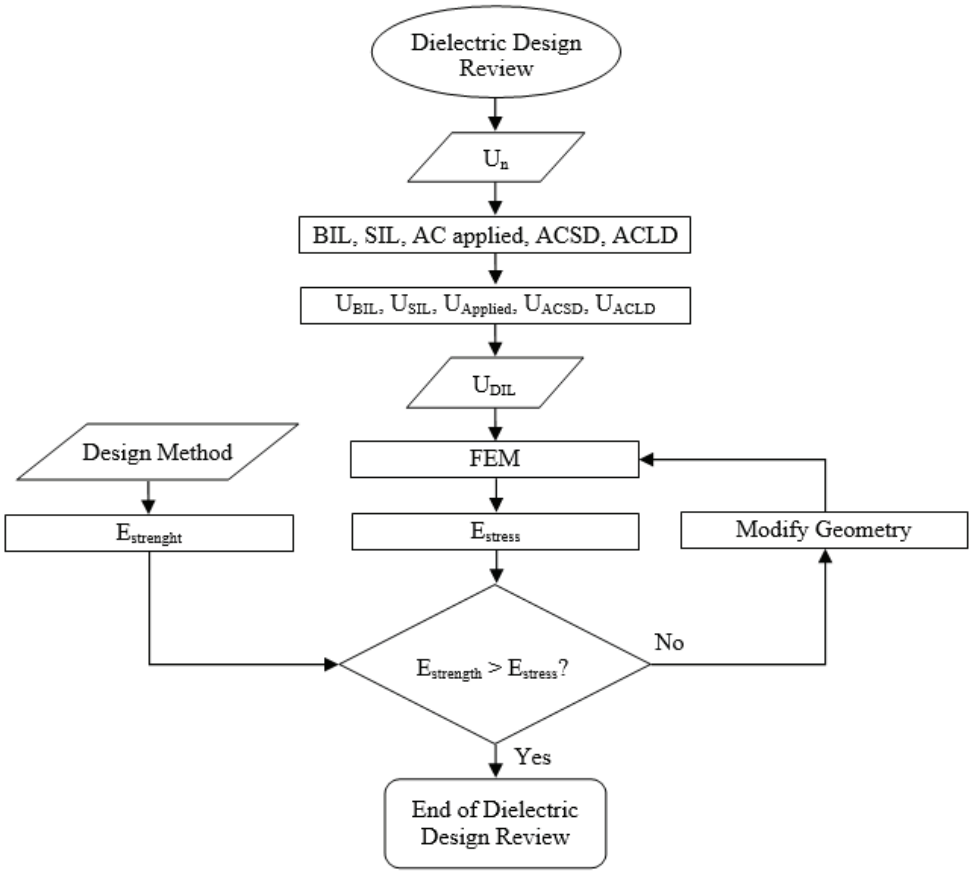


Figure 3. Flowchart for the dielectric design review.

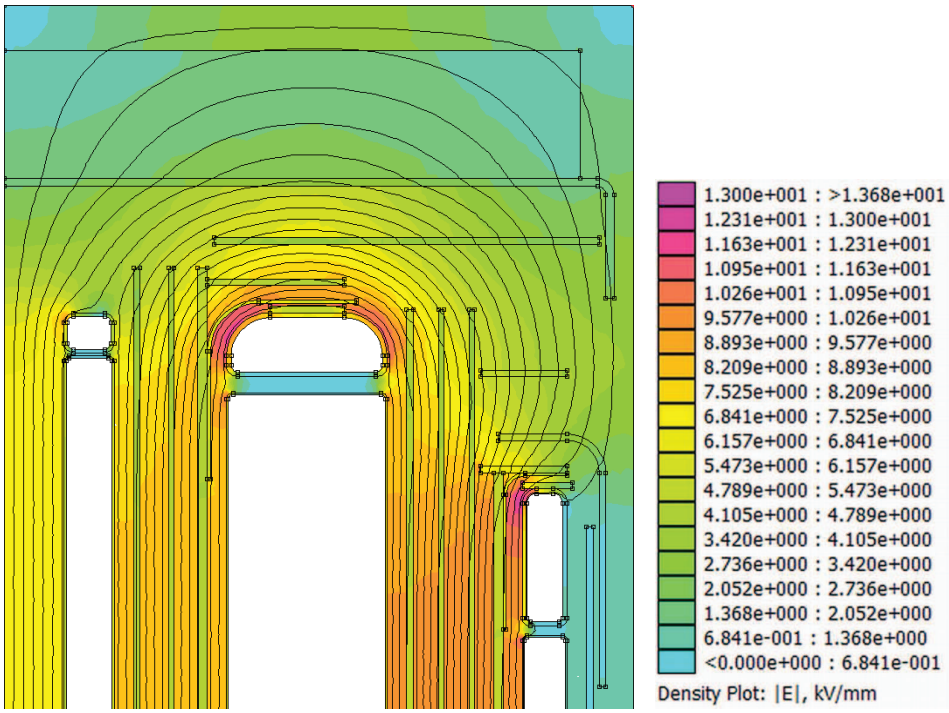


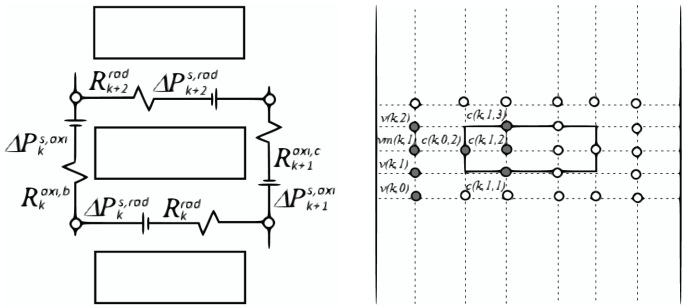
Figure 4. Electrical stress computed by FEM.

- Measurement of the ambient, bottom oil, top oil and average winding temperatures.
- Hot-spot temperature rise over ambient for all windings.
- Core surface and hot-spot rise temperature.

ISBN 978-84-617–9183–5

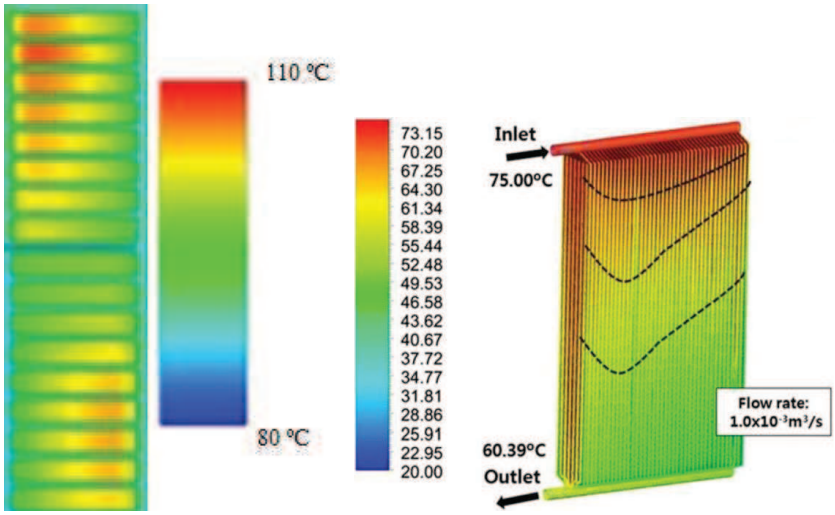
- Average temperature rise over ambient for all windings.
- Core hottest-spot temperature at full and over load with rated and over voltage.
- Oil flow in active part and heat exchangers.
- Average and top oil temperature rise in heat exchangers.
- Hot-spot temperature in the tank.
- Heating of auxiliary equipment and structural parts of the transformer.
- Parameters to calculate overload according the selected standard.
- Temperature distribution in clamping elements due to stray flux.
- Location for placing fiber optic sensors if direct measures of hot-spot temperature in windings are required.
- Accuracy of calculations through temp-run test results.
- Order of heat-run test followed by the manufacturer.

The temperature distribution on various parts of the transformer (active part, radiators, etc.) can be modelled through, the thermal hydraulic network models (THNM) and/or the computational fluid dynamics (CFD). THNM gives more information than correlation formulations but still is based on simplified models while that provided from CFD is more detailed. Fig. 5 shows a disk winding illustration and equivalent thermal hydraulic network. The oil temperature distribution example using CFD in a winding and a radiator is shown in the Fig. 6a and 6b, respectively.



(a) (b)

Figure 5. (a) Electrical analog to model the oil flow and (b) the corresponding resolution of the thermal network [10].



(a) (b)

Figure 6. Examples of CFD calculation: (a) Core-type transformer winding [11]; (b) Radiator [12].

ISBN 978-84-617–9183–5

IV.4. SHORT-CIRCUIT DESIGN REVIEW

Under short-circuit conditions, windings are subjected to high levels of mechanical forces that try to move the windings from each other. In shell-type transformers, short-circuit forces are opposites which causes them to be practically cancelled. While in core-type, those forces, *F*, have radial and axial components. The radial forces create a compression stress (causing buckling phenomenon) inward the inner winding edge and generate a hoop stress toward the outer winding edge, Fig. 7. The radial forces can also produce spiraling, which is the tangential displacement of end turns of a helical winding. The axial forces may bend the conductors placed between the spacers and produce conductor tilting as seen in Fig. 8a and Fig. 8b, respectively.

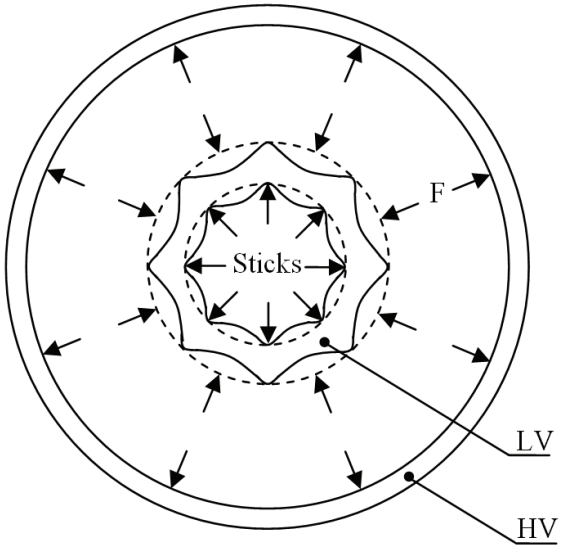


Figure 7. Cross-sectional view of the core-type winding showing the compressive and hoop stress toward the inner and outer winding, respectively, and the buckling phenomena.

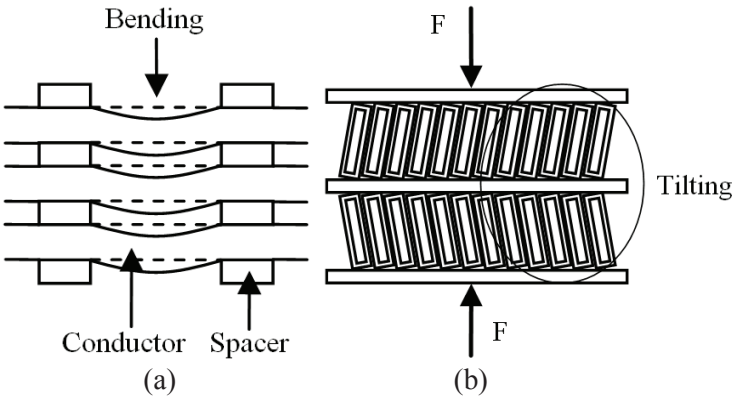


Figure 8. (a) Conductor bending between radial spacers; (b) Tilting in a layer winding.

Following are given technical aspects which could be considered for the short-circuit design review of power transformers.

- Regarding radial forces, it could be checked:
  - Hoop stress and evaluation of the circumferential support capability to avoid the failure of the winding under short-circuit conditions.

ISBN 978-84-617–9183–5

- Regarding axial forces, it could be inspected:

  - Tolerance for the electrical center alignment between the windings.
  - End thrust and calculation of the clamping pressure. Study the enhancement factors to take into account the dynamic effects of the end thrust during the short-circuit.
  - Stress calculation in the pressure ring.
  - Stress in the tie straps under lifting and short-circuit conditions. It should be less than the mechanical strength of the material.
  - Maximum calculated forces for each individual conductor strand and maximum bending stress.
  - Tilting pressure on the strands.
  - Compressive stress on the spacer blocks.

There are approximated formulas to calculate short-circuit forces in typical transformer winding arrangements [13]. However, modern calculations use FEM methods to compute short-circuit forces and obtain more reliable results. The IEC 60076-5 proposes that short-circuit withstand capability should be demonstrated by means of short-circuit test or by calculations/design considerations [14]. Manufacturer and purchaser must reach an agreement about the method to use. For the former, the test must be performed according the requirements of the selected standard. In case the standard is not applicable, manufacturer and purchaser must agree the conditions of the test. For the latter, manufacturer must provide information related to similar tested transformers in order to validate its design. In that address, the selected standard could provide guidelines to identify similar transformers. Some purchasers may have confidence about the capability of the manufacturer based on the design review. However, many others prefer short-circuit test to prove the short-circuit performance of transformers, which is a way to evaluate the quality of manufacturing processes too.

IV.5. TANK DESIGN REVIEW

The tank is the container of the core and windings, as well as the dielectric fluid insulation. It must provide structural support for the transformer elements and withstand the forces due to short-circuits and transportation, as well as pressure and vacuum loads. The tank is built from welded plates with a removable cover which allows the access to the core and windings. In order to provide mechanical resistance against stresses, there are placed bolted or even welded stiffeners on the sides and the top of the tank [15]. There are also covers for access to the bushings connections and tap changer, and supporting structures for the elements anchored on it, like the bushing turret, the conservator, the radiators, etc [16].
Technical aspects that could be checked during the review of the tank design of power transformers are:

- Tank withstand capability against the maximum pressure under all possible conditions plus the weight of the oil column inside the tank.
- Gasketed surfaces performance for proper compression of the gaskets.
- Design of stiffeners on tank walls.
- Seismic withstand capability.
- Auxiliary equipment for cooling must not hinder any objects at the transformer location.
- Calculation of the natural frequency of the tank panels to assure no resonance at twice the frequency of the exciting voltage and its harmonics.
- Intended use and location of sensors for on-line monitoring equipment, if specified.
- Worker safety policy fulfilment as well as the provision of ladders, electrical clearances, falling objects and environmental protection, if specified.

The structural design of the tank is based on the calculation of the types of stresses that it supports. These calculations are based on static and dynamic considerations. For performing design reviews to help mitigate tank rupture due to internal electrical faults it could be considered the *IEEE Guide for Tank Rupture Mitigation of Liquid-Immersed Power Transformers and Reactors* [17]. To receive guidance for establishing procedures to verify that power transformers and reactors will meet their performance requirements during an earthquake, it

ISBN 978-84-617–9183–5

might be taken into account the *IEEE Seismic Guide for Power Transformers and Reactors* [18].

IV.6. SOUND LEVEL REVIEW

The transformer vibrates during its operation due to the core vibration and its load level. This vibration usually causes noise, which is added to the noise produced by the cooling elements (fan, pumps, etc.). This noise has to be under the admissible noise level allowed by the policies of the country where the transformer is going to be installed. To perform the review of the sound level of the power transformers the technical aspects which could be considered are:

- Sound level in relation to maximum sound levels specified in the Standard.
- Level of magnetostriction and magnetic orientation of the core steel sheets. Hi-B grade could be used as it can provide from 2 to 3 dB of sound reduction as that of non Hi-B grades [16].
- Value of flux density in the core. Magnetic sheets of reduced flux density can be used to reduce the noise level [19].
- Core resonance frequencies for the core noise level.
- Level of noise in the tank. In order to lower the sound radiation it can be used sound panels outside the tank as well as enclosures.
- Transformer assembly location.
- Introduction of resilient absorbers which creates anti-vibration pads to reduce the noise. From IEEE Standard C57.136-2005, a noise level reduction between 8 and 15 dB (A) can be achieved [19].
- Level of noise emitted by cooling equipment. Low-noise pumps and fans are available in the market.
- Design of the connections between the elements that provide clamping to the active part and the tank [19].

The noise level in the windings in a range of 0-15 dB (A) can be overlooked by the methods to calculate the noise based on empirical approaches. The use of software based on numerical methods such as FEM is an interesting alternative to design "quieter" transformers through the proper management of the mechanisms of sound generation, transmission and radiation which occurs in the transformer [19]. Regarding to noise measurements, there are recognized two methods in the standards. These are the *Sound Pressure Method*, which was traditionally considered the general method of noise measurement, and the *Sound Intensity Method* to determine how to properly measure the transformer sound power level. These methods can be classified as "indirect methods" since they measure the noise as the result of the mechanical vibrations. Recently new methods based on optical fibers are being used to measure the sound [20]. The benefit of this technology is that the measurements are independent of the location of the transformer. This avoids the effect of the external noise and that of the reflected noise emitted by the transformer.

V. MANUFACTURER CAPABILITY REVIEW

Manufacturing of a power transformer is a very difficult task which involves a large amount of handwork from trained workers. The qualification of a manufacturer can only be ensured by an exhaustive knowledge of the capabilities of the proposed manufacturer plant [21]. To provide assurance on the quality of the operations and processes, the manufacturer must have a well-documented Quality Assurance and Manufacturing procedures or comply with the standard, which assures the attachability of manufacturing procedure and changes from the manufacturing process. The purchaser of the transformer should have a checklist to evaluate the manufacturer plant capability based on its technical requirements. The CIGRE WG A2.36 has created the TB "*Guide for Conducting Factory Capability Assessment for Power Transformers*" [21], which could provide guidance to the purchasers to assess the capability of the manufacturer plant.

ISBN 978-84-617–9183–5

VI. CONCLUSIONS

The typical technical requirements, methodologies and tools of key aspects of the transformer design, which are the dielectric, thermal and mechanical (short-circuit, tank and sound level) design, has been outlined. Base guidelines that might be helpful for the wide-ranging subject of reviewing the main steps of the power transformer procurement has been summarized and presented.

ACKNOWLEDGEMENT

The authors are grateful to Jewaan Puri, who passed away at the end of 2014. He provided his invaluable expertise that highly contributed to the quality of this work. In particular, Professor Xose M. Lopez-Fernandez would like to thank Jeewan Puri for the shared time discussing on transformer aspects, which were very enriching.

REFERENCES

[1] L. C. Leung and S. K. Khator, *Transformer Procurement and Relocation at a Large Electric Utility a Mixed 0-1 Linear Programming Model*, IEEE Transactions on Power Systems, Vol. 10, No. 2, p. 957-963, May 1995.

[2] X. M. Lopez-Fernandez, H. B. Ertan and J. Turowski (Editors), *Transformer: Analysis, Design and Measurements*, CRC Press, 2012.

[3] CIGRE WG A2.36, *Guidelines for Conducting Design Reviews for Power Transformers*, Technical Brochure, No. 529, 2013.

[4] CIGRE WG A2.36, *Guidelines for Preparation of Specifications for Power Transformers*, Technical Brochure, No. 528, 2013.

[5] R. K. Ladroga, D. E. Corsi, W. F. Griesacker, *Design Review and Factory Inspections*, 77th Annual International Doble Client Conference, p. 1-13, 2010.

[6] J. J. Winders, *Power Transformers. Principles and Applications*, Marcel Dekker, Inc., 2002.

[7] IEC 60076-3:2013, *Power Transformers – Part 3: Insulation Levels, Dielectric Tests and External Clearances in Air*.

[8] P. Penabad-Duran, X. M. Lopez-Fernandez and J. Turowski, *3D Methodology for the Overheating Assessment on Power Transformers Structural Parts*, proc. of the 4th International Advanced Research Workshop on Transformers, ARWtr2013, p. 40-49, Oct., 2013

[9] X. M. Lopez-Fernandez, *Hotspot Assessment on Power Transformer Structural Parts*, proc. of MyTransfo 2016, p. 1-4, Nov., 2016.

[10] H. M. R. Campelo, L. F. Braña, X. M. Lopez-Fernandez, *Thermal Hydraulic Network Modelling Performance in Real Core Type Transformers*, proc. of the XXIth International Conference on Electrical Machines (ICEM'2014), p. 2275-2281, Sept., 2014.

[11] H. M. R. Campelo, X. M. Lopez-Fernandez, P. Picher, F. Torriano, *Advanced Thermal Modelling Techniques in Power Transformers. Review and Case Studies*, proc. of the 4th International Advanced Research Workshop on Transformers, ARWtr2013, p. 6-21, Oct., 2013.

ISBN 978-84-617–9183–5

[12] A. Weinlader, S. Tenbohlen, *Thermal-Hydraulic Investigation of Transformer Windings by CFD-Modelling and Measurements*, proc. of the 16th International Symposium on High Voltage Engineering SAIEE 2009, p. 1-6, 2009.

[13] CIGRE WG 12-04, *Calculation of Short-Circuit Forces in Transformers*, No. 67, p. 29-75, 1979.

[14] IEC 60076-5:2006, *Power Transformer – Part 5: Ability to Withstand Short-Circuit*.

[15] M. J. Heathcote, J&P Transformer Book, Elsevier, 2007.

[16] S.V. Kulkarni and S. A. Khaparde, *Transformer Engineering*, Macel Dekker Inc. NY-Basel, 2004.

[17] IEEE PC57.156/D4, *Guide for Tank Rupture Mitigation of Liquid-Immersed Power Transformers and Reactors*, 2105

[18] IEEE C57.114, *IEEE Seismic Guide for Power Transformers and Reactors*, 1990.

[19] L. F. Braña, C. M. Vasques, H. M. Campelo and X. M. Lopez-Fernandez, *Quiet Transformers: Design Aspects*, 4th International Advanced Research Workshop on Transformers, ARWtr2013, p. 237-252, Oct., 2013

[20] IEC 60076-10: 2001, *Power transformers – Part 10-1: Determination sound levels,* 2001.

[21] CIGRE WG A2.36, *Guidelines for Conducting Factory Capability Assessment for Power Transformers*, Technical Brochure, No. 530, 2013.

ISBN 978-84-617–9183–5

A New Compact Smart Distribution Transformer with OLTC for Low Carbon Technologies Integration

Luis DEL RÍO ETAYO[1], Jon ALCORTA[1], Asier SOTO[1], Alena ULASENKA[1], Severo ARANAGA[1], Pablo CIRUJANO[2], Gonzalo PEREZ DE NANCLARES[2]

[1] ORMAZABAL Corporate Technology,
Parque Empresarial Boroa, Parcela nº 24 – 48340 Amorebieta (Vizcaya) - Spain
Phone: (+34) 94 630 51 30, e-mail: lre@ormazabal.com
[2] ORMAZABAL COTRADIS
Polígono El Caballo - Parcela nº 56 – 28890 Loeches (Madrid) - Spain
Phone: (+34) 91 885 15 16, e-mail: pcb@ormazabal.com

Abstract — **Over the past decade, there has been a rising awareness of use of renewable energy sources (RES) and the extension of such matters as reduction of CO2 emissions and energy consumption becoming worldwide issues. Low carbon technologies (LCT), such as electric heat pumps (EHP), electric vehicles (EV) and distributed generators (DG), can contribute to fulfil the objectives of limiting global warming. The development of a new compact smart distribution transformer with an On-Load Tap Changer (OLTC) keeps the voltage stable in distribution grids by compensating voltages instabilities in the medium voltage (MV) and can help the integration of LCT by regulating the voltage automatically to cope with the voltage fluctuations generated by new loads and DG in the low voltage (LV) side of the electric network. The smart transformer operation has been assessed in a new 'laboratory' called Demonstration and Experimentation Unit (UDEX), a real grid designed as a platform for the research, development and verification of new technologies, products, services and systems. It permits the reproduction of normal conditions and anomalous situations such as voltage instabilities or fluctuations.**

Keywords — **smart transformer, on-load tap changer, voltage control, low carbon technologies**

I. INTRODUCTION

The penetration of RES is expected to increase over the next decades. This potential rise is promoted in Europe by the European Initiative ´20-20-20´ [1][1], and globally by the last United Nations Climate Change Conference in Paris (December, 2015) [2][2]. To fulfil their commitments, lot of countries have set targets and policies to stimulate the development and integration of renewable energy into the electrical system [3]. Furthermore, the advancement in renewable energy technologies and engineering has boosted significantly the investment in clean energy, helping the deployment of RES [4]. In 2015, renewable energy expanded significantly in terms of capacity installed and energy produced, with renewable energy investments in the power sector outpacing net investments in fossil fuel power plants [3].

Furthermore, EV integration will be also an issue for the electric utilities. Whilst the integration of RES in the LV side of the network is causing overvoltages, the implementation of additional loads in the LV, such as EV or EHP, could cause voltage dips.

As the European standard EN 50160 [5] defines the voltage requirements in distribution grids, and requires that the voltage stays within a band of +/- 10% of the nominal voltage. The compliance with these statutory voltage limits would require a grid extension.

A smart distribution transformer with OLTC can keep the voltage inside the statutory limits by changing automatically the tap of the transformer, without the need of a conventional grid reinforcement [6], allowing further integration of distributed RES and EV [7, 8].

[1] To reduce CO2 emissions by 20%, to reduce primary energy use by 20%, and to increase renewable energies by 20%.
[2] Primarily aimed at reducing global greenhouse gas emissions, setting a goal of limiting global warming to less than 2 degrees Celsius (°C) compared to pre-industrial levels.

ISBN 978-84-617–9183–5

As functional testing of new solutions for voltage control is complicated in real networks, the research to assess the operation of the smart distribution transformer has been done in a new 'laboratory', UDEX, which consists in a real grid designed as a platform for the research of new products for the smart grids [9]. Network operators require high reliability products with predictable behaviour to guarantee the correct operation of the grid.

II. BACKGROUND

II.1 VOLTAGE REGULATION

Descentralised generation connected to MV or LV networks is developing very quickly in many countries. As RES are very volatile, keeping the necessary system stability in the distribution grid will become a more challenging task. New components, products, solutions and concepts try to cope with this new situation.

There are several technologies that may be applied to minimise the impacts of integration RES and to control voltage level within permissible limits. Some of them are represented in the next table along with their advantages and disadvantages:

Table I. Advantanges/Disadvantages of Technologies (Based on [10])

TECHNOLOGIES	ADVANTAGES	DISADVANTAGES
Curtail the RES (or load)	Cheap	Dissatisfied RES users
Grid extension	A better option for large loads and rural areas it can serve other local loads	Grid extension
Statcom	Removes volt spikes, fast response, harmonics elimination	Output voltage magnitude and phase angle cannot be independently adjusted in steady state due to a lack of active power
Storage	Shifts power to when it can be usefully used	Additional infrastructure and space requirements, energy lost in "round trip" inefficiencies
OFF-Load Tap Changer	Optimal solution to the problem of voltage control	Only applicable to installations in which the loss of supply can be tolerated
ON-Load Tap Changer for MV/LV	Solves LV problems, no supply interruption during a tap change	Higher capital cost than a conventional transformer

II.2 SMART DISTRIBUTION TRANSFORMERS

HV/MV power transformers equipped with OLTC have been used in electrical networks and industrial applications for the last 90 years. However, the shift towards bidirectional energy flow networks requires of an additional voltage regulation in the LV side.

There are different technologies in the market for the voltage control in the LV side based on: a magnetic voltage regulation [11], an additional booster transformer with LV contactors [12], LV vacuum and a solid-state relay [13], and finally an electromechanical device with vacuum interrupters in MV [14, 15] – such as the solution described in this paper.

Magnetic voltage regulation devices are based on the application of a magnetically controllable inductance that allows a step-less voltage regulation (see Fig.1). The main copper winding on the outside produces alternate magnetic flux within the core. A DC control winding on the inside produces a steady magnetic flux, which is perpendicular to the main one. The amount of DC flux sets the inductance value in the main winding and therefore the voltage.

ISBN 978-84-617–9183–5

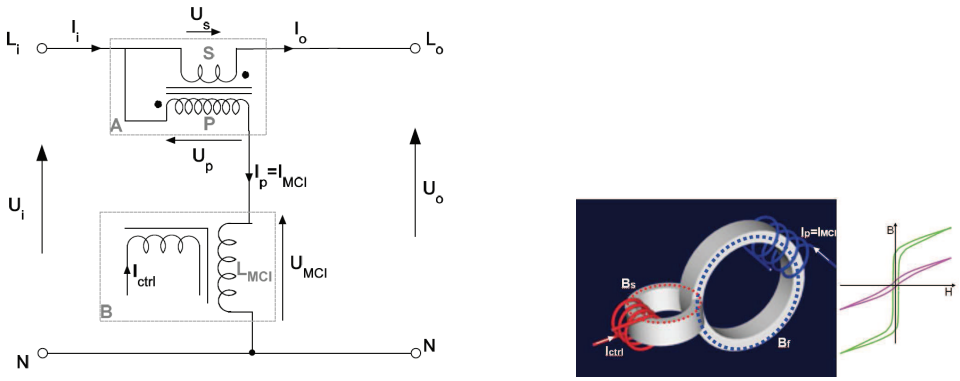


Figure 1. Single-phase magnetic voltage regulator.

Devices that use a booster transformer in series with a conventional transformer change the tap position by means of LV contactors (see Fig. 2). The on-load regulation controls up to 9 taps with up to +/- 10% and is completed with de-energized tappings to adjust the nominal voltage.

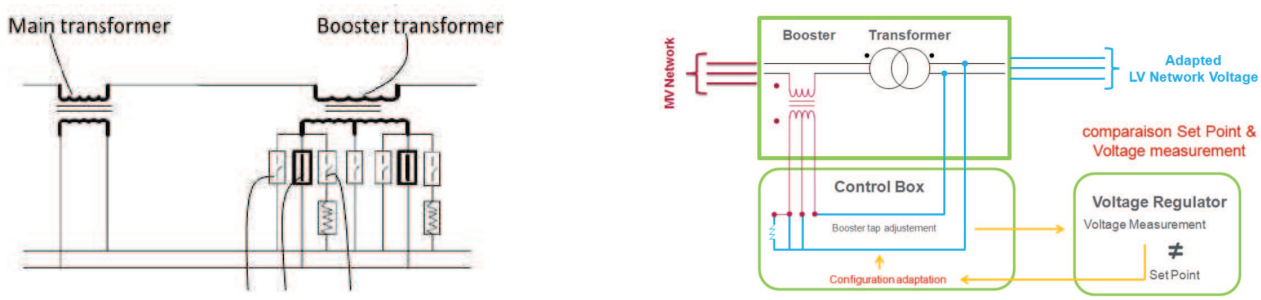


Figure 2. Conventional transformer with an additional booster transformer and contactors. Regulation principle.

There is a technology with off-load tap changer in the MV side and a LV regulation range in three steps (up to +/- 5%) by means of LV vacuum contactors, to change the tap position, and an solid-state relay (thyristor-based) that acts to ensure continuous current flow during the mechanical switching operations, limiting the current created by the momentary inter-turn short circuit with a resistor wired in series (see Fig. 3). Nowadays, this technology has evolved and air break contactors are used instead thyristors.

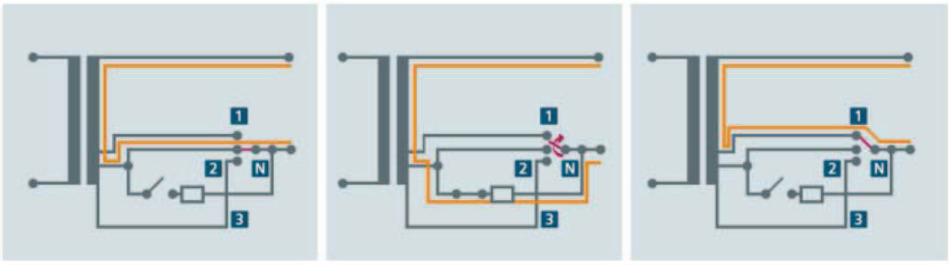


Figure 3. Voltage regulation with vacuum contactors and an air breaker bypass.

Finally, the presented solution is based on an electromechanical OLTC with vacuum interrupters in MV (see Fig. 4). OLTC enables voltage regulation by varying the transformer ratio under load without interruption. The OLTC changes the ratio of the transformer by adding or subtracting turns from the MV winding. The transformer is therefore equipped with a tap winding which is connected to the OLTC. A transition impedance bridges adjacent taps for the purpose of transferring load from one tap to the other without interruption or appreciable change in the load current. Besides, they limit the circulating current allowing, in the case of reactors, continuous loading.

ISBN 978-84-617–9183–5

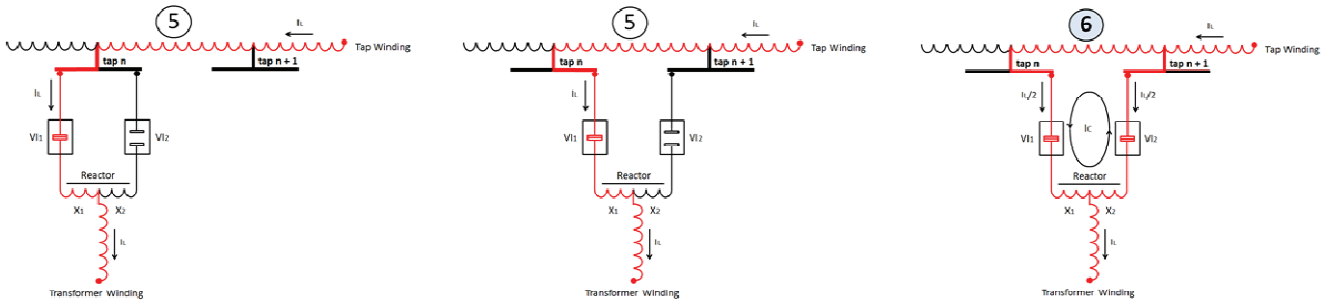


Figure 4. Voltage regulation with vacuum interrupters and movable contacts (tap-change from position 5 to position 6).

III. SMART DISTRIBUTION TRANSFORMER WITH AN ELECTROMECHANICAL OLTC IN THE MV

The new smart distribution transformer, by means of its OLTC, can adjust the transformer substation voltage so that the downstream feeder voltages can be maintained within statutory limits and this can result in an increase in capacity to cope with distributed generation or new loads without the need of new infrastructure. The implemented OLTC is able to carry out a +/-10% regulation in the LV with up to 9 steps of 2.5%.

The smart distribution transformer complies with the IEC 60076 – Power Transformers [16], IEC 60214 – Tap-Changers [17], IEC 61000 – Electromagnetic Compatibility (EMC) [18], along with the eco-design EU Directive No. 548/2014 [19]. It also can use high fire resistant biodegradable ester oil instead of mineral oil.

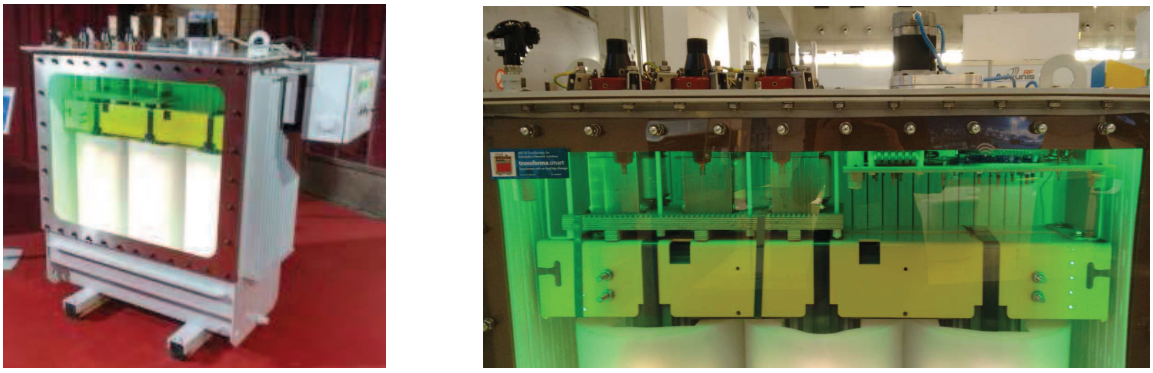


Figure 5. Smart Distribution Transformer internal view.

The flat design of the OLTC (Fig. 6) allows a compact solution, keeping the footprint of a conventional distribution transformer (to allow retrofitting).

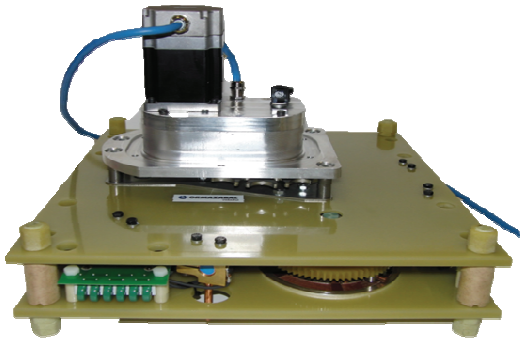


Figure 6. On-Load Tap Changer.

The OLTC is based on a electromechanical system that is able to change the tap position automatically, and with load, by means of a combination of fixed and movable contacts, along with a set of vacuum interrupters (two per phase) on the MV side of the transformer. The vacuum interrupters guarantee that the tap changing is performed safely because the arc, promoted by the switching process, is located inside the vacuum bottle - preventing oil pollution.

ISBN 978-84-617–9183–5

IV. TESTS

The functional testing is complicated without access to real networks, which is generally limited by the network operators. That is why the smart distribution transformer operation has been assessed in a new 'laboratory' called UDEX, a real grid designed as a platform for the research, development and verification of new technologies, products, services and systems.

V.1 DESCRIPTION OF THE UDEX

The main purpose of the UDEX is to make experiments in a real MV/LV network having a high flexibility, independent of the utility networks, for the development and testing of new technologies. It is able to reproduce normal conditions of existing worldwide networks as well as anomalous situations, such as MV instabilities or LV fluctuations due to LCT integration.

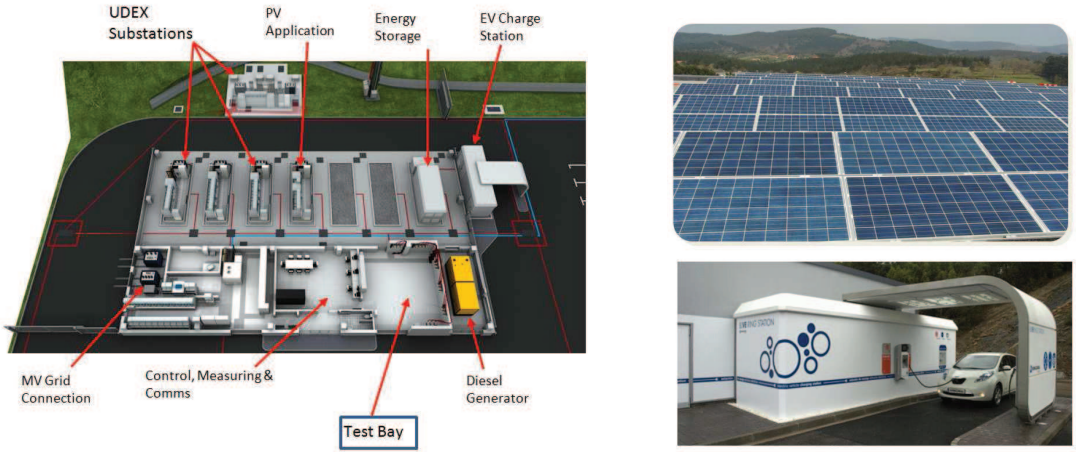


Figure 7. UDEX top view. Solar roof and EV charge station.

This concept of a highly configurable MV network for development and testing of new technologies not only contemplates equipment testing, as with standard laboratory testing, but also embraces solutions and applications for network infrastructures, such as the smart distribution transformer.

In the UDEX, several locations to place new equipment or components are available: Primary substations (CS1, CS2), transformer substations (CT1, CT2, CT3, CT4, CT5), spare test bays for new transformer substations and a test bay where the test object is located.

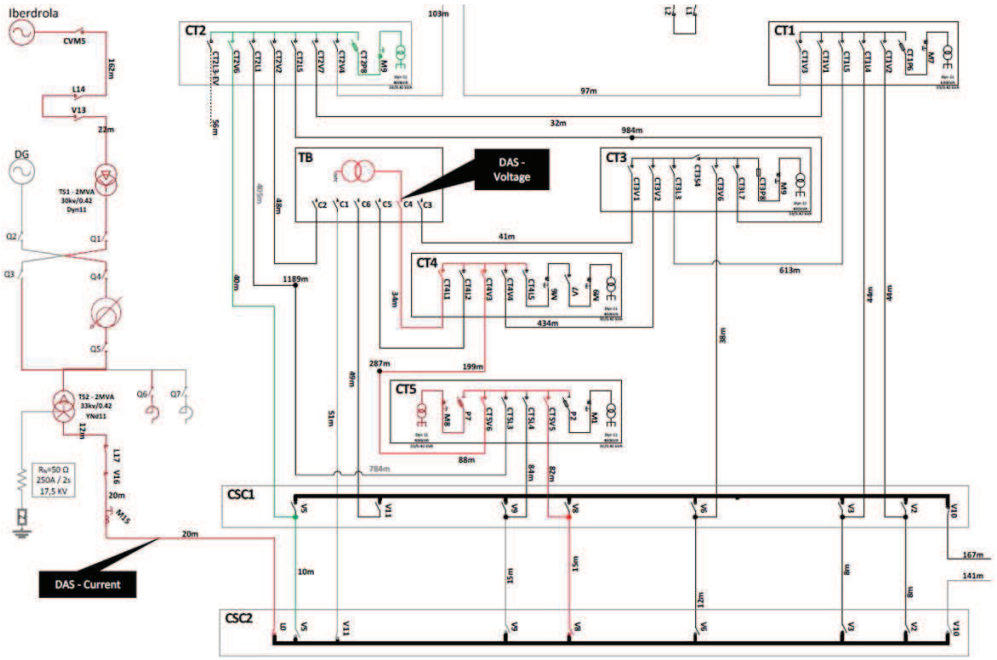


Figure 8. UDEX general lay-out.

ISBN 978-84-617–9183–5

V.2 DESCRIPTION OF THE TESTS

The smart distribution transformer is placed in the UDEX test bay.



Figure 9. Smart Distribution Transformer during a test in the UDEX test bay.

The UDEX is connected to a 36kV utility grid and is adjusted, by means of an autotransformer, to 24kV. The LV side of the smart transformer is connected to a load of 130kVA, whilst CT5 load (130kVA) is connected to the MV side.

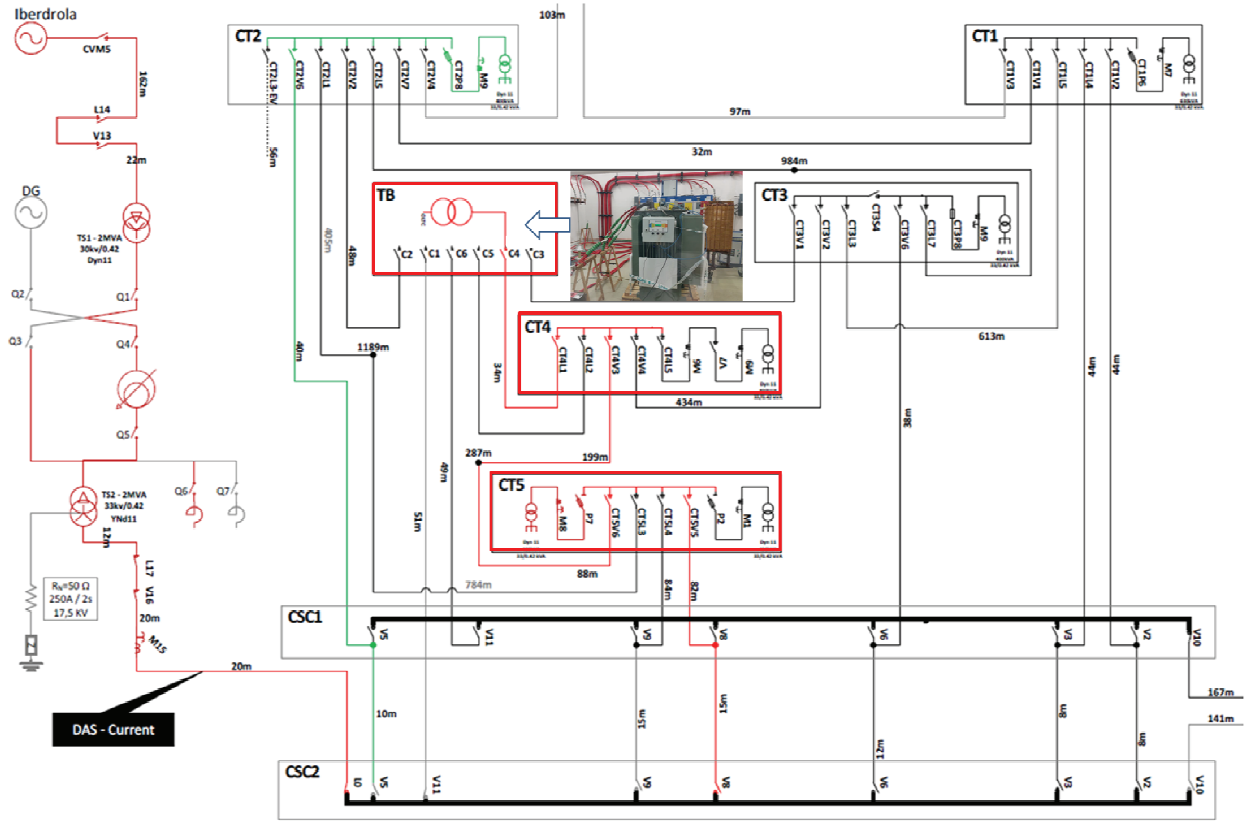


Figure 10. UDEX general lay-out (CT4 and CT5 connected) with the smart transformer in the Test Bay.

Two tests are carried out in order to assess the smart transformer operation under MV instabilities:

ISBN 978-84-617–9183–5

TEST 1. VOLTAGE DROP

A voltage drop in the LV is created by adding an extra load in the MV network: CT2 (44kVA) and CT3 (30kVA) are connected to the main MV network.

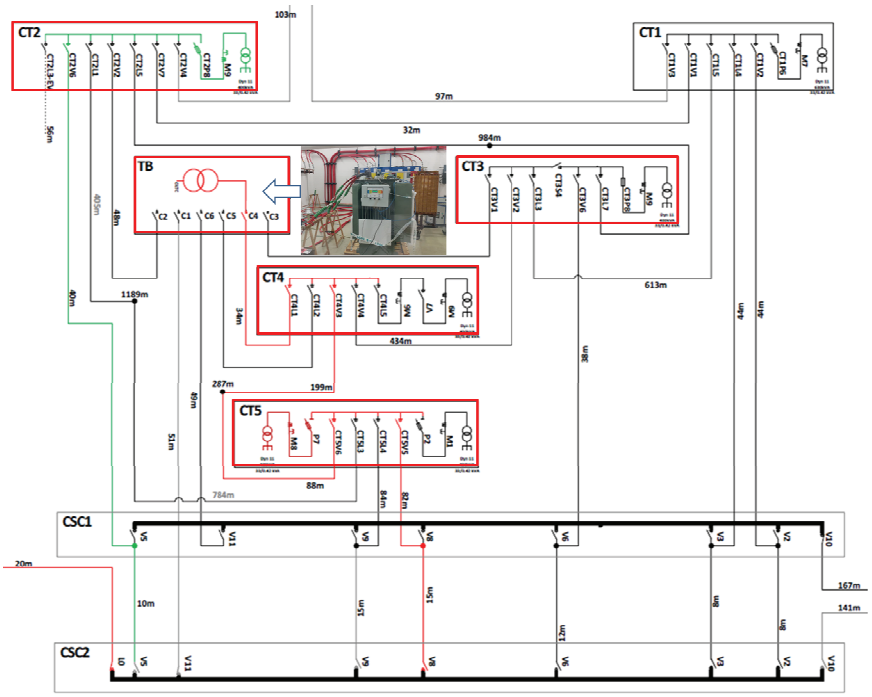


Figure 11. UDEX Test 1 lay-out (CT2, CT3, CT4 and CT5 connected) with the smart transformer in the Test Bay.

TEST 2. VOLTAGE RISE

A voltage rise in the LV is created by disconnecting the CT2 load (44kVA).

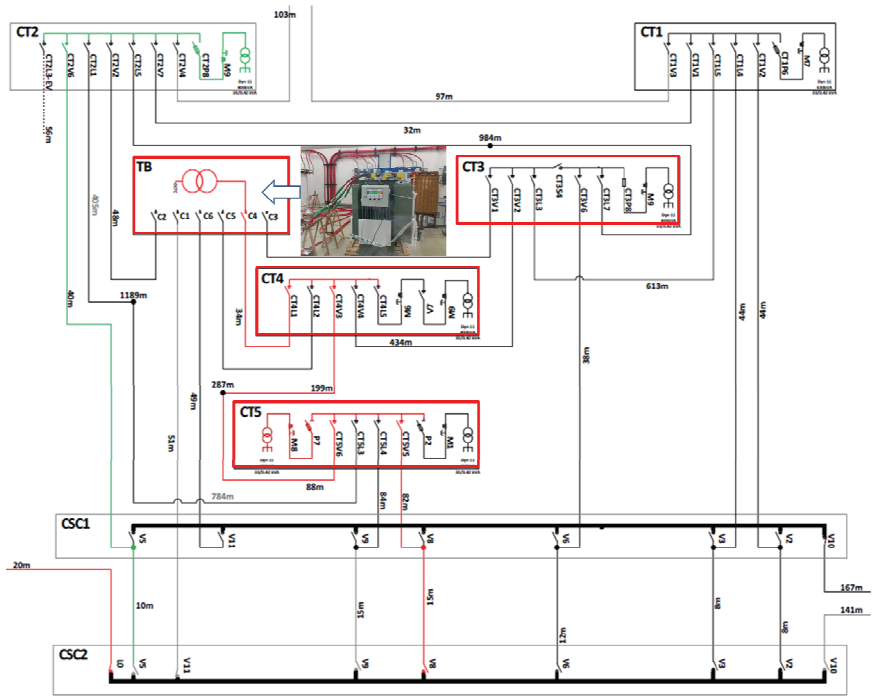


Figure 12. UDEX Test 2 lay-out (CT2 disconnection) with the smart transformer in the Test Bay.

ISBN 978-84-617–9183–5

V.2 RESULTS AND DISCUSSIONS

The smart distribution transformer operation has been assessed by means of two tests where MV voltage instabilities were reproduced. The smart distribution transformer showed its capability to cope with voltage fluctuations keeping the low voltage stable.

TEST 1. VOLTAGE DROP

The smart transformer monitoring system is able to detect such voltage drops actuating the associated OLTC to raise the voltage in two steps.

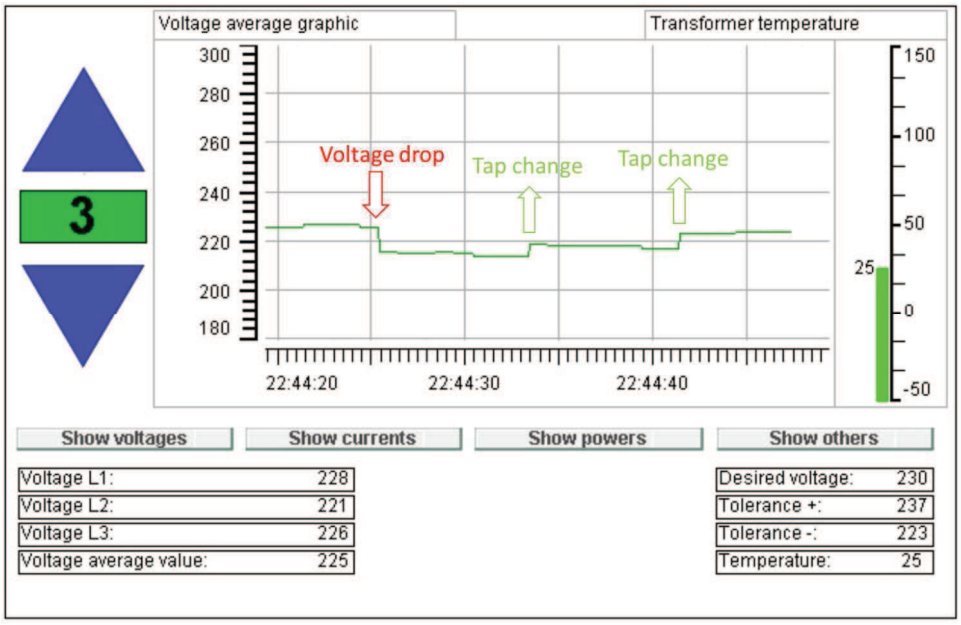


Figure 13. Voltage drop and smart transformer voltage recovery during Test 1.

TEST 2. VOLTAGE RISE

The smart transformer monitoring system is able to detect such voltage rises actuating the associated OLTC to lower the voltage in one step.

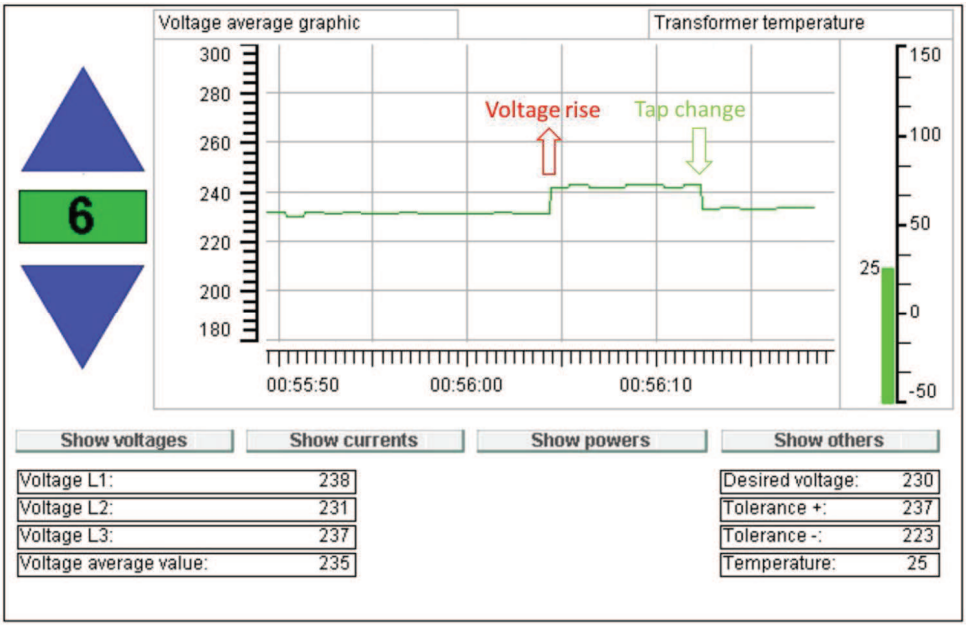


Figure 14. Voltage rise and smart transformer voltage recovery during Test 2.

ISBN 978-84-617–9183–5

V. CONCLUSIONS

The capability to control the voltage of a new compact smart distribution transformer with OLTC has been assessed in a controllable real network.

The performed tests showed that the smart distribution transformer is able to cope with voltage fluctuations, keeping the voltage within the statutory limits.

The smart distribution transformer can be considered an essential element of the network that can provide optimal grid flexibilities and reliability.

ACKNOWLEDGEMENTS

The authors of this research work wish to acknowledge I. Orue and N. Akroud for their help with the experimental set-up and measurements.

REFERENCES

[1] The "20-20-20" targets, Overview of EU climate and energy policies.

[2] COP21, Paris Climate Conference, 2015.

[3] Ren21's, Renewables 2013, Global Status Report.

[4] UNEP Collaborating Centre for Climate & Sustainable Energy Finance, Global Trends in Renewable Energy Investment 2014.

[5] EN 50160:2011. Voltage characteristics of electricity supplied by public distribution systems.

[6] J. Schmiesing, H. Beck, T. Smolka, M. Sojer. *Avoiding MV-Network Expansion by Distributed Voltage Control*, in the 22nd International Conference on Electricity Distribution, Jun 2013.

[7] T. Drizard, C. Lebosse, B. Chazottes. *Integration of Distributed PV Generation: The Nice Grid Project*, in the 23rd International Conference on Electricity Distribution, Jun 2015.

[8] S. Huang, J. Pillai, M. Liserre, B. Bak-Jensen. *Improving photovoltaic and electric vehicle penetration in distribution grids with smart transformer*. IEEE PES Innovative Smart Grid Technologies Europe 2013.

[9] I. Orue, I. Gilbert, J. Larrieta, J.A. Sánchez, *Making Faults to Protect Power Networks*, paper nº 0161, CIRED Worshop – Helsinki 14-15 June 2016.

[10] CIRED, International Conference on Electricity Distribution 2013, http://www.cired2013.org/downloads/RT1a-kaltenborn.pdf.

[11] S. Roposa, G. Stumberger, D. Lestan, M. Roser. *Application of Voltage Stabilizer in Slovenian Low Voltage Grid*. Przeglad Elektrotechniczny (Electrical Review), ISSN 0033-2097, R. 87 NR 3/2011.

[12] Y. Chollot, P. Deschamps, A. Jourdan, S. Mishra. *New Approach to Regulate Low Voltage Distribution Network*, in the 23rd International Conference on Electricity Distribution, Jun 2015.

[13] R. Schmid, R. Walz, K. Boldt, H. Müller, K. Handt, G. Hipszki. *On-load voltage regulation in the low voltage grid*, CIRED workshop 2012.

[14] T. Smolka, D. Dohnal, M. Sojer, R. Heiliger, J. Schmiesing, T. Hug, F. Sutter. *Advanced Grid Integration of Dispersed Generation by using Voltage Regulated Distribution Transformers (VRDT) – Experiences from field tests and potentials for minimizing network expansion*. CIGRE Session 2014.

[15] D. Geibel, T. Degner, T. Bülo, C. Tschendel, M. Pfalzgraf, K. Boldt, P. Müller, F. Sutter, T. Hug. *Active, Intelligent Low Voltage Networks – Concept, Realisation and Field Test Results*, in the 22nd International Conference on Electricity Distribution, Jun 2013.

[16] IEC standard 60076-1:2011. Power transformers.

[17] IEC standard 60214-1:2014. Tap-changers.

[18] IEC standard 61000-4-1. Electromagnetic compatibility (EMC).

[19] Commission Regulation (EU) No 548/2014 of 21 May 2014 on implementing Directive 2009/125/EC of the European Parliament and of the Council with regard to small, medium and large power transformers.

ISBN 978-84-617–9183–5

Smart Transformer based on Power Electronics: Current Developments and Future Trends

Alberto PIGAZO[(1)], Marco LISERRE[(2)], Tamás KEREKES[(3)] and Giampaolo BUTICCHI[(2)]

[(1)] Dept. of Computer Systems and Electronics, University of Cantabria, Santander, Spain, e-mail: pigazoa@unican.es
[(2)] Chair of Power Electronics, Christian-Albrechts University, Kiel, Germany, e-mail: {ml, gibu}@tf.uni-kiel.de
[(3)] Dept. of Energy Technology, Aalborg University, Aalborg, Denmark, e-mail: tak@et.aau.dk

Abstract — **New challenges in Smart Electical Grids, such as integration of Electric Vehicles chargers and Distributed Energy Resources, require advanced functionalities, both at power and communication levels to be provided in distribution electrical grids. The Smart Transformer is intended to replace conventional power transformers providing such advanced features but the challenge is replacing a tested and proven technology with power electronics based one. This manuscript provides an overview to ST technologies and current develpments, comparing the characteristics of the available prototypes, and gives a glimpse of future trends and required funtionalities.**

Keywords — **Smart Transformer, Solid State Transformer, Smart Grid, Distributed Energy Resources**

I. INTRODUCTION

The proliferation of Distributed Energy Resources (DERs) and active loads in distribution grids has posed many technical and operational challenges to Distribution System Operators (DSOs) [1]. The centralized generation based schemes are evolving to more decentralized ones, with an increasing penetration of renewable energy sources in LV grids, and new loads with advanced management requirements, such as charging stations for Electric Vehicles (EV), are being connected to these networks [2].

Power electronic interfaces in DERs are allowing such paradigm change but are also contributing to certain grid issues, such as power quality events. This is the case of the 50.2 Hz problem in Europe due to the simultaneous disconnection of a number of PV generators under the occurrence of a minor over frequency event [3] or the occurrence of temporary over voltages in feeders due to the formation of an electric island [4]. Due to this fact, it's commonly required that distribution generation units based on inverters include high level functionalities such as grid support (V, f, Q control) or ride-through capability under faults [5-7].

Local and national regulations are being adapted to cope with this new panorama. Among others, in California, USA, the PV inverters must provide voltage/frequency ride-through, real/reactive power control and ramp rate control [8]. In Spain, the law RD 900/2015 on self-consumption allows the customers to balance their power consumption at the PCC close to zero as a consequence of the local connection of DERs [9], which makes more difficult the voltage regulation by DSOs. The international standards are also evolving providing specific regulations for active front-ends in DERs. The interaction of power electronic converters in DERs and the electrical grid is regulated in UL 1741 [10], IEEE 929 [11], IEEE 1547 [12], IEC 61727 [13], IEC 62116 [14] standard series. Communication requirements between the electrical grid and DERs are described in IEEE 2030 [15], IEEE 1815 [16] and IEC 61850 [17]. These standards are being continuously adapted to include new requirements in electrical grids.

DSOs are facing these issues by increasing the automation of their electrical grids, stablishing new operational requirements and integrating new devices facilitating the grid decentralization. Increasing the automation level of the distribution grid is the main target of the project RedACTIVA [18], where two Spanish DSOs are collaborating with manufacturers and researching institutions/universities to develop new devices and approaches to manage the technical and operational challenges due to DERs proliferation and electrical grid decentralization. The utilization of devices/equipment such as On Load Tap Changers (OLTCs), electronic breakers, Flexible AC Transmission Systems (FACTs), High Voltage DC (HVDC), energy management devices, advanced monitoring units (i.e. synchrophasors) are allowing the management and operation of

ISBN 978-84-617–9183–5

distribution grids to be improved by providing the required advanced functionalities to deal with ad-hoc issues. The coordination of these devices/equipment among them and through the DSO control centre require real time communications to be available with different latencies, safety and security requirements.

The Smart Transformer (ST) concept due to the Project Highly Efficient and Reliable ST (HEART) [19, 20] is a Solid State Transformer (SST) that integrates the advanced features required by DSOs into distribution transformers at both power and communication levels. The SST is employed to manage power flows in distribution electrical grids and the ST behaves as a communication hub for the smart grid. Fig. 1 shows the role of the ST in distribution electrical grids.

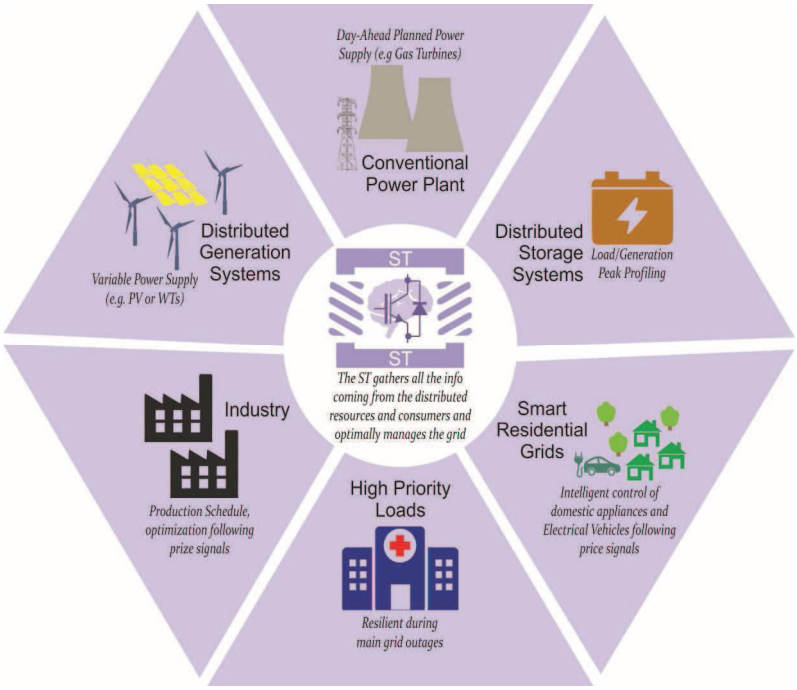


Figure 1. The role of the ST in distribution electrical grids. PV: photovoltaic, WTs: Wind Turbines [20].

This manuscript will provide the foundations of the SST, describing its current development status and future trends. The manuscript is organized in five sections: introduction, architecture/operation principles of SST, the concept and functionalities of the ST and conclusions.

II. SOLID STATE TRANSFORMERS: TOWARDS THE SMART TRANSFORMER IN ELECTRIC DISTRIBUTION GRIDS

The system level challenges described in the previous section could be properly addressed by the ST but it has to compete with the traditional transformer, based on a proven technology, in terms of cost, efficiency and reliability. Moreover, in comparison to the traditional transformer, the additional functionalities demanded to the ST would impose more restrictive operational conditions that make it more difficult to cope with efficiency and reliability requirements [20].

The first conventional three phase low frequency transformer was firstly proposed by Dobrovolsky in 1889 [21]. Conventional low frequency transformers operate with fixed voltage/current/frequency ratios and, being highly efficient and operated within the linear range, maintain active/reactive powers at both windings. Distribution transformers have evolved to cope with certain issues in smart grids. This is the case of OLTCs modifying their voltage set points when the voltage profile goes down a predefined threshold. Temporary and permanent voltage violations can be distinguished by means of a predefined time delay applied to the detection of the threshold crossing. Solutions like those adopted by Siemens in [22] are available integrating both a

ISBN 978-84-617–9183–5

mechanical switchboard plus a solid-state relay. However, the volume, weight and functionalities of these developments are limited and a higher integration of power electronics can improve their performances.

Conventional transformers are relatively inexpensive, highly robust and reliable, highly efficient (98.5% to 99.5%) and limit the short circuit current. As weaknesses, a relatively large volume and weight is required to increase their efficiency at low frequencies, the conventional transformer has power losses at no load, exhibits voltage drop under load and its performance deteriorates in the presence of harmonics, DC offset and load imbalances [23].

The concept of an SST was first introduced by McMurray in 1968 [24]. The proposed device was based on solid state switches with high frequency (HF) isolation that behaved like a traditional transformer (the output frequency matches the input one and the voltage ratio was fixed). In the 1980s, Brooks [25] highlighted the output voltage waveform-conditioning capability of a solid state transformer. First practical applications of SSTs arose in the 1990s in traction systems, where the standard frequency of 16.66 Hz imposed bulky and heavy LFTs with low efficiency. Weight and volume restrictions in this application make SSTs more practical than LFTs. The volume and weight reduction due to the SST was around 20-50 % and the system conversion efficiency was also improved, from 93% to 96%. Unfortunately, due to the frequency change in traction standards, from 16.6 Hz to 50 Hz, no actual SST development led to an industrial product because of the reduced gain margin, in terms of volume and weight at 50 Hz. It must be considered that additional control functionalities due to the SST played a limited role in traction applications.

Nowadays, the SST is considered a power electronic based solution intended to replace the standard low frequency transformer (LFT) providing galvanic isolation between the input and output of the converter, active control of power flow in both directions, compensation of power grid disturbances and ports and interfaces to connect DERs. Among the functionalities to be expected are: voltage dip and harmonic compensation capabilities, load voltage regulation, disturbance rejection, power factor correction, VAR compensation and active filtering, overload and short circuit protections. The potential to use the SST as the enabling technology for smart grid functionalities in electric distribution is much higher. The SST is supposed to replace the standard LFT, connecting the medium-voltage (MV) grid to the low-voltage (LV) grid, and offer DC connectivity and services to both LV and MV grids. In this case, the weight and volume advantages have a limited impact while efficiency and reliability are the primary requirements, as high losses and service interruption cannot be tolerated, as summarized in Fig. 2. The functionalities in question together with the need for control and communication functions make this device a smart SST or an ST. Hence, an ST is a SST behaving as a power system management node, linking diverse AC or DC infrastructures and other energy sources and supporting the infrastructures needed for the smart distribution grid deployment.

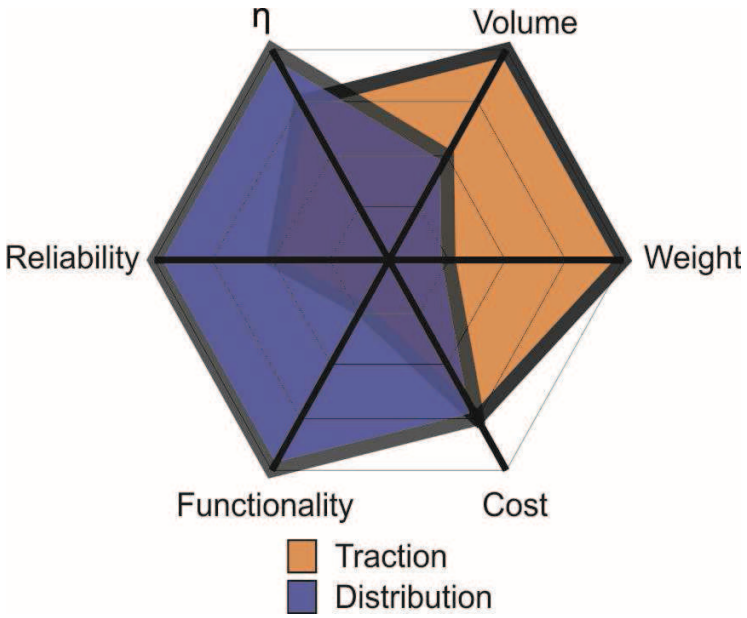


Figure 2. Comparison of SST requirements in traction and electric distribution applications [20].

ISBN 978-84-617–9183–5

The classification of SST topologies depending on the number of power conversion stages is shown in Fig. 3. One, two and three conversion stages can be employed to increase the SST flexibility and availability of intermediate voltage levels. One stage SSTs are based on Direct Matrix Converters (DMCs) or Indirect Matrix Converters (IMCs) and does not provide access to constant DC links (In the case of IMCs, a virtual DC link can be accessible). In two-stage SSTs, the separation can be applied at MV or LV sides. MVDC and LVDC levels are controlled in three-stage SSTs but such separation requires bulky storage elements.

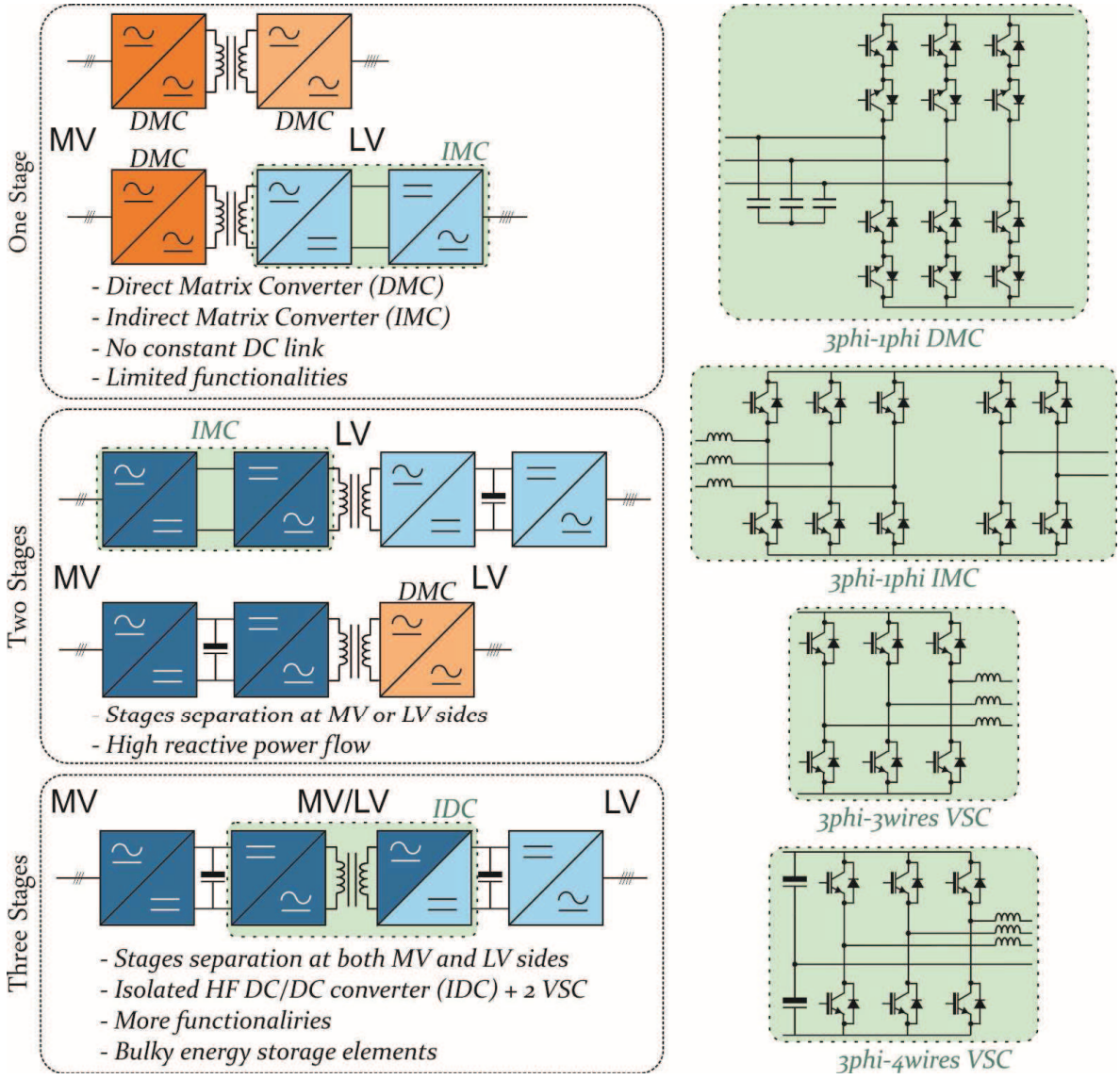


Figure 3. Classification of SST topologies based on the number of employed stages for power conversion. Dark/light colors refers to MV and LV levels respectively [20].

Three-stage SST topologies can be also classified depending on their modularity (Fig. 4). Not modular, semi-modular and modular structures are available. Not modular approaches require wide band-gap power devices to manage voltages and currents at the MV side and maintenance activities can only be carried out with the SST stopped. Semi-modular topologies consist of a unique multiwinding isolation transformer with several power converters connected to each winding. In order to achieve voltage and power scalability, the modular approach must be applied, where multiple isolation transformers are employed, typically one per stage. Modular topologies allow hot swapping of modules during maintenance tasks. Three-stage modular SST can be subdivided according to the modularity level, as depicted in Fig. 5. Depending on the modularity level more or less connection points (MVDC and/or LVDC) will be available.

ISBN 978-84-617–9183–5

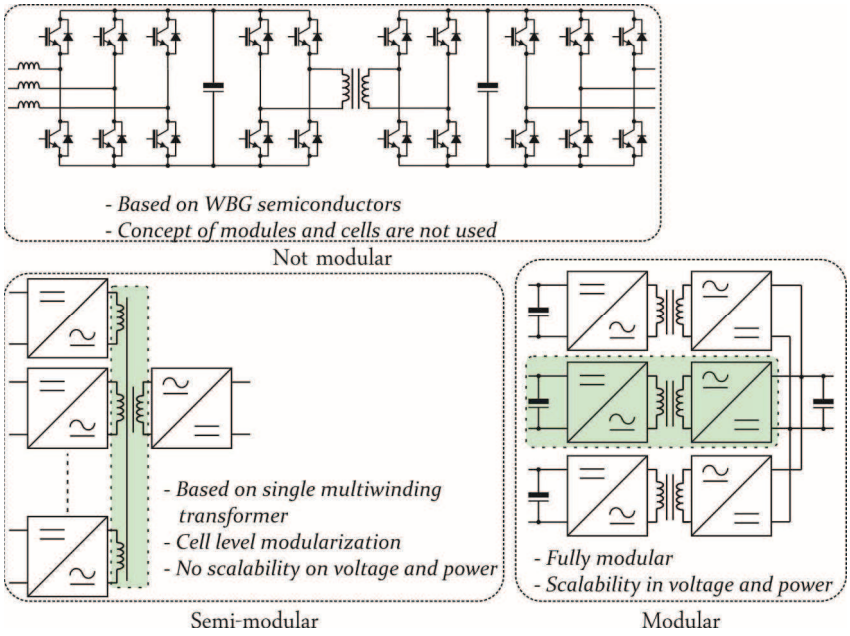


Figure 4. Classification of three-stage SST topologies based on modularity [20].

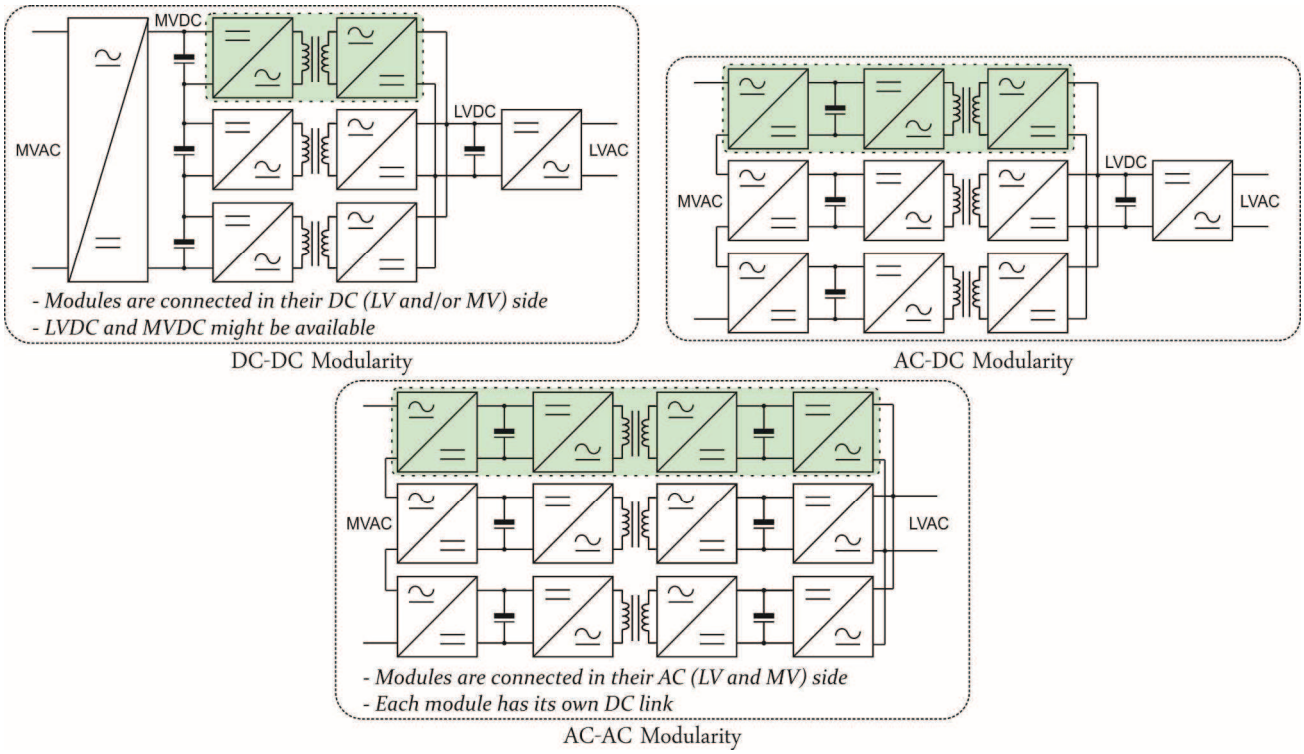


Figure 5. Classification of three-stage Modular SST topologies based on modularity level [20].

Fig. 6 shows typical MV power converter topologies employed in SSTs. The Neutral Point Clamped (NPC) topology divides the voltage stress across the employed devices connected in series, clamping diodes are employed to generate diverse output voltages at the AC side. Depending on the converter configuration, the maintenance tasks require one arm, or the whole bridge, to be replaced. This issue can be solved by means of cascaded H bridges resulting on a per-phase Multilevel Converter (MC), where each bridge regulates one floating DC voltage and these voltages are employed to generate a low distorted voltage waveform at the MV side. Modular Multilevel Converters (MMCs) extend the system modularity, providing simple cells which can be replaced without stopping the SST.

ISBN 978-84-617–9183–5

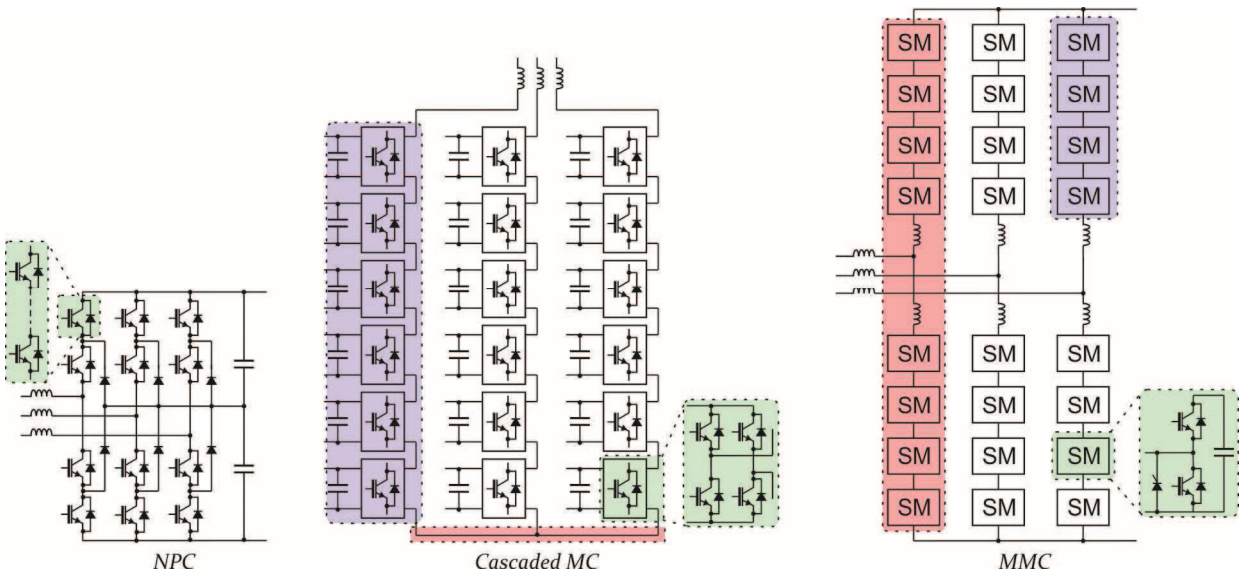


Figure 6. MV converter topologies [20].

DC-DC converters in SSTs provide galvanic isolation through a high frequency transformer (Fig. 7). Three main approaches can be found in the literature: the Dual Active Bridge (DAB) converter, the Series Resonant (SR) converter and Multiple Active Bridge (MAB) converter. In the DAB converter the conventional control strategy consists on applying square voltage waveforms to the high frequency transformer primary and secondary. Phase displacement control of these waveforms allow the power transfer to be controlled. In SR converters, the resonant tank is employed to generate a high frequency sinusoid to be applied to the transformer primary. MAB converters combine several windings in the same transformer to control the power transfer among both sides of the SST.

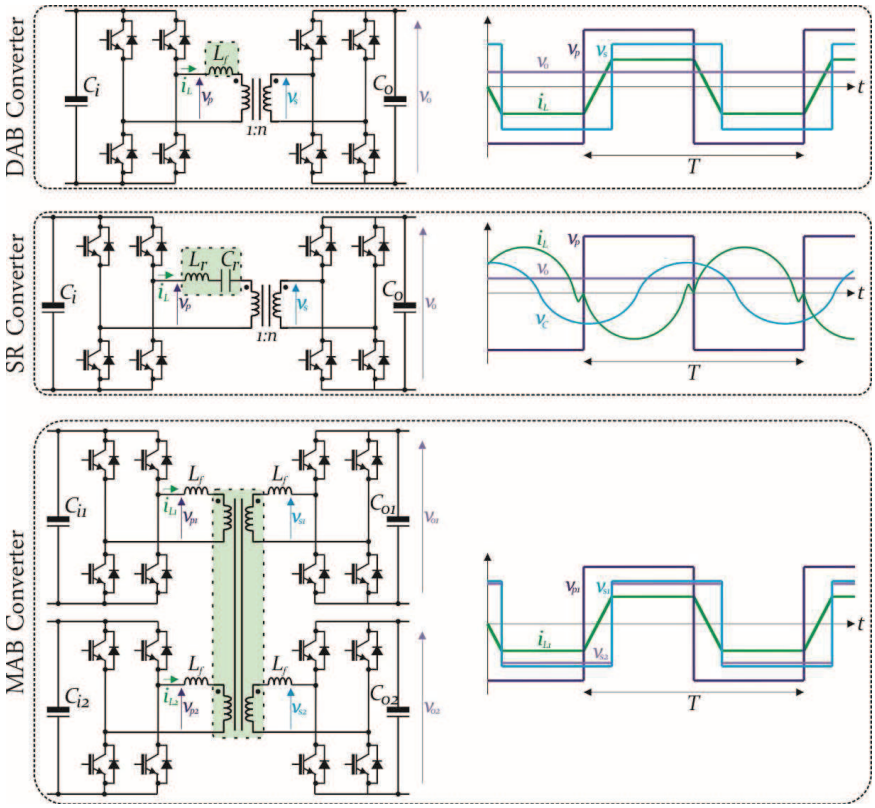


Figure 7. The most applied topologies for the implementation of the isolated DC/DC converter. DAB: Dual Active Bridge, SR: Series Resonant and MAB: Multi Active Bridge [20].

ISBN 978-84-617–9183–5

The main component in SSTs is the high frequency transformer, employed for isolation of the DC-DC converters and providing a high power density with low losses. Increasing the transformer power density requires a proper management of these losses through a cooling system. The main types are depicted in Fig. 8. The construction types are limited by the available core shapes within this dimension range. It must be considered that increasing the power of the transformer at a certain frequency increases the transformer size and, as a consequence, the parasitics in the transformer core and the employed conductors. Shell type transformers provide design flexibility with reduced parasitic components.

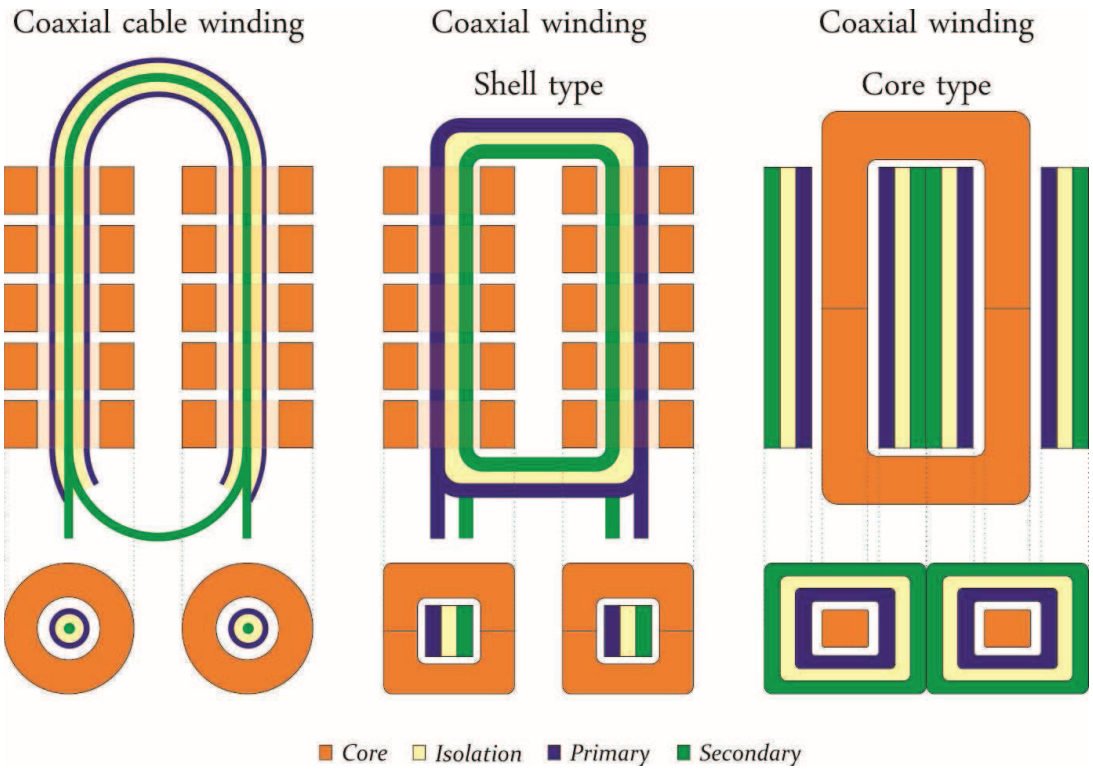


Figure 8. MF transformer types employed in SST [23].

Table I compares the main characteristics of magnetic materials employed in high frequency transformer prototypes for SSTs [26]. Nanocrystalline cores combine a high saturation flux density with low power losses but their cost is also high, which can limit certain SST designs.

Fig. 9 shows high frequency transformers prototypes applicable to SSTs. The ABB prototype consists of a coaxial cable winding providing extremely low leakage inductance and a reliable isolation due to a homogeneous electric field, however, it exhibits a low flexibility on turns ratio (1:1) and complex terminations [27]. The prototype in [28] is based on coaxial windings applied to a core type structure. It allows the leakage inductance to be adjusted and provides flexibility on the turns ratio with simple terminations but the isolation is more complex. It employs a water cooling based system. This is the approach in the GE prototype in [29], where an amorphous core provides 150 kVA in a 1.7 kV to 377.8V transformer operating at 10 kHz. The prototype from Bombardier in [30] employs coaxial windings over a shell type core, reaches 350 kW at 8 kHz, is water cooled and provides 33 kV isolation. Amorphous materials are also employed in three prototypes developed by FREEDM in [31] for 10 kVA, 3.8 kV to 400V at 3 kHz, based on Metglas SA2605SA1 with diverse saturation fluxes, reaching efficiencies around 97%. The ETHZ water-cooled prototype in [32] reaches 166 kW, at 20 kHz, and it is based on a nanocrystalline core, which allows the power density to be increased up to 32.7 W/dm^3 with a measured 99.5% efficiency. STS Induktivitaeten [33] is producing a MF Transformer for traction applications operating at 8 kHz, providing 450 kW/600 kVA powers with 99.7% efficiency and 37 kVrms isolation.

ISBN 978-84-617–9183–5

Table I. Characteristics of Magnetic Materials for High Power Applications [26]

Material	Alloy Composition	Loss (W/kg) 20 kHz, 0.2 T	Saturation [mT]	Magneto-striction (10^{-6})	Permeability (50 Hz)	Max. Working Temp. [°C]
Grain oriented Si steel	$Fe_{97}Si_3$	>1000	2000	9	2k-35k	120
Advanced Si steel	$Fe_{93.5}Si_{6.5}$	40	1300	0.1	16k	130
High performance ferrite	MnZn	17	500	21	1.5k – 15k	100/120
Fe-amourphous alloy	$Fe_{76}(Si,B)_{24}$	18	1560	27	6.5k – 8k	150
Co-amorphous alloys A	$Co_{73}(Si,B)_{27}$	5	550	<0.2	100k – 150k	90/120
Co-amorphous alloys B	$Co_{77}(Si,B)_{23}$	5.5	820	<0.2	2k – 4.5k	120
Co-amorphous alloys C	$Co_{80}(Si,B)_{20}$	6.5	1000	<0.2	1k – 2.5k	120
Nanocrystalline alloys I	FeCuNbSiB	4.0	1230	0.1	20k – 200k	120/180
Nanocrystalline alloys II	FeCuNbSiB	4.5	1350	2.3	20k – 200k	120/180
Nanocrystalline alloys III	FeCuNbSiB	8.0	1450	5.5	100k	120/180

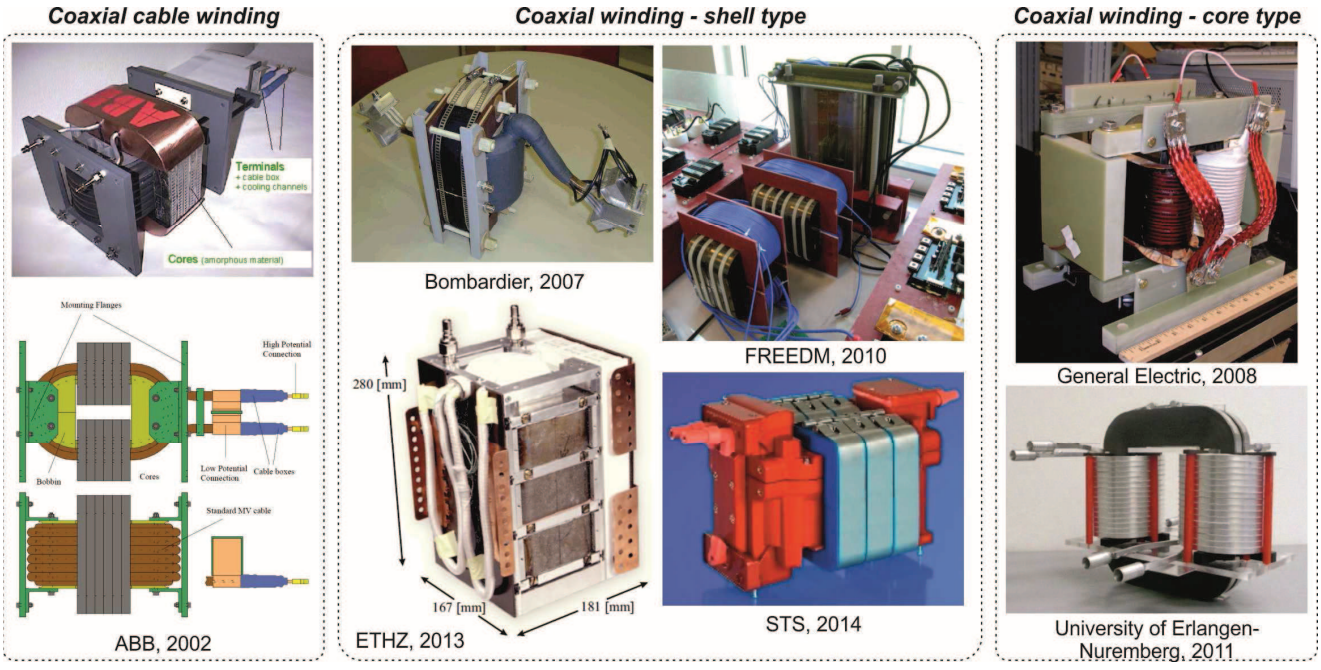


Figure 9. MF transformers for isolation of DC/DC converters in SSTs.

In order to generate the LVAC voltage, an inverter must be connected to the DC-DC converter output. Fig. 10 shows the most commonly employed topologies. NPC inverters with passive (diode) clamping to the neutral allow a low distortion voltage waveform to be generated at the LV side but with unbalanced thermal stress among the external and inner devices of each arm. This issue can be solved by means of active NPC, with active clamping. In this case, the added devices allow the stress to be balanced. The standard approach is based on voltage source converter (VSC) where the LV AC neutral is connected to a divided dc bus.

ISBN 978-84-617–9183–5

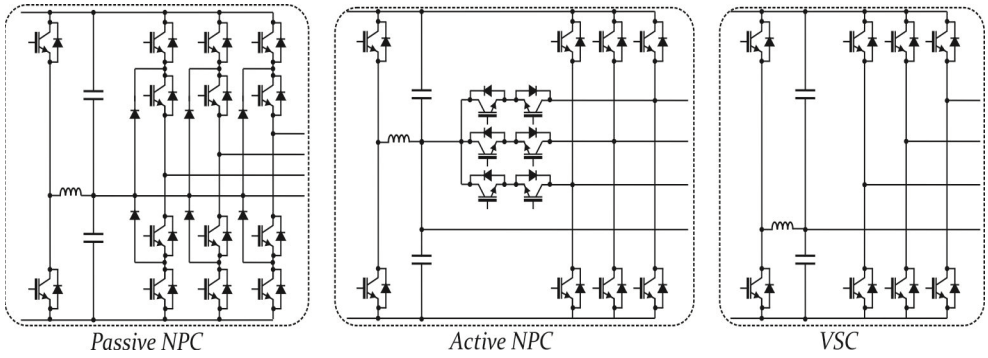


Figure 10. 3 phase 4 wires topologies employed for implementation of the LV stage of the ST [20].

III. CURRENT STATUS OF STT DEVELOPMENTS

The concepts shown in the previous section have been applied in diverse prototypes. This section provides an overview of current SST prototypes [34].

III.1 ABB (2006)

The first approach by ABB [35] consisted on one stage topology, with a cascaded configuration of DCMs in the input side and cascaded output rectifiers. The input DCMs were serialized, up to 16 modules, to reach the 15 kV/16.7 Hz input voltage. The output rectifiers were parallelized and operated with an output voltage equal to 1.8 kV. The medium frequency transformer operated at 400 Hz. Fig. 11 shows the employed topology and a picture of the developed prototype.

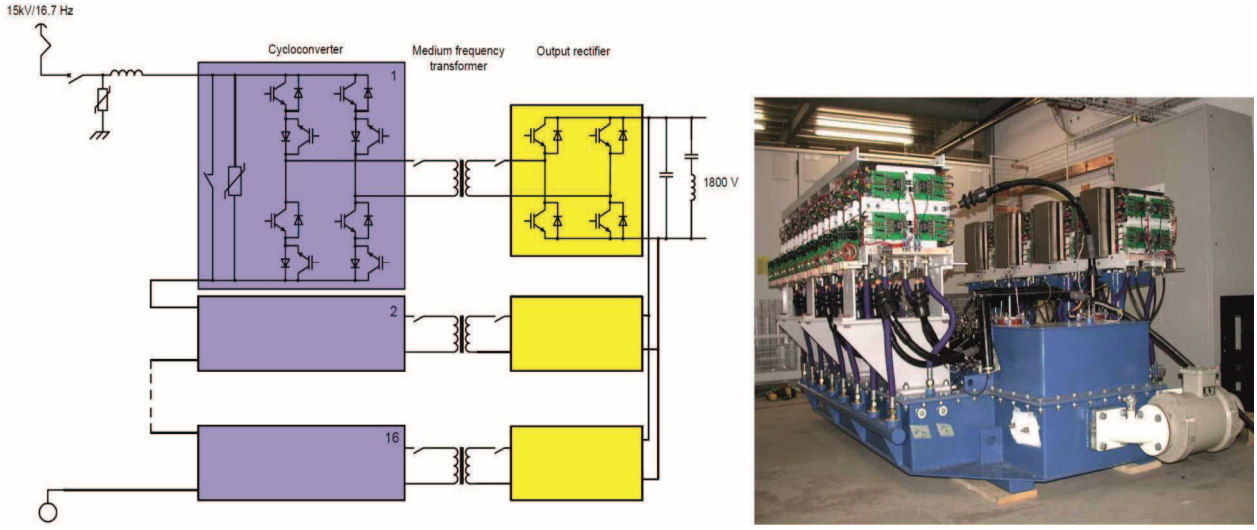


Figure 11. Power Electronics Transformer for traction applications by ABB [35].

III.2 ABB (2011)

A subsequent development by ABB [36] employed a two-stage topology, with a multilevel converter built by means of cascaded H bridges in the MV side and one SR converter as DC-DC converter, the outputs of each employed module were parallelized to increase the available LVDC power. Fig. 11 shows the employed topology and a picture of the developed prototype. Each inner high frequency transformer was rated at 150 kW (withstanding 225 kW overloads for 60 seconds) and 1.8 kHz. These transformers were built with nanocrystalline material and oil direct air forced cooling method, which provided isolation [37]. The rated power of the prototype was 1.2 MVA (8 modules + 1 redundant) and reached a 96.2% efficiency. It employed 72 semiconductors and 6.5 kV and 3.3 kV IGBTs.

ISBN 978-84-617–9183–5

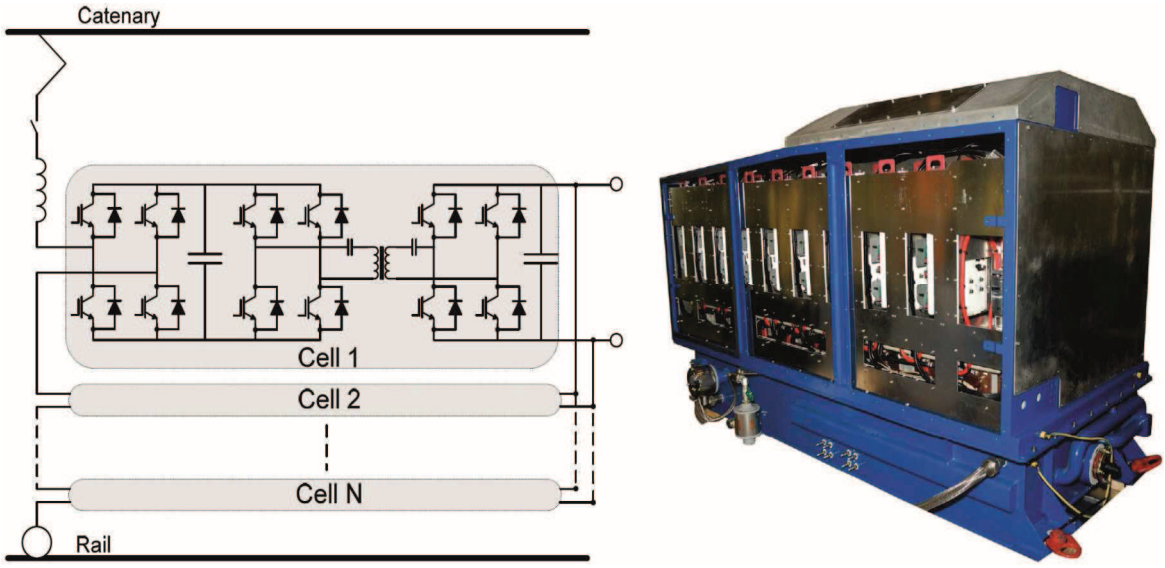


Figure 12. Power Electronics Transformer for traction applications by ABB [36],[37].

III.3 FREEDM (2013)

The approach by FREEDM consists of a three-stage architecture: a cascaded H-bridge configuration at the MV side, DAB converters for DC-DC conversion whose outputs are parallelized to increase the LVDC (200 V) power. The Fig. 13 shows the employed topology. Finally, an inverter provides the LVAC at 120 V. The prototype has approximately 3MVA power and the high frequency transformer operates at 3.6 kHz. It was built with customized 6.5 kV IGBTs, 16 semiconductors per phase, and the reached efficiency is 92% with only DC loads and 85% with AC loads.

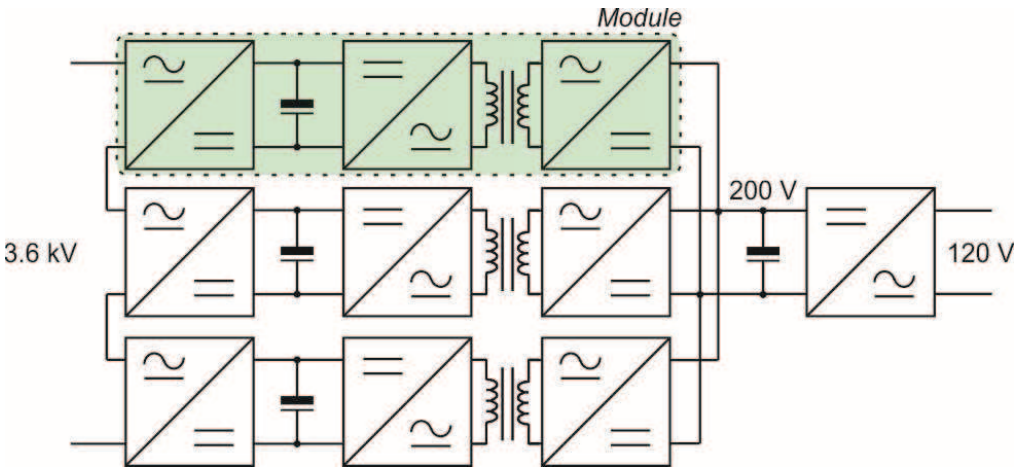


Figure 13. SST by FREEDM, North Carolina State University.

III.4 FREEDM (2015)

A second proposal of FREEDM consist on not modular three stage topology with a NPC converter in the MV side, a thre-phase-NPC-DAB in the dc-dc stage and three phase inverter in the LVAC side. The prototype employed 10 kV SiC Mosfets, a 10 kHz high frequency transformer and input and output voltages of 13.8kV and 470 V respectively [38]. The theoretical efficiency was 96.75% and the measured one 94% at 5% of load. Fig. 14 shows the employed topology.

ISBN 978-84-617–9183–5

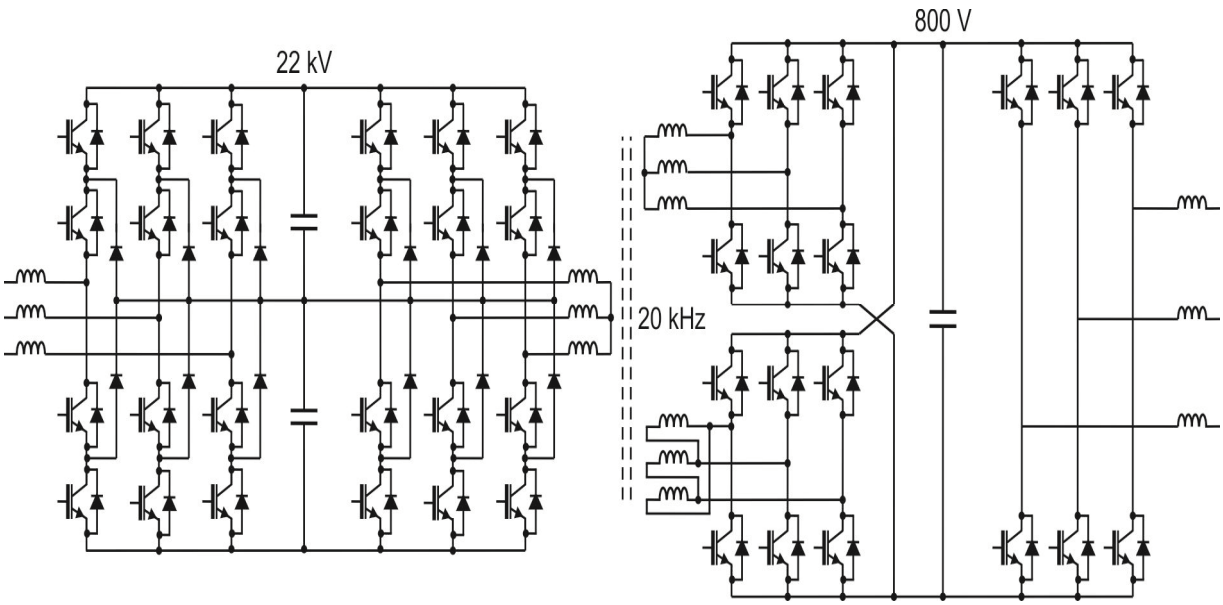


Figure 14. Not modular SST by FREEDM, North Carolina State University.

III.5 HUANG/FREEDM (2015)

A simpler structure is employed in a new prototype by FREEDM [39], again based on a three-stage topology, 13 kV SiC Mosfets allowed two H bridges to be employed in combination with a dual active bridge. The prototype was three-phase, with 3.6 kV input voltage and 120/240 V output voltages. The LVDC voltage was 400 V, the nominal frequency of the isolation transformer was 15 kHz. The maximum efficiency of the prototype was 94.59% at 40% of load. The employed topology is shown in Fig. 15.

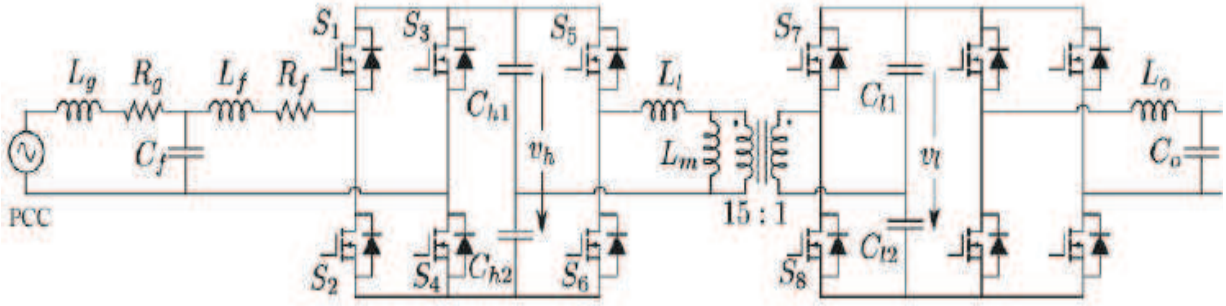


Figure 15. Simple Not SST by FREEDM, North Carolina State University.

III.6 UNIFLEX (2009)

The concept explored with UNIFLEX [40] consists of a modular multiport 5MVA SST to improve the power management with focus on distribution grids. The prototype exhibits 3 ports and cascaded H bridges are employed at both MV and LV sides, allowing the direct connection of distributed storage systems, as it is depicted in Fig. 16. The prototype was a three phase one rated at 300 kVA, with 2 kHz isolation transformers, and input and output voltages of 3.3 kV and 415 V respectively. The theoretical efficiency is 94.7%.

ISBN 978-84-617–9183–5

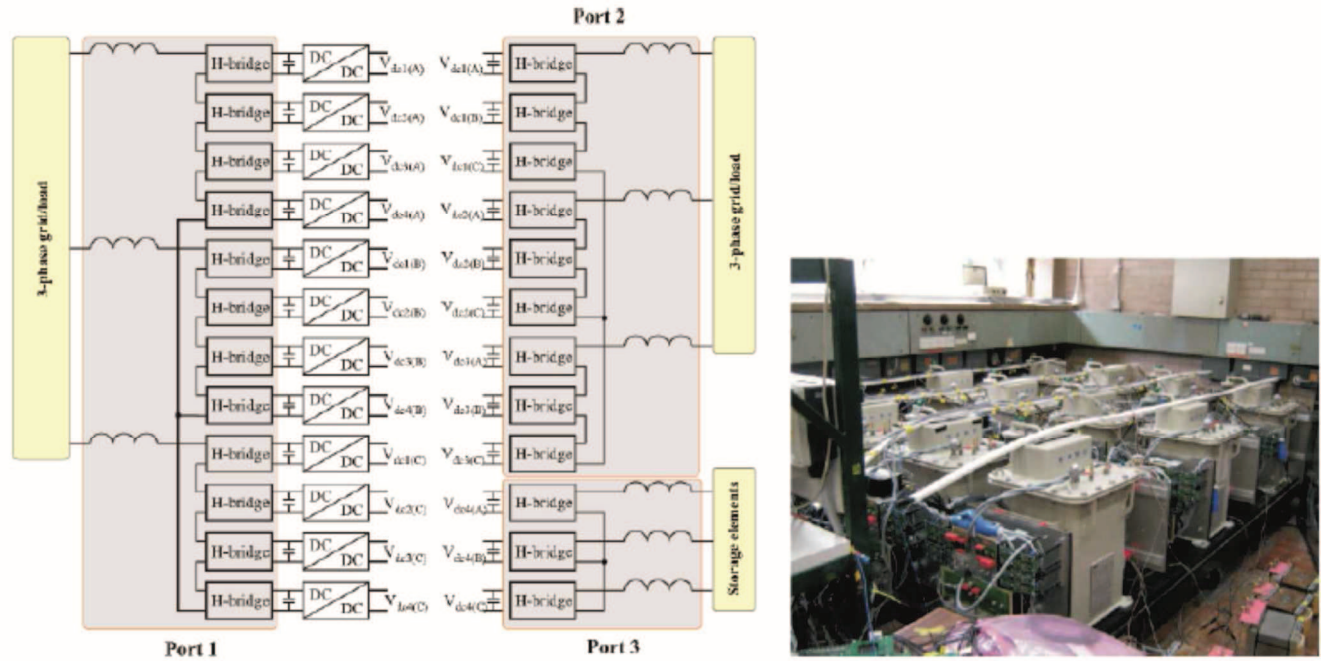


Figure 16. Multiport SST concept in UNIFLEX [40].

III.7 ETHZ MEGALINK SST

The ETHZ SST prototype [23], known as MEGAlink SST, has a rated power of 1 MVA and it is based on a three-stage topology: cascaded H bridges at the MV side with 1700 V IGBTs, DAB as DC-DC converter and the parallelized outputs are applied to two parallelized 500 kVA three phase inverters feeding the LVAC side. The LVDC is rated at 800 V and it is accessible. The employed topology is shown in Fig. 17 and provides power flow control, reactive power compensation and fault current limiting.

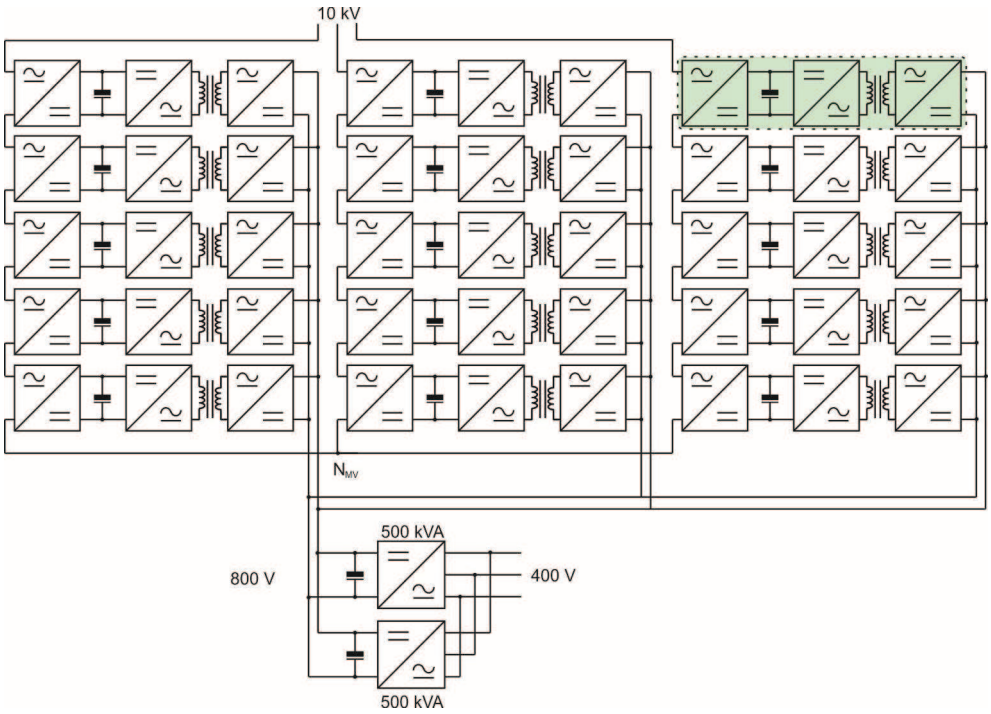


Figure 17. ETH MEGAlink.

ISBN 978-84-617–9183–5

III.8 GE (2009)

The SST proposal by GE [41] is based on IMCs with series cascaded connection at the MV side and parallelized outputs at the LV side. No MVDC or LVDC are accessible. The 1 MVA three phase prototype shown in Fig. 18 has been implemented by means of 10 kV SiC Mosfets [42] and consists of 12 modules with 3 groups of 4 modules connected in series, with isolation high frequency transformers operating at 20 kHz. The input voltage is 13.8 kV and the LVAC voltage is 415 V. The theoretical efficiency is 97%.

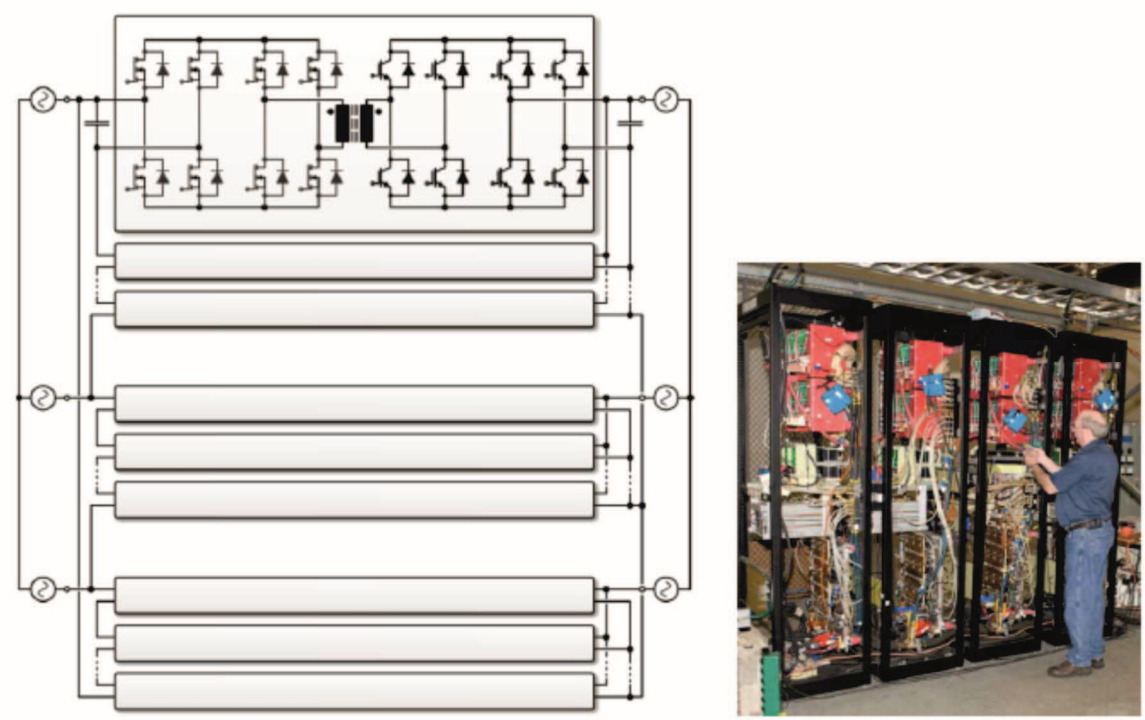


Figure 18. SST prototype by GE [41],[42].

III.9 SST Prototypes Comparison [34]

The main characteristics of the SST prototypes are compared in Fig. 19. As it can be seen, the efficiency does not only depend on the number of employed stages and SiC based converters achieves a higher efficiency with higher isolation transformer frequency.

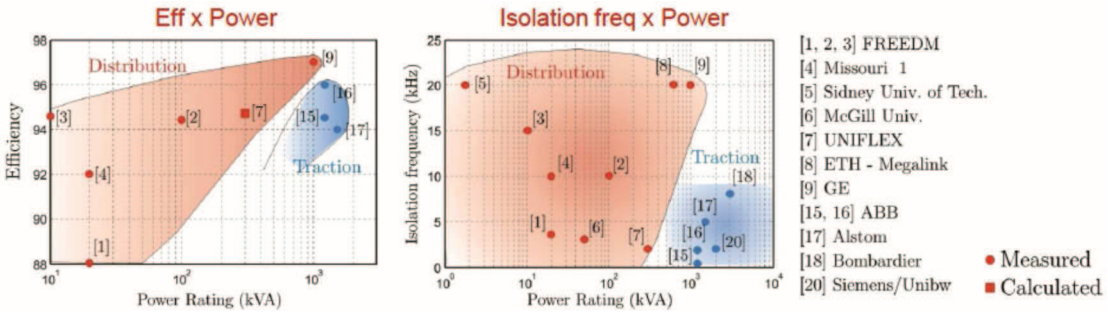


Figure 19. Comparison of SST characteristics: efficiency vs rated power and isolation frequency vs rated power [34].

IV. The Smart Transformer

The SST functionalities described in previous sections together with the need for control and communication functions make this device a smart SST or an ST. Hence, an ST is a SST behaving as a power system management node, linking diverse AC or DC infrastructures and other energy sources and supporting the infrastructures needed for the smart distribution grid deployment. The ST approach in the project HEART is based on three stage architectures with a modular or semi-modular architecture, behaving as a fault tolerant

ISBN 978-84-617–9183–5

system due to the redundancy and reconfiguration capability and allowing different power flow paths so the ST will continue working even with faulty path. It is also desirable voltage and power scalability. The power routing will take into account the aging of the modules to avoid the older ones to be stressed. The proposed ST, as it is depicted in Fig. 20, is based on quadruple active bridges (QAB) [43].

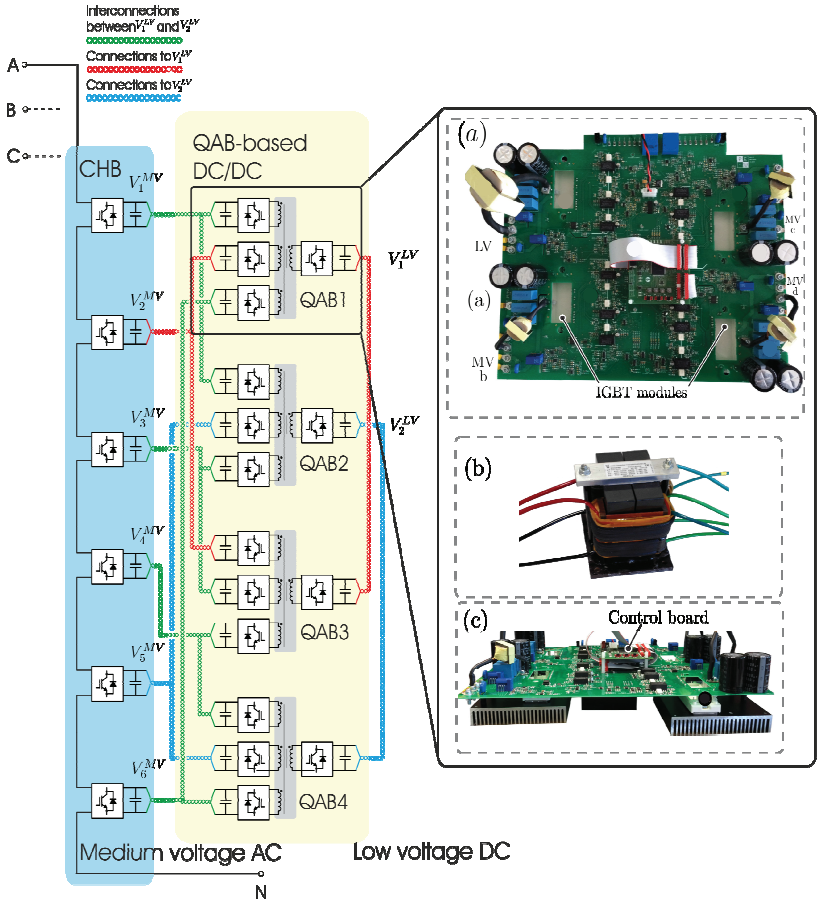


Figure 20. ST topology proposed by CAU-Kiel and QAB for DC-DC conversion [34], (a) QAB Prototype, (b) high frequency transformer, (c) front view of the prototype.

Fig. 21 shows the availability of DC links on both sides of the DC-DC converter, which allows renewable DC sources to be directly integrated without intermediate power electronics interfaces, and the system modularity would allow to operate even with faulty modules or the disconnection of certain modules under partial loading to increase the system efficiency. The DC links can integrate distributed storage systems for load peak saving, smoothing the energy demand.

The ST can regulate the LV AC voltage allowing the integration of LV distributed energy resources and balance the voltage due to single phase generation units (Fig. 22).

The presence of distributed generation sources increases the current during short circuits and breakers could not open the circuit cue to the high current, the ST can lower the voltage in order to reduce the overall fault contribution (Fig. 23).

The electrical power quality (PQ) in distribution grids cannot be ensured by conventional transformers and a limited amount of renewables and non-linear loads can be connected without deterioration of the PQ. The ST can manage the power quality so to increase the amount of connected load and renewables. The ST can also keep the LV AC grid PQ within the limits in the case of occurrence of MV voltage variations, acting like an active power filter at the LV side (Fig. 24).

ISBN 978-84-617–9183–5

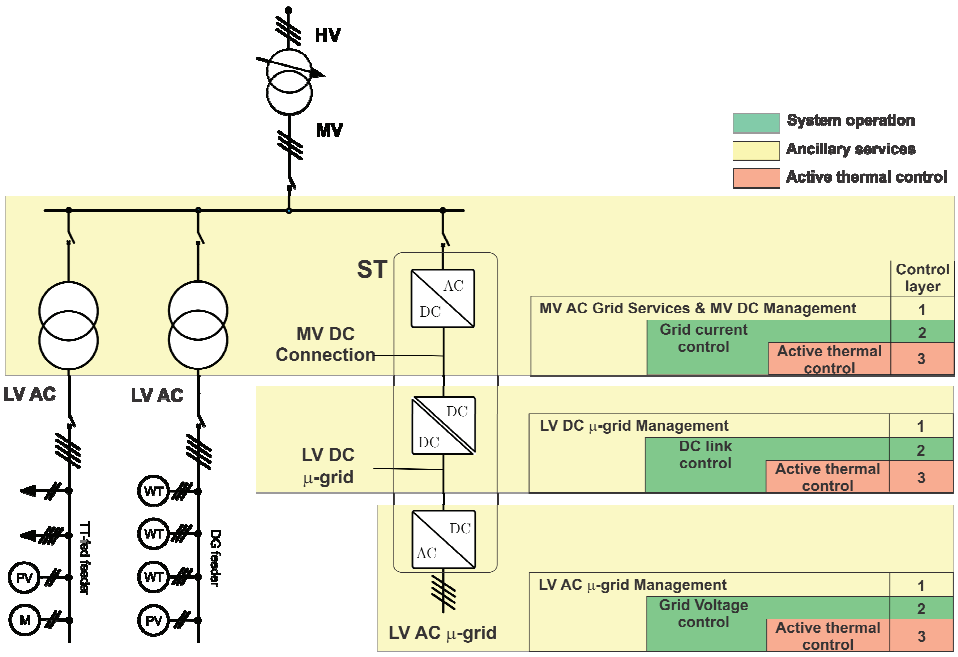


Figure 21. ST flexibility for MVDC, LVDC and LVAC services [34].

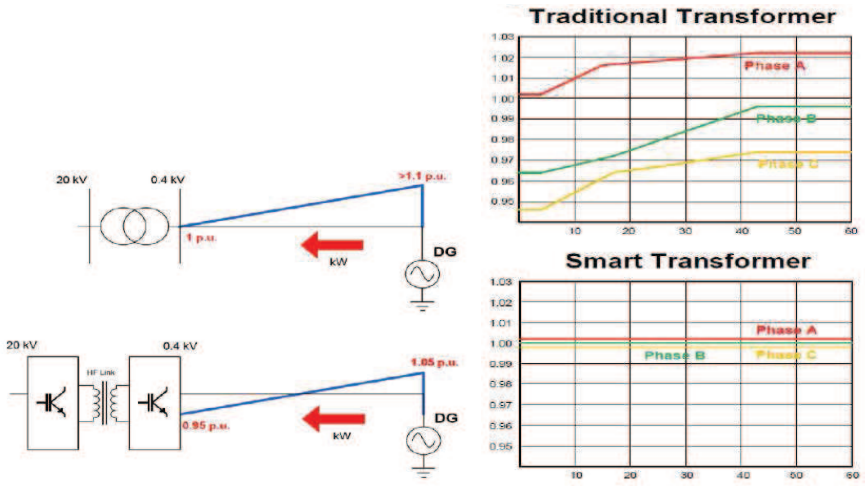


Figure 22. LVAC regulation through the ST [34].

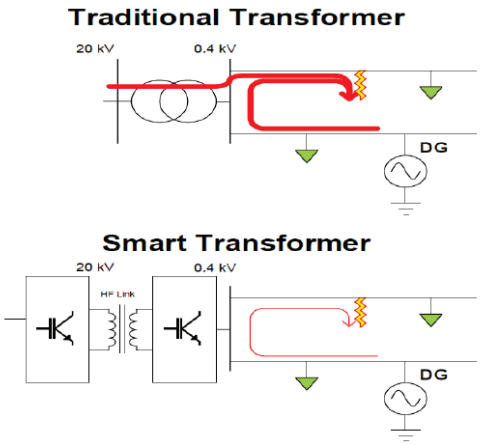


Figure 23. LVAC Fault current limiting through ST [34].

ISBN 978-84-617–9183–5

The main characteristics of the Smart Transformer in comparison to the conventional ones are summarized in Table II. The actual challenges of the ST are the life cycle, the efficiency and cost. It must be considered that the ST provides additional functionalities such as power quality enhancement ones (e.g. compensations of voltage dips, reactive power, load balancing) and replaces distributed FACTs.

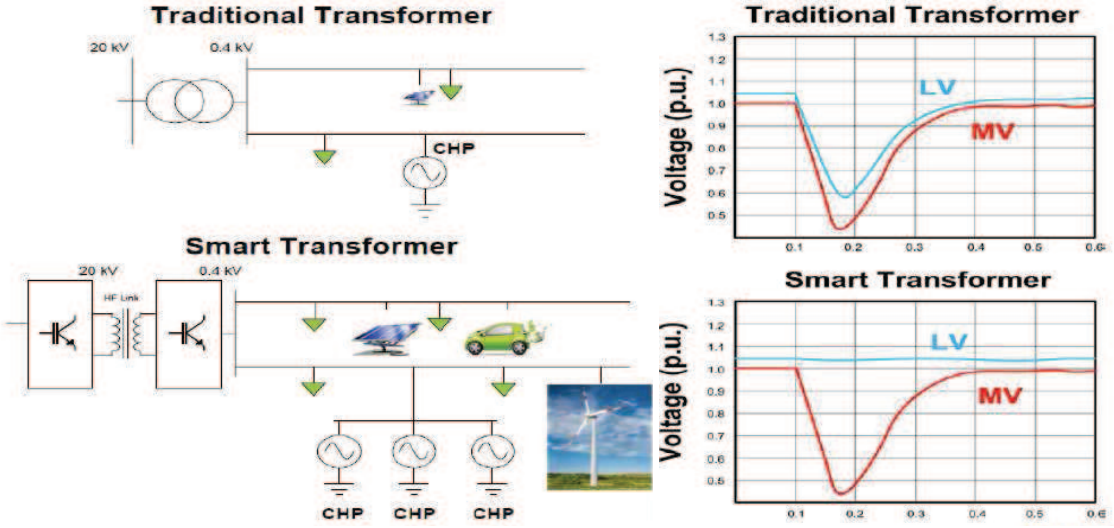


Figure 24. ST allowing generation and load integration at LV with PQ functionalities [34].

Table II. Comparison of Conventional Transformer and ST Characteristics/Functionalities [34].

Factor	TRADITIONAL TRANSFORMER	ST
Life cycle	Higher	Lower
Efficiency	Higher	Lower
Cost (incl. maintenance)	Lower	Higher
Volume/weight	Higher	Lower
DC-connectivity	No	Yes
Power Quality	Lower	Higher
Fault Management	No	Yes
Optimal energy management	No	Yes
Flexibility	Lower	Higher

V. CONCLUSIONS

The increasing penetration of distributed energy resources, both generation and storage, and new electric loads, e.g. electric vehicle chargers, makes more difficult voltage regulation and power quality improvement in LV AC grids. The Smart Transformer (ST) can address this issues but there are challenges to be solved, e.g. life cycle, efficiency and cost, prior conventional distribution transformer can be replaced by STs. This manuscript provides an overview of ST topologies, technologies and functionalities, reviewing currently available prototypes.

REFERENCES

[1] B. Olek and M. Wierzbowski, *Local Energy Balancing and Ancillary Services in Low-Voltage Networks With Distributed Generation, Energy Storage, and Active Loads*, IEEE Transactions on Industrial Electronics, Vol. 62, no. 4, p.2499-2508, April 2015.

[2] J. Hu, S. You, M. Lind and J. Ostergaard, *Coordinated Charging of Electric Vehicles for Congestion Prevention in the Distribution Grid*, IEEE Transactions on Smart Grid, Vol. 5, No. 2, p. 703-711, March 2014.

ISBN 978-84-617–9183–5

[3] R. Brundlinger, T. Strasser, G. Lauss, A. Hoke, S. Chakraborty, G. Martin, B. Kroposki, J. Johnson and E. de Jong, *Lab Tests: Verifying That Smart Grid Power Converters Are Truly Smart*, IEEE Power and Energy Magazine, Vol. 13, No. 2, p. 30-42, March 2015.

[4] H. Ghoddami and A. Yazdani, *A Mitigation Strategy for Temporary Overvoltages Caused by Grid-Connected Photovoltaic Systems*, IEEE Transactions on Energy Conversion, Vol. 30, No. 2, p. 413-420, June 2015.

[5] F. Blaabjerg, Y. Yang and K. Ma, *Power Electronics - Key Technology for Renewable Energy Systems - Status and Future*, in Proc. of the 3rd International Conference on Electric Power and Energy Conversion Systems, p.1-6, October 2013.

[6] B.-I. Cracium, T. Kerekes, D. Sera and R. Teodorescu, *Frequency Support Functions in Large PV Power Plants With Active Power Reserves*, IEEE Journal of Emerging and Selected Topics in Power Electronics, Vol. 2, No. 4, p. 849-858, December 2014.

[7] R. Teodorescu, M. Liserre and P. Rodríguez, *Grid Converters for Photovoltaic and Wind Power Systems*, Wiley 2011, ISBN: 978-0-470-05751-3.

[8] *Rule 21 Smart Inverter Working Group Technical Reference Materials*, available at http://www.energy.ca.gov/electricity_analysis/rule21/.

[9] Real Decreto 900/2015, de 9 de octubre, *por el que se regulan las condiciones administrativas, técnicas y económicas de las modalidades de suministro de energía eléctrica con autoconsumo y de producción con autoconsumo*. BOE, No. 243, p. 94874-94917. October 10th, 2015. Available at https://www.boe.es/boe/dias/2015/10/10/pdfs/BOE-A-2015-10927.pdf

[10] *UL 1741 Standard for Inverters, Converters, Controllers and Interconnection System Equipment for use with Distributed Energy Resources*, January 2010.

[11] *IEEE 929-2000 Recommended Practice for Utility Interface of Photovoltaic (PV) Systems.*

[12] *IEEE 1547 Standard for Interconnecting Distributed Resources with Electric Power Systems.*

[13] *IEC 61727 Photovoltaic systems – Characteristics of the utility interface*

[14] *IEC 62116 Utility-interconnected photovoltaic inverters – Test procedure of islanding prevention measures*

[15] *IEEE 2030 Smart Grid Interoperability Series of Standards.*

[16] *IEEE 1815 Standard for Electric Power Systems Communications- Distributed Network Protocol (DNP3).*

[17] *IEC 61850 Series on Power Utility Automation.*

[18] *RedACTIVA: Innovación en la Automatización de la Red de Distribución de Neutro Aislado*, available athttp://www.unionfenosadistribucion.com/es/redes+inteligentes/investigacion+y+desarrollo/nacionales/1297303835189/redactiva.html

[19] Kiel University ERC Consolidator Grant Project HEART. (2014–2018). *The highly efficient and reliable smart transformer*. Available at http://www.heart.tf.uni-kiel.de/

[20] M. Liserre, G. Buticchi, M. Andresen, G. de Carne, L. Ferreira-Costa and Z.-X. Zou, *The Smart Transformer. Impact on the Electric Grid and Technology Challenges*, IEEE Industrial Electronics Magazine, Vol. 10, No. 2, p. 46-58, June 2016.

ISBN 978-84-617–9183–5

[21] M. von Dolivo-Dobrovolsky, *Electrical induction apparatus or transformer*, U.S. Patent US 422746, 1890.

[22] G. Hipski, R. Schmid, R. Maier, K. Handt and G. Buchgraber, *Distribution Transformers – ready for the smart grid*, 21st International Conference on Electricity Distribution, CIRED, June 2011.

[23] J. W. Kolar and J. E. Huber, *Solid-State Transformers: key design challenges, applicability, and future concepts*. Tutorial No. 9. Tutorial at the 8th International Power Electronics and Motion Control Conference, 2016. Available at https://www.pes.ee.ethz.ch/uploads/tx_ethpublications/ECCE_Asia_2016_kolar_huber_Solid-State_Transformer_Tutorial_WEBSITE.pdf

[24] E. McMurray, *Power converter circuits having a high frequency link*, U.S. Patent US3517300, 1968.

[25] J. L. Brooks, R. I. Staab, J. C. Bowers and H. A. Nienhaus, *Solid state regulated transformer with waveform conditioning capability*, U.S. Patent US4347474, 1982.

[26] X. She, *Control and Design of a High Voltage Solid State Transformer and its Integration with Renewable Energy Sources and Microgrid System*, Ph.D. Dissertation, North Carolina State University, 2013.

[27] L. Heinemann, *An actively cooled high power, high frequency transformer with high insulation capability*, 7th Annual IEEE Applied Power Electronics Conference and Exposition, 2002, pp. 352-357.

[28] H. Hoffmann and B. Piepenbreier, *Medium frequency transformer for rail application using new materials*, 1st International Conference on Electric Drives Production, 2011, pp. 192-197.

[29] S. Prabhakaran, C. Stephens, F. Johnson, and L. Lorio, *High frequency power transformers for future military propulsion and energy systems*, Electron. Machine technology symposium, 2008.

[30] M. Steiner and H. Reinold, *Medium frequency topology in railway applications*, 2007 European Conference on Power Electronics and Applications, pp. 1-10.

[31] S. Baek, Y. Du, G. Wang, and S. Bhattacharya, *Design Considerations of High Voltage and High Frequency Transformer for Solid State Transformer Application*, IEEE IECON, 2010, no. 2, pp. 421–426.

[32] G. Ortiz, M. Leibl, J. W. Kolar and O. Apeldoorn, *Medium frequency Transformers for solid-state-transformer applications – design and experimental verification*, 10th International Conference on Power Electronics and Drive Systems, 2013, pp. 1285-1290.

[33] STS Induktivitaeten website, available at http://www.sts-trafo.com/MF-Transformer-for-Traction.338+M52087573ab0.0.html.

[34] M. Liserre, *Smart Transformer: reliability through modularity*, available at http://files.portal.aau.dk/filesharing/download/person/caj@et/aau/dk/~/pub/Smart%20Transformer%20reliability%20through%20modularity.pdf

[35] N. Hugo, P. Stefanutti, M. Pellerin and A. Akdag, *Power electronics traction transformer*, 2007 European Conference on Power Electronics and Applications, pp. 1-10.

[36] C. Zhao, S. Lewdeni-Schmid, J. K. Steinke, M. Weiss, T. Chaudhuri, M. Pellerin, J. Duron and P. Stefanutti, *Design, implementation and performance of a modular power electronic transformer (PET) for railway application*, 14th European Conf. on Power Electronics and Applications, 2011.

ISBN 978-84-617–9183–5

[37] D. Dujić, F. Kieferndorf and F. Canales, *Power Electronic Transformer Technology for Traction Applications – An Overview*, Electronics, vol. 16, no. 1, June 2012, pp. 50-56.

[38] K. Mainali, A. Tripathi, S. Madhusoodhanan, A. Kadavelugu, D. Patel, S. Hazra, K. Hatua, S. Bhattacharya, *A Transformerless Intelligent Power Substation: A three-phase SST enabled by a 15-kV SiC IGBT*, IEEE Power Electronics Magazine, vol. 2, no. 3, 2015. pp. 31-43.

[39] F. Wang, G. Wang, A. Huang, W. Yu, and X. Ni, *Design and operation of a 3.6 kV high performance solid state transformer based on 13 kV SiC MOSFET and JBS diode*, IEEE Energy Conversion Congress and Exposition 2014, pp. 4553–4560.

[40] UNIFLEX. (2013). UNIFLEX Project. Available at http://www.eee.nott.ac.uk/uniflex/Project.htm

[41] R. Raju, *Silicon Carbide High Voltage, High Frequency Conversion*, 2014 NIST High Megawatt Variable Speed Drive Technology Workshop. Available at http://www.nist.gov/pml/high_megawatt/upload/Approved-Raju-oE_NIST_HMW_VSD_GE_raju.pdf

[42] M. K. Das, C. Capell, D. E. Grider, S. Leslie, J. Ostop, R. Raju, M. Schutten, J. Nasadoski, A. Hefner, *10 kV, 120 A SiC Half H-Bridge Power MOSFET Modules Suitable for High Frequency, Medium Voltage Applications*, 2011 IEEE Energy Conversion Congress and Exposition, pp. 2689-2692.

[43] L. F. Costa, G. Buticchi and M. Liserre, *Quadruple Active Bridge DC-DC converter as the basic cell of a modular Smart Transformer*, 2016 IEEE Applied Power Electronics Conference and Exposition, pp. 2449 - 2456

ISBN 978-84-617–9183–5

Power Voltage Transformers. Applications and Particularities

Adolfo IBERO[(1)], Javier GARCIA[(1)] , Xose M. LOPEZ-FERNANDEZ[(2)] and Hugo RODRIGUEZ-IGNACIO[(2)]

[(1)] High Voltage Instruments Transformers Department, ARTECHE
Derio Bidea 28, 48100 Mungia, Spain
Phone: (+34) 946011200, fax: (+34) 946740958, e-mail: ai@arteche.es, jrg@arteche.es

[(2)] Department of Electrical Engineering, University of Vigo
Campus Lagoas-Marcosende, E 36310 Vigo, Spain
Phone: (+34) 813478, fax: (+34) 814014, e-mail: xmlopez@uvigo.es

Abstract — **In this paper the applications and particularities of the Power Voltage Transformers (PVTs) used for direct conversion of power from high to low voltage are discussed. PVTs are a power source that effectively supply to auxiliary services in substations or serving as the main transformer in a compact substation for isolated loads. Therefore, state of PVTs technology that covers the international standards and some design and testing aspects are presented. Finally, the technical features for both oil and SF_6 insulated PVT models are addressed.**

Keywords — **Power Voltage Transformer, Station Auxiliary Services, Isolated Loads, Rural Electrification.**

I. INTRODUCTION

Voltage transformer (VT) is a type of instrument transformer which has been used in substations over the last century for stepping down the system voltage to a safe value that can be fed to low ratings meters and relays [1]. A design of VT with higher kVA ratings as shown in Fig. 1, named PVT, has become an alternative to power transformers or low voltage grids for the feeding the auxiliary services in substations. An extension of PVT with more kVA ratings is also being installed to feed isolated loads due its inherent advantages of simplicity, low maintenance, compactness and low costs. These isolated loads comprise oil and gas pumping stations, mining and defense installations, cell phone towers, hospitals and railroad substations. This approach eliminates the necessity for rather complex and expensive protection and monitoring systems and by default assumes a long-term, maintenance-free operation. Recently, the PVT is being designed with much higher kVA without reaching the capacity of a power transformer, with the purpose to serve as a mini-substation, stepping down the power supply directly from the high voltage transmission line to low voltage or medium voltage output in one step. It enables providing power source to even larger isolated applications as small residential areas where there are no distribution lines and to install a traditional substation or build a grid is not competitive. PVTs can be used as a single-phase transformer either as an individual unit for supplying single-phase loads, or in a three-phase bank to support larger kVA three-phase loads as shown in Fig. 2.



Figure 1. Arteche's PVTs. Paper-oil insulated PVT (left and middle), gas insulated PVT (right).

ISBN 978-84-617–9183–5

Therefore, in this paper the benefits of this equipment and the current status of the technology, international standards and certain considerations that should be taken into account regarding its specification, design, testing and integration with the rest of the switchgear equipment that can be found in a typical substation are shown.



Figure 2. HV line-to-ground connected single-phase (left) and three-phase (right) PVT.

II. BACKGROUND

Alternatives historically used when it was necessary to feed small or isolated loads were, in general, diesel generators, distribution networks and power transformer tertiary windings. The use of a diesel generator is a fast selection due to the fact that the installation of the equipment is cheap and easy, but on the other hand the running cost is high and its reliability is low. Moreover, it demands more maintenance and adds carbon footprint and noise pollution. Distribution network is feasible when the infrastructure previously exists or when the distribution network is going to feed a certain amount of loads which justify the investment. When the distribution network is designed to feed a small load, like the auxiliary services in a substation, the installation costs makes this option expensive and non-competitive in several cases. Another solution used in substations to feed the auxiliary services is the use of the tertiary winding of a power transformer. This is effective and cheap if the transformer already exists but it hampers the design of main power transformer as well as reduces its reliability by the fact of adding one more winding. In addition a second step-down transformer may be required for low voltage. Overmore, the utilities cannot be operated if the transformer is de-energized. PVTs were conceived more than 30 years ago as a reliable and convenient mean for taking power off the HV bus and so to meet the requirements of power supply within electrical substations [2]. Nowadays, PVTs are applicable for providing power supply to the substation and the isolated loads when a transmission line is not accessible or the investment on a complete substation is not justified [3]. PVTs may also provide the electricity required for the construction of a substation and so eliminates the need to obtain long-term power from an outside supplier. Once the substation is concluded, the PVT can be used as an auxiliary power supply, or be easily moved to another location. Also, during emergency situations as natural disasters, mounting PVTs in containers or trucks allow for mobile power supplies. Those can be easily and rapidly deployed and put into service where are more needed. In case of a failure of the distribution transformer or a need to de-energize the power transformer, a PVT could operate as secondary power supply as it is directly connected to the HV line. This would eliminate the need for a diesel generator. It can also be used as a primary power source in switching substations without power transformers to supply the substation and SCADA control systems.

At the design stage, the electric field stress control is a key enabler to guarantee the long-term dielectric integrity of the transformer. In the bushing, at high voltage electrode, this is done using conductive foils, typically aluminum or copper, whose lengths and diameters at which they are positioned are such as to create a more uniform radial-voltage distribution [4]. Fig. 3 shows the equipotential lines in an oil-filled bushing.

ISBN 978-84-617–9183–5

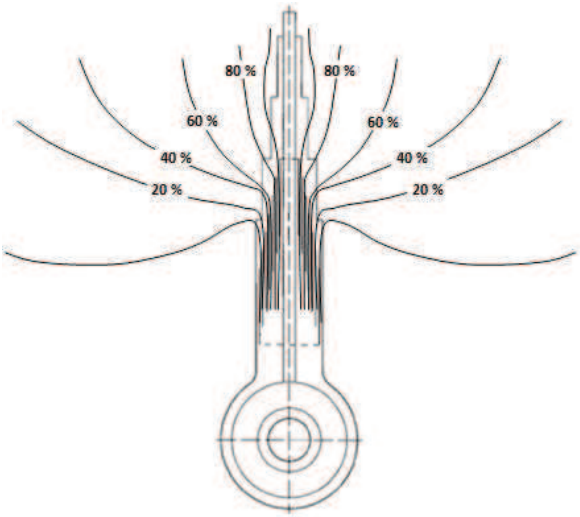


Figure. 3 Electric field stress control at high voltage electrode.

In the literature, there are a few published works related with PVTs since their principle of operation and design is very similar to existing inductive voltage transformer and this technology is in hands of manufacturers. Indeed, the fact that PVTs are derived from instrument transformers make them "install-and-forget" equipment and enhances them with all their features and developments such as extremely high reliability, being maintenance-free, explosion safety designs, etc. Most of the manufacturers base their designs in the *closed-core* type one from inductive voltage transformers but, in [5, 6] are presented the properties and advantages of the *open-core* design concept, available only for paper-oil insulated PVTs. Studies on the PVT performance or behavior with regard to voltage quality, stability, and capacity constraints are shown in [7] where it is compared the PVT penetration on a transmission network with the constructed Surge Impedance Loading curves. The technical features and parameters for both oil and SF6 insulated PVT as well as different kinds of substation applications from using PVT as a power source are described in [8]. This paper also presents an alternative power source in various kinds of substation applications. Reference cases for such applications in Uruguay and DR Congo are shown as good examples on how the rural electrification concept using PVTs can be implemented as alternative power source which provide benefits and support how to use power grid smartly and efficiently. Fig. 4 depicts the rural electrification concept, which consists in applying the PVT to serve as a mini-substation, stepping down the power supply directly from the high voltage transmission line to low voltage output in one step to provide power source to small residential areas without the large investment. A business case, as well as a real project, is presented and described in [2] to illustrate the application of the PVT as a power source to more effectively enable the people living in small African villages to access electricity. Recently, the installation of a unique substation that uses as a main source of power a 123 kV – 100 kVA PVT to provide energy to the town of Tubares, Mexico at a total cost of one third compared to a traditional substation is described in [9].



Figure 4. Rural electrification concept using PVTs.

ISBN 978-84-617–9183–5

In this paper, the authors highlight the benefits and the applications of the PVT, as well as design aspects of both paper-oil and gas insulated PVTs. International standards and certain considerations that should be taken into account regarding its specification are shown too.

III. POWER VOLTAGE TRANSFORMERS (PVTS) DESIGN

PVT provides reliable power from any high voltage transmission giving the user the full control of the energy supply directly from the constantly available transmission grid. PVTs design is close to an inductive voltage transformer to satisfy the dielectric requirement, coupled to a larger core similar to that used in distribution transformers. Using advanced materials and design, a fully rated compact dielectric design is developed (Fig. 5). Such design is very akin between all kinds of PVTs despite there are different characteristics between them. PVTs are developed in both the oil and SF_6 insulated format. In the following subsections the oil and SF_6 insulated PVTs models are introduced.

1. Primary terminal
2. Pressure relief device
3. High-voltage electrode
4. Insulation (porcelain or silicone)
5. Low-voltage electrode
6. Manometer
7. Primary windings
8. Secondary windings
9. Core
10. Secondary terminals box
11. Filling valve

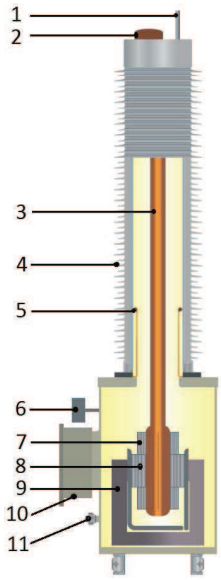


Figure 5. Arteche's UG type (up to 550 kV) cross section, showing the main components.

III.1 OIL INSULATED POWER VOLTAGE TRANSFORMERS (PVTS)

For low power applications, the internal design of this kind of transformers is almost identical to the internal design of a voltage instrument transformer. A schema of this transformer is shown in Fig. 6. Its main components are the core inside a metallic tank, the primary winding, the secondary winding and the paper-oil insulation. The core is of the stepped type, in order to have the maximum cross-section. It is made of grain-oriented silicon steel with low losses to limit the no-load losses and the temperature rise. Around the core is the secondary winding, made of enameled copper strip, and around it the primary winding is placed to reduce the leakage inductance. The primary winding is made of enameled copper wire, and is a "non-resonant" type, where the layers of coils adopt a trapezoidal shape in order to optimize the voltage distribution in the coil for both power-frequency and transient voltages. Between the layers of coils, an oil impregnated paper is used as insulation and between windings and core there is an insulating cylinder. Around the active part, oil impregnated paper is used to isolate the HV from the earth voltage. High electrical stresses outside the insulation can develop tracking on its surface while inside the paper-oil insulation it can lead to premature ageing of the transformer insulation. Dielectric strength of paper-oil insulation is influenced by the amount of dissolved air and other gasses. Arteche's PVTs are hermetically sealed to avoid any air ingress. Oil compensation is accomplished using metallic bellows with oil level indication.

ISBN 978-84-617–9183–5

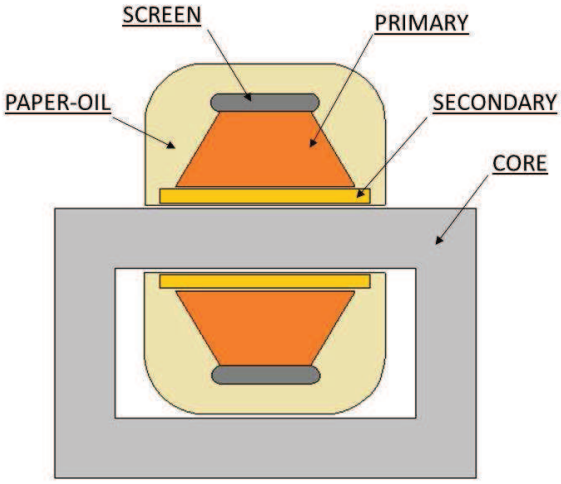


Figure 6. Oil immersed PVT.

The oil immersed PVT is a suitable solution to be used when the voltage and the load is equal to or below 245 kV and 10-15 kVA, respectively. The simplicity of the design provides this kind of transformer a long and maintenance-free life. When the load is higher than 20 kVA per phase, a possible alternative can be the Arteche's UTP type (Fig. 7). UTPs cover the range of 50 to 333 kVA and from 100kV to 362 kV. The design of an UTP is an especial version of the traditional instrument transformer but it has several differences in order to improve the heat evacuation generated in the transformer. UTPs are designed to be directly connected to the high voltage line and to feed high burdens by the secondary winding. The coil used is a disk wound design and the internal insulation is less compact to be able to transmit more power meeting the standards.



Figure 7. Arteche's UTP type installed in a substation.

As the design of the PVT is related to the design of an instrument transformer, the most suitable standard is the one applicable to instrument transformers, which is the IEC61869-1 [10] for general requirements and the IEC61869-3 [11], for the specific requirement used in voltage transformers. Following the IEC61869-3 standard, the maximum power of an instrument transformer is defined by the concept "thermal limiting output".

ISBN 978-84-617–9183–5

The thermal limiting output is the value of the apparent power at rated voltage which can be taken from a secondary winding without exceeding the limits of temperature rise. In order to be included in the IEC61869, the secondary windings must comply with an accuracy class. Because of that, the secondary windings used in the PVTs must be defined with a specific accuracy class. The temperature rise of windings, magnetic circuits and any other part of instrument transformers shall not exceed the appropriate value, which varies between 50 and 65 K for oil immersed instrument transformers. The heat generated inside the transformer is evacuated through natural convection to the atmosphere.

III.2 GAS INSULATED POWER VOLTAGE TRANSFORMERS (PVTS)

When the power required is higher than 20 kVA, gas insulated PVTs are the adequate choice (Fig. 8). Arteche's gas insulated PVTs portfolio covers the high voltage range up to 550 kV, with a maximum power of 100 kVA. The internal construction of this kind of transformer is alike to the internal construction of the oil immersed PVTs. It is built with its primary and secondary windings around a magnetic core inside a metallic tank. These windings are made of heat-resisting electric wires coated in synthetic resin and a layer of plastic with high dielectric strength and excellent thermal and mechanical performance. The SF_6 and the plastic layer form the electrical insulation. An input valve for SF_6 gas is provided on a side of tank together with a manometer for monitoring gas pressure and to allow the detection of potential leakages. The core is also of the stepped type and the secondary winding is made of enameled copper strip. The primary winding is around the secondary winding and a metallic shield is placed in the core to control the electric field. The main difference with the oil immersed PVT is that there is no oil impregnated paper to insulate the HV parts, so all the elements are immersed in SF_6 gas inside a pressurized vessel. The lack of paper and oil reduces the size and weight of the active part making this transformer format to feed bigger loads connected to higher voltage lines up to 550 kV compared to paper-oil insulated ones due to the amount of insulation required which forces for bigger equipments with large quantities of oil. With this design, the heat generated in the active part is transferred through the gas to the tank and from it to the atmosphere. The cross section of the gas-insulated PVT is shown schematically in the Fig. 9.



Figure 8. UGP transformer.

Gas insulated designs can be applied on both gas-insulated switchgears (GIS) and air-insulated switchgears (AIS). In the first case, they are directly connected as a standard voltage transformer, and in the second case a bushing with composite insulator is used to comply with the air side insulation requirements. Currently, there are single-phase units for both GIS and AIS, and three-phase units for GIS. It is worth mentioning that for the same total power, the single-phase units are more compact than the three-phase, and therefore this solution should be prioritized in GIS. In principle, both insulation technologies can achieve similar power ratings and it is up to the customer to choose among them. Being that true, it must be pointed out that for very small power, until 10-15 KVAs, oil immersed PVT is more compact and cost effective.

ISBN 978-84-617–9183–5

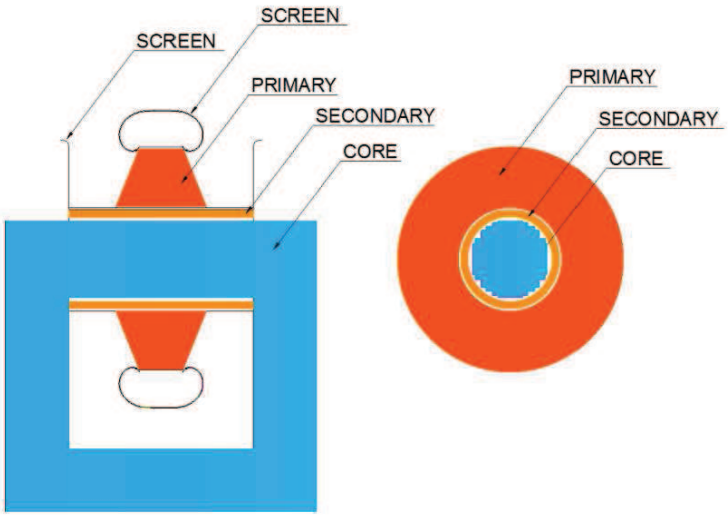


Figure 9. Gas insulated PVT.

IV. CONSIDERATIONS FOR SPECIFYING AND SELECTING POWER VOLTAGE TRANSFORMER (PVTS)

The specification of a PVT is not difficult but the lack of an international reference standard can arise some doubts when it comes to define which tests are the most adequated to ensure manufacturing quality. In the IEEE there is, currently, a working group (WGC57.13.8) which is developing a standard (*IEEE Standard Requirements for Station Service Voltage Transformers* [12]), while in the IEC there is no running project. According to the primary purpose of a PVT, which is power supply, the applicable standard could be IEC60076. But, if we analyse the design of this equipment, the IEC61869 for instrument transformers seems more adequated. The application of both standards simultaneously is undesirable, due to the huge differences between them, mostly of the testing part, with different procedures, requirements or in the consideration of a given test as type, routine or special test. For instance, let us focus on the dielectric test as they are the ones intended to guarantee the quality of the main insulation. If we compare to IEC61869, ACSD (IEC60076-3: 7.3 [13]) is quite similar to power-frequency voltage withstand tests on primary terminals and partial discharge measurement test (IEC61869: 7.3.1 and 7.3.2). Main differences are that partial discharge limits are significantly higher than the ones for instrument transformer: 100 *pC* on IEC60076 for 10 *pC* on IEC61869. Also, another difference worth noting is that lightning impulse (LI) test and switching impulse (SI) test are routine tests for power transformers. For instrument transformers they are type tests, but voltage levels are significantly higher. Apart from applicable standards and tests, an important point to bear in mind in this type of equipment is the circuit they will be part of, and protections required to guarantee a safe and reliable operation. An example of what could be a typical installation is depicted in the schematic shown in the Fig. 10. PVTs don't have a tap changer on the secondary side to compensate for voltage oscillations on the line or due to the loading degree of the burden. So, in the installation of the Fig. 10, a voltage stabilizer is used on the secondary side before the connection to auxiliary services cabinet. Regarding protection devices, the installation of the Fig. 10 consist of the following:

- MCB (89G) for protection against short-circuits in the secondary side.
- Voltage transformer (VT) to measure secondary voltage of the PVT, and together with the CT allows for energy measurements (kWh).
- Current transformer (CT) connected to an overcurrent relay (51) to protect against overloading.
- Breaker for manual disconnection of the transformer (mainly for maintenance purposes).
- Fuse (89-1) for additional short-circuit protection.

Also, other accessories, such as thermocouple sensors on the secondary windings to allow for real-time monitoring and overload control are feasible.

ISBN 978-84-617–9183–5

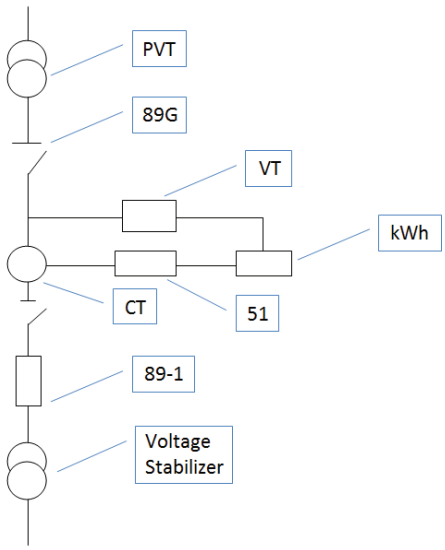


Figure 10. Typical equipment of an installation with a PVT.

V. CONCLUSIONS

Several kinds of substation applications with PVTs are presented in this paper. PVTs can be used to provide control/auxiliary power source in switching substation and in lieu of tertiary winding of power transformer as well as for remote substation, mining and emergency areas. In addition, PVTs can also be used to provide a very fail-safe alternative for providing the much needed increase in electrification rates in the developing countries. Their applicability for rural electrification is shown through several referenced examples of economically lightweight substation solutions. Another thought of the paper is that PVTs can be labeled as "*install-and-forget*" units which are proven to operate reliably in all conditions. Because of these advantages, the substation design can also be simplified and made more financially attractive. Therein lays the potential for a more widespread use of PVTs as primary units for power supply and distribution to remote areas in the vicinity of overhead power lines.

REFERENCES

[1] *Transformer: Analysis, Design and Measurements*, Editors: X. M. Lopez-Fernandez, H.B. Ertan and J. Turowski. CRC Press 2012.

[2] D. Xu, N. Powers and W. Sae-Kok, *Development of a Power Source for Rural Electrification*, IEEE Global Humanitarian Technology Conference (GHTC), 2015, p. 340-347, Oct. 2015.

[3] Arteche Catalogue, *Auxiliary Services Voltage Transformers. Oil-Paper and Gas Insulation*.

[4] *Electric Power Transformer Engineering*, Editor: J. H. Harlow, CRC Press 2004.

[5] I. Ziger, *Open-core Power Voltage Transformer. Concept, Properties, Application*, IEEE International Energy Conference (ENERGYCON), 2014, p. 246-253, May 2014.

[6] I. Ziger, *Power Voltage Transformers – Expanding Beyond Station Service*, IEEE Power & Energy Society General Meeting, p. 1-5, Jul. 2015.

[7] M. J. Saulo and C. T. Gaunt, *Implication of Using Auxiliary Service Voltage Transformer Sub-Stations for Rural Electrification*, International Journal of Energy and Power Engineering, Vol. 4, No. 2, p. 1-11, March 2015.

ISBN 978-84-617–9183–5

[8] D. Xu, N. S. Powers, M. Paul and W. Sae-Kok, *Alternative Power Source in Various Substation Applications*, IEEE Innovative Smart Grid Technologies – Asia (ISGT ASIA), 2015, p. 1-4, Nov. 2015.

[9] O.R. Calvo, R.G. Ibarra, A. Solano and E. Acosta, *Rural Electrification in Chihuahua, Mexico at One Third of the Cost vs a Conventional Substation*, World Energy Congress, Montreal, Canada, Sep. 2010.

[10] IEC 61869-1:2009, *Instrument Transformers – Part 1: General Requirements*.

[11] IEC 61869-3:2009, *Instrument Transformers – Part 3: Additional Requirements for Inductive Voltage Transformers*.

[12] IEEE PC57.13.8, *IEEE Standard Requirements for Station Service Voltage Transformers*, IEEE Engineering Society. Unpublished

[13] IEC 60076-3:2013, *Power Transformers – Part 3: Insulation Levels, Dielectric Tests and External Clearances in Air*.

ISBN 978-84-617–9183–5

Toroidal Transformer for Full-Wave Rectifier Cooperation - Design and Properties

Boguslaw GRZESIK, Mariusz STEPIEN

Department of Power Electronics, Electrical Drives and Robotics, The Silesian University of Technology
2 Boleslawa Krzywoustego str., 44-100 Gliwice, Poland
Phone: (+48) 322371247, fax: (+48) 322371304, e-mail: mariusz.stepien@polsl.pl

Abstract — **The paper is devoted to toroidal transformer dedicated for DC spot welding system. The transfomer is based on amorphous magnetic core with very high magnetic permeability, shaped as a toroid. Primary winding, classical one, is made of copper wire. The secondary is made of copper strips shaped in proper way. The secondary consists of two parts, each is separate winding with one common lead. Such arrangement is required for cooperation with full wave, two diode rectifier. Very high permeability of magnetic core and proper arrangement between windings results with high coupling ratio, which is required by supplying inverter. The transformer operates with high turn-to-turn ratio of 70:1 and the output current at the frequency of 10 kHz is about 9 kA. The output power and efficiency obtained by FEM calculations are 43 kW and 92%, respectively.**

Keywords — **DC spot welding, toroidal transformer, amorphous magnetic material.**

I. INTRODUCTION

Novel trends in power electronics are focused on more efficient and operating with higher energy density devices. The way to find devices fulfilling such requirements is increasing frequency of operation and usage of novel materials. Large group of devices considerably influencing on properties of electrical systems are transformers. Properties of transformers like higher energy density can be obtained by increasing of frequency, but higher efficiency requires more sophisticated approach. Use of new materials parallel with improvement of transformer construction can result with higher coupling ratio and small power losses. These two parameters influence on transformer efficiency.

The paper is focused on design and analysis of properties of power electronic transformer operating at 10 kHz. The transformer is current boosting transformer operating with full-wave rectifier at the system of DC spot welding. Structure of the system is shown in Fig. 1. The output current of the transformer is about 9 kA at the voltage of 5 V. Reported here results are a part of broad research focused on welding transformers [1]. The transformer is investigated in the paper basing on the numerical FEM analysis and laboratory experiments.

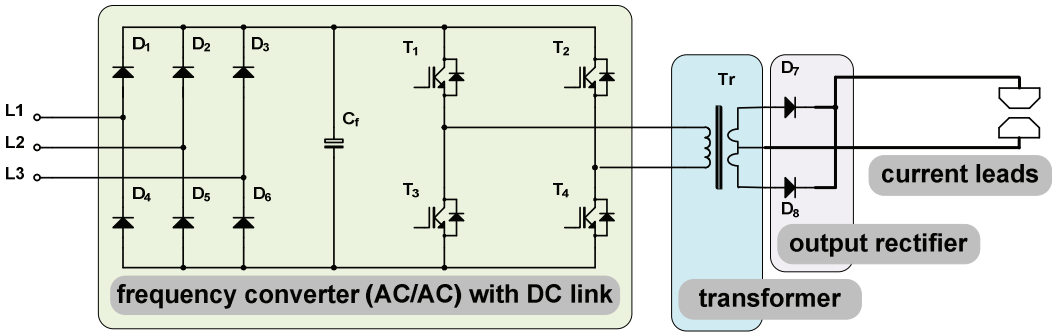


Figure 1. Scheme diagram of DC spot welding system with transformer and two diode rectifier.

Transformers are one of the most important elements in energy transmission and conversion. Welding systems require very high output current, so the transformer boosting current should be located possibly close to the electrodes [2]. Transformer should transfer energy with possible high density. Additionally the transformer is supplied by the bridge inverter with relative small duty ratio. It causes very high required coupling ratio. Some

ISBN 978-84-617–9183–5

works carried out shows that promising solution is a toroidal transformer [3]. Presented here results confirms this prediction.

II. IDEA OF THE TRANSFORMER

The transformer is based on well-known design of toroidal transformer. The main difference is the secondary winding which has two specific features. The first is single turn (all turns of secondary are connected in parallel) and the second one is that the secondary is divided in two parts, respectively to operation with full wave two diode rectifier. Model of the secondary windings which reflects also general shape of the transformer is shown in Fig. 2. One can observe three output clamps (middle clamp common for both secondaries).

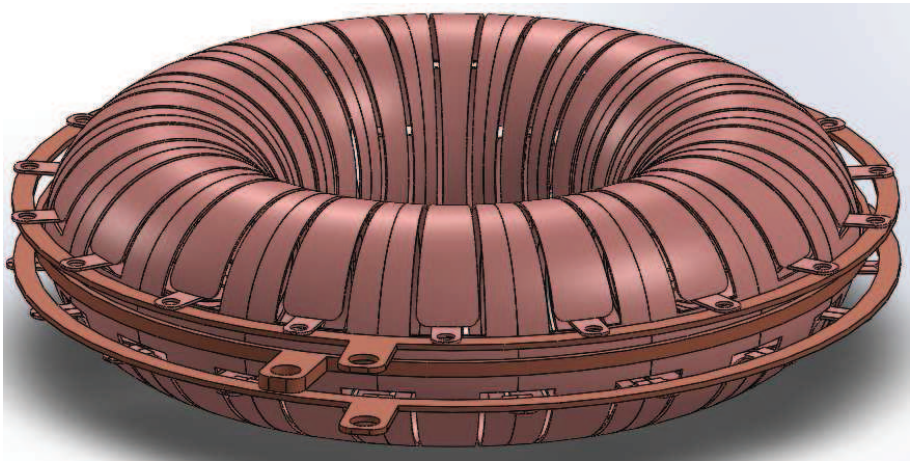


Figure 2. Model of the secondary winding in the toroidal transformer.

General dimensions of the transformer are shown in Fig. 3. The final turn-to-turn ratio of transformer is about 70:1. It reflects number of turns in the transformer. The primary is 70 turns wounded on the toroidal core and the secondary is single (parallel turn). Transformer operates at 10 kHz supplied by voltage inverter with rectangular voltage waveform.

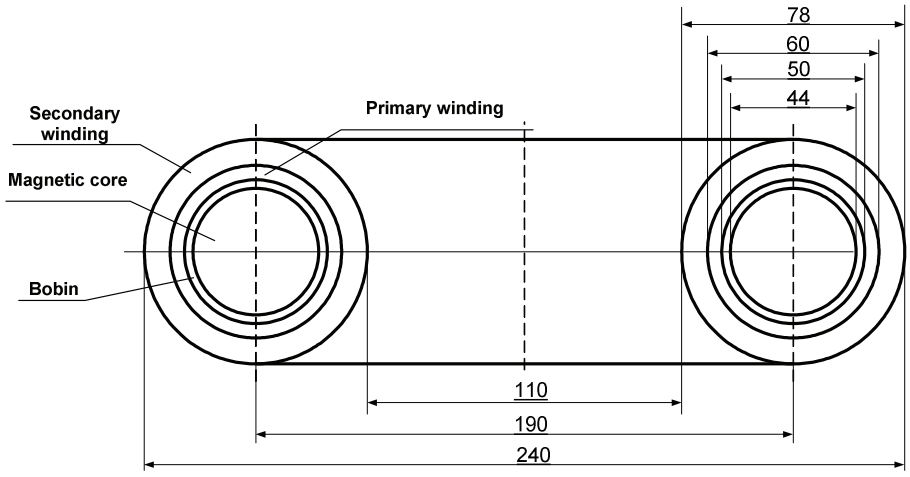


Figure 3. General dimensions of the toroidal transformer.

III. DESIGN AND STRUCTURE OF MAGNETIC CORE AND SECONDARY WINDING

The originality of the transformer lies in a combination of two features: novel material of magnetic core and proper design of secondary windings resulting with very high coupling ratio. This section describes those features with more details.

The magnetic core of the transformer, toroidal in the shape with near circular cross-section area is made of Metglas 2605 SA1 amorphous material. Such material has very high relative magnetic permeability (1000 -

ISBN 978-84-617–9183–5

10000). The cross section of magnetic material is, in fact, not exactly circular, because it is made of thin tapes of 20 m each. Photograph of the magnetic core (without housing) and general cross-section of magnetic core is shown in Fig. 4.

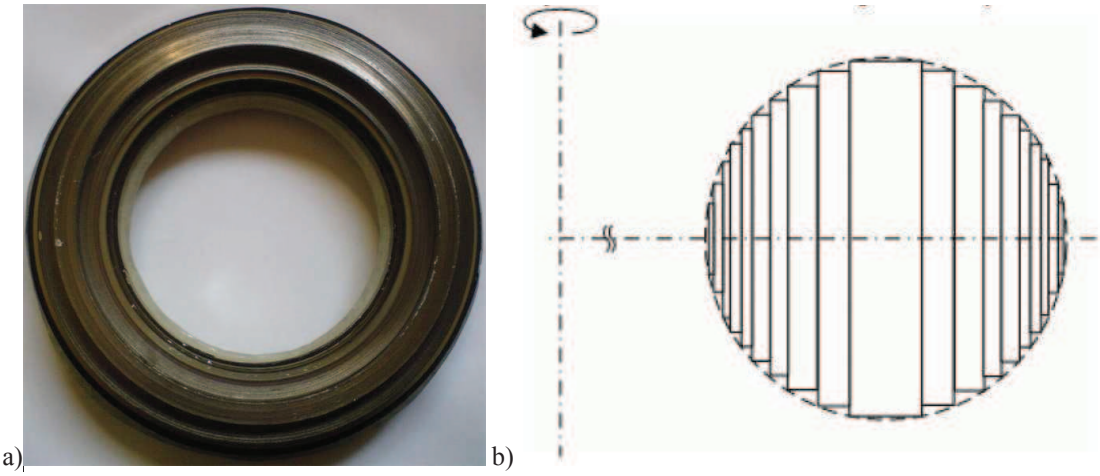

a) b)

Figure 4. Photograph of the magnetic core and the real shape of the cross-section.

Very high magnetic permeability is not only advantage of the amorphous magnetic material. Very important is also specific power loss. Comparative analysis shows that power loss in amorphous material is about 0.15 kW/kg and it is more than 5 time smaller in comparison with silicon steel (power loss in silicon steel usually exceeds 1 kW/kg). Proper analysis has been carried out and reported by authors [4], [5].

As was mentioned above, the transformer is toroidal in the shape and it has two, single turn secondary windings, which allows cooperation with unidirectional full-wave rectifier as a part of welding system. The structure of the secondary windings (front and back side) and system of connections is schematically shown in Fig. 5. The transformer in welding system is a step down transformer (boosting output current) and the secondary is a single turn winding. Because of two diode rectifier winding is made of proper number of copper strips forming two separate windings. Output clamps *A* and *B* are connected to proper diodes and the common belt *C* creates neutral point for rectifier.

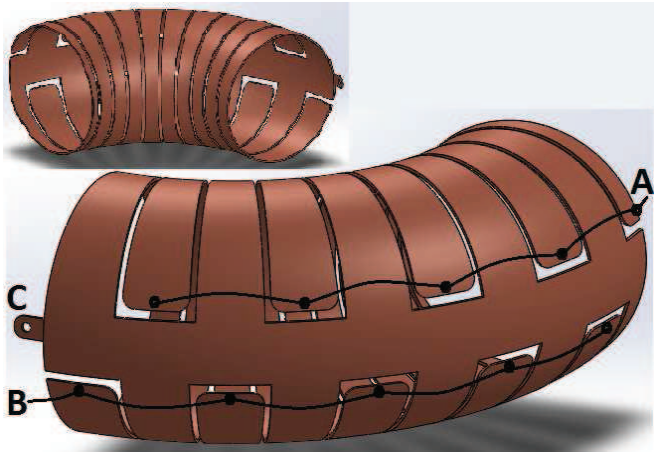


Figure 5. Structure of turns in the secondary winding.

IV. PROPERTIES OF THE TRANSFORMER

Properties of transformer has been examined in the first step by numerical modelling. A commercial ANSYS software has been used. The results of numerical modelling obtained for supplying voltage of 400 V_{RMS} and load resistance of 5 mΩ are presented in Fig. 6. One can observe distribution of the current density, where one turn of secondary winding is carrying current and the second one is at idle state (connected with blocking diode). The output current calculated at such operational condition is 8.9 kA. The input current is 128 A. It gives current ratio 70:1 which is equal to turn-to-turn ratio. Distribution of the current in secondary windings shows that at 10 kHz and given dimensions, skin and proximity effects influence on the current distribution

ISBN 978-84-617–9183–5

causing with increased ohmic losses. The output power is 43 kW and the transformer efficiency 92.1%. Because the transformer operates near of short circuit state the main source of power losses are ohmic losses.

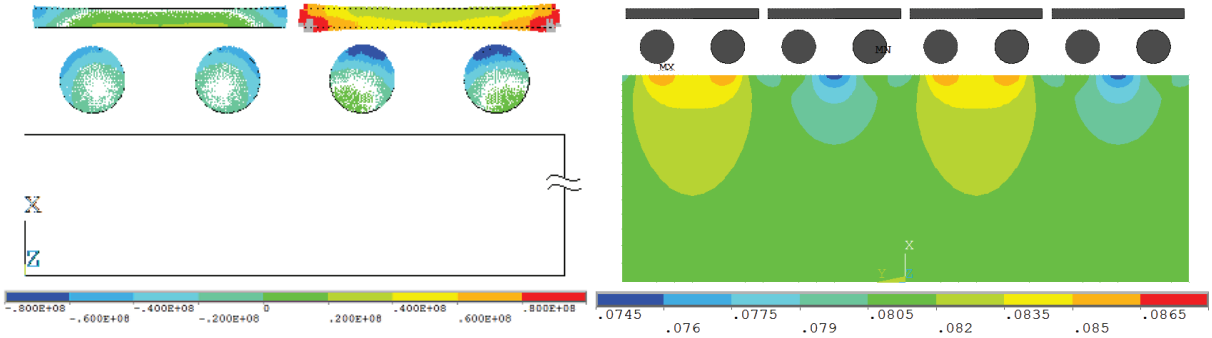


Figure 6. Results of numerical modelling, distribution of the current density (left) and magnetic flux density (right).

One can observe that the magnetic flux density in magnetic core is near uniform. The level of magnetic flux density at given operational point (considered as rated one) is very small (below 100 mT). It means operation of magnetic core far from saturation. Magnetic flux density in real transformer is more inhomogeneous because the modelling has been carried out using linearized 2D model of transformer (infinitely long cylinder).

V. CONCLUSIONS

Following conclusions can be drawn concluding the consideration presented in the paper:

- Toroidal transformer dedicated for welding system has been proposed in the paper. It has conventional primary winding and special secondary one turn windings (two sections).
- The transformer is made of amorphous magnetic core with very high magnetic permeability. It allows to obtain high coupling ratio.
- At rated voltage of 400 V_{RMS} and 10 kHz the transformer operates with output power of 43 kW and 92% of efficiency. The output current is 8.9 kA (results obtained by numerical calculations).
- The transformer is very good candidate for system of DC spot welding because of possible cooperation with two diode rectifier. Ratings of transformer allows to use it as a single device for DC welding. It can be also arranged in a modular way to increase output current.

ACKNOWLEDGEMENT

Results presented in the paper have been obtained under work supported by the Polish National Centre for Research and Development (NCBR) with the project no. PBS3/B4/12/2015.

REFERENCES

[1] M. Stępień, B. Grzesik, H. Kołodziej, T. Biskup, *HF Transformer for two diode full-wave rectifier*, 18th International Symposium on Power Electronics - Ee2015, October 28-30, 2015, Novi Sad, Serbia.

[2] Z. Mikno, M. Stępień, B. Grzesik, *Optimising the operation of servomechanical force systems used in the joining of thin-walled metal elements in the automotive industry*, 2015 International Conference on Sustainable Mobility Applications, Renewables and Technology (SMART), November 23-25, 2015, Kuwait City, Kuwait.

[3] B. Grzesik, M. Stepien, R. Jez, *Toroidal HTS transformer with cold magnetic core - analysis with FEM software*, Journal of Physics. Conference Series, Article no. 032018, vol. 234, part 3, 2010.

[4] B. Grzesik, M. Stępień, *Toroidal superconducting transformer with cold magnetic core - results of analysis and measurements*, Journal of Physics: Conference Series, 507 (2), 032043, 2014, pp. 1-4

[5] B. Grzesik, M. Stepien, *Characteristics of new magnetic materials in LN2 for HTS transformers*, Proc. of the 6th International Conf. ELMECO-6 Electromagnetic Devices and Processes in Environment Protection joint with 9th Seminar Applications of Superconductivity AoS-9, 2008, pp. 14-15.

Environmental Protection for Larger Onshore and Offshore Wind Turbine Transformers

Lorena CEBRIÁN, Rafael MURILLO, Miguel CUESTO

Technology Center for Transformers, ABB
Ctra. de Madrid km 314, 50012 Zaragoza, Spain
e-mail: lorena.cebrian@es.abb.com

Abstract — **It is well known that windmill technology for both onshore and offshore applications is under continual development, leading the size and power rating of each turbine to higher values [1]. Because of this increase, the ratings of the transformers located either inside or outside the turbine's nacelle are also increasing. Considering the technical complexity and the high cost of each square meter built on the windmill, having optimized solutions is very important for transformer selection.**

A key driver for transformer design is the level of environmental protection that is dependent on the geographical location of the windmills themselves. The degree of the ambient corrosivity will determine the amount of environmental protection from humidity, salt and pollution when considering life expectancy and maintenance activities. Solving this problem from a technical and economical viewpoint is a major challenge due to the location of most of today's wind farms.

Based on these previous reasons, achieving a robust and at the same time efficient environmental protection of transformers is a key technical challenge for design. This is especially the case for higher voltage rated wind transformers (36 kV) where the combination of reduced ambient dielectric withstand and high electrical stresses need to be very well evaluated.

This paper will start presenting the state of the art regarding environmental protection of dry-type transformers and describing the main technical challenges together with the innovative solutions developed to design, using the adequate state-of-the-art tools, 36 kV dry-type transformers robust enough for different corrosive environmental conditions. The paper will continue describing the manufacturing of several 36 kV and testing prototypes performed at world-class laboratories. Results of the tests will also be presented. The document will end explaining the conclusions of the development and proposing some recommendations that may be considered of interest; taking into account that the IEC standard of transformers for windmill turbine applications [2] is currently under revision.

Keywords — **Wind transformer, dry-type power transformer, environmental protection, onshore, offshore, windmill**

I. INTRODUCTION

There is a continued interest in developing transformer solutions which aim at ensuring their robustness against harsh environments, so as to make them suitable for all types of onshore and offshore applications in the Windmill industry.

In addition to this and considering the importance of the space occupied within the turbine's nacelle, the robustness should be achieved in the most efficient way.

With this two motivations, a project was started to deal with this particular topic.

II. STATE OF THE ART REGARDING ENVIRONMENTAL PROTECTION OF DRY-TYPE TRANSFORMERS

The first task to be performed in order to properly approach the project consisted on evaluating the current design intended for windmill applications regarding its environmental withstanding, according to the classification established by the IEC60076-11 standard for dry-type power transformers.

ISBN 978-84-617–9183–5

In clause 13.2 of the mentioned standard, the different environmental classes in which a transformer can be classified are described. In short, the range varies from E0 (no condensation or pollution expected over the transformer) to E2 (frequent condensation/pollution expected). Current windmill transformers are typically designed for E2 environmental class, which guarantees that the transformer can withstand the severe environmental conditions of the validation test, which include a relative humidity of above 93% with a water conductivity between 0.5 and 1.5 S/m. Therefore, the first step was to verify this point. In order to do this, the standard describes in its clause 26 the procedure of the test to be performed to the desired design.

The performance of an environmental test is as follows:

- The transformer is placed in a test chamber with controlled temperature and humidity, achieved by periodically atomizing water in the chamber.
- The transformer is kept in the chamber for not less than 6 hours without being energized.
- Within 5 minutes after this period, and while the transformer is still in the testing chamber, it is submitted to a test with induced voltage. There are two types of tests depending on the type of system they are intended for:
  1. Transformers with windings intended for connection to a system which are solidly earthed or earthed through a low impedance shall be energized at a voltage of 1.1 times the rated voltage for a period of 15 min.
  2. Transformers with windings intended for connection to systems which are isolated or earthed through a considerable impedance shall be submitted to a test with induced voltage for 3 successive periods of 5 min. During the test, each high voltage terminal in turns shall be connected to earth and a voltage of 1.1 times the rated voltage shall be applied between the other terminals and earth.
- The test is considered as passed when no flashovers occur during the voltage application and no serious tracking marks are shown in a subsequent visual inspection.

As it was verified on several previous occasions, the second type of test described is much more demanding than the first one. Also, it is important to note that most windfarms have the second type of grounding system for transformers, and therefore our aim became in all cases to validate our designs for this more demanding second type of test.

A 2500 kVA 30/0.582 kV transformer for windmill was manufactured in order to be E2 tested according to the described standard and validate the current solution. The values of the transformer were selected as similar as possible to the ones required by the windmill market, in order to perform a realistic validation. The main characteristics of this type of transformers, which are intended for an optimal behavior for windmill applications are:

- Modified distance from main terminals to ends of coil
- Reduced HV-LV air gap, by using an improved insulation
- Supporting blocks manufactured with improved material
- Special design for the structural clamps

The described transformer was therefore tested at an independent high-voltage laboratory in the Netherlands, where the complete E2 test sequence for the more demanding type of test was successfully passed and an official certificate was issued.

ISBN 978-84-617–9183–5

III. PROJECT DESCRIPTION AND TECHNICAL CHALLENGES

The second part of the project and also its main motivation was to implement a design which cannot only be suitable for E2 environmental conditions, but also for the more restrictive E3 conditions described in the new standard IEC60076-16. This standard, currently under revision, is specific for power transformers intended for wind turbine applications, which is our main target for this project. It includes one more stage on the environmental class classification of transformers, taking into account the harsh environments in which windmill transformers have to operate on many occasions. On its clause 7.4.5, the standard describes the more demanding environmental characteristics of the test to be carried out on transformers intended for an E3 validation. These include a relative humidity of above 95% and an increased salinity of the vaporized water in the range of 3.6 to 4 S/m.

Table I. Environmental Conditions for Tests E2 and E3

	E2	E3
humidity	above 93%	above 95%
salinity	0.5 to 1.5 S/m	3.6 to 4 S/m

These more demanding test conditions present a challenge in transformer design. The first task performed was to internally carry out a prototype (not official) test equivalent to the E3 test described by the standard, to the current solution for windmill transformer design intended for E2 in order to evaluate the results obtained and find out the principal weak points towards which the design enhancement should be directed.

The selected transformer was again a 2500 kVA 30/0.582 kV design, in order to facilitate comparison between results already obtained and future tests. The transformer did not pass the test, but several very interesting conclusions were reached.

When the defined test voltage was applied, several flashovers were observed on the transformer between some of its components. After a while, the continuous discharges stopped but some sparkling continued around various parts of the transformer, which were identified in order to improve their behaviour in the future design.



Figure 1. Flashovers observed during first tests.

After the test, the transformer was inspected to analyse the consequences of the test over it. The main issue were various tracking marks, which are not accepted at an E3 test evaluation. The tracking marks were found in several components, made from different materials.

ISBN 978-84-617–9183–5



Figure 2. Traces of the flashovers observed during inspection.

Once this test was performed, the main weak points of the transformer´s design were identified, and a series of internal tests were defined where different changes would be introduced to evaluate whether or not they solved and/or improved the performance of the transformer on the E3 test. For every test, one of the phases of the transformer was left unchanged so as to use as reference in relation to the design changes made. The design changes involved concepts such as materials, distances and addition of new components.

A total of six internal tests were carried out in which several design changes were applied. Here below, the different modification areas, their motivation and the results obtained are summarized:

Supporting block material

It was decided to perform a first test using supporting blocks manufactured with two different materials and shapes. After the test, the type-1 blocks presented permanent burning marks all over their surface, whereas the type-2 blocks showed no marks, performing completely different.

Therefore, it was validated that it is mandatory for the supporting blocks to be manufactured with an improved material suitable for severe environmental conditions.



Figure 3. Type-1 supporting block with burning marks after E3 test.



Figure 4. Type-2 supporting block after E3 test presents no burning marks.

Antitracking coating

The first new concept tested was to include the usage of an antitracking coating for the surfaces which presented some problems during the test, and had been marked or burned by the tracking occurring over them. This type of coating will expectedly allow the varnished surfaces to withstand tracking without burning, along with providing them with hydrophobic properties.

Several antitracking coating brands were tried, as well as different combinations of varnished/non varnished surfaces on the transformer, keeping the target of an efficient use of this coating.

ISBN 978-84-617–9183–5



Figure 5. HV-LV barrier with antitracking coating.



Figure 6. Coating supporting blocks and silicones.



Figure 7. Transformer with coated HV dome areas in two of its phases.

Unalike results were obtained with the usage of antitracking coatings, concluding that they enhance performance when applied over some surfaces but can also worsen it on others. Moreover, it was observed that this kind of coatings do not adhere optimally to all surfaces of the transformer, so extra care has to be taken when deciding upon their application in order to obtain the desired results.

Block silicone pad material

The original silicone pads could show in some cases some tracking marks after the tests. Therefore, an intense search of different types of silicones was carried out to find a suitable material that would not result burnt by the tracking but will still maintain the same required mechanical characteristics as the current solution.

HV design

One of the main problems observed during the test were the flashovers taking place between the HV coils and some grounded components, due to the high conductivity of the water present over the transformer surfaces during the test. Therefore, in order to comply with it, there was a need of somehow increasing the tracking distance, the surface behavior, or both. So several different solutions intended to improve, and at the same time avoiding to overdimension in order to make the solution efficient, were tested to validate them and find one that enhanced the dielectric performance and avoided the occurrence of flashovers during the test.

Magnetic core columns

Many of the flashovers happening during the previous tests were directed from the HV to the section of the magnetic core columns which is left exposed between the coils and the clamps. Therefore, focus was also directed to solving this problem by means of testing several solutions until the dielectric behavior was improved.

IV. TEST RESULTS

After the described internal tests were performed and all the information was gathered, a final prototype was prepared including all the validated improvements that had proved to enhance the dielectric behavior of the transformer when exposed to severe environmental conditions. This transformer was officially tested at the same independent high-voltage laboratory in the Netherlands, where an E3 test condensation test according to IEC60076-16 standard, in its more demanding version (intended for connection to systems which are isolated or earthed through a considerable impedance), was performed. The results were successful and the prototype passed the test without any issues, validating the proposed design solution for these very restrictive environmental conditions and therefore making it suitable for the windmill market in all aspects.

ISBN 978-84-617–9183–5



Figure 8. Transformer ready to be tested after 6 hours condensation period.

V. CONCLUSIONS

There is a real need of an in-depth analysis and redesign of transformer characteristics to make them suitable for the very demanding test conditions that the new standard for transformers intended for wind turbine applications defines for environmental withstanding.

During the course of this project it was verified that the standard solution for E2 does not comply with E3 requirements, and by means of a set of experimental tests and design enhancements, the changes required to obtain this validation were identified, defined considering an efficient use and finally applied in a prototype that successfully complied with the test, therefore obtaining a dry-type transformer design solution for voltages up to 36kV suitable for the most demanding windmill applications, that ABB can offer to the market.

The next steps of this project would be to increase the power rating and voltage of this kind of dry-type transformers, going over 36kV, i.e. 72 kV insulation level. In order to achieve this, the challenge of their dimensions will need to be re-addressed, since their larger size would once again become the main problem for these dry-type designs to be used for windmill applications. ABB is already working on this new challenge with a project to make it feasible.

REFERENCES

[1] Andrew Ho, Ariola Mbisrtrova and Giorgio Corbetta, *The European offshore wind industry - key trends and statistics 2015*, EWEA (European Wind Energy Association) report, Feb. 2016.

[2] IEC 60076-11, *Dry-type transformers*. First edition 2004 – 05.

[3] IEC 60076-16, *Transformers for wind turbine applications.* Edition 1.0 2011-008 (currently under revision).

ISBN 978-84-617–9183–5

Cooling Ability of Insulating Liquids

B. PAHLAVANPOUR , J. WEESMAA and C.P. WOLMARANS

Nynas Naphthenics
Raffinaderivagen 21, 149 82, Nynashamn, Sweden
Phone: (+44) 7876508740, e-mail: bruce.pahlavanpour@nynas.com

Abstract — **An important function of insulating liquid in a transformer, apart from insulation, is cooling. In this paper heat transfer calculations are done based on a simplified model of a transformer radiator system, simulating the type used on larger transformers, where forced convection is used to increase heat transfer. The results from calculations show that high end naphthenic transformer oil and paraffinic oils have similar heat transfer properties. Calculations were also performed for a high end synthetic ester, and in comparison it has limitations for use as a transformer fluid in power transformers.**

***Keywords* — transformer, cooling, oil, insulation**

NOMENCLATURE

λ	Thermal conductivity.	Nu	Nusselt Number.
T	Temperature.	Re	Reynolds Number.
h	Heat transfer coefficient.	Pr	Prantl Number.
L	Characteristic Length.	Gr	Grashof Number.
D	Diameter of a pipe.	$\Delta\theta$	Temperature difference between surface and bulk.
Cp	Specific heat capacity.	l	Pipe length.
μ	Dynamic viscosity.	ρ	Fluid Density.
u	Fluid velocity.	Δp	Pressure drop.
v	Kinematic viscosity.		
α	Thermal diffusivity.		
g	Gravity constant.		
f	Darcy Friction factor.		

I. INTRODUCTION

Dielectric material is used in the construction of transformers to separate and insulate active parts. The most common insulating materials used in transformers are pressboard and Kraft paper and/or Crepe paper, on the coils, together with an insulating fluid, which most commonly is mineral oil. The insulating fluid is the only material in the transformer that is in contact with all other interior materials. This is one major reason for using oil analysis as a useful monitoring tool to keep track of what is happening inside the transformer.

In this article, the focus is on transformer fluid properties and how these affect the heat transfer coefficient of the fluid. The heat transfer coefficient of a fluid describes its ability to transfer heat to/from itself from/to another medium; in the case of a radiator this is to/from metal surfaces. In transformers, heat is generated due to losses coming partly from the magnetization of the iron core (no-load losses) and most importantly the losses depending on the load of the transformer (load losses).

The no-load losses are generated from hysteresis and eddy currents in the iron core and depend on the properties of the materials. The major part of heat generation in transformers is depending on the load. The load losses consist of resistance loss in the copper coil and stray losses. Stray losses are coming from the alternating flux of the transformer and may also link with other conducting parts, like the core or the transformer tank. As alternating flux links with these parts of the transformer, there will be a locally induced electric current. These currents will circulate locally at parts of the transformer and will not contribute to the output of the transformer, but will dissipate as heat.

ISBN 978-84-617–9183–5

Heat is generated in the core and windings (coils) of transformers due to losses, and then heat is transferred to the surface of the material, in the core and coils, via conduction [1]. Then from the surface of the core and coil having contact with oil, the heat is transferred via convection to the surrounding oil. There are other losses that generate excess heat, like the component of stray flux in metal parts. The heat transfers via convection through the oil and increases the temperature of the oil. When the oil is heated up, its density decreases, and so the fluid will rise and circulate upwards [2]. When the circulating fluid meets a cold sink, like a radiator or cooler outer surface, the oil will cool down and the density of the oil increases again, which makes it fall and circulate downwards. In this oil circulation the heat generated inside the main tank of a transformer is transported to cooler surfaces outside of the main tank, and a thermal circuit is formed. In the radiator the heat is transferred first via convection to the metal surface, then via conduction through the walls of the radiator, and via convection by ambient air [3].

II. HEAT TRANSFER VIA CONVECTION

The convective heat transfer coefficient (1) is a function of the Nusselt number (2).

$$Heat\ transfer\ coefficient;\ h = \frac{Nu * L}{\lambda} \tag{1}$$

$$Nusselt\ number; Nu = \frac{h \times L}{\lambda} \tag{2}$$

The Nusselt number is dimensionless, and is a mathematical correlation based on experimental data, it depends on other dimensionless numbers, namely the Reynolds number (3), Prantl number (4) and Grashof number (5) [2, 3, 4, 5, 6, 7, 8].

$$\boldsymbol{Reynolds\ number;\ Re = \frac{u \times L}{\nu}} \tag{3}$$

$$Prantl\ number; \mathrm{Pr} = \frac{\mu \times C_p}{\lambda} \tag{4}$$

$$Grashof\ number;\ Gr = \frac{\alpha * g * \Delta\Theta * \rho^2 * L^3}{\mu^2} \tag{5}$$

The Nusselt number is calculated using the Prantl number and either the Grashof number (for natural convection cooling) or the Reynolds number (for forced convection cooling) as shown in (6) and (7).

$$For\ natural\ convection;\ Nu = f(Pr, Gr) \tag{6}$$

$$For\ forced\ convection;\ Nu = f(Pr, Re) \tag{7}$$

III. OIL PROPERTIES IMPORTANT FOR HEAT TRANSFER

i. Viscosity

The viscosity of a fluid is a measure of its resistance to gradual deformation by shear stress or tensile stress. A deeper understanding of the viscosity of a fluid requires an examination of the motion of a fluid on a molecular basis [4]. One of the major functions of oil in transformers is that it should absorb, circulate, and dissipate the heat in the cooling system. The specific heat for most mineral oils fall into a narrow range, so for mineral oil based insulating liquids it is the viscosity that mostly impacts the efficiency of cooling (given one type of cooling system). The viscosity of an oil decreases with lower average molecular size, as does vapour pressure. Therefore, the limit in flash point (which is there for fire safety reasons) effectively also puts a limit on how low the viscosity of the oil can be. From a producer's perspective this can be optimised by narrowing the

ISBN 978-84-617–9183–5

distillation range of the oil, which is depending on the molecular size range. Both the relevant ASTM and the IEC standards set the upper limit of viscosity at 12 mm2/s (40 ˚C). However, it is not necessarily 40°C where the most effective cooling is needed, but at the transformer's top oil temperature. A low viscosity at top oil temperature ensures higher heat transfer.

ii. Viscosity index

Depending on the cooling system type in the transformer it is often also an advantage if the viscosity of the insulating oil decreases significantly with temperature, because then the speed of circulation will also increase. This in turn increases heat dissipation and contributes to cooling the whole of the equipment. In general, the viscosity of oils with a higher content of naphthenic molecules plummet faster – those with a low VI (Viscosity Index) than the viscosity of oils dominated by paraffinic structures (high VI) [5]. This is one property that sets insulating oils apart from most lubricating oils (which are produced in much larger volumes) where it is desirable to maintain a high VI to ensure equal lubrication at a wide range of temperatures, e.g. in engines. VI is not specified in any of the two standards, but it is implicit since the maximum viscosity allowed is given at two different temperatures.

iii. Pour Point

In cold climates naphthenic oils have another advantage with their naturally low pour point. In practice this means that even when the oil is very cold shortly after start-up of a transformer, it flows and can transport heat away from windings and core. Low pour point is easier to achieve with naphthenic oils than it is with paraffinic oils, which often need to use so called pour point depressant additives (usually large polar polymeric type molecules) for this reason [5].

IV. HEAT TRANSFER IN FLUIDS

In all transformers in-service there will be heat generation which means that the local temperature will rise. The heat transfer in transformers is possible via convection (flowing media). In smaller units, like a distribution transformer with no pump, the fluid is cooled through natural convection which means that when the fluid temperature rises the density decreases and the warmer fluid rises upwards. Transformers with a higher load normally have oil pumps and an external cooling unit installed. This type of system, where the fluid is pumped through the transformer to increase heat transfer, is called forced convection or directed cooling (if it includes internal oil guides). Forced convection is an effective method to increase the cooling capacity, especially when turbulent flow is induced. However, there are limitations on fluid velocity in transformers due to generation of static charges or electrostatic charging tendency (ECT), when the fluid has linear flow velocity over 1 m/s [9]. In practice OEMs manufacturing large power transformers have designed for a bulk velocity around 0.5 m/s (in the transformer tank) to avoid generation of ECT. So there is an upper limitation on the fluid´s bulk velocity, but there are still differences in the heat transfer due to the fluids own properties [1].

V. PROPERTIES OF INSULATING FLUID

Important properties of a transformer fluid that influence heat transfer ability are: thermal conductivity, density, specific heat capacity and viscosity. (Thermal conductivity (λ) is derived from Fourier´s law [3], which describes a mediums ability to conduct energy from one point to another at a given temperature, the unit for λ is [W/m*K]. Specific heat capacity (C_p) describes how much heat needs to be transferred to 1 kg of mass at a given temperature and increase the temperature by 1 °K, the unit for C_p is [J / g °C]. The Reynolds number (3) is a dimensionless tool that describes what forces dominate in the flow, the inertia or viscosity [2, 3, 4, 8]. In the case of a cylindrical pipe the characteristic length (L) would be its diameter (D).

For fluid flowing in pipe, transition from laminar to turbulent flow occurs at Re= 2300, and beyond Re=3000 turbulent fluid flow is dominant [3]. The mass and heat transfer increase significantly when turbulent flow is dominant. The formed eddies mix the fluid more efficiently than in laminar flow, see Fig. 1.

ISBN 978-84-617–9183–5

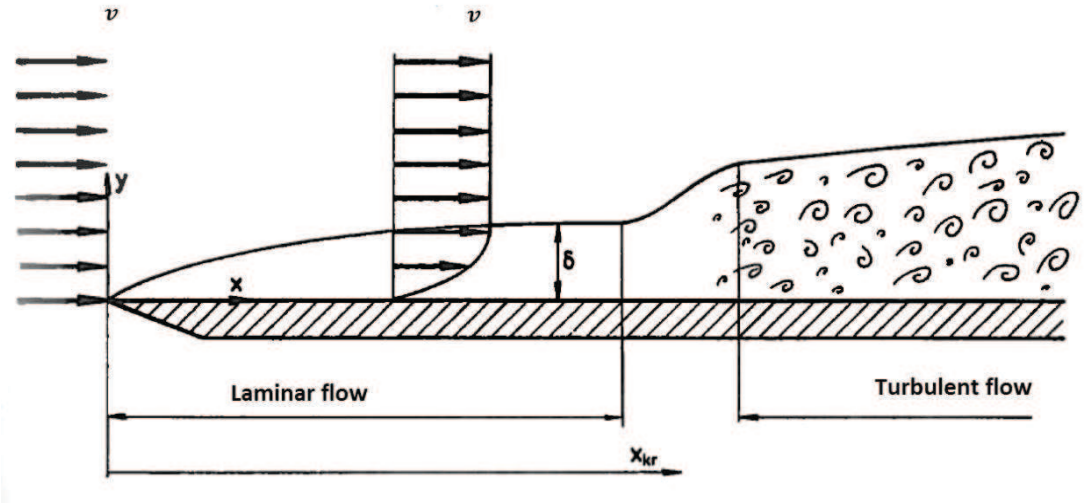


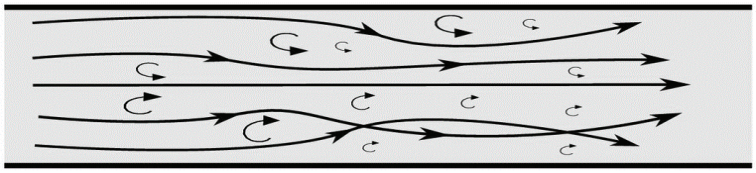
Figure 1. Fluid flowing over a flat surface with flow velocity at x_{kr} transition from laminar to turbulent flow occurs [3].

In close proximity to the wall there is a thin film (boundary layer) with lower flow velocity, due to friction.

In order to simplify the calculations, an external cooler (heat exchanger) can be modelled as a pipe. The hot oil is entering inside the pipe and on the outside of the pipe another colder media is used to remove excess heat from the flowing oil in the pipe. At low flow velocity there is mainly a parallel flow profile (laminar flow) and at higher flow velocity a turbulent flow pattern will develop, and this is good for increasing heat transfer (see Fig. 2 and 3).



Laminar Flow



Turbulent flow

Figure 2. Laminar versus Turbulent flow.

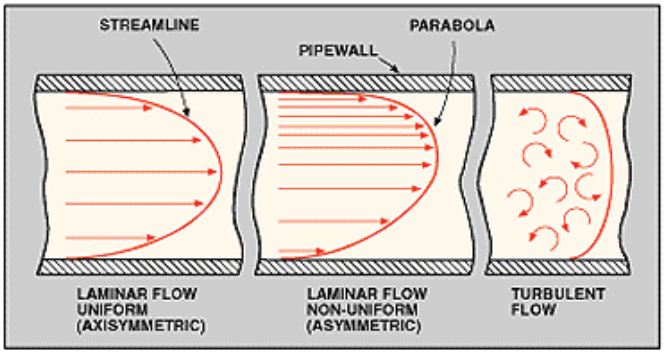


Figure 3. Turbulent flow mixes fluid in the tube´s radial dimension with the help of eddies and increases heat transfer significantly for the fluid.

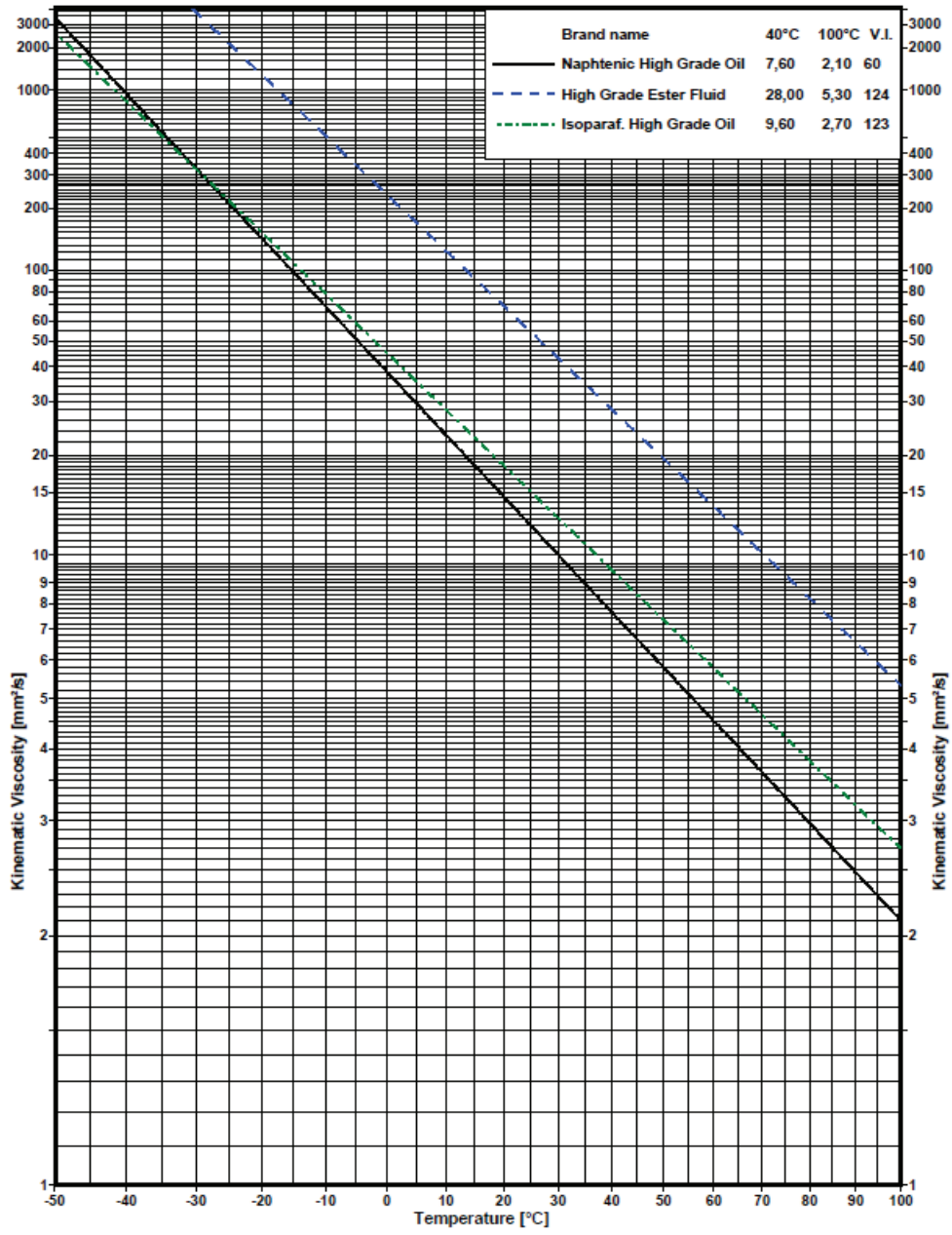
ISBN 978-84-617–9183–5

VI. HEAT TRANSFER OF DIFFERENT FLUIDS

To calculate the heat transfer coefficient, physical data (kinematic viscosity and density) is needed for the fluid at different temperatures. Thermal conductivity and specific heat capacity also need to be measured.

The Reynolds number can be calculated at different temperatures if the fluid's bulk velocity in the cooler is known, and the hydraulic diameter of the cooler. In this instance values of D=10 cm and various cooler flow velocities are used in the calculations – the actual oil velocities at different points in the transformer will differ between a wide range for different transformer designs. In the transformer tank, many transformer manufacturers work with a common bulk flow limit due to ECT of 0.5 m/s, but the flow rate in the external cooler can be of higher velocity depending on the arrangement of the unit [9].

A viscosity diagram, shown in Fig. 4, compares the viscosity versus temperature (and therefore VI) for a synthetic ester transformer fluid, a paraffinic transformer oil and a naphthenic transformer oil. The naphthenic oil below has a steeper decline in viscosity when temperature rises, compared to the ester fluid and the paraffinic oil.



ISBN 978-84-617–9183–5

Figure 4. Viscosity versus Temperature diagram for different oil types.

The data used in the calculations for three different fluids mentioned in this paper are shown in Table I and II below.

Table I. Kinematic Viscosity

Kinematic Viscosity [cSt]	Naphthenic	Paraffinic	Synthetic Ester
ν @ 40°C	7.49	9.51	28
ν @ 50°C	5.59	7.19	19.5
ν @ 60°C	4.34	5.59	14
ν @ 70°C	3.48	4.49	10.5
ν @ 80°C	2.85	3.68	8
ν @ 90°C	2.39	3.08	6.5

Table II. Density

Density [kg/m^3]	Naphthenic	Paraffinic	Synthetic Ester
ρ @ 40°C	859	794	956
ρ @ 50°C	852.3	789	948
ρ @ 60°C	845.7	783	941
ρ @ 70°C	839.1	777	934
ρ @ 80°C	832.4	770	928
ρ @ 90°C	825.7	764	919

When fluid is flowing in tubes, there is a shift to turbulent flow when the Re number is higher than 2300, and fully developed turbulent flow over 5000. The Nusselt number is a dimensionless number describing the heat transfer. For a fluid in tubes the Nusselt number (2) is used as a base for the calculations [3].

In order to calculate the heat transfer (1) for a certain fluid over temperature, the Nusselt number needs to be calculated. This can be done via a mathematic correlation using empirical data for heat transfer in tubes. Gnielinski's correlation is valid for fluids in a steady state flow in tubes.

$$\text{Gnielinski's correlation;} Nu = \frac{\frac{f}{8}*(Re-1000)*Pr}{1+12.7*\sqrt{\left(\frac{f}{8}\right)}*(\sqrt[2/3]{Pr}-1)} \quad (8)$$

The Prantl number (4) is a dimensionless parameter describing how the fluid behaves in the thermal boundary layer [3].

Gnielinski's correlation is valid if: $0.5 \leq Pr \leq 2000$ and $3000 \leq Re < 500000$ are fulfilled [2].

Gnielinski's correlation also uses the Darcy friction factor *f*, which can be calculated from the pressure drop for fluid flowing in a pipe, Δp [3]:

$$\Delta p = 4 * f * \left(\frac{1}{2} * \rho * v^2\right) * \left(\frac{l}{D}\right) \quad (9)$$

The Darcy friction factor decreases with higher Re number, and increases with rougher surface structure inside the tube. Due to the lack of experimental data on measurements of pressure loss in pipes, an empirical formula can be used or a Moody [10] diagram.

ISBN 978-84-617–9183–5

The Blasius formulae [6] for a smooth pipe surface can be used for Re = 3000 to 10^5 to approximate the friction factor, f (10).

$$f = \frac{0.079}{R_e^{0.25}} \tag{10}$$

In order to conduct calculations for the models described earlier, thermal data for the fluids is needed, thermal conductivity and specific heat capacity at different temperatures were obtained, shown in Table III and IV below.

Table III. Thermal Conductivites

Thermal Conductivity [W/m*K]	Naphthenic	Paraffinic	Synthetic Ester
λ @ 40°C	0.1402	0.165	0.143
λ @ 50°C	0.1432	0.166	0.1422
λ @ 60°C	0.1462	0.167	0.141
λ @ 70°C	0.1492	0.167	0.14
λ @ 80°C	0.1522	0.168	0.139
λ @ 90°C	0.1552	0.168	0.137

Table IV. Specific Heat

Specific Heat [J / g °C]	Naphthenic	Paraffinic	Synthetic Ester
C_p @ 40°C	1.8711	2.05	1.93
C_p @ 50°C	1.9225	2.16	1.959
C_p @ 60°C	1.9684	2.2	1.99
C_p @ 70°C	2.0188	2.24	2.01
C_p @ 80°C	2.0711	2.27	2.02
C_p @ 90°C	2.1173	2.33	2.04

Example calculations on heat transfer coefficient (h) are presented in Fig. 5 and Fig. 6 below for the three different fluids. Here it was assumed that the cooler unit is a basic pipe and has a diameter of 10 cm and the results here show heat transfer coefficient versus temperature for flow velocity in the pipe of 0.2 m/s (Fig. 5) and 5 m/s (Fig. 6). In all the calculations the pipe is assumed to have a smooth surface on the inside of the radiator. Note that at lower flow speed, the synthetic ester is flowing in laminar mode. The heat transfer coefficients were also calculated at 80°C for a number of other flow velocities and compared between the different liquids as shown in Fig. 7.

Note that the calculations have been done on the fluids only. It can be seen that a lower viscosity will facilitate better heat transfer and a lower top oil temperature, hence also the possibility of longer service life for the transformer materials. Comparing Figure 3 and Figure 4 show that the naphthenic oil, having a steeper slope in the viscosity diagram (lower viscosity index or VI), seem to offer a higher heat transfer coefficient than the paraffinic type of oil, with higher VI, that have almost similar viscosity properties at 40°C.

ISBN 978-84-617–9183–5

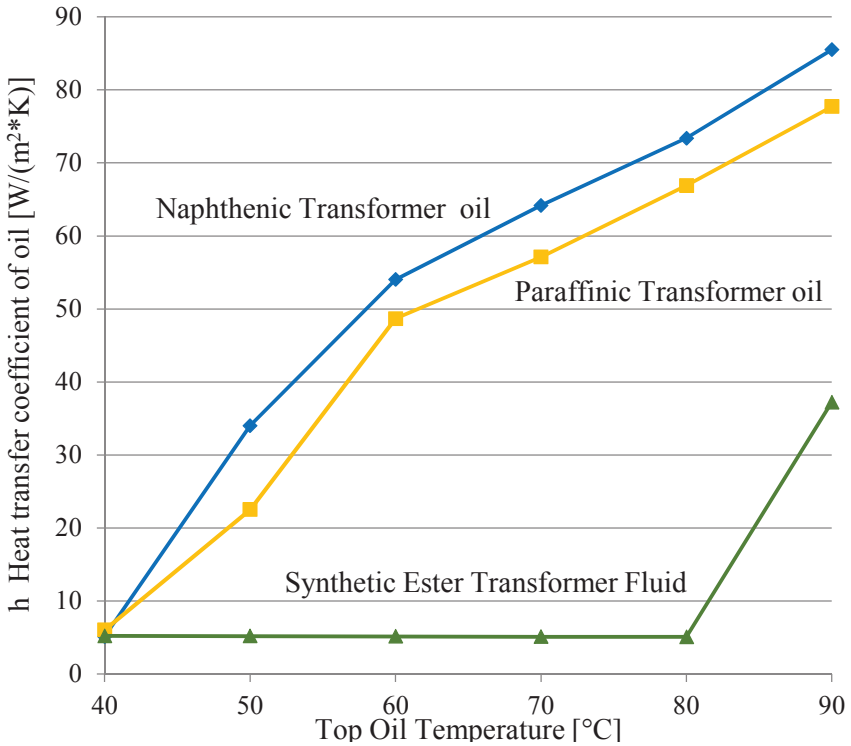


Figure 5. Calculated heat transfer coefficient versus temperature for flow velocity in a smooth pipe D = 10cm for a flow rate of 0.2m/s.

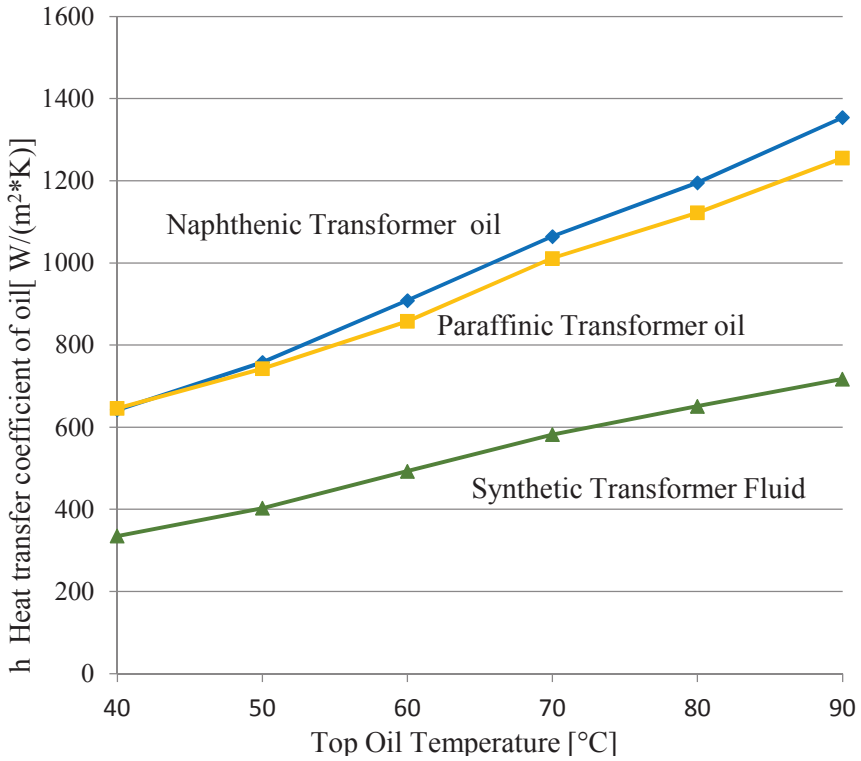


Figure 6. Calculated heat transfer coefficient versus temperature for flow velocity in a smooth pipe D = 10cm for a flow rate of 5 m/s.

ISBN 978-84-617–9183–5

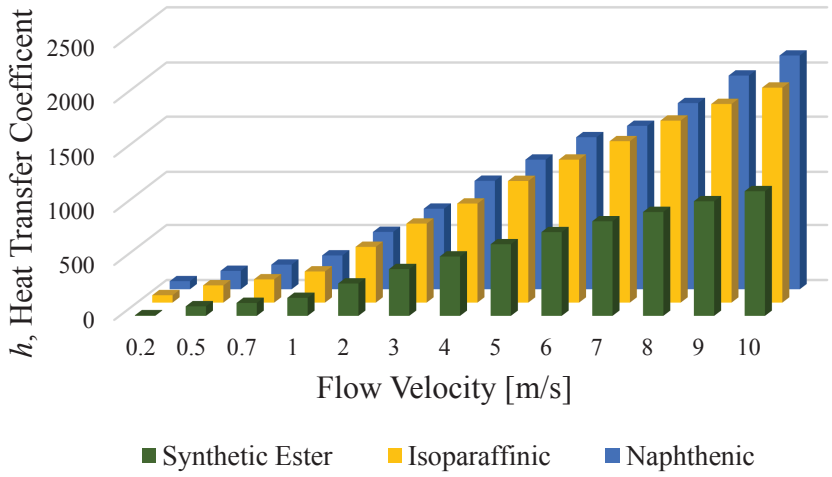


Figure 7. Heat transfer at a fixed temperature, here 80°C, and variation in fluid velocity shows that naphthenic oil has higher values for the heat transfer coefficient than iso-paraffinic oil and synthetic ester at all flow rates.

VII. CONCLUSION

The calculations presented in this paper show that the naphthenic oil has a significantly better heat transfer coefficient in forced convection than the synthetic ester. As observed in Figure 4 and Figure 5, the naphthenic oil and the iso-paraffinic have slightly different physical properties, but similar heat transfer coefficients overall, in this study, with a slightly better performance shown by the naphthenic oil. Low viscosity is one main parameter for a higher heat transfer coefficient, along with thermal conductivity, specific heat capacity and density.

REFERENCES

[1] W.M. Flanagan, *Handbook of transformer design and applications*, 2nd ed., McGraw-Hill

[2] G.F.C.Rogers et al., *Engineering thermodynamics work and heat transfer*, 1967, Longman

[3] A.D. Kraus et al. , *Introduction to thermal and fluid engineering*, 2010, CRC Press

[4] J.R. Welty et al. *Fundamentals of momentum, heat and mass transfer*, 1984, John Wiley & Sons

[5] R.M. Mortier et al., *Chemistry and technology of lubricants, Blackie Academic & Professional*, 2nd ed., 1997

[6] Massey, B.S. , *Mechanics of fluids* (1991)

[7] F.P. Incropera; D. P. DeWitt, (2007). *Fundamentals of Heat and Mass Transfer* (6th ed.). Hoboken: Wiley

[8] H. Y. Wong, *Heat transfer for engineers* (1977), Longman

[9] S.V. Kulharni et al., *Transformer Engineering*, 2004, Marcel Dekker Inc.

[10] Moody, L. F. (1944), *Friction factors for pipe flow*, Transactions of the ASME 66 (8): 671–684

ISBN 978-84-617–9183–5

Enhancing Transformer Liquid Insulation with Nanodielectric Fluids: State of the Art and Future Trends

Víctor A. PRIMO[(1)], Belén GARCÍA[(1)], Juan Carlos BURGOS[(1)], Ricardo ALBARRACÍN[(2)]

[(1)]Department of Electrical Engineering
Universidad Carlos III de Madrid, Spain.
Phone: (+34) 916249972, fax: (+34) 916249972
e-mail: vprimo@ing.uc3m.es, belen.garcia@uc3m.es, jcburgos@ing.uc3m.es

[(2)]Department of Electrical, Electronics and Automation Engineering and Applied Physics
Universidad Politécnica de Madrid, Spain
Phone: (+34) 916249972, fax: (+34) 916249972, e-mail: rasbarracin@gmail.com

Abstract — **In the last years several, works have proposed the use of nanodielectric fluids as an improved insulation for different elechtrotecnical applications. The behaviour of nano dielectric fluids has been evaluated from the point of view of the dielectric and thermal properties. Although the results of the different authors are in any cases not in complete agreement, most investigations report promising performances for these new liquids. In this paper, a literature survey on this field is presented.**

Keywords — **Insulating liquids; Nanoparticles; Nanodielectric fluids Nanofluid; Ferrofluid**

I. INTRODUCTION

Recently, nanodielectric fluids have been proposed to be used as transformer liquid insulation. These materials are obtained by dispersing nanoparticles in a matrix fluid. The addition of particles seeks to improve the dielectric and thermal properties of the base liquids, giving rise to a new generation of insulating fluids. Several authors claim that the performance of nanodielectric fluids as insulators and coolers is superior to that of the base liquids.

The interest on these type of fluids has risen exponentially over the last years, as can be derived from the number of scientific works published in international journals and conferences (Fig. 1).

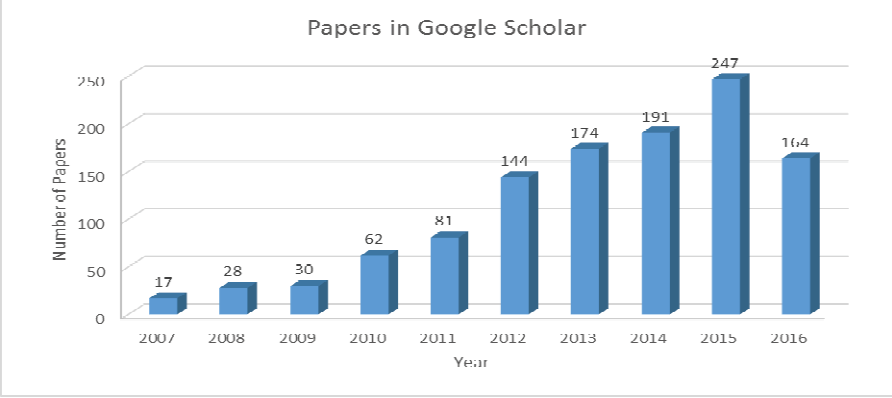


Figure 1. Papers dealing with the subject "nanofluids for application in transformers", from 2007 to July 2016. Source, Google Scholar.

Nanodielectric fluids are not a feasible technical solution nowadays. Some issues related to their stability, the interaction with the magnetic fields present in the transformer, the effect of the nanoparticles on the transformer solid insulation performance, and the production costs should be studied and addressed before they could be applied in real transformers.

ISBN 978-84-617–9183–5

The aim of this paper is to present a state of the art on Nanodielectric fluids for electrotechnical use. The experimental results obtained by different authors are reviewed and compared. Additionally, practical issues, such as the manufacturing process of the liquids, and basic theoretical aspects are reviewed.

II. MANUFACTURING OF NANODIELECTRICS FLUIDS.

Although some companies, such as General Electric, have already registered patents related with the use of nanodielectric fluids in electric devices, those liquids are not commertially available nowadays. The investigations reported in literature are mostly based on fluids manufactured at laboratory scale. Dıfferent types of particles and base fluids have been proposed and tested to date. Nanofluids can be classified according to the type of nanoparticles disperssed in the base fluids, and by the base fluds used.

2.1 Nanoparticles

The selection of the nanoparticle is one of the most important issues when preparing a nanofluid. Nanoparticles can be categorized according to their conductivity into three groups [1]

- Conductive nanoparticles: Fe_3O_4, Fe_2O_3, ZnO,…
- Semiconductive nanoparticles: TiO_2, CuO, CuO_2,...
- Insulating nanoparticles: Al_2O_3, SiO_2, BN,…

Works have been published dealing with fluids manufactured using different conductive, semiconductive and insulating particles, reporting positive effects for most of them. Sima explains in [2] that the physical phenomena that takes place when an insulating fluid doped with particles is subjected to an electric field is the same, independently of the particle nature. This finding could seem to contradict the traditional theory of liquid dielectric breakdown, which assumes that the contamination of an insulating fluid with conductive particles or impurities would lead to a degradation of its performance.

Sima [2] states that, under the effect of an electric field, the electrons in the nanoparticles are orientated in a direction opposite to that of the electric field, generating a positive and negative charge distribution on the surface of the conductor (Fig. 2).

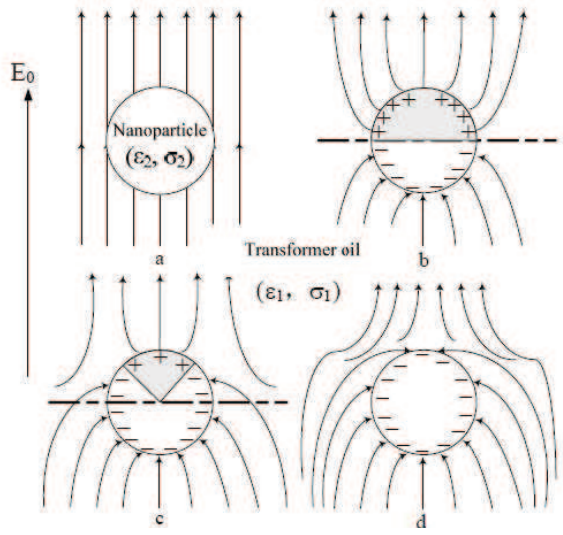


Figure 2. Electric field lines after a uniform z-directed electric field is activated at t = 0 around a Nanoparticle with radius R, permittivity ε_2, and conductivity σ_2. This nanoparticle is surrounded by transformer oil with permittivity ε1 and conductivity σ_1. Taken from [2].

ISBN 978-84-617–9183–5

2.2 Base Fluid

The base fluid is the liquid in which the nanoparticles are dispersed. Although most of the works in the field of Nano-dielectric fluids are focused in mineral-oil based liquids, some investigations have also been reported on the use of natural ester or synthetic ester based nanofluids [3], [4] or [5]. Dombek in [6] compares the enhancement in the thermal properties that can be achieved by adding nanoparticles to Mineral oil and Synthetic esters. Other authors as Wang [7] have also tested Natural-Ester based fluids.

The development of ester-based nanodielectric fluids could be an important area in the future, since the addition of nanoparticles can lead to an improvement of the cooling properties of the fluid, which are one of the weak points esters fluids.

2.3 Manufacturing procedure

In the vast majority of the cases, the nanoparticles to be dispersed in dielectric fluids are prepared outside the fluid or purchased to nanotechnology companies. This is known as a two-step manufacturing process. The particles are dispersed in the matrix fluid by sonication or magnetic stirring, being precise, in most cases, to add a surfactant to prevent particle agglomeration or sedimentation [6].

It must be also highlighted that appropriate health and safety measures must be implemented in the laboratories in order to manipulate the nanoparticles, being advisable to protect or isolate the workers from them to prevent their being breathed.

2.4 Stability

One of the main problems when working with nanofluids, is to guarantee the stability of the nanoparticles dispersed in the oil in the long term. Nanofluids stabilities have been reported to go from a few weeks to several months. As mentioned before, it is common to use surfactants and dispersants to prevent the agglomeration of the nanoparticles by coating its surface with a layer of specific products. One of the major surfactants employed to this end is oleic acid [8], [9].

III. THERMAL PROPERTIES

Thermal properties are important for transformer oils, since, as it is well known, the oil also acts as a coolant in transformers. The main thermal properties of dielectric oil are the viscosity and the thermal conductivity of the fluid.

3.1 Thermal Conductivity

Several researchers have reported experimental studies dealing with the thermal conductivity of nanofluids. In Yanijao Li's paper [10], three factors that influence the nanofluids' thermal conductivity are highlighted. These factors are the properties of the nanoparticles, the liquid matrix and the liquid-solid interface.

The influence of nanoparticles in the thermal conductivity of the nanofluid mainly depends on the effect of the volume fraction of particles, the thermal conductivity of the particles, their morphology and the Brownian motion. Many investigations have revealed a large increase on thermal conductivity as the volume fraction of nanoparticles rises. This improvement in some cases is not linear. This may be due to an organized structure in the solid-liquid interface.

The influence of the base liquid has been less studied than the influence of the nanoparticles concentration and type. It can be summarized that thermal conductivity experiments show an increase with increasing temperature and this in turn depends on the type of matrix liquid used.

ISBN 978-84-617–9183–5

Finally, the influence of the solid-liquid interface is one of the important factors affecting the thermal conductivity. Several studies claim that the interfacial layer between the nanoparticle and the fluid has a very important role in improving the thermal properties of nanofluids. According to Choi [11] in particles smaller than 10 nm, the nano-layer is more important than the nanoparticles used to manufacture the nanofluid.

Donbek [6] published an experimental study in which the thermal properties of different nanofluids were determined. Fig. 3 shows the increase of thermal conductivity of a mineral oil modified by nanoparticles TiO_2 and surfactant about mineral oil as a function of temperature.

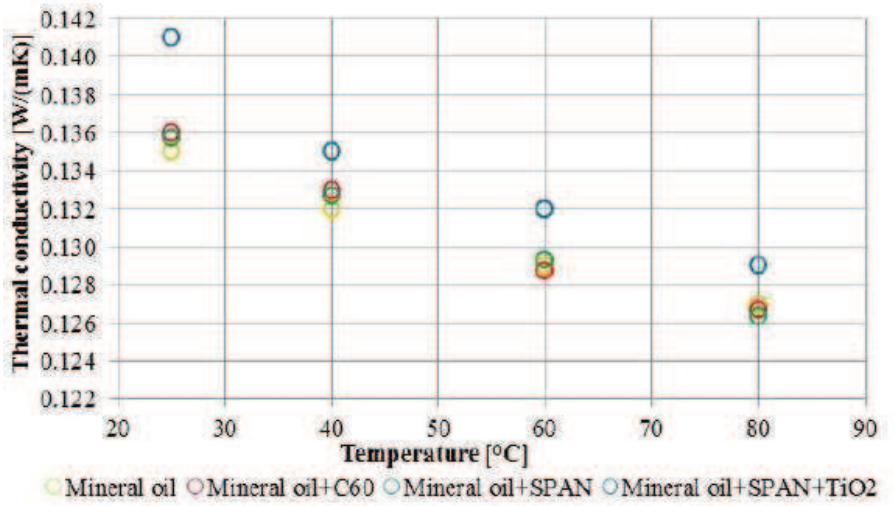


Figure 3. Thermal conductivity coefficient of mineral oil and nanoliquids formed on its basis, as a function of temperature. Take from [6].

3.2 Viscosity

The viscosity of nanofluids has been little studied, despite of being a thermal property as important as the thermal conductivity for the cooling performance of the fluids. The vast majority of studies are focused on the factors influencing the viscosity of those liquids, such as the concentration or size of nanoparticles and the temperature.

Li [12] showed that the viscosity of nanofluids decreases with increasing temperature and increases with the increase of the concentration of the nanoparticles, being much greater the effect of temperature.

Fig. 4 shows how viscosity of a mineral oil varies with the addition of several nanoparticles as a function of temperature. As can be seen the viscosity of all the included fluids decrease as temperature increase, but not a big variation is observed when the particles are added.

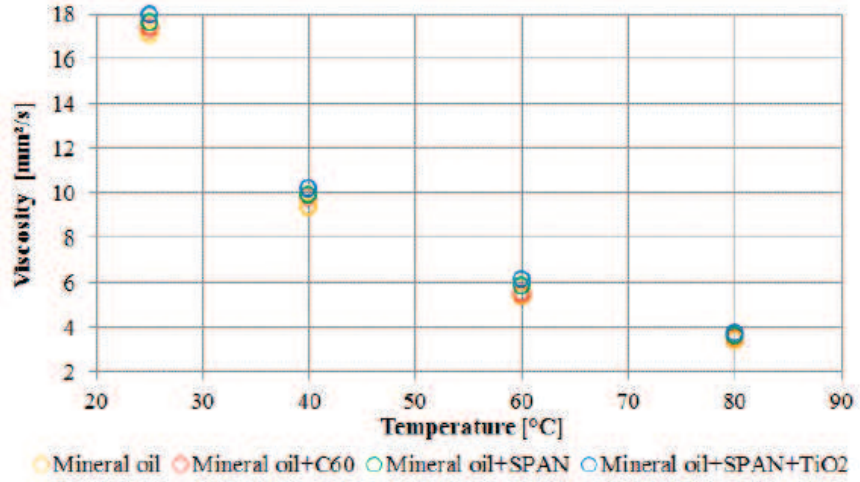


Figure 4. Viscosity of mineral oil and nanoliquids formed on its basis, as a function of temperature. Taken from [6].

ISBN 978-84-617–9183–5

IV. DIELECTRIC PROPERTIES

Several authors have tested the dielectric properties of nanofluids comparing them with those of base fluids. This section discusses the results obtained by the different authors:

4.1 AC Breakdown Voltage

AC Breakdown voltage has been measured on several nanodielectric fluids obtained by mixing mineral oil with insulating, semiconductive and conductive particles.

Table I compares the results reported by different authors, including details of the experiments such as the particles added to the oil, the particle size or the concentration of the nanoparticles in the base fluid. As can be seen, an improvement was observed in all cases. An author, [13] reports an increase of more than 40 % on the AC Breakdown voltage.

Table I. Increase in AC Breakdown Strength Reported by Several Authors.

Nanoparticle/ Oil System	Nanoparticle Size (nm)	Nanoparticle loading	% Increase in AC Breakdown Strength	Ref
Fe_3O_4/MO	10	-	42,8%	[13]
Fe_3O_4/VO	30	-	19.8%	[14]
ZnO/MO	34	0.0005 % vol	8.3%	[15]
TiO_2/VO	20	0.00625 % vol	31%	[4]
SiO_2/MO	15	0.0074 % vol	17%	[16]
TiO_2/MO	<20	0.006g/L	15%	[17]
SiO_2/MO	15	0.01 % vol 0.02% vol	19% 26%	[18]

Y. Zhou [1], states that a clear increase in the AC Breakdown Strength of Mineral Oil based nanofluids containing Fe_3O_4 nanoparticles is observed. This improvement is especially noticeable when the moisture content of oil is high. The authors suggest that this effect might be due to the formation of water clusters that are attached by the surface of the nanoparticles. A similar improvement in dielectric properties was observed when the particles added were TiO_2, as Du et al [19] report.

Table II shows a study presented by Du Yue-fan et al [17] where the effect of adding TiO_2 nanoparticles in the AC (50Hz) Breakdown Voltage of mineral oil was determined. As can be seen, a certain improvement is reported for low concentrations of particles, although it must be noted that for concentrations greater than 0.03 g/L the performance of the nanofluid is similar or even worse than that of mineral oil. This same effect has been also reported in other works and it seems clear that depending on the nanoparticle concentration in oil, their effect can be even detrimental.

Table II. Comparison of AC Breakdown Voltages Between Nanofluid and Transformer Oil Reported by [17].

Samples	Mean Breakdown Voltage (KV)	% Increase in Breakdown Voltage
Transformer Oil	71,59	0%
TiO_2 (0.003g/L)	67,33	-5,9%
TiO_2 (0.006g/L)	82,48	15,2%
TiO_2 (0.01g/L)	77,82	8,7%
TiO_2 (0.03g/L)	71,76	0,2%
TiO_2 (0.05g/L)	53,25	-25,6%

One of the most widely used nanoparticle is magnetite (Fe_3O_4). In [20] Nytro Libra mineral oil is mixed with magnetite nanoparticles with a volume concentration of 0.1-0.6%. The breakdown voltage measured according to IEC 60156 standard [23] for mineral oil was 60.44 kV, while for volume concentrations of nanoparticles

ISBN 978-84-617–9183–5

0.2%, 0.3% and 0.6% was 63.76 kV, 70.16 kV and 53.84 kV, respectively. So, increasing the volume concentration may increase the voltage breakdown, but up to a limit in which the magnetic nanoparticle concentration could result in a decrease of the breakdown voltage due to the form of conducting chains close to the electrodes. In this case, the optimal nano oil volume concentration for having the higher breakdown voltage is around 0.2-0.3% [20], [21].

In [22], the statistical behaviour of the AC breakdown voltage is compared in mineral, synthetic and natural ester oils according to IEC 60156 standard [23]. The breakdown voltage of insulating oils, generally follows a Normal distribution and its average value is higher in natural esters than in mineral oils. Besides, this value is also higher for natural esters at the risk levels of 1%, 10% and 50% ($U_{1\%}$, $U_{10\%}$, and $U_{50\%}$). As an additional result, the dielectric strength of ester oils is generally greater than that of mineral oils under AC voltages.

Another effect that must be taken into account [24] is that the AC breakdown voltage rises with the size of the nanoparticles up to a certain limit that depends on the nanoparticles concentration in the fluid. As an example, for the ester fluid FR3, the breakdown voltage is 55.1 kV, while for the same fluid containing 40.7 nm Fe_3O_4 is 68.5 kV, an increase of 24.5%. Besides, in [25] it is found that the AC breakdown voltage also depends on the chemical composition of the nanoparticles.

Additionally, in [13] is found that the improvement on the AC breakdown voltage, in Fe_3O_4 mineral oil-based nanofluids, is greater as the water content of the oil increases, Fig. 5.

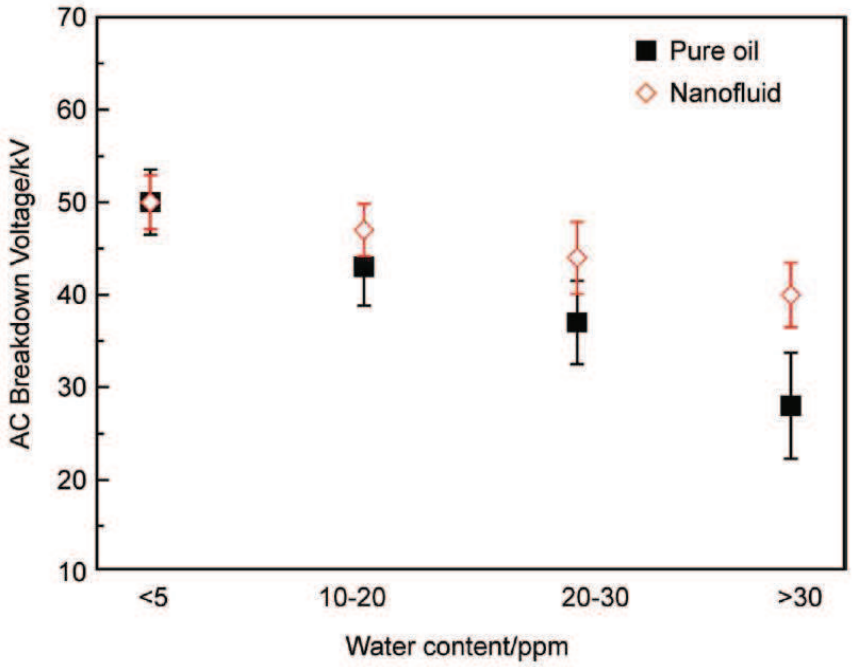


Figure 5. AC breakdown for mineral oils and Fe_3O_4 mineral oil-based nanofluids as function of water content. Taken from [1] that adapted it adapted from [13].

Finally, [24] shows that the polarization of the surfactants that coat the particles can significantly influence the electron trapping depth of natural ester based nanofluids. The results have shown that the breakdown strength increases for nanofluids with a smaller thickness ratio of surfactant. Besides, in [1] it is shown that the choice of a certain surface modifying agent can increase or decrease the AC breakdown strength of mineral oil-based ferrofluids. According to this, Fig. 6 shows the influence of two TiO_2 nanoparticle surface modification agents compared with the AC breakdown voltage of TiO_2 mineral-oil based nanofluids related to the TiO_2 concentration.

ISBN 978-84-617–9183–5

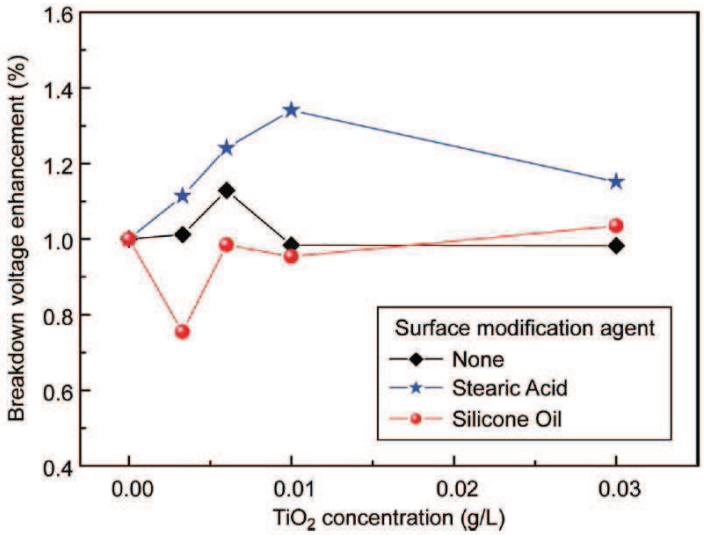


Figure 6. AC breakdown voltage dependency of surfactants for different mineral oil-based TiO_2 nanofluids compared with different TiO_2 concentrations [1] adapted from [26].

4.2 DC Breakdown Voltage

Several authors have reported an increase of the DC Breakdown Voltage of insulating fluids when nanoparticles are added [1]. As shown in Fig. 7, the DC breakdown voltage showed an increases as the concentration of Fe_3O_4 nanoparticles increased from 0.2-2 vol%. Besides, in some tests, the specimen was subjected to a 20 mT external magnetic field, and this effect reduced the DC breakdown voltage compared to the same concentration without external magnetic field applied [27]. The authors sustained that the reason for this observation is the formation of a micrometer-sized aglomerated Fe_3O_4 particles in the nanofluid as a result of magnetic dipole-dipole interaction between each nanoparticle under the external magnetic field [1].

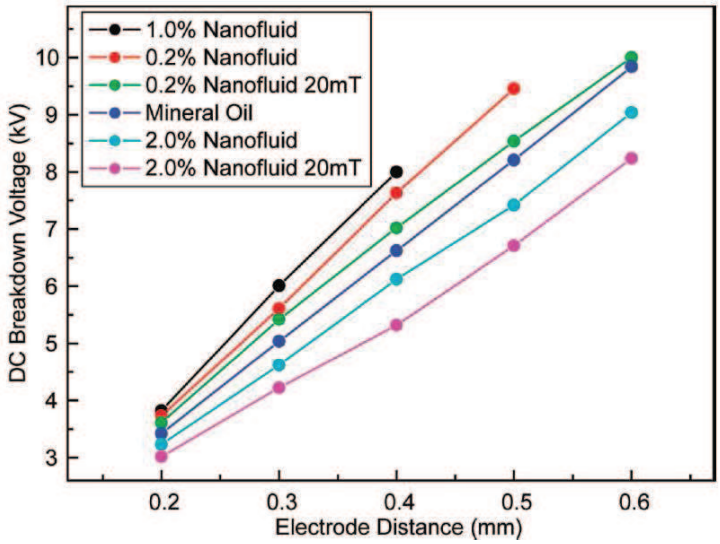


Figure 7. DC breakdown voltage compared with electrode distance for mineral oil and different concentrations of Fe3O4 oil-based nanofluids, some of them are subjected to a 20 mT external magnetic field [1] adapted from [27].

According to [28], it is found that the DC breakdown behaviour it is very different from positive to negative DC applied voltage, i.e. for mineral oil compared with TiO_2 nanoparticles (0.075 vol%), the positive DC breakdown is quite similar for mineral oil and for nanofluid, however, the negative DC breakdown showed a significant increase, according to Table III.

ISBN 978-84-617–9183–5

Table III. DC Breakdown Voltage of Mineral Oil and Nanofluid. Taken from [29].

Samples	DC(+) Breakdown Voltage(KV)	Standard Deviation (KV)	DC(-) Breakdown Voltage(KV)	Standard Deviation (KV)
Mineral oil	49.1	2.6	66.3	4.0
Nanofluid	45.1	1.8	84.6	6.4

4.3 Streamer propagation in nanofluids. Lightning impulse.

A streamer discharge is a transient electrical discharge that can appear when an insulating medium, e.g. insulating oil, is exposed to a large voltage drop, such as in the case of a lightning impulse.

Streamer propagation in transformer fluids depends on the field ionization and thus, as many of the mobile electrons produced by ionization are trapped before they can be swept away from the ionization region, the electrodynamics involved in the development of the streamer in the nanofluid will be significantly slower than that of pure oil. Besides, nanofluids have slower positive streamer velocities and higher positive voltage breakdown than that of pure conventional oil [30]. In [13] the effect of the nanoparticles on the propagation velocity of positive streamers was studied, observing that that parameter was reduced by as much as 46% by the addition of the particles. The effect of reducing the propagation velocity of streamer is higher as the nanoparticle conductivity increases [30]. A slower propagation velocity allows more time for the impulse voltage to be extinguished, so the positive voltage breakdown must be higher than that obtained in conventional transformer oil. Note that positive streamer implies a greater risk for the insulation of electrical equipment than negative streamers.

In [3], the average breakdown voltage for positive lightning impulse of a natural ester was found to be 73.9kV, while for the Fe_3O_4 based nanofluid it rose to 101.5kV, a 27.2% increase. In the case of the negative lightning impulse, the average values for the breakdown voltage were 83.8 kV for the base fluid vs. 93.7 kV for the nanofluid, a 10.6% increase. In addition, the breakdown time also increased for the nanofluid compared with the base liquid [14], i.e. 9.9 μs for vegetal oil and 12.0 μs in nanoparticle's oil-based, which represents a 17.5% increase of the breakdown time.

Finally, O'Sullivan [31], Sima [2] and [30] implemented several mathematical models in Finite Elements to study streamer phenomena in insulating fluids when different types of nano-particles are dispersed in them.

4.4 Partial discharges (PD) in nanofluids

Breakdown occurs after discharge initiation and propagation across the oil. Besides, the breakdown voltage measurement alone provides little information on the discharge process. Therefore, it is important to investigate the details of the discharge mechanisms in mineral oil and in nanofluids. In [32], the PD inception voltage (PDIV), PD duration, PD rise time, total discharge magnitude and PD voltage amplitude is compared for mineral oil, silica nanofluid and fullerene nanofluid (with an average particle size of 15 [nm] and 1 [nm], respectivelely) under DC voltage. The discharge mechanism in mineral oil depends strongly on the polarity of the applied DC voltage. Under negative DC polarity, inception voltage and discharge magnitude are quite similar between nanofluids and the reference mineral oil. However, under positive DC voltage, the nanofluids show an increased inception voltage and a reduction of the total discharge magnitude compared to the reference mineral oil, [33].

According to [29] the dielectric withstand of partial discharge of mineral oil can be improved by the addition of TiO2 nanoparticles. The PDIV is increased and the PD magnitudes and numbers of PD pulses are reduced, as it is shown in Table IV [1], [29].

ISBN 978-84-617–9183–5

Table IV. PDIV, PD Magnitudes, and Numbers of PD Pulses Acquired at 1.0 and 2.0 PDIV During 10 Minute Measurements Intervals in Mineral Oil and TiO_2 Nanofluids.

Sample	PDIV (kV)	Std. Deviation (kV)	Measured at 1.0 PDIV		Measured at 2.0 PDIV	
			Pulse number	Mean discharge magnitude (pC)	Pulse number	Mean discharge magnitude (pC)
Mineral oil	30.6	2.7	9	435	245	6062
TiO_2 Nanofluid	33.1	1.8	6	245	168	5180

Finally, in [33] three different nanofluids, silica ferrofluid 0.2, graphene oxide, and SiO_2, DC and AC withstand capability are compared with mineral oil. As a result, for all nanofluids, nanoparticle concentrations around 0.2 g/l enhance dielectric withstand properties under quasi uniform fields. Under divergent fields, partial discharge characteristics are improved under AC conditions. Under DC conditions silica nanofluid performs better than mineral oil, but the other two nanofluids do not perform well.

V. CONCLUSIONS

From the year 2010, interest in nanodielectric fluids applications has increased significantly. Several research groups are working with different materials (both fluid and particle type), focusing their studies on the thermal and dielectric properties of these liquids.

Authors have observed that the addition of nano-particles to the oil improves the dielectric behavior of the fluid increasing its breakdown voltage and the AC pulse and other thermal properties. The application of such liquids could achieve more compact designs of transformers and improve the reliability of the new high voltage transformers for AC (UHVAC-ultra-high voltage alternating current) or DC (Ultra-high voltage direct UHVDC- current).

Although the results reported in good number works are promising, more research is necessary to make nanofluids a feasible industrial solution. Investigations should be carried out to determine aspects such as influence of the applied materials and techniques, the long term stability of the fluids, the thermal and dielectric properties under different conditions or the interaction of the particles with other elements of the transformers.

VI. ACKNOWLEDGEMENT

This work has been supported by the Spanish Ministry of Economy and Competitiveness within the project DPI2015-71219-C2-2-R.

REFERENCES

[1] Y. Lv, Y. Zhou, C. Li, Q. Wang, and B. Qi, *Recent progress in nanofluids based on transformer oil: Preparation and electrical insulation properties*, IEEE Electr. Insul. Mag., vol. 30, no. 5, p. 23–32, 2014.

[2] W. Sima, J. Shi, Q. Yang, S. Huang, and X. Cao, *Effects of conductivity and permittivity of nanoparticle on transformer oil insulation performance: Experiment and theory,* IEEE Trans. Dielectr. Electr. Insul., vol. 22, no. 1, p. 380–390, 2015.

[3] J. Li, R. Liao, and L. Yang, *Investigation of natural ester based liquid dielectrics and nanofluids,* ICHVE 2012 - 2012 Int. Conf. High Volt. Eng. Appl., vol. 56, no. 2 mm, p. 16–21, 2012.

[4] Y. Zhong, Y. Lv, C. Li, Y. Du, M. Chen, S. Zhang, Y. Zhou, and L. Chen, *Insulating properties and charge characteristics of natural ester fluid modified by TiO2 semiconductive nanoparticles,* IEEE

Trans. Dielectr. Electr. Insul., vol. 20, no. 1, p. 135–140, 2013.

[5] P. Krishna Kumar, S. Senthil Kumar, and M. Ravindran, *Investigation on mixed insulating fluids with nano fluids and antioxidants,* 2014 Int. Conf. Adv. Electr. Eng. ICAEE 2014, p. 6–9, 2014.

[6] G. Dombek, Z. Nadolny, and P. Przybyłek, *The Study of Thermal Properties of Mineral Oil and Synthetic Ester Modified by Nanoparticles TiO 2 and C 60,* Ichve, p. 1–4, 2014.

[7] B. Wang, J. Li, B. Du, and Z. Zhang, *Study on the stability and viscosity of Fe3O4 nano-particles vegetable insulating oils,* ICHVE 2012 - 2012 Int. Conf. High Volt. Eng. Appl., p. 307–310, 2012.

[8] M. V. Avdeev, M. Balasoiu, V. L. Aksenov, V. M. Garamus, J. Kohlbrecher, D. Bica, and L. Vekas, *On the magnetic structure of magnetite/oleic acid/benzene ferrofluids by small-angle neutron scattering,* J. Magn. Magn. Mater., vol. 270, no. 3, p. 371–379, 2004.

[9] L. Pislaru-Danescu, A. M. Morega, G. Telipan, M. Morega, J. B. Dumitru, and V. Marinescu, *Magnetic nanofluid applications in electrical engineering,* IEEE Trans. Magn., vol. 49, no. 11, p. 5489–5497, 2013.

[10] Y. Li, J. Zhou, S. Tung, E. Schneider, and S. Xi, *A review on development of nanofluid preparation and characterization,* Powder Technol., vol. 196, no. 2, p. 89–101, 2009.

[11] W. Yu and S. U. S. Choi, *The role of interfacial layers in the enhanced thermal conductivity of nanofluids : A renovated Maxwell model,* p. 167–171, 2003.

[12] N. Suspensions, *Experimental Viscosity Measurements for Copper Oxide Nanoparticle Suspensions,* Vol. 7, no. 2, p. 198–201, 2002.

[13] V. Segal, a. Hjortsberg, a. Rabinovich, D. Nattrass, and K. Raj, *AC (60 Hz) and impulse breakdown strength of a colloidal fluid\nbased on transformer oil and magnetite nanoparticles,* Conf. Rec. 1998 IEEE Int. Symp. Electr. Insul. (Cat. No.98CH36239), vol. 2, p. 619–622, 1998.

[14] J. Li, Z. Zhang, P. Zou, S. Grzybowski, and M. Zahn, *Preparation of a vegetable oil-based nanofluid and investigation of its breakdown and dielectric properties,* IEEE Electr. Insul. Mag., vol. 28, no. 5, p. 43–50, 2012.

[15] M. Hanai, S. Hosomi, H. Kojima, N. Hayakawa, and H. Okubo, *Dependence of TiO 2 and ZnO nanoparticle concentration on electrical insulation characteristics of insulating oil,* p. 780–783, 2013.

[16] J. Liu, L. Zhou, Y. Luo, X. Huang, and G. Wu, *Dielectric Frequency Response of Oil-paper Composite Insulation with Transient Moisture Distribution,* p. 1380–1387, 2013.

[17] D. U. Yue-fan, L. V Yu-zhen, Z. Jian-quan, L. I. Xiao-xin, and L. I. Cheng-rong, *Breakdown Properties of Transformer Oil-based TiO 2 Nanofluid,* p. 3–6, 2010.

[18] H. Jin, T. Andritsch, P. H. F. Morshuis, and J. J. Smit, *AC breakdown voltage and viscosity of mineral oil based SiO2 nanofluids,* Annu. Rep. - Conf. Electr. Insul. Dielectr. Phenomena, CEIDP, p. 902–905, 2012.

[19] Y. Du, Y. Lv, C. Li, Y. Zhong, M. Chen, S. Zhang, Y. Zhou, and Z. Chen, *Colloids and Surfaces A : Physicochemical and Engineering Aspects Effect of water adsorption at nanoparticle – oil interface on charge transport in high humidity transformer oil-based nanofluid,* Colloids Surfaces A Physicochem. Eng. Asp., vol. 415, p. 153–158, 2012.

[20] J. Ghasemi, S. Jafarmadar, and M. Nazari, *Journal of Magnetism and Magnetic Materials Effect of magnetic nanoparticles on the lightning impulse breakdown voltage of transformer oil,* J. Magn. Magn.

ISBN 978-84-617–9183–5

Mater., Vol. 389, p. 148–152, 2015.

[21] M. Nazari, M. H. Rasoulifard, and H. Hosseini, *Journal of Magnetism and Magnetic Materials Dielectric breakdown strength of magnetic nano fl uid based on insulation oil after impulse test,* J. Magn. Magn. Mater., vol. 399, p. 1–4, 2016.

[22] V. Dang and A. Beroual, *Comparative Study of Statistical Breakdown in Mineral , Synthetic and Natural Ester Oils under AC Voltage,* No. November 2011, p. 1508–1513, 2012.

[23] IEC 60156 Ed. 2, *Insulating liquids – Determination of the breakdown voltage at power frequency – Test method*, 1995.

[24] J. Li, B. Du, F. Wang, W. Yao, and S. Yao, *The effect of nanoparticle surfactant polarization on trapping depth of vegetable insulating oil-based nanofluids,* Phys. Lett. A, vol. 380, no. 4, p. 604–608, 2016.

[25] J. A. Mergos, M. D. Athanassopoulou, T. G. Argyropoulos, and C. T. Dervos, *Dielectric Properties of Nanopowder Dispersions in Paraffin Oil,* p. 1502–1507, 2012.

[26] Y. Lv and X. Li, *Preparation and breakdown strength of TiO 2 Fluids Based on Transformer Oil,* p. 2–4, 2010.

[27] J. Kudelcik, P. Bury, P. Kopcansky, and M. Timko, *Dielectric breakdown in mineral oil ITO 100 based magnetic fluid,* vol. 9, no. 2, p. 78–81, 2010.

[28] Y. Du, Y. Lv, C. Li, M. Chen, Y. Zhong, J. Zhou, X. Li, and Y. Zhou, *Effect of semiconductive nanoparticles on insulating performances of transformer oil,* IEEE Trans. Dielectr. Electr. Insul., vol. 19, no. 3, p. 770–776, 2012.

[29] B. Du, J. Li, B. M. Wang, and Z. T. Zhang, *Preparation and breakdown strength of Fe3O4 nanofluid based on transformer oil,* ICHVE 2012 - 2012 Int. Conf. High Volt. Eng. Appl., p. 311–313, 2012.

[30] J. G. Hwang, M. Zahn, F. M. O'Sullivan, L. A. A. Pettersson, O. Hjortstam, and R. Liu, *Effects of nanoparticle charging on streamer development in transformer oil-based nanofluids,* J. Appl. Phys., vol. 107, no. 1, p. 1–17, 2010.

[31] F. M. O'Sullivan, *A model for the initiation and propagation of electrical streamers in transformer oil and transformer oil based nanofluids,* Thesis (Ph. D.)--Massachusetts Inst. Technol. Dept. Electr. Eng. Comput. Sci. 2007., p. 309, 2007.

[32] H. Jin, P. Morshuis, A. R. Mor, J. J. Smit, and T. Andritsch, *Partial Discharge Behavior of Mineral Oil based Nanofluids,* vol. 22, no. 5, pp. 2747–2753, 2015.

[33] A. Cavallini, R. Karthik, and F. Negri, *The effect of magnetite, graphene oxide and silicone oxide nanoparticles on dielectric withstand characteristics of mineral oil,* IEEE Trans. Dielectr. Electr. Insul., vol. 22, no. 5, p. 2592–2600, 2015.

ISBN 978-84-617–9183–5

Optical and Numerical Investigation of Oil Flow Velocities Inside a Zigzag Cooled Winding Model

S. TENBOHLEN[1], N. SCHMIDT[1], C. BREUER[2], S. KHANDAN[1], R. LEBRETON[3]

[1]University of Stuttgart, Germany
[2]GE Grid Solutions, Germany
[3]GE Grid Solutions, France

Institute of Power Transmission and High Voltage Technology,
Pfaffenwaldring 47, 70569 Stuttgart, Germany
Phone: +49 (0)711 685-67 870, fax: +49 (0)711 685-67 877,
e-mail: stefan.tenbohlen@ieh.uni-stuttgart.de

Abstract — **In this contribution the oil speed in horizontal ducts of an OD cooled winding is investigated by experimental and numerical methods. The presented winding model offers insight into the horizontal cooling channels perpendicular to the main oil flow direction. To visualize the oil flow, tracing particles were added to the cooling oil and illuminated by high power LEDs. The particle velocities were then determined by taking photographs with a defined exposure time. The design of the sophisticated winding model is described in the contribution. In addition to the experimental results, this contribution presents a comparison with respective numerical results from 3D CFD calculations. Finally, numerical results from the 3D winding model concerning the oil flow distribution inside the winding at various operating conditions are presented. The investigation indicated a strong inhomogeneous oil flow distribution on the horizontal channels. The presented results give a deep insight into the oil flow and temperature behaviour of windings enabling the designer to optimize the cooling of power transformer windings.**

Keywords — **Power Transformer, OD Cooling, Optical Investigation, Thermal Modelling, Computational Fluid Dynamics, Oil Flow Rate**

I. INTRODUCTION

Power transformers are key components applied in transmission and distribution systems. Their power rating and life-cycle characteristics are strongly dependent on thermal aspects. The higher the evolving temperature levels at a given loading rate are settling, the faster the insulation materials will age at that loading rate. Therefore, a profound knowledge about the temperature distribution inside a transformer is crucial for an appropriate assessment of the component's power rating and for that reason offers the opportunity to cut costs in the production process. In the past, and still today to some extent, analytical and empirical methods have been used to predict the temperature distribution in the transformer components and to determine the hot-spot value; however these methods have inherent limitations [1]. For the investigation of the temperature distribution within the windings of an oil cooled transformer, different approaches can be pursued [2]. In this contribution, the oil speed in horizontal ducts of an OD cooled winding is investigated by experimental and numerical methods.

Representatively for often used winding types, a so-called "zigzag" arrangement of a disc-type winding was investigated. In such a case, winding discs are layered above each other, while so-called spacers keep the axial distance between the discs and determine the height of the horizontal ducts for the oil. The sticks ensure the proper fixation of the spacers and keep the radial distance between the discs and the outer cover. The vertical ducts are formed by the space between discs and outer cover. The oil is led from the bottom into the vertical ducts and flows from there upwards, while it distributes into the particular horizontal ducts. To ensure a proper distribution of the oil to the horizontal ducts, which should be as equal as possible, the vertical duct is intermitted -alternating between the inner and the outer duct- after a specified number of discs by so-called washers. This leads to an oil flow in a "zigzag" manner.

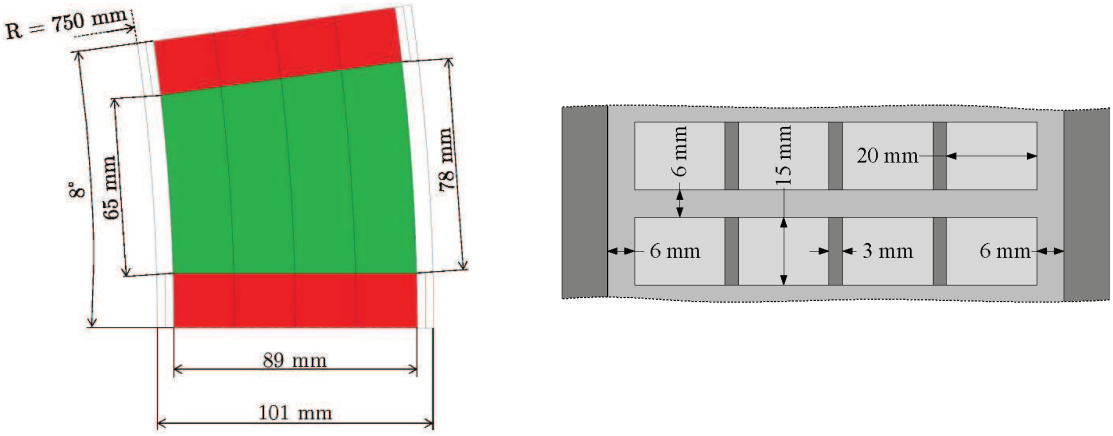
ISBN 978-84-617–9183–5

In order to confirme the suitability of a numerical 3D winding model to predict the realities in transformer windings accurately a comparison between experimentally determined oil flow velocities with corresponding numerical data is presented in the paper.

II. Development of an Experimental Model for a Disc Winding

The design of disc type transformer windings shows a strong symmetry in the circumferential direction and can be subdivided into symmetrical sections. Consequently, all windings models investigated below represent one symmetrical section of a disc winding. As carried out in the introduction, a winding design with characteristics being representative for an OD-cooled disc winding is chosen as a common basis for all investigated winding models. A top view of a symmetric section of this chosen winding design, including all relevant geometric details to assess this design, is shown in Figure 1a). Since common transformer design rules usually refer to entire windings, the properties given in this contribution, to reference investigated operating conditions, are transferred accordingly. For example, instead of specifying the heating power per conductor model representing a section of 8 ° in circumferential direction of on entire winding turn, the corresponding losses per complete winding turn are referenced. Analogous considerations are applied for the oil flow rate. For that reason, the actually applied heating power per conductor model and the oil flow rates passing the winding models are 8 °/360 ° = 1/45 times the referenced values pointed out in the figure captions.

The paper wrapping typically applied around conductors in transformer windings for purposes of an electrical insulation is substituted by solid blocks of plastic (Polyvinylidenefluoride) located only in between the conductors of a disc. Prior experimental investigations showed a great sensitivity to the evolving temperature levels on the exact thickness of the applied paper wrapping. Unfortunately, this property, especially with regard to the comparably short experimental conductor models, is difficult to keep within small tolerances. To eliminate respective detrimental influences but still allow a realistic thermal decoupling of the conductor models in one disc, the paper is substituted, as illustrated in detail in Figure 1b).



a) Top view on winding segment b) Cross section of winding model

Figure 1. Design characteristics of the modelled winding geometry and the winding model [3].

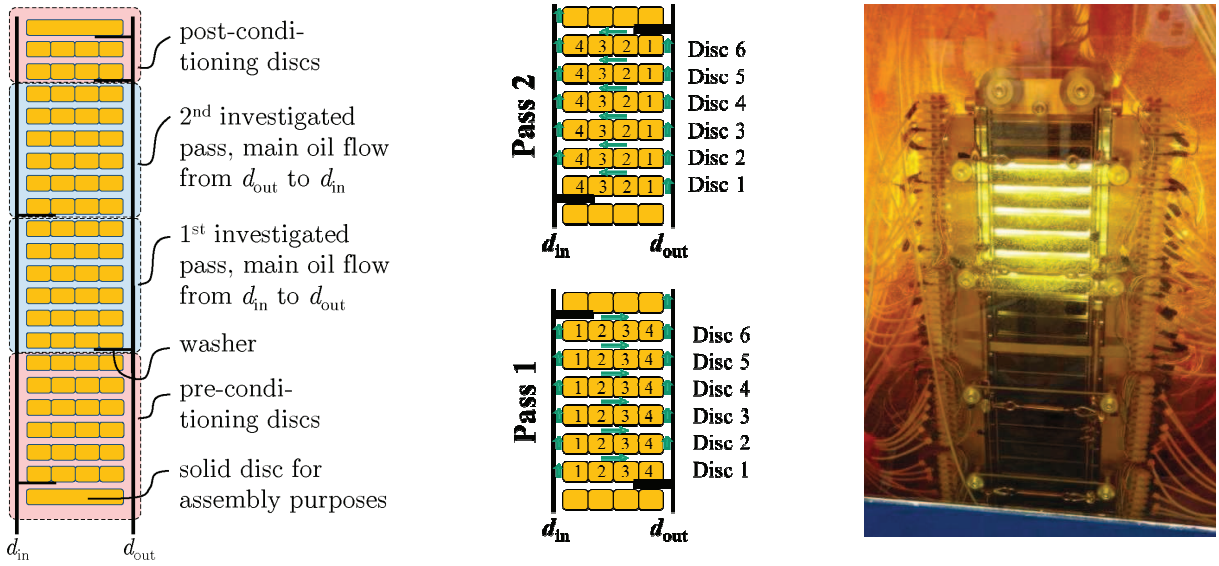
To provide the heating power normally dissipated in the winding turns of a power transformer during operation, heating cartridges are injected into each conductor model through a borehole. An accurate measurement of the individual conductor temperatures is accomplished with temperature sensors located inside the conductor.

The cooling system of OD-cooled disc windings is usually subdivided into so-called passes in the axial direction. By periodical placement of washers inside the vertical channels alternating between the inner and outer winding diameter, two different types of passes result. Therefore, the experimental winding model must consist of at least two consecutive passes. In addition, representative entering and exiting conditions are required before and after the investigated passes. This ensures thermal and hydraulic conditions that are representative for every pass throughout the complete cooling system of the modelled winding. Integrating these considerations, Figure 2a) shows the chosen winding model layout in a schematic view. To its right, Figure 2b) provides a clear reference for the pass, disc and conductor numbering the presented post analysis

ISBN 978-84-617–9183–5

relies upon. Finally, Figure 2c) contains a photo of the experimental winding model during operation. Although this picture gives no detailed insight into the chosen mechanical design of the winding model, comprising its sealing and insulation concept, it already offers a first impression of the required technical efforts.

Next to a representative winding design, also the operating conditions of the modelled winding are chosen accordingly with respect to the winding type and dimensions. To control the relevant boundary conditions precisely, a laboratory setup was applied [3]. In order to clarify better the experimental setup, in Figure 3 the laboratory setup illustrated schematically. It allows an accurate control over the mass flow rate $\dot{m}_{oil}$, the oil temperature at the model inlet ϑ_{in} and the heating power of each conductor $P_{losses,\,i}$. While the oil inlet temperature is set via a controlled flow heater, the initially provided oil flow rate from a gear pump is limited to a defined value by a controlled valve processing data from a flowmeter. To minimize the heat leakage from the winding model to its surroundings, the entire model is submerged in an open experimental tank filled with oil of the same temperature as provided by the flow heater. Finally, the individual power supplied to each heating cartridge is set by software controlled power electronics. Due to the chosen laboratory setup, a total measuring tolerance concerning the temperatures of approximately 0.5 K is achieved. Consequently, temperature gradients can be determined with an accuracy of around 1 K. The occurring deviations concerning the mass flow measurement and heating power control are below 1 %.



a) Schematic layout of experimental winding model

b) Numbering of discs and conductors in investigated passes

c) Experimental winding model in tank during operation

Figure 2. Components of a conductor model for the experimental winding model [3].

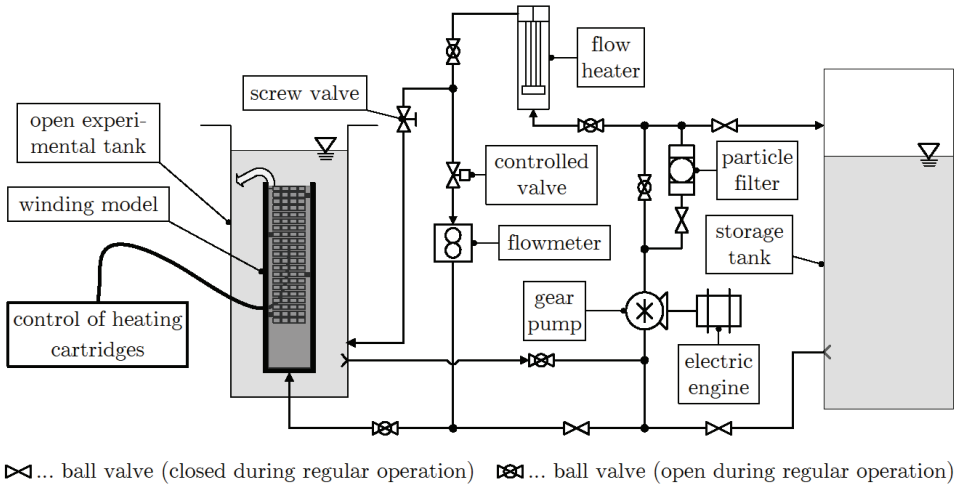


Figure 3. Piping and instrumentation diagram of the laboratory setup designed to create strictly controlled boundary conditions inside the winding model.

ISBN 978-84-617–9183–5

Because oil is a transparent liquid, the investigation of the oil flow requires additional measures. For that purpose, tracing particles were added to the oil of the experimental setup. These particles were chosen according to the material properties of the mineral oil and the application conditions of the investigation. To make the particles visible, a strong source of light has to be applied. High power LEDs were mounted directly in front of the horizontal channels, as indicated in Figure 4. A digital camera was then mounted in a defined alignment of the horizontal channels and focused on the investigated area in the middle of the horizontal channels. Due to the chosen optical equipment and the connected setup, the depth of field defining the investigated area in the *z*-Dimension shown in Figure 4 is limited to approximately 6 mm. The particle velocities within the investigated area were then determined by taking photographs applying a defined exposure time. After measuring the particle track lengths in the taken pictures, the particle velocities can be calculated with the relation as follows:

$$\text{Local velocity of particle } v_i = (\text{Length of path line of particle } i\ l_i) / (\text{Selected shutter speed } \Delta t) \quad (1)$$

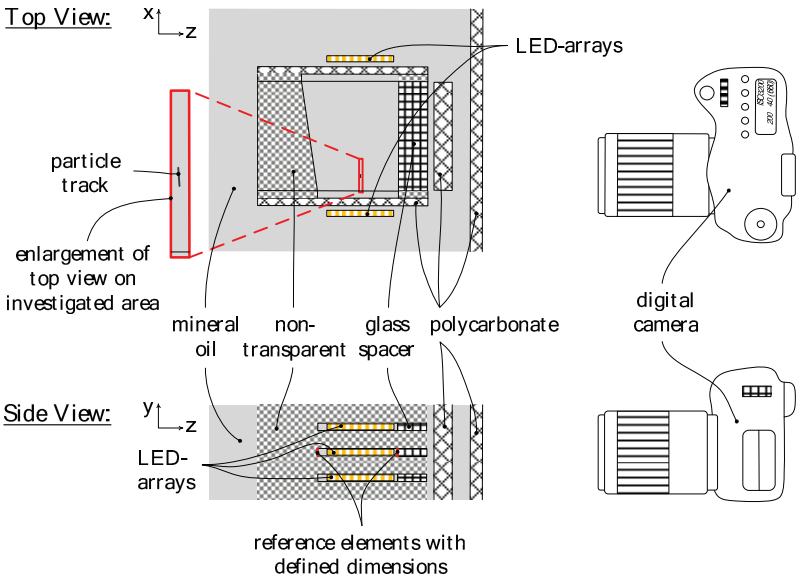


Figure 4. Experimental setup of the optical analysis.

As demonstrated in Figure 5, the analysed area is also limited in the *y*-Dimension to the inner third of the horizontal channels and in the *x*-Dimension to the exit location of the oil inside the horizontal channels. For that reason, only particles inside a volume of approximately 20 mm × 2 mm × 6 mm ($x \times y \times z$) were analysed within each channel. This restriction is necessary since the oil flow velocities are not expected to be homogeneously distributed. Consequently, the investigated area should be as small as possible. However, since the velocities might also fluctuate over time due to effects of turbulences, a certain number of particle tracks need to be considered for each investigated area. Since the number of particles captured on photograph inside a certain area is directly dependent on the size of the investigated area, a compromise between restricting the investigated area and the resulting number of available particle tracks recorded for post analysis had to be made.



Figure 5. Example of a photograph of particle tracks with contrast enhancement and enlargement of the investigated area in the taken pictures and further enlargement of one particle track.

ISBN 978-84-617–9183–5

III. Results of the Optical Analysis Comparing with CFD Calculations

After determining the particle velocities in a certain channel at specific operating condition, the gathered data is further post-processed. To illustrate this process, Figure 6 shows the distribution of measured particle velocities in channel 6 at the defined operating conditions in the context of an idealized Gaussian distribution function. Since this distribution function appears suitable for the collected measurement data, it is applied for the post-processing of the experimental results. Figure 7 gives the results at specified operating conditions in pass 1. Next to the averaged, minimum and maximum values the displayed boxes illustrate the amount of scattering experienced during post-processing the measurements. For that purpose, the boxes enclose the range of measured values comprising 80% of all conducted measurements according to a Gaussian distribution. It can be noted, that especially the first and last channel show a wider distributed velocity distribution within the investigated area.

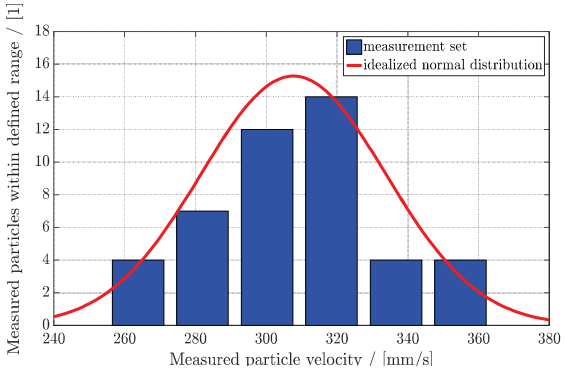


Figure 6. Distribution of measured velocities in channel number 6 of pass 1 at $\dot{m}_{oil}$ = 9.0 kg/s, ϑ_{in} = 40°C and P_{loss} = 8 W with illustration of an idealized distribution according to a Gaussian distribution function.

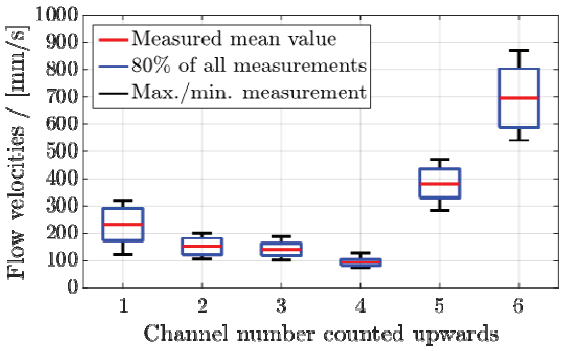


Figure 7. Distribution of the determined oil flow velocities in pass 1 at $\dot{m}_{oil}$ = 18.0 kg/s, ϑ_{in} = 80°C and P_{loss} = 8 W including the average.

While the experimental determination of the oil flow distribution is extensive, the corresponding numerical data can be extracted from the CFD-result files. Since the numerical models apply turbulence models [3, 4], only the averaged values of the oil flow velocities are suited for comparison. Figure 8 shows the comparison of the experimental results and numerical post analysis at various operating conditions in pass 1 of the winding model. In addition to the numerical results at the exact location the optical measurements were conducted, the respective numerical data at ±5 mm in the z-Dimension are given as well. This should show how the oil velocity can vary within a duct. Especially in the first channel the analysed location is of great influence on the determined velocity. This can be attributed to separation eddies at the duct entrance (see Figure 9). The measured mean values agree impressively well with the numerical results in middle position at all operating conditions.

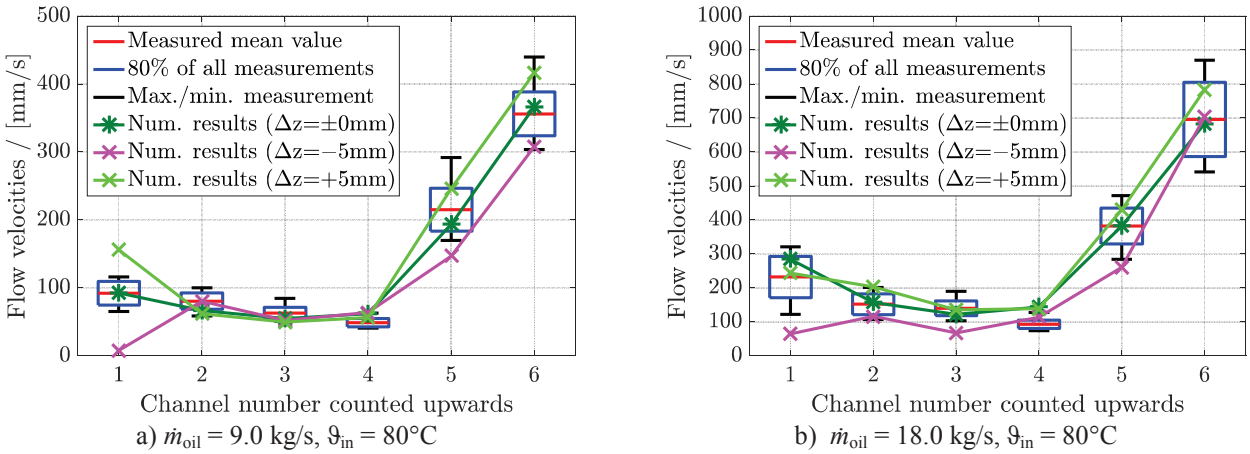


Figure 8. Comparison of measured and calculated mid channel velocities in pass 1 with oil going through widening horizontal channels of the experimental model at various oil flow rates and inlet temperatures at P_{loss} = 8 W.

ISBN 978-84-617–9183–5

Since the thermal investigation showed great agreement between experimental and numerical results [3] and the respective results for the oil flow velocities are also in good agreement, the numerical results for the oil flow distribution are consequently also assumed to be valid.

In order to investigate the reason for the uneven distribution of oil velocities Figure 9 shows the streamlines of the oil flow for a flow rate of 9 kg/s. It gets obvious that separation eddies are blocking a portion of the entrance for horizontal channels, especially at the lower region, because the oil washer equipped at the top prevents oil flowing up, effectively forcing them turn to the horizontal channels, and thus the eddies at these channels are largely suppressed. Mainly the flow in the ducts at lower position is getting very small and can even turn to backflow. In Figure 10 the maximum oil velocity in the middle of each horizontal channel of pass 2 and the hot spot temperature of the respective disc are shown. The velocity is proportional to the oil mass in the channels. The distribution of oil onto the horizontal channels is visibly asymmetrical for both flow rates. Most of the oil flow (app. 70%) passes through the top two ducts. This is what was indicated by the streamline plot in Figure 9, in which it got visible that separation eddies are blocking the lower ducts of the pass in the case with such a high flow rate. It is therefore obvious that simple decomposition of the pass into primitives as straight channels, branches and confluences, as it is done by means of thermal network models, is only applicable for low Reynolds Numbers [5, 6]. Due to the higher oil velocity in the upper channels the cooling of these turns is improved and the hot spot occurs in the lower turns of the pass.

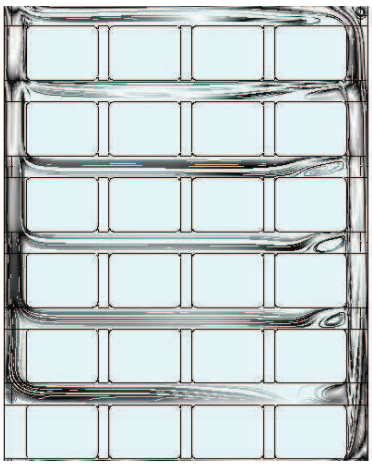


Figure 9. Streamlines at a flow rate of $\dot{m}_{oil}$ = 9.0 kg/s.

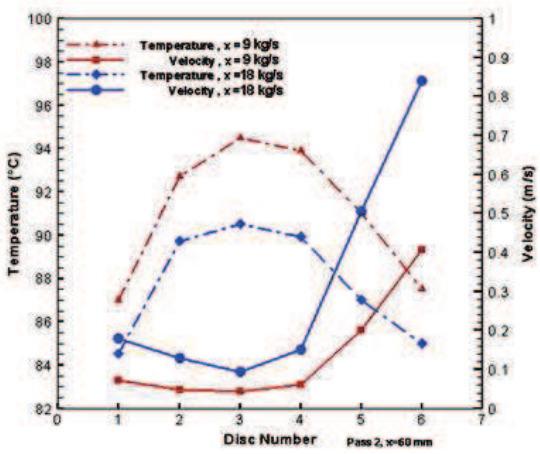


Figure 10: Velocity of oil flow and hot spot temperature for flow rates of $\dot{m}_{oil}$ = 9.0 kg/s and $\dot{m}_{oil}$ = 18.0 kg/s.

IV. Conclusion

In this contribution the oil speed in horizontal ducts of an OD cooled winding is investigated by experimental and numerical methods. The presented winding model offers insight into the horizontal cooling channels perpendicular to the main oil flow direction. The optical investigation of oil velocities confirmed the suitability of 3D numerical winding models to calculate the thermal behaviour accurately. The comparison between the experimentally determined oil flow velocities showed a good agreement with the corresponding numerical data. The investigation indicated a strong inhomogeneous oil flow distribution on the horizontal channels. The presented results give a deep insight into the oil flow and temperature behaviour of windings enabling the designer to optimize the cooling of power transformer windings.

References

[1] A. Skillen, A. Revell, H. Iacovides and W. Wu, *Numerical Prediction of Local Hot-spot Phenomena in Transformer Winding*, Applied Thermal Engineering, 36(2012)96-105.

[2] P. Picher, F. Torriano, M. Chaaban, S. Gravel, C. Rajotte, B. Girard, *Optimization of transformer overload using advanced thermal modelling*, CIGRE 2010, Paris, A2-305.

ISBN 978-84-617–9183–5

[3] S. Tenbohlen, N. Schmidt, C. Breuer, F. Devaux, R. Lebreton, T. Stirl, *Evaluation of the Thermal Performance of Transformer Windings by Numerical Investigations and Measurements*, CIGRE 2016, Paris, A2-309.

[4] F. R. Menter, *Two-Equation Eddy-Viscosity Turbulence Models for Engineering Applications*, AIAA Journal 32 (8): 1598–1605, August 1994.

[5] J. Zhang, X. Li, *Coolant Flow Distribution and Pressure Loss in ONAN Transformer Windings. Part I: Theory and Model Development*, IEEE Transactions on Power Delivery, 2004, vol. 19, pp. 186-193.

[6] A. Weinläder, W. Wu, S. Tenbohlen, Z. Wang, *Prediction of the Oil Flow Distribution in Oil-immersed Transformer Windings by Network Modelling and CFD*, IET Electric Power Applications, Vol. 6, Issue 2, 2012.

ISBN 978-84-617–9183–5

Installation of 250 MVA Mobile Transformers as Strategic Reserve Units at REE (Red Eléctrica de España)

Ana AZNAR, Sergio QUINTÍN

Department of Substation Maintenance, REE (Red Eléctrica de España)
Paseo Conde de los Gaitanes 177, 28050 Alcobendas (Madrid), Spain
Phone: (+34) 916508500, e-mail: aaznar@ree.es ; squintin@ree.es

Abstract — **Transformers are critical components of HV transmission networks. Any outage, planned or accidental, means a long period till service recovery due to repair times and transportation difficulties (given their dimension and weight).**

As an efficiency measure to guarantee the power supply through the whole HV grid, REE (Red Eléctrica de España), the system operator in Spain, has three 400 kV (250 MVA) mobile ("fast-deployable") transformers with hybrid insulation as strategic reserve units, which allow to reduce both the downtime in case of failure and the associated costs.

This paper presents the definition process of these strategic reserve units as well as the advantages of this solution describing two real cases.

Keywords — **power transformer, mobile transformers, fast-deployable, strategic reserve units**

I. INTRODUCTION

REE is the Spanish transmission system operator, managing a fleet of 345 transformers. Of these, 252 are single-phase transformers and 93 are three-phase transformers.

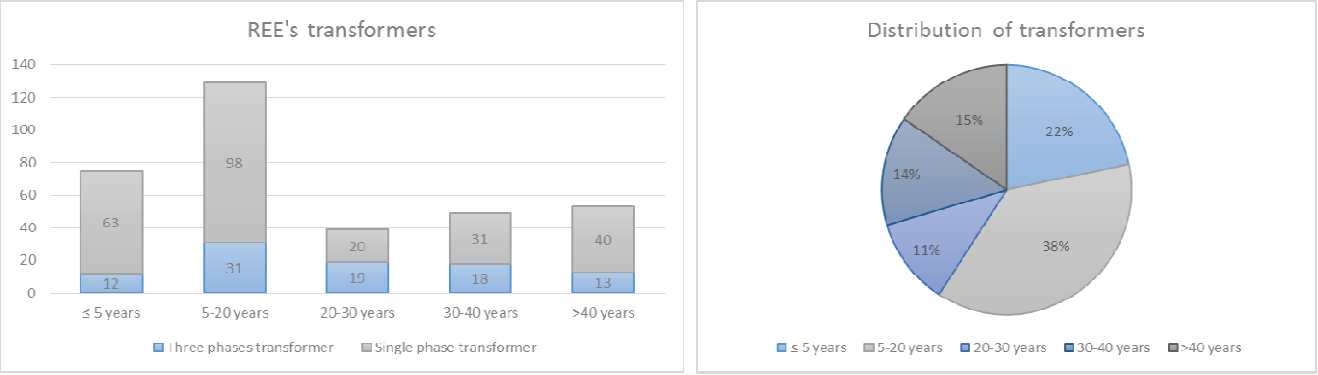


Figure 1. REE's transformers and distribution by age.

Given the number of units under management and their age, it is necessary to define a strategic plan that includes reserve units for emergency situations and brings drivers of economic and technical efficiency.

II. BACKGROUND

REE was founded in 1985 as the first TSO (Transmission System Operator). Consequently, many of its assets belonged and came from the companies that were responsible for the HV transmission networks till that year, providing a very heterogeneous fleet of transformers.

Moving forward, REE established a strategy for the homogenization of the fleet, with the goal of standardising the transformer design for all new acquisitions as an additional measure of efficiency:

ISBN 978-84-617–9183–5

- Standardisation and development of 200 MVA single-phase transformers: A technical specification has been developed containing all electrical and design parameters, and must be followed in the purchase of transformers. All new transformers, both for new substations and for replacement of older ones, have to comply with this norm. This means that transformers from different manufacturers are electrically compatible and interchangeable, facilitating the substitution of units in case of failure without altering the operating conditions.

Table I. 200 MVA Standard Single-Phase Transformer Characteristics

HV winding	LV winding	Tertiary winding	Rated power	Frequency	Vector group
400 kV	230 ±15% kV	33-26.4-24 kV	200 /200/40 MVA	50 Hz	YN, a0, d11



Figure 2. 200 MVA standard single-phase transformer.

- Standardisation and development of the 500 MVA poly-transformer (2004-2012): Although REE prefers the single-phase transformer over the three-phase one due to its dimensions and cost of repair, there is a significant number of three-phase transformers installed. The poly-transformer was defined as the corresponding strategic reserve unit for these three-phase transformers. In order to cover the maximum number of compatible units, it was designed with the possibility of three levels of LV.

Table II. 500 MVA Standard Poly-Transformer Characteristics

HV winding	LV winding	Tertiary winding	Rated power	Frequency	Vector group
400 kV	230 +3,5% -3,8 % kV 138 + 9 % - 9,8 % kV 110 +12,7 % - 13,5 % kV	33-26.4-24 kV	500/500/60 MVA 350/350/60 MVA 280/280/60 MVA	50 Hz	YN, a0, d11

ISBN 978-84-617–9183–5



Figure 3. 500 MVA standard poly-transformer.

- Development of the 400 kV (117 MVA) mobile ("fast-deployable") transformer (2008-2009): The main problem in case of failure, for either the single-phase or the three-phase transformer, was the transportation of the transformer itself, both in terms of time and cost. To deal with this problem, REE defined the necessity of a transformer of reduced dimensions and weight which could be transported without special conditions. This transformer was designed and manufactured by ABB with the following characteristics:

Table III. 400 kV (117 MVA) Mobile Transformer Characteristics

HV winding	LV winding	Tertiary winding	Rated power	Frequency	Vector group
400 kV	230 kV 138 kV	33-26.4-24 kV	116,66/116,66/15 MVA 65/65/15 MVA	50 Hz	YN, a0, d11

- Developed of 400 kV (250 MVA) mobile ("fast deployable") transformer with hybrid insulation (2010-2013): The first mobile transformer's power was conditioned by the dimensions and weight required for shipping; in this case the bank power was limited to 351 MVA, which means 58.5% of standardised 600 MVA REE substation's capacity (200 MVA per phase). Thus, if one phase had to be replaced it was necessary to install two units in parallel.



Figure 4. Two 400 kV (117 MVA) mobile transformers installed in parallel.

ISBN 978-84-617–9183–5

The need of a mobile transformer of higher power was the reason to develop the 400 kV (250 MVA) mobile transformer with hybrid insulation.

Table IV. 400 kV (250 MVA) Mobile Transformer with Hybrid Insulation Characteristics

HV winding	LV winding	Tertiary winding	Rated power	Frequency	Vector group
400 kV	230 kV 138 kV 110 kV	33-26.4-24 kV	250/250/30 MVA 120/120/30 MVA 110/110/30 MVA	50 Hz	YN, a0, d11

- Development of three-phase power transformers with dissociated phases (2012 -2103): This is a three-phase transformer where phases are dissociated, which means easier transportation and repair in case of failure. These units were defined to replace the three-phase transformers in the substations where it wasn't possible to substitute them for a bank of three 200 MVA standard single-phase transformers due to lack of space.

Table V. Three-Phase Power Transformer with Dissociated Phases Characteristics

HV winding	LV winding	Tertiary winding	Rated power	Frequency	Vector group
400 kV	230 ± 8% kV	33-26.4-24 kV	Sp (*)/Sp (*)/40 MVA	50 Hz	YN, a0, d11

(*) Sp: 150 or 200 MVA depending final substation



Figure 5. Three-phase power transformer with dissociated phases installed in REE.

ISBN 978-84-617–9183–5

III. DESCRIPTION OF THE 400 KV (250 MVA) MOBILE TRANSFORMER WITH HYBRID INSULATION

The development of the 400 kV (250 MVA) mobile transformer with hybrid insulation was a R&D joint project between REE and the manufacturer ABB, which arose from: 1) the need defined by REE of a transformer of reduced dimensions and weight but high rated power for its contingency plans, and 2) ABB's knowledge in transformer manufacturing, materials, technology and design.

The solution offered to reduce dimensions and weight was the use of high-temperature insulation materials, which allow to operate at higher temperatures without degradation, becoming the oil the limiting factor. This type of insulation is a well-known concept, widely used up to 245 kV, but its application to 400 kV required additional changes as there weren't any references in the world so far.

The main parameters of the final design are the following [1]:

- Single phase autotransformer
- Core construction: shell type
- Outdoor type for continuous service
- Rated voltage:
    - HV winding: 400 kV
    - LV winding: 220-138-110 kV (polytransformer)
    - Tertiary winding: 33-26.4-24 kV
- Rated power: 250 MVA at 230 kV, 120 MVA at 138 kV and 110 MVA at 110 kV.
- Frequency 50 Hz
- Vector group: YNa0d11 (for a three-phase bank)
- Cooling: ODAF
- Temperature rises:
    - Top oil: 60ºC
    - Average winding: 95 ºC
    - Hot spot winding: 120 ºC

Being a development based on a new design, a live temperature-capture system (optic fibre) was added to the transformer to monitor the hot spot as well as a complete monitoring system (DGA, temperatures, currents, cooling system, etc.) to check the correct thermal and dielectric operation.



Figure 6. 400 kV (250 MVA) mobile transformer with hybrid insulation.

ISBN 978-84-617–9183–5



Figure 7. conventional transport of the 400 kV (250 MVA) mobile transformer.

IV. PLACEMENT AS STRATEGIC RESERVE UNITS

As important as the definition of these transformers' design parameters is their location as strategic reserves to optimise the time to restore service. The process for defining the best location was as follows:

- Carrying out a study of electrical compatibility of the fast-deployable transformer with REE's fleet of single-phase transformers to determine the number of units serving as reserve. The peculiarity of having different secondary voltages gives us greater flexibility, proving to be compatible with 195 units, i.e., 77% of single-phase transformers. Three-phase transformers weren't included because their strategic reserves are poly-transformers.
- The 50 most critical transformers of these compatible units were selected, eliminating those that already had a reserve unit at the substation. Two main concepts were taken into account for this estimation of criticality: state and condition of the transformer (which define the probability of failure) and the impact in the operation in case of failure. Furthermore, we have evaluated the age and the probability of failure by historical fault on older transformers with the same construction characteristics.
- Those transformers with scheduled maintenance that need a reserve unit to minimise downtimes were included in the list of critical units. On the other hand, the transformers whose replacement is already planned according to our strategic renewal plan were removed from this list. In addition, those locations which permit maximum utilisation of transformers' capacity were prioritised for the installation of the mobile transformer.
- Using the final list of critical transformers compatible with the mobile transformer, four areas were selected where the density of critical transformers was high. At the time of the study only three mobile transformers were available, so only three areas were chosen: those with higher distance in case of not having reserve units.
- In order to find the optimal substation for each area both shipping criteria and space availability were taken into account. Mobile transformers are stored completely assembled and filled with oil, so a preliminary selection included locations where space was available considering the transformer's dimensions and weight and the container for components. Preference was finally given to those with an available oil pit, but this was not a limiting factor because each unit is provided with a collecting oil tray to avoid possible spills.

ISBN 978-84-617–9183–5



Figure 8: areas with high concentration of critical transformers

V. CASE 1

The first 400 kV (250 MVA) mobile transformer was used to perform the overhaul of three units in a bank (ATP1) with the following electrical characteristics:

Table VI. Electrical Characteristic of the Old Bank

HV winding	LV winding	Tertiary winding	Rated power	Frequency	Vector group
400 kV	230 ±15% kV	33-26.4-24 kV	150/150/50 MVA	50 Hz	YN, a0, d11

Due to the age of such units (dating from 1972), refurbishment was mandatory to ensure service under reliability and safety conditions.

The required time for the reconditioning of each unit was 20 days, which implied an outage time for the bank of 60 days. In order to reduce such downtime it was decided to install the fast-deployable transformer replacing one phase. This phase was reconditioned first and then used to replace the next unit, and so on to have the three units finished. The length of each change was 7 days, only 21 days in total.

At Operation level it was necessary to establish the functioning implications and limitations as a result of replacing one 150 MVA unit in the bank with the 250 MVA mobile transformer, because it created an imbalance in the phase currents of both the transformer and the elements connected to 400kV and 200kV due to its different power and design compared to the original units.

The calculation of the resulting imbalance in the ATP1 and ATP2 substations banks was made on different taps of the ATP1, with different loads and peak and valley scenarios. It was concluded that the operation under this configuration was feasible with the following limitations:

- Preferential tap of the tap changer must be specified to minimise the imbalance and possible margin of taps that can be used.

ISBN 978-84-617–9183–5

- The 150 MVA units limit the unbalanced operation of the ATP1. Overcurrent restriction is imposed on the side of HV, which implies not exceeding 75% of the 450 MVA assigned to the ATP1. The mobile unit does not limit the operation.
- Changes in the protection settings in order to work correctly with this unbalanced operation.



Figure 9: 400 kV (250 MVA) mobile trasnformer installation

The time that the mobile transformer was in service allowed, thanks to the monitoring system installed, to confirm its correct operation and thus to validate this new design.



Figure 10: 400 kV (250 MVA) mobile transformer installed instead of a 400 kV (150 MVA) single-phase transformer

ISBN 978-84-617–9183–5

VI. CASE 2

In Brovales substation, owned by REE, an incident in the ATP1 bank took place in April 2016, causing the bank outage because of a short circuit in the tertiary of phase 0.

The fault involves disassembling the transformer and transporting it to factory to determine the scope of the failure and the corrective actions.

The estimated length for in-factory repair ranges from 5 months (assuming only tertiary winding is affected) to 7 months (assuming also HV/LV winding is affected). To restore the service as soon as possible it is decided to replace phase 0 by the mobile transformer reserve of its area during the reparation period.

The failed transformer is a 200 MVA standard REE unit so the 400 kV (250 MVA) mobile ABB transformer is electrically compatible to work with the other two units from another manufacturer. In this case, unlike the previous one, the transformers were electrically identical so it was not necessary to establish any limitation on operation, except for the fact that the regulation is disabled given that the mobile transformer doesn't have a tap changer because of dimensional reasons.

The following figure shows a comparison among the outage times associated with the replacement of the transformer according to different alternative solutions:

- Use of mobile ("fast-deployable") reserve unit.
- Completion of faulty transformer repair.
- Acquisition of a new transformer.

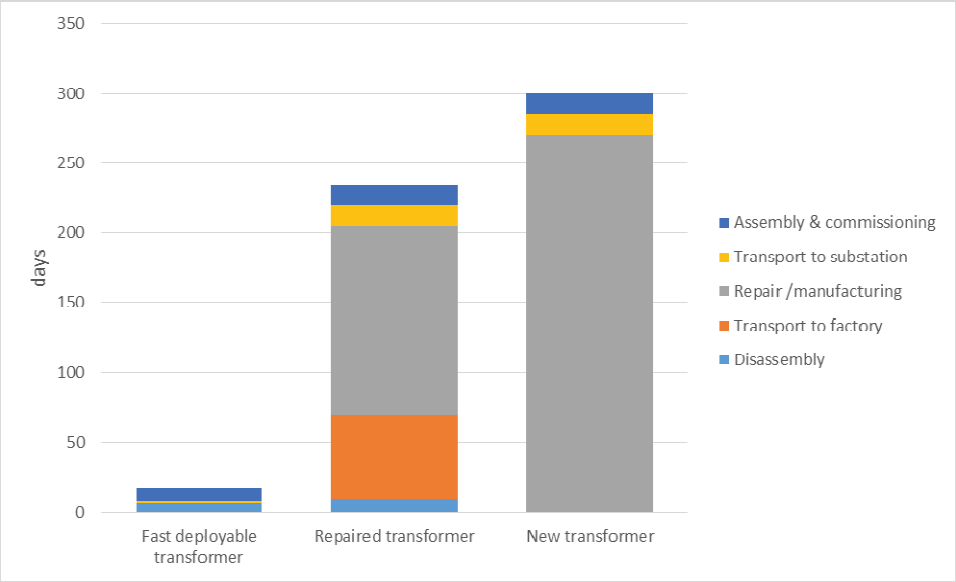


Figure 11: comparison of outage time for the different solutions

This figure shows that transportation and repair or new manufacturing are the activities that consume more time. In the transportation case, this is due to the procedure to obtain special-transport authorization and the restrictions on the circulation of such special transport. In the case of repair or new manufacturing, it involves adjusting these works within the factory schedule, which means dependence of the manufacturer. By providing mobile transformers as a strategic reserve the manufacturer dependency disappears and special-transport authorization is not required.

In this case, the service has been restored in 2 months and 11 days; this time includes not only the transformer's

ISBN 978-84-617–9183–5

replacement but the whole process from transformer's trigger until the service is restored (internal field inspection, decision making for service replacement, engineering for new transformer adaptation, safety study, etc.). The use of the mobile transformer has reduced the outage time by 65%.



Figure 12: 400 kV (250 MVA) mobile transformer installed instead of a 400 kV (200 MVA) single-phase transformer

VII. CONCLUSIONS

With its strategic plan to guarantee the service, REE identified the need of having single-phase transformers with reduced dimensions and weight to serve as a strategic reserve and thus cover any type of incident within its fleet of transformers, reducing downtimes and costs in case of failure. This transformer was developed in a joint project with ABB, being the first reference worldwide of a hybrid-insulation transformer up to 400 kV.

The use of this transformer, both in the case of bank's refurbishment because of maintenance and in the case of failure, has allowed to validate the new design and to confirm the advantages of this solution for the efficient management of a fleet of transformers.

REFERENCES

[1] M. Cuesto, M. Oliva, A. Prieto, J.C. Sanchez and L. Navarro, *Fast-deployable HV network transformer with hybrid insulation: a solution against major events,* 54-PS3 CIGRE2013.

ISBN 978-84-617–9183–5

Transformer Maintenance Planning through Continuous Insulation Condition Monitoring

Laurentiu-Viorel BADICU[1], Wojciech KOLTUNOWICZ[1], Victor Lozano SANCHEZ[2], Boris BATLLE[2]

[1]OMICRON Energy Solutions GmbH, 5 Lorenzweg, Berlin, Germany
[2]OMICRON Technologies, Calle la Caléndula, 93, Edificio L, 28109 Alcobendas, Madrid, Spain
Phone: (+49) 3031160985143, fax: (+49) 3031160985104, e-mail: laurentiu-viorel.badicu@omicronenergy.com

Abstract — **The maintenance and operation recommendations based on the results obtained from continuous monitoring on two identical old transmission transformers are presented. The 130 MVA 230/115 kV transformers have been in service in similar load conditions for more than 40 years. A monitoring system for bushings and active part insulation was installed on these transformers. Additionally, oil sampling for lab DGA was performed. The monitoring data was processed to obtain an Insulation Health Index value, which is a number indicating in this case the poor condition of the insulation systems. This information triggered a detailed monitoring data evaluation in order to find the potential defect type and its location – information not provided directly by the Insulation Health Index algorithm.**

Keywords — **power transformers, on-line monitoring, partial discharge, insulation health index**

I. INTRODUCTION

CIGRE recently published a technical brochure in which 964 major transformer failures occurring between 1950 and 2009 are analysed [1]. Transmission and distribution transformers, as well as shunt reactors and generator step-up transformers (GSU), were considered in this analysis. Their overall failure rate was within 1%. Only GSU units in the voltage class from 300 kV to 500 kV exceeded this 1% failure rate. Dielectric failures were the most significant in all transformer classes (Fig. 1) [1]. The windings, bushings and lead exits are affected by this failure mode.

The maintenance resource allocation should be done after a careful transformer fleet analysis. Fig. 2 indicates a group of activities that need to be undertaken in order to identify transformers subjected to failure that require either immediate actions or to be included in a medium-term maintenance plan. The main activity is the calculation of an Insulation Health Index (IHI). The IHI is a single value from 0 % (highest failure probability) to 100 % that indicates the overall dielectric condition of the transformer taking into consideration the most relevant diagnostic indicators [2-3].

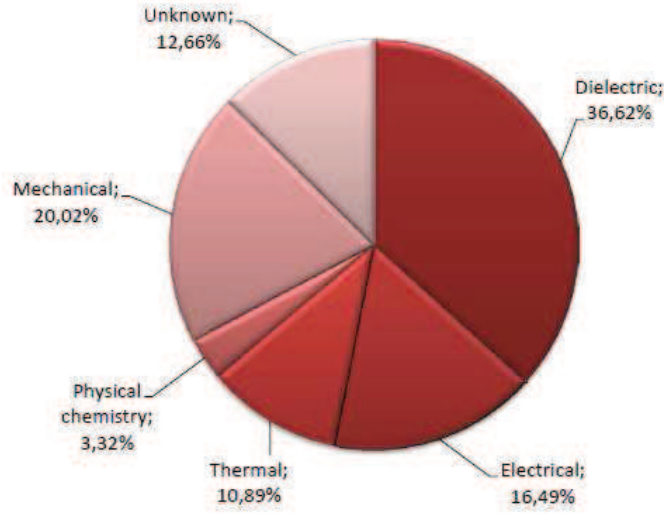


Figure 1. Failure mode analysis based on 964 major failures.

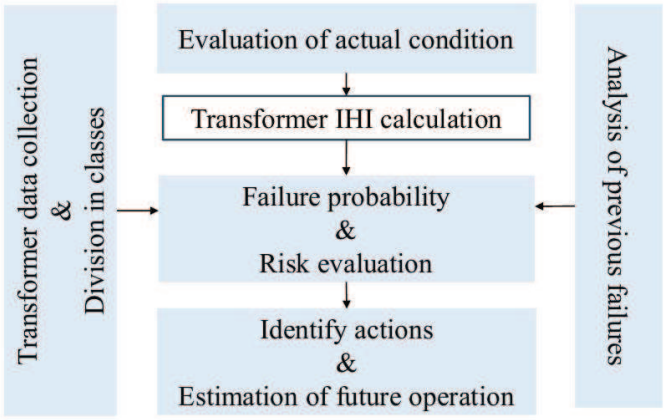


Figure 2. Transformer fleet management approach.

ISBN 978-84-617–9183–5

Information related to the transformer rated voltage, its design and other historical data coming from the unit under consideration or any other identical units need also to be considered. In the case of large transformer fleets, the use of IHI will give the asset manager the possibility to identify the units with the highest failure probability and prioritize the actions and investments. This powerful tool represents just a stage of a process to increase the transformer operation reliability, as indicated in Figure 2, and is especially useful when comparing the dielectric condition of the transforms belonging to a similar class (of rated voltage, power, manufacturing year, type, designated use, etc.) that operate in similar conditions and environments. The difficulty increases when two transformers show similar (critical) IHI values, but the input data indicates the presence of different defects. This is an issue addressed by this paper, as well.

II. TRANSFORMERS UNDER INVESTIGATION

The monitoring system was installed on two identical transformers T1 and T2 (Fig. 3 and Table I). In particular, the partial discharges (PD), dissipation factor (DF) and capacitance (C) of the bushings insulation as well as PD of the active part were monitored. The monitoring system architecture is presented in [4]. The transformers are operated by the same utility, in similar load conditions. T1 – in service since 1967 – was relocated in 1984 from one substation to another, and in 1993 the active part was rewound. Further, in 2005 the oil reclamation was done and in 2010 the bushing of phase U was replaced because of the bad condition of its insulation system. Transformer T2 – in service since 1973 – has not undergone any major revision, only regular tap changer maintenance and replacement of some fans motors and gaskets were done instead.



Figure 3. One of the transformers under monitoring.

Table I. Name Plate Data of the Transformers

Type	Free breathing transmission transformers
Power [kVA]	130000
Nominal voltage HV [V]	230000
Nominal voltage LV [V]	115000
Nominal current HV [A]	326.5
Nominal current LV [A]	652.5
Connection group	Yy0/d5
Cooling system	OFAF

III. TRANSFORMERS CONDITION ASSESSMENT

For both transformers, the IHI values of the bushings and active parts were calculated (Fig. 4) according to the procedure presented in [5]. For both transformers, the IHI values of the bushings are above 76%, while for the active parts the IHI values are 27 % (T1) and 41 % (T2) respectively. According to [6], the IHI values indicate that T1 can no longer be safely operated while T2 needs further investigations to derive proper condition-based maintenance actions.

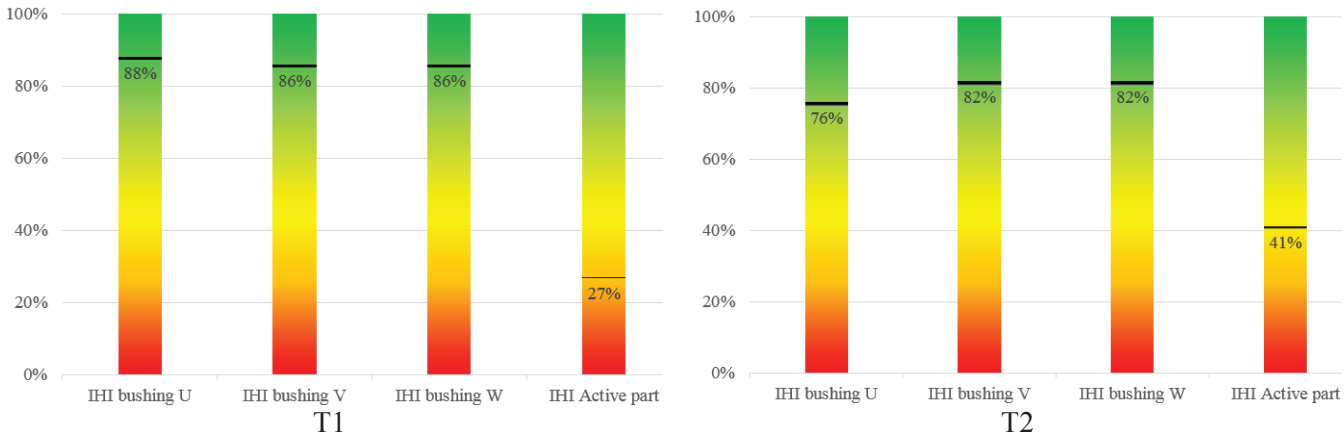


Figure 4. IHI values for bushings and active parts of the transformers under investigation.

ISBN 978-84-617–9183–5

Partial discharges

The PD activity was monitored for both transformers based on the conventional method (at the bushing measuring taps) and unconventional ultra-high frequency (UHF) method (by placing a sensor inside the transformer tank). These methods have a complementary character. The conventional type measurements indicate the defects in both bushing and winding insulation, while the UHF measurements are only sensitive to detect winding problems.

Conventional PD monitoring

The PD signal was synchronously detected at the measuring tap of each bushing via a special coupling unit. It includes several levels of redundant over-voltage protections and the measuring tap is automatically grounded when the communication with the acquisition unit is interrupted. After installation, the PD system was calibrated for different measuring frequencies and bandwidth, so no further calibration is needed even if the frequency of the measurement is changed during monitoring. Traditional phase-resolved PD (PRPD) patterns are recorded and used for detailed data evaluation (Fig. 5) as well. This helps to identify the PD defect type and gives its rough location. The PRPD patterns are complex with overlapped signals from different PD sources (Fig. 6). In order to separate clusters of different PD sources and noise, a synchronous multi-channel PD evaluation technique is applied – 3PARD [7]. The separation between multiple PD sources and noise based on 3PARD can be both manually (T1) and automatically (T2) applied.

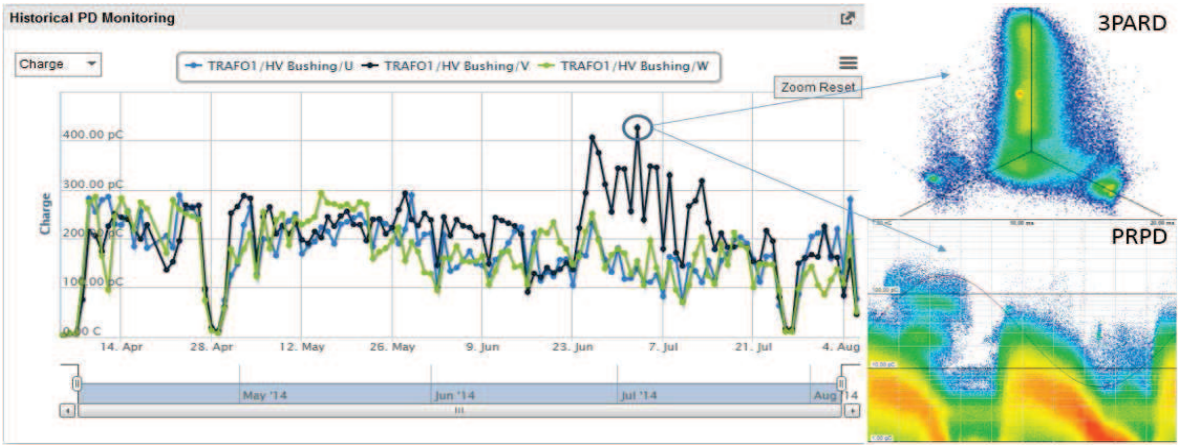


Figure 5. Three phase PD trend.

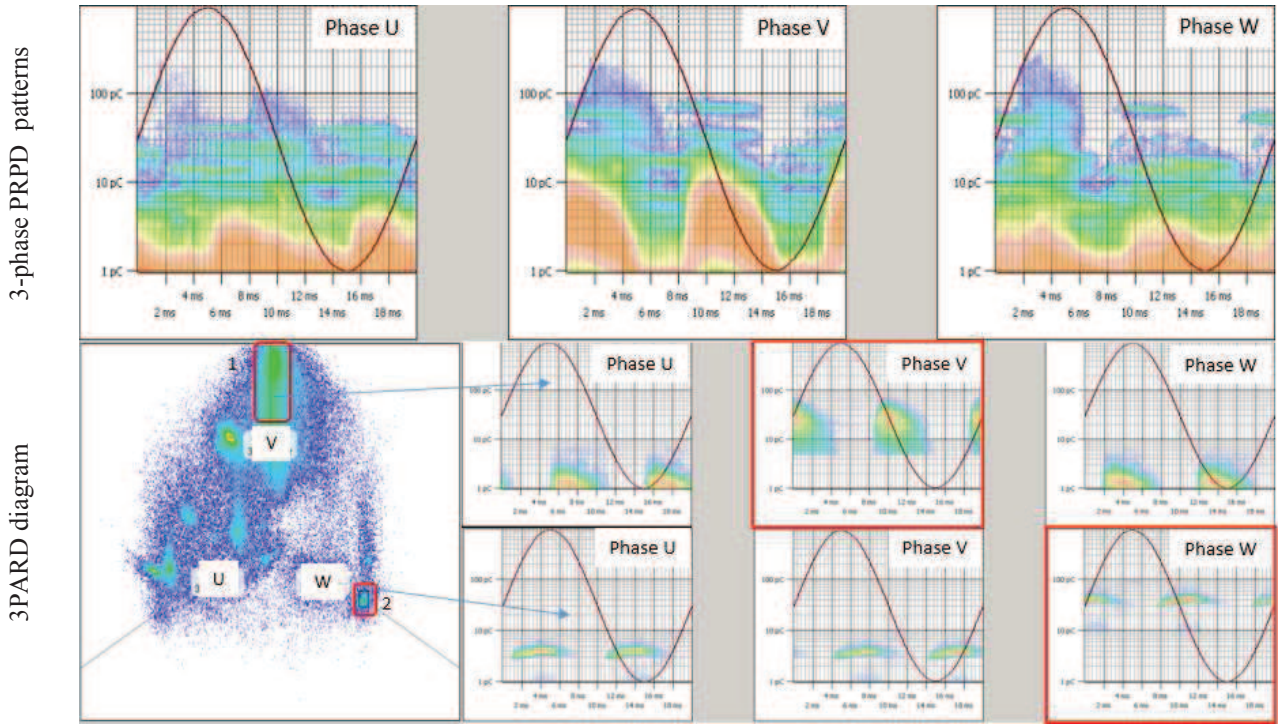


Figure 6. Separation of PD sources using 3PARD.

A detailed analysis of the 3PARD diagram of T1 is presented in Fig. 6. By selecting each cluster, a separation between noise and PD signals is possible. The back transformation to PRPD patterns of clusters 1 and 2 is also presented. The pattern of the cluster 1 indicates the presence of PD activity at the phase V of the transformer. The highest amplitude of the signal is detected at the phase V, but signal cross talk to the phase U and W is also visible. The PRPD pattern of cluster 2 appears to be generated by PD activity in the vicinity of phase W. The other clusters visible in the 3PARD diagram are generated by external noise. An increase (by factor of 3) of the PD signal magnitude over the last three months of monitoring was noticed (Fig. 7), indicating the necessity of immediate maintenance. This is presented in chapter IV of this paper.

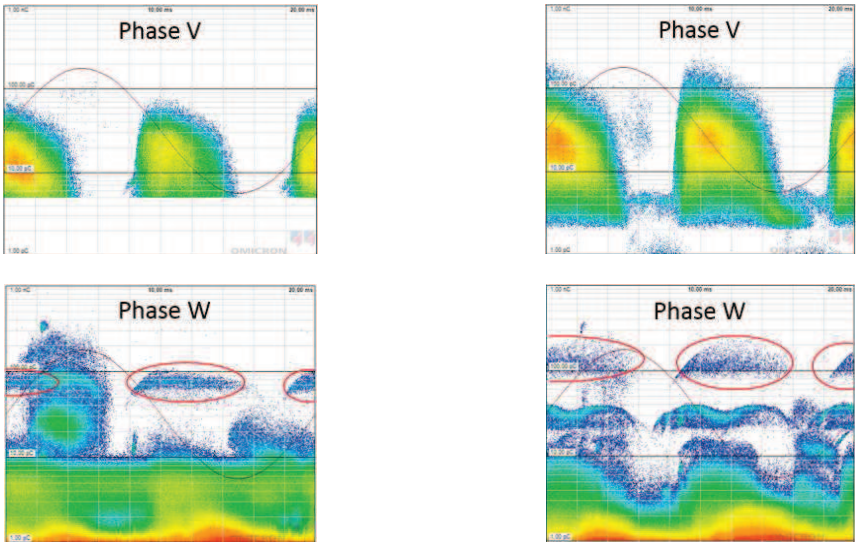


Figure 7. Increase of the PD pulse amplitude detected at the phases V and W.

For T2, the automated separation of the clusters in the 3PARD diagram was used. The Monitoring Software automatically performs cluster separation on a regular basis and whenever a warning level is exceeded (red triangles in Fig. 8 - left). For such a measurement, a PD data set (streams) with all significant data is saved for additional expert analysis or future comparisons. The back transformation to PRPD patterns is visualized by clicking on the identified clusters from the 3PARD. The cluster under investigation and the PRPD pattern of the signal origin will be surrounded by a red and blue rectangle respectively (Fig. 8).

A number of eight clusters were automatically identified and separated in the 3PARD diagram. Only two of them are generated by PD signals – located in the vicinity of the phases V (cluster 2) and W (cluster 8) – Fig. 9. Both sources of signals are intermittent and do not appear simultaneously. The presence of the PD signal at phase W had been identified since the monitoring system was installed and the amplitude remained constant. The PD signal of the phase V started being visible after a planned outage, when the transformer was reconnected to the transmission grid.

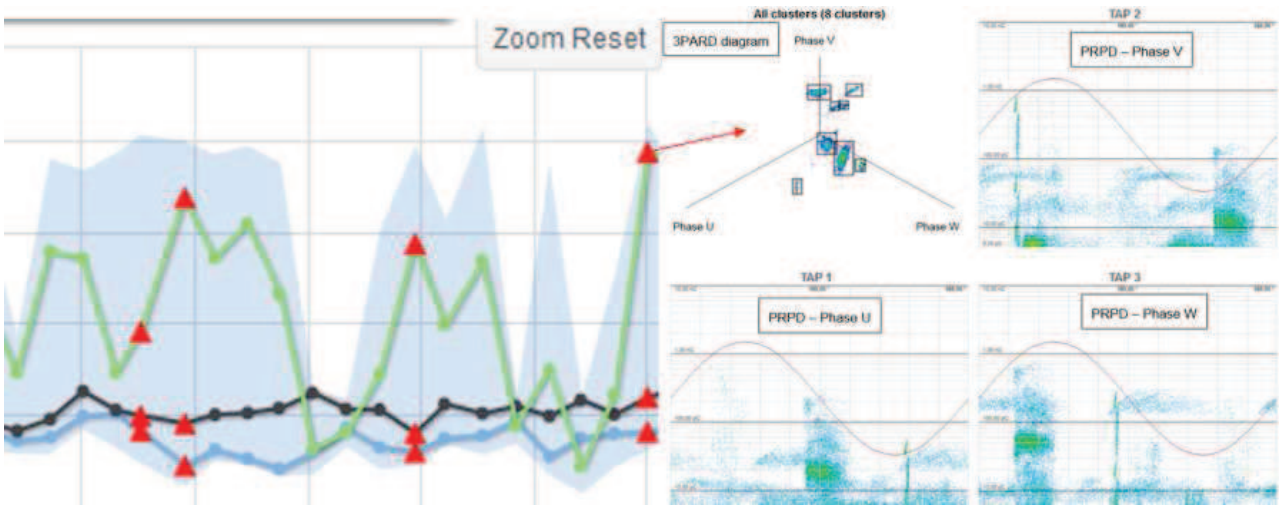
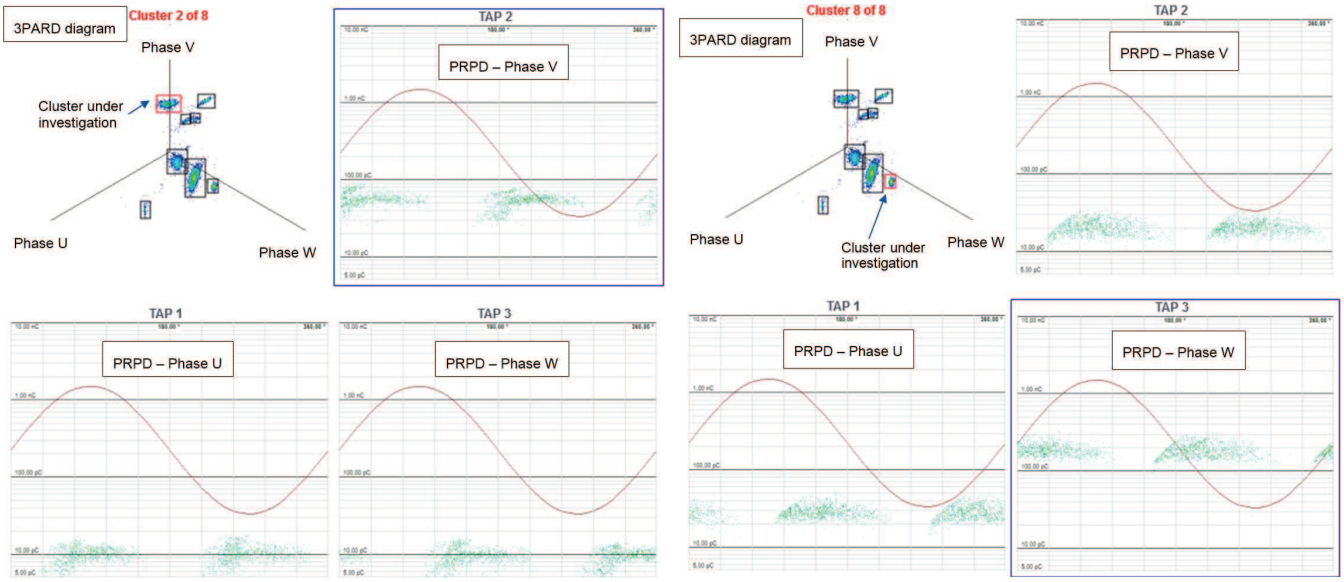


Figure 8. Automated PD and noise separation in the 3PARD diagram.

ISBN 978-84-617–9183–5



PRPD pattern of the PD signal at phase V PRPD pattern of the PD signal at phase W

Figure 9. Automated cluster separation with the identification of the signal origin phase (blue square).

Unconventional UHF PD monitoring

The UHF PD signal was measured in the frequency range from 0.1 to 2 GHz by antenna type sensors (one for each transformer) installed inside the tank. In order to gain more information about the frequency content of the UHF signal, off-line and on-line frequency sweeps were performed (Fig. 10). In the frequency sweep diagram, two spectra of the signal are shown. The upper spectrum is based on the maximum amplitude of the time domain signal acquired at each value of the frequency during the sweep. The lower spectrum corresponds to the minimum amplitude. PD activity is always visible on the upper spectrum while noise with external interferences, like e.g. corona discharge, radio waves, and GSM, are visible on both spectra. An off-line frequency sweep was performed during the installation of the monitoring system, while the transformers were de-energized. The off-line spectra gives information about the sources of interferences produced by other equipment in the substation. These sources are discarded when the analysis of the detected on-line PD signal is performed.

In case of T1, the on-line sweep indicates the PD activity in the frequency range from 450 to 650 MHz. An increase of the PD signal amplitude was noticed in the last two months of monitoring of T1. This was an indication of the continuous development of the defective area in the transformer. The pattern of the UHF PD signal is presented in Fig. 11 as well. Having the PD signal detected in the UHF range is a confirmation of the PD activity inside the transformer tank (excluding the bushings).

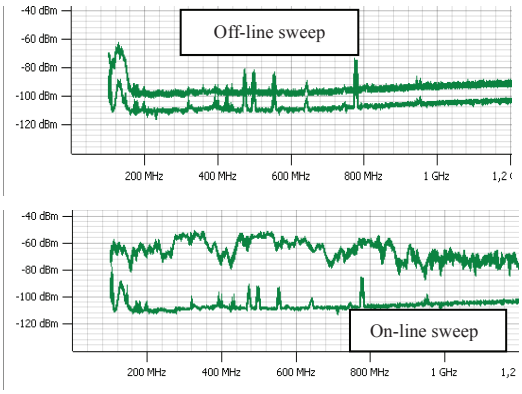


Figure 10. UHF signal spectra taken with the transformer in off- and on-line mode.

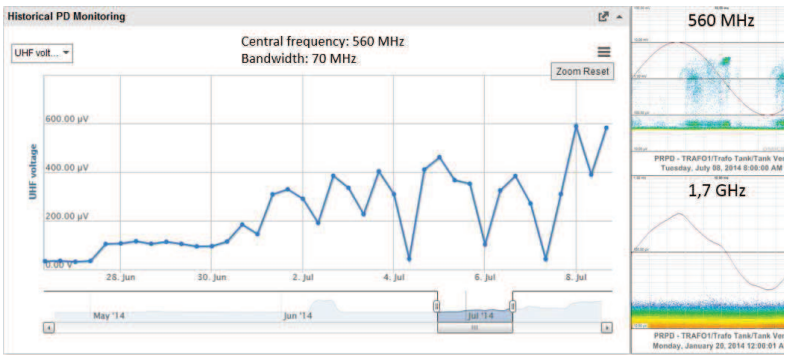


Figure 11. UHF PD trend and PRPD pattern of the PD signal (560 MHz) of transformer T1.

In case of T2, the intermittent character of the PD signal is confirmed by the UHF trend presented in Fig. 12. The measurements are performed at a central frequency of 280 MHz and a bandwidth of 650 kHz. The detected UHF signals were synchronized with the 50 Hz signal taken from the bushing measuring tap of phase V. This

ISBN 978-84-617–9183–5

enables the identification of the origin phase of the signals visible in the UHF PRPD pattern. The presence of the PD activity inside the transformer tank is confirmed. However, the trend is stable and no increase in the signal amplitude was recorded within the last year of monitoring of T2.

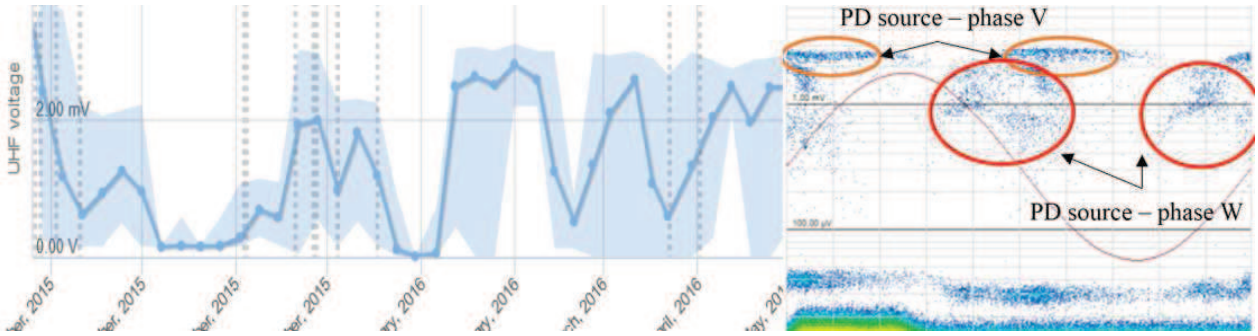


Figure 12. UHF PD trend (right) and PRPD pattern (right).

Dissolved gas analysis

In parallel with PD monitoring, regular oil sampling for DGA lab tests was performed (Table II). For T1, the increase of H_2 and CH_4 concentrations confirms the presence of the PD activity, while the increase of the CO concentration indicates the paper deterioration, probably as an effect of the on-going PD activity. The most popular DGA interpretation methods were applied in order to gain more information about the fault nature, but no agreement could be found between their results – especially in case of transformer T1 – Table III. The lack of result consistency is most probably caused by the presence of more on-going defects of different types.

Given their proven reliability [8], a deeper investigation of the DGA results based on Duval Triangles 1, 4 and 5 was performed. The theory behind these interpretation methods is clearly presented in [9]. For transformer T1, Triangle 1 indicates a mixture between a sparking electrical fault and a thermal fault, with more sparking formed in May 2014. This information is consistent with results of PD monitoring. From Delta values between May and June, Triangle 4 suggests overheating of oil in April-May, then suggests PDs in June with only H_2 produced. These PDs may have occurred in voids in the paper insulation. Triangle 5 suggests a hot spot in oil.

For T2, the lab DGA results are presented in Table II as well. In comparison with the gas pattern of T1, the presence of the "hot metal gases" can be noticed – C_2H_4 and C_2H_6. Duval Triangle 1 indicates the presence of a thermal fault in T3. Proceeding with the analysis as recommended in [9] and applying the Triangle 4 and 5 the thermal fault involving paper carbonization is indicated (confirming the presence of CO). The thermal heating of the paper is also confirmed by the values of CO2/CO higher than 10. The same interpretation is given by Dörnenburg ratios while Roger ratios indicates the presence of core and tank circulating currents – Table III.

Table II. DGA Results for Both Transformers

	Sampling date	H_2 (ppm)	CO (ppm)	CO_2 (ppm)	CH_4 (ppm)	C_2H_2 (ppm)	C_2H_4 (ppm)	C_2H_6 (ppm)
T1	Apr 2013	576	557	3821	150	11	116	19
	Apr 2014	433	416	3016	115	9	92	15
	May 2014	966	835	5952	226	21	179	32
	Jun 2014	1212	808	5797	225	21	171	30
T2	Dec 2014	187	865	9232	512	4	1148	274
	Mar 2015	157	863	9616	513	8	1134	274
	Jul 2015	216	879	9360	500	5	1050	263
	Jun 2016	118	989	10180	540	7	1076	290

Table III. Results of Popular DGA Interpretation Methods

Interpretation methods		Transformer T1	Transformer T2
Duval Triangles	Triangle 1	Mixture of sparking electrical fault and thermal fault (300 ºC < T < 700 ºC)	Thermal fault T3 (T > 700 ºC)
	Triangle 4	Oil overheating	Paper Carbonization
	Triangle 5	Hot spot in oil	Paper Carbonization
Roger's ratios		Fault not identified	Core and tank circulating currents, overheated joints
Dörnenburg's ratios		Fault not identified	Thermal decomposition
IEC ratios		Discharge of high energy	Thermal fault of high temperatures
Key gas		PD in the oil	Overheated oil and cellulose

ISBN 978-84-617–9183–5

IV. MAINTENANCE RECOMMENDATIONS

A summary of the findings for both transformers is presented in Table IV. Based on these facts, recommendations were given to the utility regarding the maintenance strategy.

In case of T1, acoustic PD localization was recommended to confirm the location of the PD source before conducting the internal inspection, which was also recommended. The crucial indicator of the transformer critical condition was shown by the strong increase of PD and H_2 levels within 3 months of monitoring. In the next step, the transformer was de-energized and just the bushing of phase V was initially dismantled for the internal investigation. PD activity traces around the phases V and W were found using an endoscope (Fig. 13). Having the proof of the on-going PD activity, the utility decided to lower the oil level and dismantle all other bushings for a detailed investigation. Off-line bushing C and DF measurements were also performed, confirming the results of the monitoring system. Several carbonization traces on the surface of the HV lead exits were found at phase V (Fig. 14) and phase W (Fig. 15). Carbonization traces were identified on the inner layers of the insulation, as well. After conducting the detailed internal investigation, the utility concluded that the transformer must not be returned to service as its safe operation is no longer guaranteed. Because a complete rewind of the active part would not be economically justified, the utility decided to replace the transformer T1 to prevent an in-service failure.

Transformer T2 – identical design with T1– shows intermittent PD activity at phases V and W. When it occurs, the amplitude of the signal of both PD sources is constant. The PRPD pattern of the signal detected at phase V may be the result of PD activity in the oil bubbles, which explains the presence of CH_4. The pattern shape and phase position of the PD pulses detected at phase W indicate the presence of a floating potential or a contact problem at the tap selector. This theory is also supported by the presence of C_2H_4 and C_2H_6, which indicate the oil decomposition around hot metals. Such a defect could be easily identified by performing a winding resistance measurements during the next planned outage.

Table IV. Recommendations of Maintenance Actions Based on Monitoring and Diagnosis Findings

<table>
<tr><th colspan="4">Transformer T1 (47 years of service)</th><th colspan="4">Transformer T2 (43 years of service)</th></tr>
<tr><td colspan="8">Insulation Health Index</td></tr>
<tr><td>Bushing U [%]</td><td>Bushing V [%]</td><td>Bushing W [%]</td><td>Active part [%]</td><td>Bushing U [%]</td><td>Bushing V [%]</td><td>Bushing W [%]</td><td>Active part [%]</td></tr>
<tr><td>88</td><td>86</td><td>86</td><td>27</td><td>76</td><td>82</td><td>82</td><td>41 %</td></tr>
<tr><td colspan="8">Monitoring and diagnosis findings</td></tr>
<tr><td colspan="4">PD monitoring:
- Defects in Phase V and W confirmed by conventional and UHF measurements
- PRPD pattern of surface discharge and discharges in gas bubbles
- PD trend increased by a factor of 3 over three months
- PD activity continuous</td><td colspan="4">PD monitoring:
- Defects in Phase V and W confirmed by conventional and UHF measurements
- PRPD pattern of floating potential, surface discharge and discharges in gas bubbles
- PD trend stable
- PD activity intermittent</td></tr>
<tr><td colspan="4">DGA measurements:
- Key gases: H_2, CO, CH_4
- PD defect (electrical sparking), thermal fault</td><td colspan="4">DGA measurements:
- Key gases: CO, CH_4, C_2H_4, C_2H_6
- PD defect, thermal fault with paper carbonization</td></tr>
<tr><td colspan="8">Recommended maintenance actions</td></tr>
<tr><td colspan="4">- Acoustic PD measurements to confirm the location of the defects.
- Internal inspection to assess the root cause of the steep PD level increase of the.</td><td colspan="4">- Acoustic PD measurements to confirm the location of the defects with a particular focus on the tap changer area.
- Winding resistance measurement to be performed at the first planned outage
- Keep under close observation</td></tr>
<tr><td colspan="8">Operation decisions</td></tr>
<tr><td colspan="4">Transformer to be replaced</td><td colspan="4">Transformer remains in operation</td></tr>
</table>

ISBN 978-84-617–9183–5



Figure 13. Preliminary internal inspection for defect location confirmation of Transformer T1.



Figure 14. Traces of PD activity at phase V of T1.



Figure 15. Traces of PD activity at phase W of T1.

V. CONCLUSIONS

- Insulation Health Index indicates the condition of the transformer, but it does not provide information about the location and type of the defects.
- The results from PD and DGA evaluation provide a complementary information about transformer condition.
- By combining conventional and UHF PD monitoring techniques, PD defects localization can be more accurately performed.
- A synchronous multi-channel PD evaluation technique (3PARD) enables effective separation between multiple PD sources and noise and can be performed automatically.
- Based on PD monitoring and DGA measurements the appropriate operation decisions can be taken.

REFERENCES

[1] "*Transformer reliability survey*", CIGRE Technical Brochure 642, December 2015.

[2] J. Vines, B. Banh, C. Stiegemeier, P. Patel, L.V. Cheim, „*Transformer Health in the Real World*" ABB Review – the Corporate Technical Journal, Issue 3, 2015.

[3] A.N. Jahromi, R. Piercy, S. Cress, J.R.R. Service, "*An Approach to Power Transformer Asset Management Using Health Index*", IEEE Electrical Insulation Magazine, Vol. 25, No. 2, pp. 20-34, 2009.

[4] L.V. Badicu, U. Broniecki, W. Koltunowicz, S. Körber, M. Krüger and E. Voegel, "*Prevention of transformer failure through continuous monitoring*", Proceedings of the 19th International Symposium on High Voltage Engineering, Paper 274, Pilsen, August 23-28, 2015.

[5] L.V. Badicu, U. Broniecki, W. Koltunowicz, „*Increased transformer operation reliability through continuous monitoring*", Proceedings of International conference on Condition Monitoring Diagnosis and Maintenance – CMDM2015, Paper 118, October 5-8, Bucharest, Romania, ISSN 2344-245X.

[6] G. Anders, S. Otal, T. Hjartarson. "*Deriving Asset Probabilities of Failure: Effect of Condition and Maintenance Levels*", Power Engineering Society General Meeting, IEEE 2006, pages 1-7.

[7] W. Koltunowicz, R. Plath, "*Synchronous multi-channel PD measurements*", IEEE Transactions on Dielectrics and Electrical Insulation, Vol. 15, No. 6, p.1715-1723, December 2008.

[8] A. Abu-Siada, S. Hmood and S. Islam "*A New Fuzzy Logic Approach for Consistent Interpretation of Dissolved Gas-in-Oil Analysis*" IEEE Transactions on Dielectrics and Electrical Insulation Vol. 20, No. 6; p. 2343-2349, December 2013.

[9] M. Duval, "*Use of Duval Pentagons and Triangles for the interpretation of DGA in Electrical Equipment*", Proceedings of TechCon North America 2016 – Albuquereque, February 23-25, 2016.

ISBN 978-84-617–9183–5

Fast Front Transients in Transformer Connected to Gas Insulated Substations: (White+Black) Box Models and TDSF Monitoring

Luis ROUCO[1], Xose M. LÓPEZ-FERNÁNDEZ[2, 3], Casimiro ALVAREZ-MARIÑO[3] and Hugo GAGO[4]

[1]Instituto de Investigación Tecnológica (IIT), E.T.S. de Ingeniería ICAI, Universidad Pontificia Comillas
Alberto Aguilera, 23, 28015 Madrid, Spain
Luis.Rouco@iit.comillas.edu
[2]Departamento de Ingeniería Eléctrica, Universidad de Vigo
Campus Lagoas-Marcosende, 36310 Vigo, Spain
xmlopez@uvigo.es
[3]Spanish Association for Innovation in Transformer
A Xunqueira, 20, 36378 Gondomar, Spain
csmalvarez@gmail.com
[4]Iberdrola Distribución
Federico Salmón, 5, 28016 Madrid, Spain
hgago@iberdrola.es

Abstract — **Protection to fast front transients of power transformers connected to Gas Insulated Substations (GISs) requires not only detailed model of the GIS but also of the power system components connected to it including the power transformers themselves. Transformer models with different degree of modeling detail have been proposed in the literature. However, there is no single model able to represent at the same time the transient performance both outside and inside transformer when connected to the power system. This paper reports an investigation that shows the valuable information obtained when a white+black box representation is used to model the transformer in fast front transient simulations. Precisely, transient overvoltages will be simulated and the time domain severity factor (TDSF) will be monitored in an actual GIS model in the ATP/EMTP program.**

Keywords — **Fast Front Transients, Gas Insulated Substations, Transformer Models, Time Domain Severity Factor**

I. INTRODUCTION

Protection to Fast Front Transient (FFTs) [1] of power transformers connected to Gas Insulated Substations (GISs) requires not only detailed model of the GIS but also of the power system components connected to it including the power transformers themselves. An appropriate model of the transformer should therefore be applied in transient simulations to determine not only the overvoltages in its terminal but also in each coil. There are several approaches with different levels of sophistication for obtaining such models [2] [3].

Generally speaking, mathematical models of dynamic systems can be of two types: white-box (or physical) models and black-box models.

The white-box model allows assessing the internal transformer dielectric stress. However, it is based on information normally only available to manufacturers [4]. Hence, the use of white-box model is not feasible in simulation of fast front transients.

An alternative model is the black-box models. Such models have no physical meaning, since its structure is just a mathematical equation that matches the model output with the observed data. These models reproduce the transformer behaviour as seen from its terminals, over a wide frequency band. Black-box models are particularly suitable for studying the high-frequency interaction between a transformer and the network such as insulation coordination studies and the analysis of transferred overvoltages between transformer winding terminals.

ISBN 978-84-617–9183–5

On the other hand, there are many examples in the literature and in the engineering practice describing simplified models for representing power transformers. Generally such practice uses models valid only in certain a range of frequencies. This range is chosen depending of the desired application. It can be viewed between white and black as a kind of gray-box model since the structure is built primarily on the equipment physic and the parameters obtained by calculation or measurement tests. The advantage of these simplified models is that they are easy to implement in electromagnetic transient programs (EMTP), suitable and sufficient for a first transient analysis in the substation.

The International Electrotechnical Commission (IEC) has developed modelling guidelines of power system components for FFT simulations [5] . There are recommendations for modelling transformers by simplified models with their winding capacitances to ground and the capacitances between windings. A simplified approach is proposed in [6] to obtain and use a reduced capacitances transformer model developed from the node capacitance matrix provided by the manufacturer instead of using the measured capacitances.

The utility on its side could need to make evaluation studies on interaction between the transformer and the power system in case of fast front transients to monitor the severity of the risks. Such monitoring can thus help to analyse and prevent failures due to upon incoming transients from the system to transformer either design review stages or manoeuvres, change of grid topologies, protection coordination, etc. This paper proposes to monitor the mentioned situations via the time domain severity factor (TDSF), which assesses the severity supported by transformer windings due to transient events occurring in the power system [7].

The TDSF can be considered as tool in substation design studies, complementary to standard insulation coordination analyses, as well as information to the manufacturer of the transient electrical environment of the substation.

This paper presents a new approach for interactive protection system simulation. In this approach, the power system network is modeled in the ATP/EMTP program while the “compiled foreign model” mechanism of MODELS language is employed to implement the transformer in a White+Black box package. This permits to monitor the interaction between power system network and transform model in a ATP/EMTP environment. A case study is included to demonstrate the protection system simulation against overvoltages [8] in a GIS and the transformer subjected to a lightning impulse using the proposed new approach. It shows the capabilities of reproducing the internal transformer behaviour for high frequency in simulations within ATP/EMTP program. A prominent advantage of this approach is the easy interfacing between the power system network models and the transformer model because the MODELS are inherently embedded in ATP/EMTP program.

II. SIMPLIFIED TRANSFORMER MODELS

Traditionally, in very fast transients, such as lightning surge studies into the network, only the capacitive behaviour of the power transformer is consider relevant as first approach. So, the mutual capacitive coupling between phases is ignored, leaving only a capacitive per-phase equivalent. Such a model could be used for representing the impact of a transformer on an incoming wave on a cable or overhead line, but it is a way too simple for capturing the detailed high-frequency interaction between the transformer and the network, or the transfer of overvoltages between inner windings.

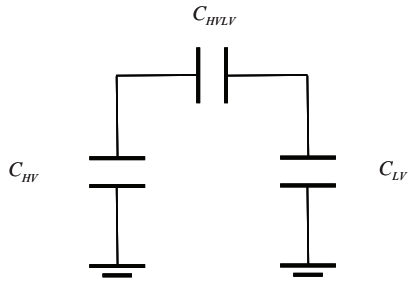


Figure 1. Simplified transformer model representation (two terminals).

ISBN 978-84-617–9183–5

A typical simplified transformer model is shown in Figure 1. The parameters C_{HV}, C_{LV} and C_{HVLV} are the surge capacitances and will depend upon the range of frequencies considered. The parameter C_{HV} can be provided by the manufacture or calculated from impedance frequency response measurements. If these values are not available from measurements or from manufactures typical values are suggested in the literature. For example see Table 4.1 in [9]. Typical capacitance values for auto-transformers can be found in Table 4.2 in [10]. This subject is also discussed in [11] and in [12] where a list of typical values are also provided.

Also IEC [5] recommends to represent transformers in FFT simulations by the winding capacitances to ground and the capacitances between windings as shown in Fig. 1.

Reference [6] has obtained and used a reduced capacitances transformer model developed from the node capacitance matrix provided by the manufacturer instead of using the measured capacitances. The capacitance transformer model can be written in the frequency domain as:

$$j\omega \mathbf{C}\mathbf{V}_n = \mathbf{I}_n \tag{1}$$

The reduced capacitance matrix $\mathbf{C}_R$ is firstly obtained by performing the Kron reduction to the high and low voltage terminals of the transformer. The windings capacitances are obtained from the reduced capacitance matrix $\mathbf{C}_R$ according to:

$$\mathbf{C}_R = \begin{bmatrix} C_{R11} & C_{R12} \\ C_{R12} & C_{R22} \end{bmatrix} \tag{2}$$

$$\left.\begin{array}{l} C_{R11} = C_{LV} + C_{HVLV} \\ C_{R12} = -C_{HVLV} \\ C_{R22} = C_{HV} + C_{HVLV} \end{array}\right\} \begin{array}{l} C_{HVLV} = -C_{R12} \\ C_{HV} = C_{R22} - C_{HVLV} \\ C_{LV} = C_{R11} - C_{HVLV} \end{array} \tag{3}$$

III. WHITE+BLACK BOX TRANSFORMER EMTP/ATP PACKAGE

The ATP (Alternative Transient Program) is the public domain version of EMTP (Electromagnetic Transient Program). It is based on the original version of the EMTP program and it is the most widely used version of EMTP.. This software allows simulating electromagnetic transient phenomena, taking into account, among other features, sophisticated models for transmission lines, circuit components and control elements. However the transformer model is based on simplify one usually without option to analyze the performance inside in the windings excited by a transient voltage. That is the reason that this work proposed a white+black box for the transformer as a package easy to use in the ATP/EMTP environment connected to the all components of the substation. A demonstrative case was implemented in ATP/EMTP, since it offers the option of programming function through MODELS. By recompiling the ATP/EMTP program, it is possible to create sub-routines and function programming models by foreign programming languages.

The white+black box ATP/EMTP package proposed in this work is constructed from a white-box model. Their parameters are frequency dependent and calculated from transformer geometric dimensions and material physical of the transformer. Series capacitances interturns, earth capacitances of the turn to core, to tank and to yoke, and shunt capacitances between turns of adjacent windings have been included for modeling the electrostatic couplings. Self-inductance of each turn and mutual inductance between turns of all windings has been considered for taking all inductive couplings into account. The dielectric losses and copper losses caused by the eddy currents (skin and proximity effects) have also been included. The white+black box ATP/EMTP package can simulate any type of multi-phase, multi-winding transformer.

This approach is particularly useful for enhancing the understanding of the internal transformer transient behavior connected to the power system, since the transformer model and the network model of the power system can interact during the simulation. As a result, the interaction between the power system network model and the transformer model make the overall power system simulation more powerful.

ISBN 978-84-617–9183–5

IV. TIME DOMAIN SEVERITY FACTOR (TDSF) MONITORING

To take decisions on the risk level supported by power transformer, in this work focused to overvoltages, when connected in the grid an evaluation tool is necessary to manage capable to bring the internal transformer voltages stress information. The guide published by Cigre JWG A2/C4.38 [2] recommends the time domain severity factor (TDSF) [13] which is useful when combined with "online" monitoring either in the simulation stage or physically implemented in the real network, as indicator of increased transient risks for a unit.

A severity factor assesses the dielectric stress of a transformer winding considering the incoming transient overvoltage. It determines the safety margin regarding the standard acceptance tests either in the frequency or time domain.

In the case of the TDSF gives further detailed information in the time domain on the severity supported by the transformer windings due to the transient event coming from the power system, regarding the internal transient response due to dielectric tests in the time domain. The TDSF is formulated as [13] :

$$TDSF(i) = \frac{\Delta V_{sw}(i)}{\Delta V_{env}(i)} \tag{2}$$

where $\Delta V_{sw}(i)$ is the maximum voltage drop along the ith dielectric path due to the transient events and $\Delta V_{env}(i)$ is the maximum voltage drop along the same ith dielectric path for all standards dielectric tests.

Since each transient waveform depends on the electrical interaction between transformer and the power system, it implies that each of those combinations is characterized by a TDSF. To obtain the TDSF implies the use of two different models of the transformer under consideration. First, a terminal model (black box model) of the transformer is built to compute the transient voltage waveform at the transformer terminals during the transient event that occurred in the power system where the transformer is connected. Then, a detailed model (white box model) of the transformer is used to compute the internal transient voltage distribution along transformer windings.

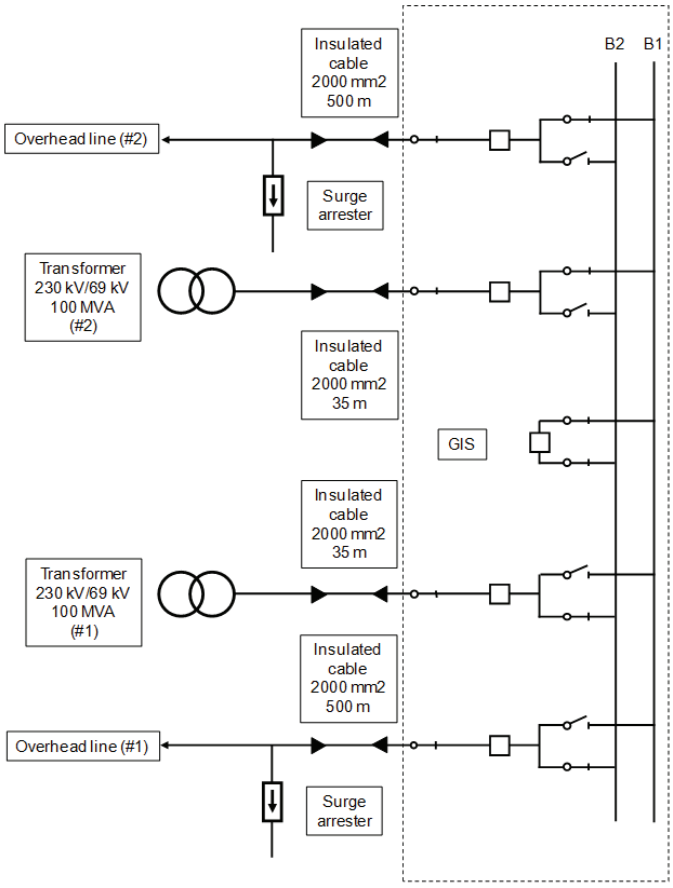


Figure 2. Substation layout.

ISBN 978-84-617–9183–5

V. TIME DOMAIN SIMULATIONS. CASE STUDY

The performance of the white+black box EMTP/ATP package and the simplified model have been compared using them for modelling a 220 kV/66 kV transformer in an actual substation equipped with 220 kV GIS with five bays (two overhead line bays, two transformer bays and a bus bar coupling bay) and simulating a direct lightning stroke in a phase conductor of one of the two overhead lines (#2) [8] . The layout of the substation is shown in Figure 2. The ATP/EMTP model of the GIS and the power system components connected to it is displayed in Figure 3. The white+black box ATP/EMTP package has been used to represent transformer #2.

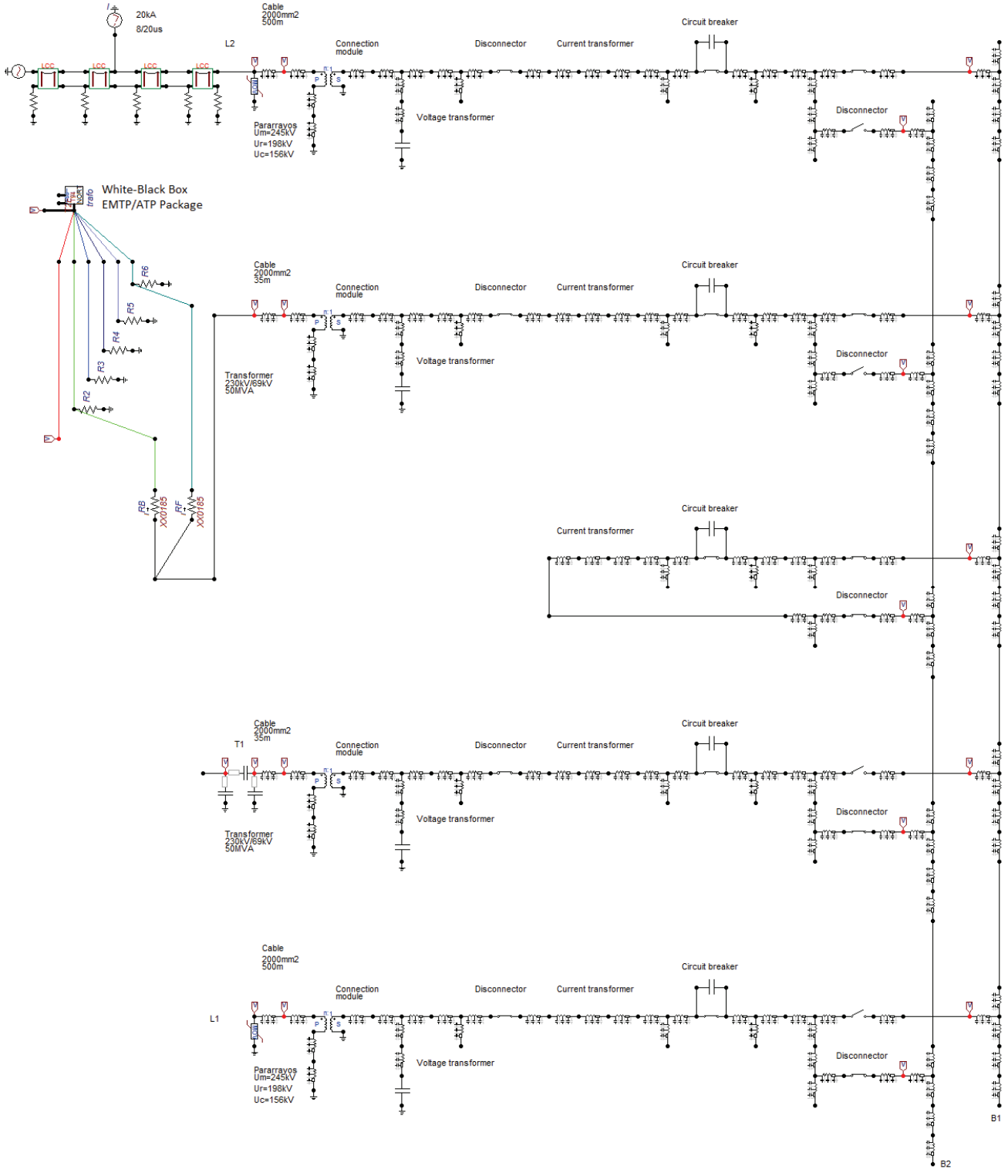


Figure 3. Substation EMTP model with transformer white+black box package.

ISBN 978-84-617–9183–5

Results were obtained running the substation EMTP model simulating a direct lightning stroke in a phase conductor of one of the two overhead lines (#2).

Figure 4 compares the high voltage (HV) terminal voltages provided by both the white+black box package and the simplified model when surged arrested is connected. Voltages provided by both model agree. It confirms the value of the simplified model. Moreover, as the maximum voltage is below the transformer BIL (850 kV). Figure 5 compares the low voltage (LV) terminal voltages provided by both the white+black box package and the simplified model. It must be noted the great difference between the voltages of provided by the white+black box package and the simplified model. However, the voltage provided by the white+black box package is below the BIL of the low voltage winding (325 kV).

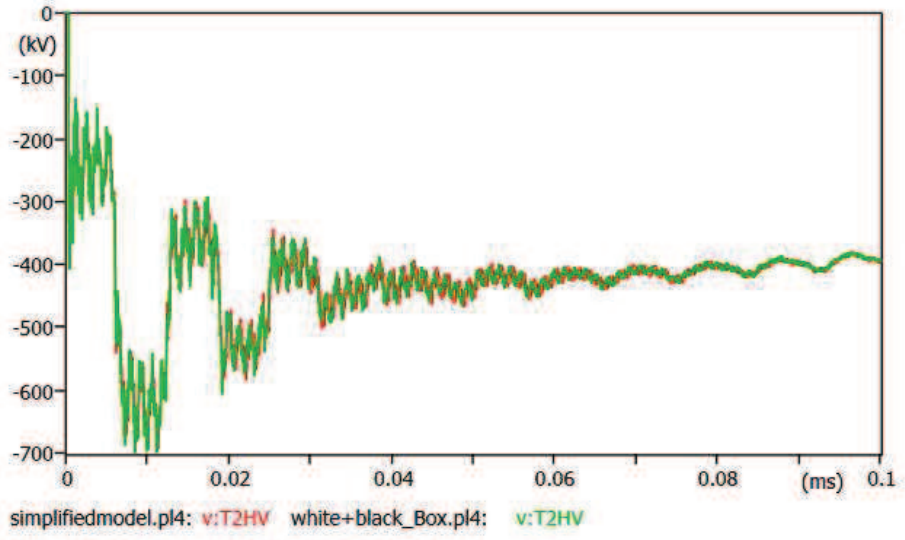


Figure 4. Comparison between white+black box EMTP/ATP package and simplified: HV terminal.

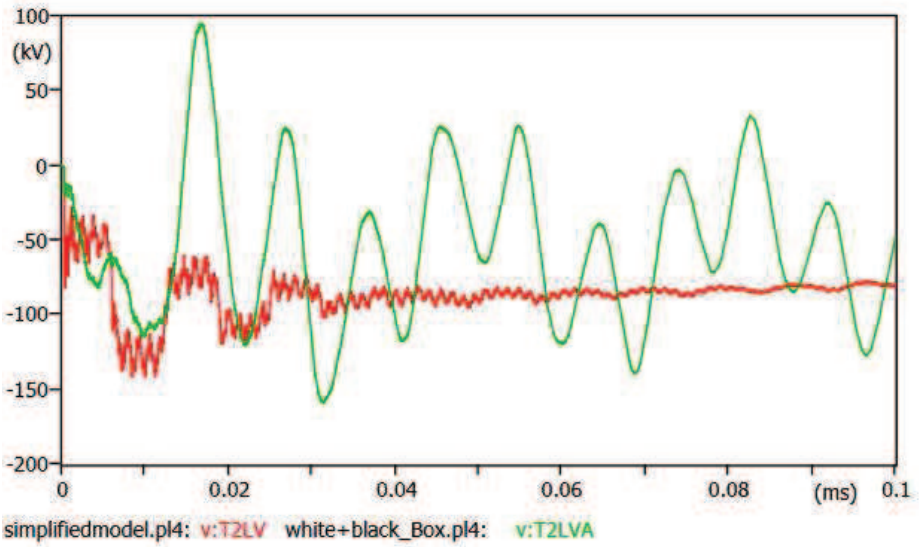


Figure 5. Comparison between white+black box EMTP/ATP package and simplified model: LV terminal.

The distribution of voltages within the high voltage winding provided by the white+black box package are displayed in Figure 6. The internal node voltages are scaled with respect to the terminal node voltage. The distribution of voltages within the low voltage winding provided by the white+black box package are shown in Figure 7. No node exhibit voltage higher than the low voltage transformer winding BIL (325 kV).

The TDSF monitoring both with and without surge arrester protection (MOV) are shown in Figure 8 and Figure 9 respectively. It is remarkable that without protection the TDSF goes to near unit value, which means that the transformer is close to potential risk.

ISBN 978-84-617–9183–5

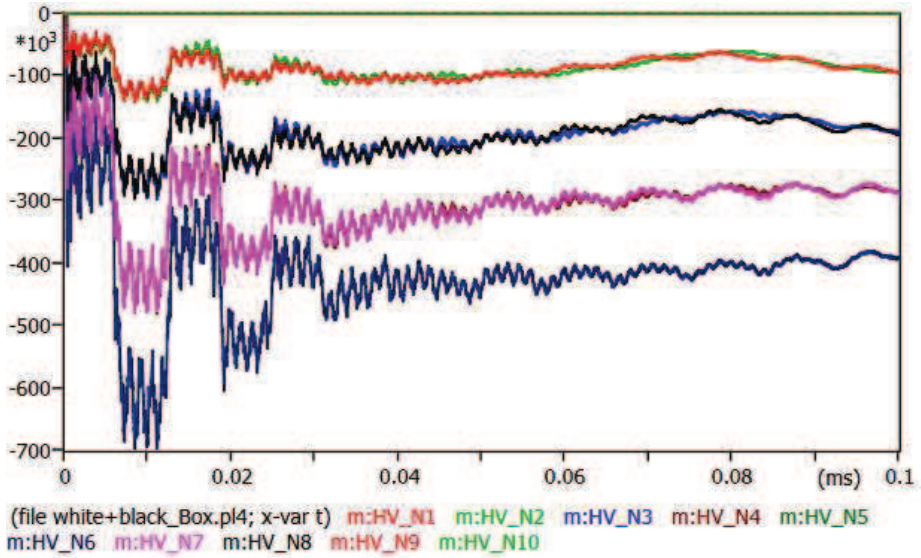


Figure 6. White+black box package: HV winding voltages.

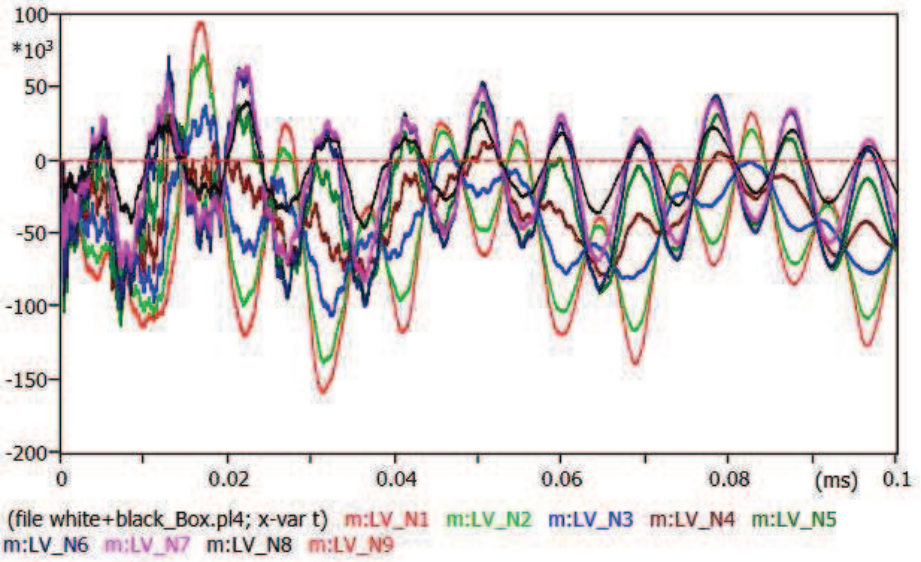


Figure 7. White+black box package: LV winding voltages.

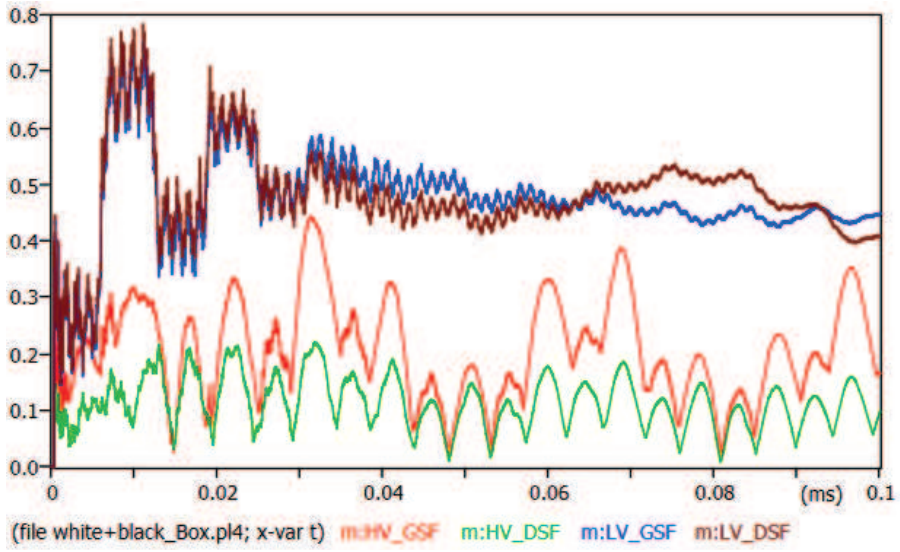


Figure 8. White+black box package: TDSF at HVand LV windings with protection (MOV).

ISBN 978-84-617–9183–5

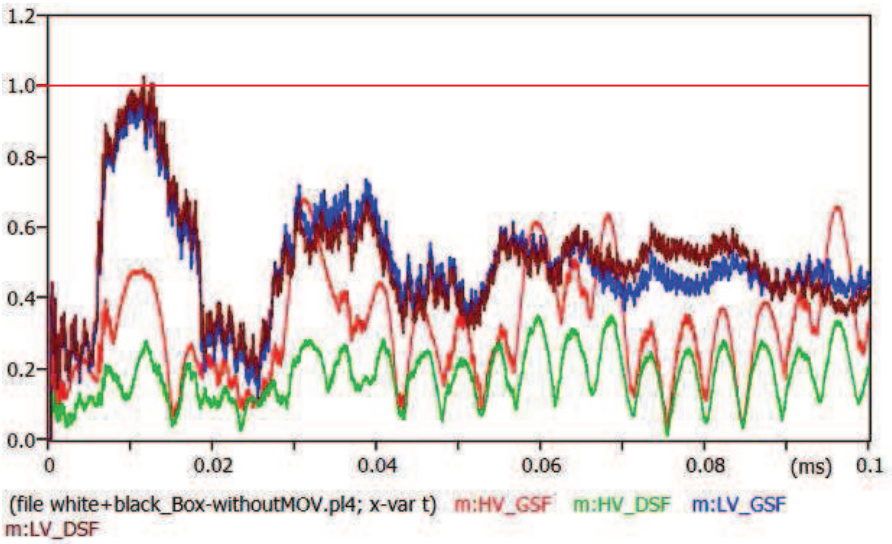


Figure 9. White+black box package: TDSF at HV and LV windings without protection (MOV).

VI. CONCLUSIONS

This paper has investigated the use of white+black box package in simulation of FFT. A white+black box package has been incorporated to a detailed model of a GIS. The terminal voltages provided by both the white+black box package and the simplified model have been compared. High voltage terminal voltage provided by both model agree. In contrast, low voltage terminal voltages provided by both the white+black box package and the simplified model exhibit great differences.

The TDSF monitoring was implanted into the proposed white+black box package, which offers valuable information to take decisions on the risk level supported by power transformer interacting with the power system during fast transient conditions.

REFERENCES

[1] IEC, International Standard IEC 71-1: *Insulation Coordination, Part I: Definitions, Principles and Rules*, 17th Edition, 1993-12.

[2] Joint Working Group SC A2 CIGRÉ, *Electrical Transient Interaction Between Transformers And Power Systems,* Tech. Brochure JWGA2/C439, Part-1 Expertise&Part-2 Case Studies Apr. 2014.

[3] Xose M. Lopez-Fernandez, H.B. Ertan and J. Turowski, Editors, *Transformer: Analysis, Design and Measurements*, CRC Press 2012.

[4] Xose M. Lopez-Fernandez and C. Alvarez-Mariño, *Computation Method for Transients in Power Transformers with Lossy Windings*, IEEE Transactions on Magnetics, Vol. 45, No. 3, p. 1863-1866, March 2009.

[5] IEC, Technical Report IEC TR 600071-4, *Insulation Coordination, Part 4: Computational Guide to Insulation Coordination and Modelling of Electrical networks*, First Edition 2004-06.

[6] L. Rouco, H. Gago and A. Prieto, *Detailed and Reduced Transformers Models in FFT Simulations*, 3rd International Advanced Research Workshop on transformers, ARWtr 2010, Santiago de Compostela, España, 3-6 October 2010.

ISBN 978-84-617–9183–5

[7] Xose M. Lopez-Fernandez and C. Alvarez-Mariño, *Induced Transients Voltage Performed Between Transformers and VCB. Severity Factors and Case Studies*, IEEE Transactions on Power Delivery, Vol. 30, No. 3, p. 1137-1144, January 2015.

[8] L. Rouco, L. Sigrist, H. García, E. Palazuelos, J. Bernal, M.A. Jimeno, *Protection of Power Transformers Connected to GIS Against Lightning Overvoltages*, Cigre 2014 Session 45, Paris, France, 24-29 August 2014, Paper C4-205.

[9] CRIEPI, *Lightning Protection Design for Power Stations, Substations and Underground Transmission Lines*, CRIEPI Report T40, 1995 (in Japanese).

[10] IEEE TF Report, *Modeling Guidelines for Fast Front Transients*, IEEE Trans. on Power Delivery, Vol. 11, No. 1, pp. 493-506, 1996.

[11] A. Greenwood, *Electrical Transients in Power Systems*, Second edition, Jon Willy & Sons Inc., ISBN 0-471-62058-0, 1991.

[12] CIGRE WG 33.02, *Guidelines for Representation of Network Elements when Calculating Transients*, CIGRE Technical Brochure 39, 1990.

[13] C. Álvarez-Mariño, X. M. Lopez-Fernandez, A. J. M. Jácomo-Ramos, R. A. F. Castro-Lopes, J. M. Duarte-Couto, Time Domain Severity Factor (TDSF): *Induced Transient Voltage Between Transformer and Vacuum Circuit Breakers*, COMPEL: The International Journal for Computation and Mathematics in Electrical and Electronic Engineering, vol.31 no.2, pp.670-681, 2012.

ISBN 978-84-617–9183–5

Equipment Condition Monitoring (ECM) Using Smart Sensors for Power Transformers with Special Focus on Real Time Asset Diagnosis and Prognosis

Marcos E. G. ALVES

Department of R&D Electrical Engineering, RADICE
Praça Claudino Alves, 141 - Atibaia, Brasil
Phone: (+55) 11 2410 1190, fax: (+55) 11 4413-5991, e-mail: marcos.alves@radiceconsultoria.com

Daniel P. SANTOS

Development Engineering, TREETECH
Praça Claudino Alves, 141 - Atibaia, Brasil
Phone: (+55) 11 2410 1190, fax: (+55) 11 4413-5991, e-mail: daniel.pedrosa@treetech.com.br

Gilberto A. MOURA

Application Engineering, TREETECH
Praça Claudino Alves, 141 - Atibaia, Brasil
Phone: (+55) 11 2410 1190, fax: (+55) 11 4413-5991, e-mail: gilberto.amorim@treetech.com.br

Abstract — **The high voltage equipment engineers face the challenge of providing increased reliability and availability of power transformers in the scenario of new applications of electricity, such as electric cars as well as in distributed generation and renewable energy sources. In this scenario, the Equipment Condition Monitoring Systems (ECM) for on-line and continuous monitoring and diagnostic of high voltage equipment condition, during normal operation, are essential tools for more effective and intelligent management of those assets, by enabling predictive maintenance, based on actual condition, to replace preventive maintenance, based on time.**

This paper presents the experience of Treetech with the design, implementation, operation and maintenance of on-line monitoring systems composed of smart sensors, communications and data processing software for diagnostics and prognostics of high voltage equipment condition, mainly for power transformers.

The centralized and decentralized architectures for sensors data acquisition are analyzed and their characteristics, advantages and disadvantages are presented, as well as case studies resulting from a large amount of monitoring systems deployed in field.

Keywords — **Transformer, On-Line monitoring, Diagnosis, Equipment Condition Monitoring ECM**

1. INTRODUCTION

Electricity is becoming increasingly more essential to society, which leads to an increasing demand for greater reliability and continuity of supply. New applications of electricity, such as electric cars and also the distributed generation and renewable energy sources, for example, confirm this trend. These needs are reflected in industry regulations, which provide heavy financial penalties in case of interruption of supply or unavailability of transmission equipment, even if scheduled in advance.

The current scenario of electric energy markets worldwide has taken companies in the sector to operating in an unprecedented competitiveness context, forcing high voltage equipment engineers into a permanent search for new technologies able to fulfill with higher efficiency, better supply quality and at lower costs. Some of the first equipment to operate under this new change are power transformers, since, in addition to being essential for transmission and distribution grids, they are also usually the biggest and highest value assets in substations.

In consequence, Equipment Condition Monitoring Systems (ECM) are being implemented as one of the main tools that provide answers to this change without jeopardizing transformer operating safety and reliability, allowing operators to know their actual condition and diagnosing or prognosticating eventual problems.

The experience already acquired by the market through the development, specification and purchase of on-line monitoring systems, in addition to their subsequent operation and maintenance, allows the main philosophies used in systems building to be identified, as well as analyses of the practical results and the selection of the solutions that feature the best results at the lowest costs.

ISBN 978-84-617–9183–5

In this way, even though initially monitoring systems were deployed only on large scale power transformers, the choice and specification of appropriate philosophies and architectures can render viable the application of on-line monitoring systems even on small and medium scale transformers.

Accordingly, in the following sections this paper presents the experience of Treetech with the design, implementation, operation and maintenance of on-line monitoring systems composed of smart sensors, communications and data processing software for diagnostics and prognostics of high voltage equipment condition, mainly power transformers.

The centralized and decentralized architectures for sensor data acquisition are analyzed and their characteristics, advantages and disadvantages are presented, as well as case studies resulting from a large amount of monitoring systems deployed in field.

II. Typical Topology of On-Line Monitoring Systems

Typically, power transformer on-line monitoring systems adopt the topology shown in the block diagram in Fig. 1, where the following main components can be defined:

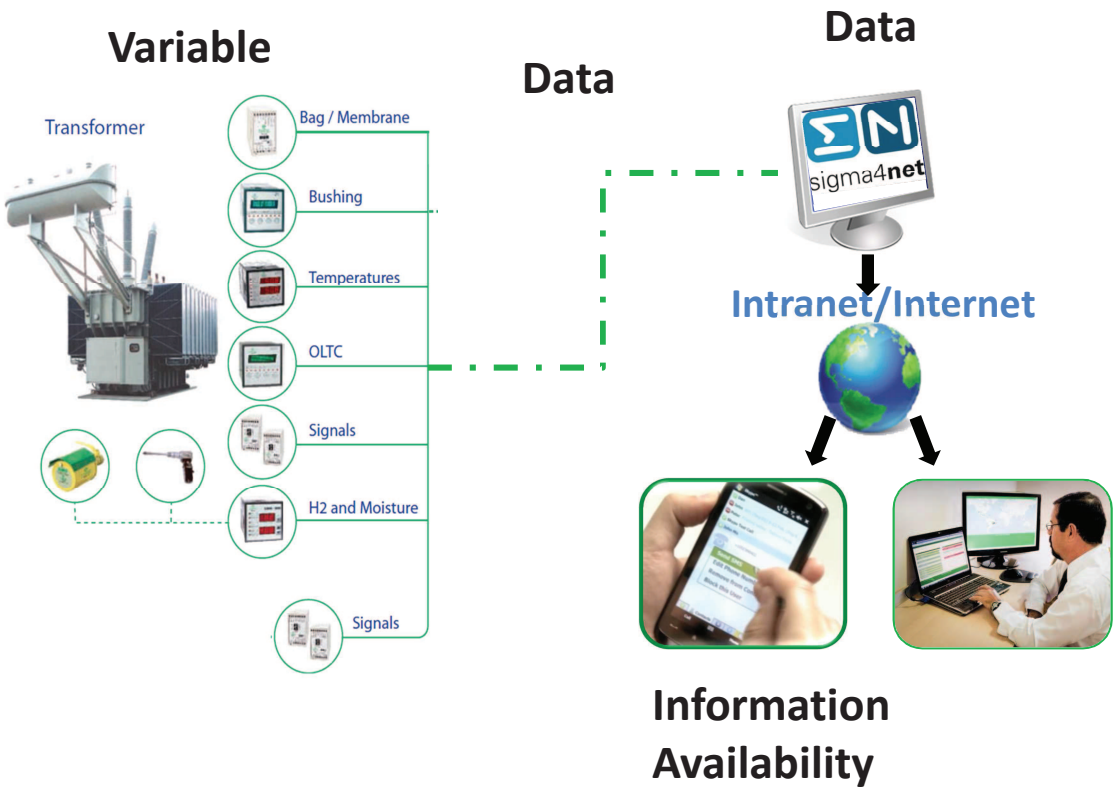


Figure 1. Typical Topology of a Transformer Monitoring System.

- **Variable Measurement** – Measurement of the different variables considered to be important in order to know the condition of the equipment performed via sensors and/or transducers, in general located on the transformer. If the architecture adopted is centralized, there will also be a measurement concentration device (PLC).
- **Data Transmission** – Consists in transmitting data from measurements taken by sensors, obtained in the preceding stage, to the stage of data storage and processing, using the most convenient physical medium for the purpose.
- **Data Storage and Processing** - Data Storage and Processing for readings issued by sensors digital boards obtaining useful information for asset maintenance and management, such as diagnosis and

ISBN 978-84-617–9183–5

prognostics of the state of the different subsystems and overall condition of the transformer. This also avoids overloading maintenance engineering with a high volume of data, not always easily interpreted.

- **Information Availability** – For monitoring systems to deliver their objectives, information related to the state of the equipment must be made available to the different interested sectors, while simultaneously maintaining data integrity and access security.

Specification for an on-line monitoring system must take into account the necessary characteristics and the options to meet and address them in each of these. The main issues to be observed are described below.

II.1 VARIABLE MEASUREMENT

Specification of Variable Measurement for the monitoring system must take into account: (1) the variables to be measured and (2) the architecture to be adopted for these readings.

2.1.1 Variable Selection

Below is a list of the typical variables measured in on-line monitoring systems for power transformers, but it is possible to use just a part of them:

1. Ambient temperature
2. Oil temperature
3. Winding temperatures
4. Load tap changer temperature
5. Condition of conservator bag/membrane
6. Water content and relative saturation in transformer oil
7. Water content and relative saturation in load tap changer oil
8. Bushing capacitance and tangent delta
10. Hydrogen in oil
11. Load Currents and Voltages
12. Tap changer position
13. Load tap changer working instant
14. Number of tap changer operations
15. LTC motor currents and voltages
16. Transformer oil level
17. Tap changer oil level

The choice of variables to measure through the monitoring system will be conditioned to the following main factors:

- Applicability on the transformer in case of point, considering the existence or absence of accessories such as on load tap changer, oil circulation pumps, etc.
- The variables required to perform the diagnostic functions considered important for the application. This factor is directly linked to the Data Storage and Treatment block, and will be detailed in item 2.3.

2.1.2 Architecture for Variable Measurements

Measuring variables during operation of the transformer is performed by way of sensors and/or signal conditioners, which may be connected in one of two main architecture options:

- One based on a centralizer element located on the transformer casing, usually a PLC (Programmable Logic Controller), or,
- A decentralized architecture, based on IEDs (Intelligent Electronic Devices) also located on the transformer casing.

The choice of architecture to be used for measuring variables must take into account the inherent characteristics to each of the options, shown in Table I.

ISBN 978-84-617–9183–5

Table I. Comparison of Centralized and Decentralized Architecture Characteristics

Centralized Architecture	Decentralized Architecture
▪ Centralized system – PLC concentrates information received from all sensors and sends them to the next block in the monitoring system.	➢ Decentralized system, where sensors are IEDs (*Intelligent Electronic Devices*) that send the information directly to the next block of the monitoring system.
▪ Centralized system, expansions and maintenance more difficult.	➢ Naturally modular system, making expansions and maintenance easier.
▪ Sensors must be dedicated to the connection to the PLC, resulting in the need for eventual duplication of sensors and additional costs for monitoring systems.	➢ Existing IEDs in control and protection systems can be integrated to the monitoring and data acquisition systems, avoiding the costs of additional sensors.
▪ Centralizer element (PLC) represents additional costs in installing, programming and maintenance for the system.	➢ There is no centralizer element – eliminating additional costs.
▪ Failure in PLC may lead to loss of all functions offered by system.	➢ Failure in one IED leads to loss of just a part of the functions – other IEDs continue in service.
▪ Centralizer element (PLC) is an additional failure point for the system	➢ There is no centralizer element, thus eliminating a possible failure point.
▪ Typical maximum PLC operating temperature is 55ºC [1]. Installing on main equipment (ex.: transformers) is not advisable.	➢ Operating temperature -40 to +85ºC, suitable for installing in yard on main equipment.
▪ Installation recommended in control room – large number of connection cables between device and yard.	➢ Typical installation on main equipment, in yard – only serial communication (twisted pair or optic fiber) for link to control room.
▪ Typical insulation level 500V – not suitable for high voltage substation environments [1].	➢ Typical insulation level 2.5kV – designed for high voltage substation environment.
▪ Serial communication ports do not tolerate surges, impulses and induction found in substation, mandating the use of optic fiber in communication with the control room – high installation cost.	➢ Serial communication ports designed for substation environment, allowing deployment of twisted-pair cables for communication with control room – low set up cost. Allows optional use of optic fiber cabling, with self-powered external converters.
▪ Usually operate using industrial communication protocols [1].	➢ Specific communication protocols for deployment in power systems (time-stamp, clock synchronicity, etc.).

Monitoring system topologies using centralized and decentralized architectures can be seen in the examples of Fig. 2 and 3. Fig. 2 shows, for example, the duplication of oil temperature and load current sensors which does not occur in Fig. 3.

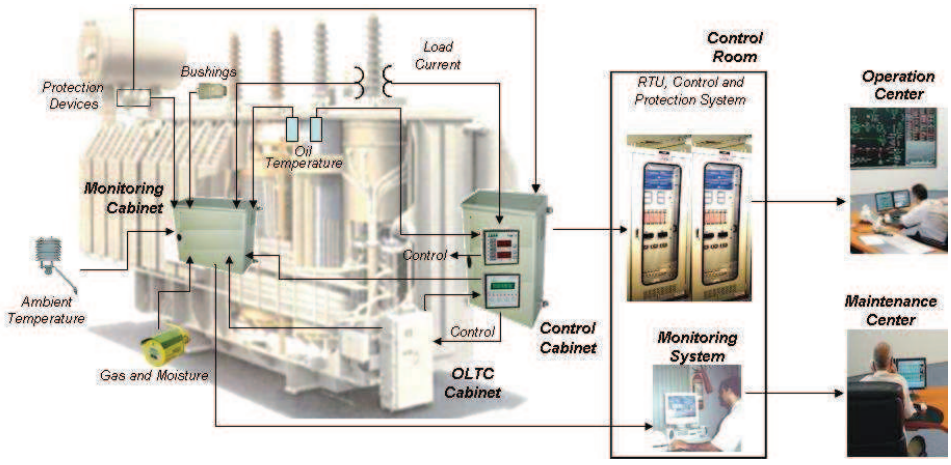


Figure 2. Topology using Centralized Architecture.

ISBN 978-84-617–9183–5

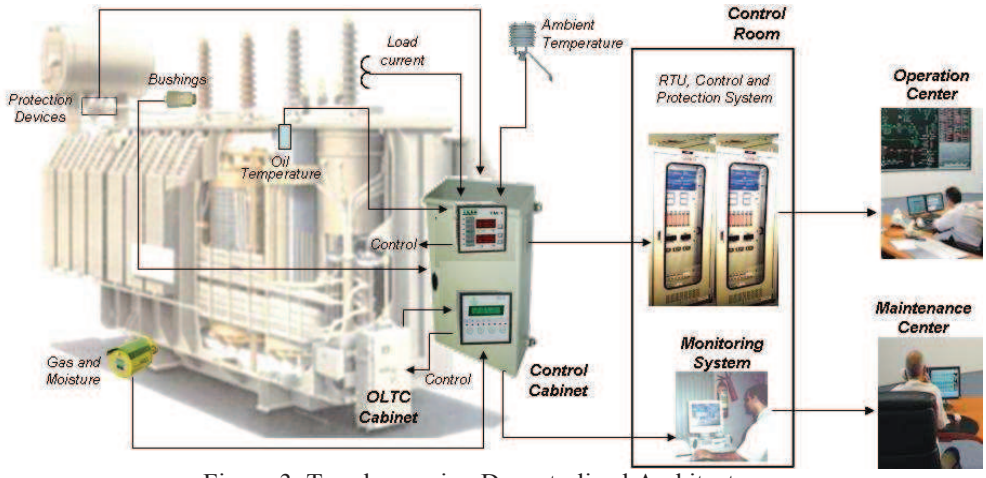


Figure 3. Topology using Decentralized Architecture.

The different benefits obtained from the use of decentralized architecture make it advisable, therefore, in monitoring systems specifications, given the higher level of reliability and lower maintenance costs, in addition to the ease in specifying for small scale monitoring systems and reduced costs. To this end, a contribution is made by the possibility in deploying existing IEDs already installed on the transformer for supervision and control functions as data sources (sensors) for the monitoring system. In some cases, like the examples shown in item 3, monitoring systems can actually have zero sensor acquisition costs.

II.2 Data Transmission

Transmission of data from the measurement equipment (item 2.1) to the substation control room can be achieved via a range of different means of communication, obviously addressing the requirements of the type of architecture deployed in measuring the variables, as shown in Table I. In systems with centralized architecture for measuring variables, optic fiber cables are usually deployed.

In systems with decentralized architecture, on the other hand, in addition to the option for optic fiber cabling, it is possible to use RS485 serial communication standard cables, with the advantage of the lower costs and shorter installation times, thus contributing to reducing costs and increasing financial feasibility for monitoring systems in small scale transformers. Thus, under this aspect also, deploying decentralized architecture becomes advisable in specifying monitoring systems.

Other communication options can also be studied, depending on the characteristics of the facility, such as for example, dedicated radio links or wi-fi wireless networks.

If the computer that stores and treats the data (item 2.3) is located in the substation control room, the equipment data transmission connection can be direct. However, if the computer is in another remote facility, transmissions of measurement data can also be done via the company intranet, by internet or even by cellular phone modem GPRS.

II. 3 Data Storage and Processing

The data supplied by the IEDs located on the transformer, both raw readings and those supplied resulting from the pre-treatment of the data, are received by a computer, which can be located in the substation control room or at a remote location, running the monitoring software.

More than a system for simple digitizing of sensor measurements, a monitoring system must be able to transform these data into useful information for transformer maintenance, which are equipment condition diagnosis and prognosis. In order to comply with this function, the monitoring system must be equipped with an “Engineering Module”, which contains the algorithms and mathematical models for diagnostics and prognostics.

Table II summarizes the main diagnostic modules that can be specified for a monitoring system, as well as the variables needed for their operation [2], [3].

ISBN 978-84-617–9183–5

Table II. Examples of Diagnostic Modules and Variable Measurements Needed

Diagnostic Module	Variables Necessary
- Insulation Loss of Life	- Winding temperatures (hot-spot) - Water content in paper (from the diagnostic module)
- Forecast of future temperatures - Cooling system efficiency	- Ambient temperature - Top oil temperature - Percent load - Cooling stage in operation
- Cooling Maintenance Assistant	- Cooling stage in operation
- Water in Oil and in Paper - Bubbling temperature - Free water formation temperature	- Percent relative water saturation in oil - Water content in oil in ppm - Oil temperature at the point of measurement - Winding temperatures - Ambient temperature
- Gas in transformer oil	- Hydrogen in oil concentration - Concentration of combustible gases in oil (off-line or on-line)
- Load tap changer temperature differential	- Top oil temperature - Tap changer oil temperature - Tap position
- Load tap changer operation time	- Tap position - Tap changer in operation
- LTC motor torque	- Tap position - Tap changer in operation - Tap changer motor current - Tap changer motor voltage (optional)
- LTC Maintenance Assistant	- Tap position - Tap changer in operation - Load current
- Water in LTC oil	- Percent relative water saturation in oil - Water content in oil in ppm - Oil temperature at the point of measurement

In systems with decentralized architecture, the modularity of the IED sensors is extended to the diagnostic modules to be used, since modules can be specified to cover just the variables listed in the column “Variables Required” in Table II.

This contributes to reducing costs and increasing financial feasibility for monitoring systems in small scale transformers. Thus, under this aspect also, deploying decentralized architecture becomes advisable in specifying monitoring systems. In item 3, a few examples of monitoring subsystems are given where, deploying few sensors, it is possible to diagnose the different transformer functions.

II. 4 INFORMATION AVAILABILITY

In order to create availability of the information from the monitoring system, usually the computer used to run the monitoring software will be connected to the company Intranet or even the Internet. In order to allow access to the monitoring system without the need to install specific software in all remote computers, the solution usually employed is access via internet browsers.

In addition, in order to avoid the need for ongoing follow up of the system, which would lead to major time consumption (and respective cost) for maintenance engineering, the monitoring system can be specified with an automatic alert message sending functionality in the event any abnormality is registered. Alerts can be sent by email or by SMS text messages on cell phones, according to definitions previously recorded on the system.

ISBN 978-84-617–9183–5

III. EXAMPLES OF MONITORING SYSTEM CONFIGURATION

In order to illustrate the specification of different configurations for monitoring systems, below a few examples of application using monitoring modules with relatively few variables are given.

Examples consider the use of decentralized architecture, taking advantage of supervision and control equipment already found on many transformers with sensors for variable measurement for the monitoring system.

III.1 TEMPERATURE MONITORING SUBSYSTEMS

Fig. 4 brings an example of a Temperature monitoring sub-system that uses as sensor for measurement of variables only one temperature monitor, frequently already found on transformers for the functions of forced ventilation supervision and control. With this simple configuration, several monitoring functions are possible, as shown in the list found in the figure.

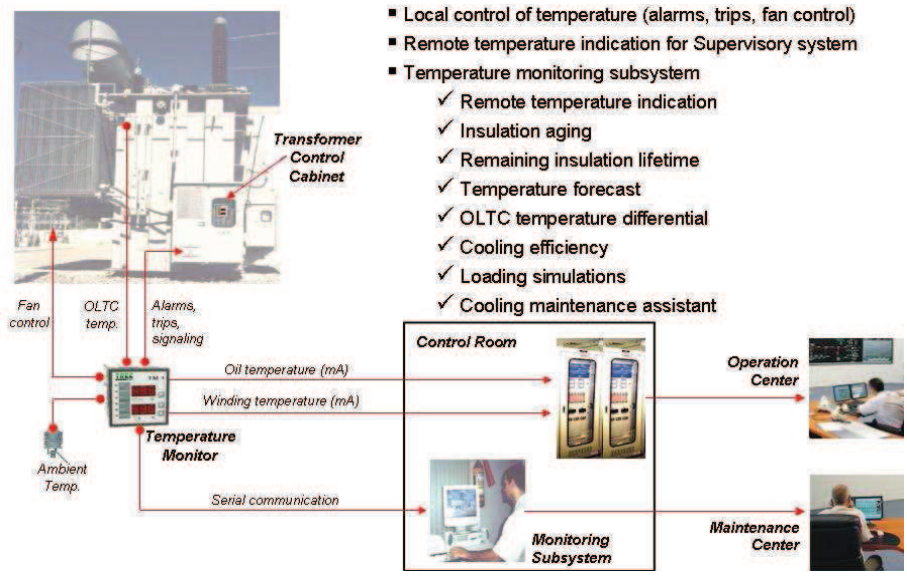


Figure 4. Temperature Monitoring Subsystem.

III.2 TEMPERATURE AND MOISTURE MONITORING SUBSYSTEMS

Fig. 5 brings an example of Temperatures and Moisture monitoring subsystem that uses as sensors for measuring variables a temperature monitor, frequently already found on transformers for the functions of forced ventilation supervision, and control, and one moisture in oil sensor of relatively low cost. With this simple configuration, several monitoring functions are possible, as shown in the list found in the Fig. 4, with addition of the functions of the moisture monitoring subsystem listed in Fig. 5.

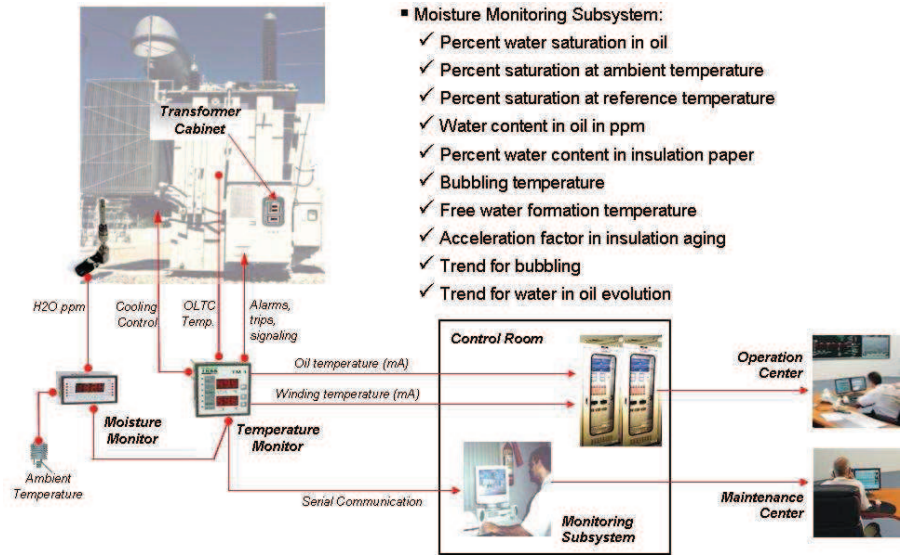


Figure 5. Temperature and Moisture Monitoring Subsystems.

ISBN 978-84-617–9183–5

III.3 TEMPERATURE, MOISTURE AND BUSHING MONITORING SUBSYSTEMS

Figure 6 brings an example of a monitoring subsystem for Temperatures, Moisture and Bushings that uses as sensors for measuring variables a temperature monitor, frequently already found on transformers for the functions of forced ventilation supervision and control, one moisture in oil sensor and a bushing monitor. This configuration allows all the functions of the temperatures and moisture monitoring subsystems shown in figure 5, plus the functions of the bushing monitoring subsystem listed in figure 6.

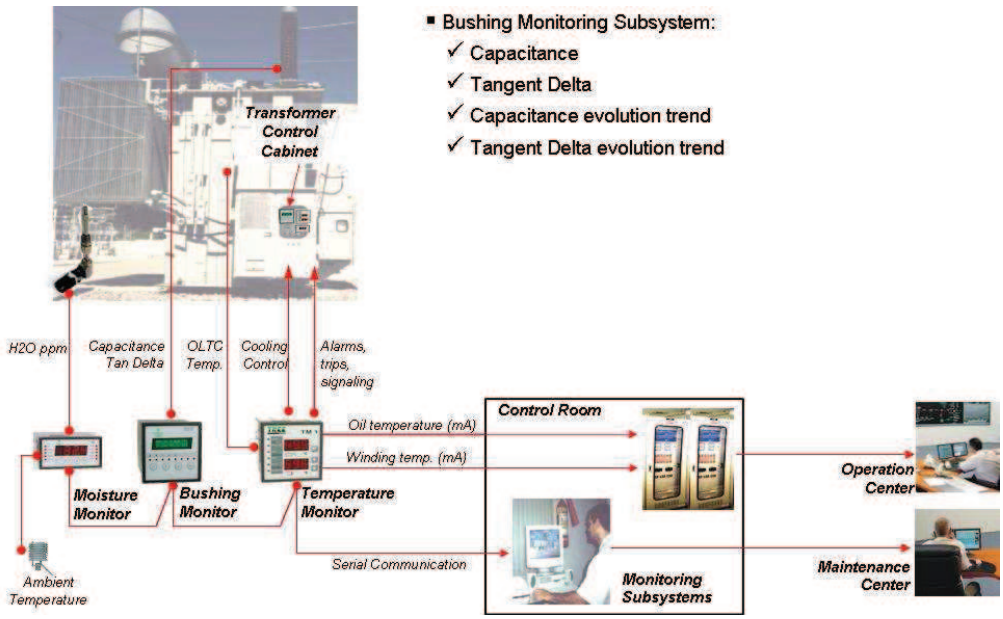


Figure 6. Temperature, Moisture and Bushing Monitoring Subsystems.

III.4 TEMPERATURE AND LOAD TAP CHANGER MONITORING SUBSYSTEMS

Fig. 7 brings an example of a Temperatures and On Load Tap Changer monitoring subsystem that uses as sensors for measurement of variables a temperature monitor and a voltage regulation, frequently already found on transformers for the functions of forced ventilation supervision and control and of the tap changer. This configuration allows all the functions of the temperatures monitoring subsystems shown in Fig. 4, plus the functions of the on load tap changer monitoring subsystem listed in Fig. 7.

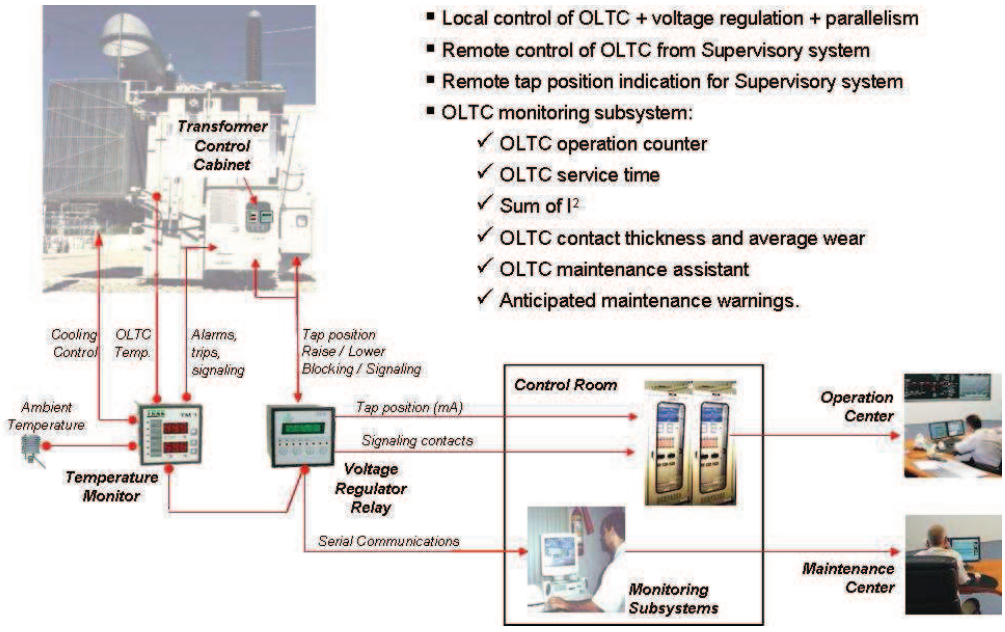


Figure 7. Temperature and Load Tap Changer Monitoring Subsystems.

ISBN 978-84-617–9183–5

IV. SUCCESSFUL CASE STUDIES

Several successful case studies, described below, demonstrate the benefits of using ECM systems as long as built with the appropriate architecture. In all cases following, a decentralized architecture is used.

A) SERRA DA MESA HYDROELECTRIC PLANT

In FURNAS, a transmission utility, taking advantage of the modularity feature of the decentralized architecture, a monitoring system was installed dedicated solely to on-line monitoring of bushings, with the possibility of future expansion.

Fig. 8 shows details of the installation, which included the following equipment [4]:

- Three bushings 550 kV and three 245 kV in a bank of single phase auto transformers;
- Three 550 kV bushings on a bank of single-phase shunt reactors.



Figure 8. Details of bushing monitoring system installed [3].

A few months after being installed the monitoring system issued an alarm by an increase in the capacitance of the 550 kV bushing of the autotransformer phase A, as shown in Fig. 9.

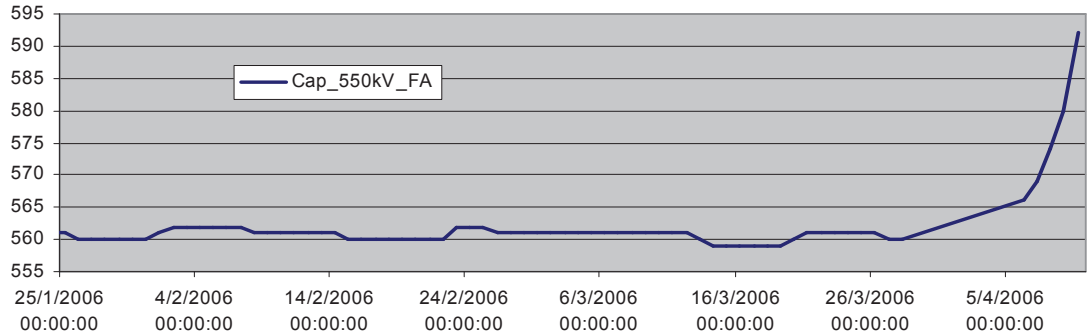


Figure 9. Capacitance increase of 550 kV bushing of autotransformer phase A.

Consequently, the monitoring system prevented a catastrophic failure, with possible fire and serious damage to the transformer [3][4].

The experience of Furnas maintenance engineering with the operation and maintenance of a large number of transformer online monitoring systems has shown that the architecture used to build the systems plays a decisive role for their reliability and ease of maintenance. The decentralized architecture based systems showed better results than those with centralized architecture, which had a high incidence of defects and require high maintenance burden.

ISBN 978-84-617–9183–5

B) IBIÚNA CONVERTER SUBSTATION

Ibiúna is the substation where ±600 kV DC from HVDC transmission system of Itaipu hydroelectric plant is converted to 345 kV AC for supply in the Sao Paulo area, with installed capacity of 7200 MVA distributed among 24 single-phase converter transformers (Fig. 10).

In the first stage of implementation of online monitoring, the temperature supervision systems of all 24 converter transformers have been modernized, with the replacement of all original oil and winding mechanical thermometers by digital temperature monitors, as illustrated in Fig. 11. As a result, the incidence of defects in the temperature monitoring system was reduced from an average of 7 defects /years to virtually zero, releasing the maintenance staff for other tasks and reducing maintenance costs and downtime of the transformer [5].



Figure 10. View of a single-phase converter transformer



Figure 11. Replacement of mechanical thermometers of the converter transformers for digital temperature monitors for the online monitoring system.

The monitoring system deployed includes also the online monitoring of capacitance and tangent delta of the direct current bushings on the converter transformers, a novel application in the world [6].

C) A 343MVA 230kV TRANSFORMER WITH TWO OLTCs

In 2001, the first commercial online power transformer monitoring system in Brazil was installed at Alumar, one of the largest aluminium production complexes in the world. The monitoring system was installed on a three phase 343MVA 230-34.5kV transformer with two OLTCs (On-Load Tap Changers), one on the high voltage and another on the medium voltage side (Fig. 12). The system's architecture is based on a decentralized data acquisition philosophy and using intelligent devices, and also its monitoring and diagnosis features.

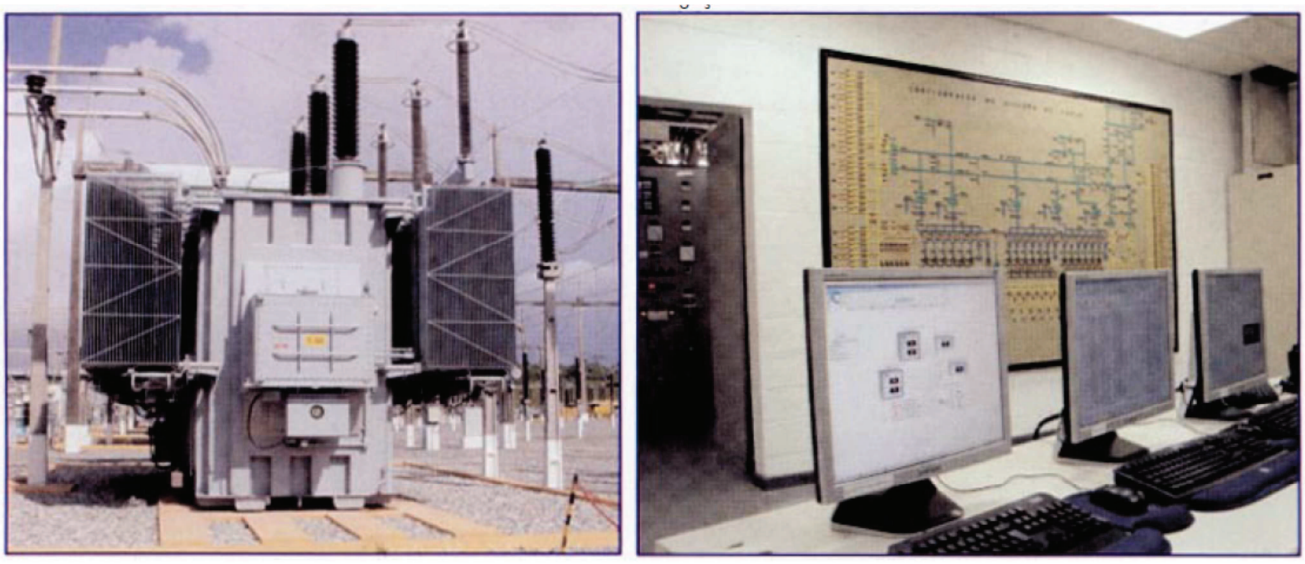


Figure 12 - Transformer monitored on-line and the control room – decentralized architecture, modularity and economy

ISBN 978-84-617–9183–5

Because this monitoring system was, at the time, the first online transformer monitoring system to operate commercially, there were many expectations around the system . In fact, shortly after it went into operation, facts evidenced the gains achieved with the installation of the system, when it detected a defect in an On Load Tap Changer that, under other conditions, would remain unnoticed and might have caused severe future losses [7].

This fact shows that the savings that can be obtained from using an online monitoring system to avoid severe failures are substantial, and the price, often used as an excuse to not install monitoring systems is actually low.

D) ENGIE: COMPARISON OF THE EFFICACY OF OFF-LINE TESTS vs. ON-LINE MONITORING

On-line monitoring of the bushing conditions has been adopted by Tractebel for all the step-up transformers 550 kV at ENGIE hydroelectric power plants (UHE) of Machadinho, Itá and Salto Santiago, with the purpose of reducing the probability of failures, increasing the plant`s reliability, reducing maintenance costs and eliminating unnecessary interventions, which pose potential risk of inserting defects formerly absent, especially in case of chromatography gas tests. Three years after the operation startup, on-line monitoring indicated increase of capacitance and tangent-delta of a bushing at UHE Itá. With the transformer out of operation, off-line capacitance and tangent-delta measurements were made, as well as chromatography gas tests on the bushing oil. Although the latter tests have undoubtedly confirmed the insulation degradation and veracity of on-line alarms, the off-line capacitance and tangent-delta measurements presented results virtually unchanged, and therefore in an apparent conflict.

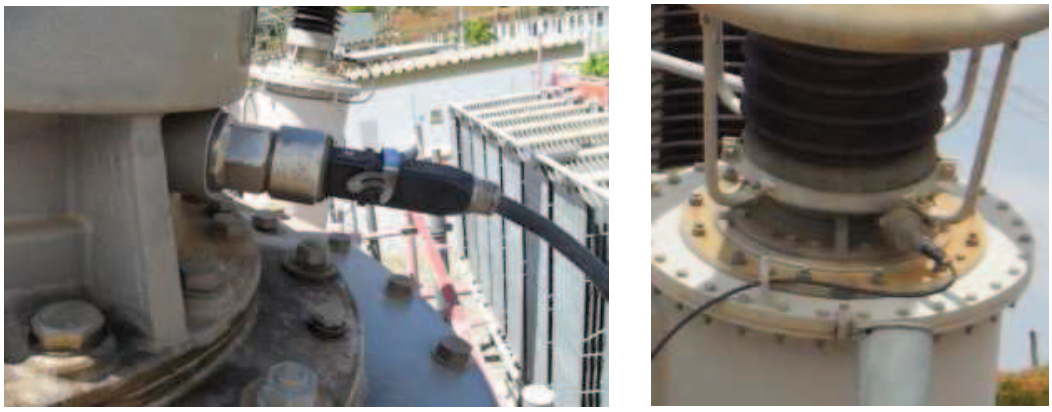


Figure 13. Example of tap adapter installation. Source: [8].

Approximately three years after installing the on-line monitoring of bushings on the step-up transformers at UHE Itá, the bushing monitor generated alarms for the phase-B bushing in the transformer TR1. A warning of capacitance increase trend was initially exhibited, although the capacitance value had not reached the thresholds set for high and very high capacitance alarms. A few time later, on 08/08/2012, the capacitance reached an alarm threshold of high capacitance, thus confirming the trend previously indicated by the bushing monitor.

The chart in Fig. 14 shows the capacitance evolution within the one-year period, from its initial value of 290 pF until reaching on 08/08/2014 the alarm threshold value for high capacitance, set at 295.8 pF, that is, 2% increase on the initial value. In parallel to the capacitance shown, there was also an increase in the on-line value calculated for tangent-delta, from the initial value of 0.39% to a final value close to 1.2%, that is, three times its initial value.

ISBN 978-84-617–9183–5

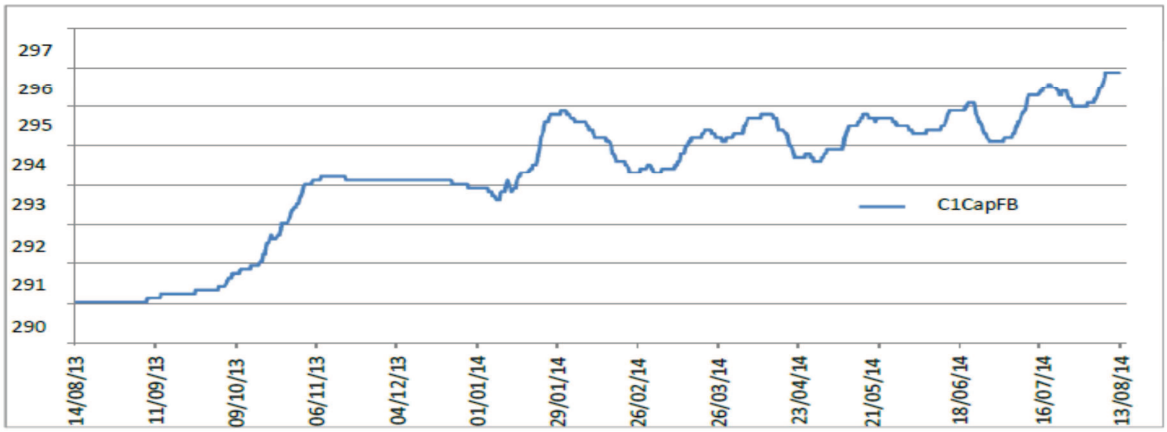


Figure 14. Capacitance evolution of the phase-B bushing, transformer TR1.

It is interesting to observe that the stability of the on-line monitoring system enabled to set the alarm threshold with a relatively low value, only 2% when compared to the suggested value of 5% provisioned in ANSI/IEEE C57.19.100-2012 [9] standard, in order to provide great sensitivity to detecting defects in the on-line monitoring system, without generating undue alarms.

ENGIE scheduled a shutdown of the equipment, in order to enable the conduction of off-line tests that could evidence the bushing conditions. It included off-line measurements of capacitance and tangent-delta and gas chromatography in the bushing oil, obtaining the results shown in Tables III and IV below.

Table III. Off-Line Measurements of Capacitance and Tangent-Delta on the Suspected Bushing

Magnitude	Measure	Variance	Test conditions	Partial diagnostic of the test
Capacitance	279.8 pF	279.8 / 290 = -3.5 %	Temperature 16 ℃ Test voltage 10 kV	Variance within the limits accepted by the standards
Tangent-delta	0.52 %	0.52 / 0.39 = +33.3 %	Temperature 16 ℃ Test voltage 10 kV	Variance within the limits accepted by the standards

As we can see in Table III, the capacitance and tangent-delta values achieved in the off-line test, when analyzed individually, would indicate that the bushing is in good conditions, as they do not present any correlation with the on-line monitoring indications. However, the analysis of dissolved gases in the suspected bushing oil, according to the data shown in Table IV, and the analysis below indicate a very different conclusion. In this same table we also inserted the results from the analysis conducted on the phase-C bushing of the same transformer, for reference purposes only.

Table IV. Dissolved gases in the suspected bushing oil and the reference bushing oil

Gas	H2	O2	N2	CH4	CO	CO2	C2H4	C2H6	C2H2	TGC
Suspected bushing (ppm)	639	1548	11256	479	291	3457	248	76	8	1741
Reference bushing (ppm)	21	2148	86320	9	40	216	ND*	1	ND*	71

* Note: ND = Not detected.

The analysis of these gas measurements in the oil, in accordance with IEC 60599-2007 [10] standard, reveals that combustible gases Hydrogen (H2), Methane (CH4), Ethylene (C2H4), Ethane (C2H6) and Acetylene (C2H2) present values very above the ones considered as typical (acc. to Table I). According to this standard, the diagnosis of the type of defect on bushings leads to "T – Thermal Fault" diagnostic (Fig. 15).

As presented above, although the diagnostics provided by the on-line capacitance and tangent-delta monitoring, and by the analysis of dissolved gases, has exhibited coherence between each other and confirmed the existence of a bushing defect, the diagnostic achieved by the off-line measurement of the same

ISBN 978-84-617–9183–5

variables measured by on-line monitoring (capacitance and tangent-delta) was different, as it did not detect significant variances in relation to the initial reference values.

Thus, off-line capacitance and tangent-delta measurements exhibited low efficacy for the correct diagnostic of the bushing conditions. In the analysis performed with the data available to the time, the reasons listed below were pointed out as the most probable ones for this fact:

- Dielectric temperature

As widely known, the tangent-delta value of the oil-impregnated paper (OIP) type insulation, which is the case of the bushing in question, has strong dependence with the dielectric temperature, even on insulations in good conditions. This is a characteristic that tends to worsen when the insulation presents increase of tangent-delta value.

- Voltage applied on the dielectric

Another great difference between the capacitance and tangent-delta measurements made off-line in relation to on-line monitoring is the voltage applied on the bushing's dielectric. While in the on-line monitoring during the normal operation of the bushing, this is powered at the nominal voltage, 550 kV / $\sqrt{3} \approx 318$ kV in the case being studied, for off-line tests, the voltage usually applied has an order of 10 kV, i.e. 3% of the nominal one.



Figure 15. Bushing disassembly in a repair shop.
1º - Disassembly, 2º - Smooth surface, 3º - Surface with bubbles, 4º - small carbonization, PD activity.

To conclude, the experience at field presented herein of detecting a defect on a 550 kV bushing in a step-up transformer at UHE Itá enabled to prove the efficacy of on-line monitoring of bushings installed in this and other power plants near 3 years before, thus meeting the objectives for reducing the risk of catastrophic failures, eliminating the very high cost of these failures and increasing the installation reliability, in addition to the increase of maintenance efficiency and reduction of maintenance costs by preventing unnecessary interventions for off-line tests.

By the other side, this experience also enabled to checking the efficacy of test techniques being widely used for decades in the industry for the diagnostic of the conditions of operating bushings, confirming the low sensitivity of off-line capacitance and tangent-delta measurements for the defect detected in the bushing being studied.

ISBN 978-84-617–9183–5

Although this analysis has confirmed the great sensitivity of the analysis of dissolved gases in the oil for detecting defects in bushings, the risks of defect insertions in the bushing make the utilization of this test applicable to special situations only, such as the final confirmation of a defect diagnosis.

The evidences presented above, associated to the need for continuous and on-line diagnostic during the whole equipment operation time, without any "blind zones" during the intervals between tests, in addition to the difficulties to power the equipment off, confirm that the on-line capacitance and tangent-delta monitoring of the bushings fully meets the needs of the power utility company.

V. CONCLUSIONS

In order to achieve the expected outcomes for using power transformer condition monitoring systems (ECM), special care must be taken in drafting the specifications for the features of the system, such as the variables to measure, the architecture that will be used in measuring the variables and the desired diagnostic modules.

By specifying a decentralized architecture for measuring variables, based on intelligent devices (IEDs), it is possible to deploy specific diagnostic modules, as shown in the examples given in item 3, taking advantage of the IEDs already installed on the transformer for supervision and control functions as data sources (sensors) and at a zero cost for the monitoring system. This architecture also allows the gradual implementation and expansion of the monitoring system, respected the availability of company resources and allowing their implementation on a larger number of transformers. The cases of successful use of systems based on decentralized architecture also demonstrated the importance of online monitoring systems to avoid catastrophic failures of equipment, increase equipment availability and reduce maintenance costs.

Thus, the deployment of online monitoring systems, in the past usually limited to large scale transformers due to their high costs, also becomes possible in small and medium scale transformers.

REFERENCES

[1] Lavieri Jr., Arthur, Hering, Ricardo, *"New Concepts in Energy Systems of High Reliability", Encarte Especial Siemens Energia,* http:// mediaibox.siemens.com.br/upfiles/232.pdf, January/2001.

[2] Alves, Marcos, *"On-Line Monitoring System for Power Transformers", Eletricidade Moderna Magazine*, May/2004.

[3] Amom, Jorge, Alves, Marcos, Vita, André, Kastrup Filho, Oscar, Ribeiro, Adolfo, et. al., *"Sistema de Diagnósticos para o Monitoramento de Subestações de Alta Tensão e o Gerenciamento das Atividades de Manutenção: Integração e Aplicações", X ERLAC - Encontro Regional Latinoamericano do CIGRÉ*, Puerto Iguazu, Argentina, 2003.

[4] Melo, Marcos A. C., Alves, Marcos, *"Experiência com Monitoração On-Line de Capacitância e Tangente Delta de Buchas Condensivas", XIX SNPTEE – Seminário Nacional de Produção e Transmissão de Energia Elétrica*. Rio de Janeiro, Brasil, 2007.

[5] Peres, Edilson, Duso, Wilson, Latenek, J., Alves, Marcos, *"Monitoração On-Line de Transformadores Conversores do Sistema de Transmissão HVDC na SE Ibiúna", XIII ERIAC*, Puerto Iguazu, Argentina, Maio/2009.

[6] Peres, Edilson, Alves, Marcos, "*Field Experience with On-Line DC Bushing Monitoring in HVDC System at Ibiúna Substation", 2009 HVDC User's Conference*, Foz do Iguaçu, Brasil, 2009.

[7] Alves, Marcos and Silva, Gilson, *"Field Experience in on line Monitoring of one 343mva 230kv Transformer With 2 Load Tap Changer", Eletricidade Moderna Magazine*, April/2006.

[8] Araújo, D. C. P., Alves, M. E. G., Teixeira, R. M., Silva, J. C., Moreira, C. R. N., *"Prevenção de Falha em Transformador Trifásico 525 kV pela Monitoração On-Line de Tangente Delta de Buchas", XXII SNPTEE – Seminário Nacional de Produção e Transmissão de Energia Elétrica*. Brasília, Brazil, 2013.

[9] The Institute of Electrical and Electronic Engineers, ANSI/IEEE Std C57.19.100-2012, "IEEE Guide for Application of Power Apparatus Bushings", February/2013.

[10] International Electrotechnical Commission, IEC 60599 Edition 2.1, "Mineral oil-impregnated electrical equipment in service - Guide to the interpretation of dissolved and free gases analysis", 05/2007.

ISBN 978-84-617–9183–5

Risk of Contamination of the Oil During the Different Processes After Testing a New Transformer. Detection and Analysis of this Contamination and Description of the Process to Remove it Successfully.

Miguel MARTÍNEZ RONDEROS mmartinezr@iberdrola.es
Carlos VILA MONTAÑÉS cvila@iberdrola.es
Diego LUMBRERAS BASAGOİTİ dlumbreras@iberdrola.es
Laura HERNÁNDEZ FERNÁNDEZ lhernandezf@iberdrola.es
Emilio SIERRA GÓMEZ

IBERDROLA DISTRIBUCION ELECTICA
Transformers Standardization and Maintenance Department
Federico Salmón nº 5 28016 Madrid

Abstract — **Between F.A.T (factory acceptance test) and commissioning test take place several processes in which dielectric oil is involved. An incorrect oil handling and store could alter its characteristics and reduce the dielectric strength of the insulation system or result in acceleration of the rate of ageing of the insulation system. In this paper some cases are described in order to demonstrate how easy it is to make a mistake and how complicate is to solve it.**

Keywords — **Oil quality, RVM, FINGERPTINT,**

I. INTRODUCTION

Expected lifetime in Power Transformers (PT) depends significantly on their initial condition previous the first commissioning onsite. Then is when fingerprint tests play a crucial role as these tests are the milestone which marks the start of transformer service life. In addition to that from contractual point of view these tests are the last milestone prior to accept the transformer by the custome.

During the period between FAT (factory acceptance test) and commissioning tests (fingerprint test) a power transformer is subjected to multiple key operations, some of them related to the dielectric insulation system, such us: oil draining in factory, filling with dry air, power transformer and oil shipping, PT oil filling and others.

The purpose of this article is to highlight the importance of the oil handling during these operations, and the consequences of improper procedures

II. OIL HANDLING

Dielectric oil shipping between factory and substation can be done in several ways.

- Oil filled shipping
- Oil draining and later filling.

Once it is located on the plinth at its final destination and in case the transformer has been shipped with dry air, this option includes other two possibilities to fill the transformer with dielectric oil:

- Filling the transformer with the dielectric oil used during FAT
- Ordering new dielectric oil which will be delivered directly to the substation

Within the entire transportation of a transformer from the factory to site, several process related to the dielectric oil are included:, racking, storage in tanks, pumping into tankers, treatment process, etc. It is important to note that, most of these processes are carried out by third companies hire by transformer manufacturer or the Utility, which sometimes are not precautious enough regarding oil handling, leading to potential contaminations of the oil. Some of the possible mechanisms to contaminate the oil are obvious:

- Contamination with the lubricating oil from the pumps of the Treatment plant, during oil filling or reconditioning.
- Contamination with other products previously stored in the tanks and tanker used.
- Contamination with other products present in the treatment equipment due to an improper cleaning

ISBN 978-84-617–9183–5

III. CONTAMINATION DETECTION

As indicated in the introduction, fingerprint tests are the latest milestone prior to commissioning and acceptance of a new PT and its connection to the network. Part of these fingerprint tests are mainly focused on detecting problems in both solid and liquid insulation and they are commonly applied in the industry. They are commonly applied in the industry, and are added to the specific and mandatory tests defined by each Utility. In the case of Iberdrola Distribución these are:

- Oil specifics
  - Moisture content
  - Dielectric dissipation factor and conductivity
  - Spectroscopy infrared
  - Acid Neutralization Number
  - Colour

- General to the PT
  - Insulation power factor test f(V, f)
  - Insulation resistance and polarization index
  - Core insulation resistance measurement
  - Recovery Voltage Measurement (RVM)

These tests are considered sufficient to detect issues and/or contaminations; however it is worth to highlight the importance of the technician who analyzes the results. In a huge percentage of cases the results are correct, so it is the technician duty to distinguish and detect the few that present an issue, which is usually showed only by small deviations in the results, as the proportion between contaminant and dielectric oil is minimum.

Real cases proving these situations are reflected in the present documents, where small variations in spectroscopy infrared conductivity depending on polarity or relative maximums in dielectric spectroscopy test, as well as others, led to detect a problem in the transformer before its commissioning.

IV. CASE STUDY I

Power transformer characteristics:

Data	Value
Rated voltage	30/13,8 kV
Rated power	25 MVA
Oil volume	7600 Kg

During commissioning tests the existence of a contaminant was detected by Laboratory technicians in physicochemical tests. Electrical tests were very sensitive to that contaminant.

IV.1 TEST SEQUENCE

Although all physicochemical parameters achieved the required values by IBD, a discrepancy was observed in the spectroscopy infrared test. An abnormal band at 1749 cm^{-1} wavelength was founded, being that band related with a pure mineral oil, but more typical of a band of carbonyl groups.

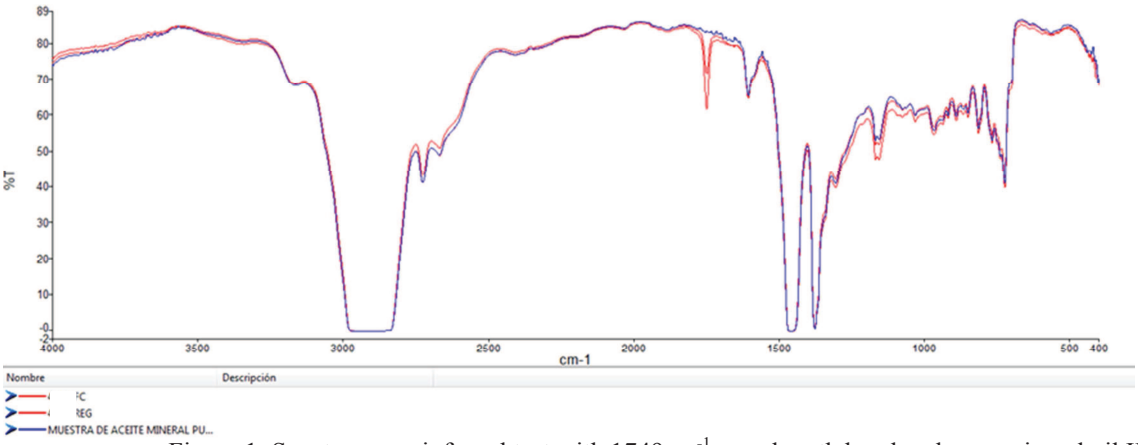


Figure 1. Spectroscopy infrared test with 1749cm^{-1} wavelength band and pure mineral oil IR.

ISBN 978-84-617–9183–5

In this case electrical tests were very sensitive to contaminants, because dielectric DC spectroscopy does not show polarization processes. In addition to that power factor test exceeded the required values by standard, although FAT results were correct.

Table I. Power Factor Test @ 10kV 50Hz

Date	ICHL[1]	ICH[2]	ICL[3]	Temperature ºC
FAT	0,241	0,222	0,290	20
Finger Print-Test	0,140	0,854	0,365	11

1- CHL represents the insulation between the high- and low-voltage winding.
2- CH represent the insulation between de high-voltage winding conductor and the grounded tank and core
3- CH represent the insulation between de low-voltage winding conductor and the grounded tank and core

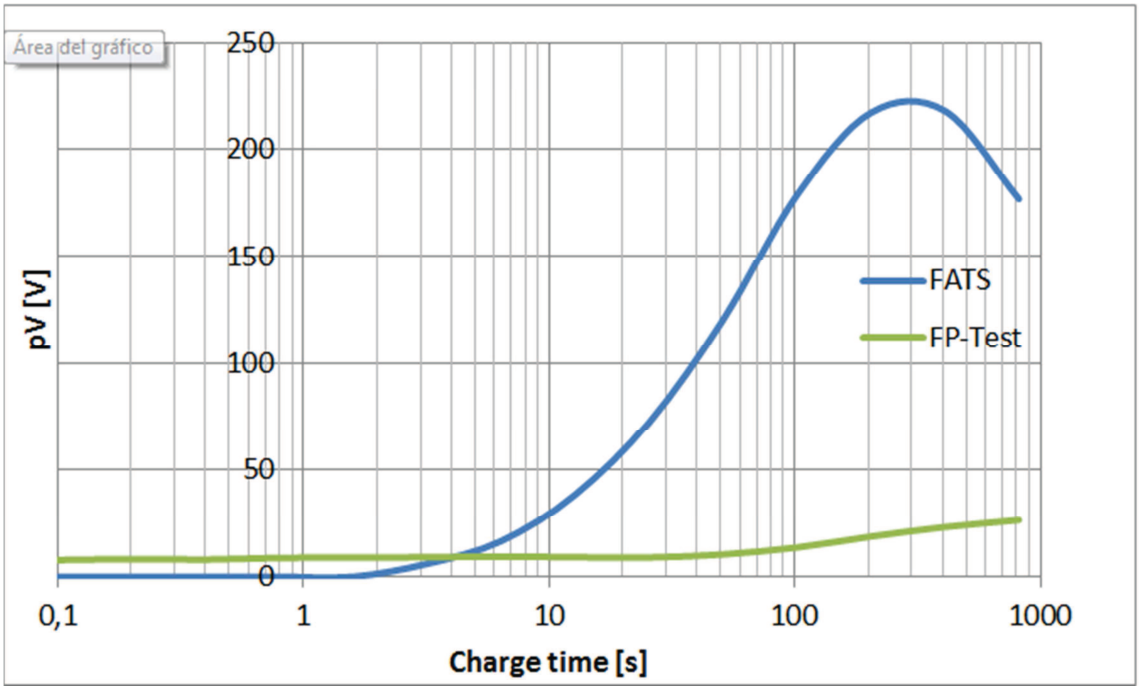


Figure 2. RVM test results.

It should be noted that in this particular case if data would not have been analyzed exhaustively, obtained test values would had been considered as correct, except for power factor values in CH configuration above standard accepted values. Even the extremely poor RVM test analyzed by the software indicates a time constant 819.2 seconds, which is an excellent result. This proves that physicochemical tests require a very strict evaluation to detect an anomaly in spectroscopy infrared test.

Considering these results and with the collaboration of the transformer manufacturer, it was possible to follow oil traceability, discarding contamination in the manufacturer facilities as the same oil had been used to fill another transformer, which had been recently and successfully commissioned for Iberdrola. Therefore, it was concluded that contamination happened either during oil shipping or oil treatment, in this particular case the analysis concluded in this second option as the contamination took place by residues at hoses owned by treatment company.

IV.2 DECONTAMINATION

Decontamination process consisted in several and consecutive steps of contaminated oil draining and spraying transformer active part with clean oil, using as acceptance milestone the spectroscopy infrared test about the “sacrificed” oil coming from the cleaned process, the process finished when spectroscopy infrared test of sacrificed oil did not show contamination traces.

In this occasion the decontamination process was easy due to windings impregnation oil was clear, and contaminated oil did not have opportunity of impregnated cellulosic insulation.

ISBN 978-84-617–9183–5

IV.3 AFTER DECONTAMINATION TEST

Once power transformer was decontaminated, new fingerprint tests confirmed that decontamination was satisfactory, as it could be observed that the band at 1749cm^{-1} wavelength in spectroscopy infrared test disappears.

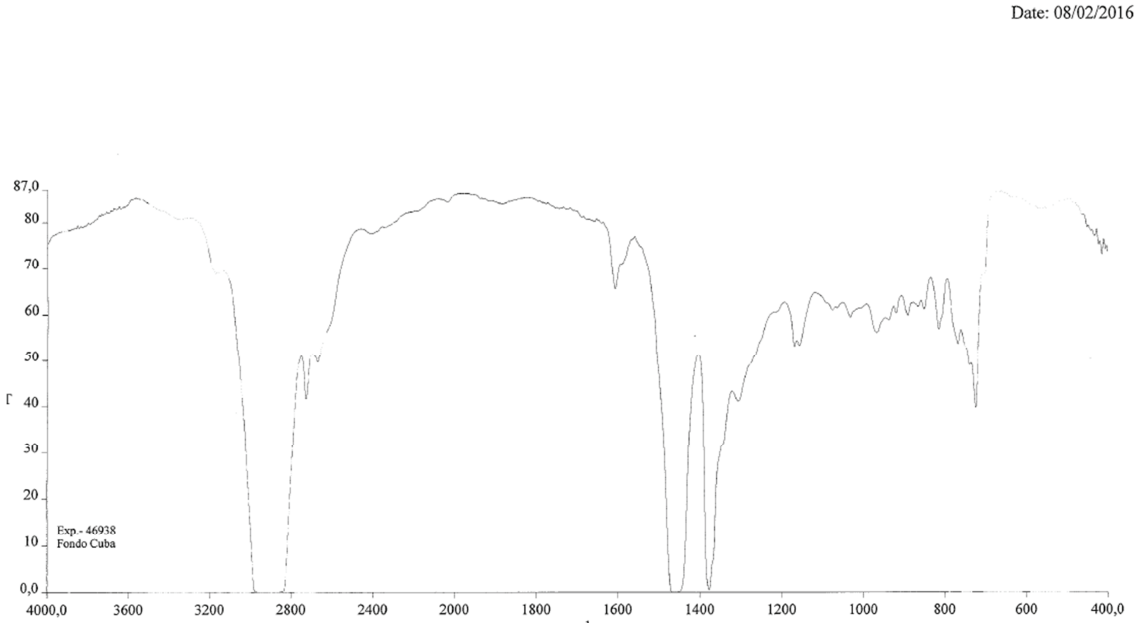


Figure 3. Spectroscopy infrared test without 1749cm^{-1} wavelength band.

Additionally electrical test were performed and the results obtained were adequate and similar to f.a.t.

Table I. Dielectric Power Factor Test @ 10kV 50Hz

Date	ICHL[1]	ICH[2]	ICL[3]	Temperature ºC
FAT	0,241	0,222	0,290	20
Fingerprint-Test	0,140	0,854	0,365	11
Fingerprint-Test (2)	0,247	0,337	0,262	23

1- CHL represents the insulation between the high- and low-voltage winding.
2- CH represents the insulation between de high-voltage winding conductor and the grounded tank and core.
3- CH represents the insulation between de low-voltage winding conductor and the grounded tank and core.

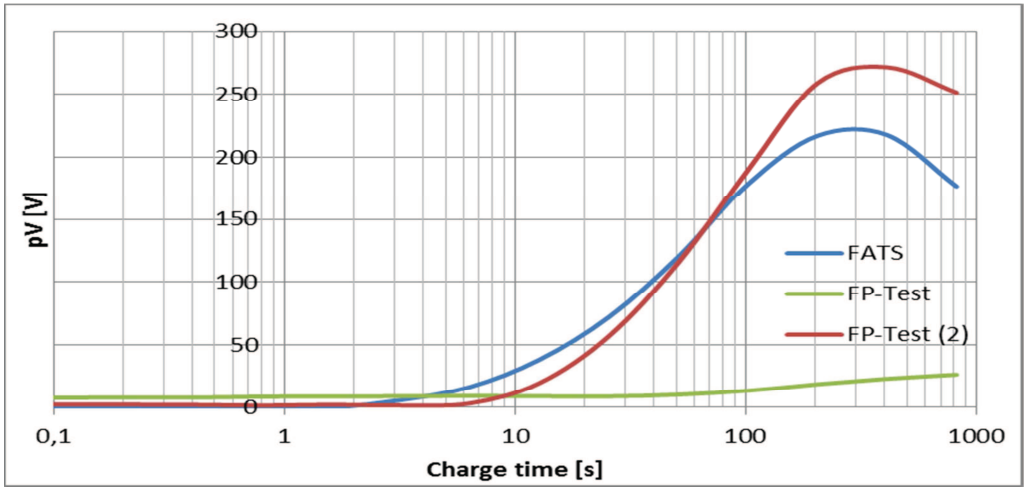


Figure 4. RVM test results.

ISBN 978-84-617–9183–5

V. CASE STUDY II

Power transformer characteristics

Data	Value
Voltage	132/21,5 kV
Power	20 MVA
Oil volume	13900 Kg

The transformer commissioning was long and tedious, because after fingerprint test were done, it was decided to ship back this transformer to factory due to the very low insulation values obtained. These were caused by the presence of polar components impregnating the cellulosic insulation. After dielectric characteristics were recovered due to a factory process, in a new commissioning test, once again, at the substation a new insulation problem was discovered, joined with inhibitor traces presence in the oil, which is not allowed under Iberdrola standards for new oils, after the second commissioning, it was observed that oil dielectric dissipation factor increased quickly due to polar contamination migration from cellulosic insulation to oil, and it was decided to decontaminate transformer onsite.

V.1 TEST PHASE

In this case several phases are going to be detailed, paying attention to the individual tests results.

V.1.1 First Commissioning

When first fingerprint tests, dielectric test values were unsatisfactory while physicochemical oil analysis were correct.

It was suspected that polar contamination should be impregnated in the cellulosic insulation and it was not mixed with oil. Finally and after a long investigating process was determined that polar contamination came from the lubricating oil in the dry air pump And for this reason it was decided to return transformer to its factory.

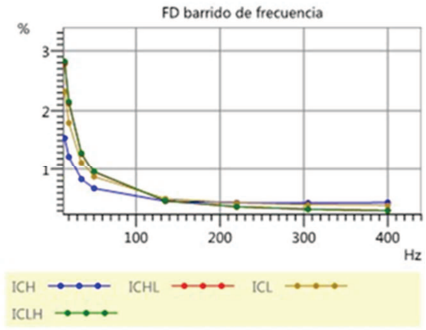


Figure 5. Power factor test which shows abnormal values at low frequencies.

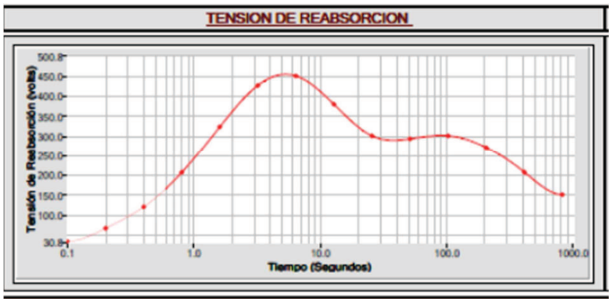


Figure 6. RVM test which shows a polar contamination proper maximum.

V.1.2 Second Commissioning

The power transformer came back from the factory, and new fingerprint tests were performed. The results of these were not as bad as the first ones but there were not as satisfactory as we desire. By other hand inhibitor traces were detected in the oil. This is a new example proving that during the shipping of oil from transformer factory to substation is essential to avoid accidents by improperly oil handling. Finally it was accepted to connect the transformer to the network.

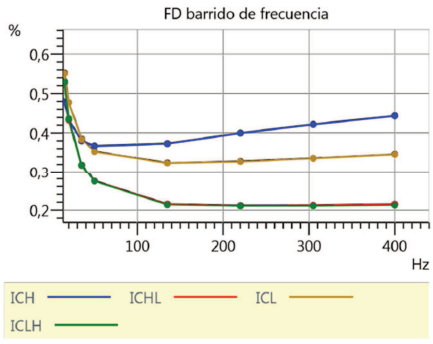


Figure 7. Improvement in dielectric loss at low frequency.

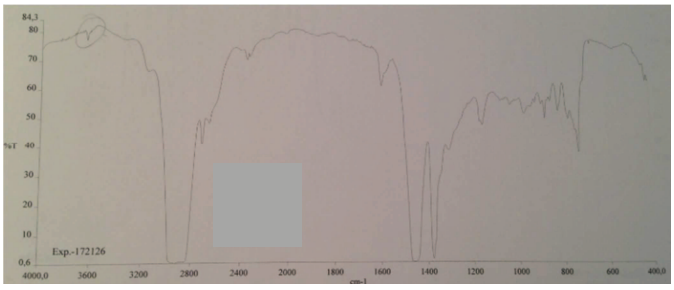


Figure 8. inhibitor proper band at 3600 cm-1 which could means that it is regenerated oil.

ISBN 978-84-617–9183–5

After transformer commissioning our suspicions were confirmed, due to a very soft decontamination polar contaminants from windings insulation migrated to the oil, whose dielectric properties rise down rapidly.

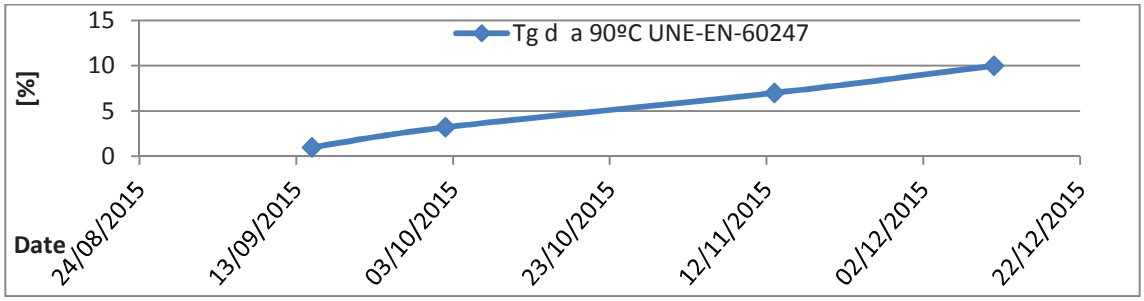


Figure 9. oil disipation factor evolution.

V.2 DECONTAMINATION

In this case it was chosen a deeper decontamination process, being necessary to drain all the oil including windings impregnation oil, and based on that proceeding to replace the oil.

Due to the latter migration of the contamination to the oil, the physicochemical test were not sensitives until the migration process of polar components from windings to oil, therefore it was decided to use RVM test to identify the presence of polar components.

The decontamination and cleaning process consist in:

- Initial dielectric test
- Oil draining
- 12 hours vacuum application
- Oil draining under vacuum
- 12 hours vacuum application
- Oil draining under vacuum and spaying with sacrifice oil
- 24 hours vacuum application and Oil draining under vacuum
- Dielectric tests
- Oil filling with pre-treated new oil and later oil treatment
- Dielectric tests

RVM test has been used to determine polar components inexistence and the results obtained are showed in the following table.

Table II. Obtained RVM values

Time	09/05/2016 a Initial state	09/05/2016 b Oil drained	12/05/2016 Oil drained	16/05/2016 Final state
0,1	22,88	32,93	29,35	0
0,2	47,6	58,11	16,75	2,54
0,4	88,73	98,67	22,07	7,74
0,8	155,28	173,42	33,74	5,89
1,6	254,52	277,28	16,06	8,43
3,2	375,37	404,14	32,81	10,4
6,4	**455,43**	**454,62**	**32,46**	**20,91**
12,8	444,23	414,3	29,35	50,1
25,6	340,02	326,5	40,09	92,63
51,2	283,87	297,96	35,93	150,87
102,4	285,25	254,41	34,31	230,39
204,8	276,93	108,72	15,83	300,09
409,6	232,34	10,74	14,79	355,41
819,2	166,83	31,54	13,17	360,33

ISBN 978-84-617–9183–5

RVM curve showed a maximum at 6,4 seconds time constant, which has been identified as key constant for polar compounds, thus 6,4 seconds would be the value uses to determine the recovery efficiency. In the several curves obtained shows:

- (09/05/2016 a) Two maximums: One absolute maximum which represent the polarization process of the contaminant substance, and a relative maximum which represent insulation condition.
- (09/05/2016 b) After oil draining, relative maximum disappeared and only polar substances impregnated in windings are detected in the RVM test.
- (12/05/2016) when the polar substance is drained, there is not any substance which response to RVM test.
- (16/05/2016) Transformer after oil filling and treatment presents a good condition in the RVM results obtained.

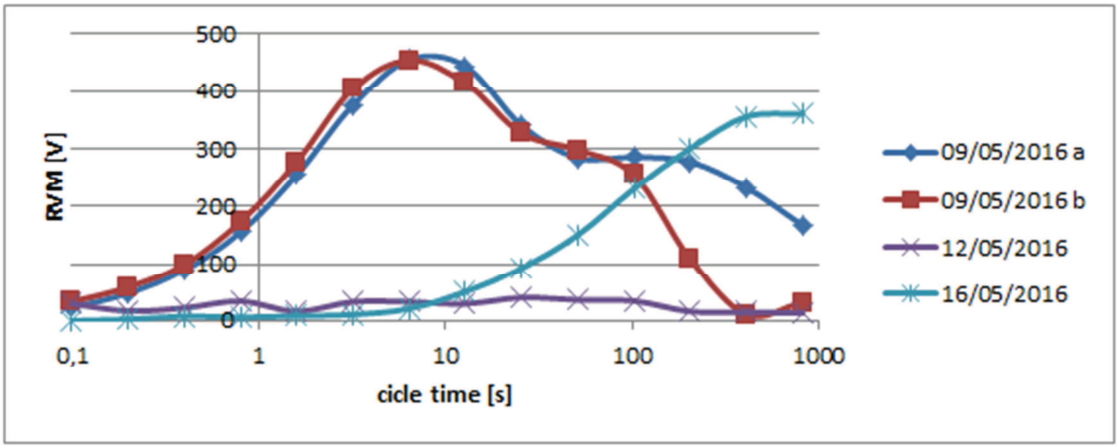


Figure 10. Obtained RVM curves.

VI. CONCLUSIONS

As shown in the case studies detailed in this document, the different processes involved between FAT and commissioning test at the substation is critical for oil condition, and the lack of quality during these processes can affect dramatically the performance and reliability of a new transformer.

Two examples have been explained; In the first one the oil was contaminated by residues at hoses owned by treatment company, and in the second one windings were impregnated with polar contamination from the lubricating oil in the air pumps. Both cases could have been avoided following the correct procedure in oil draining, dry-air filling, PT and oil shipping, PT oil filling with dielectric oil process control.

In the case of some of these tasks were performed by a third company which has been contracted by PT manufacturer, we strongly recommend, increased control during all these process in order to avoid this kind of problems.

On the other hand it highlights the the importance of an exhaustive fingerprint test set, although FAT has been satisfactory. There are several processes in which power transformer oil can be contaminated prior to its network connection, and it is critical to ensure that the initial condition is the optimum, as it will greatly contribute to the durability of the asset during its lifetime

REFERENCES

[1] UNE-EN 60247:2004 *Líquidos Aislantes. Medida de la Permitividad Relativa, del Factor de Disipación Dieléctrica (tan d) y de la Resistividad en Corriente Continua.*

[2] UNE-EN 60814:1999 *Líquidos Aislantes. Papeles y Cartones Impregnados en Aceite. Determinación del Contenido en Agua por Valoración Culométrica Automática de Karl Fischer.*

ISBN 978-84-617–9183–5

[3] UNE-EN 60666:2011 *Detección y Determinación de Aditivos Específicos en Aceites Minerales Aislantes.*

[4] Gusztav Csépes, *Practical Foundations of the RVM (Recovery Voltage Method for Oil/Paper insulation Diagnosis,* Electrical Insulation and Dielectric Phenomena, 1998. Annual Report. Conference on (Volume:1), p 345-35, Oct 1998

[5] Tapan K. Saha, *Deriving an Equivalent Circuit of Transformers Insulation for Understanding the Dielectric Response Measurements*, IEEE Transactions on Power Delivery, Vol. 20, No. 1, January 2005

[6] Ruijin Liao, *Quantitative Analysis of Ageing Condition of Oil-paper Insulation by Frequency Domain Spectroscopy,* IEEE Transactions on Dielectrics and Electrical Insulation Vol. 19, No. 3; June 2012

[7] Rainer Patsch, *Dielectric Time Constants – the Key to the Interpretation of Return Voltage Measurements on Cellulose-Oil Insulated Power Equipment,* Proceedings of the 9th WSEAS International Conference on POWER SYSTEMS

[8] Rainer Patsch, *Return voltage measurements Diagnostic interpretations based on the dielectric time constants,* Materials Science-Poland, Vol. 27, No. 4, 2009

[9] M. H. Li, *Return Voltage Measurements of Oil Impregnated Paper Insulated Transformers,* Proceedings of 2005 Intemattonal Symposium oil Electricdl Insulating Materink, June 5-9, 2005. Kitakyushu, Japan

[10] P. R. S. Jota, *Modeling the Polarization Spectrum in Composite Oil/Paper Insulation Systems*, IEEE Transactions on Dielectrics and Electrical Insulation Vol. 6 No. 2, April 1999

[11] ABB Power Products, *Service Handbook for Transformers,* 3rd edition 2007

[12] J.M. Abella Martin, *Física de dieléctricos*, SA MARCOMBO Barcelona 1984

[13] Ninas AB, *Transformer oil handbook*, 3er edition 2010, Sweden

[14] J. Aubin, E*ffect of Particles on Transformer Dielectric Strength*. Working Group 12.17 CIGRÉ, June 2000

ISBN 978-84-617–9183–5

BAT/BEP Diagnostics & Treatments for Smart Life Cycle Management of Oils & Transformers (Smart LCM-O&T): Case Histories of DBDS/Corrosion & PCBs

Vander TUMUATTI*, M. TUMIATTI, C. ROGGERO, R. ACTIS and R. MAINA

Sea Marconi Technologies S.a.s.
Via Ungheria 20, 10093 Collegno (Turin) – Italy
*Founder and General Partner of Sea Marconi and Ass. Secretary IEC TC 10
e-mail: tumiatti@seamarconi.it

Abstract — **This paper describes the "State Of the Art" for inventory, control, management, decontamination of electrical equipment and insulating liquids containing DBDS/Corrosion & PCBs. The Best Available Techniques (BAT) and Best Environmental Practices (BEP) for Life Cycle Management (LCM) of electrical equipment impregnated with insulating liquids, according to the prescriptions of the Stockholm Convention on Persistent Organic Pollutants (POPs) entered into force on May 17th 2004, are presented, according to art. 5 Annex C and IEC and CENELEC standards. The quantitative determination of total corrosive sulfur (TCS) in insulating liquids permits an objective ranking of sulfur compounds according to their corrosiveness towards copper. Case Histories of Diagnostics & Treatments are presented in according to IEC & CENELEC include On -Load treatments in power transformers and shunt reactors, in Brazil, South America, Europe and worldwide. The integrated treatment normally runs at 80-100 °C and has the capability to decontaminate equipment on-site through continuous circulation of the oil a closed system (without draining the oil or using auxiliary tanks) using the solvent capability of the oil for continuous extraction of PCBs and DBDS from solid materials inside the equipment (according IEC 60422 art. 11.4.4).**

Keywords — **Transformer, Mineral insulating oil, Additive, PCBs, Diagnosis, Countermeasure, CDP Process, Dehalogenation, Dibenzodisulfide DBDS, Corrosive Sulfur, insulating liquids, Quantitative determination, Total Corrosive Sulfur – TCS, Selective Depolarization, C1 – DBDS & Corrosive Sulfur, C2 – NON DBDS & Corrosive Sulfur, C3 – SDBP & Corrosive Sulfur (SCBP – Sulfur Combustion By Products), C4 – NON Sulfur corrosion & Metal dissolution**.

I. INTRODUCTION

Mineral insulating oils and other insulating fluids have a strategic role in electrical equipment (transformers, shunt reactors, tap changers, bushings, etc.) regarding generation, transmission, distribution and end-use of electrical power. Such equipment represent key assets for the oil and gas industry, mines, heavy industry, manufacturing, drinking water production and distribution, civil and defense infrastructures (hospitals, harbors, airports, railways, households, etc). The diagnostics and integrated treatments (such as depolarization, dehalogenation, reclamation etc.) are the key factor for Life Cycle Management of Oil & Transformer (LCM-O&T) focalized on loss prevention and environmental protection.

II. DBDS / CORROSION SCENARIO

Insulating liquids may contain corrosive sulfur compounds that, having detrimental effects on electrical equipment, such as transformer, have been investigated and classified in some macro classes that include elemental, inorganic and organic sulfur. The Total Corrosive Sulfur (TCS) is related to the origin of the oil, the refining processes and the presence of additives. Insulating mineral oils are comprised of paraffinic and naphthenic bases, synthetic iso-paraffins, esters, poly α-olefins, poly alkylene glycol. Most of the additives act as electrostatic discharge depressants, metal deactivators, metal passivators, antioxidants, such as polysulfides and disulfides (e.g. dibenzyl disulfide - DBDS).

Some sulfur species that have antioxidant properties are corrosive and react with metal surfaces. Examples of these species are elemental sulfur, mercaptans and disulphide. Since their presence has been linked to failures of electrical equipment, the IEC standard for mineral insulating oils states that corrosive sulfur compounds shall not be present in unused and used insulating liquids (see IEC 60296 ed. 4 2012)[1].

ISBN 978-84-617–9183–5

Among the several corrosive compounds, one in particular, DBDS, is currently in the limelight, as its presence has been connected to copper sulphide formation on the surfaces of copper conductors under normal operating conditions of electrical equipment. Copper sulphide, which is a semiconductor, is held responsible for several short-circuit faults and windings deformation, through its build-up on paper [2-9].
Current standard test methods for detection of corrosive sulfur are ASTM D1275, methods A and B, and DIN 51353. In case of potentially corrosive sulfur, in used and unused insulating oil, the IEC 62535 standard is employed. All these methods are purely empirical and qualitative, as they depend on a visual and subjective perception of color [10-13], do not produce any quantitative result and are totally unreliable if a metal passivator is contained in the oil under investigation. As a matter of fact, in this latter case, a "False Negative" result can be produced, even if sulfur corrosive compounds are present. Contrarily, a "False Positive Result" can be returned when aging oils, acidic oils, undergoes the aforementioned test methods. Therefore, further confirmative analyses are required. IEC 62535 specifies that in case of doubts in the interpretation of the results from the inspection of paper analyzed by other methods (for example by SEM-EDX).
The International Electrotechnical Commission founded in the 1906 (IEC – www.iec.ch) give the most advanced standards worldwide in the field of electrotechnical and electronic field and include more than 60 members and 23 associates members. The Technical Committee 10 (TC 10) set up a working group (WG-37) aimed at developing methods for the unambiguous quantitative determination of corrosive sulfur compounds in unused and used insulating liquids. Because of the complexity of such determinations, the test method was divided into three parts:

Part 1 – Test method for quantitative determination of the corrosive sulfur compound dibenzyldisulfide (DBDS).

Part 2 – Test methods for quantitative determination of Total Corrosive Sulfur (TCS).

Part 3 – Test methods for quantitative determination of total thiols and disulfides (TMD) and other targeted corrosive sulfur species, such as elemental sulfur [14].

The analytical and diagnostic activities can achieve a full significance if contextualized in a broader scenario, where depolarization treatments are also included. Monitoring and maintaining the quality of insulating fluids and equipment is essential to guarantee a reliable functioning of electrical equipment. Therefore, codes of practice have been established by electrical power authorities, power companies and industries in many countries.
A few maintenance techniques are available for protecting metal surfaces from corrosion, such us adding metal passivators, replacing the oil or processing it through a Selective Depolarization treatment. In Table I an evaluation between oil replacement and Sea Marconi's Selective Depolarization is shown. It is evident that Selective Depolarization is economically and technically preferable to oil replacement. It does not require unused oil refilling, oil reconditioning, oil disposal, and guarantees the full recovery of chemical and physical properties. It's free from cross contaminations and can be performed keeping the transformer energized (On Load). In Table II the comparative evaluation between Selective Depolarization and simple Fuller's Hearth treatment (new and thermally regenerated) is also shown. Fuller's Hearth are totally unable to remove DBDS from the oil and when regenerated can impart corrosiveness to oil that are originally non-corrosive. Furthermore the regeneration steps represent an environmental issues being a possible source of POPs (PCBs, PCDDs-Dioxins, PCDFs- Furans, PCA, etc.), if emission control measures are not efficient.
Metal passivators additives, such as triazole derivatives (e.g. benzotraizole, toluyl triazole, Irgamet®30, Irgamet® 39), can only offer a temporary protection for metal from corrosion. Not only heat, but moisture and acidic conditions also, quickly degrade the mentioned molecules, impairing their passivating properties and exposing again the metal surfaces to the action of corrosive compounds. In CIGRE document 378/2 – 2009 it is stated: "*..the addition of metal passivators is not a guarantee against failures. For instance, in Brazil, more than 200 shunt reactor oils in service were passivated (in most cases between ½ and 2 years after going into service). It has been reported that 9 of these units failed between one and 24 months after passivation…*" And in document 378/1- 2009 it is reported that "t*here are a significant number of reports of increased hydrogen and carbon dioxide formation when the passivator is added to oil already in service".*

ISBN 978-84-617–9183–5

Furthermore triazole derivatives are classified as Harmful and Environmental Hazardous substances and can pose a serious threat to health and safety of workers (Suspected Carcinogenic) [15-16].
In this paper, methods and best practices for Life Cycle Management (LCM) of oils and transformers based on the State of the Art, IEC standards, CIGRE Guidelines Best Available Techniques (BAT) and Best Environmental Practices (BEP) are presented together with a significant set of case histories [17, 18, 19, 20].
One priority topic is represented by the "DBDS & Corrosion Free Program – Tumiatti's Square", a comprehensive diagnostic and processing tool, addressing four different types of corrosion:

- C1 – DBDS & Corrosive Sulfur
- C2 – NON DBDS & Corrosive Sulfur
- C3 – SCBP & Corrosive Sulfur (SCBP – Sulfur Combustion By Products)
- C4 – NON Sulfur corrosion & Metal dissolution

III. PCBs / POPs SCENARIO

The identification of PCBs, as a harm to the environment, is symptomatic of a typical application scenario common to many other synthetic chemical compounds (i.e. POPs – Persistent Organic Pollutants). The risks generated by PCBs in the ecosystem resulted in the promulgation of numerous rules at international level on the prohibition and use of these substances (1976 – EEC Directives 76/405 and 76/769; USEPA 1979 40 CFR Part 761). Also, international agreements were reached finalised toward the elimination of these toxic and persistent compounds within established time limits. These include the water resources of the Great Lakes Region (18% of the global reserve of drinking water) several European Directives and the Protocol of Stockholm of May 2001 on POPs.

It must be noted that the term "PCBs" as defined in art. 2 of Directive 96/59 EC, for the first time includes also other halogenated compounds, besides the 209 possible congeners of the Polychlorinated biphenyls. They are the PCTs equivalent (8557 possible congeners) and PCBTs (several thousand congeners) with a concentration exceeding the limit of 0.005% by weight (50 mg/kg or ppm). These compounds are classified as dangerous, persistent and bio-accumulable, creating an unreasonable risk for the environment and Human Health (such as contamination of food, as occurred in June 1999, in Belgium, France and Italy).
Recently the PCBs was classified "Class 1 – Cancergenic for Human (1st April, 2013). – www.iarc.fr
In the event of uncontrolled thermal oxidation, during the operation of transformers (hot spots > 150-300 °C) or in case of failures (arching of electrical systems) with explosions and fires, significant concentrations of very dangerous compounds occur, such as PCDFs- Furans (135 congeners) and PCDDs-Dioxins (75 congeners).
The use of PCBs as insulating liquid in electrical equipment, particularly transformers and capacitors, caused a significant contamination of the environment. It is estimated PCBs production from 1929 until 1989 the 1.5 million of tons of pure PCBs. Only in Brazil it is estimated about 8.1 million of the equipment contain some level of PCBs (ANEEL 2014).

Significant amount of 3.8 million of distribution transformers are contaminated by PCBs in Brazil (ABDEE 2014).

The equipment and materials contaminated represent a high strategic and investment value of several billion dollars. The obligation for PCBs inventory, decontamination and/or disposal (by 2028) such a mass of equipment and materials involves risks and costs connected with technical and logistic critical factors.
The Best Available Techniques (BAT) and Best Environmental Pactices (BEP) for Life Cycle Management (LCM) of electrical equipment impregnated with insulating liquids, according to the prescriptions of the Stockholm Convention on Persistent Organic Pollutants (POPs) entered into force on May 17th 2004, are presented, according to art. 5 Annex C and IEC and CENELEC standards.
This paper analyses the PCBs problem, the technological options for the decontamination and/or disposal, the asset management options as well as the description of the performance and functional features of a continuous mode dehalogenation process designated as CDP Process® by SEA MARCONI TECHNOLOGIES.
The efficiency of this process was demonstrated successfully on the 2,3,7,8 TCDD (dioxin) in the Seveso accident (starting from 1982), through laboratory experiments and field industrial applications (since 1989) for the dehalogenation/detoxification of PCBs/PCTs/PCBTs/PCDDs/PCDFs on electrical transformers.

ISBN 978-84-617–9183–5

IV. THE MAIN NORMATIVE REFERENCES-IEC & CENELEC

The International Electrotechnical Commission (IEC) and European Standards (CENELEC) cover terms and definitions, specification for mineral insulating oils.

Decontamination - Regulatory References:

- IEC 60296 Ed.4-2012"unused mineral insulating oils for transformers and switchgear "
- IEC 60422 Ed. 4 2013 Supervision and maintenance guide for mineral insulating oils in electrical equipment (Art.12.4)
- IEC 61619 – EN 12766 Insulating liquids – Contamination by PCBs, (PCBs, PCT and PCBsT). Methods of determination by capillary column Gas chromatography
- CENELEC CLC/TR 50503 February 2010 "Guidelines for the inventory, control, management, decontamination and/or disposal of electrical equipment and insulating liquids containing PCBs.";
- CIGRE 413 Working Group D1.01(TF 12)April 2010"Insulating Oil Regeneration and Dehalogenation".
- Stockholm Convention on Persistent Organic Pollutants (POPs/PCBs) (http://chm.pops.int/Implementation/PCBs/Overview/tabid/273/Default.aspx)

V. STRATEGIES AND OPPORTUNITIES

Life Cycle Management (LCM) of insulating Oils & Transformer (LCM-O&T) has been developed, in 10 key steps, in accordance with the following objectives:

A. Prevention and/or mitigation of losses (direct and indirect) and risks for workers, assets, public health and environment, arising from human error, malfunction, or failures of the equipment that cause fires or spillage of hazardous compounds (Oils, PCA, etc.) and Persistent Organic Pollutants (POPs; PCBs, etc.);
B. Implementation of "State of the Art", IEC Standards, "Best Available Techniques" (BAT), "Best Environmental Practices" (BEP) and methodologies available for safety, whilst taking into account the surroundings and the criteria of self-sufficiency and functional recovery;
C. Technical feasibility of the activities within the prescribed time schedules, according local regulations, based on cost/benefit analysis and economical feasibility. (CENELEC CLC/TR 50503 – February 2010, etc.).

The key steps for Life Cycle Management (LCM-O&T) are:

I. **Inventory**
II. **Requirements**
III. **Acceptance**
IV. **Factory Test**
V. **Commissioning and Prior Energization**
VI. **Energization**
VII. **Infancy**
VIII. **Operation**
IX. **Aging**
X. **End of Life**

VI. DBDS/CORROSIVE SULFUR AND PCBS LIMIT

The DBDS/Corrosive Sulfur equivalent for unused mineral insulated oil the concentration is < 5mg/Kg [IEC 60296 Ed 4-2011 - Table 2 not detectable (<5mg/kg) test Method IEC 62697-1-2,3 (in preparation)] and prior of energization in the transformer (IEC 60422 Ed. 2013 – Table 3).

ISBN 978-84-617–9183–5

The PCBs for unused mineral insulated oil the concentration is < 2mg/Kg according with IEC 60296 Ed 4-2012- Table 2 – test method IEC 61619 and prior of energization in the transformer (IEC 60422 Ed. 2013-Table 3).

For oil in service the PCBs concentration is below 50mg/kg [Stockholm Convention on Persistent Organic Pollutants (POPs/PCBs)] or less depending of the local regulations (< di 0.5 mg/kg in Japan; < 2 mg/kg in Buenos Aires – Argentina; etc.) and internal environmental policy of the holder.

VII. SUSTAINABLE SOLUTIONS: DIAGNOSTICS & TREATMENTS

This paper present Sustainable Solution based on Diagnostic and Treatments for Smart Life Cycle Management of Oils & Transformers (Smart LCM - O&T) that is tailored-made on the procurement and life phase of the asset and uses insulating fluids to diagnose and treat transformers' criticalities (functional and environmental). This is a novel management approach developed by industry experts in the field of transformers oil treatment to meet the needs of the energy market – producers, distributors and users - for a reliable, life-cycle based approach to the management of these devices that are the backbone of the electricity distribution grid. This solution provides a one-stop shop for the diagnosis of the health of transformers through innovative testing on insulating materials and comparison with a wealth of information on previous cases as well as providing a treatment solution to prolong the life of this expensive and highly dependable devices. This is an innovative way of managing existing information and capturing new data, through the introduction of innovative testing and treatment procedures and devices. It uses insulating fluids to detect problems area within the transformers as if it were blood, checking for the problems most common to the age of the transformers, and delivering the solution – the therapy – through the "blood" itself.

Sustainable Solution is composed of:

- a **powerful dynamic ICT platform based on bayesian and semantic technology** for automated smart diagnosis based on a proprietary metric of the functional health of this important structural asset on the basis of a large dataset of previous cases;
- **testing procedures ready for patenting** that study specific markers within insulation materials to diagnose criticalities and identify the causes; these take into account the phase of the life of the device and its procurement, according to a ten steps approach to be introduced for the first time with this product
- **multitesting devices and associated protocols** for electric and chemical properties testing that can be used in the lab, on site, in line and on load (i.e. with the transformer energised and fully running);
- a **novel Decontamination Modular Unit (Smart DMU)** for oil Integrated Treatments (Physical Decontamination, Selective Depolarization of DBDS and corrosive compounds, Dehalogenation/Detoxification PCBs, Transformer Desludging, Transform Dehydration, etc.) for the reduction of DBDS, Corrosive Sulfur and PCBs content in and the overall recovery through treatment of oil & transformers on site, on line and on load;

The web platform relies on and it is an evolution towards functionalization of a large database of 200,000 diagnoses on 70,000 transformers, built up by Sea Marconi (since 1968), who specializes in providing insulating fluids testing and treatment services to the major transformers users/maintainers throughout the world. This wealth of information is to be made dynamically accessible through natural language queries, dynamically enhanced through semantic-based analysis of the web and interactive thanks to smart devices installed with the transformer. A predictive, big data analysis model combining bayesian networks and statistics uses the ten step metric:

I. Anamnesis-Family;
II. Anamnesis-Subjective;
III. Signs (Visual evidence and/or onsite tests);
IV. Symptoms-analysis (markers to be analyzed);

ISBN 978-84-617–9183–5

V. Trends;
VI. Outlook;
VII. Certainty Factors;
VIII. Case histories;
IX. Criticalities - functional and environmental with priorities and index;
X. Actions – prevention and/or mitigation with priorities and index) to automatically deliver the diagnosis.

The integrated testing devices deliver common platform modules for undertaking at once multiple analysis of electrical and chemical properties and markers. The Decontamination Modular Unit (DMU) allows for either a continuous mode or batch integrated treatment (CDP Process, CHEDCOS, etc.) of insulating fluids: the patented technology lowers the halogens concentration to below the 0.5 mg/kg limit set by Japan, content ratio that is a hundredth of the limit established by the Council Directive 96/59/EC on the disposal of polychlorinated biphenyls and polychlorinated terphenyls (PCB/PCT) – the PCB Directive, the Stockholm Convention on Persistent Organic Pollutants (POPs/PCBs), IEC and CENELEC standards.

VIII. TECHNOLOGY FOR INTEGRATED TREATMENTS

The Chemical Dehalogenation Process (CDP ®) in continuous mode by closed circuit, integrated in Decontamination Mobile Units (DMU), is a technique in compliance with BAT / BEP definition of the Italian Ministry of Environment, - D.M. 29/01/2007 - G.U. no. 133 of 7/06/2007 art. D.2.2.2.3 and art. E.3, applicable for transformers and electrical equipment contaminated by PCBs. Units can be operated on transformers on site and in operation filled with mineral insulating oils contaminated by PCBs. The interventions could be carried out with the On-load option keeping the transformer in operation, energised and under load; this means keeping the transformer in operation during the intervention without losses of production.

The CDP and DMU units are capable to decontaminate PCBs-containing oils to concentrations below legal limits such as by local regulation, international standards and technical guidelines (such as re-classification of oil and transformers as “PCBs-FREE” according local regulation).

This solution satisfies the European regulations and standards in terms of BAT/BEP and sustainability (technical feasibility, economic-cost/benefits, environmental benefits and social-green jobs), safety (for workers, public health and environment-emissions CO2 etc.),proximity, self-sufficiency and functional recovery through the integrated treatments (off load and on load conditions) for life cycle management (LCM) of insulating liquids and transformers, and includes the following key aims:

A. Dehalogenation and detoxification of PCBs in oil below the limits prescribed by local regulations or internal specifications (< 50; < 25; < 10; <2 mg/Kg of PCBs, determined with IEC 61619 Ed.1-1997). This process uses a solid reagent (S/CDP) consisting of a high molecular weight glycol mixture, a mixture of bases and radical promoter or other catalyst for chemical conversion of organic halogen to inert salts on a high surface area particulate support. This process normally runs typically at 80-100 °C and has the capability to decontaminate equipments on site, through continuous circulation of the oil in a closed system (without draining the oil or using auxiliary tanks), using the solvent capability of the oil for continuous extraction of PCBs from solid materials inside the equipment (IEC 60422 Ed.4- 2013-01 art.11.4.4; CENELEC CLC/TR 50503 – 2010 art. 8.4.2.3; CIGRE 413 – 2010 art. 10.1.4.);

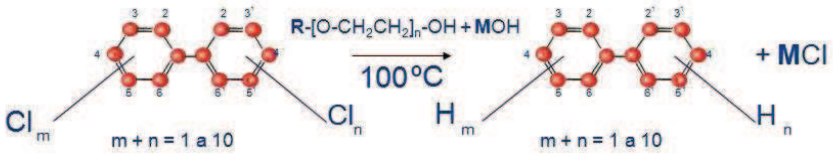
B. Selective depolarization of oil, with the reagents S/CDP and S/CHED, through elimination of oxidation by products, corrosive sulfur compounds-DBDS and organic-metal compounds with improvement of oil properties (electrical, physical and chemical according IEC 60422 ed. 4 2013-01; § Table 5);

C. Decontamination of transformers and electrical equipment (extraction of PCBs, DBDS, moisture, sediments and sludge from solid materials inside the equipment).

ISBN 978-84-617–9183–5

Criticality	Solution- Integrated Treatments		
	Physical Decontamination CHEDCOS®	Selective Depolarisation CHEDCOS®	PCBs Dehalogenation CDP PROCESS®
H_2O, gases, particles	✓ YES	✓ YES	✓ YES
Acidity, Tg delta, colour		✓ YES	✓ YES
DBDS [1], Corrosive sulphur [2]		✓ YES	✓ YES
Dissolved metals [3]		✓ YES	✓ YES
PCBs/PCTs/PCBT/POPs			✓ YES

The CDP and DMU technique was classified as BAT/ BEP by the Italian Ministry of the Environment, the Territory and the Seas Decree 29/01/2007 – Published on the Official Gazette n.133 titled Guidelines for the identification and utilisation of the Best Available Techniques on Treatment of PCBs, apparatuses and wastes containing PCBs and stocking systems. The CDP and DMU is the solution for dehalogenation in continuous mode by closed circuit process and uses a solid reagent (S/CDP) and runs at 80-100°C and solving the major critical operational factors of the others PCBs decontamination methodologies (change of insulating liquid-refilling CENELEC CLC/TR 50503 -2010 art.8.4.1; batch process using sodium, lithium and derivate at 150-300 °C with risk of fire or explosion-art. 8.4.2.1; batch process using KPEG at 130-150 °C- art. 8.4.2.2) or waste disposal by incineration. The main innovation is the use of a granulate solid reagent (S/CDP) , not mixable with the oil, formed by mixtures of polyethylene glycols and solid polypropylene glycols with high molecular weight, a mixture of bases and a radical initiator or other catalysers placed in a column to de-chlorinate progressively at low temperature (80-100°C) the aromatic halides also when particularly stable (PCBs. PCTs, PCBTs, PCDDs, PCDFs). This reagent operates, at the same time, the depolarisation of the oil and the decontamination from other contaminants (oxidation by products, corrosive sulfur compounds-DBDS and organic-metals compounds). This dehalogenation method uses for the reaction a mixture of glycols (R-[O-CH2CH2]n-OH + MOH) , alkaline base (MOH) ,catalyser and solid support that reacts with the halogenated compounds (PCBs) present in the oil and progressively replace the atoms of halogens in the molecules into hydrogen (dehalogenation / detoxification by mechanisms of nucleophilic replacement and radical reaction – catalytic hydro dehalogenation). Residual by-products of such reaction are normal, non-toxic salts (MCl), absorbed by proper sorbent materials.



For the continuous technique, the active principles, mixed in the appropriate proportions, are absorbed by a particle solid support with a high surface area. The reagent (S/CDP Reagent) obtained in this manner, is pre-packaged in cartridges creating a reaction bed on which the oil to be decontaminated flows, pre-heated to temperature of 80° - 100°C.
By operating CDP and DMU in closed loop it results fully complying with Directive 76/769/CE of 26 July 1976. The use of the CDP Process – both with mobile units near the equipment (cabins, electric substations etc.) and at equipped Centres for the decontamination of PCBs - is comparable to maintenance activities (IEC 60422 ed. 4 2013-01) when the electrical equipment have not reached the end of operational life.
This type of multifunctional process is performed in a continuous manner by the closed-loop circulation of the oil, without draining the contaminated equipment; the latter is simply connected to a decontamination mobile unit (DMU), with a variable flow from 500 through 5.000 l/h. These mobile units are modular systems with compact dimensions equipped with automatic safety and process control systems capable of operating under all operational conditions (power generating stations, primary and transformation cabins, bunkerised substations

[1] Corrosive sulfur-DBDS
[2] Corrosive sulfur-Non DBDS
[3] Metal corrosion –No Corrosive sulfur

ISBN 978-84-617–9183–5

etc.). Also, the mobile units can be equipped with spill protection systems (Spill Guard), self-cleaning systems also capable of eliminating critical emissions into the atmosphere (Emx-Clean) and automatic supervision and control systems for all the safety parameters of the process to prevent the origin of possible critical conditions (functional and environmental).
During the continuous circulation, the insulating liquid is subject to decontamination operations proceeding simultaneously, as described here below:

- heating of the oil at a temperature between 80 and 100 °C;
- chemical dehalogenation by percolation under pressure on the solid reagent, pre-prepared in filtering cartridges contained in appropriate containers (columns);
- depolarisation by percolation under pressure on adsorbent particle supports with a high surface;
- decontamination with degassing, dehumidification under vacuum and micro filtration

The DMUs are connected to the transformer by hoses, then the decontamination processes are started: the insulating mineral oil circulates through the DMUs where it is heated, degassed, de-humidified, filtered, decontaminated and then returns into the transformer, which is never drained, even partially. The continuous circulation of the insulating liquid in the closed system transformer-DMU-transformer creates a constant flow of liquid in the transformer favouring the elimination of deposits (sludge) on the papers and in the tank. The activities are carried out under safe conditions thanks to the low operational temperatures, the use of patented reagents that do not create dangers for explosions or fire, the use of special pipes (SpillGuard®) capable of cutting off the process in case of accidental spills and also thanks to a control system software capable of verifying at any given time that the process proceeds under safe conditions and under quality control rules, 24 hour a day, even when working unmanned.
The interventions are carried out with the On-load option keeping the transformer in operation, energised and under load; this means keeping the transformer in operation during the intervention without losses of production (international experiences also in nuclear power plants and on transformers up to 760 MVA and up to 500 kV).
On distribution transformers, typically of power 250 kVA (about 800 kg as total weight of the equipment with 200 kg of oil), the process is implemented in continuous and closed-loop, providing the simultaneous decontamination of 4-6 or more transformers, properly grouped in batches, in a Unit and a Specific Multiple Connection.

CDP and DMU - Dehalogenation in continuous mode diagram

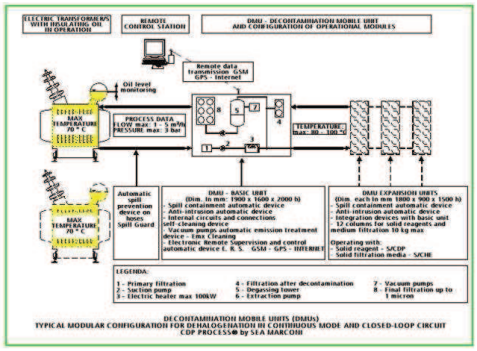


TABLE I. COMPARISON BETWEEN SEA MARCONI'S SELECTIVE DEPOLARIZATION AND OIL REPLACEMENT.

Key Factors	Sea Marconi Closed loop treatment	Replacement of Oil
On-Load Operation	**Yes** ✔	✖ **No** Off-Load for Draining and Refilling
Requirement of Unused Oil	**No** ✔	✖ **Yes** 125%/150% of original mass of oil
Compatibility of Unused Oil vs original	**Safety** ✔	⚠ **Warning** base Oil, additives, others

ISBN 978-84-617–9183–5

Recovery: Physical Properties KV, DGA, H_2O	**Yes**	**Warning** only after reconditioning of Unused Oil in closed loop §11.2.3 (IEC 60422 Ed. 4 2013)
Recovery: Chemical Properties TAN, DF, IFT	**Yes**	**Warning** only after reconditioning + reclam. treatments of Unused oil in closed loop §11.3 (IEC 60422 Ed. 4 2013)
Removal: DBDS & Corrosive Sulfur	**Yes**	**Warning** only if initial DBDS is < 80 mg/Kg or reclamation with special adsorbent
Desludging & Dehydration Solid Insulation	**Yes**	**Warning** only after reconditioning + reclamation of Unused oil in closed loop §11.3 (IEC 60422 Ed. 4 2013)
Decontamination: Dissolved Metals	**Yes**	**Warning** only after reclamation with special adsorbent. Initial value 8/10 times higher than target limit
Dehalogenation: PCBSs/POPs in Oils	**Yes**	**Warning** only if initial PCBs is 8/10 times higher than the target limit
Self-cleaning unit from: DBDS, PCBs/POPs	**Yes**	**No** cross contamination
Cross contamination by DBDS, PCBs/POPs	**Safety**	**Warning** depending on the used oil mainly in the solid insulation
Partial Discharges: air bubble & moisture	**Safety**	**Warning** especially for wet insulation
Environmental Risks for Oil handling	**Safety**	**Warning** high logistical impact
Oil & PCBs Waste disposal	**No**	**Yes** especially if PCBs is higher than limit

TABLE II. COMPARISON BETWEEN SEA MARCONI'S SELECTIVE DEPOLARIZATION AND FULLER'S HARTH TREATMENT.

Key Factors	**DMU & Integrated Treatments Sea Marconi Patented**	Treatment with typical Fuller Earth	Treatment with typical Fuller Earth and regeneration > 600-700 °C
Recovery: Physical Properties KV, DGA, H_2O	**Yes**	**Yes**	**Yes**
Recovery: Chemical Properties TAN, DF, IFT	**Yes**	**Yes**	**Yes**

ISBN 978-84-617–9183–5

Removal: DBDS & Corrosive Sulfur	Yes	No	No
Decontamination: Dissolved Metals	Yes	No	No
Dehalogenation: PCBs/POPs in Oils	Yes	No	No
Classification: BAT/BEP - Best Available Techniques/Best Environmental Practices (PCBs/POPs)	Yes	No	No
Self-cleaning unit from: DBDS, PCBs/POPs	Yes	No	No
Cross contamination by DBDS, PCBs/POPs	Safety	Danger	Danger
Corrosion by Sulfur Degradation byProducts (SDBP) as H_2S, RSH etc. due to high temperature	Safety	Safety	Danger
Dioxins Emissions (PCDDs, PCDFs) due to high temperature degradation by products	Safety	Safety	Danger

Example Process Systems

CDP and DMU -Typical configuration rendering and pictures



CDP and DMU- Containerized unit connected with shunt reactor (500 kV) on-load treatment

ISBN 978-84-617–9183–5



CDP and DMU- FIELD SCREENING TEST and DIAGNOSTIC IN LABORATORY

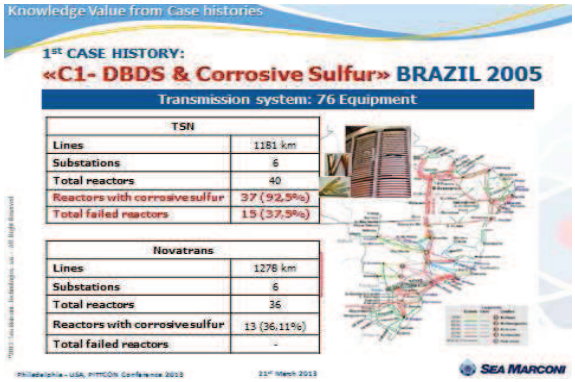
The CDP and DMU use the preliminary determination of the content of total chlorine ,trough SM-TCPs KIT ; SM-TCPS test kit by Colorimetric; SM-TCS Test Kit; Sea Marconi and total acid number SM-TAN KIT by Sea Marconi.
Some representative samples of insulating liquids to be taken before, during and after the treatments to be analyzed in accreditated Laboratory (SEA MARCONI has the accreditation N. 0899 by ACCREDIA). Test for total PBSs , Acid number, gases, breakdown voltage, dissipation factor, particles, moisture, DBDS, additives content , etc according to IEC 60422 and diagnostic reports to be reclassify "NO PCBs Oil and Transformer ".

IX. TYPICAL APPLICATIONS AND CASE HYSTORIES

The CDP Process® developed by Sea Marconi Technologies – Italy, since 1982 (first patent), has been successfully used for the for the complete dehalogenation /detoxification of the 2,3,7,8 TCDD (Dioxin of the "Seveso Case" in the 1983) .

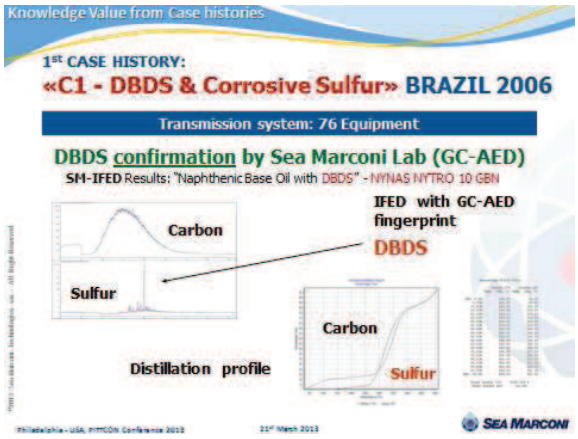
The CDP PROCESS has been used for years, also on large fleets of transformers, without causing any accident. In France, such technical maintenance technique is normally applied with DMU mobile systems for power and distribution transformers (Ref. Prefecture de Meurthe et Moselle, Direction des Action Interministerielles, Bureau de l'Environment, Arrete n. 2002/01 of 17/01/02, SEA MARCONI TECHNOLOGIES France, Nancy).
The CDP and DMU solution is available since 1988 on over 8.000 transformers (mainly power transformers up to 760 MVA , 500 kV and 100.000 kg of oil each), shunt reactors, and electrical equipments filled with mineral insulating oils contaminated by PCBs in more than 20 countries in Europe, South America (Argentina, Brazil, Colombia, Chile, etc.) Africa and Asia(Japan, etc.).
The PCBs initial concentration range (85 % of the cases) was >50-< 500 mg/kg of PCBs; some special applications (5 % of the cases) > 5.000 - <50.000 mg/Kg of PCBs, in case of refilling of power transformers initially filled with pure askarel-PCBs. Other international references were obtained by several tenders issued by international organisations on strategic electric networks. This solution increases the value of functional resources in operation, without disposing of PCBs waste, resulting as the best solution also in terms of CO_2 equivalent (5 Kg of di CO_2 saved for each kg of oil not incinerated).
Since 2001 the total amount of decontaminated tons by Sea Marconi owned plants more than 30.000 tons of mineral insulating oil and more than 120.000 tons of transformers on-site.

DBDS & Corrosion Sulfur (Brazil 2005): Shunt reactors 500 KV.

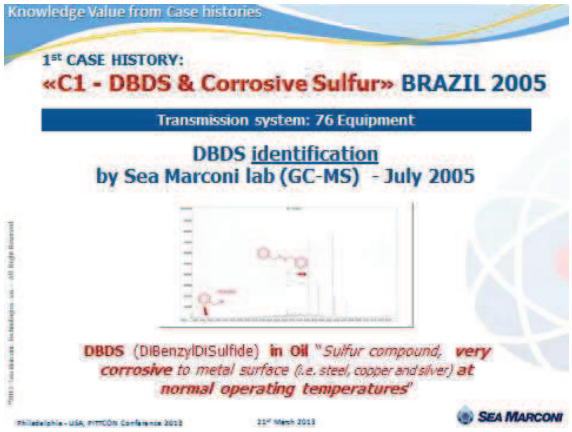


ISBN 978-84-617–9183–5

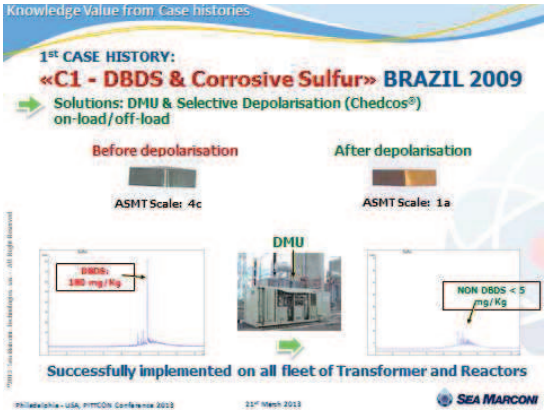
DBDS & Corrosion Sulfur (Brazil 2005): Shunt reactors 500 KV.



DBDS & Corrosion Sulfur (Brazil 2005): Shunt reactors 500 KV



DMU & Selective Depolarisation (Brazil 2009): shunt reactors and GRID transformers 500 KV

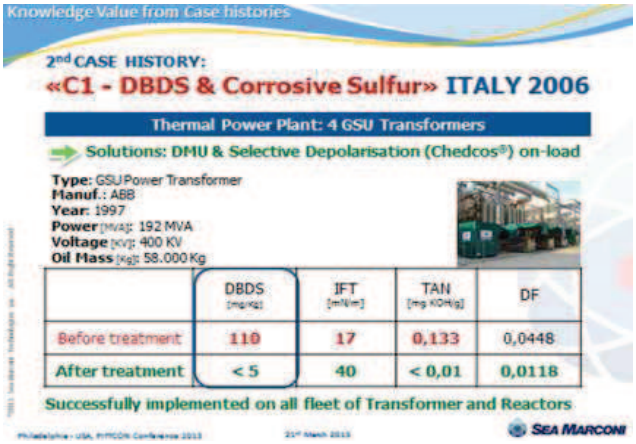


ISBN 978-84-617–9183–5

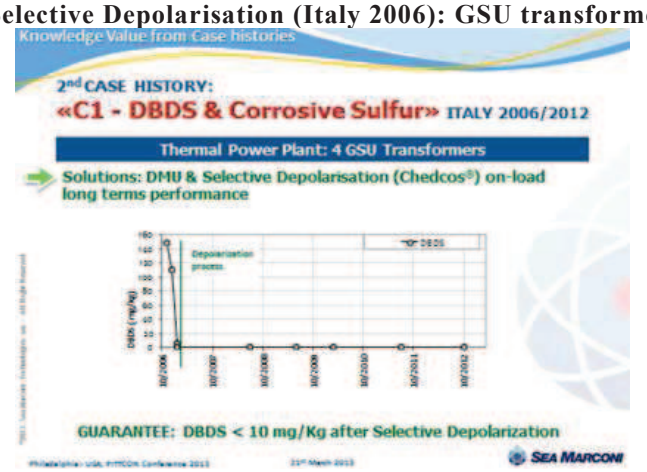
DBDS & Corrosion Sulfur (Italy 2006): GSU Transformer 400 KV.



DMU & Selective Depolarisation (Italy 2006): GSU transformers 400 KV



DMU & Selective Depolarisation (Italy 2006): GSU transformers 400 KV



NON DBDS & Corrosion Sulfur (Middle East 2009): GSU Transformer 400 KV

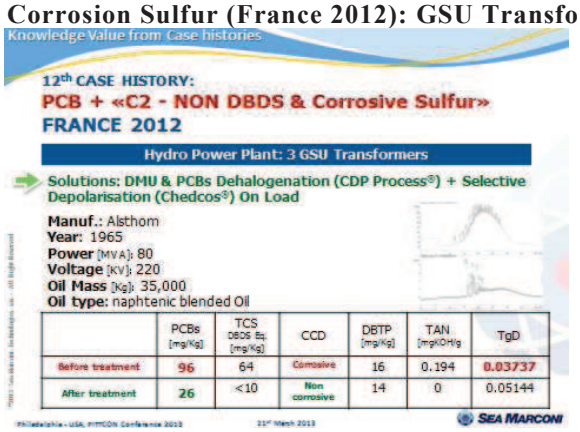


ISBN 978-84-617–9183–5

NON DBDS & Corrosion Sulfur (Middle East 2009): GSU Transformer 400 KV



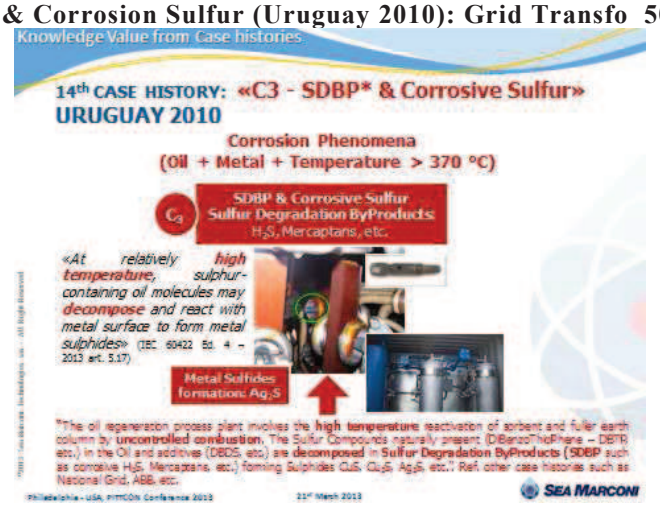
NON DBDS & Corrosion Sulfur (France 2012): GSU Transformer 220 KV



SDBP & Corrosion Sulfur (Uruguay 2010): Grid Transfo 500 KV

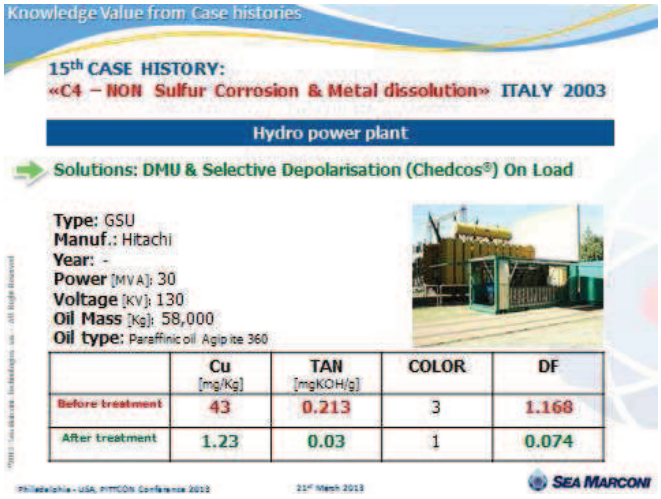


SDBP & Corrosion Sulfur (Uruguay 2010): Grid Transfo 500 KV

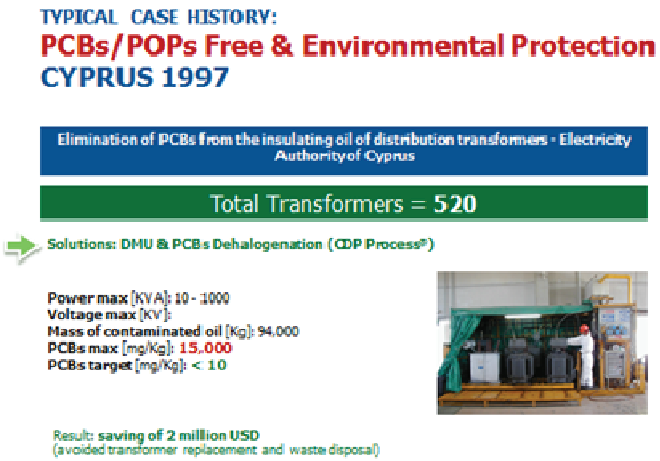


ISBN 978-84-617–9183–5

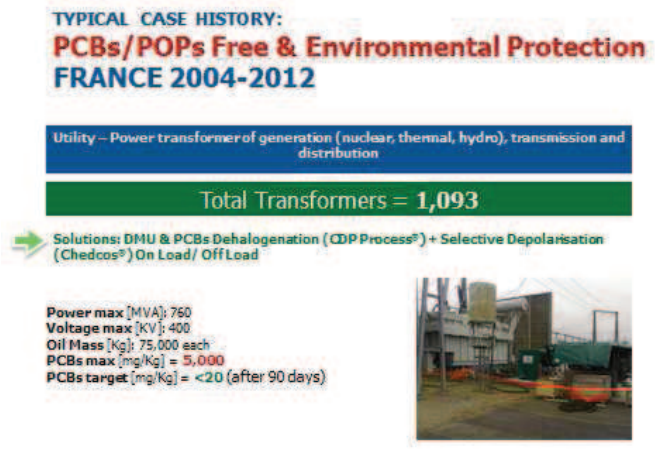
NON Sulfur Corrosion & Metal dissolution (Italy 2003): GSU Transfo 130 KV



CDP and DMU- Typical applications for distribution transformers on-site (Case History Cyprus - 1997)

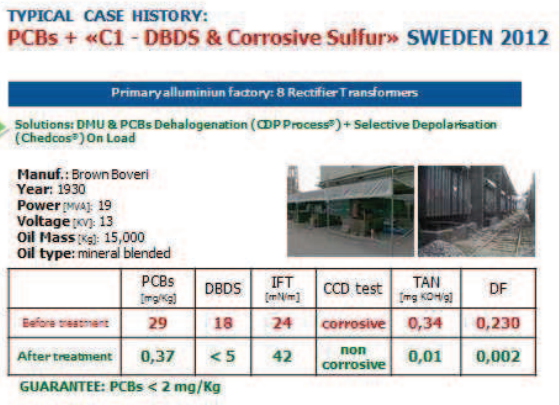


CDP and DMU- Typical applications for power transformers on-site (Case History France - 2004/2012)



ISBN 978-84-617–9183–5

CDP and DMU- Typical applications for power transformers on-site and on-load (Case History Sweden - 2012)



	PCBs [mg/Kg]	DBDS	IFT [mN/m]	CCD test	TAN [mg KOH/g]	DF
Before treatment	29	18	24	corrosive	0,34	0,230
After treatment	0,37	< 5	42	non corrosive	0,01	0,002

CDP and DMU- Typical applications for power transformers on-site and on-load (Case History France - 2013 , Hydro power Plant - generation)







Manufactures	Jeumont Schneider
Year	1969
Power	105 MVA
Voltage	225 KV
Oil Mass	29.000 Kg
Total Mass	126.000 Kg
Oil Type	Mineral



OIL PROPERTY (IEC 60422 ed. 4 2013-01)	BEFORE	AFTER
Colour (ASTM D1500-07)	> 8	2,7
Breakdown Voltage (kV)	73,1	75
Water content (mg/Kg)	6	2
Acidity (mg KOH/g)	0,294	< 0,01
Dielectric Dissipation Factor at 90°C	1,023	0,09211
TCS - Total Corrosive Sulfur - DBDS equivalent (mg/Kg)	69	8
Interfacial tension (mN/m)	18,8	33,3
2-FAL (mg/Kg)	0,583	< 0,05
Total PCB content (mg/Kg)	71	25
Copper dissolved (mg/Kg)	64	2
Particles (ISO 4406:1999)	23 / 20 / 14	17 / 15 / 10
Note: PCBs Garantee < 50 mg/Kg		

X. CONCLUSION

This Sustainable Solution, based on Diagnostic and Treatments for Smart Life Cycle Management of Oils & Transformers (Smart LCM - O&T), represent the Best Available (BAT) and Best Environmental Practices (BEP) for loss prevention and environmental protection.
Therefore, Life Cycle Management (LCM) is an indispensable tool for the prevention and/or mitigation of direct and indirect losses and associated risks for workers, assets, public health and environment, that can arise from human errors, malfunctioning, or failures of the equipment and be a source of fires and/or spillage of hazardous substances (Oils, PCA, etc.) and Persistent Organic Pollutants (POPs; PCBs, etc.).
This approach guarantees knowledge added value for Customers, Holders and Partners in terms of best innovative technologies, reliability, quality control, traceability, economics, environmental protection, social and stakeholders relationship.

ISBN 978-84-617–9183–5

REFERENCES

[1] IEC 60296:2012, Fluids for electrotechnical applications – Unused mineral insulating oils for transformers and switchgear.

[2] Lewand R.L., Corrosive Sulfur in Transformer Systems, Chemist's perspective, DOBLE ENGINEERING COMPANY - NETA WORLD, U.S.A., 2003.

[3] Wilson A.C.M., *Insulating Liquids: their use, manufacture and properties*, IEEE, New York and UK, 1980.

[4] Lewand R. L., *The Negative Effects of Corrosive Sulfur on Transformer Components*, DOBLE ENGINEERING COMPANY - NETA WORLD, U.S.A., 2004.

[5] Scatiggio F., *Corrosive Sulfur*, Proceedings of IEC TC 10 Plenary meeting, Cape Town, 2005.

[6] Tumiatti V., Maina R., Scatiggio F., Pompili M., and R. Bartnikas, *Corrosive Sulfur in mineral oils: its detection and correlated transformer failures*– IEEE International Symposium on Electrical Insulation, Toronto (Canada), 2006.

[7] Maina, R., Scatiggio, F., Kapila, S., Tumiatti, V., Tumiatti, M. and Pompili, M., *Dibenzyl disulfide (DBDS) contaminant in used and unused mineral insulating oils. CIGRE SC2, 2006* (http://www.cigre-a2.org).

[8] CIGRE Technical Report 378: *Copper Sulphide in Transformer Insulation*, April 2009.

[9] K. Anderson, S. Kapila, V. Flanigan, V. Tumiatti, R. Maina, and M. Tumiatti, *Determination of corrosive sulfur species in mineral insulating oils using GC –AED, GC-MS-MS – FTMS*. Abstract No. 800-2; presented at PittCon 2009, Chicago, IL, March, 2009.

[10] IEC 62535:2008, insulating liquids – Test method for detection of potentially corrosive sulphur in used and unused insulating oil.

[11] ASTM D1275, Methods A and B, Standard test method for corrosive sulphur in electrical insulating oils.

[12] ASTM D130, Standard test method for corrosiveness to copper from petroleum products by copper strip test.

[13] DIN 51353, Testing of insulating oils: detection of corrosive sulphur; silver strip test.

[14] Tumiatti V., Roggero C.M., Kapila S., et. al., IEC 62697 – 2012: State of the Art Methods for Quantification of DBDS and Other Corrosive Sulfur Compounds in Unused and Used Insulating Liquids, IEEE transactions on dielectrics and electrical insulation, Vol 19, Issue 5, pag 1633 10/01/2012

[15] Stouten, H, Rutten, AJL, van de Gevel, IA, De Vrijer, F, 2000. Nordic Expert Group for Criteria Documentation of Health Risks from Chemicals and the Dutch Expert Committee on Occupational Standards: 126. 1,2,3-Benzotriazole. National Institute for Working Life. Stockholm, Sweden

[16] National Cancer Institute Technical Report Series No. 881978 *Bioassay of 1H- Benzotriazole for possible carcinogenicity CAS No. 95-14-7*, NCI-CG-TR-88 - U.S. department of Health, Education, and Welfare Public Health Service National Institutes of Health

[17] Tumiatti V., Smart Life Cycle Management of Oils & Equipment Pittcon 2013, Philadelphia.

ISBN 978-84-617–9183–5

[18] IEC 60422 ed4.0 *Mineral insulating oils in electrical equipment - Supervision and maintenance guidance*. Pub. Date 2013-01-10

[19] V. Tumiatti, R. Maina, F. Scatiggio, M. Pompili and R. Bartnikas, *In service reduction of corrosive sulfur compounds in insulating mineraloils*, ISEI 2008.

[20] Tumiatti V. Kapila S. Roccero C.M., et al. *Integrated Methods for corrosivity, ageing and fingerprinting determination, as well as diagnosis, decontamination, depolarization and detoxification of oils*, Int. Pub. Num. WO 2010/070590 A1, 24 June 2010



Vander Tumiatti is the Founder and Owner of SEA MARCONI TECHNOLOGIES (since 1968), Torino, Italy, an international company that is involved in research, technologies, products, and services for energy & environment. He has developed BAT & BEP Sustainable Solutions for Life Cycle Management (LCM) of insulting liquids & transformers focalized on inventory, control, diagnosis, decontamination, depolarization (DBDS, TCS, Polar Compounds) end dehalogenation /detoxification (PCBs/POPs).
He has more than 40 international patents and is the author of many international technical and scientific publications. He has been the Assistant Secretary of IEC TC10 since 2000. He is also a member of several international groups, with major participation in technical normative activities (CEN, IEC, CIGRE ,IEEE).
2009 June -"1906 Award", Award IEC for “the precious contribution to the understanding of the potentially corrosive behaviour of mineral insulating oil used in power transformers and for his discoveries, recognised worldwide, in the development of diagnostic chemical analyses”.

ISBN 978-84-617–9183–5

Partial Discharge Detection Method BlueBOX® Technology for Cable Boxes in Power Transformers

Cristina MEDEL OSUNA. Carlos DELGADO REDONDO. Ángel M. GONZALO CHICOTE

Regulated Electricity Business. Unión Fenosa Distribución. Gas Natural Fenosa
Phone: (+34) 915676000, fax: (+34) 915507793, e-mail:
cmedel@gasnatural.com, cdelgado@gasnatural.com, agonzaloc@gasnatural.com

Abstract –**The occurrence of incidents in the interconnecting elements, like insulated cable links of power transformers to their respective bays in a GIS system of the High Voltage Grid, may lead into a prolonged unavailability of equipment and produce important solicitations due the short circuits to the transformer and also to the enclosure that contain it.**

Union Fenosa Distribucion (UFD), in order to comply with the regulatory requirements in terms of electricity supply quality in urban areas, improved the technology developed with Polytechnic University Madrid (UPM), which is generally applied in the field of High Voltage insulated power lines for detecting partial discharge (PD) by advanced methods, to use it not only in cables but also in the transformer. So that, through an online monitoring it was achieved the necessary quality levels for the repairs and upgradings carried out.

Moreover it was essential to confirm the perfect state and condition of the transformer for a safe reconnection through the necessary discrete electrical measurements, tests and analysis, which are adapted to the characteristics of the system and counting with the restricted accessibility to active parts. Also, the infrastructure of the enclosure where the transformer is content it was revised and strengthened in order to enhance the resistence against the overpressures generated by internal explosion of any element, retaining the early detection of the fire protection systems, ensuring the electrical disconnection of the switchgear and activating the automatic fire extinguishing system at the right time.

Therefore, it is important to highlight the efforts on the adaptations and the evolutions of the early detection methods to diagnose and locate possible failures in power transformers and its associated elements, which will also lead to carry out a proper follow up or monitoring of operating conditions through an optimum combination of sensors and equipment.

Keywords – **insulated cable, partial discharge, monitoring, transformer enclosure**

I. INTRODUCTION

Union Fenosa Distribución (UFD) is responsible for the regulated electricity distribution activity of Group Gas Natural Fenosa (GNF). It currently manages 384 electrical substations and 778 power transformers with 27.391MVA of installed capacity in Spain.

The grid operation management and, in particular, the maintenance management performed by Union Fenosa Distribución have the strategic objective of being the most effective and efficient as possible.

One of the most important issues that may occur in power transformers and insulated cable links are internal defects in the insulation. These faults generally produce partial discharges of magnitude and / or an increasing rate before failure. An uncontrolled failure of insulation as well as causing a loss of power can also cause serious equipment failures in a very violent mode, resulting in dangerous explosions or fires affecting the entire installation, for which it should be designed.

The measurement of partial discharge (PD) is being increasingly used for the diagnosis of the insulation condition of equipment. Therefore, this article explores the combination of several techniques of online PD

ISBN 978-84-617–9183–5

measurement tools that are appropriate for monitoring electrical networks of high voltage applied at a substation, for example in transformer cable links systems and its terminals at both ends of the transformer and GIS gear.

This measurement technology aims to detect the activity of PD, discriminating noise, automatically locating their source points, distinguishing different generating sources and correlating each PD source with a determined phase resolved pattern associated to the triggering factors.

II. DESCRIPTION OF THE TECHNOLOGY

In Fig. 1, the simplified program flow identifies the measuring method developed by UPM and UFD, based on a technological research project called ENERGOS between 2009 -2014 within the CENIT technical research program. The procedure consists of taking synchronised and regular samples of PD through specific sensors and measurement devices arranged in the network (step 1). Following the acquisition of the signals the noise suppression process is applied (step 2) where the non desired noise is removed by a powerful digital filter based on the transformed Wavelet.

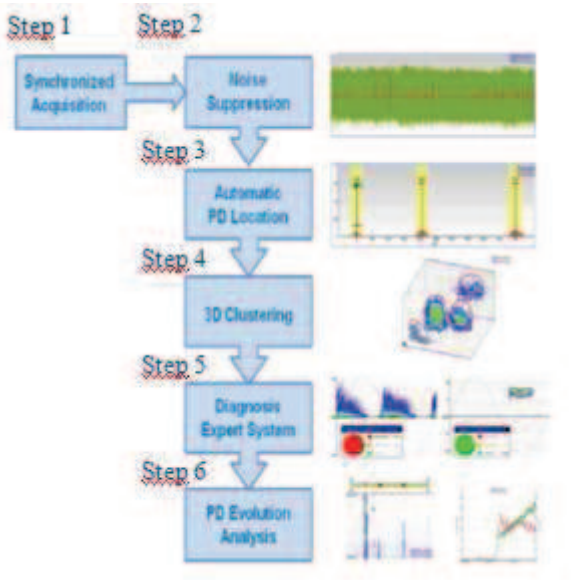


Figure 1. Measure procedure flow.

The filtered data of the measurement devices allow for the correlation of PD generated pulses with the location from where they were generated by an automated tool (map position PD). The location of the site of the source of the PD is defined by the delay of the arrival of the PD pulse to each sensor travelling through the network (step 3).

When different defects appear in the same location (cable accessory, transformer, etc.), it is required to distinguish them and analyse the importance of each one. The tool "3D Waveform Clustering" (step 4) allows to distinguish different sources of PD located in the same place. The waveform of each PD pulse is identified by three characteristic pulse parameters: main frequency of pulse fi and αi y βi parameters that define the asymmetry of the envelope associated to each pulse, allowing a three-dimensional representation of each PD pulse in correlation with its waveform. Spatial representation (3D) of the three parameters related to the waveform (fi, αi and βi), allows for the identification of different PD groups, located in 3D space. By appropriate choice of parallelepiped volumes in the 3D representation, a group of PD is selected when the phase resolved pattern corresponds to a kind of pattern associated with PD type generating signals (step 5). The temporal evolution of the PD associated with a type of defect allows for the assessment of the associated risk of failure (step 6).

ISBN 978-84-617–9183–5

a. Captación de las señales de DP

For the selection of sensor to deploy, it was considered, the different sources of PD signals in the different parts of the system.

An example is shown in Fig. 2, for a system in a substation of 220 kV, where the transformer and GIS are connected through a cable link of 30m.

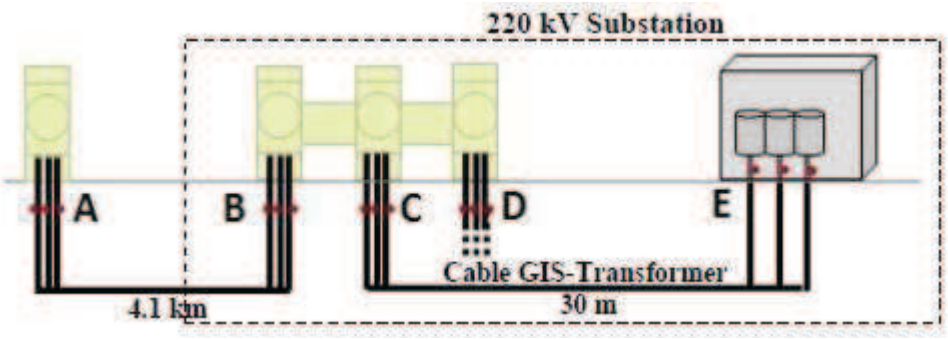


Figure 2. Simplified sketch of 220kV substation under PD monitoring.

The electromagnetic screening of the housing structure in switchgear type GIS and power transformers, as is in the case that this paper refers to, allow in combination of the measurement in the UHF (Ultra High Frecuency) band, reduce substantially outside interference. Thus the noise that can pass through these structures can weaken rapidly (e.g. corona discharge), or is easily recognisable (e.g. mobile communications).

Therefore UHF sensors allow correct detection of the PD, but with its measure it is not possible to determine the apparent load (as is defined in IEC 60270). This phenomenon is explained on the basis that detection methods according to IEC 60270 are sensitive to the current, which is integrated to obtain apparent load, while UHF methods are more sensitive to variations of the current. However, it is possible to verify the detection sensitivity of a UHF system comparing the measurements with the obtained by a detection system according to IEC 60270.

Among the advantages of the application of UHF method for PD measure, it can be highlighted:

- High sensitivity in capturing accurate, high noise resistance from electromagnetic or corona interference
- Ability to accurately locate PD sources when more than one sensor is used in a GIS (already installed for discrete measures in 220kV GIS property of UFD) or in a power transformer (measuring the time of flight of signals to each sensor)
- Ability to differentiate between internal defects or external in GIS, or the power transformer, and the detection of located defects in the case of applying the method in cables or cable accessories

On the other hand, there are disadvantages of the method that uses sensors in UHF:

- Poor selectivity in the location of a defect. In cables, the higher frequency components are significantly weakened with distance
- Requirement to be properly positioned and oriented
- Requirement to be fixed rigidly to the test object (GIS , transformer, cable)
- Requirement to also be properly screened

Due to the increase in PD signal weakness in UHF with distance, for detecting PD in the cable, High Frequency Current Transformers (HFCT) sensors were used.

ISBN 978-84-617–9183–5

Apart of the different types of sensors suitable for each part of the installation, there is the challenge of selecting a single equipment that collect all signals for a single measurement.

The BlueBOX® system works with HF ranges (from 1 kHz to 50 MHz), so it was necessary the study and development of an adapter to convert UHF into HF. This bridge of frequency transformation allows for an expansion of the measurement range of the BlueBOX equipment to more than 300MHz.

Therefore, if the captured filtered and amplified signal, is also converted to a lower frequency pulse by UHF-HF converter, it can be registered by the BlueBOX system. These pulses have a very similar characteristic waveform and by the BlueBOX system clustering tool, they can be grouped and easily filter noise interference present in the measuring system.

The UHF-HF converter is placed at the outlet of the sensors and this enables the conventional measurement equipment to be responsive to signals received in UHF.

This will permit to take full advantage of different existing sensors in the installations, and also make use of the powerful tools that the BlueBOX system offers, unifying the use of a single measuring system for different AT equipment in a substation.

Online PD measurements require a previous calibration check in order to determine the characteristic of sensors (verify the detection sensitivity of a UHF system comparing the measurements with the obtained by a detection system according to IEC 60270).

With the Bluebox system, the received pulses with the UHF sensor might not be processed unless they are integrated. This is because the signal has a very high frecuency waveform and the measuring system has a receiving band between 1 kHz and 50 MHz. Therefore, the received signal will be processed and recorded by the Bluebox system once it is captured, filtered, amplified and also converted into a lower frecuency pulse through the UHF-HF converter, as the Fig. 3 shows.

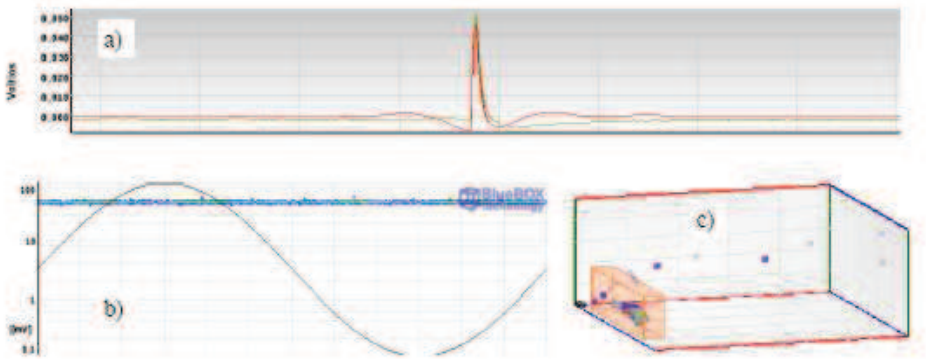


Figure 3. a) y b) Calibration pulse measurement using UHF-HF converter for BlueBox c) PD Cluster selection.

III. Application on Power Transformers

It is possible to make a temporary PD measurement with BlueBOX technology using HFCT and UHF sensors installed at the cable end terminations of the GIS (HFCT), compartments of cable housing inlets in the GIS (UHF), the transformer cable end terminations (HFCT + UHF) and grounding of the transformer tank (HFCT) .

IV. Case Study

In the case study, the measurements taken were on a 220kV cable link and a transformer 220/15-15 kV in an urban area, after an incident by failure of a termination in the cable end of the connection to the transformer. In

ISBN 978-84-617–9183–5

addition to the standard measurements to be performed in a transformer in the case of an incident of near short circuit to ensure the integrity and good condition, it can also be supplemented with others that detect PD activity in the transformer and the cable origin of the incident.

A. Substation features

Within the Spanish capital city, Madrid, GNF operates a 220kV network, the studied substation being part of this grid Installation is sited in a dense area. In recent years, the premise was subject to refurbishment/retrofit works according to GNF plans to improve safety, space utilization and the environment in its urban substations. It is a compact installation equipped with SF6 switchgear. It transforms 220kV to 15kV, based on double busbar configuration, with 7 HV positions. Three separate 15kV double busbars systems are linked to the 220kV level through three similar four-winding power transformers with a quaternary winding connected in delta for compensation purposes.

B. Substation background

A failure of a 220kV oil-immersed sealing end (phase R) occurred in January 2014 in a 220/15-15kV transformer bridge circuit, which led to service interruption and destruction of the failed asset. GNF decided to advance with a thorough investigation to find out the root cause of failure and, hence, avoid similar faults in the future.

This failure was preceded by another fault that occurred two years earlier at the same bridging circuit (phase T), which had indeed a higher impact. Fire reached neighbouring cables and damaged the transformer's enclosure. All the sealing ends in the bridge circuit for the referred position were installed in 2002. The cable manufacturer personnel was in charge of the installation of the bridging link. In 2008, GNF proceeded with the retrofitting of the transformer and the associated circuit and re-commissioning tests consisted solely of sheath tests and PD measurements at nominal voltage were carried out on December 2008, in circuit cables and accessories. No PD activity was reported.

However, in January 2014 a single phase fault in the transformer phase R sealing end took place. As the sealing end of phase T had already failed on 2012, GNF opted to replace simultaneously sealing ends for the failed phase R and the non-failed phase S.

The inspections of the sealing ends - failed and non-failed - were held on July 2014 cable manufacturer facilities.

A failure investigation was carried out, obtaining the following conclusions:

- The failure was the result of an insufficiently chamfered edge of the semi-conducting insulation screen
- It was key to determine whether the failure was caused by careless installation practices or by an inherent property of the cable
- In order to obtain insight into the scale of the issue, it was recommended to determine which cables (and the accompanying accessories) are of the same type
- When the population of potentially suspect accessories were determined, it was recommended selecting a representative sample group of accessories and subjecting them to an offline partial discharge test at elevated voltage
- It was also recommended reviewing the on-line partial discharge measurements techniques that have been applied thus far and assess their efficacy, in order to determine whether they can be used for future monitoring of suspected sealing ends

ISBN 978-84-617–9183–5



Figure 4. Damage caused by the failure sealing end.

C. Events During the Failure

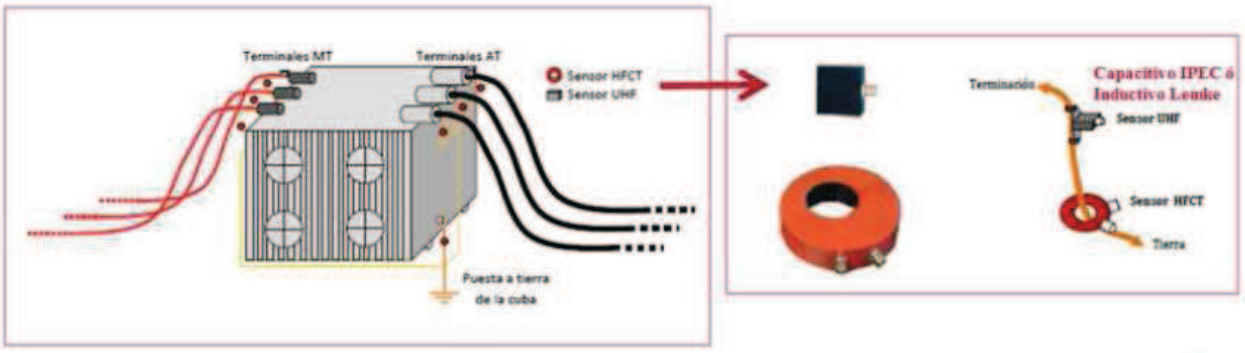
A single phase fault in transformer phase R sealing end took place on January 2014. The fault was cleared in 60 ms with the activation of transformer's differential protection (ANSI 87T), overcurrent phase protection (ANSI 50) and lockout function (ANSI 86). Noteworthy, sealing end are within the jurisdiction of the differential protection.

The short circuit current magnitude reached 30kA at steady state, 150 times more than the rated current of CTs (200A). In conformance with the failure report produced by GNF, the transient peak current could have been as much 34kA.

The distance protection for the remaining feeders has been activated as expected. Moreover, the fire detection system detected the presence of flames and the overpressure relief mechanism was timely activated.

D. Components of the continuous PD measurement system

BlueBOX Technology Continuous PD Monitoring System consists of three types of elements compounding the measuring network. These elements are the 'Control and Analysis System (CAS)' containing a CPU and a synchronization system, the 'Measurement System (MS)' acquiring the PD signals of the three phases simultaneously synchronized by the CAS and the 'PD sensors' type UHF or HFCT. In addition, two calibrators, one HFCT and the other UHF, for performing response testing.



ISBN 978-84-617–9183–5

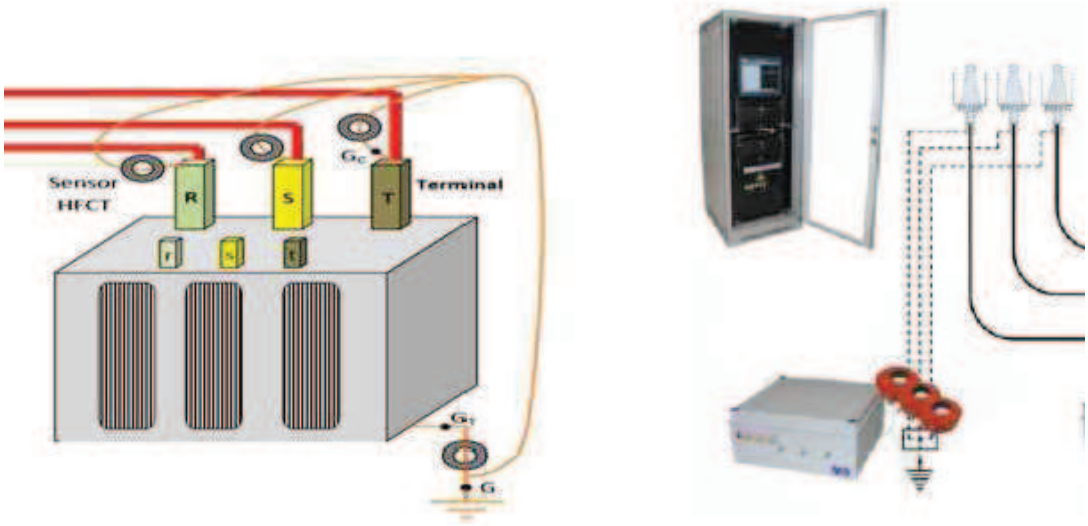


Figure 5. UHF y HFCT sensor configuration for Transformer y GIS sealing end.

Fig. 6 shows the layout of the PD monitoring configuration for a substation made up of one 220kV GIS position and 220kV Transformer

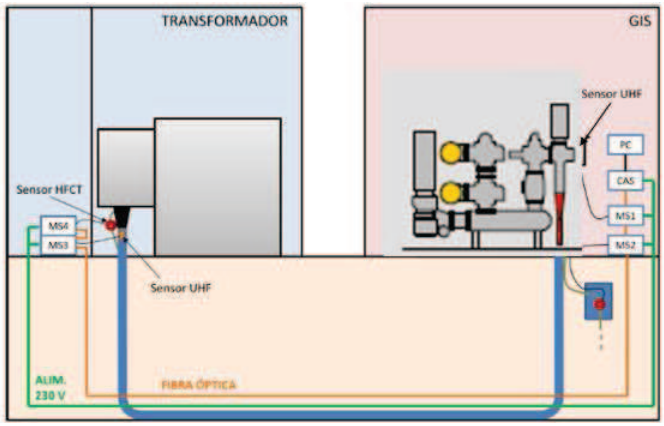


Figure 6. Testing circuit for UHF y HFCT sensor located in transformer y GIS sealing end.

Measurements with BlueBOX system:

1. Simultaneous measurement using the HFCT sensor in GIS terminal.
2. Simultaneous measurement using the UHF sensor in GIS terminal (cable box, preinstalled)
3. Simultaneous measurement using the UHF sensor in GIS terminal, phase R
4. Simultaneous measurement using the HFCT + UHF sensor in transformer terminal.
5. Simultaneous measurement using the UPM quadruple described in the previous section, in the coupling capacitor in HV and in LV**.
6. Simultaneous measurement using the HFCT sensor on the grounding of the transformer.

** using the UPM quadruple in the LV coupling capacitor for UHF signal

The monitoring is made continuously for one month, from right before performing the energization of the system until one month after.

The diagnosis of the measurements indicates that the monitored cable system is free from PD in the internal insulation.

ISBN 978-84-617–9183–5

The system detected characteristics of floating potential PD in the S phase at the end of the GIS for at least one minute at the time of the maneuvers at the beginning of energization. Since such discharges have not been detected for the rest of monitoring, it is considered that they do not represent a risk for insulation.

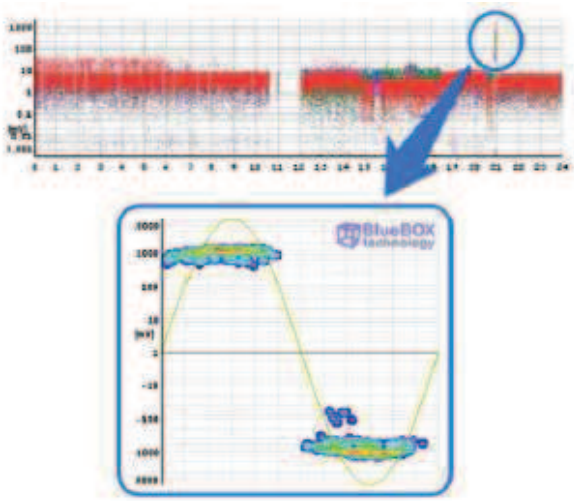


Figure 7. Floating potential PD in the S phase.

The PD patterns acquired by means of the sensors are show in the below Fig. 8:

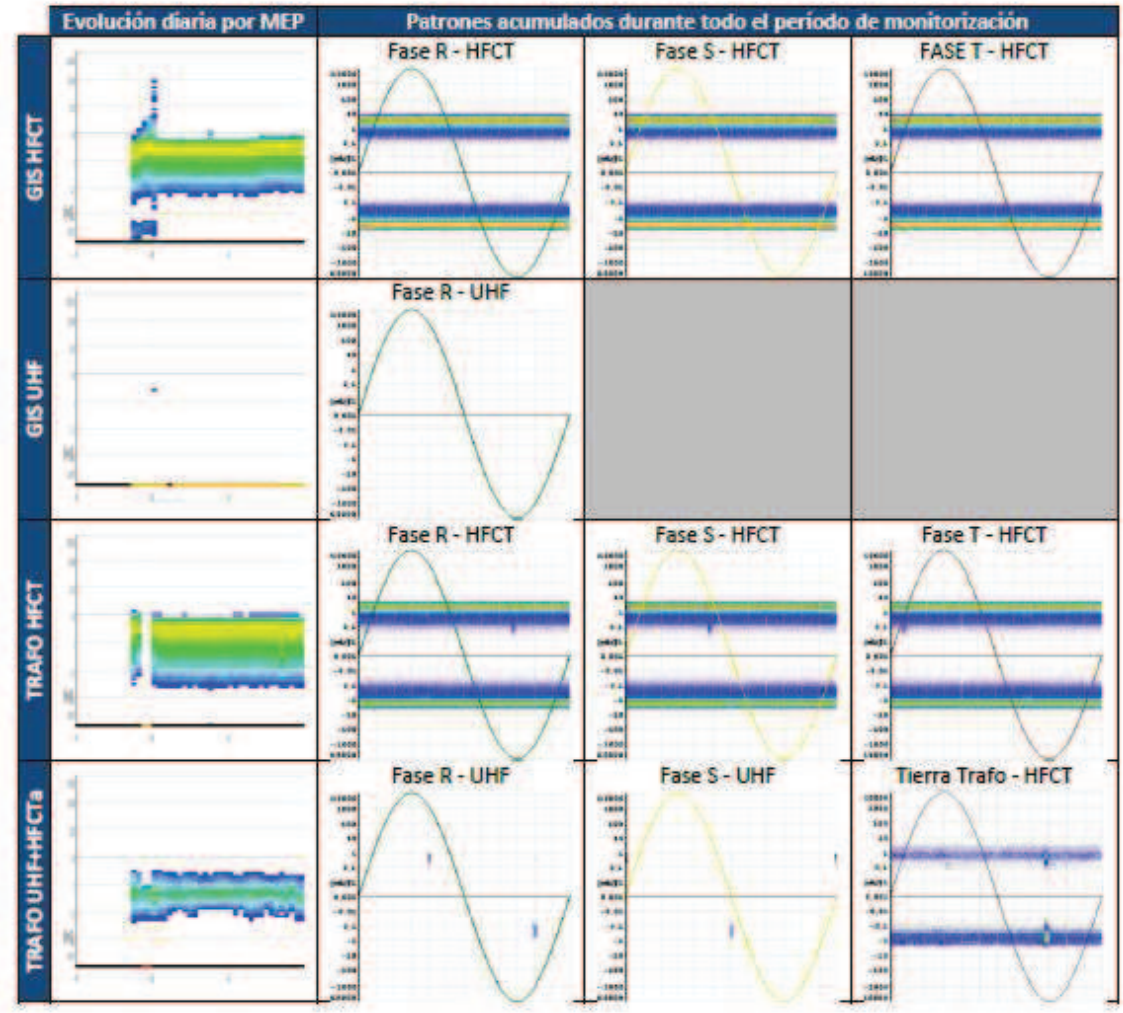


Figure 8. Phase patterns acquired.

ISBN 978-84-617–9183–5

For the detected activity, it could be concluded:

a) Non-significant noise for a few days (not constant) along the 33 meters of cable.
b) Repetitive electrical pulse noise produced by any machine located at both ends.

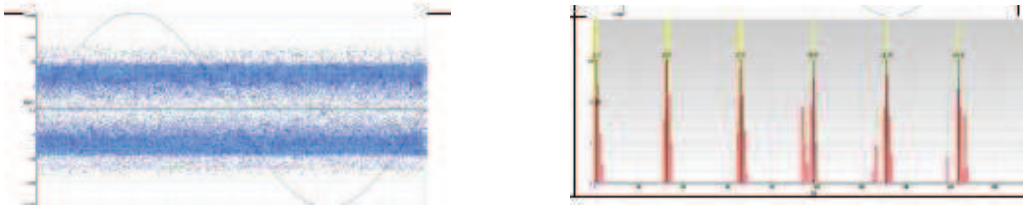


Figure 9. Pattern resolved uniform phase noise and Reflectometry analysis.

Appropriate actions within the facility were proposed, once repaired cable and accessories, which include among others:

- Electrical tests of the transformer
  As soon were available HV end connections (link within cable termination compartment and bushings to inside transformer container for connection to windings) to verify that it has not been damaged, due to the estimated 34kA of short circuit current according to data provided by the records of 220kV feeder circuit in other ends to the substation. The main electrical tests performed on the transformer were Frequency Response Analysis (FRA), Capacity and loss tangent δ, transformation ratio, static and dynamic winding resistance. The results of the tests showed the appropriate values to allow the energization of the transformer.

- Perform analysis of transformer oil
  Dissolved Analysis Gases (tank and cable box) were evaluated in laboratory and Hydran M2, and the results were correct.

- Perform analysis of SF6 condition in the GIS position circuit breaker compartments
  In the first analysis, decomposition products were detected, which is usual after a fault of this type, but verification is required that the proper regeneration and performance of the absorbent compartment is adequate.

- Study different on-line monitoring systems to detect evolution of defects, after replacement of the damaged elements, since performing specific tests does not guarantee early detection.
  Another measure of PD was performed by cable manufacturer during a week. The measuring system was compounded of an ultra wide band (UWB) sensor, an integrated signal acquisition and processing system, storage and data transmission (PriCAM Grids).

  The results only showed a pattern of accumulated PD. Only noise signals from the electromagnetic environment were detected. The average noise level was approximately 11 mV.

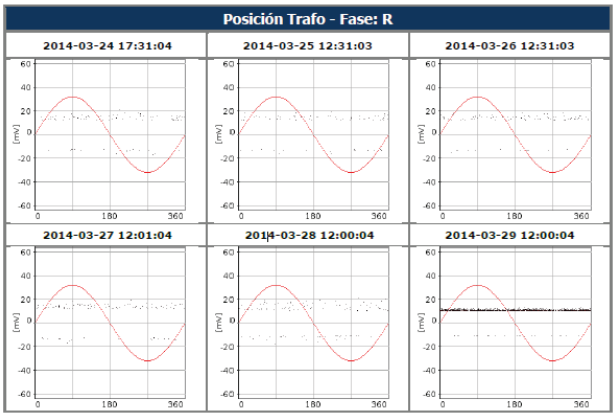


Figure 10. PD pattern on R phase, Pos.Trafo.



Figure 11. A) PryCAm B) Traf Sensor C) GIS Sensor.

ISBN 978-84-617–9183–5

- Check the design of the "pass through" of the cable link to the other chambers to guarantee the perfect fire sealing.
- While the incident was under analysis period by cable manufacturer due a similar case with another client, the cable manufacturer reported to GNF the need to perform a re-commissioning to the stored terminals by the laboratory of origin in DELFT (Holland) before mounting them to confirm their correct state.

V. CONCLUSIONS

The periodic maintenance, the commissioning and the receiving of an installation after a major repair by a specific PD measurement can detect sources of PD in the insulation. The BlueBOX technology provides characteristic indicators for each detected PD source to evaluate the importance of the defect by: phase resolved pattern, PD pulse amplitude, PD rate per period, defect type and location. All of which are performed with a single measuring system and different sensors.

PD monitoring should be further developed and improved since it is an effective technique for the diagnosis of electrical insulation of equipment and installations of HV.

For online PD measures, it is essential to have PD measuring instruments able to remove the superimposed electrical noise to the PD signals and effective locating, classifying and identification tools for the different PD sources. Therefore, PD pattern recognition associated with each PD source is also essential for proper diagnosis.

UHF measures are less affected by this electrical noise in the system and are effective in the task of locating defects.

These tools help to correct misdiagnosis of nonexistent defects or to locate defects that had gone unnoticed in the other measurements and begin their PD activity after weeks of the installations being energized.

The final analysis of measures requires great experience and knowledge by the analysts that provide the diagnosis.

However, it remains to improve the automatic recognition of PD groups associated with pattern types in transformers (for example in the insulating paper/oil) as a simple and reliable synchronisation technique for PD measurements made by more than a unit of measure.

REFERENCES

[1] *High-voltage test techniques – Partial discharge measurements*. IEC 60270-2000

[2] Alberto Gonzalez, *Proyecto ENERGOS: Tecnologías para la gestión automatizada e inteligente de las redes de distribución energética del futuro*." Programa para el fomento de la creación de Consorcios Estratégicos Nacionales de Investigación Técnica. PROGRAMA CENIT-2009

[3] *High Voltage On-site Testing with Partial Discharge Measurement CIGRE,* Brochure Nº 502. WG D1.33. June 2012.

[4] Garnacho, M.A. Sánchez-Urán, J. Ortego, F. Álvarez, A. González , D. Prieto, *Experiencias Españolas en monitorización de DP en redes eléctricas de AT.*

[5] "Guidelines for Unconventional Partial Discharge Measurements" CIGRE Brochure Nº 444. WG D1.33. December 2010

ISBN 978-84-617–9183–5

[6] *Informe técnico DIAEL de Monitorización y diagnóstico de Descargas Parciales Online* Documento nº: 20140307-1, 2014

[7] *PFI ON A 220 KV OIL-IMMERSED SEALING END – DNV-GL-* Gas Natural Fenosa Report No.: P14-R-070-PA, Rev. 0

[8] *Informe técnico PRYSMIAN Monitorización de Descargas Parciales Online* Referencia: _IF.104.14_, 2014

ISBN 978-84-617–9183–5

Experiences in the Diagnosis of High Voltage Current Transformers by Dielectric Frequency Response (DFR) and Oil Analysis

Roberto LIÑAN GARCIA, Arali GUZMAN LOPEZ, Daniel PEREZ DORANTES.

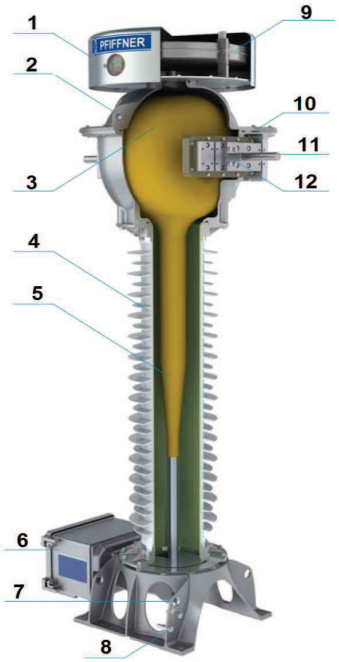
Instituto Nacional de Electricidad y Energías Limpias (INEEL), Reforma No. 113, Col. Palmira, CP 62490, Cuernavaca, Morelos, México,
rlinan@iie.org.mx, aguzman@iie.org.mx daniel.perez@iie.org.mx

Abstract – This paper presents the experiences in the application of a diagnostic methodology for ranking the operating condition of current transformers (CT´s) developed by the Instituto Nacional de Electricidad y Energías Limpias (INEEL) in 2008. For the development of this methodology, an experimental setup was used that allowed the evaluation of current transformers of different models and rated voltages. The diagnostic methodology is based on measurements of the dielectric properties as a function of frequency (DFR) and its correlation with the dielectric breakdown strength of the oil, moisture content in the oil and dissolved gases in oil (DGA). The analysis of the results allowed to establish four risk zones: Zone 1: Good condition, Zone 2: Periodic Inspection, Zone 3: Schedule replacement and zone 4: Immediate Replacement. The methodology is effective to detect the main failure mechanisms in CT´s. It also allows evaluating the operating condition of the insulation system of the CT´s efficiently, so that where it has been used there have not been catastrophic failures.

Keywords — Current Transformer, Dielectric Frequency Response (DFR), Moisture content, Dielectric Breakdown Strength, Dissolved Gas Analysis in Oil (DGA)

I. INTRODUCTION

Current transformers (CT´s) are used to transform high level currents into safe level currents used for measurement and protection in the transmission and distribution network. Constructively, the insulating system used in CT´s is the oil impregnated paper with external insulation of porcelain. In Fig. 1 the main components of a paper/oil system CT are shown.



1. Bellows cover with oil level indicator
2. Lifting lugs
3. Active parts with iron cores, secondary windings an HV insulation
4. Porcelain or silicon composite insulator
5. Bushing
6. Terminal box with rating plate
7. Oil drain valve
8. Main earth connection
9. Expansion bellows
10. Housing with drainage area
11. Primary connection
12. Primary changeover

Figure 1. Main parts of a CT, courtesy of Pfiffner.

The CT´s compared to other substation equipment, are considered low cost and for its design, are maintenance free. However, the occurrence of failures generates costs due to damage to adjacent equipment, purchase of a

ISBN 978-84-617–9183–5

new CT, replacement costs, interruption of service costs and the effect on personnel safety. The estimated total cost of a CT catastrophic failure is approximately one million dollars.

Up to date, the Transmission Network in Mexico has 17.954 CT´s installed in 399 substations. Approximately 20% of the total fleet of CT´s has an age of 25 years in operation [1]. On the other hand, in the period 2000 to 2009, in the CFE transmission network, the occurrence of catastrophic failures in these CT´s increased substantially, presenting 167 failures.

According to failure statistics, the main causes of failure of CT´s in operation, in order of priority are: moisture, arcing/external events, manufacturing defects, partial discharge and overheating [2, 3]. The presence of moisture inside of the CT is due to loss of its hermetic sealing, where moisture enters through defective seals and membranes, due to thermal degradation of paper during operation.

To date, worldwide conventional diagnostic techniques (thermography, visual inspection, measurement of power factor and insulation resistance) are used for the evaluation of CT´s [4]. The results show that these are not effective for assessing the insulation condition of the CT´s. The limitation of these measurements is that at frequencies of 60 Hz have low sensitivity to changes in moisture in the system.

INEEL in 2008 demonstrated that moisture is the main root cause of failure of CT´s in Mexico. For this, laboratory experiments were done on CT´s removed from operation, by using the measurement of Partial Discharges. The CT´s were subjected to different temperatures causing moisture migration between solid and liquid insulation. As a result, a reduction in the dielectric strength was observed in areas of high electrical stress, until a dielectric failure occurred. With these results, INEEL developed a methodology to detect the main failure and assess the condition of the insulation system.

II. EXPERIMENTAL DEVELOPMENT

The methodology developed by the INEEL is based on the results obtained in the experimentation in which the behavior of the paper/oil insulation system was analyzed in two CT models under different operating conditions. This allowed us to establish correlations between the dielectric and physicochemical properties of the insulating system of the CT´s.

Fig. 2 shows the experimental setup used for the development of the diagnostic methodology. The arrangement simulates thermal conditions, the moisture content in the paper and oil flow. It has an oil preservation system and is instrumented to measure current, temperatures at different points of CT´s and moisture content in the oil.



Figure 2. Experimental arrangement used for the development of the diagnostic methodology.

The two CT´s used for the experimental stage were an upper module of a CT of 400 kV removed from service and a new CT of 245 kV. On the CT 400 kV, its initial moisture content in the paper was unknown and it was humidified until 3 % weight in the paper (WCP). The CT of 245 kV had initial moisture content in the paper of 0.3 % and it was humidified to a 0.5 % and 0.6 % of the weight on paper. In both CT´s humidity process was carried out gradually to avoid saturating the oil and the formation of free water inside of the CT. During experimentation, monitoring the water content in the oil (WCO), dissolved gas content and oil dielectric strength was performed. In addition, dielectric characterization was performed by dielectric frequency response (DFR) at different moisture levels.

ISBN 978-84-617–9183–5

RESULTS

The results of the characterization of the dielectric properties of the insulating system paper/oil in the CT´s under different thermal and moisture profiles, showed that at frequencies lower than 10 Hz the variables are more sensitive to changes of moisture in the insulation than the measures taken at rated frequencies. In Fig. 3 it is shown that the power factor increases with respect to the moisture content in the CT insulation [5].

The impact of moisture in the CT insulation has the following consequences: changing the characteristics of grading materials of electric field, water bubbles generation, decrease in dielectric strength of the insulation, premature saturation of insulating oil, increased level and PD's activity at temperatures above 70 °C, deterioration of the semiconductor paper from PD's activity and presence of circulating currents, and increasing the value of Tan δ and power factor.

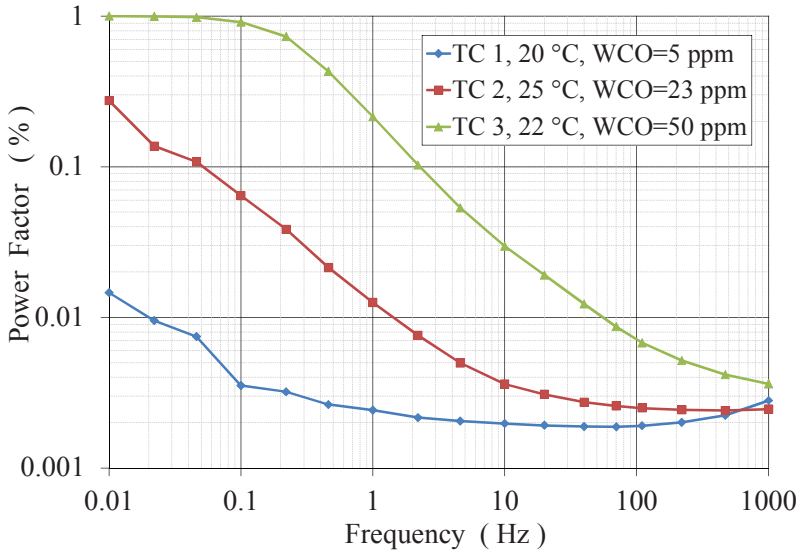


Figure 3. Power factor as a function of moisture content in the CT´s.

III. Development Of The Methodology

Based on the results obtained during the experimental stage, a multivariable analysis was done using the dielectric parameters (dielectric spectroscopy as a function of frequency) and physicochemical (dissolved gas analysis, dielectric strength and moisture content in the oil) in the insulation system of CT´s. Correlations between these parameters were established, which in turn allowed to establish criteria for diagnosis and classification of the operating state of the insulating system. Four risk zones were established and corresponding actions for each of these were defined, in order to reduce the rate of catastrophic failures (see Table I).

Table I. Classification of Insulation in CT´s.

Risk Zone	Colour	Recommended actions
Good condition	**Green**	Good condition, normal inspection
Regular inspection	**Yellow**	Low risk of failure, six months inspection
Schedule replacement	**Orange**	Medium risk of failure, schedule replacement
Immediate replacement	**Red**	High risk of failure, immediate remove from service

IV. Application Of The Methodology In The Field

Since its development, the diagnostic methodology to classify the operating condition of CT´s, has been applied to 555 transformers, of which 152 were classified in green zone, 128 in yellow zone, 129 in orange zone and 146 in the red zone.

In this section the results obtained in 2015 during the application of the methodology to 114 CT´s installed in the Transmission Network of the Comision Federal de Electricidad are presented. The population of CT´s evaluated consists of 13 CT´s models from five different manufacturers, in three voltage levels (115, 230 and 400 kV). The designs of the CT´s are of the type top core and hair pin and with preservation systems of metal bellows, expansion tank and elastic membrane.

ISBN 978-84-617–9183–5

The results of the 114 CT´s were analyzed using the method of Principal Components Analysis (PCA) to classify CT's with the greatest degradation in the oil/paper insulation system. This statistical technique used to find the causes of the variability of a data set and sort them by importance; it also permits the determination of the correlation and variance between variables. For the results of the 114 CT´s the variables analyzed were: Dielectric strength, moisture content, permittivity, resistivity, Power Factor and dissolved gases content. The variables that have higher correlation are: Power Factor and Resistivity for DFR and Hydrogen and Carbon Monoxide for dissolved gases. In Fig. 4 the classification for Principal Components Analysis of DFR for the 114 CT´s is presented. It is observed that 6 CT´s (numbers 44, 45, 46, 47, 48 and 49) have a high probability of failure as they are grouped in the top left of the graph. In the bottom right section of Fig. 4 are grouped the CT´s (example: 14, 95, 104 and 105) have good condition in the insulation system based on DFR measurements.

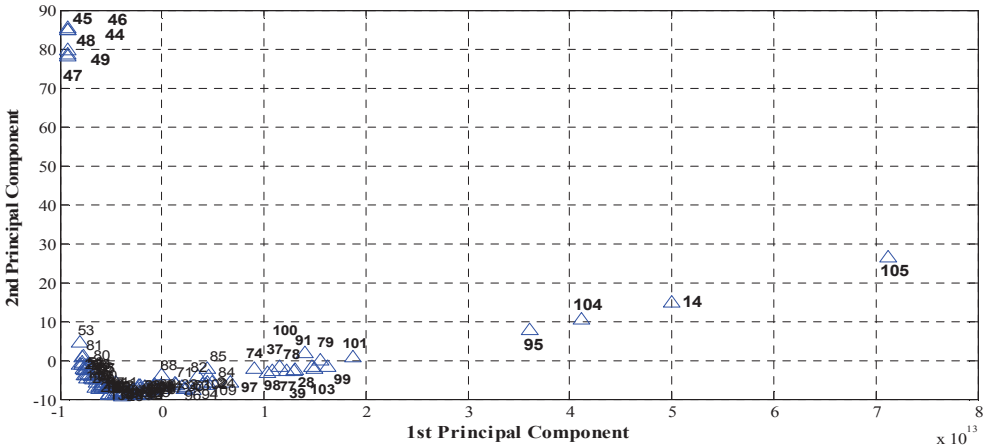


Figure 4. Classification of DFR measurements for the 114 CT´s evaluated by Principal Components Analysis, where the first component is the power factor and the second is the resistivity.

On Table II the values for dielectric parameters and dissolved gases for 13 CT´s evaluated with PCA for DFR are presented. The CT´s 44, 45, 46, 47, 48 and 49 have a high value of power factor and they were classified in the red zone. CTs 44, 45 and 46 present high concentrations of Ethane indicating overheating of oil. CT´s 38 and 53 have high contents of Ethane and the results of DFR classify them in the orange zone. CT´s 14, 95, 104 and 105 are found in green zone according to PCA by DFR and they do not have high concentrations of dissolved gases. CT number 22 has a permittivity and a power factor with high values and a low resistivity so it is classified in the orange zone.

Table II. Values of the Dielectric Parameters and Dissolved Gasses of 13 CT´s Classified by Principal Components Analysis in the DFR Measurements.

CT Number	H_2 (ppm)	CO (ppm)	CO_2 (ppm)	C_2H_4 (ppm)	C_2H_6 (ppm)	CH_4 (ppm)	C_2H_2 (ppm)	Permittivity	Resistivity (Ω-m)	Power Factor	Diagnostic
14	11	215	289	3	4	7	1.5	1.03	5.93E13	0.29	
22	4	346	339	2	3	6	0.4	1.12	1.2E12	13.14	
38	4	55	239	6	**149**	26	0	1.01	1.4E12	12.63	
44	0	57	227	3	**108**	20	0	1.06	2.5371E10	98.91	
45	0	55	236	4	**92**	0	0	1.16	2.8066E10	98.41	
46	0	54	242	4	**133**	21	0	1.62	2.2942E10	97.92	
47	17	180	144	2	3	0	0	1.06	7.2474E10	91.97	
48	13	177	161	1	3	2	0	1.20	5.8175E10	93.23	
49	11	181	191	2	6	2	0	1.01	8.0754E10	91.05	
53	0	52	269	9	**153**	57	0	1.06	1.1686E12	14.31	
95	0	171	171	4	8	3	0	1.01	4.5368E13	0.39	
104	5	194	202	3	7	4	0	1.02	2.425E13	0.73	
105	6	225	185	2	4	6	0.5	1.02	5.045E13	0.35	

ISBN 978-84-617–9183–5

Fig. 5 shows a graph of the power factor of three CT´s located in the green, orange and red zones. At frequencies higher than 10 Hz, a linear behavior of the power factor is observed. However, at frequencies below 1 Hz, a variation is observed in the power factor between CT´s. CT number 44 located in the red zone presents values of the power factor to be the highest, this is indicative of the presence of moisture in the insulation system.

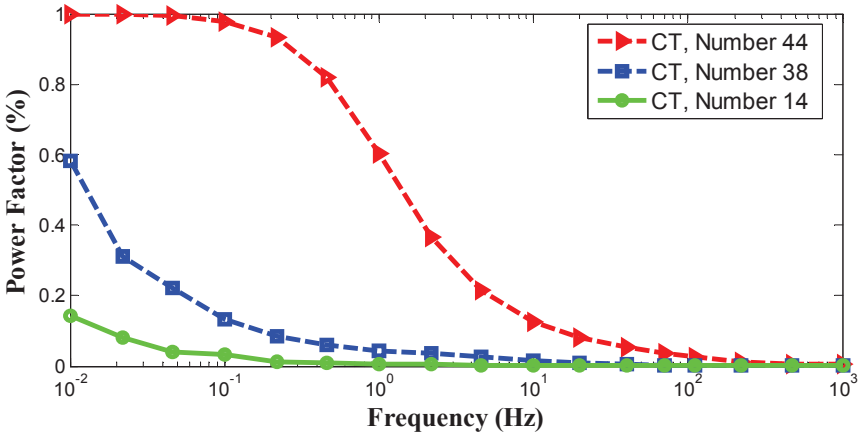


Figure 5. Measurement of power factor with DFR.

Fig. 6 shows the Principal Components Analysis for dissolved gases. CT´s 3, 80, 81, 82, 89 and 92 are found outside of normal behavior for the population. In Table III the results of the dissolved gases content of these equipment are presented.

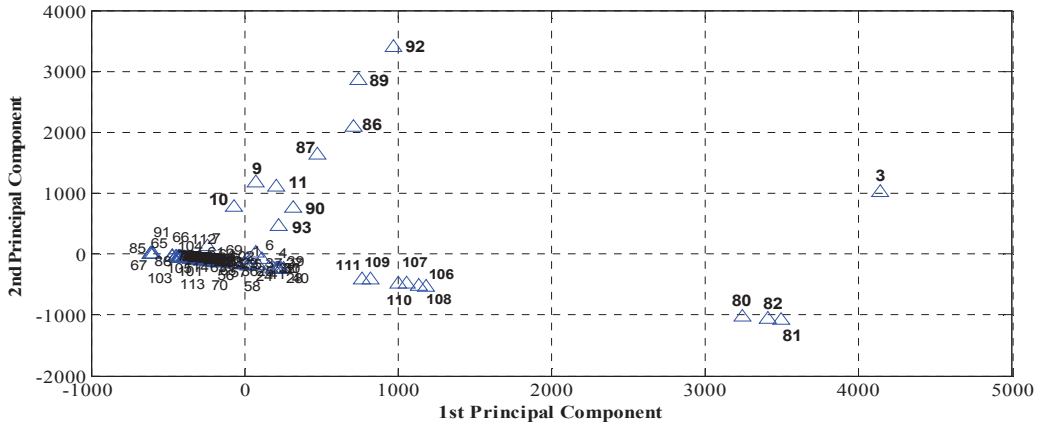


Figure 6. Classification of the measurements with DGA for 114 CT´s using Principal Components Analysis, where the first component is the Hydrogen and the second is the Carbon Monoxide.

Table III. Values of Dielectric Parameters and Dissolved Gasses for CT´s Classified by Principal Components Analysis with a Greater DGA Value

CT Number	H_2 (ppm)	CO (ppm)	CO_2 (ppm)	C_2H_4 (ppm)	C_2H_6 (ppm)	CH_4 (ppm)	C_2H_2 (ppm)	Permittivity	Resistivity (Ω-m)	Power Factor	Diagnostic
3	**2189**	**628**	**4303**	6	11	17	0	1.06	2.92E12	5.8	
80	13	**981**	**3865**	7	7	9	0	1.06	1.463E12	11.51	
81	24	**984**	**4133**	1	13	13	0	1.05	1.513E12	11.28	
82	18	**959**	**4046**	3	15	15	0	1.02	1.28E13	1.37	
89	**3118**	149	547	3	15	12	0	1.01	8.57E12	2.07	
92	**3697**	183	614	4	11	7	0	1.03	2.43E12	7.15	

Upon analyzing the contents of the dissolved gases individually it was found that CT´s 89 and 92 had high concentration of hydrogen, which indicates the existence of partial discharges in these CT´s. No other gas in these CT´s outside normal operating conditions was found. Both CT´s were classified in the red zone by dissolved gases although the dielectric parameters are classified in yellow and orange zone respectively. CT´s,

ISBN 978-84-617–9183–5

80, 81 and 82 exceed the normal operating limits on the concentrations of carbon monoxide and carbon dioxide; however, this may be because they have been operating more than 30 years. Upon completion of the analysis of these CT´s with the results of DFR, the units were placed in the orange zone. CT number 3 presented excessive generation of Hydrogen and carbon oxides, this is an indication that there are partial discharges that affects the solid insulation (cellulose). All these CT´s were removed from operation by a high probability of failure.

During the application of the methodology it was found that in CT´s of a certain model and vintage, the concentration of Ethane exceeds the limits of normal operation. It was determined that the above is due to design problems in the CT´s, causing oil overheating. No other gas was found above the normal range.

In Table IV, the classification of the operating status of the 114 CT´s evaluated with diagnostic methodology during 2015 is presented. 30% of the population has a significant damage in its insulation system. All equipment ranked in orange and red zone were removed from service.

Table IV. Classification of CT´s Evaluated.

Risk Zone	Colour	CT´s	CT´s (%)
Good condition	**Green**	39	34
Regular inspection	**Yellow**	41	36
Schedule replacement	**Orange**	8	7
Immediate replacement	**Red**	26	23

V. CONCLUSIONS

The developed methodology considers the variables that are of the major impact on the degradation of insulation system for CT´s. It is effective to detect the main failure mechanisms (moisture, partial discharge and overheating). Using the method of Principal Components Analysis it is possible to analyze the correlation of variables and to determine the limits of the diagnostic areas of CT´s. As well, the diagnostic is composed of two evaluations, the dielectric performance of the solid insulation (DFR) and the oil (dissolved gases, dielectric strength and moisture).

The application of the methodology has reduced the failure rate, increase the reliability of the transmission network, increasing personnel safety, reduce costs interruption, minimize the economic impact caused by catastrophic failures and prepare replacement plans based on the CT´s condition. It also allows efficiently evaluate the operating condition of the insulation system of the CT´s, so that where it was used there have not been catastrophic failures. In CFE the implementation of the methodology has reduced the number of major faults in CT´s per year, from an average of 19 faults in the period 2004 to 2009 to an average of 3 failures in the period 2010 to 2015.

REFERENCES

[1] SUBDIRECCIÓN DE TRANSMISIÓN CFE*, Estadística de Fallas de Transformadores de Potencia, Reactores de Potencia y Transformadores de Instrumento*, México, D.F, 2015.

[2] T. V. Oommen, Moisture Equilibrium in Paper-Oil Insulation System, Proc. Electrical Insulation Conference, Chicago, Illinois, October 1983.

[3] V. Davidov, Moisture Assessment in power transformers: Lessons Learned, Monash University, Australia; O. Roizman, IntellPower, Australia; TechCon 2002 Asia-Pacific.

[4] B. K. Gupta, J. Densley, A. Narang, Diagnostics practices used for instrument transformers, Electrical Insulation 2008, ISEI 2008, Vancouver B.C, Conf. 239-242.

[5] S.M. Gubanski, P. Boss, G. Csepes, V.D. Houhanessian,J. Filippini, P. Guuinic, U. Gafvert, V. Karius, J.Lapworth, G. Urbani, P. Werelius and W.S. Zaengl, Dielectric response methods for diagnostics of power transformers, CIGRE Technical Brochure, No. 254, Paris, 2004.

ISBN 978-84-617–9183–5

Experımental Method for Evaluatıng Electrıc and Magnetıc Properties of Structural Steel Used in Power Transformer Tank

Phamella R. T. PICCOLI [1], Sérgio H. L. CABRAL [2], Luiz F. de OLIVEIRA [3], Odirlan IARONKA [3], Diogo HARMEL [3], João E. SAPELI [2], João P. VIEIRA [3]
[1] Católica de Santa Catarina, [2] Universidade de Blumenau, [3] WEG T & D
[1] Joinville, [2,3] Blumenau
phamella.piccoli@catolicasc.org.br , scabral@furb.br, luizo@weg.net, odirlan1@weg.net, diogoh@weg.net, joaoesapeli@gmail.com, jooen.blu@gmail.com

Abstract — **Structural steel is the basic material of the tank of any oil filled power transformer that has an obvious role to play. On the other hand, when in operation, the tank is subjected to magnetic flux leakage from the transformer windings. Thus, eddy currents are induced in it and lead to undesirable losses in the mass of the tank that not only compromise the efficiency of the transformer as well as may cause hot spots. For mitigating these problems, the transformer designer must know in advance some specific properties of the structural steel that are the dependence of both volumetric losses and magnetic permeability in function of the density of magnetic flux. However, data like these are not usually available by the manufacturer of structural steel plates whereas the use of the Epstein frame is not feasible, because of the incompatibility between the sizes of the Epstein frame and the samples of steel plate to be tested. Thus, this work presents the proposition of a new experimental method for obtaining these necessary data, which details are given through an example for testing the steel ASTM A36.**

Keywords — **power transformer; structural steel; volumetric losses; magnetic permeability.**

I. INTRODUCTION

The search for the increase in the efficiency of power transformers has made the transformer tank and the other steel parts as the prominent candidates for cutting the operating losses[1,2]. This is because when in operation the magnetic flux leakage of the transformer windings reaches all these steel elements and induces eddy currents that generate undesirable losses and hot spots that can condemn any transformer design. Thus, in view of mitigating these problems, a transformer designer should have available some basic but essential information about some of the electric and magnetic characteristics of the steel plates to be chosen. For example, the volumetric losses and the relative magnetic permeability, both in function of the incident magnetic flux density, as well as the AC magnetisation curve. Once available, data of these characteristics allow computer simulation programs mapping the magnetic fields inside the tank plates and other steel parts like bolts, nuts and clamps and thus allow the transformer designer evaluating the associated losses as well as temperatures, in view of properly deciding for better solutions, by including the adoption of magnetic shields[3,4]. However, the availability of such a kind of data is quite unusual for this type of steel but only for the laminated steel that is used in the magnetic circuit of the transformer. On the other hand, to obtain these data by testing samples of this type of steel through a conventional Epstein frame is not feasible because of the dimensional incompatibility between it and any representative sample of the structural steel. Thus, as an alternative way, this work presents the proposal of a new experimental method to determine those so desired electrical and magnetic characteristics of a structural steel. To exemplify the use of the proposed method, results for the ASTM A36 steel are presented.

II. BASIC PRINCIPLES

Although the use of a conventional Epstein frame is not adequate for measuring losses in a sample of structural steel, to observing its principles of operation for creating an alternative method may be very useful. In fact, to involve a sample of a structural steel plate with a continuous winding for establishing a uniform magnetic field strength over the cross section of the steel core is not a difficult task. With this purpose, two identic samples of the ASTM A36 structural steel were cut from a plate with a thickness of 6.35 mm. For the sake of practicality,

ISBN 978-84-617–9183–5

each of the two samples had the shape of a toroid with the dimensions as shown in Fig. 1.a. The so-called practicality of the toroidal shape lies in the fact that it fits very well to the winding machinery process available for winding bushing current transformers that have also a toroidal shape. In this way, the winding process can be performed with a significant uniformity. Thus, by taking into account that the proposed method requires two windings for each toroid, each of these windings was uniformly distributed along the whole perimeter of each toroid, by forming one layer with 800 turns. Therefore, each toroid has two layers of winding, with one layer per winding, as schematically shown in Fig. 1.b.

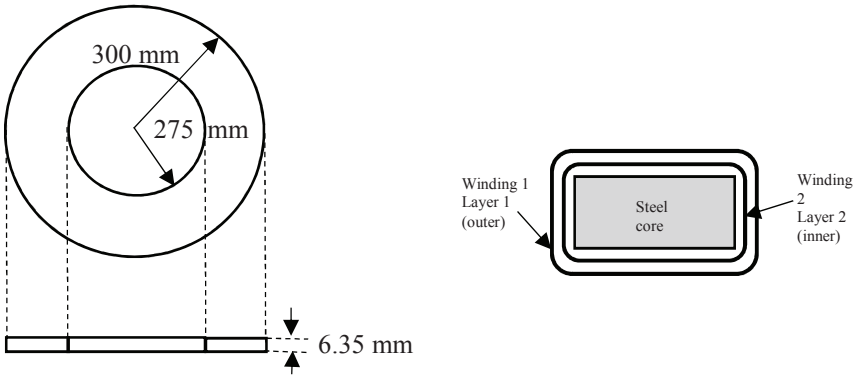


Figure 1. a. Top and front views of a toroidal sample obtained from a ASTM A36 structural steel plate.
b. The view of the cross section of the toroid with each winding per layer.

In this way, each of the two identic toroids becomes a 1:1 toroidal transformer. The reason for taking two identic toroids is to allow separating the winding and core losses [7]. After all, because of the magnetising current circulating through the windings and its inherent harmonic content, the additional losses may become significant and thus determining the winding losses becomes more complex and difficult. In fact, one of the key steps of this proposed method is how to take into account these additional losses[7]. For example, the two identic toroidal transformers should be connected in the same way as it is schematically shown in Fig. 2, that corresponds to one of the transformers connected with additive polarity, whereas the other is with subtractive and both are submitted to an AC/60 Hz voltage. In this case, the transformer with additive polarity can be exactly taken as being under the condition of the no-load test, whereas the other, with subtractive polarity, taken as being under the condition of the short-circuit test, simultaneously. In this circuit, the resistors R_S indirectly represent the Joule losses in the windings, whereas the resistors R_N represent the core loss of each toroidal transformer. Both the component of the losses is evaluated from the measurement of voltage and current, as indicated, and thus active and reactive power.

Thus, for each level of applied voltage the value of each of the parameters of the winding circuit is obtained from the same usual way that it is performed for the no-load and short-circuit tests of transformers and this allows obtaining the desired electric and magnetic characteristics of the material of the core of toroidal transformer, the ASTM A36 steel. The details of this process are described in the sequence.

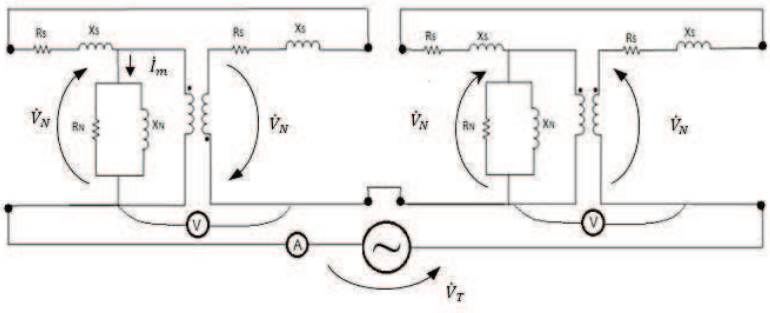


Figure 2. The equivalent circuit of the connection of the two toroidal transformers. The left one is connected with additive polarity whereas the right one with subtractive.

ISBN 978-84-617–9183–5

III. SEPARATION OF LOSSES

The process of separation the winding losses from the core losses is performed in two tests, with the connection of the transformers as shown in Fig. 2. In the first test, one of the toroidal transformers, marked as A, is connected with additive polarity whereas the other, marked as B, is with subtractive. After this, for the second test is done with each of the transformers, A and B, with an opposite polarity. In both the tests, the AC voltage is applied at various levels of RMS amplitude, which makes the RMS value of the series current to range from few hundreds of milliamps to a little bit more than seven (7) amps. For each of the levels of the applied voltage the values of winding voltage and current, and thus power, as also indicated in Fig. 2, are measured with oscilloscopes and recorded. Tables I.a and I.b show the obtained result for the first and second tests.

Table I. a. Test with Toroid A with Additive Polarity and B with Subtractive Polarity
b. Test with Toroid B with Additive Polarity and A with Subtractive Polarity.

Vtotal (V rms)	I (A rms)	V (V rms)	P (W)	I (A rms)	V (V rms)	P (W)
	Toroid A - Additive			Toroid B - Subtractive		
5.47	0.332	5.3	1.35	0.332	0.273	0.0327
10.51	0.496	10.3	4.26	0.5	0.411	0.208
15.43	0.65	15.2	8.32	0.648	0.538	0.359
20.34	0.818	20	13.8	0.815	0.672	0.557
25.77	1.02	25.2	22.1	1.02	0.842	0.88
30.96	1.27	30.4	33.1	1.26	1.04	1.35
35.72	1.51	35.2	45.2	1.54	1.24	2
41.7	1.85	40.5	63.9	1.85	1.52	2.85
46.7	2.22	45.1	84	2.22	1.78	3.9
52.1	2.62	50.2	111	2.62	2.1	5.58
57.4	3	55.4	140	3.02	2.42	7.35
62.6	3.41	60.4	175	3.4	2.85	9.86
67.8	3.61	65.6	197	3.59	2.93	10.7
72.9	4.08	70.5	239	4.04	3.3	13.5
78.1	4.51	75.4	282	4.48	3.67	16.7
83.9	5.01	80.9	337	4.99	4.07	20.6
88.9	5.44	85.4	384	5.39	4.48	24.4
94.1	5.75	90.6	423	5.66	4.73	27
99.3	6.14	95.4	475	6.1	5.01	32.1
104.9	6.63	101	537	6.54	5.49	36.6
109.5	6.91	105	580	6.84	5.81	40.5
115	7.27	110	607	7.15	6.06	44

V_{total} (V rms)	I (A rms)	V (V rms)	P (W)	I (A rms)	V (V rms)	P (W)
	Toroid B - Additive			Toroid A - Subtractive		
2.63	0.205	2.58	0.394	0.2	0.165	0.0333
6.56	0.378	6.46	1.98	0.379	0.313	0.12
10.6	0.506	10.5	4.46	0.51	0.42	0.217
14.86	0.639	14.7	8.03	0.642	0.53	0.342
20.1	0.835	20.1	14.5	0.835	0.692	0.588
28.2	1.16	28.1	28.2	1.17	0.965	1.15
38.8	1.64	38.6	54	1.64	1.36	2.27
42.9	1.87	42.4	68.1	1.87	1.56	2.96
47.3	2.15	46.3	85	2.14	1.78	3.85
51.1	2.41	50.2	103	2.4	2.03	4.94
55.4	2.73	54.4	126	2.72	2.27	6.34
59.7	2.96	58.4	146	2.95	2.48	7.45
64.4	3.28	62.9	174	3.27	2.75	9.15
68.3	3.52	66.8	198	3.51	2.97	10.5
72.2	3.81	70.5	224	3.81	3.13	12.1
76.3	4.08	74.2	252	4.07	3.36	13.9
81	4.42	78.9	291	4.42	3.66	16.4
85	4.64	82.9	317	4.65	3.85	18.1
89.3	4.97	86.8	355	4.98	4.19	21.2
93.3	5.26	90.5	390	5.25	4.43	23.6
101.2	5.83	98.1	460	5.8	4.92	28.8
107.6	6.08	104	502	6.04	5.16	31.4

Thus, based on the procedures of the no-load and short-circuit tests of transformers, the values of P (active power, in watts) for each of the toroids when with subtractive connection represent its respective winding losses, whereas the values of P for each of the toroids with additive connection represent the sum of the winding and core losses. Therefore, in principle, for separating both losses only one test would be enough by subtracting from each of the values of losses of the toroid with additive polarity the respective values of losses of the other toroid, which polarity is subtractive. However, since it is not possible to be sure that both the toroids are absolutely equal this method proposes to proceed the subtraction by using the same toroid under the two different polarities, which explains why the two tests should be performed. Nonetheless, with this aim, the values chosen for applying AC voltage to the transformers should be the same in both the tests, which can be a somehow time-consuming task. Alternatively, the losses with the subtractive connection of each toroid can be analytically adjusted in function of the current and thus the subtraction can be performed in the sequence, for each value of the same current. This is the procedure taken in this work and the adjustment is done in the following way:

$$P_e = A\, I^n \tag{1}$$

In which A and n have constant values that are obtained by numerical techniques of adjustment. P_e corresponds to the losses in the windings of the toroid as a function of the current, I. The choice of (1) is based on the fact that the losses in the windings are predominantly caused by the Joule effect. In this case, A has the same value as of the electrical resistance of the winding whereas n has the value of 2. However, because of the presence of current harmonics and their consequent additional losses the value for both of these constants may differ from these expected values. Fortunately, along the tests, it was noticed that for the samples of the ASTM A36 steel the harmonic distortion was low enough to consider the value of n as equal to 2. In consequence, the value obtained for A was 0.84. As a reference, the value of the sum of the DC resistance of the windings of the toroid A was 0.6 Ω for the DC current ranging from 3 to 8 A, whereas the value for the toroid B was 0.64 within the same range.

ISBN 978-84-617–9183–5

The graphics of Fig. 3 show the comparison between the measured (last column of Table I.b) and adjusted winding losses for the toroid A as a function of the rms current.

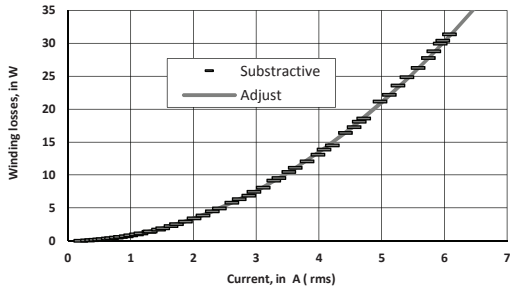


Figure 3. Comparison between measured and adjusted losses in the winding of toroid A with the same current as the basis.

As a complement and for the giving an idea of how significant can be the harmonic content of the current in the windings and its influence on the winding losses, graphics of Fig. 4.a show the wave shape of the instantaneous current for the two extreme levels of applied voltage, lower and higher (Tables I.a and I.b), whereas Fig. 4.b show the respective spectrum of current amplitudes.

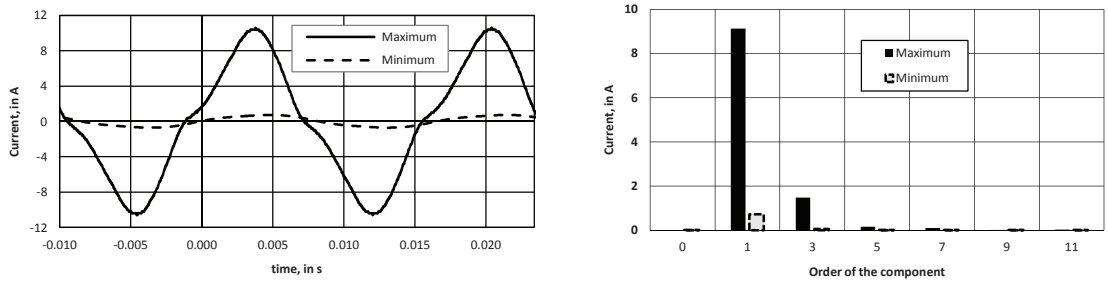


Figure 4. a. Instantaneous current wave shape for lower and higher level of applied voltage;
b. Amplitude spectra of harmonic components of current

The graphics of Figs. 5.a and 5.b show the behaviour of the separated losses as a function of the current for the toroids A and B, respectively.

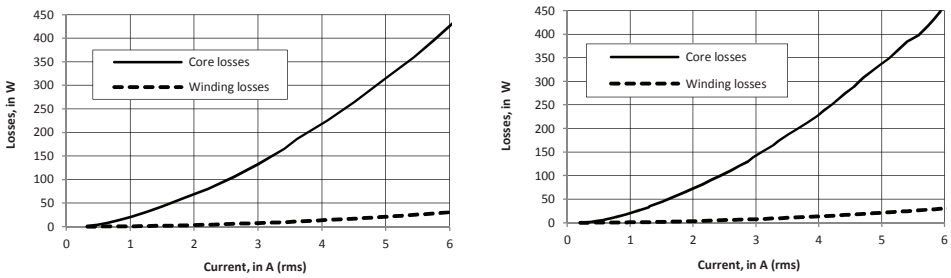


Figure 5. Separation of core and winding losses - a. Toroid A ; b. Toroid B

From the comparison between the graphics of the Fig. 5 it is noticeable that despite all the efforts for the total similarity of the two toroids, differences do exist. In fact, for any same value of current, the value of losses for the toroid B is always slightly higher. Thus, once the windings and core losses have been separated, the same principles of the short-circuit and the no-load tests are applied to determine the value of the parameters of the classical circuit of the toroidal transformers. Based on Fig. 2, these values are of the resistors R_S and R_N as well as of the inductive reactances, X_S and X_N. In consequence, from the basics of electric circuits, it is possible to evaluate the voltage drop, $\dot{V}_N$, across the branch with R_N and X_N in parallel. Thus, it is possible to determine the maximum value of the applied magnetics flux density, B_{peak} :

$$B_{peak} = \frac{2|\dot{V}_N|}{4{,}44\,.\,60\,.\,800.\,A} \tag{2}$$

in which A is the area of the cross section of the toroids that is equal to $1.59_{x}10^{-4}$ m^2, as depicted from Fig. 1.a.

ISBN 978-84-617–9183–5

On the other hand, for each value of current, the average value of the maximum magnetic field strength in the core can be evaluated by

$$H_{peak} = \frac{\sqrt{2}\,800\,|\dot{I}_m|}{\ell_m} \tag{3}$$

in which $|\dot{I}_m|$ is the rms current that flows through the branch of paralleled R_N and X_N and ℓ_m is the average path of the magnetic circuit of the toroids that from Fig. 1.a is equal to 0.9 m.
Based upon these calculations, important results are achieved for the ASTM A36 steel. The first one is shown in Fig. 6.a that is the behaviour of the volumetric core loss magnetic in function of the magnetic flux density for both the toroids. In addition, the graphics of Fig. 6.b show the AC magnetisation curve, or the behaviour of the magnetic flux density in function of the magnetic field strength, for the tested toroids. At last, regarding the magnetic permeability of the ASTM A36 steel, the graphics of Fig. 6.c show the behaviour of its relative value as a function of the magnetic flux density. For obtaining these graphics, each of their points was calculated by the ratio between the values the magnetic flux density and the magnetic field strength, from graphics of Fig. 6.a, per unit of the vacuum permeability, μ_o.

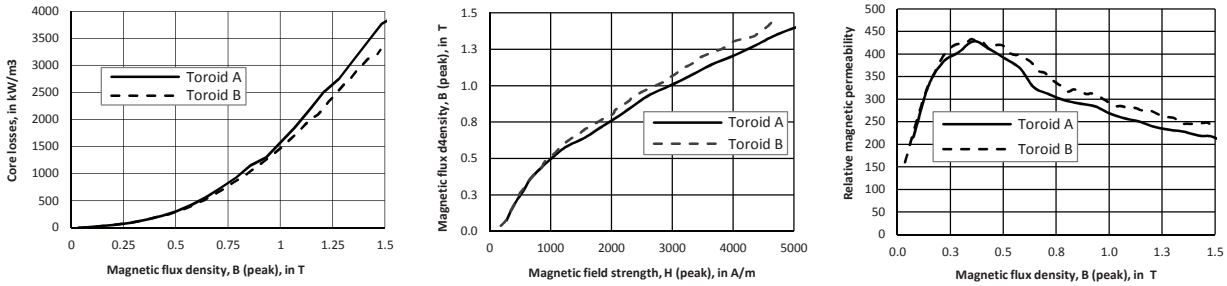


Figure 6. a. The volumetric core losses per toroid.
b. The AC Magnetisation curves per toroid.
c. The relative magnetic permeability per toroid.

IV. ANALYSES OF THE RESULTS

From the graphics of Figs. 5 to 7 it is clear that despite all the concerns for the two samples to be the more similar as possible to each other there are noticeable differences in their behaviour of the two toroids. However, these differences are not so significant and thus the analyses of the results can be performed with basis on their average behaviour. With respect to the results that characterise the ASTM A36 steel, electrical and magnetically, it is important to consider that the volumetric losses have a somehow predictable behaviour that is the approximately quadratic dependence on the magnetic flux density. Similarly, the AC magnetisation curves and the correlate magnetic permeability present predictable behaviour, according to [7] literature, by showing the effect of magnetic saturation and the corresponding decrease in the value of the magnetic permeability. In fact, the real importance of the results presented are not properly on the confirmation of the expected behaviour but exactly on the obtained values. In other words, information such as, for example, under a magnetic flux density of 1T the value for the volumetric losses is 1500 kW/m^3 for the ASTM A36 steel, the magnetic field strength is 3000 A/m and the relative magnetic permeability is about 280. Objective data like these as well as all the many other obtained by the proposed methodology and shown through Figs. 5 to7 have significant importance to any transformer designer in view taking measures towards the efficiency of any power transformer design. The application of the proposed method for other types and/or thickness of structural steel will substantially help the transformer designer.

At last, as some criticising comment for the results and the proposed methodology, it is important to mention the possible influence of the skin effect on the results, which was not taken into account. This because of the cross-section of the toroids with dimensions 6.35 mm x 25 mm that favours the occurrence of skin effect on the distribution of the magnetic flux in the cross section of the toroids, definitely. However, it also is important to consider that thanks to magnetic saturation, the magnetic skin effect has some compensating effect towards the uniform distribution of the magnet flux over the cross section of the steel toroid. This so because despite the skin effect naturally causes a tending of the magnetic flux to concentrate in the outer perimeter of the cross

ISBN 978-84-617–9183–5

section, an increase in the applied magnetic flux density also tends to cause the magnetic saturation of the region close to the outer perimeter of the cross section, which forces this increasing magnetic flux to prefer the inner area of the cross section. As a global result, the distribution of the magnetic flux over the cross section tends to be somehow uniform. The real evaluation of how this process takes place and its influence on the behaviour of items like the volumetric losses, the AC magnetisation curve and the magnetic permeability is a consequent proposition for future works.

V. CONCLUSIONS

The results obtained by the proposed method are shown as potentially interesting for the electric and magnetic characterization of structural steel used in tanks transformers and other metal shields. The procedures for preparing and testing steel samples is not so complex and can be adopted by transformer manufacturers to not only giving good and important information to the transformer designer but also to serve as a procedure for checking the quality of structural steel received in order to guarantee that the designed transformers have a so desired efficiency. Besides the mentioned likely influence of the skin effect, application of the proposed method for other structural steel types with different plate thickness arise as natural future items to be explored.

REFERENCES

[1] A. Lotfi, H. Hoidalen, E. Agheb and A. Nysveen, *Characterization of Magnetic Losses in the Transformer Tank Steel*, in IEEE Transactions on Magnetics, vol. 52, no. 5, pp. 1-4, May 2016.

[2] G. Bertotti, *General Properties of Power Losses in Soft Ferromagnetic Materials*, in IEEE Transactions on Magnetics, vol. 24, no. 1, pp. 621-630, Jan 1988.

[3] Y.M. Xu, C. Du and D.W. Meng, *Eddy Current Loss and Shielding Research of the Tank in Power Transformer*, Advanced Materials Research Vols. 468-471, p. 1086-1089, 2012.

[4] J.C. Olivares, R. Escarela-Perez, S.V. Kulkarni, F. de Leon, E. Melgoza-Vasquez and O. Hernandez-Anaya, *Improved Insert Geometry for Reducing Tank-Wall Losses in Pad-Mounted Transformers*, in IEEE Transactions on Power Delivery, vol. 19, no. 3, pp. 1120-1126, July 2004.

[5] C. Simão, N. Sadowski, N.J. Batistela and J.P.A Bastos, *Evaluation of Hysteresis Losses in Iron Sheets Under DC-biased inductions*, in IEEE Transactions on Magnetics, Vol. 45, no. 3, pp. 1158-1161, March 2009.

[6] C. Simão, N. Sadowski, N.J. Batistela and P. Kuo-Peng, *Simplified Models for Magnetic Hysteresis Losses Evaluation in Electromagnetic Devices*, Electric Machines and Drives Conference, 2009. IEMDC '09. IEEE International, Miami, FL, 2009, pp. 876-880.

[7] S.V. Kulkarni and S.A .Khaparde, *Transformer Engineering, Design and Practice*, NewYork, Marcel Dekker, 2004.

[8] Xose M. López-Fernández, P. Penabad-Durán and J. Turowski, *3-D Methodology for the Hazard Assessment on Heating Transformer Covers,* Electrical Machines (ICEM), 2010 XIX International Conference on, Rome, 2010, pp. 1-6.

ISBN 978-84-617–9183–5

Use of Specific Finite Element Methods to Compute Load and no Load Losses in Power Transformers.

Guillaume LAI, Vincent LECONTE

ALTAIR
38450 Meylan Cedex, France
Tel : +334 76 90 50 45 ; email : vincent.leconte@cedrat.com

Abstract — **New European directives for the "eco-design" represent a challenge for many transformer manufacturers. Simulation tools can help them to reach the required efficiencies, by computing accurately all the losses in the transformer. Different modeling methods based on Finite Element Analysis are presented. Some results and measurements comparisons will be given in the full paper.**

Keywords — **Power transformer, No load Test, Load test, Special Losses, Finite Element Analysis**

I. INTRODUCTION

Losses in power transformers are one of the main preoccupations of transformer manufacturers. Re-designs and optimizations are necessary to reach the new requirements of European directives in terms of energy efficiency. For many years, analytical formulae have been used to design transformers. Today, these methods show some limitations with the accuracy requested by new standards. Finite Element Analysis allows improving computation possibilities, being able to reproduce virtually the classical tests done to characterize the losses in transformers. Moreover, simulation tools are able to locate losses, in particular special losses, and are very useful to give indications on how to reduce them.

Nevertheless, several modelling difficulties arise when simulating the transformer. Some specific methods based on 2D and 3D FE calculations are described below, for an efficient evaluation of the losses in copper and in iron parts.

II. NO LOAD LOSSES

During a no-load test, the main losses are concentrated in iron. To reproduce this test, a 3D magneto-harmonic FE computation is performed, in which saturation of materials is taken into account [1] as well as the connection with the electric circuit, to impose a voltage drop on the HV coils

In this part, I will use several methods and several modelling in order to establish No load losses accurately in a 150 MVA transformer.

Modelling the core with FEA requires using local and global model. Firstly, I simulated a simple case with different configurations (Fig. 1). The aim of these local modellings was to determine the real effect of an air gap on the losses computed.

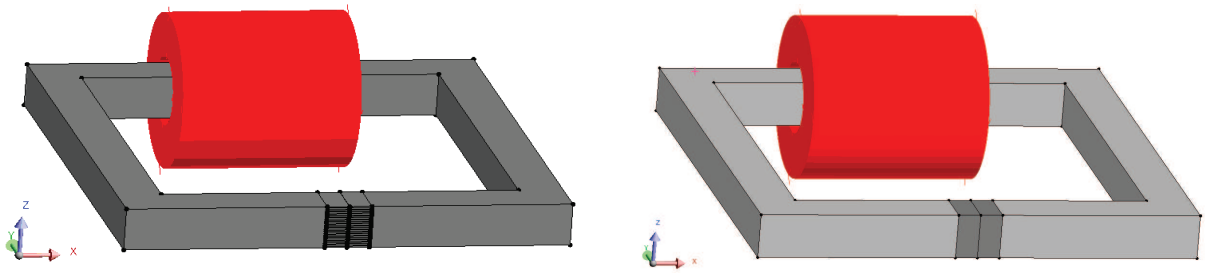


Figure 1. Simple case of a magnetized core, with laminated core (left), with no conducting model (right).

ISBN 978-84-617–9183–5

With considering the mesh size of the laminated problem, and the solving time, I decided to study only a cube of 1000 mm3 of laminated region around the air gap (Fig. 2).

The complete geometry had been compared to the same project with physical model used in the global modelling, in order to revaluate the Eddy losses.

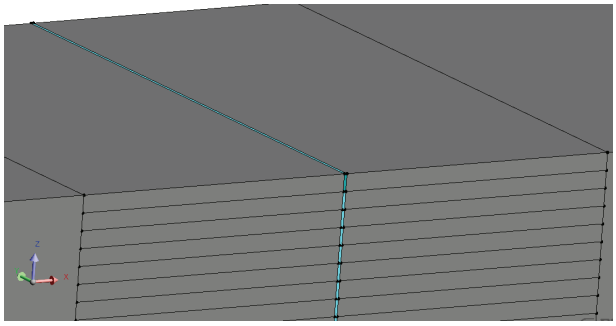


Figure 2. Air gap in the study part of core.

The massive part of the laminated model is constituted by 33 sheet of oriented magnetic steel, with a thickness of 0.3 mm and an air gap of 0.05mm. The second order mesh used to model inducted current is constituted at least by 8 nodes in the sheet thickness and by 3 nodes in the air gap (Fig. 3). This density allowed modeling all rotating current inside the lamination part, and to have accurate result of eddy current around the air gap [3]. This accurate model had been compared to the model used in the global modelling (Fig. 1)

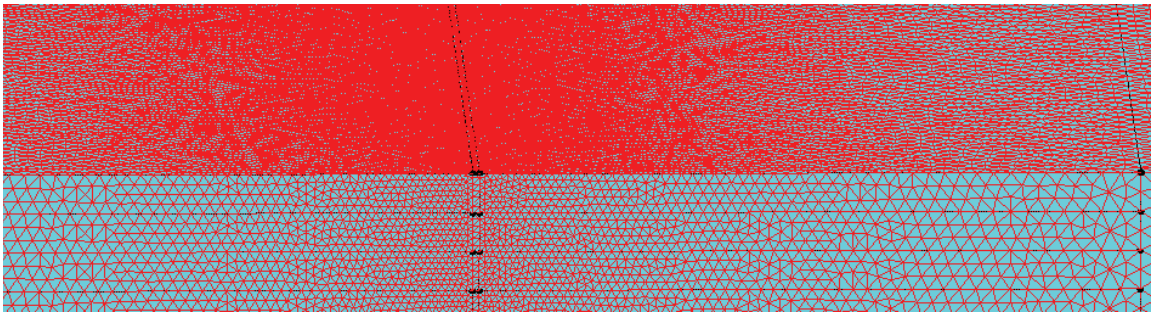


Figure 3. Zoom on laminated part mesh.

As no linear anisotropic is not authorized in FEA software, magnetic characteristics of the material used in the laminated model is anisotropic linear. This model could be considered as right, if the steel was not saturated. So voltage used at the terminal of winding is 0.24V in order to have an induction of 1.05T.

Between each magnetic sheet, there is a perfect insulator face region. These one had no thickness, so, the section of core is not changed comparing to the section used for the rest of core.

As the mesh density is high, the time solving for reference value is about 2 days for the complete model.

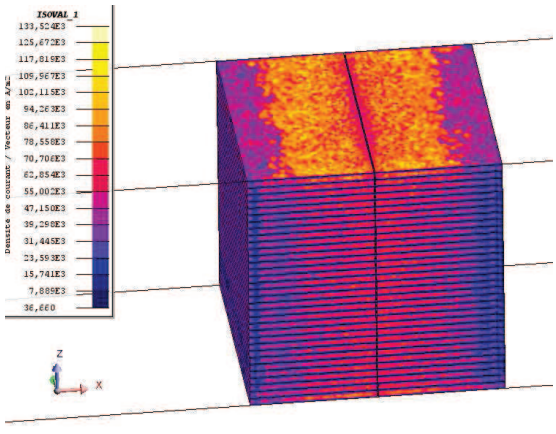


Figure 4. Current density on laminated part [A/m²].

ISBN 978-84-617–9183–5

Results [Table I and Fig. 4] were compared to models without lamination:

- Classical non conducting magnetic volume region without air gap (reference).
- Classical non conducting magnetic volume region with air gap (reference).

Losses are computed with Bertotti [2] extended formula (1). This model separates losses generated by hysteresis, classical losses, and losses in excess. That allows comparing only excess and classical losses.

$$dP=\underbrace{c_1 * \bar{B}^{c_2} * f}_{\text{Hysteresis}}+\underbrace{\pi^2 * \sigma * d^2 * (\bar{B} * f)^{c_3} / 6}_{\text{Classical losses}}+\underbrace{\sqrt{(c_4 * \sigma * S * V_0)} * (\bar{B} * f)^{c_5}}_{\text{Losses in excess}} \quad (1)$$

where:

- B :is the peak value of induction [T]
- f: is the frequency [Hz]
- σ: is the electric conductivity of the magnetic material[$\Omega^{-1}.m^{-1}$]
- Vo: is a constant field, which depends on the difference of coercitive magnetic field strength between two magnetic objects according to the theory of Bertotti.
- S: is the cross section of the sheet[m²]
- D : is the thickness of magnetic sheet (lamination) [m]
- c_1, c_2, c_3 , c_4, c_5: coefficient determined in order to superimposed measured and theoretical curve of W/kg (Fig. 5)

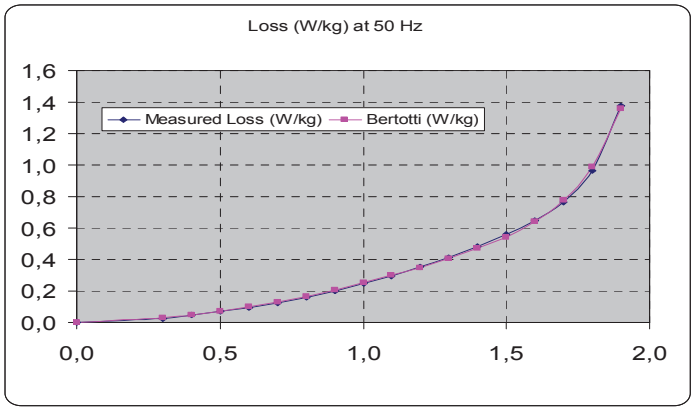


Figure 5. Measured W/kg vs Bertotti W/kg determined by varying c_1, c_2, c_3 , c_4, c_5.

Table I. Symbols for Magnetic Properties

	Losses in excess [W]	Classical losses [W]
MODEL WITH LAMINATED GEOMETRY WITH AIR GAP	2.67E-3	4.29E-5
CLASSICAL MODEL WITH AIR GAP	2.33E-3	3.92E-5
CLASSICAL MODEL WITHOUT AIR GAP	1.39E-3	2.75E-5

Finally, classical losses and losses in excess found in complete model are respectively 31.6% and 31.9% above losses computed on the classical model with air gap.

After that I considered a 150 MVA transformer core with air gap (Fig. 6) and I computed no load losses with Bertotti in function of the size of air gap. The original computation was under the measurement, and so, I multiplied losses in excess and classical losses by coefficient found in the first part (Fig. 7).

ISBN 978-84-617–9183–5

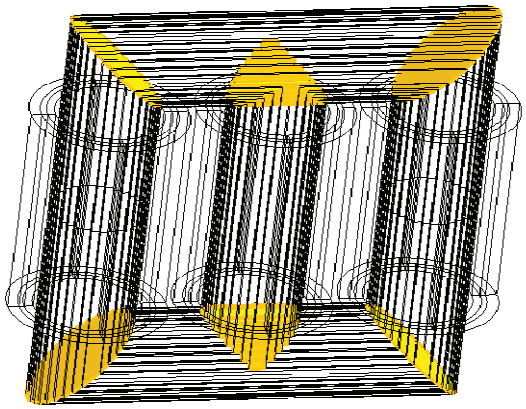


Figure 6. Air gap localization.

In conclusion, losses computed in the global model need to be revaluated in order to take account of the local effect of air gap. However, result is always under measurement, and other local modeling, as model of manufacturing hole, are needed to evaluate more accurately the no load losses.

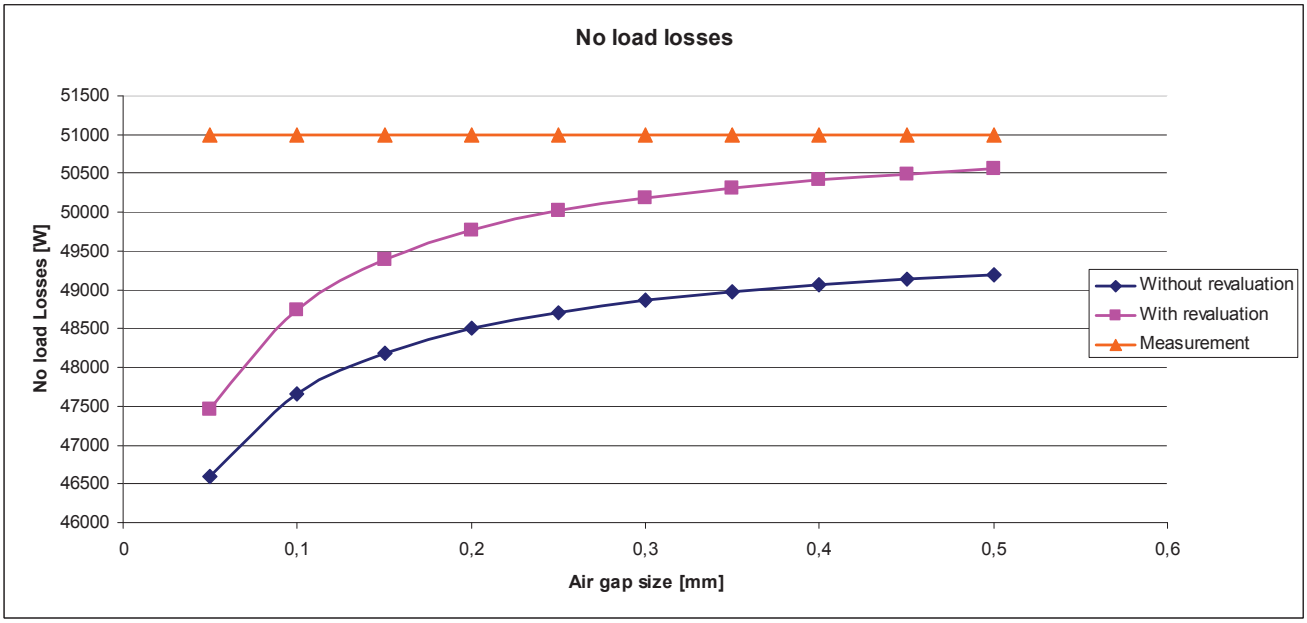


Figure 7. No load losses in a 150 MVA transformer in function of air gap size [mm].

III. LOAD LOSSES, AND HOT POINT COMPUTATION

Load losses are usually identified using a short-circuit test in which rated current is imposed. If measurements are only able to give global numbers, the 3D modeling allows localizing the losses accurately and separating the different contributions.

Special losses in connections, mechanical parts and tank are computed separately from the windings losses. A first computation is done in 3D using non-meshed coils. These ones are used to create the excitation magnetic field around the transformer (Fig. 8) and in the core, without meshing the coils themselves, reducing the model size and providing an easier mesh creation process. Because the tank is made of sheet metal, a special FE region with only a surface mesh may also be used to represent it, to avoid meshing its volume, and then gain in model size, without compromising with the accuracy [4].

ISBN 978-84-617–9183–5

In windings, skin and proximity effect have to be evaluated, which is a challenging task in 3D, and which is not computed during the solving when using non-meshed coils.

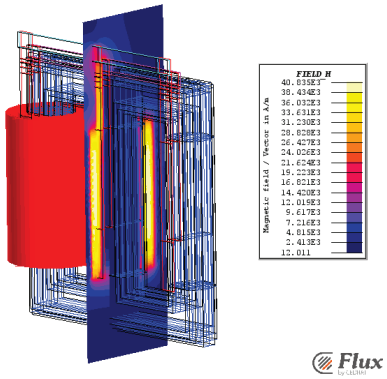


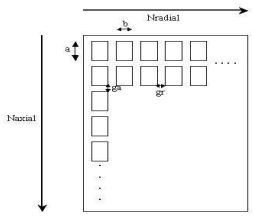
Figure 8. Field H generated by no mesh coil and connection [A.m^{-1}].

Therefore, to evaluate the power losses due to eddy currents in the turns, it is necessary to use a formula such as (2) in post-processing [5].

$$P(eddy) = \frac{1}{\sigma \mu_o^2}\left[\frac{b}{\delta}\frac{\sinh(a/\delta)-\sin(a/\delta)}{\cosh(a/\delta)+\cos(a/\delta)}Brad^2 + \frac{a}{\delta}\frac{\sinh(b/\delta)-\sin(b/\delta)}{\cosh(b/\delta)+\cos(b/\delta)}Bax^2\right] \quad (2)$$

where:

- P(eddy) : is losses density [W/m^3]
- δ : is the skin depth [mm]
- σ : is the electric conductivity of the magnetic material [Ω^{-1}.m^{-1}]
- B : is the magnetic field [T]
- a,b : are dimensions of the wire [m]
- μ_0 : is the vacuum permeability
- f : is the frequency [Hz]



If the dimensions of the wires are small comparing to skin depth, formula (2) can be simplified using a limited development (3):

$$P(eddy) = \sigma\pi^2 f^2 (b.a^3 .Brad^2 + a.b^3 .Bax^2)/6 \quad (3)$$

In this situation, another numerical method that is available is to use a homogenization technique as shown in [6].

To compute special losses in foils, the above formulae do not apply. In 3D, once again, thin conducting regions may be used [7]. Nevertheless, in most cases, this would lead to a very big 3D model. A more efficient way is to model all the turns in 2D (Fig. 9), and to consider them as solid conductor regions coupled through an electric circuit. It is a very accurate method although it requires high mesh densities in the foils, which is affordable in 2D.

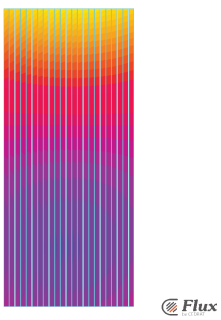


Figure 9. Current density J with solid conductor modeling in HV pancake.

ISBN 978-84-617–9183–5

This modeling allows computing hot point position inside the winding. After exporting result and compute the thermal aspect with an Electromagnetic coupled thermal application, we obtain the position of hot point (Fig. 10)

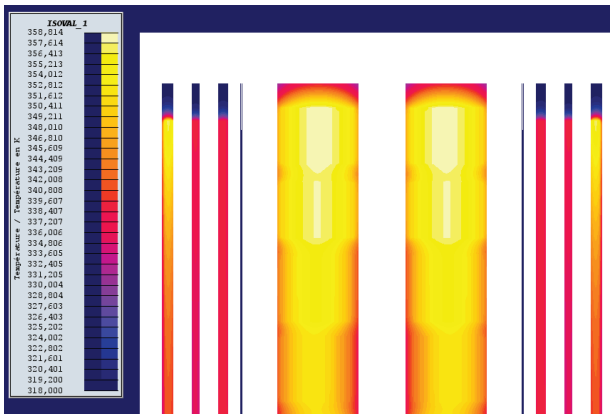


Figure 10. Temperature in the winding [°K].

In conclusion, several 2D and 3D model are needed to compute losses in transformer. These one can be used in a thermal simulation in order to determine the hot point, and the temperature.

IV. CONCLUSION

Transformer modelling is always a big challenge for all transformer manufacturers. Modelling local phenomenon allows having a better idea from the transformer behaviour and can be used in order to revaluate the losses computed in a global modelling.

REFERENCES

[1] E. Vassent, G. Meunier, and J.C. Sabonnadiere, *Simulation of induction machine operation using complex magneto-dynamic finite elements*, IEEE Transactions on Magnetics, vol. 25, no. 4, pp. 3064–3066, 1989

[2] F.Fiorillo, A.Novikov *An improved Approach to power Losses in Magnetic Laminations under Nonsinusoidal Induction waveform* IEEE Transactions on Magnetics, vol. 26, no. 5, pp. 2904–2910, 1990.

[3] C. Guerin, G. Tanneau, G. Meunier, X. Brunotte, and J. B. Albertini, *Three dimensional magnetostatic finite elements for gaps and iron shells using magnetic scalar potentials*, IEEE Trans. Magn., vol. 30, no. 5, pp. 2885–2888, 1994.

[4] *3D eddy current losses calculation in transformer tanks using the finite element method*, IEEE Trans. Magn., 29(2):1419 - 1422 , 1993

[5] T.Ngneugueu Calculation of Extra losses in shell transformers windings*, IEEE Trans Magn,* vol. 24, no. 6, pp. 2673-2675, *1988*

[6] J. Gyselinck and P. Dular, *Frequency-domain homogeneization of bundles of wires in 2D magnetodynamic FE calculations*, IEEE Trans. Magn., vol. 41, no. 5, pp. 1416-1419, 2005.

[7] 3-D Magnetic Scalar Potential Finite Element Formulation for Conducting Shells Coupled With an External Circuit, IEEE Trans. Magn., vol 48, no.2, pp 323-326, 2012

ISBN 978-84-617–9183–5

Implicit and Explicit State Space Models of Power Transformers for Fast Front Transient Simulations

Luis ROUCO and Alfredo del RÍO

Instituto de Investigación Tecnológica (IIT), E.T.S. de Ingeniería ICAI, Universidad Pontificia Comillas
Alberto Aguilera, 23, 28015 Madrid
Luis.Rouco@iit.comillas.edu

Abstract - Design of power transformers with respect to fast front transients requires appropriate simulation models. Transformer manufacturers have developed detailed transformer modes for their internal use. Such models are described in terms of node capacitance and coil inductance matrices of the windings. This paper describes implicit and explicit state space models of power transformers for fast front transient simulations. Simulation of time and frequency domain responses with such models is detailed. The paper shows simulation results obtained with a manufacturer model of a power transformer using the proposed models.
Keywords - Fast Front Transients, Transformer Models, Implicit State Space Models, Explicit State Space Models.

I INTRODUCTION

Fast Front Transients (FFT) [1] occur in power networks due to direct incidence of lightning in power lines. Design of power transformers with respect to FFT requires appropriate simulation models.

Transformer manufacturers have developed detailed transformer modes for their internal use. Such models are described in terms of node capacitance and coil inductance matrices of the windings [2]. As the resulting set of differential equations is linear, time domain simulations are computed using the exponential of the state matrix which is also called transition matrix. As many programs developed by transformer manufacturers dated from the sixties of the last century, they use iterative algorithms to compute the exponential of the matrix based on truncations of its series expansion of until the error is below a selected threshold [3].

This paper describes implicit state space models of power transformers for fast front transient simulations. Implicit state space models are described in general by sets of non-linear differential and algebraic equations. Implicit state space models are very common in other fields of power system simulation like power system stability [4]. The advantage of such models is that they can accommodate easily other devices that interact with power transformers such as surge arresters in case of time domain simulations. Moreover, computation of response in the frequency domain is greatly simplified. Of course, linear explicit state space models can be obtained from implicit linear space models. The paper illustrates the simulation models with results obtained from a manufacturer model of a power transformer.

II MODELS OF DYNAMIC SYSTEMS

Let us consider a dynamic system described by a set of non-linear differential and algebraic equations:

$$\begin{aligned} \dot{\mathbf{x}} &= \mathbf{G}(\mathbf{x}, \mathbf{z}, \mathbf{u}) \\ \mathbf{0} &= \mathbf{H}(\mathbf{x}, \mathbf{z}, \mathbf{u}) \end{aligned} \tag{1}$$

where $\mathbf{G}$ y $\mathbf{H}$ are vectors of non linear functions, $\mathbf{x}$ are the state variables, $\mathbf{z}$ are the algebraic variables and $\mathbf{u}$ are the input variables.

A dynamic system expressed in terms of the state and algebraic variables is called to be written in implicit form.

If the system of non-linear differential and algebraic equations (1) is linearized around a stable operating point $\mathbf{x} = \mathbf{x}_0, \mathbf{z} = \mathbf{z}_0, \mathbf{u} = \mathbf{u}_0$, it becomes:

ISBN 978-84-617–9183–5

$$\begin{bmatrix} \Delta\dot{\mathbf{x}} \\ \mathbf{0} \end{bmatrix} = \begin{bmatrix} \left.\frac{\partial \mathbf{G}(\mathbf{x},\mathbf{z},\mathbf{u})}{\partial \mathbf{x}}\right|_{\mathbf{x}=\mathbf{x}_0,\mathbf{z}=\mathbf{z}_0,\mathbf{u}=\mathbf{u}_0} & \left.\frac{\partial \mathbf{G}(\mathbf{x},\mathbf{z},\mathbf{u})}{\partial \mathbf{z}}\right|_{\mathbf{x}=\mathbf{x}_0,\mathbf{z}=\mathbf{z}_0,\mathbf{u}=\mathbf{u}_0} \\ \left.\frac{\partial \mathbf{H}(\mathbf{x},\mathbf{z},\mathbf{u})}{\partial \mathbf{x}}\right|_{\mathbf{x}=\mathbf{x}_0,\mathbf{z}=\mathbf{z}_0,\mathbf{u}=\mathbf{u}_0} & \left.\frac{\partial \mathbf{H}(\mathbf{x},\mathbf{z},\mathbf{u})}{\partial \mathbf{x}}\right|_{\mathbf{x}=\mathbf{x}_0,\mathbf{z}=\mathbf{z}_0,\mathbf{u}=\mathbf{u}_0} \end{bmatrix} \begin{bmatrix} \Delta\mathbf{x} \\ \Delta\mathbf{z} \end{bmatrix} + \begin{bmatrix} \left.\frac{\partial \mathbf{G}(\mathbf{x},\mathbf{z},\mathbf{u})}{\partial \mathbf{u}}\right|_{\mathbf{x}=\mathbf{x}_0,\mathbf{z}=\mathbf{z}_0,\mathbf{u}=\mathbf{u}_0} \\ \left.\frac{\partial \mathbf{H}(\mathbf{x},\mathbf{z},\mathbf{u})}{\partial \mathbf{u}}\right|_{\mathbf{x}=\mathbf{x}_0,\mathbf{z}=\mathbf{z}_0,\mathbf{u}=\mathbf{u}_0} \end{bmatrix} \Delta\mathbf{u} \quad (2)$$
$$= \begin{bmatrix} \mathbf{A}_1 & \mathbf{A}_2 \\ \mathbf{A}_3 & \mathbf{A}_4 \end{bmatrix} \begin{bmatrix} \Delta\mathbf{x} \\ \Delta\mathbf{z} \end{bmatrix} + \begin{bmatrix} \mathbf{B}_1 \\ \mathbf{B}_2 \end{bmatrix} \Delta\mathbf{u}$$

where:

$$\Delta\mathbf{x} = \mathbf{x} - \mathbf{x}_0, \Delta\mathbf{z} = \mathbf{z} - \mathbf{z}_0, \Delta\mathbf{u} = \mathbf{u} - \mathbf{u}_0$$

If the algebraic variables $\mathbf{z}$ are eliminated from (2), then the dynamic system becomes described just by the state variables $\mathbf{x}$ and the input variables $\mathbf{u}$:

$$\Delta\dot{\mathbf{x}} = \mathbf{A}\Delta\mathbf{x} + \mathbf{B}\Delta\mathbf{u} \quad (3)$$

where:

$$\begin{aligned} \mathbf{A} &= \mathbf{A}_1 - \mathbf{A}_2\mathbf{A}_4^{-1}\mathbf{A}_3 \\ \mathbf{B} &= \mathbf{B}_1 - \mathbf{A}_2\mathbf{A}_4^{-1}\mathbf{B}_2 \end{aligned} \quad (4)$$

A dynamic system expressed only in terms of the state variables is called to be written in explicit form.

III TRANSFORMER MODEL

The detailed model of a transformer at high frequencies is characterized by the node capacitance and the coil inductance matrices. Both the node capacitance and the coil inductance matrices are determined from the physical layout of the transformer windings and magnetic circuit.

The capacitance matrix $\mathbf{C}$ relates the node voltages $\mathbf{v}_n$, the departing node currents $\mathbf{i}_n$ and source injected currents $\mathbf{i}_s$ according to:

$$\mathbf{C}\frac{d\mathbf{v}_n}{dt} = -\mathbf{i}_n + \mathbf{i}_s \quad (5)$$

Each term of the capacitance matrix C_{ij} is determined as:

$$\begin{aligned} C_{ii} &= c_i + \sum_k c_{ik} \\ C_{ij} &= C_{ji} = -c_{ij} \end{aligned} \quad (6)$$

where c_i is the capacitance of node i to ground and c_{ij} is the capacitance between nodes i and j. Figure 1 shows the node voltages and currents in an example circuit. Such example circuit only exhibits capacitive couplings between adjacent nodes. Although real transformers exhibit additional capacitive couplings, the capacitance matrix is still sparse.

ISBN 978-84-617–9183–5

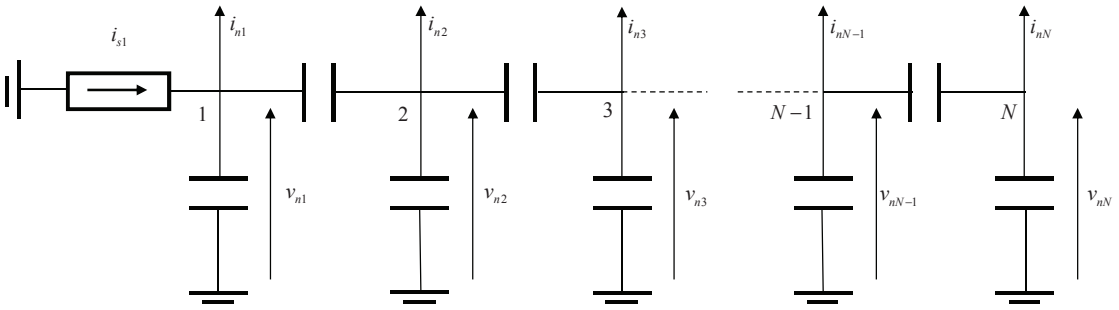


Figure 1. Capacitive component of the transformer model.

The coil inductance matrix $\mathbf{L}$ relates the coil voltages $\mathbf{v}_c$ and the coil currents $\mathbf{i}_c$ according to:

$$\mathbf{L}\frac{d\mathbf{i}_c}{dt} = \mathbf{v}_c \tag{7}$$

Each term of the coil inductance matrix L_{ij} is determined as:

$$\begin{aligned} L_{ii} &= l_i + \sum_k l_{ik} \\ L_{ij} &= L_{ji} = -l_{ij} \end{aligned} \tag{8}$$

where l_i is the self inductance of mesh i and l_{ij} is the mutual inductance between meshes i and j. Figure 2 shows the coil voltages and currents in an example circuit. Such example circuit exhibits inductive couplings among all meshes which is the actual situation in real transformers.

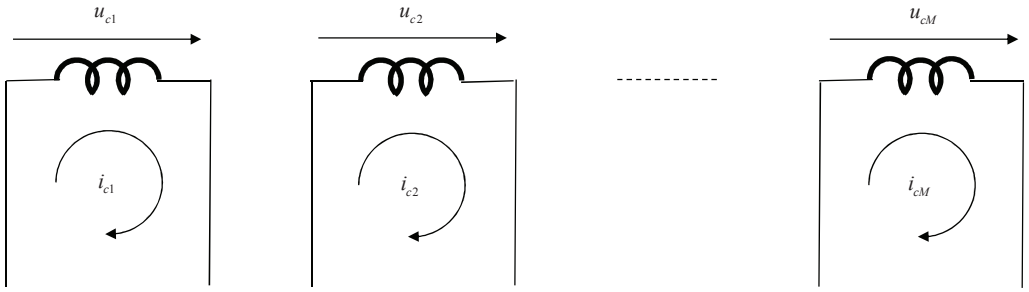


Figure 2. Inductive component of the transformer model.

and the node and coil voltages are related according to:

$$\mathbf{v}_c = \mathbf{T}\mathbf{v}_n \tag{9}$$

The node and the coil currents are related according to:

$$\mathbf{i}_n = \mathbf{T}^T\mathbf{i}_c \tag{10}$$

Equations (5)-(9) can be written as a set of differential-algebraic equations of the form (2) where the state variables $\mathbf{x}$ are the node voltages $\mathbf{v}_n$ and the coil currents $\mathbf{i}_c$, the algebraic variables $\mathbf{z}$ are the node currents $\mathbf{i}_n$ and the coil voltages $\mathbf{v}_c$ and the input variables $\mathbf{u}$ are the currents supplied by the excitation sources $\mathbf{i}_s$.

ISBN 978-84-617–9183–5

$$\begin{aligned}
\frac{d\mathbf{v}_n}{dt} &= \mathbf{C}^{-1}\left(-\mathbf{i}_n + \mathbf{i}_s\right) \\
\frac{d\mathbf{i}_c}{dt} &= \mathbf{L}^{-1}\mathbf{v}_c \\
\mathbf{i}_n &= \mathbf{T}^T\mathbf{i}_c \\
\mathbf{v}_c &= \mathbf{T}\mathbf{v}_n
\end{aligned} \tag{11}$$

IV TIME DOMAIN SIMULATION

The model of the transformer is built assuming that node number 1 is ground. Hence,

$$\begin{aligned}
v_{n1} &= 0 \\
\frac{dv_{n1}}{dt} &= 0
\end{aligned} \tag{12}$$

In addition, it considers that bus number 2 is the node to be disturbed. The lightning impulse is modeled as a combination of two exponential functions. Therefore:

$$\begin{aligned}
v_{n2} &= V_0\left(e^{-\alpha t} - e^{-\beta t}\right) \\
\frac{dv_{n2}}{dt} &= V_0\left(-\alpha e^{-\alpha t} + \beta e^{-\beta t}\right) \\
V_0 &= 1.035319, \alpha = 0.072786/5\cdot 10^6, \beta = 13.04424/5\cdot 10^6
\end{aligned} \tag{13}$$

Taking into consideration (12) and(13), the set of differential equation of node voltages becomes:

$$\begin{bmatrix} \frac{dv_{n3}}{dt} \\ \vdots \\ \frac{dv_{nN}}{dt} \end{bmatrix} = \mathbf{C}^{-1}\left(3:N,:\right)\left(-\mathbf{i}_n + \mathbf{i}_s\right) = \mathbf{C}^{-1}\left(3:N,:\right)\left(-\mathbf{i}_n + \begin{bmatrix} 0 \\ i_{s2} \\ 0 \\ \vdots \\ 0 \end{bmatrix}\right)$$

where:

$$i_{s2} = \frac{1}{\mathbf{C}^{-1}\left(2,2\right)}\left(\frac{dv_{n2}}{dt} + \mathbf{C}^{-1}\left(2,:\right)\mathbf{i}_n\right)$$

As the transformer model is linear, time domain simulation can be performed either using numerical integration algorithm of the implicit model like Runge-Kutta or the solution of the explicit model in terms of the eigenvalues and eigenvectors of the state matrix. The appendix details both approaches. Figure 3 shows the layout of an actual shell type transformer which data were provided by a manufacturer. Figure 4-left shows the transformer node voltages. Figure 4-right compares node 12 voltage computed using Runge-Kutta numerical integration algorithm or the solution in terms of the eigenvalues and eigenvectors. There is no difference at all between the results provided by both methods.

V FREQUENCY DOMAIN SIMULATION

Many frequency responses can be calculated in a transformer. We illustrate the method considering the transfer function between the current injected at node number 2 and the voltage of node number 2 as well which is actually the short circuit impedance. The frequency response first requires to convert in the Laplace domain (11). The frequency response is calculated by solving for each frequency $s = j\omega$ the following set of complex algerbraic equagtions:

ISBN 978-84-617–9183–5

$$\begin{bmatrix} j\omega\mathbf{I}_{2-N} & \mathbf{C}^{-1}(2:N,2:N) & \mathbf{0} & \mathbf{0} \\ \mathbf{0} & j\omega\mathbf{I}_N & -\mathbf{L}^{-1} & \mathbf{0} \\ \mathbf{0} & -\mathbf{I}_N & \mathbf{0} & \mathbf{T}^T \\ \mathbf{T} & \mathbf{0} & -\mathbf{I}_M & \mathbf{0} \end{bmatrix} \begin{bmatrix} \mathbf{v}_{n,2-N}(\omega) \\ \mathbf{i}_n(\omega) \\ \mathbf{v}_c(\omega) \\ \mathbf{i}_c(\omega) \end{bmatrix} = \begin{bmatrix} j\omega \cdot \mathbf{e}_{2-N} \\ \mathbf{0} \\ \mathbf{0} \\ \mathbf{0} \end{bmatrix} \tag{14}$$

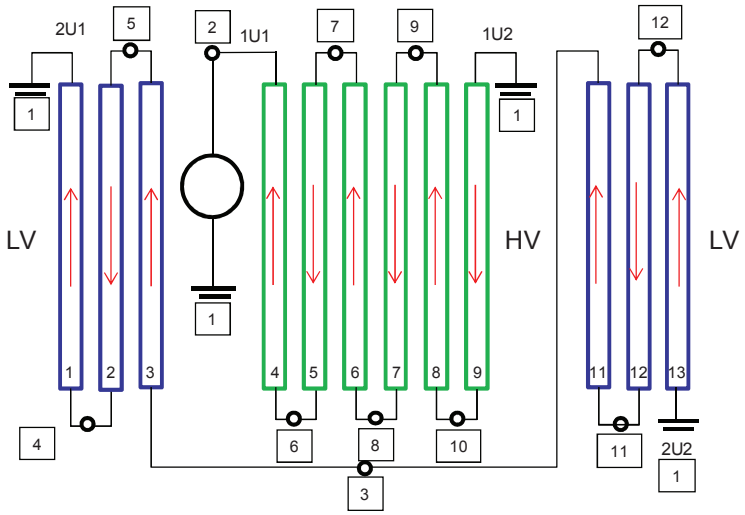


Figure 3. Layout of an actual shell type transformer.

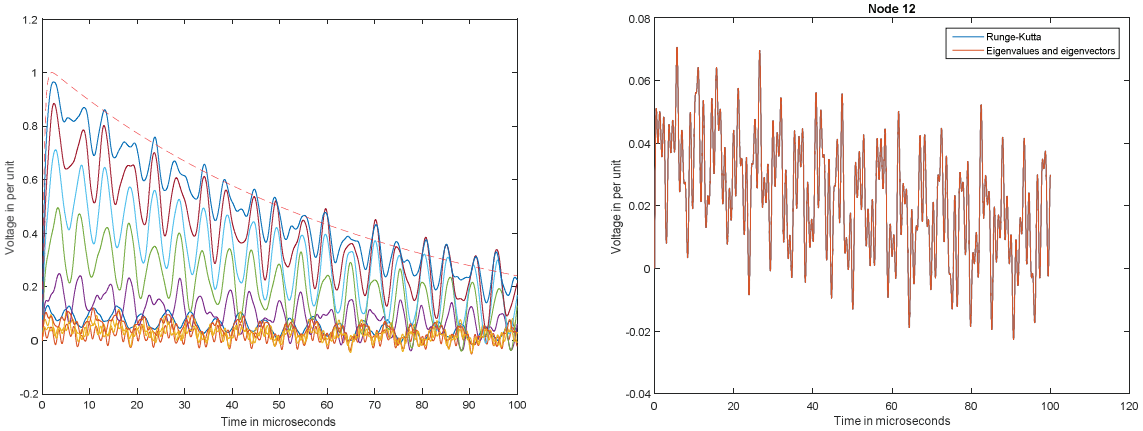


Figure 4. Node voltages (left) and comparison of node 12 voltage computed using two approaches (right).

Figure 5 show the Bode diagram (magnitude and phase) of the transfer function between the current injected at node number 2 and the voltage of node number 2. The natural frequencies of the transformer model are seen as peaks in the magnitude plot.

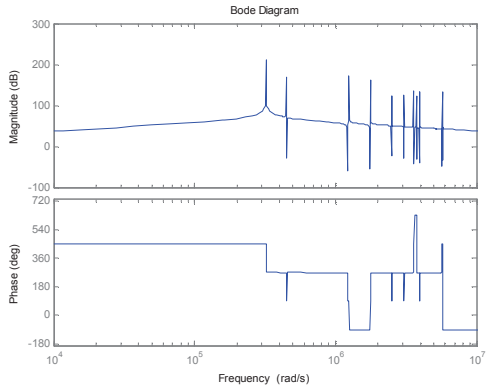


Figure 5. Frequency response.

ISBN 978-84-617–9183–5

VI CONCLUSIONS

This paper has presented implicit state space models of power transformers for fast front transient simulations. Implicit and explicit models have been connected. Moreover, the paper has highlighted the value of implicit state space models for both time and frequency domain simulations. Time and frequency domain of an actual shell time transformer have been shown to illustrate the model use.

REFERENCES

[1] IEC, International Standard IEC 71-1: "Insulation Coordination, Part I: Definitions, principles and rules", 17th Edition, 1993-12.

[2] J. H. McWhirter, C. D. Fahrnkopf, J. H. Steele "Determination of Impulse Stresses within Transformer Windings by Computers, Transactions of the American Institute of Electrical Engineers, Part III, Power Apparatus and Systems, Volume 76, No. 2, February 1957, pp. 1267-1274.

[3] C. Moler and C. Van Loan, "Nineteen Dubious Ways to Compute the Exponential of Matrix". SIAM Review, Vol. 20, No. 4, October 1978, pp. 801-836.

[4] L. Rouco, F.L. Pagola, G.C. Verghese, I.J. Pérez-Arriaga, "Selective Modal Analysis", Power system Coherency and Model Reduction, Editor J. H. Chow, Springer, 2013.

APPENDIX

Let us consider a set of non linear differential equations $\dot{\mathbf{x}} = \mathbf{F}(\mathbf{x}, u)$, the Runge-Kutta method of order 4-5, computes the state variables in step *k+1* $\mathbf{x}_{k+1}$ from the state variables is step *k* $\mathbf{x}_k$ according to:

$$\begin{aligned}
\mathbf{x}_{k+1} &= \mathbf{x}_k + \frac{1}{6}(k_1 + 2k_2 + 2k_3 + k_4) \\
k_1 &= \mathbf{F}(\mathbf{x}_k, u_k) \\
k_2 &= \mathbf{F}\left(\mathbf{x}_k + \frac{k_1}{2}, u_k\right) \\
k_3 &= \mathbf{F}\left(\mathbf{x}_k + \frac{k_2}{2}, u_k\right) \\
k_4 &= \mathbf{F}(\mathbf{x}_k + k_3, u_k)
\end{aligned}$$

Let us consider a set of set of linear differential equations $\Delta\dot{\mathbf{x}} = \Delta\mathbf{x} + \mathbf{b}\Delta u$ resulting from linearizing the set of non linear differential equations $\dot{\mathbf{x}} = \mathbf{F}(\mathbf{x}, u)$. Let us assume that $\mathbf{\Lambda}$, $\mathbf{V}$ and $\mathbf{W}$ are respectively the matrices of eigenvalues and right and left eigenvectors

$$\begin{aligned}
\mathbf{AV} &= \mathbf{V\Lambda} \\
\mathbf{WA} &= \mathbf{\Lambda W} \\
\mathbf{WV} &= \mathbf{I}
\end{aligned} \tag{15}$$

Then, the time response to zero initial conditions and an input change can be computed according to:

$$\Delta\mathbf{x}(t) = \int_{t_0}^{t} \mathbf{V} e^{\mathbf{\Lambda}(\tau - t_0)} \mathbf{W}\mathbf{b}\Delta u(\tau)\, d\tau \tag{16}$$

ISBN 978-84-617–9183–5

Non Invasive PD Monitoring for Power Transformers

Fernando GARNACHO (1), Javier ORTEGO (2)
Fernando ÁLVAREZ (3), Miguel A. SÁNCHEZ-URÁN (3)

(1) LCOE- FFII; C/ Eric Kandel, nº1, Getafe, Madrid, Spain
(2) DIAEL S.L. C/ Peñuelas nº 38, 28005, Madrid, Spain
(3) Department of Electrical Engineering, Polytechnic University of Madrid, Spain
Phone: (+34) 91562516, e-mail: fgarnacho@loce..etsii.pm.es

Abstract — **A new on line electromagnetic PD method using non-invasive sensors in the HF range is described in this paper. A powerful signal processing filtering tool developed on the basis of wavelet transform removes noise interferences preserving the original PD pulse waveform. The preservation of the original waveform of the PD pulse allows knowing the real pulse polarity, and with this information the PD source emplacement, inside or outside the transformer, is determined. A PD clustering is performed using arrival times and amplitude ratios of the pulses acquired. On line PD experiences show the efficiency of this new on line PD approach.**

Keywords — **On line PD measurements, PD pulse polarity, HFCT sensors, PD clustering.**

I. INTRODUCTION

PD activity in power transformers can be detected by means of the analysis of dissolved gases in the insulating oil, known as "dissolved gas analysis" (DGA). When PD activity is detected in DGA the next step is to identify the physical phenomenon involved in the PD source. The phase-resolved PD (PRPD) pattern is crucial for a correct diagnosis. The evolution of the PRPD pattern versus other parameters, such as, transformer temperature, load current and grid voltage give us a better understanding of the insulation problem.

Although in accordance with [1] PD patterns can be obtained applying the conventional electromagnetic PD method described in [2], that operates in the frequency range of not more than 1 MHz. This method requires no electromagnetic noise during the PD test. However, in practice there is a high level of background noise in power substations where on-line PD measurements are needed. The new technical specification IEC 62478 TS [3] and the new Electra Brochure [4] advise about how to perform conventional PD measurements by triggering of the PD measurement according to IEC 60270 using an invasive antenna UHF sensor installed inside of the power transformer, through the oil valve. The acquired UHF signals are used to identify the instants in which PD pulses appear within the power transformer under test. This criterion is very efficient when the electrical noise is due to repetitive interferences in short time intervals that do not matched PD pulses. However, in the rest of cases, the PD pulse is mixed with noise and both noise and PD pulse are together measured when the UHF signal triggers the conventional IEC 60270 PD measurement. For this reason this method is not able to detect small PD pulses hidden below the noise level . In addition, this approach is not applicable for the existing transformers with oil valves different to DN50 and DN80, because a straight input is required to enter the UHF antenna in the transformer tank. These disadvantages can be avoided by PD measurements in the HF range and if the noise is removed by signal processing tools without modify the waveform of the original PD pulse.

II. NOISE IN POWER SUBSTATIONS AND WAVEFORM DISTORTION CAUSED BY NOISE FILTERING

Usually, there is a high level of electrical noise in electrical substations, in special in outdoor substations, where on-line PD measurements are required. For instance, amplitude levels of 800 mV

ISBN 978-84-617–9183–5

of background noise were acquired by a HFCT sensor placed on an earth connection of a 400 kV substation. Many small PD pulses can appear below the electrical noise: e.g. a PD pulse of 0.01 mV is below background noise level in Fig. 1. The noise frequency spectrum depends on the particular substation in which the PD measurement must be performed, but in every substation, the zone with higher amplitudes appears in the lower frequency ranges (< 1MHz), where standardized PD measurements should be carried out. For this reason, IEC 60270 measurements are not possible in these emplacements.

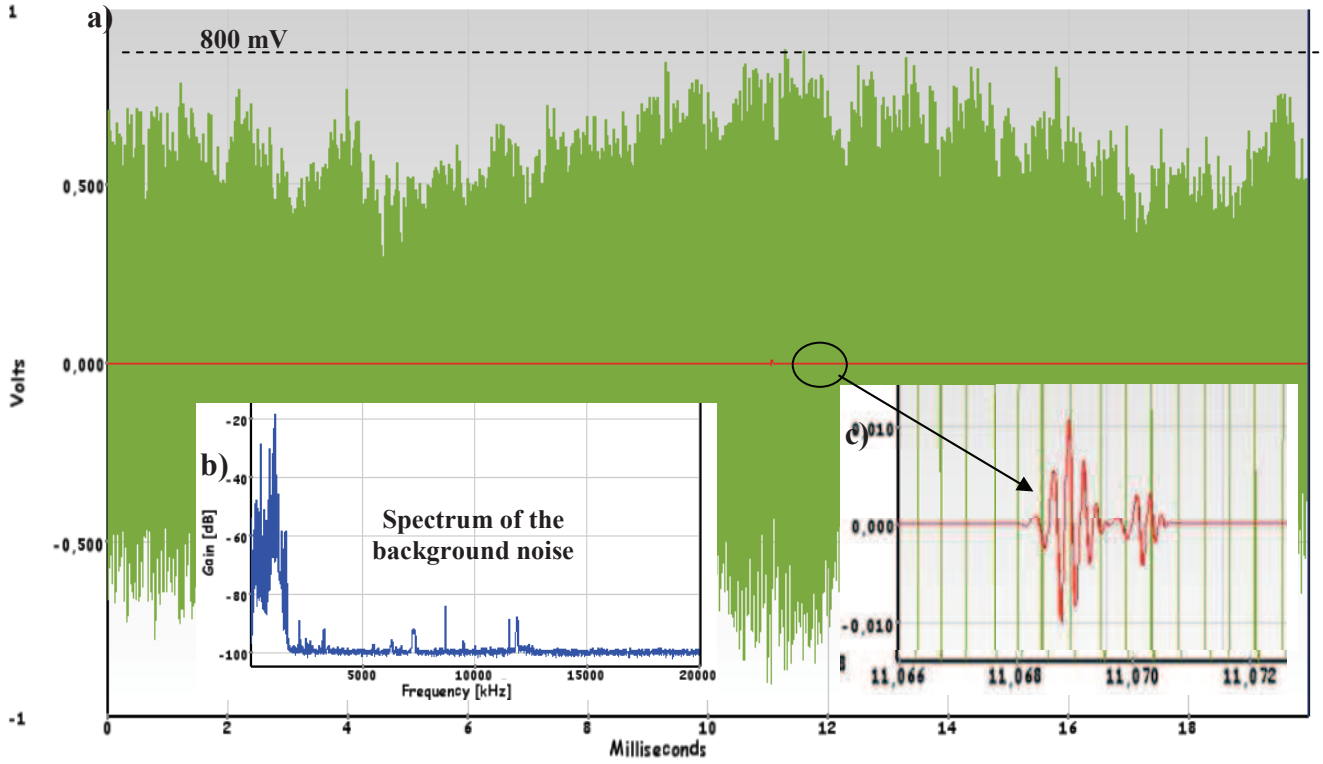


Figure 1. a) Background noise acquired by a HFCT sensor installed in an earth connection of a transformer tank. b) Spectrum of the background noise. c) Small PD pulse hidden below the noise.

When UHF measurements are performed (300 MHz – 3 GHz), only the UHF content of the original PD pulse is detected and consequently an important waveform distortion is caused to the original wave-shape. Also when the measuring frequency is chosen on the basis of the best signal/noise ratio an important signal distortion is provoked to the real PD pulse, converting a unidirectional PD pulse in an oscillating pulse where the polarity is missed. For this reason, the noise filtering technique to be applied should preserve the original waveform of the PD pulse.

III. PD SOURCE LOCATION USING PD POLARITY

The analysis of the PD pulse polarity is an efficient way for determining if the PD source is placed inside or outside the power transformer. The current pulse of a PD measured through the earth connection of the transformer tank flows in a different way depending on where the PD source is sited. When the PD source is inside a power transformer (T), the PD pulse flows from the transformer tank (TT) to the earth (E) through the grounding cable where the HFCT is installed, (see S_G in Fig. 2). Then the pulse of the HFCT is considered positive. However, when the PD pulse occurs in an insulation outside the transformer (e.g. in a cable terminal) the PD pulse flows from the earth (E) to the power transformer tank (TT) through the grounding cable. Then the pulse is considered negative

ISBN 978-84-617–9183–5

such it is shown in Fig. 2. If an additional HFCT sensor (Sc) is placed at the earth connection of the cable sheath an opposite current will be detected.

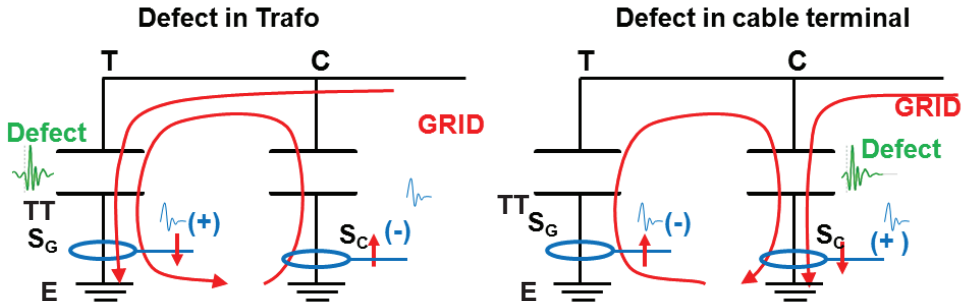


Figure 2: a) Pulse polarity of the PD signal when the defect is in the transformer, b) Pulse polarity of the PD signal when the defect is in the cable terminal.

IV. Description of the New PD Measuring Approach an Practical Case

The new on-line PD measuring approach presented in this paper uses external HFCT sensors installed on the cable sheath terminals or on the measuring taps of the bushings. Capacitive sensors connected on the measuring taps can be also used instead of HFCT sensors when bushings are installed in power transformers. The HFCT sensors used operate in the frequency range from 0.1 MHz to 20 MHz, where the most relevant frequency content is found if an internal PD source appears in a power transformer. According to references [5] and [6] the frequency spectrum of the conducted PD pulses caused by an internal defect in transformer windings is in the frequency range of few MHz. For this reason PD measurements in the HF range are very appropriate provided that the noise is eliminated. Additional external non-invasive UHF sensors based on patch type couplers placed on each bushing close to the tank are recommended, but not mandatory, in order to analyze if the PD signals are close to the transformer bushing. The operation frequency range from 0.3 GHz to 0.8 GHz is chosen for the UHF sensors, in order to avoid telecommunications interferences and to analyze if any PD source radiating UHF signals is close. UHF signals are amplified and converted to HF signals in order to use the same PD monitoring system (MS) as the one used for HF measurements.

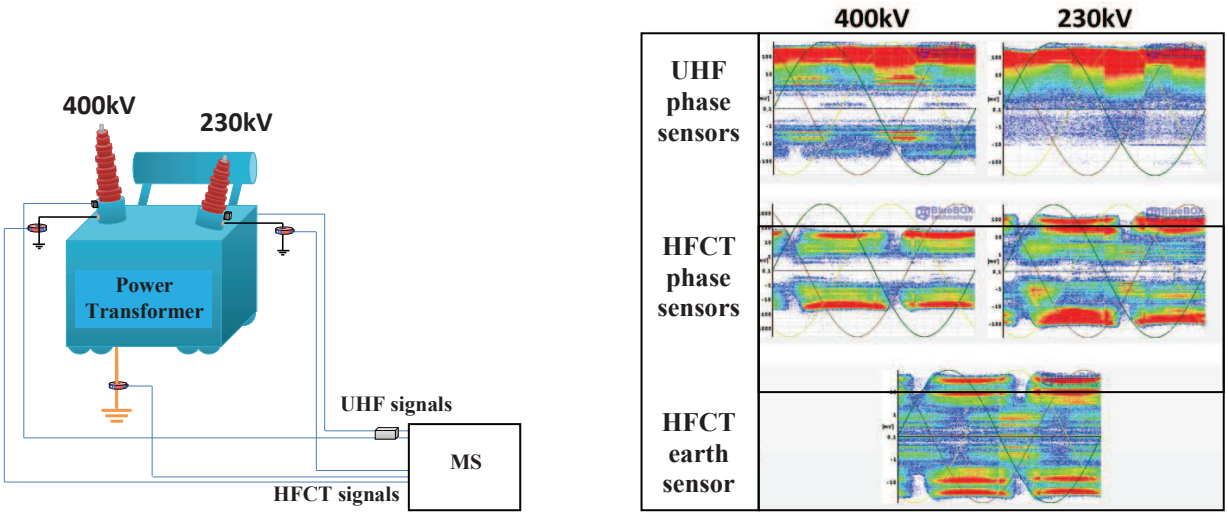


Figure 3: a) Sensors emplacement b) PRPD patterns acquired by the PD sensors

Fig. 3 shows a practical case of PD measurements in an autotransformer with the emplacement of the PD sensors and the PRPD patterns obtained. The synchronized signals acquired by the HFCT sensors placed in the HV and LV transformer sides and on the grounding connection of the tank are treated by

ISBN 978-84-617–9183–5

means of signal processing tools to recognize pulse polarity of the PD signal (see Fig. 4). Using the wavelet transform and statistical analysis the electrical noise is removed [7]. Numerical algorithms allow determining arrival time, polarity and amplitude of each PD pulse. The pulse polarity is used to discriminate if the PD source is inside or outside the power transformer.

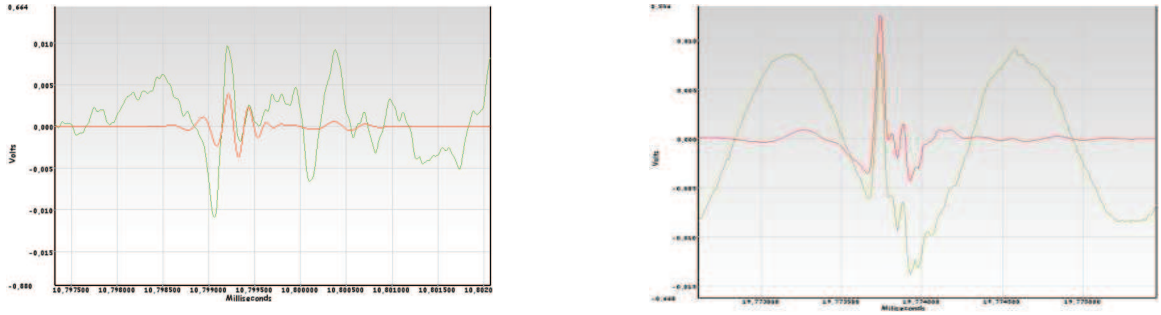


Figure 4: PD pulse polarity acquired by the HFCT sensor connected between tank grounding and earth: a) Negative PD pulse means PD source is outside the power transformer; b) Positive PD pulse means PD source is inside the power transformer.

Analyzing the arrival times of the PD pulses and the amplitude ratios between the PD pulses acquired by the HFCT sensors different PD clusters are distinguished (Fig. 5.B). The PRPD pattern of each PD cluster is then displayed in order to recognize what defect is involved (Fig. 5.C).

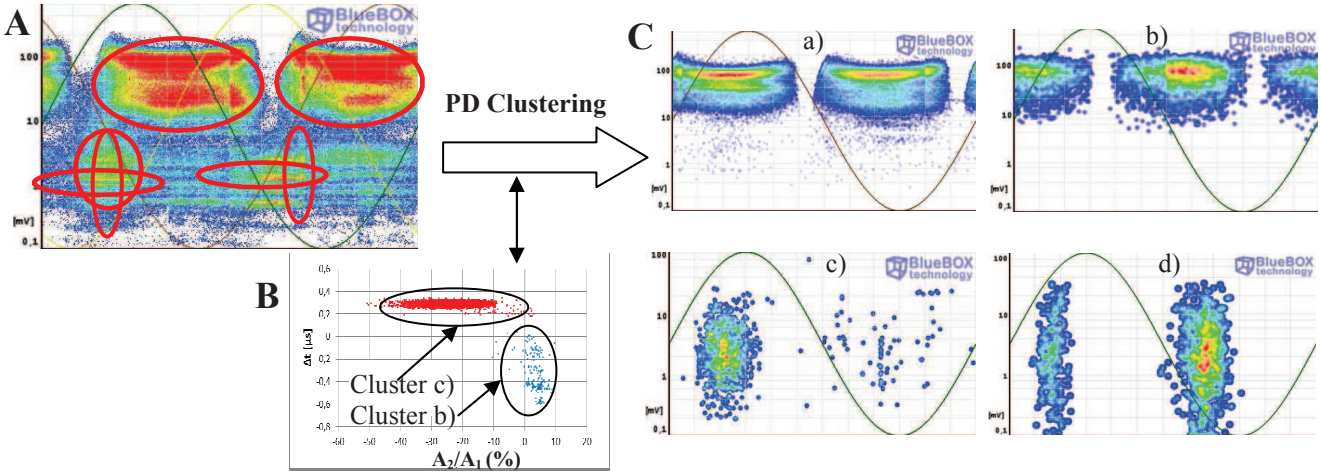


Figure 5: I) PD pulses acquired by a sensor HFCT: II) Clustering: arrival times (Δt) /Amplitude ratio (A_2/A_1) of external PD sources of phase U. III) PRPD patterns: a) Floating potential in phase A, b) External floating potential in phase V, c) External surface PD in phase V, d) Internal surface PD phase V.

The PD patterns shown in Fig. 5.C correspond to four different PD sources: three of them are external PD sources: a) external floating potential in phase U, b) external floating potential in phase V and external surface PD in phase V, because the PD pulses detected by the HFCT of the earth connection of tank had negative polarity. However, an internal PD was detected in the phase V (pattern d) Fig. 5.C), that was associated to an internal surface PD. After a opening an internal defect was found in the 230 kV bushing.

The recognition of PRDP patterns of each PD source and its evolution versus climatic conditions and electrical stress (current and voltage) is also used for final diagnosis [7] and [8]. The temporal evolution of PD activity along the 24 h of the day is an useful information to evaluate if the PD source is critical for the transformer integrity.

ISBN 978-84-617–9183–5

V. CONCLUSIONS

Unconventional PD measurements are required for on-line PD testing of power transformers. Invasive UHF antenna sensors are not always permitted. The new approach for PD monitoring introduced in this paper works in the HF range with non-invasive HFCT sensors. The background noise is removed by means of a filtering tool developed on the basis of wavelet transform that preserves the original PD pulse waveform. The pulse polarity of the PD signals acquired through the earth connection of the transformer tank allows determining whether the emplacement of the PD source is inside or outside of the transformer. A PD clustering performed on the basis of arrival times and amplitude ratios of acquired pulses allows discriminates the different PD sources and using the PRPD pattern of each PD cluster an efficient insulation diagnosis about PD can be performed.

REFERENCES

[1] IEC 60076-3 Power transformers - Part 3: Insulation levels, dielectric tests and external clearances in air.

[2] IEC 60270 High-voltage test techniques – Partial discharge measurements.

[3] IEC 62478TS "High Voltage Test Techniques. Measurements of Partial Discharges by Electromagnetic and Acoustic Methods"

[4] Guidelines for Partial Discharge Detection using conventional (IEC 60270) and unconventional methods WG D1.37 CIGRE Brouchure-2016

[5] S. Okabe, G. Ueta and H. Wada, "Partial discharge signal propagation characteristics inside the winding of gas-filled power transformer - study using the equivalent circuit of the winding model," IEEE Transactions on Dielectrics and Electrical Insulation, pp. 1668-1677, 2011

[6] A. Pfeffer; S. Tenbohlen; S. Kornhuber, "Influence of PD Location and Frequency Ranges on measured Apparent Charges," International Symposium on High Voltage Engineering (ISH), Hannover, Germany, 2011.

[7] F. Garnacho *et al*. "PD Monitoring System for HV substations", CIGRE Session, Paris, France 2014, paper B3-210.

[8] F. Garnacho, *et al.* "On line Partial Discharge Measurements by means of Signal Processing Tools Integrated in Micro-Procressing Hardware" 19th International Symposium on High Voltage Engineering – ISH 2015 Pilsen, Czech Republic. 2015.

ISBN 978-84-617–9183–5

Network Modelling on Dry-Type Transformer Cooling Systems

Andrea CREMASCO[1], Wei WU[2], Andreas BLASZCZYK[3], Bogdan CRANGANU-CRETU[4]

[1]ABB-Trasfor Development Center, Lugano, Switzerland, e-mail: andrea.cremasco@ch.abb.com
[2]ABB Inc., Raleigh, NC, USA, e-mail: wei.wu@us.abb.com
[3]ABB Corporate Research Center, Baden, Switzerland, e-mail: andreas.blaszczyk@ch.abb.com
[4]ABB Transformers, Zürich, Switzerland, e-mail: bogdan.cranganu-cretu@ch.abb.com

Abstract — **The application of dry-type transformers is growing in the market because the technology is non-flammable, safer and environmentally friendly. However, the unit dimensions are normally larger and material costs become higher since no oil is present for dielectric insulation or cooling; therefore, one of the primary tasks of a transformer manufacturer concerns how to design a dry-type transformer with good balance between dimension and cost, dielectric, mechanical and thermal performances. At designing stage, a transformer thermal model used for predicting temperature rise is fundamental and the modelling of cooling systems is particularly important. Dry-type transformer cooling systems include several categories of fans, enclosures, heat exchangers and their combinations. The present paper introduces a fast-calculating thermal network model for modelling the cooling systems; by a preliminary verification from analytical methods and advanced CFD simulations, the model shows acceptable accuracy, confirmed by final validation with experimental results.**

Keywords — **Dry-type transformer, temperature rise, network model, cooling system**

I. INTRODUCTION

Dry-type transformers avoid using oil for dielectric insulation or cooling and thereby are non-flammable, safer and environmentally friendly in comparison with their liquid-filled alternatives. These advantages make dry-type transformers' market share gradually increasing especially in applications that request high standards of safety and reliability, for instance urban areas, buildings, marine ships, offshore platforms, etc. Compared to liquid-filled transformer, one of the disadvantages of dry-type is that, since oil is absent for insulation or cooling, they require larger dimensions to have sufficient cooling. In this context, one of the primary tasks of a dry-type transformer manufacturer is to optimize the cooling design and predict temperature rises more accurately in order to reduce material usage and transformer cost.

The growing computational resource offered by computer technology allows to predict temperature rise by numerical models with increasing complexity, from those based on equivalent thermal networks [1]-[3] to Computational Fluid Dynamics (CFD) analysis [4]-[5]. The higher level of discretization used in CFD makes possible to study more in depth the thermo-fluid dynamic phenomena occurring in the transformer, but the high computational cost prevents it from being used systematically as a design tool. Compared to CFD, thermal network models employ a lumped parameter approach based on the analogy to electric circuits. The network model abstracts fluid dynamics and heat transfer phenomena into a group of interconnected lumped elements whose formulation is based on physics principles. The reasonably low computational cost required by network models justifies their widespread usage for transformer design.

In this paper, we focus on the network model of the cooling system. Comparing with [3] the model includes new elements like core cooling duct, roof and floor ventilation openings, horizontal barrier limiting the bypass flow outside of the coils and the heat exchanger unit. The calculated temperatures, heat and mass flows have been verified based on a simple CFD model as well as heat-run tests. For selected examples we have shown that the network model performs with accuracy that is acceptable in transformer design.

II. BASIC CONCEPT

The network model of a transformer can be divided in two major components: active parts and cooling system, see Figure 1. The active parts include coils, core, leads and bus-bars representing the heat sources whereas the cooling system consists of all other parts supporting or preventing the heat dissipation. An interface between both enables to separate model creation and reusing all created components in arbitrary configurations. This

ISBN 978-84-617–9183–5

interface ensures that the mass flows in pressure network (PN) branches and the heat flows in the thermal network (TN) branches are properly interconnected. The basics of both pressure and thermal networks are

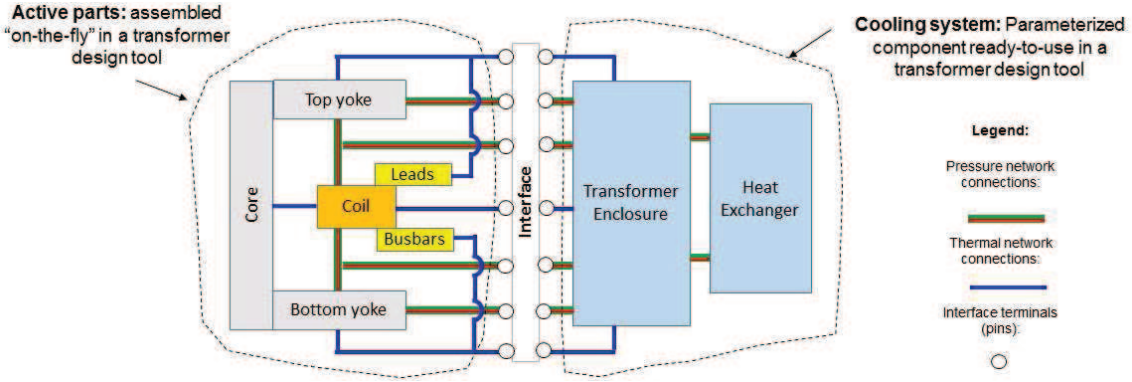


Figure 1. Thermal model concept: active parts and cooling system components.

presented in [1].

The sub-components of the cooling system can be combined according to the cooling concept. The most important cooling configurations related to ventilated enclosure and the heat exchanger have been presented in the following two sections. For configurations without heat exchanger, the ventilation openings are either open by connecting them to ambient pressure/temperature or closed by imposing zero mass flow. For sealed enclosures, all openings are closed. The heat exchanger is always connected to side inlet/outlet openings whereas the roof inlet/outlet are closed. The extremal case of a transformer without enclosure follows the same interface to the active parts, but internally all terminals are connected to ambient pressure and temperature.

The active parts model represents typically one coil of the transformer. Therefore, in the model of enclosure the surface areas for convection/radiation as well as flow cross section areas (like for ventilation openings) are divided by the number of coils. For the heat exchanger model instead of adjusting its geometrical parameters, we multiply/divide the mass rates coming from/to transformer by the number of coils (it is convenient since the heat exchanger is connected with enclosure only by the pressure network interface as shown in Figure 1).

An important advantage of a well-defined interface between the active part and the cooling system model is the ability to create them separately. The active parts are typically created "on-the-fly" in a transformer design tool based on a transformer specification, whereas the cooling system can be created by thermodynamic experts as a "ready-to-use" parametrized sub-circuit to be integrated into the full network of the transformer.

III. ENCLOSURE WITH VENTILATION OPENINGS

Dry-transformers commonly operate inside a ventilated enclosure, which is installed to provide protection against external objects. Cold air enters from inlet vents and flows through cooling ducts in the coil and in the core. For natural cooling (AN) the fluid is driven by buoyancy only, while for air forced cooling (AF) its major part is blown by fans installed directly below the coils or in correspondence to the enclosure vents. In both AN and AF cases, air circulates from the bottom to the top of the coils and then leaves the enclosure through the outlet vents taking the heat away. For the configurations with fan installed at the ventilation openings, a horizontal barrier is installed outside the coils to avoid bypass flows and to direct the airflow inside cooling ducts.

These air and heat flows have been preliminarily examined by CFD analysis of simplified 2D-axisymmetric models by ANSYS Fluent, in order to identify the main physical phenomena to be reproduced in the network model. An example of such analysis is shown in Figure 2-left in form of the temperature and velocity field plots with arrows indicating the direction of the air streams denoted by S1, …, S13. The CFD analysis provides reference results for the accuracy verification of the developed network models. It is important to mention that even if the CFD analysis is performed on a simplified model, the corresponding network model is designed with the same assumptions and therefore the comparison is consistent.

ISBN 978-84-617–9183–5

The topology of the enclosure PN, shown in Figure 2-right, follows the air streams identified in the CFD velocity plot. The cold air enters the enclosure at inlets (S1) and is directed into the core and coil ducts with (AF) or without (AN) the support of the fans. Both heated streams (S9) and (S10) merge together at the top and leave the enclosure through the outlets (S12) and (S13). The flow rates in PN are strongly influenced by the flow resistance of the ventilation grids, which can be calculated from the pressure loss formula equation (1). The friction coefficient ξ can be obtained for different ventilation grids from literature [6] or derived from dedicated experiments. The experimental estimation is required if the grids include louvers and/or filters.

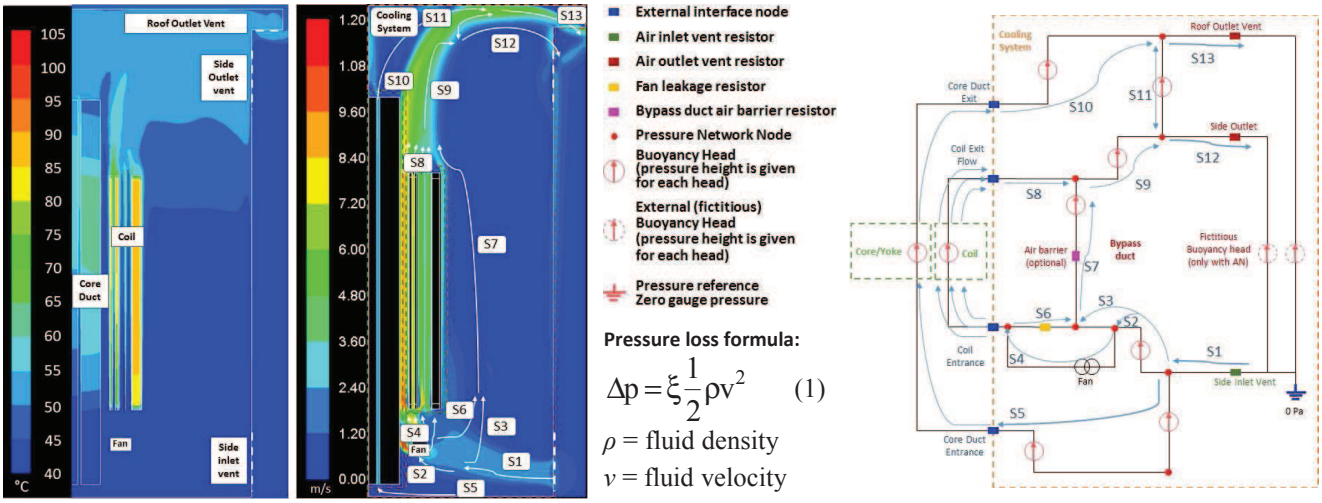
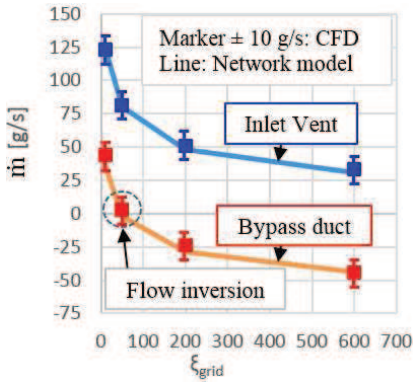


Figure 2. Left - thermal and fluid flow distributions for AF cooling. The transformer includes a core duct and cooling system with side and roof vents. Right - corresponding PN model following the path flow observed by CFD: the fan is part of a loop to reproduce the bypass flow around it. Friction resistors are included to introduce the concentrated pressure loss due to ventilation grids and air barriers. The cooling system is connected to the interface pins of the active part section.

Based on a properly defined PN it is possible to reproduce flow inversion outside the coil for enclosure with increasing grid friction factors (thanks to the bi-directionality of the PN [1]), as shown in Figure 3-left. The deviation between the CFD and the equivalent network model is reasonable for design purpose, as shown in Figure 3-right.



Temperatures [°C]			
ξ_{grid} = 100	CFD	Network model	Diff.
Secondary Winding (LV)	85.9	89.6	3.7
Primary Winding (HV)	90.2	91.8	1.6
Iron Core	58.4	58.5	0.1
Enclosure Sidewall	48.0	47.8	-0.2
Fluid outlet	57.1	56.4	-0.7

Figure 3. CFD vs Network model result comparison for AF ventilation with side and roof vents. Left - mass flow rate at enclosure inlet and bypass duct. Negative mass flow rate in the bypass duct represents a flow inversion from the top to the bottom due to very dense grid. Right - result comparison for the case presented in Figure 1.

The network of the cooling system includes the wide region separating the enclosure wall to the coil, called here “bypass duct”. In case of AN ventilation, this region is characterized by buoyant flow for which it is difficult to estimate its equivalent airflow resistance since the stream velocity is not uniform across the bypass duct. In order to prevent excessive flow due to very low resistance in this part of the equivalent network, we placed fictitious buoyancy head outside the enclosure model (dashed line) to counteract buoyant flows in the bypass duct, as shown in Figure 2-right. The formulation of these buoyancy sources is based on the enclosure design parameters and has been interpolated according to CFD results. These fictitious elements are used only for AN cooling and are disabled for AF.

ISBN 978-84-617–9183–5

In case of fans placed at the side openings the enclosure includes horizontal barrier with a narrow gap around the coil circumference to direct the airflow into the coil cooling ducts. This gap is represented in the PN by a non-linear flow resistor that can be computed according to Eq. (1), with $\xi = 1.7$ [6], where the velocity is computed from the volume flow in the bypass duct divided by the cross section area of the gap. A significant leakage of the barrier may increase the cross section area and reduce the efficiency of the cooling.

IV. HEAT EXCHANGER

Heat exchanger units are commonly used for applications requiring strong cooling or when the heat dissipation to ambient needs to be limited. For dry-type transformers, the heat exchanger system generally consists of two separated fluid circuits, one with air, the other with a coolant, such as water. Hot air is forced through the heat exchanger matrix, consisting of a metallic structure with baffles and fins providing direct contact to the coolant circuit, which takes heat losses away. The heat exchanger unit is delivered together with the fans mounted at the enclosure openings, as shown in Figure 4.

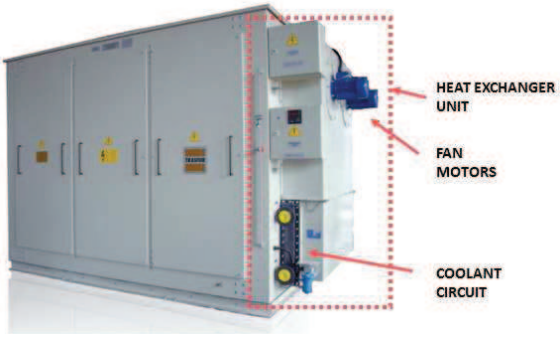
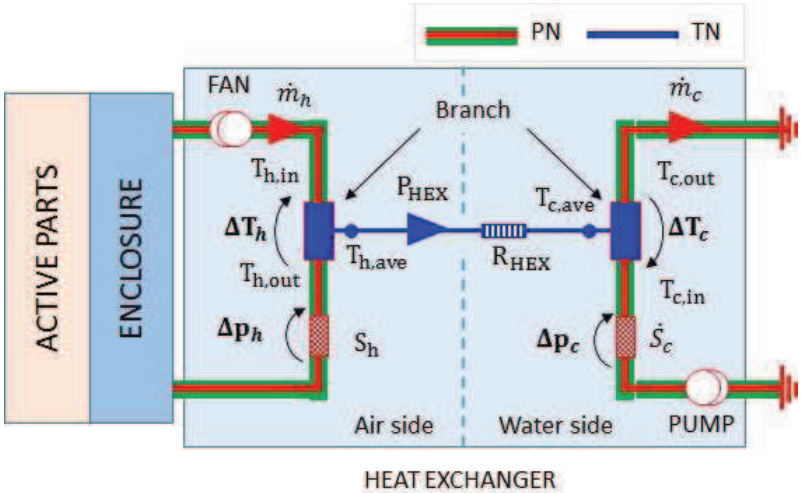


Figure 4. 3000 kVA transformer with water heat exchanger. The unit is installed at the transformer enclosure side and includes two fans in parallel. The coolant circuit openings are visible whereas air circuit openings, not visible, are in correspondence to the transformer enclosure vents.

The network model of the heat exchanger represents both the air and the coolant circuits, in order to predict not only the cooled air temperature $T_{h,out}$ re-entering the transformer enclosure, but also water temperature rise ΔT_c, which can be a subject of operational restrictions. The pressure networks of air and coolant are connected by a thermal network that enables to transfer heat between both fluids, as shown in Figure 5.



$$\Delta T_x = T_{x,out} - T_{x,in} \quad (2)$$

$$T_{x,ave} = \frac{T_{x,in} + T_{x,out}}{2} \quad (3)$$

$$P_{HEX} = \frac{T_{h,ave} - T_{c,ave}}{R_{HEX}} \quad (4)$$

$$T_{x,out} = T_{x,in} + \frac{P_{HEX}}{\dot{m}_x c_{xp}} \quad (5)$$

$$S_x = \frac{\Delta p_x^*}{\dot{m}_x^*} \quad (6)$$

c_p = fluid specific heat capacity

Figure 5. Network topology of the heat exchanger model. Index *x* represents the hot air "*h*" or the coolant "*c*".

Each PN includes a "current source" in form of a fan or a pump as well as flow resistors representing the internal pressure drop calculated according to formula (6). The resistor S_h is essential for the selection of the fan parameters. Together with the pressure drop across the transformer, it allows to obtain the total operating pressure and the corresponding volume flow rate of the fan.

ISBN 978-84-617–9183–5

The connecting TN includes so-called "Branch" elements [1], that put in relationship the transferred power P_{HEX} with the outlet temperature of both air $T_{h,out}$ and the coolant $T_{c,out}$ as well as the corresponding inlet temperatures $T_{h,in}$ and $T_{c,in}$, and the mass flow rates $\dot{m}_h$ and $\dot{m}_c$, according to the first law of thermodynamics.

The TN-pins of the two "Branch" elements expose the average temperatures $T_{h,ave}$ and $T_{c,ave}$ between the inlet and outlet of the air and the coolant circuit respectively. The main element of the model is the equivalent thermal resistor R_{HEX} representing the heat transfer effectiveness of the heat exchanger; this resistor is connected between the two aforementioned pins and is defined according to the heat exchanger rated parameters , identified in Eq. (7) by a star:

$$R_{HEX} = \frac{1}{P^*_{HEX}} \cdot \frac{\left(T^*_{h,in} + T^*_{h,out}\right) - \left(T^*_{c,in} + T^*_{c,out}\right)}{2} = \frac{T^*_{h,ave} + T^*_{c,ave}}{P^*_{HEX}} \quad (7)$$

This definition ensures that for rated mass flow rates and rated inlet temperatures of both fluids the power transferred through R_{HEX} is equal to the rated cooling capacity P_{HEX}^* of the heat exchanger.

The operating conditions of the heat exchanger are not always the rated ones; for instance when the unit is installed on a transformer whose losses are lower than the cooling capacity of the heat exchanger. In order to verify the reliability and the accuracy of our formulation, we identified a 30 kW shell and tube heat exchanger as reference. Next, we compared results coming from our equivalent model with those obtained by the effectiveness-Number of Transfer Units (ε-NTU) method [7], applied to the reference heat exchanger, for different operating conditions. Results are shown in Figure 6.

$T_{c,in}$	30.0	°C
Q_h	2.1	m^3/s
m_c	1.4	kg/s

$T_{h,in}$	60.0	°C
Q_h	2.1	m^3/s
m_c	1.4	kg/s

$T_{h,out}$	40.0	°C
$T_{c,in}$	30.0	°C
m_c	1.4	kg/s

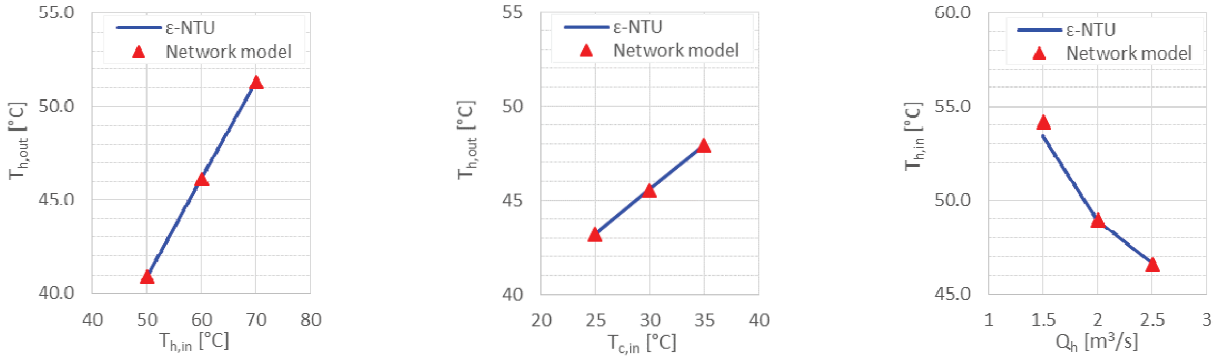


Figure 6. Result comparison between network model formulation and ε-NTU method, at different operating conditions.

These results confirm reasonable accuracy of our heat exchanger model formulation in our range of application, compared to results obtained by the ε-NTU method.

V. EXAMPLES

The presented network method was applied to real transformer units with different cooling system components; Table 1 summarizes four example units.

Table 1 Temperature Rise (K) Comparison Between Heat-Run Test Measurements and Equivalent Network Model.

	Secondary winding (LV)			Primary winding (HV)		
	Meas.	Calc.	Diff.	Meas.	Calc.	Diff.
Enclosure with light grid ventilation (NEMA1) – AN	58.0	57.0	-1.0	70.9	70.2	-0.7
Enclosure with outdoor grid ventilation (NEMA3R) – AN	44.4	50.0	5.6	64.1	65.7	1.6
Enclosure with fans inside underneath the coils – AF	87.2	83.3	-3.9	95.8	93.5	-2.3
Enclosure with an external water based heat exchanger	43.3	37.9	-5.4	73.3	69.0	-4.3

ISBN 978-84-617–9183–5

The pressure loss factors of different types of ventilation grids were measured in our laboratories. For the first three examples the deviation between the measurement and the modelling results can be caused by uncertainties in the bypass duct model. The fourth example has more uncertainties related to heat exchanger description, because manufacturers usually consider safety margins and the cooling capacity derived from its inlet, outlet temperatures and flow rates will differ from the rated cooling power in the specification. In addition, the tested transformer may have been affected by leakage air paths in the outer air barrier due to manufacturing tolerances, not included in our model yet. These factors may be the reason why the predicted temperatures are lower than the tested values. On the other hand, the real characteristics of the heat exchanger fans are not presented in the specification either; thereby it should be concerned in the next step how to obtain as accurate as possible heat exchanger data for the network modelling.

VI. CONCLUSIONS

The network approach presented in this paper provides an efficient numerical method to model the cooling system of dry-type transformers. In comparison with CFD simulation approaches the network model runs much faster and the accuracies still fall in acceptable range; therefore one is able to utilize this method in optimization procedures included in transformer design systems. The accuracy of network modelling of the cooling systems relies on the accuracies of the enclosure ventilation description, the fan characteristics and the heat exchanger specifications, etc. Therefore it is significant to obtain these data more accurately.

REFERENCES

[1] A. Blaszczyk, R. Flückiger, T. Müller, C. O. Olsson: *Convergence behavior of coupled pressure and thermal networks*. Compel journal, Vol. 33, No. 4, p.1233-1250, 2014.

[2] E. Morelli, P. Di Barba, B. Cranganu-Cretu, A. Blaszczyk: *Network based cooling models for dry transformers*, ARWtr Conference, Baiona, Spain, 2013.

[3] A. Cremasco, P. Di Barba, B. Cranganu-Cretu, W. Wu, A. Blaszczyk: *Thermal Simulations for Optimization of Dry Transformers Cooling System*, Scientific Computing in Electrical Engineering: SCEE 2014, Wuppertal, Germany. Springer International Publishing, Vol. 23, p.103-113, 2016.

[4] A. Skillen, A. Revell, H. Iacovides, W. Wu: *Numerical prediction of local hot-spot phenomena in transformer windings*, Applied Thermal Engineering, Vol. 36, pp. 96-105, 2012.

[5] W. Wu, A. Nogues, J. Kern: *OpenFOAM CFD modelling on forced air cooling dry-type transformers*, OpenFOAM User Conference 2015, Stuttgart, Germany, 2015.

[6] I. E. Idel'chik: *Handbook of Hydraulic Resistance*, 3d ed., CRC Press, Boca Raton, FL, 1994.

[7] R. K. Shah and A. C. *Mueller, Heat Exchanger Basic Thermal Design Methods, in Handbook of Heat Transfer Applications*, 2d ed., W. M. Rohsenow, J. E Hartnett, and E. N. Gani~ (eds.), Chapter 4, Part 1, pp. 1-77, 1985.

ISBN 978-84-617–9183–5

The Development of 400kV Transformers with Ester-based Dielectric Liquids

Mark LASHBROOK, Attila GYORE, Manjunath RAMAKRISHNA, Russell MARTIN

M&I Materials Ltd
Hibernia Way, Trafford Park, Manchester, M32 0ZD, UK
Phone: (+44) 161 864 5429, fax: (+44) 161 864 5444, e-mail: MarkLashbrook@mimaterials.com

Abstract — **Ester-based fluids offer the potential for safer and more environmentally friendly power transformers. This can save considerable civil costs in installations, but in order to use these fluids in 400kV transformers their dielectric and thermal behaviour must be understood. Over ten years of laboratory research and full scale testing have been carried out to evaluate the dielectric performance of ester-based fluids. This has included studies of fundamental behaviour as well as a wide range of dielectric testing of realistic insulation structures. Work has been carried out by both academic institutions and equipment manufacturers, which has led to a better understanding of the design implications of using these fluids. The large body of research conducted on the electrical behaviour of ester-based fluids has come to the conclusion that design changes are necessary for higher voltage transformers and this leads to a higher price for an ester transformer. Despite this the overall project cost can be reduced by full utilisation of the benefits of fire safe ester fluids and a number of recent projects are using this in practice.**

Keywords — **ester, 400kV, impulse**

I. INTRODUCTION

Mineral oil has been used in transformers to provide electrical insulation and cooling since the early days of electrical networks. While mineral oil is an effective coolant and dielectric medium, it is, however, inherently flammable and environmentally damaging if leaked or spilled. There have been numerous instances of large mineral oil transformer fires and in each case substantial damage has been caused, along with costly clean-up of the surrounding area if the tank has ruptured in a catastrophic manner. The answer to these problems lies in the use of alternative, far less flammable fluids for power transformers (and in the case of ester fluids, much more environmentally friendly).

The behaviour of mineral oil in higher voltage transformers is generally understood and designers have established rules for the construction of transformers through research, as well as trial and error, over many years. In modern times the design of power transformers has become more and more sophisticated, with magnetic, electrical and thermal computer modelling now widely used. This allows designers to push the designs to their limits, whilst being relatively confident that the transformer will pass final test if the manufacturing process is without fault.

At higher voltages, the use of esters insulating liquids in transformers has developed greatly over the thirty five years since their introduction. It is now the case that large power transformers used for transmission projects can and are being successfully designed and built with esters. This paper outlines the development history of ester-based transformers and discusses the latest projects that will see synthetic ester utilised for a number of 400kV transformers.

II. APPLICATION HISTORY OF ESTERS

A. Synthetic Esters

Synthetic ester dielectric fluids were developed to answer a difficult problem in the electrical industry, when PCB based fluids were effectively banned in the late 1970s. In the early days synthetic esters were used for retrofilling PCB units and to produce replacement transformers for locations of high fire risk. An early adopter of synthetic ester in the UK was British Steel, who installed a number of ester filled furnace transformers back in 1979. This was followed soon after by the Royal Mint who again had a need for fire safe transformers for

ISBN 978-84-617–9183–5

their furnaces. Many UK and European projects then followed in hospitals, airports, public buildings and offshore oil and gas platforms, where transformers with high levels of fire safety were vital.

Another early adopter of synthetic ester transformers was the railway industry, starting with the retrofilling of PCB transformers on Amtrak rolling stock in the USA during the 1980s. The use of synthetic ester in rolling stock has continued over the last 30 years in a wide range of locomotive and electric multiple unit (EMU) transformers, including freight and high speed train sets. Standards in Europe now require the use of high fire point fluids, such as esters, in trains and recent developments in China will see ester fluids in transformers for 500km/h trains, working at the cutting edge of railway development (Fig. 1).



Figure 1. CRH-5 High Speed Train with Synthetic Ester Transformers.

B. Natural Esters

Another development in the late 1990s was the introduction of natural esters to the transformer market. These fluids, based on renewable seed oils, aimed to provide the ultimate in environmentally friendly transformer oil. Natural esters gained users in distribution transformers, predominantly in the USA and South America. There then followed development of power transformer applications with natural esters, including a number of retrofills where mineral oil was directly replaced with the alternative fluid. Since this time the use of natural esters has increased, with several utilities taking the step to change over from mineral oil to natural ester across their distribution fleet.

Laboratory studies have also shown that ester-based fluids have the potential to significantly increase the lifetime of insulating paper. This has been utilized by some manufacturers to produce more compact distribution transformers, which provide a higher kVA output from a reduced footprint.

C. Ester Differences

It is worth noting that despite both these fluids being named ester there are fundamental differences between synthetic and natural types. The key difference between the two is that natural esters can only be used in sealed transformers, while synthetic esters are suitable for either sealed or breathing configurations.

III. ESTER FILLED POWER TRANSFORMERS

The development of synthetic ester and natural ester power transformers has been conducted almost in parallel, with the majority of the natural ester projects being carried out in the USA and Brazil, while the synthetic ester transformers are mainly installed in Europe. With synthetic ester the approach taken has been to design and install new transformers, rather than retrofilling older units. Table I shows a short selection of the power transformer references for both synthetic and natural ester over the last 25 years. [1]

ISBN 978-84-617–9183–5

Table I. Ester Power Transformer References

SYNTHETIC ESTER			NATURAL ESTER		
High Voltage	**Rating**	**Year**	**High Voltage**	**Rating**	**Year**
110kV	25MVA	1999	115kV	15MVA	2004
151kV	110MVA	2002	161kV	200MVA	2004 (retrofill)
238kV	135MVA	2004	230kV	8MVA	2005 (retrofill)
220kV	100MVA	2010	161kV	25MVA	2006
154kV	200MVA	2011	110kV	40MVA	2008
400kV	240MVA	2016	138kV	40MVA	2009
433kV	120MVA	2016	420kV	300MVA	2014

IV. COST BENEFIT OF ESTER FILLED TRANSFORMERS

One barrier in the past to the more widespread adoption of ester fluids has been their price, which is higher than mineral oil. However in more recent times users are realising that there are significant savings to be made in overall installation costs if ester-based fluids are used in place of mineral oil. The fire safety benefits alone mean that fire barriers can be removed and active fire suppression systems are no longer required, since the safety is effectively built into the transformer. Factoring in the reduction in civil engineering costs and the potential longer life of ester transformers this solution starts to look very attractive.

KWO in Switzerland realised the considerable savings to be made and after an intensive risk assessment by the safety institute SWISSI they installed four synthetic ester filled converter transformers, without fire suppression systems, as shown in (Fig. 2). This saved them money not only in civil engineering, but also more importantly removed the need for large amounts of invasive maintenance on the firefighting systems, which will save a substantial amount of expenditure and downtime over the full life of the installation.

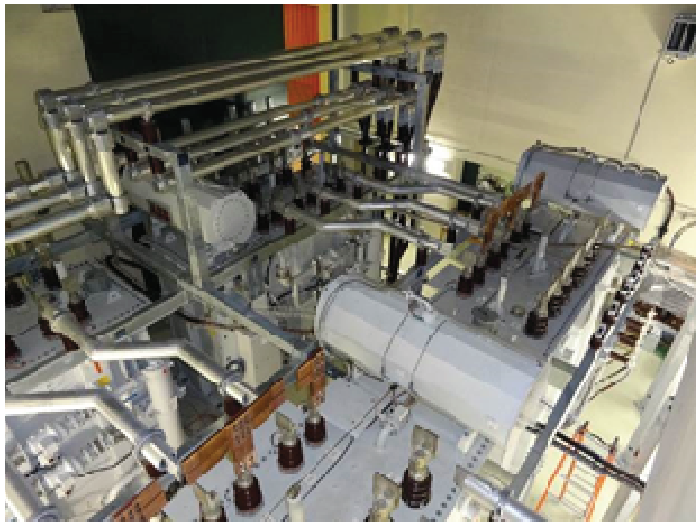


Figure 2. KWO Synthetic Ester Transformer Installation.

Another key area where ester-based fluids can have a positive impact is in environmental protection. Ester fluids are classed as readily biodegradable, meaning that if they are spilled into the environment they are expected to quickly degrade to water and carbon dioxide through the action of micro-organisms found in nature. In contrast mineral oil is poorly biodegradable and likely to persist for far longer. This environmental benefit can be utilised in some cases to reduce the complexity and volume of containment required. Considering an installation with multiple mineral oil transformers, separate containment would be needed for each unit, along with oil separators for each. With ester-based fluid one combined containment system could be used, significantly cutting down civil engineering costs.

ISBN 978-84-617–9183–5

V. LABORATORY RESEARCH FOR 400KV AND ABOVE

Such is the demand for ester transformers at higher voltages that university research into alternative fluids has been conducted in many different research centres around the world. One example of a large scale collaborative project was the 8 year joint research project between National Grid, Alstom Grid, M&I Materials and a number of UK utilities which studied the fundamental behaviour of ester fluids in comparison to mineral oil. The aim of this project was to define what was necessary to use esters at 400kV. This research project incorporated five PhD theses on the subject of ester behaviour under electrical conditions and included both synthetic and natural esters. The outcome of this project was a vast amount of information on the electrical, thermal and ageing behaviour of esters.

Various other institutions have published work on ester fluids, in Europe the other notable independent researchers are Stuttgart University and the Schering Institute at Hannover University. Much of their work mirrored that carried out at the University of Manchester and discovered very similar results. Various other large transformer manufacturers have also carried out their own extensive research work into the use of esters, including Siemens and ABB.

In order to effectively use esters in large power transformers designers first needed to understand their fundamental behaviour, in comparison to the better understood characteristics of mineral oil.

The first factor which affects the design of ester transformers is the difference in permittivity between esters and mineral oil. This brings advantages within winding structures as the permittivity of ester is closer to that of paper, giving a more homogeneous electrical field distribution. Stress in the fluid is also lower with esters, for a given structure, with higher stress in the solid insulation. Since the impregnated solid is a stronger dielectric than the fluid alone this is also beneficial. On the other hand the difference in permittivity also means that peak stress in certain structures can be higher with esters, so small adjustments may be needed to reduce this stress to acceptable levels.

One of the key differences coming out the laboratory research is the behaviour of ester fluids under impulse conditions, where a somewhat lower dielectric strength than mineral oil has been observed. An example of this comes from testing carried out by the University of Manchester using the 1-shot per step (IEC method) and 3-shot per step (ASTM method), with the results shown in Fig. 3 [2].

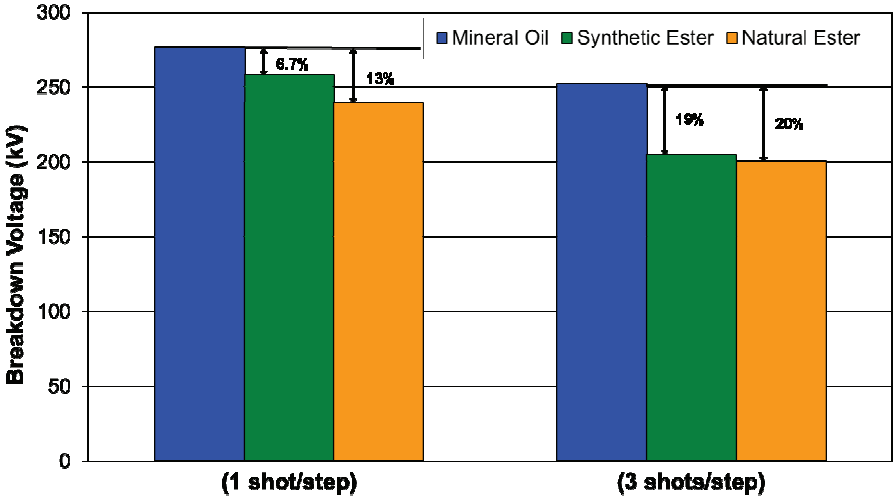


Figure 3. Impulse Breakdown Results.

The larger difference in the ASTM method is most likely due to a higher chance of breakdown, caused by more impulse shots at each level. In simple terms these results indicate that design changes might be needed to make sure a power transformer with ester passes impulse test.

ISBN 978-84-617–9183–5

Larger differences were found in experiments using very divergent fields, with electrode setups such as needle to plane and needle to sphere. These were designed to produce focussed electrical fields, in order to exaggerate the effects and observe fundamental behaviours. In these experiments ester fluids were shown to have similar discharge inception voltages to mineral oil, meaning insulation structures would be similar, but propagation of streamers appears to happen more readily in esters. For design this indicated that adjustments needed to be made with long oil gaps and divergent fields in esters.

Observations such as faster discharge propagation in divergent fields give a clue to how esters will behave in real transformers, but does not give the full picture. In addition to the fundamental research a large amount of testing has been conducted on more realistic insulation structures, to feed into design calculations. This testing and experience gained by transformer OEMs with ester suggest that the differences between mineral oil and ester can be accommodated with some adjustments in design. These changes do add some cost to the transformers, when compared to standard mineral oil units, but this is still far outweighed by the potential cost saving benefits.

In terms of thermal behaviour the higher viscosity of ester fluids mean that cooling channels may need to be widened, in order to maintain the same operating temperature rises. This in turn impacts electrical design to a degree. Although esters will give a higher temperature rise than mineral oil for a particular design a large amount of laboratory work has also shown that insulating paper ages more slowly in esters than it does in mineral oil. Since the lifetime of the insulating paper is often the life limiting factor for a transformer this is critical. In designing transformers well established temperature limits are applied for mineral oil and cellulose combinations. The evidence published in IEC 60076-14 [3] and IEEE C57.154 [4] over the last two years indicates that higher temperatures can be accepted with esters, without loss of life. This can work to offset the difference and perhaps even allow the design of more compact power transformers if the full benefits of esters indicated in the standards are used.

VI. Case Study 1: National Grid UK

It is clear from the past history and laboratory work that ester fluids behave in a different way to mineral oil at higher voltage levels; however, the challenges are not insurmountable. The benefits that esters can bring in fire protection and increased transformer life can financially outweigh the extra cost of using an ester.

This is illustrated by the fact that there are a number of large transformer projects under development globally, using both synthetic and natural esters. One key project for synthetic ester which directly followed the NIA funded research is being carried out by National Grid in the UK. Following the many years of research and development, as well as the full scale test rig made by Alstom Grid, the decision was made to install three 400kV synthetic ester transformers in a critical substation located in Highbury, in the centre of London. This substation is part of the London Tunnels project which is aiming to provide long term security of electrical supply to the UK capital.

One of the hurdles to conducting any project on this scale in a dense urban area is obtaining planning consent, which requires many adjustments to the design in order to meet the needs of local residents and the immediate community. The plan for the London site in Fig. 4 shows the main transformer and switchgear building, along with a range of residential buildings surrounding the site. [5][6]

VII. Case Study 2: Letsi Hydropower Station Sweden

Swedish power company Vattenfall has used synthetic ester power transformers since 2002, when it installed a unit rated at 151kV and 110MVA. Since then the company has steadily increased its fleet of synthetic ester generator units, moving up to 238kV in 2004. Following the positive experience with these transformers, Vattenfall decided to utilize synthetic ester for a major refit project at the Letsi hydro power station. This hydropower plant has been in operation for over 40 years and the underground mineral oil transformers were ready for replacement.

Due to current safety standards it was deemed unacceptable to have new underground mineral oil transformers, specifically for fire safety reasons. After careful consideration the decision was taken to install synthetic ester

ISBN 978-84-617–9183–5

transformers, in order to significantly increase fire safety. There will be four 433kV 120MVA single phase units installed during 2016 [6]

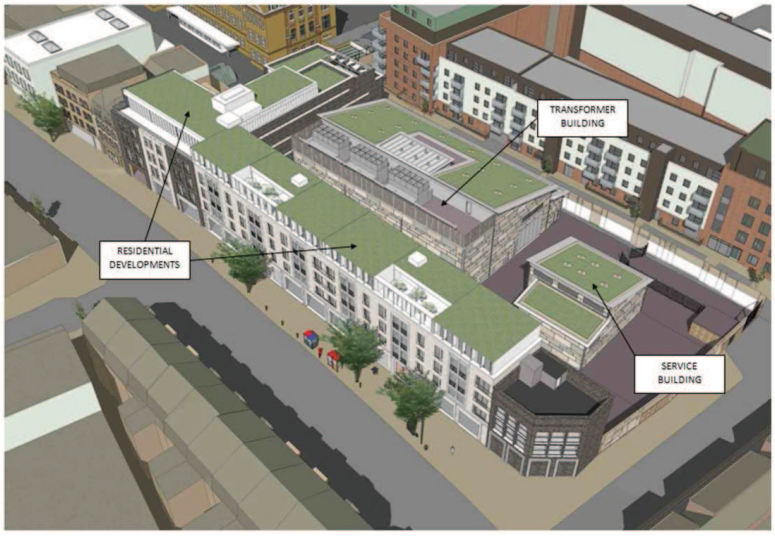


Figure 4. Plans for National Grid Highbury Development.

VIII. CONCLUSIONS

For over thirty five years ester-based transformer fluids have been successfully employed in a wide range of transformer applications. Most of these have been at distribution voltage levels or for specialist applications such as traction and wind turbines. The use of ester fluids in larger power transformers has developed over the last 20 years and for the last 10 years synthetic esters have been used successfully in units at up to 238kV. The large body of research work that has been conducted on esters also gives an excellent background for design adjustments and the understanding of ester behaviour is increasing all the time. All this means that nowadays a range of equipment manufacturers are able to offer ester transformers for transmission projects, moving the use of esters to the 400kV level.

The built in fire safety of ester fluids offers asset managers an excellent solution to reduce overall installation costs, as well as lifetime running costs when factoring in the removal of fire protection systems. The fact that pool fires cannot occur with ester fluid means that the complexity of containment systems can possibly be reduced, for example having single containment pits for multiple transformers. The favourable environmental behaviour of ester fluids may also offer the opportunity to reduce containment systems, further reducing civil engineering costs.

The culmination of this work will see two major projects in 2016 where synthetic ester filled 400kV transformers will be installed. More projects at this voltage level and higher are expected to follow as users recognize the benefit of deploying ester-based fluids.

REFERENCES

[1] Medium and Large Power Transformer Users List Envirotemp FR3 Fluid Retrofill and New Installations, Cooper Power Systems, January 2007.

[2] Q. Liu, Z.D. Wang, F. Perrot, *Impulse breakdown voltages of ester-based transformer oils determined by using different test methods,* IEEE CEIDP 2009

[3] IEC 60076-14 2013, Power Transformers – Part 14: Liquid-immersed power transformers using high temperature insulation materials

[4] C57.154-2012 - IEEE Standard for the Design, Testing, and Application of Liquid-Immersed Distribution, Power, and Regulating Transformers Using High-Temperature Insulation Systems and Operating at Elevated Temperatures

[5] London Power Tunnels, Seven Sisters Road, public information leaflet, 2012

[6] Siemens Transformers Case Study, Alternative insulation for a hydro power plant, Siemens AG 2015

ISBN 978-84-617–9183–5

Two-Dimensional Methodology for the Optimized Design of Power Transformer Insulation System

Hugo RODRIGUEZ-IGNACIO[(1)], Xose M. LOPEZ-FERNANDEZ[(1)(2)] and Casimiro ALVAREZ-MARIÑO[(2)]

(1) Department of Electrical Engineering, University of Vigo
Campus Lagoas-Marcosende, E 36310 Vigo, Spain
Phone: (+34) 813478, fax: (+34) 814014, e-mail: xmlopez@uvigo.es
(2) Spanish Association for Innovation in Transformers

Abstract — **In this paper, a 2-D methodology for automating the optimized design of power transformer insulation system structures based on an analytical optimizer linked with electric finite element method (FEM) is presented. The objective is to offer a practical tool to compute in an automated way the optimal geometry of transformer insulation system structures for the safety margin adopted by the transformer designer. The accuracy of the analytically obtained geometry is validated by means of the electric FEM. An iterative procedure is introduced to asssure the closeness between the numerical safety margin of the optimized geometry and the adopted safety margin.**

Keywords — **Automated Design, Finite Element Method (FEM), Genetic Algorithms, Optimization Algorithm, Power Transformer, 2-D Methodology.**

I. INTRODUCTION

Power transformer is one of most important and expensive electrical apparatus in power system [1]. It plays a vital role for contributing to the reliability of whole power system, which strongly depends on the safe operation of transformer insulation system [2]. The task of transformer insulation designer is to make an optimum design decision between the inter-electrodes minimum distance and an acceptable safety margin (SM) [3]. Such insulation design would cope with the ever demanding task for cost reduction and maintaining the profit margin [4]. Here, a computer-based tool play a key role for assisting to designer in the automated insulation design process addressing crucial issues that networks of the future demand on the design insulation level (DIL) [5]. Such a tool can be properly considered when it is coupled with a numerical dielectric analysis. Commercial finite element method (FEM) software packages are readily available; however, in the case of the optimized design of power transformer insulation system structures, FEM becomes particularly complex to apply. It is because a huge number of calculations are required to compute the electrical stress along all the considered insulation structures in the search space of the optimization problem.

Therefore, in this paper, a computer-based automated methodology linking an analytical optimizer that incorporates the use of Genetic Algorithms (GAs), with the electric FEM to assess electrical stress in insulation system structures is presented. Thus, the problems to compute the electrical stress along the insulation structure for the wide range of unexplored choices are overcome analytically. Meanwhile, the electric FEM easily allows checking the obtained results. An important aspect in the proposed methodology is to guarantee the accuracy of the computed results for any safety margin selected as reference (SM_{Ref}). This is ensured by including an iterative procedure, which identifies the deviation of the computed results and modify the parameters involved in the computation.

II. BACKGROUND

Issues about the research in transformer insulation design procedures have come out since the early 1990s. Tschudi et al. in 1995 review the state of the art of transformer insulation design assessment, highlighting the stages of a design process that iteratively leads to an optimized solution [6]. In 1995, Maleski et al. describe a procedure for calculating the safety margin (SM) in critical parts of the paper-oil insulation system using commercial field calculation programs [7]. Also, Tschudi in 1996 provides an overview on oil-paper insulation design practiced in Weidmann engineering offices [8]. Schultz et al. in 1998 emphasize the still high potential

ISBN 978-84-617–9183–5

of design optimization leading to increase the dielectric strength of oil-barrier systems and discuss the design of high voltage AC insulation systems [9]. Lopez-Fernandez et al. in 2010 propose a practical modeling and design methodology for evaluating the insulation system structures under fast transient voltages [10]. Ziomek et al. in 2011 summarize details of insulation design procedure for its optimization [11]. Portillo, in 2013, gives a practical overview of the complete insulation design process of high voltage core-type power transformers focused in the design procedure [12]. The precedent papers are concerned with optimal design criteria and procedures based on experience of trial-and-error approach.

Nelson, in 1994, illustrates the main principles of automated dielectric design; furthermore, he indicates that there is some rational basis for aiming at computer-based system for automating the dielectric design assessment and optimization [5]. Nelson et al., in 1995, describe a computer based automated insulation design tool for evaluate the integrity of insulation system structures [13]. Di Barba et al., in 1998, show how the optimal insulation design of the HV winding can be reached more efficiently in an automated way [14]. Bramanti et al., in 2002, present a case study of optimal design of the end insulation system where an optimization strategy to automate the optimization design was incorporated linked to FEM [15].

In the last decade there is a lack of publications by persuading in the strategy of automated optimal design of power transformers insulation system. Still, recently papers are based on trial-and-error approach conditioned by personal expertise. Therefore, there is a wide range of unexplored possibilities leading to a concealed high potential of design optimization implementing algorithms based on automated computation for selecting optimal design of insulation system structures.

III. PROPOSED 2-D METHODOLOGY

The 2-D methodology proposed in this paper is aimed to obtain the optimized insulation design of transformer insulation system structures for a reference safety margin (SM_{Ref}). Its computational procedure is based on a link between an analytical optimizer with the FEM. In this way, the optimal insulation structure geometry can be readily calculated with the analytical optimizer, and then, the accuracy of the electric field distribution calculation is checked by means of the electric FEM. The flowchart can be followed in Fig. 1. The methodology starts with the analytical model that allows the computation of the optimal insulation structure geometry. After introducing geometric dimensions, materials property data, and the source voltage value, an analytical optimal insulation structure is obtained applying analytical formulation of the electric field. From that analytical solution, the optimized geometry is introduced in the electric FEM model. The numerical solution gives the electric field distribution, which permits the computation of the numerical safety margin (SM_{Num}) linking the two models. The analytical model may not be accurate enough and so the SM_{Num} differs from the SM_{Ref}. Therefore, in the proposed methodology, models are adjusted in an automated way by means of an iterative procedure which identifies the appropriate input data for the analytical optimizer to match the SM_{Ref} with the SM_{Num} obtained in the electric FEM. In the next sections, the physical–mathematical aspects of the proposed methodology are explained in detail.

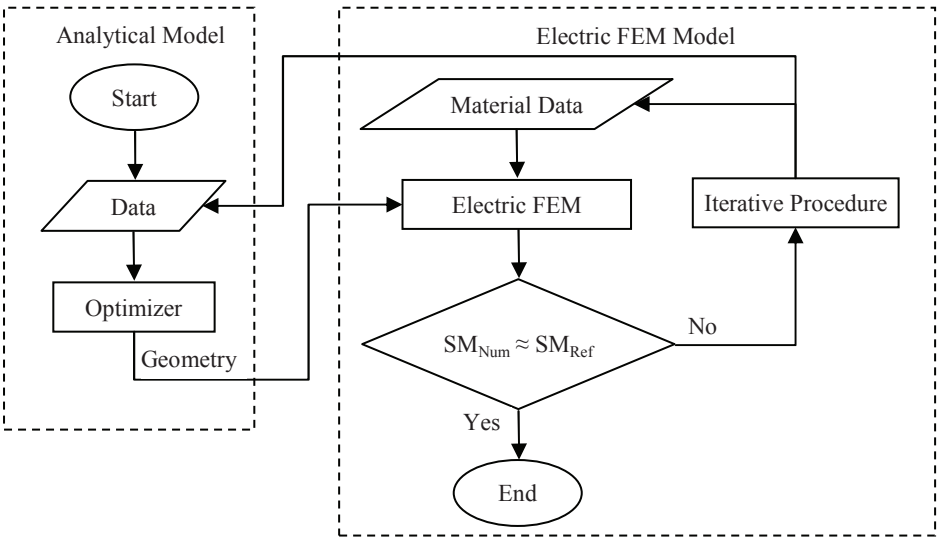


Figure 1. Flowchart corresponding to the 2-D proposed methodology for the analytical and electrical linked models.

ISBN 978-84-617–9183–5

III.1 ANALYTICAL OPTIMIZER

In this sub-section, the proposed optimization method that incorporates GAs to automate the insulation design process is described.

III.1.1 Optimization Algorithm

In this optimizer the well-known GA is implemented as search & optimization method based on the Darwin's principle of Survival of the fittest [16]. It starts with a set of randomly chosen solutions or individuals called population. These solutions are usually coded in binary strings which are known as chromosomes. Each solution is assigned a fitness which is directly related to the objective function of the search and optimization problem. Thereafter, the population is modified to a new one by applying three operators similar to natural genetic operators: reproduction, crossover, and mutation [17]. It works in an iterative manner by successively applying these three operators in each generation until some condition (e.g. number of iterations or improvement of the best solution) is satisfied. A simple working principle of the GA is reflected in the flowchart as shown in Fig. 2.

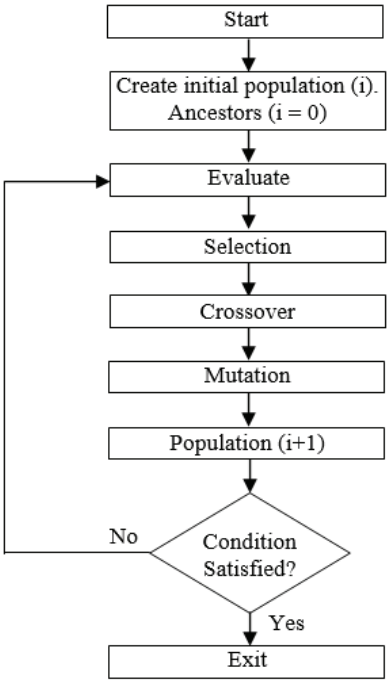


Figure 2. The flowchart of GA.

III.1.2 Optimization Problem Description

The problem of designing an insulation system structure suitable for a prescribed performance can be solved in an automated way by minimizing the objective function subject to geometrical and physical constraints [14]. The objective function proposed in this methodology can be represented by the deviation between actual and reference SM of each element that forms the insulation structure formulated by:

$$F = \sum_{i}^{n} \left(SM_i - SM_{Ref} \right) \tag{1}$$

where n is the number of elements that forms the insulation structure, SM_i the i-element SM and SM_{Ref} the reference SM. Accordingly, SM_i is defined as the quotient of the admissible dielectric strength and the electrical stress in the i-element [18]. The admissible dielectric strength of the insulating material is that established by

ISBN 978-84-617–9183–5

the oil design curves, which express the maximum admissible dielectric strength as a value of low probability of partial discharge (PD) inception [19], whereas the electrical stress is calculated analytically.

Then the problem reads: starting from an initial design x_0, find x such that the objective function F is minimum,

$$\min_{\Omega} (F) \tag{2}$$

subject to constraints; Ω is the controlled sub-region where the optimization process was focused on. For the main insulation structure shown in Fig. 3, oil gap width and pressboard barrier thickness have been selected as design variables (layers). The vector of design variables in this case of main insulation structure where $n = 7$ layers is (d_1, d_2, d_3, d_4, d_5, d_6, d_7).

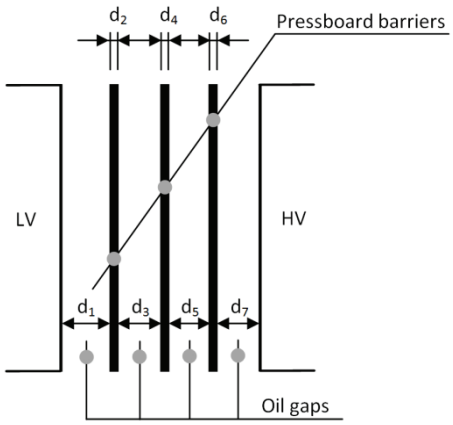


Figure 3. Typical main insulation system structure. Detail of the sub-region, showing the seven design variables with three barriers and four gaps (ducts).

III.2 ELECTRIC FEM

In this sub-section, the numerical model used to validate the previous analytical approaches is described.

III.2.1 Computer Implementation

The numerical model is solved as an electrostatic 2-D plane model applying FEM to solve the electric field for the optimized insulation structure geometry. The governing equation for electrostatic finite element analysis is the Laplace's equation given below:

$$\nabla^2 V = 0 \tag{3}$$

where V is the scalar potential. To simplify the computation of fields the electric FEM employs the electric scalar potential, V, defined by its relation to E as:

$$E = -\nabla V \tag{4}$$

Substituting into Gauss Law and applying the constitutive relation for dielectric materials, yields the second order partial differential equation:

$$-\varepsilon \nabla^2 V = \rho \tag{5}$$

which applies over regions of homogeneous ε. The electric FEM solves (5) for voltage V over a user-defined domain with user-defined sources and boundary conditions.

ISBN 978-84-617–9183–5

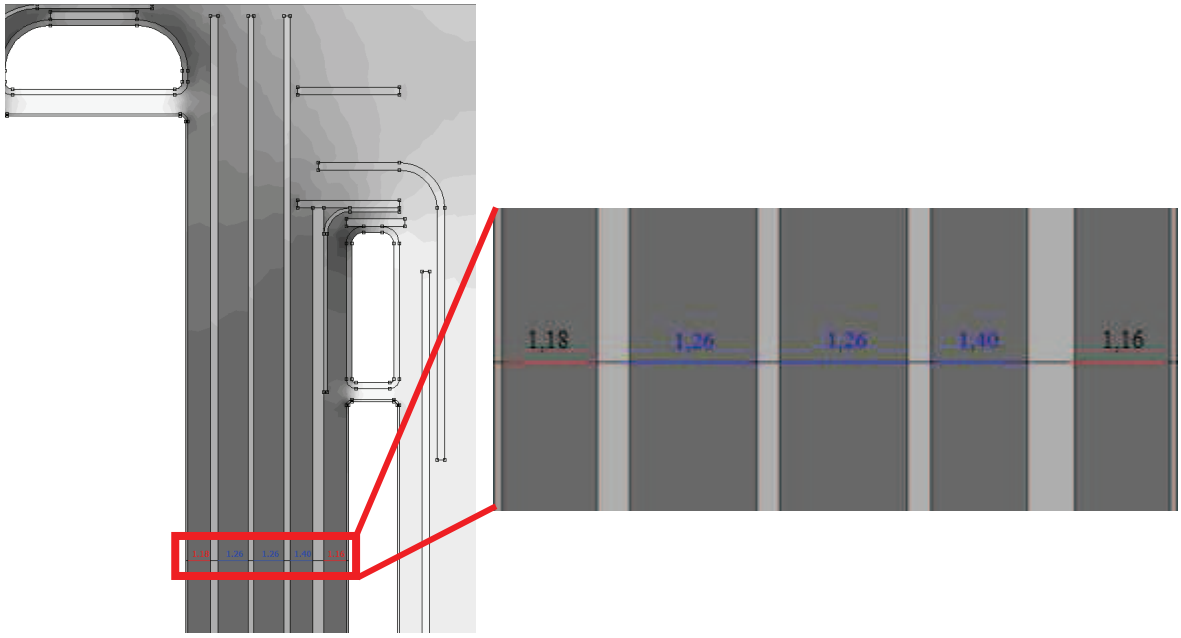


Figure 4. Safety margin analysis. a) Optimal insulation geometry obtained with the optimizer. b) Detail of the safety margin analysis into the HV-LV gap.

III.2.2 Electric FEM Solution

The electric FEM automatically runs the following three major stages: pre-processing, solving, and post-processing. In the pre-processing stage, the optimal insulation structure geometry obtained with the analytical optimizer is taken as geometrical description of the device, which together with the material properties, boundary conditions and voltage sources completely defines the problem. In the Fig. 4 is depicted the safety margin analysis of the main insulation structure represented in Fig. 3, showing in red the SMs below SM_{Ref}. Once the solution is accomplished, the post-processor automatically extracts the required results from the solution. In particular, the post-processor conducts an automated safety margin analysis that allows the SM_{Num} calculation.

III.3 Iterative Procedure for the Automated Optimal Design

In the proposed methodology is introduced an iterative procedure that automatically runs when the SM_{Ref} does not match with the SM_{Num} of the optimized insulation structure geometry obtained with the electric FEM. Its objective is to iteratively update the adopted SM_{Ref} in the analytical optimizer until the current SM_{Num} and the first selected SM_{Ref} fulfill the stopping criterion.

IV. Conclusions

A 2-D methodology has been proposed as a practical tool to automatically obtain the optimized design of transformer insulation system structures. The optimal insulation system structure geometry is calculated by means of the analytical optimizer based on GAs. The results are numerically validated with the electric FEM by comparing the SM_{Num} of the optimal insulation geometry with the selected SM_{Ref}. An iterative procedure is introduced in the methodology to ensure that SM_{Num} draws close to SM_{Ref}. The proposed 2-D methodology reduces the computation time during the design stage of power transformers due to the introduction of the analytical model, whilst the accuracy of the results is assured by the electric FEM computation.

References

[1] A. Ma and Z. Zhang, *End Insulation Electric Field Analysis and Design Optimization of 500 kV Power Transformer Based on ANSYS*, presented at the International Conference IEEE PES Innovative Smart Grid Technologies ASIA (ISGT ASIA), Tianjin, China, 2012.

ISBN 978-84-617–9183–5

[2] A. Mehta, R. Sharma, S. Chauhan and S. Agnihotri, *Study the Insulation System of Power Transformer Bushing*, in International Journal of Computer and Electrical Engineering, Vol. 3, No. 4, p. 544-547, Aug. 2011.

[3] S. V. Kulkarni and S. A. Khaparde, *Transformer Engineering: Design and Practice*, 1st ed., NY: Marcel Dekker, 2004.

[4] G. Youhua, G. Dan, L. Yanbin, G. Shuqiu and W. Guogang, *Improvement of Main Insulation Structure for 110kV Electric Power Transformer based on Electric Field Analysis*, presented at the International Conference on Electrical Machines and Systems, p. 4427-4430, 2008.

[5] J. Nelson, *Some Steps toward the Automation of the Design of Composite Dielectric Structures*, IEEE Transactions on Dielectrics and Electrical Insulation, Vol. 1, No. 4, p. 663-671, Aug. 1994.

[6] D. Tschudi, V. Dahinden and F. Derler, *Dielectric Strength Assessment of Power Transformer Insulation*, presented at the 9th International Symposium on High Voltage Engineering, Graz, Austria, p. 1081.1-4, Aug-Sept. 1995.

[7] J. Aubin and R. Malewski, *Safety Margin of Internal Insulation of EHV Power Transformers*, International Symposium on High Voltage Engineering, ISH'95, Graz, Austria, p. 8095.1-4, Aug. 1995.

[8] D. Tschudi, *AC Insulation Design. Paper-Oil Insulation Systems*, presented at the WICOR Insulation Conference, Rapperswil, Switzerland, 1996.

[9] V. Dahinden, K. Schultz and A. Kuchler, *Function of Solid Insulation in Transformers*, TRANSFORM98, Germany, p. 41-54, Apr. 1998.

[10] X. M. Lopez-Fernandez, C. Alvarez-Mariño, D. Couto, R. Lopes and A. Jacomo-Ramos, *Modelling and Insulation Design Methodology in Power Transformer under Fast Transients*, presented at the XIX International Conference on Electrical Machines, Rome, Italy, 2010.

[11] W. Ziomek, K. Vijayan, D. Boyd, K. Kuby and M. Franchek, *High Voltage Power Transformer Insulation Design*, presented in the Electrical Insulation Conference, Maryland, EEUU, p. 211-215, 2011.

[12] A. Portillo, *AC Insulation Design of Power Transformers*, International Advanced Research Workshop on Transformers, ARWtr2013, Spain, p. 70-88, 2013.

[13] A. Tahani, et al., *Automated Dielectric Design of Oil/Cellulose Structures. A Computer Implementation*, Computation of Electromagnetic Fields, Belin, 1995.

[14] P. Di Barba, U. Piovan, A. Savini, *Optimal Shape Design of the HV Winding of a Test Transformer*, COMPEL, Vol. 17, No. 1, p. 128 – 134, 1998.

[15] A. Bramanti, P. Di Barba, U. Piovan and A. Savini, *Design Optimisation of Transformer Insulation*, in Electromagnetic Fields in Electrical Engineering – ISEF'2001, IOS Press, Amsterdam, p. 170-173, 2002.

[16] D. Gupta, S. Ghafir, *An Overview of Methods Maintaining Diversity in Genetic Algorithms*, presented in the International Journal of Emerging Technology and Advanced Engineering (IJETAE), Vol. 2 No. 5, 2012

[17] P. Guo, X. Wang and Y. Han, *The Enhanced Genetic Algorithms for the Optimization Design*, *presented* at the International Conference on Biomedical Engineering and Informatics (BMEI), 2010.

[18] X. M. Lopez-Fernandez, H. Bülent Ertan and J. Turowski, *Transformers: Analysis, Design, and Measurement*, CRC Press, 2004.

[19] H. P. Moser et al, *Transformerboard*, Scientia Electrica, 1979.

ISBN 978-84-617–9183–5

Estimation of the Condition of Power Transformers and Shunt Reactors with Corrosive Sulphur

Arali GUZMAN LOPEZ, Roberto LIÑAN GARCIA, Horacio FLORES SANCHEZ.

Instituto Nacional de Electricidad y Energías Limpias (INEEL), Reforma 113, Cuernavaca, Morelos, México
aguzman@iie.org.mx, rlinan@iie.org.mx, horacio.flores@iie.org.mx

Abstract— **INNEL's experiences and development work are presented on this paper by in the application of a methodology for estimating the risk of failure in power transformers and Shunt Reactors with the presence of corrosive sulphur. Experimental arrangements were designed on a reduced scale to simulate corrosive sulphur phenomena under different operation conditions. The arrangements were submitted to an accelerated aging process and different measurements techniques were applied, to determine their sensitivity to changes in the dielectrical behavior. The most sensitivity techniques were applied in 10 shunt reactors in operation in two different periods. From results obtained, a methodology was developed capable of ranking the condition in four diagnostic zones. This methodology was applied on 31 different assets determining their health indexes. The evaluation shows the following zones: 2 in red, 19 in orange, 6 in yellow, 2 in green and 2 did not show the corrosive DBDS molecule. It was also proven that the equipment in red and orange zones, failed due to severe damage in the winding.**

Keywords— **Corrosive Sulphur, Health Indexes, Dielectric Spectroscopy, Dissolved Gas Analysis, DBDS**

I. INTRODUCTION

Worldwide, failures in power transformers and shunt reactors had been recorded without evidence of degradation caused by Dibenzyl Disulphide (DBDS) in the insulating oil [1]. Due to winding temperature, DBDS reacts with the copper conductor forming Copper Sulphide (Cu_2S), which adheres to the conductor and later migrates towards the paper layers, reducing the dielectric distances and causing the failure. This issue is of interest because it affects relatively new equipment with no early degradation signs that could have prevented these failures.

In Mexico, this issue affects a considerable amount of transformers and shunt reactors rated at 230 kV and 400kV installed in Transmission Network of Comisión Federal de Electricidad (CFE) [2, 3]. CFE has taken actions to mitigate this issue, by passivating the oil in the affected equipment. This solution is temporary, because the passivator is consumed and doesn't reverse the depositing of Copper Sulphide in insulating paper of winding conductor [4]. For this reason, CFE and INEEL developed a methodology based on health indexes to classify the degree of damage in windings in equipment with corrosive sulphur issue.

II. EXPERIMENTAL DEVELOPMENT

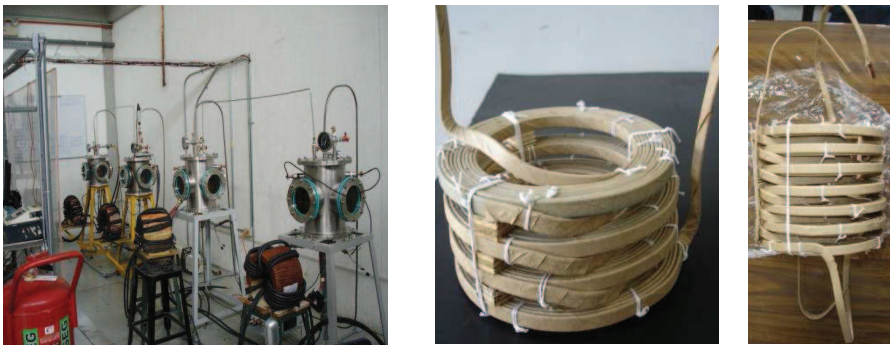
Due to the failures presented in power transformers and shunt reactors with corrosive sulphur issue, between 2010 and 2012, the INEEL developed an experimental setup to determine the most sensitive measurement techniques, electrical and physcochemical, to evaluate the winding damage. Additionally, the impact of DBDS in the oil, moisture content in the paper, oil condition, operating time without passivator and electric field interaction were evaluated.

SET UP

Four 20 L experimental arrangements were made from stainless steel, shown in Fig. 1a. A coil of four disks manufactured with copper conductor wrapped with three layers of Thermally Upgraded Paper (TUK) was placed in the interior of each arrangement. Thermocouples were installed in different places of the coil to monitor the temperature. New oil was used in all arrangements (Nynas Nytro 11 GBX). Each arrangement used tubing for recirculation, pressure monitoring, temperature control, oil preservation with Nitrogen blanket and a current supply system for heating. The experimental arrangements were submitted to a 140° C in the hottest spot of the coil and aging occurred in different stages.

ISBN 978-84-617–9183–5

During the experimental stage two types of coils were used. The coil for the experiment development was made out of four disks, Fig. 1b. For the experiments evaluating the effect of the electric field on the mobility of Copper Sulphide, a double conductor coil was used, shown in the Fig. 1 c.



(a) (b) (c)

Figure 1. (a) Experimental arrangements used for the development of the methodology, (b) coil of 4 disks and one conductor and (c) coil of 7 disks with double conductor, used during the experimental stage.

The following conditions were evaluated:

- Systems free of DBDS
- System with DBDS (1000 ppm)
- System with DBDS and passivator
- System with application of electric field

Before and during each aging stage, electrical measurements were taken: DC Winding Resistance, Insulation Resistance, Dielectric Spectroscopy, Partial Discharges, Frequency Response Analysis and Low Voltage Impulse. Oil quality measurements were taken as well: moisture content, DBDS, Passivator and Dissolved Gas Analysis in the oil. Finally, the arrangements were submitted to tests for lightning impulse with wave of 1.2/50 μs and physical inspection afterwards looking for damage in the coils.

RESULTS

Results showed that the systems with DBDS and without passivator, deposits of Copper Sulphide in the conductor started at 300 h of aging and at 450 h this was transferred to the first layer of paper. At 600 h of aging detaching flakes were observed. The migration of Cu_2S to other paper layers was not visible. Fig. 2 shows the process of depositing of Cu_2S a function of time.



(a) (b) (c)

Figure 2. Cu_2S deposits in coils as results of ageing at 140°C: (a) 300 h, (b) 450 h and (c) 600 h.

Passivator´s effect was evaluating adding 136 ppm of passivator to the system at 300 h and 450 h. In the experiments were the passivator was added at 300 h, it was observed that after 1,623 h of aging, the deposits did not advance through the rest of the layers of paper. When the passivator was added at 450 h, it was observed that after 1737 h of aging, the first layer of paper was covered with Copper Sulphide, but there was no migration to other layers. Also, a reduction of the rate of consumption of DBDS was observed (see Fig. 3). This was due to the passivator's slowing the reaction of DBDS in the formation of Copper Sulphide. Nevertheless passivator is consumed over time.

ISBN 978-84-617–9183–5

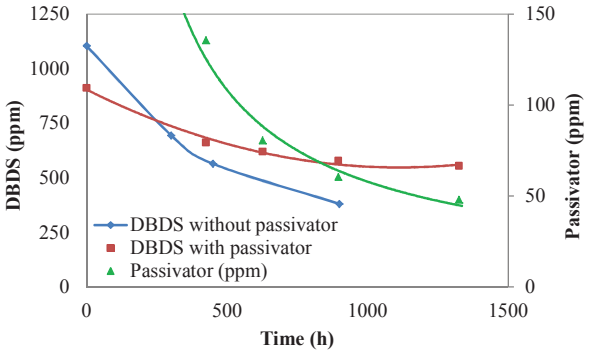


Figure 3. The effect of the passivator in the reaction of DBDS.

Because the Copper Sulphide did not migrate to other paper layers it was decided to evaluate systems with double conductor coils. For this, the system with DBDS was aged during 300 h, to reach the depositing only in the copper conductor and 6 kV were applied to the coils during 6 h. Finally, the experiment showed Copper Sulphide has migrated to the second and third layer of the paper.

Regarding sensitivity of electric measurements, dielectric spectroscopy showed important changes in the experiments. Fig. 4 shows the measurement of Tan δ, at four different aging stages: at the beginning, at 300 h, 450 h and 600 h respectively. At 300 h, an improvement of Tan δ, was observed, because at the beginning the DBDS behave as an antioxidant. At 450 h the response is similar to the zero time, indicating that the capacity of oxidation of the DBDS diminished. At 600 h a drastic reduction in dielectric response was observed.

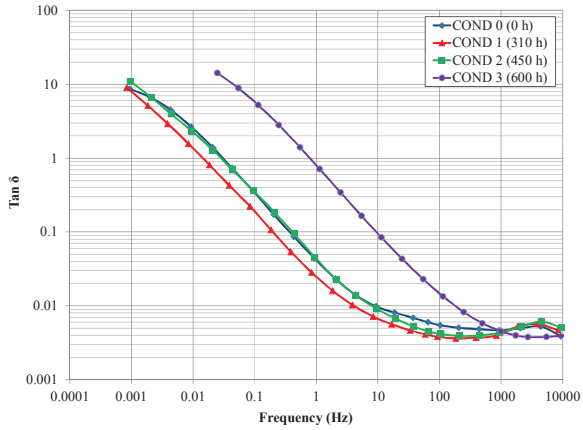
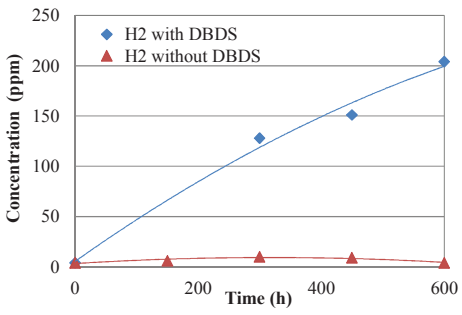


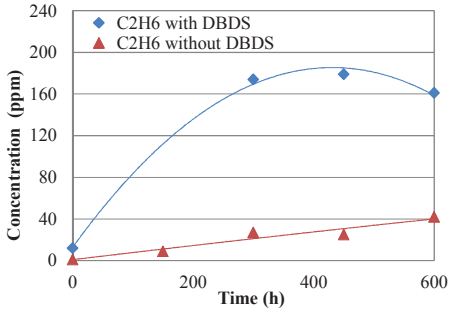
Figure 4. Dielectric response as a function of the frequency of experimental set up with DBDS submitted to the aging at 140°C at 300 h, 450 h and 600 h.

Regarding dielectric withstand of lightning impulse of the coils, it was determined that when the deposition of Copper Sulphide is only in the conductor, there was a reduction in the dielectric withstand of 5%. Nevertheless, when the depositing increased in the first layer of paper, the dielectric withstand was reduced by 35%.

Finally, regarding the generation of dissolved gases in the experimental set up, the presence of DBDS caused an increase in the gases of Hydrogen, Ethane, Carbon Dioxide and Monoxide. This is shown in Fig. 5.

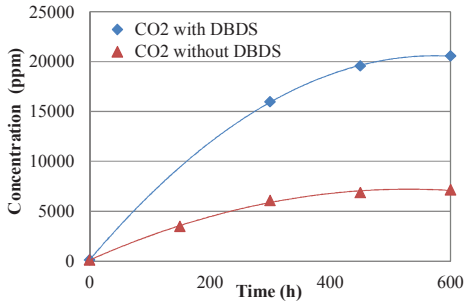


(a)

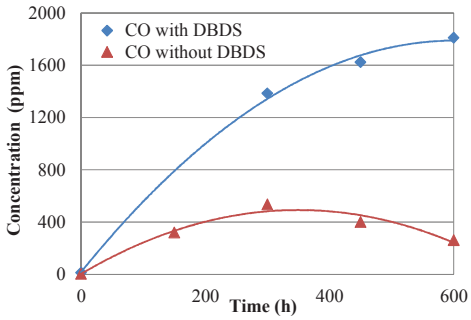


(b)

ISBN 978-84-617–9183–5



(c)



(d)

Figure 5. Behavior of the gases: (a) Hydrogen, (b) Methane, (c) Carbon Dioxide and (d) Carbon Monoxide in insulated systems with and without DBDS.

III. DEVELOPMENT OF THE METHODOLOGY

From 2011 to 2013, the INEEL adapted procedures and techniques of the experimental stage to apply in the field to transformers and shunt reactors with issues of corrosive sulphur. Ten apparatus were chosen rated at 230 and 400 kV and 18 to 50 MVAr and an annual testing program was defined for 2 years.

The apparatus were evaluated with electrical measurements of Insulation Resistance, Dielectric Spectroscopy and Frequency Response Analysis, while the oil was analyzed through the technique of Dissolved Gas Analysis, DBDS, moisture and passivator content. The apparatus operating temperature was registered. The values of the electric measurements of Insulation Resistance and Dielectric Spectroscopy were corrected by temperature.

The development of the diagnostic methodology was considered on the basis the index of health method of the Toronto Hydro-Electric System Limited [5]. The variables of the electrical measurements, physicochemical, contents of DBDS and Passivator and the maximum operating temperature, were collected in parameters of condition, assigning ranges, weights, and punctuations that served to estimate the health index of the apparatus. The calculation of health indexes was done using the following equations:

$$\text{Overall Factor} = \frac{\sum \text{Score}_i \times \text{Weight}_i}{\sum \text{Weight}} \quad (1)$$

$$CPS = \frac{\sum_{n=1} \beta_n \, (CPF_n \times WCPF_n)}{\sum_{n=1} \beta_n \, (CPF_{n.máx} \times WCPF_n)} \quad (2)$$

$$HI = \frac{\sum_{m=1} \propto_m (CPS_m \times WCP_m)}{\sum_{m=1} \propto_m \, (CPS_{m.máx} \times WCP_m)} \quad (3)$$

Where:
Overall factor: Factor which defines the impact of the variable in the health index of the apparatus
Score: Score assigned to the variable in evaluation as a function of measured values
Weight: Score assigned to the variable in function of sensitivity to depositing of Cu_2S
HI: Health Index
CPS: Condition Parameter Score
WCP: Weight of Condition Parameter
CPF: Sub-Condition Parameter Factor
WCPF: Weight of Condition Parameter Factor
αm: Data availability coefficient for condition parameter (=1 when data available, =0 when data unavailable)
βn: Data availability coefficient for condition factor (=1 when data available, =0 when data unavailable)

Three parameters were defined for evaluation: solid insulation, oil, and rate of aging. In each parameter the sensitivity variables of depositing were grouped, assigning each a score and a weight. In Table I an example of the score and weight of each parameter is presented.

ISBN 978-84-617–9183–5

Table I. Example of the Score and Weight of Sensible Variables in the Depositing of Copper Sulphide

Parameter/Variable	Scores						Weight
	1	2	3	4	5	6	
Solid insulation/Tan δ	≤1	>1-1.5	>1.5-2	>2-3	>3-4	>4	5
Oil/C_2H_6 (ppm)	≤100	101-150	151-180	181-210	211-250	>250	5
Aging rate/DBDS (ppm)	≤5	>5-50	>50-100	>100-150	>150-200	>200	5

With scores and weights of each variable defined, equations 1 to 3 were applied to obtain a health index of the apparatus under study. The health index has a value of between 0 and 1 on a scale of classification that permits interpretation of the condition of the apparatus as indicated in Table II.

Table II. Scale of Classification of the Health Index

Risk	Color	Range	Level of risk for corrosive sulphur
Good condition	**Green**	>0.75-1.0	Without operational risk. Scheduled monitoring
Regular revision	**Yellow**	>0.50-0.75	Low risk of failure. Six months monitoring
Schedule replacement	**Orange**	>0.25-0.50	Medium risk of failure. Schedule replacement/monthly monitoring
Immediate replacement	**Red**	0.0 to 0.25	Critical risk of failure. Schedule immediate replacement

In Table III the health index is shown for 10 shunt reactors during 2 years (1 measurement per year). It can be seen that in 8 apparatus an increase in damage was seen causing 4 apparatus to move from major risk zone to a failure zone. In two of the shunt reactors, the health index did not show any changes, because one of them was a spare unit and the other only operated for 6 months during the evaluation period.

Table III. Health index of 10 apparatus evaluated during the development of the methodology

Shunt reactor	R1	R2	R3	R4	R5	R6	R7	R8	R9	R10
M1	**0.45**	**0.45**	**0.55**	**0.9**	**0.63**	**0.56**	**0.53**	**0.5**	**0.3**	**0.38**
M2	**0.45**	**0.45**	**0.48**	**0.8**	**0.58**	**0.51**	**0.48**	**0.4**	**0.2**	**0.28**

IV. Experiences in the Application of the Methodology in the Field

In 2015, the INEEL determined the health index of 31 power apparatus using the methodology described. Three-phase and single-phase shunt reactors, transformers and autotransformers, installed in the Transmission network of CFE were evaluated.

The estimation of the health index of 31 apparatus indicated that 2 apparatus were in the red zone, 19 were in the orange zone, 6 were in the yellow zone, 2 were in the green zone and 2 did not have corrosive DBDS molecule. The application of the methodology on apparatus without the presence of DBDS resulted in an inaccurate diagnosis, because the methodology considers unique conditions of apparatus of corrosive types.

V. Case of the Failed Reactor

In March 2016 a three-phase shunt reactor of 25MVAr, 400 kV failed. This unit was evaluated in 2013 with the methodology developed. The unit was classified on the orange zone. After its evaluation, this shunt reactor was submitted to a process of elimination of corrosive compounds in the fluid until negligible concentrations for DBDS were obtained. The apparatus continued in operation and in November 2015, DBDS content was 11.6 ppm, this DBDS came from oil that was impregnated in the winding of the shunt reactor.

This failure highlights that once the apparatus is classified in the red and orange zones, replacement is necessary because severe damage to the winding is expected, and the removal of corrosive compounds is not an option for extending it´s operating life. The removal of corrosive compounds is recommendable for apparatus in the yellow and green zones

ISBN 978-84-617–9183–5

VI. CONCLUSIONS

The passivator slows down the DBDS reaction with the copper conductor of the winding for the formation of Copper Sulphide. However, the passivator is consumed as a function of temperature, for this, it is important to re-passivate the oil.

The application of the lightning impulse with 1.2/50 μs wave in the experimental set up allowed to make evident the degree of damage to insulation in function to the Copper Sulphide deposits in the coils. When the Cu_2S is found only in the copper conductor, the dielectric withstand has a reduction of 5% with respect to a system free of corrosive species. However, when the deposit has covered completely the first layer of paper the dielectric withstand is reduced by 35%.

The dielectric spectroscopy measurement is sensitive to the depositing of Copper Sulphide at the moment in which this compound has covered the first layer of paper. Previous to this, an improvement in the insulating system caused by the effect antioxidant of DBDS was observed. As well, with corrosive compounds, the effect of moisture in the response to frequency is negligible.

It was observed, in the laboratory, that the presence of DBDS in the oil provoking the generation of the gases Hydrogen, Ethanol, Dioxide and Monoxide of Carbon in abnormal concentrations. However, in the equipment evaluated in the field, only concentrations of Ethane and Carbon Dioxide were elevated.

The methodology was developed on the basis of unique conditions that occur in corrosive systems, so it is not applicable in equipment without this issue.

If it has been determined that equipment was diagnosed in red or orange zones, it is necessary to replace it and it is not viable to realize the elimination of corrosive compounds in the oil because any amount of DBDS remaining in the solid insulation attacks the winding until causing a failure.

To date the CFE plans to apply the methodology to all transformers and shunt reactors fleet with the issue of corrosive species, with the intention of taking necessary action to avoid failures.

REFERENCES

[1] Working Group A2.32 CIGRÉ. *Copper sulphide in transformer insulation* (Technical Brochure 378, ISBN: 978-2-85873-065-0, April 2009).

[2] *Estadística de fallas de transformadores y reactores de potencia y transformadores de instrumento* 1999 – 2008. (Coordinación de Transmisión de la Comisión Federal de Electricidad, México).

[3] E. Blanco, A. Vallejo, R. Cruz, G. Aguirre and R. Huizar, *Estudio de Falla de un Transformador Trifásico de 161 kV, 50 MVA por deposición de Azufre Corrosivo, en México,* (IEEE Reunión de Verano de Potencia y Aplicaciones Industriales, RVP-A1, Acapulco, Gro., México, julio 2007).

[4] Working Group A2.40 CIGRÉ, *Copper Sulfide Long-term Mitigation and Risk Assessment* (Short Summary, July, 29, 2010).

[5] Report No: K-015466-RA-0001-R01. "Toronto Hydro-Electric System Limited 2010 Asset Condition Assessment Audit". Kinectrics Inc. July 23, 2010.

ISBN 978-84-617–9183–5

Partial Discharge Monitoring of Power Transformers by UHF Sensors

S. TENBOHLEN[1], M. SIEGEL[2], M. BELTLE[2]

[1]Institute of Power Transmission and High Voltage Technology (IEH), University of Stuttgart
Pfaffenwaldring 47, D-70569 Stuttgart, Germany
e-mail: stefan.tenbohlen@ieh.uni-stuttgart.de

[2]BSS Hochspannungstechnik GmbH
Hohenheimer Str. 9, D-70184 Stuttgart, Germany
e-mail: martin.siegel@bss-hs.de, michael.beltle@bss-hs.de

Abstract — **The reliability of electrical energy networks depends on both, the quality and the reliability of its electrical equipment, e.g. power transformers. Local failures inside their insulation can lead to breakdowns and hence to high outage and penalty costs. Usually, power transformers are tested on partial discharge (PD) activity before commissioning. UHF PD monitoring can be used to prevent these events during service. Continuous monitoring exceeds the benefits of singular diagnostic measurements. Diagnostic PD measurements can provide snapshot information but no trend information. Also, temporary measurements can cause misleading interpretations due to the volatile nature of PD as measurements performed during low PD activity do not prove the general absence of PD. These drawbacks can be avoided by using continuous PD monitoring. In the first part, this contribution presents two different types of ultra-high frequency (UHF) sensors for PD measurement and their installation at power transformers including an UHF PD monitoring system. The second part is about a use case providing three years of UHF PD monitoring data of a power transformer, where the PD data is correlated with the transformer's load, temperature and the dissolved gas analysis.**

Keywords — **Power Transformers, Monitoring, Partial Discharge, UHF Sensors**

I. INTRODUCTION

Power transformers can be considered as an essential part concerning the reliability of the electrical grid. Hence, the reliable operation of power transformers is important for supply security because transformer failures tend to lead to significant damage with accordant costs. Therefore, all kinds of internal damages should to be recognized as early as possible. Different diagnostic methods have been established to meet the deriving demands for on- and offsite measurements [1]. Partial discharges (PD) measurement for example has been developed to detect local defects in the insulation that can be initiated and enlarged by the destructive nature of PD. Mainly, there are three different ways of PD monitoring: indirect detection by dissolved gas analysis (DGA), directly by either electrical PD measurements according to IEC 60270 [2] or by electromagnetic measurements in the ultra-high frequency range (UHF: 300 MHz –3 GHz) [3]. As DGA only provides an indication about PD being active, an increasing number of transformers are monitored using one of the direct measurement methods. PD measurement is suitable to detect damages in the insulation of power transformers at an early stage and thereby helps minimizing the risk of failure [4]. Its importance is accommodated by standardized electrical measurement according to IEC 60270 which is required for acceptance certificates at routine testing. The apparent charge Q_{IEC} has become an indicating factor for transformer quality. Especially in terms of monitoring and onsite diagnostic measurements, the electromagnetic UHF method gains in importance [5]. The electromagnetic emission of PD is measured using an UHF antenna which is inserted into the transformer tank. The generalized propagation paths of the methods are shown in Figure 1. Electrical signals travel through the galvanic coupling along the winding and are decoupled at the measurement capacity of the bushing (for online monitoring) or with an external coupling capacitor (not shown). Electromagnetic signals are not bound to the galvanic coupling and can radiate directly through the oil filled transformer. Usually, UHF PD measurements are shielded electromagnetically against external disturbances due to the Faraday shielding of the transformer tank [6] and low-pass filters provided by high voltage bushings. Therefore, UHF is less sensitive to external interferences compared to the electrical method. This creates an advantage for measurements in noisy environments, for example at on-site/online measurements and for monitoring. Cigré Working Group WG A2-27 recommends in brochure 343 to install DN50 valves in order to ensure highest flexibility for the later fitting of UHF probes. Alternatively, dielectric windows can be used for UHF sensors [7]. UHF sensors for installation at DN50 valves and dielectric windows are presented in the next chapter.

ISBN 978-84-617–9183–5

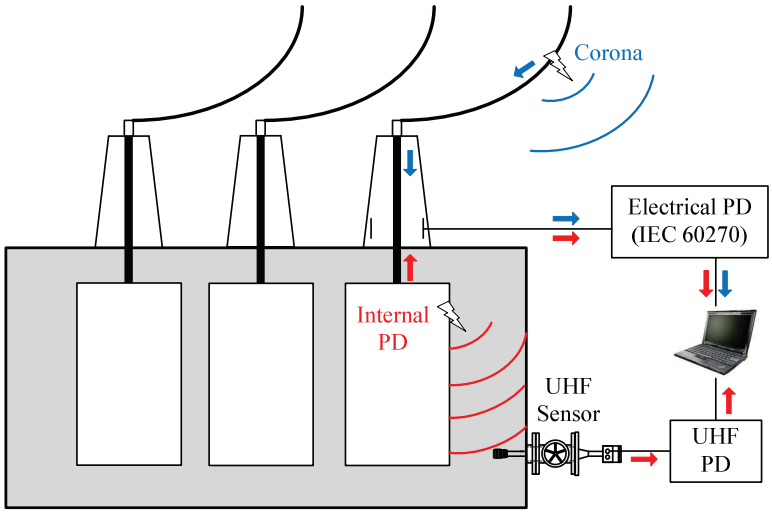


Figure 1. Signal propagation of UHF and conventional PD measurement at a power transformer with internal PD (red) and external PD (blue) [8].

II. UHF SENSORS

An UHF sensor for power transformers consists of a broadband antenna suited for the UHF frequency range radiated by PDs and of its mechanical adaption for the installation at power transformers. Mainly two UHF sensor technologies for internal PD measurement at transformers are used for practical applications.

a. UHF DRAIN VALVE SENSOR

An UHF drain valve sensor is designed as retrofit solution for transformers which have standardized DN50 or DN80 gate valves, see Figure 2 a). A standardized gate valve with straight duct where an UHF drain valve sensor can be installed is shown in Figure 2 b). Ball and guillotine valves can also be used for sensor installation. Figure 2 c) demonstrates a counterexample that is not suitable for drain valve sensor application. It illustrates a globe valve without straight opening. Other valve types without straight opening (diaphragm and butterfly valves) are also popular in some regions. As they are not applicable for UHF sensor installation, it is recommended to use only straight opening valves at new transformers.

a) b) c)



Figure 2. a) UHF drain valve sensor for installation at standardized DN50/DN80 gate valves [9]
b) Gate valve as example for oil valves suited for UHF sensor installation
c) Globe valve as example for oil valves not suited for UHF sensor installation.

Sensor application can be done even at transformers in service. At first, the UHF sensor is mounted on the valve. Secondly, the valve is opened slowly and de-aerated by a small ventilation valve on the sensor's mounting plate. Afterwards, the oil valve can be opened completely in order to insert the sensor into the transformer tank. The head of UHF sensor (the RF antenna) has to reach into the transformer for sufficient sensitivity. Usually, an insertion depth of approx. 50 mm has been proven as reasonable value. An installation of the RF antenna inside the pipe of the gate valve leads to low sensitivity due to electromagnetic shielding [3]. Besides sensitivity considerations, a minimum distance between UHF sensor and parts on high potential must be preserved to ensure save operation. UHF drain valve sensors are mainly used during diagnostic measurements on-site because their design allows them to be installed at power transformers in service. Nevertheless, permanent installation as part of an online PD monitoring system is possible as well.

ISBN 978-84-617–9183–5

b. UHF PLATE SENSOR

UHF plate sensors as shown in Figure 3 a) can be mounted directly to the tank wall which is suitable e.g. for newly built transformers. A dielectric window is integrated into the tank wall. It consists of a stainless-steel welding ring and a high-performance plastic which resists mineral oil and high temperatures. The plastic has a permittivity similar to mineral oil which allows UHF signals to pass through to the UHF sensor with low damping. The plate sensor is mounted into the dielectric window. Its RF antenna reaches into the transformer tank through the window that acts as oil barrier. In contrast to the drain valve sensor, plate sensors allow UHF measurements and sensor swapping without oil handling. Figure 3 b) shows a dielectric window and welding ring for installation at transformer tank walls. Plate sensors can be included into the transformer tank at any suited position. Even if no sensors are installed at the delivery of a transformer, oil-sealed dielectric windows with a blank cover can be mounted onto the tank wall during production to allow an easy retrofit of UHF PD monitoring during service. In Figure 3 c), a test installation of three UHF plate sensor prototypes at a power transformer is shown.

a) b) c)

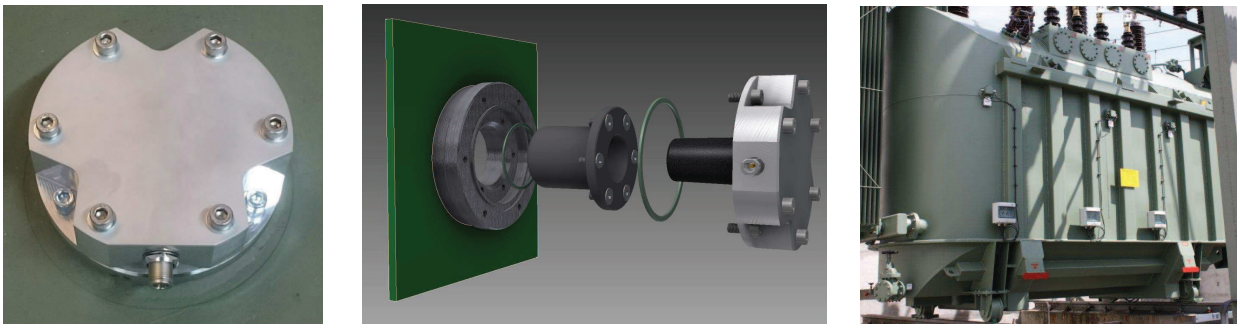


Figure 3. a) UHF plate sensor for direct installation at transformer tank wall [9]
b) 3-dimensional drawing of welding ring (left), dielectric window with gasket (middle) and UHF plate sensor (right) [9]
c) Test installation of UHF plate sensor prototypes at a power transformer.

III. UHF MONITORING SYSTEM

This chapter presents a synchronous 4-channel UHF monitoring system which can be used to either monitor one transformer with up to four UHF sensors or up to four transformers with each only one UHF sensor in a substation. Figure 4 shows the monitoring system with one UHF drain valve sensor installed at a transformer.

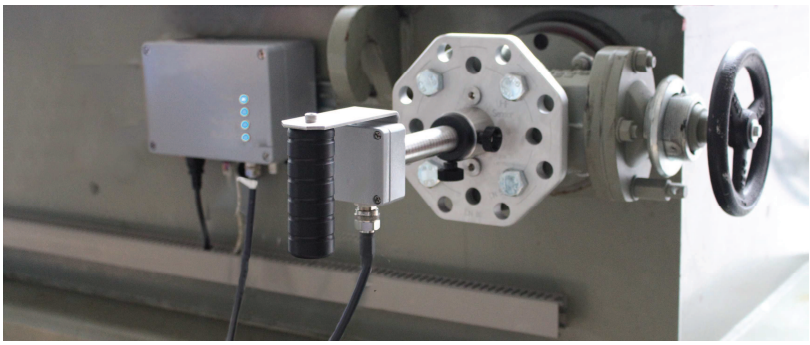


Figure 4. UHF monitoring system installed at a transformer with UHF drain valve sensor at a DN50 gate valve.

The 4-channel monitoring system uses a vertical resolution of 12 bit per channel. It is able to synchronously detect UHF signals between noise level at approx. $U_{noise} = 1$ mV and $U_{max} = 2000$ mV at all 4 channels. The phase resolution in 50 Hz and 60 Hz systems is $\varphi = 1°$. Therefore, detailed phase resolved partial discharge patterns (PRPDs) can be recorded for expert evaluation [10]. A trend view of UHF amplitude and PDs/min is provided for long term evaluation and correlation with other measured values (voltage, load, temperature). A more detailed trend view can be used for tracing of PD patterns: a time-resolved PRPD pattern allows recognizing changes in PRPDs in direct correlation with other measured values. A description of this time-resolved PRPD including example is given in the next chapter.

ISBN 978-84-617–9183–5

The UHF monitoring system is connected to a server or a desktop PC via Ethernet for storage and evaluation. The monitoring system can be accessed easily by a graphical user interface (GUI) used for system parametrization (including alarm/warning thresholds) and visualization of the measured real-time data. Figure 5 shows a screenshot of the UHF PD monitoring GUI. Real-time UHF PRPDs (left) and trend views (right) of two UHF sensors are presented. All diagrams can be parametrized and exported into standard images (jpg-files) either for single measurements or periodically (e.g. a snapshot can be exported every hour). Alarm thresholds can be defined for signal amplitude and counted PDs per interval. The trend data can be exported to csv-files for post-correlation with other operational data (e.g. on load tap changer (OLTC) position). There is also the option to reimport historical trend data for replay and PRPD generation. The provided toolset can assist asset managers to surveil and evaluate the actual status of transformers in service. It also helps PD experts for a better understanding of PD failures by continuous observing of PD and possibility of correlation to other measured data.

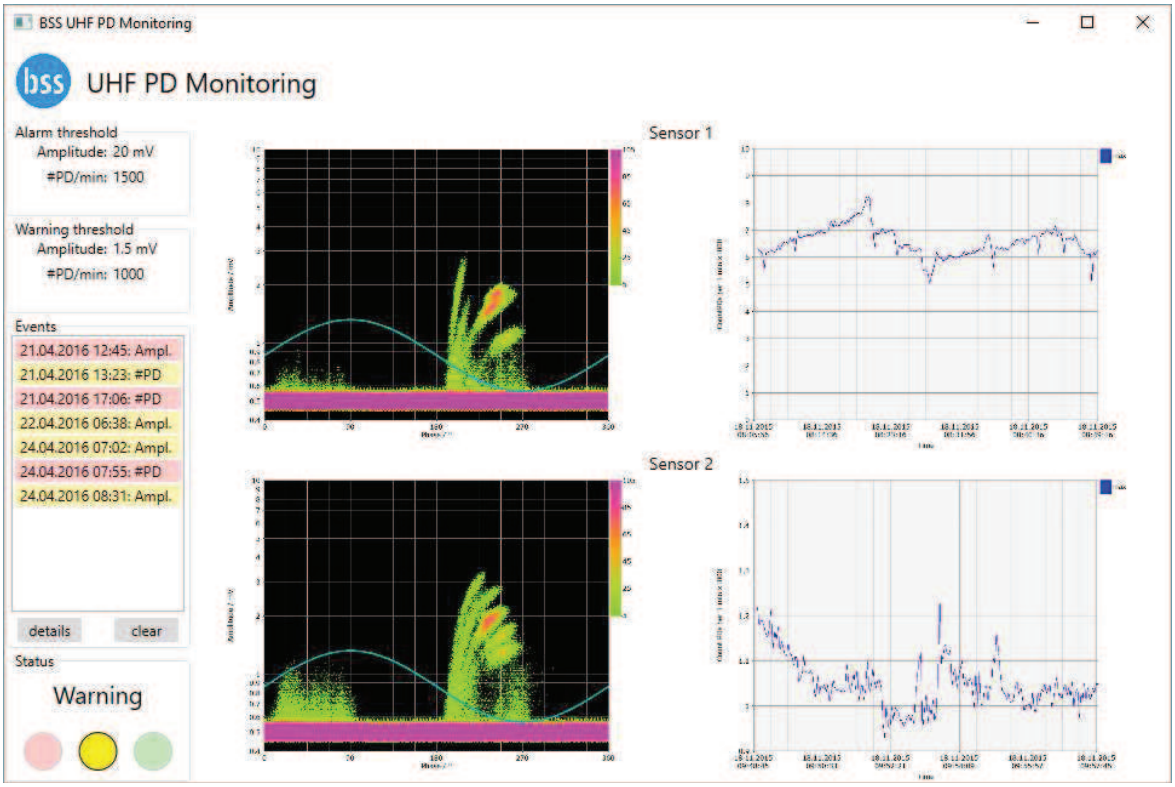


Figure 5. GUI of UHF PD monitoring software with real-time visualization of PRPD and trends (screenshot) [8].

IV. USE CASE: 120 MVA GENERATOR STEP-UP-UNIT

This use case presents PD monitoring data of an approx. 50-year-old unit generator transformer with 110/10 kV rated voltage and 120 MVA rated power, which is by now monitored for more than six years. Prior to this, the transformer was out of service for 8 years. A condition assessment before bringing the unit back into service indicated PD: conventional PD measurements according to IEC 60270 were performed using external coupling capacitors. PRPD patterns indicated that the transformer has more than one active PD at nominal voltage.

Due to the lack of common rules and threshold values for aged transformers, it was decided that the unit can only be put back into service if it is monitored continuously. For permanent observation of PD data, an online UHF PD monitoring system with an UHF drain valve sensor was installed. Furthermore, voltages, load currents, top-oil/ ambient temperatures, mechanical vibrations and dissolved gases (using a Hydran sensor) were recorded. The PD trend is used as indicator if the insulation defects are getting worse. PRPD monitoring data confirms the presence of more than one PD source. The PDs are not present permanently at constant voltage conditions. As the measured PDs show no clear trends, alarm thresholds are set slightly over the "normal" PD behavior. Alarm parameters are given by the maximum signal amplitude of UHF PD (in mV) and by the counted PD events per minute.

ISBN 978-84-617–9183–5

The following represents a case with exceeded alarm levels. Figure 6 a) shows a UHF PRPD pattern and Figure 6 b) PRPD data over time whereas the color gradient in a) represents the number of recorded PD per minute and in b) the UHF amplitude in mV.

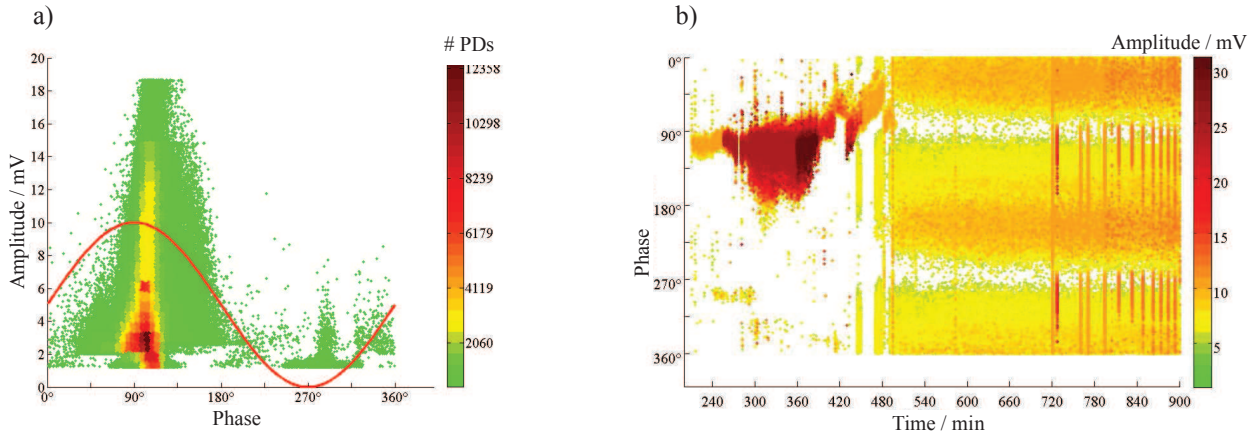


Figure 6. a) UHF PRPD (240 min – 420 min in b))
b) 2-dimenisonal simplification of time domain PRPD (no #PDs shown).

The UHF PRPD pattern in Figure 6 a) shows the PRPD data from Figure 6 b) from $t_1 = 240$ min to $t_2 = 420$ min. High UHF signals occur in this timeframe which triggered the amplitude alarm of the system. During the observation of the event, the amplitude and number of PDs stayed constant and did not worsen so it was decided to keep the transformer in service. After 3 h of high amplitudes, the PD event vanished and PD activity normalized. The measured combined dissolved fault gases represented by the Hydran value started to increase approx. 4 h after the PD event was over. Figure 7 shows the trend view of the PD amplitude correlated to the Hydran value.

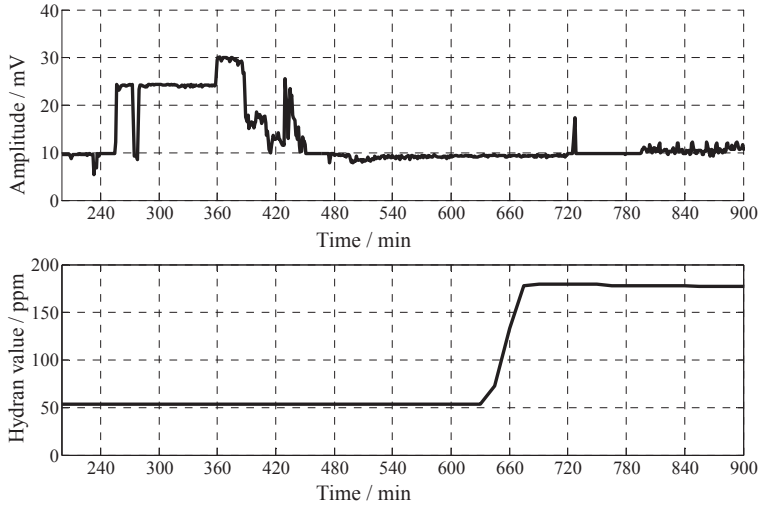


Figure 7. Max. UHF PD value (in mV) correlated with Hydran value (in ppm).

The alarm threshold for the fault gas value was exceeded approx. 7 h after the PD event started. This delay between generating H_2 and the increased values at the gas sensor is due to the gas solubility and dispersion in the transformer. This example shows the advantage of direct PD monitoring. The UHF PD monitoring system gives a real-time alarm in case of PD events and the PD can be observed using PRPDs and trend views. In contrast, the DGA monitoring only gives an alarm with several hours delay (in this case) and no detailed information about the PD itself.

V. CONCLUSION

Partial discharge measurement is common practice for transformer type tests and diagnostic measurements. It represents a suitable tool to detect local defects in the insulation before these defects can emerge to a breakdown. Hence, the method suggests itself for asset management in terms of continuous monitoring.

ISBN 978-84-617–9183–5

Monitoring exceeds the benefits of conventional diagnostic (singular) measurements. Diagnostic PD measurements can provide snapshot information, but do not provide any trend information. Also, temporary measurements can cause misleading interpretations due to the volatile nature of PD as measurements performed during low PD activity do not prove the general absence of PD. These drawbacks can be avoided by using continuous PD monitoring.

PD can be detected directly by electrical, standardized PD measurements according to IEC 60270 or by UHF measurements using antennas. The UHF method is advantageous for monitoring of on-site/online transformers, because UHF sensors are not galvanically coupled to the high voltage, do not require bushing measurement taps and are less affected by external PD sources (e.g. corona at bus bars). Sensors can either be applied at transformers online/on-site using UHF drain valve sensors at DN50/DN80 valves or at new/refurbished transformers at the factory using UHF plate sensors with a dielectric window.

A case study illustrates PD monitoring at a generator step-up unit in combination with gas-monitoring over several years. Long-term evaluation proves PD being highly volatile. A severe rise of fault gases correlates with a significant gain in PD activity which caused both monitoring systems to raise alarms. The systems differ in their alarm delay: the PD alarm was triggered 7 hours earlier than the gas alarm (due to the high time constants of dissolving gases). Hence, a combined monitoring is considered as ideal asset management. PD monitoring can provide the fastest response times. Correlations, e.g. with gas measurements, can be used to affirm the transformer's status. After such an incident, the historical databases of monitoring systems can help asset managers and experts to decide the next steps.

REFERENCES

[1] S. Tenbohlen, M. Heindl, M. Jovalekic, A. Müller, M. Siegel, *Trends of the Diagnosis of High Voltage Equipment (Trends in der Diagnostik von Hochspannungs-Betriebsmitteln)*, in ETG Diagnostik Elektrischer Betriebsmittel, Fulda, Germany, 2012.

[2] International Electrotechnical Commission (IEC), *IEC 60270 High Voltage Test Techniques - Partial Discharge Measurements*, Geneva, Switzerland, 2000.

[3] S. Coenen, *Measurements of Partial Discharges in Power Transformers using Electromagnetic Signals*, Universität Stuttgart: Books on Demand GmbH, ISBN 978-3-84821-936-0, 2012.

[4] J. Fuhr, *Procedure of Identification and Localization of Dangerous PD Sources in Power Transformers*, IEEE Transactions on Dielectrics and Electrical Insulation Vol. 12, No. 5, 2005.

[5] M. Judd, *Power Transformer Monitoring Using UHF Sensors: Installation and Testing*, IEEE International Symposium on Electrical Insulation, Anaheim, USA, 2000.

[6] M. Judd, *Partial Discharge Monitoring for Power Transformers Using UHF Sensors Part 2: Field Experience*, IEEE Electrical Insulation Magazine, Vol. 21, No. 3 May/June 2005.

[7] CIGRE WG A2.27, *Recommendations for Condition Monitoring and Condition Assessment Facilities for Transformers*, Cigre Brochure 343.

[8] S. Tenbohlen, M. Siegel, M. Beltle, M. Reuter, *Suitability of Ultra High Frequency Partial Discharge Measurement for Quality Assurance and Testing of Power Transformers*, CIGRE SC A2 & C4 Joint Colloquium, Zürich, Switzerland, 2013.

[9] BSS Hochspannungstechnik GmbH, *online datasheet*, 19.07.2016, www.bss-hochspannungstechnik.de

[10] CIGRE WG.21.03, *Recognition of Discharges*, CIGRE Electra, No.11, December 1969.

ISBN 978-84-617–9183–5

Analysis of Highly Coupled Transformers for Resistance Welding Systems Operated with Increased Frequency

Mariusz STEPIEN[1], Bogulaw GRZESIK[1], Zygmunt MIKNO[2]

[1]Silesian University of Technology, B. Krzywoustego 2, 44-100 Gliwice, Poland
[2]Institute of Welding, Blogoslawionego Czeslawa 66-68, 44-100 Gliwice, Poland
Phone: (+48) 32 237 12 47, fax: (+48) 32 237 13 04, e-mail: mariusz.stepien@polsl.pl

Abstract — **The paper is focused on the analysis of transformers that are devoted for resistance spot welding DC machine. The analysis is carried out in order to get information about such parameters of transformers like minimized leakage inductances as well as maximized coupling coefficient between windings, which are used to select suitable design of transformer. The analysis is also aimed at the influence of the design (shape of the cross-section of the magnetic core and also the way the windings are wounded) on the power properties of transformer (power loss and power density). The magnetic material taken into analysis is a ferrite one. The transformers are connected to two diode full-wave rectifier. Such connection requires special design of transformer – with two secondary windings. The transformers operate at 10 kHz of the frequency. Rating parameters are output current 10 kA, turn-to-turn ratio 50:1 and load resistance 0.8 mOhm.**

Keywords — **highly coupled transformer, resistance spot welding, planar transformer.**

I. INTRODUCTION

Intensive development of mobile welding systems requires very efficient transmission of the power from a source to the load with extremely high density of energy during the conversion [1]. One of the most important element in such system is a transformer. In order to convert energy with high efficiency and high power density higher frequency of energy conversion can be applied. Such operation requires proper power converter unit (inverter) and cooperation between converter and transformer requires additionally very high coupling ratio in transformer.

The most common frequency for energy conversion in DC welding systems is 1 kHz. Typical system contains power converter, transformer, high current rectifier and welding arms with electrodes. The energy is transferred with high current in the circuit between secondary winding of transformer and electrodes. In order to reduce ohmic power losses in this loop the transformer is located at possibly short distance to the electrodes (reducing length of welding arms). In movable systems, e.g. automotive industry welders, the transformer is located at movable part and the main requirement is reduced weight of transformer. One of the simplest way to reduce weight at the same delivered power (increasing power density) is increasing frequency of operation [2]. Analysis and optimization of design is a main goal of the analysis presented in the paper.

The results presented in the paper are based mainly on numerical modelling, but final designs are tested under operational conditions in the laboratory. Authors considered several different configurations of transformer arrangement. They can be divided in three main groups, namely coaxial transformer, planar transformers and pot-core transformers. Two first groups are described in the paper. Finally planar transformer has been selected for final consideration and prepared as a prototype for laboratory tests. Very important aspect of final selection was feasibility of transformer and difficulty/cost of fabrication – the transformer is considered as a device for mass production. Very promising design is also pot core transformer, which exhibit very good properties, but those practical aspects of its fabrication have to be solved making this transformer more practical design.

The family of transformers presented in the paper are dedicated to spot welding process. It means operation at very high output current and large transformer ratio [3]. Practically it is n1:1 ratio, where the secondary is single turn winding or multiple turns connected in parallel. Additionally transformers have two secondaries connected to two diode rectifier [4]. Such specific operation and design causes that proposed transformers and results of their analysis have been reported in literature very occasionally and selectively.

ISBN 978-84-617–9183–5

II. TRANSFORMERS AND THEIR DESIGNS

In the section two transformer proposed for DC welding system are described. They are coaxial transformer and planar one. The idea of design of both transformers is shown in Fig. 1. Both transformers are made of the same shape of magnetic core. The E65/50/15 Ferroxcube magnetic core of 3F3 material has been used [5]. Two E-shaped cores formed magnetic core 50 mm long and 30 mm high. Total length of transformers was higher because of windings ends and it was about 90 mm.

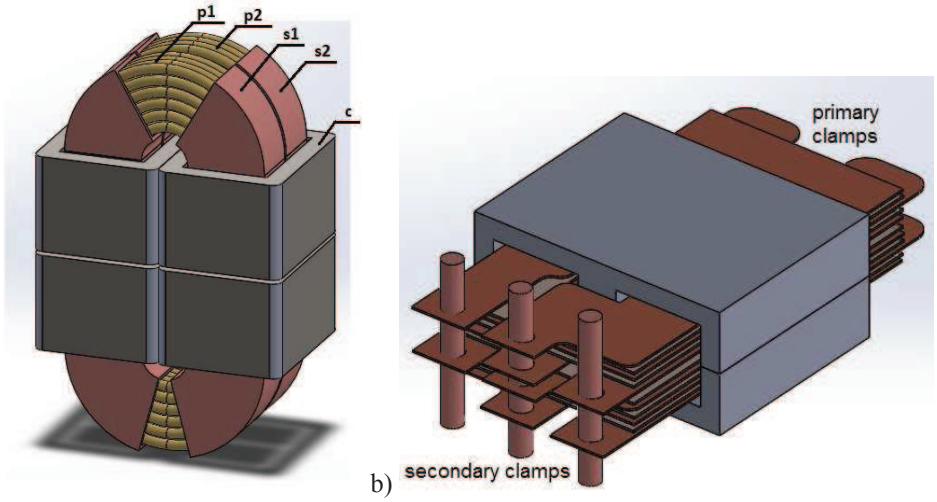


Figure 1. Idea of design of transformers for DC spot welding, a) coaxial transformer, b) planar transformer.

The transformer called as coaxial one is made as two separate transformers operating at common magnetic core. The primary winding *p*1 (c.f. Fig. 1a) is made of litz wire and located inside (coaxially) with corresponding secondary winding *s*1 which is made as a copper tube with rectangular cross-section. The secondary is connected to one of diodes in the output rectifier. The second pair, primary *p*2 and secondary *s*2, is made in the same way, while secondary *s*2 is connected to the second diode in the output rectifier. The turn-to-turn ratio of the transformer is 18:1. Such transformer is constructed to output current of 3.3 kA and it is considered as one of three module of the transformer with rating output current of 10 kA.

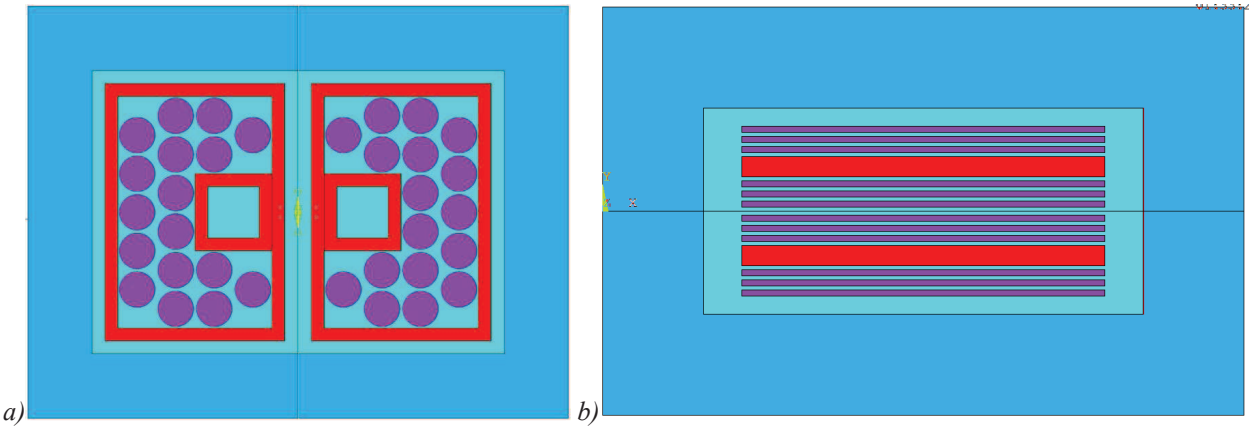
The planar transformer is made using the same shape of core but different arrangement of windings. Windings are made of copper sheets formed in rectangular loop. Each primary turn is located between two sheets of secondary turns, each connected with different diode in rectifier. Total windings are made of 18 such "sandwiches". Turns of primary winding are connected in series and turns of secondary are connected in parallel creating two separate windings connected with two diodes in the rectifier (inner clamp is common for both secondary windings – c.f. Fig. 1b). The turn-to-turn ratio is the same like in coaxial transformer. Full transformer is made of three single transformers (modules) having the same rating output current of 10 kA.

The first examination of proposed transformer was numerical analysis. Several variants of the base design has been considered to find the best properties of transformer. The second step was construction and examination of prototypes in real operational conditions. Results of both steps are described in the next sections.

III. PROPERTIES RESULTED FROM NUMERICAL ANALYSIS

Numerical analysis based on FEM has been carried out using commercial software ANSYS v. 15. Mechanical APDL (Ansys Parametric Design Language) interface allowed to prepare parametrical models of transformers and comparative analysis in respect of geometry and load parameters [6]. The analysis has been carried out assuming linear parameters of materials (including magnetic material) and harmonic excitation (sinusoidal loads). The geometry of numerical models (selected) is shown in Fig. 2. The geometry represents finite elements area. The numerical model include also circuit part. It contains loads and excitation (source). One can observe 2D geometry of models. It is considered as a planar model (infinitely long) and results have been obtained per unit of length.

ISBN 978-84-617–9183–5

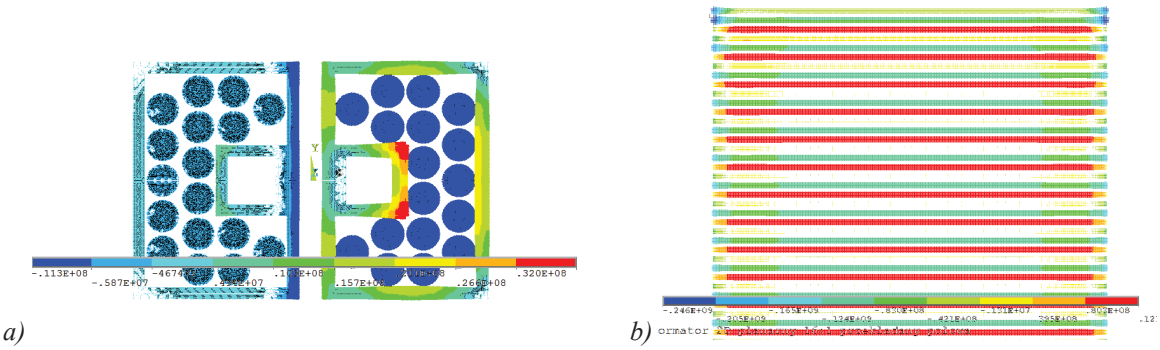


a) b)

Figure 2. Geometry of numerical FEM models, a) coaxial transformer, b) planar transformer; violet – primary, red – secondary, blue – magnetic core, light blue – air.

Geometries presented in Fig. 2 corresponds to two main transformer structures. The first one is a coaxial transformer. One can observe circular litz wires of primary and rectangular secondary. Additionally cooling channel is inserted inside of secondary. It is made of copper and it is a part of winding (since the current is flowing in the channel part it increases coupling ratio between windings). The second geometry represents planar transformer. One can observe that the secondary is a copper wire with higher thickness than primary (solid massive block) and it is located in middle part of primary. The coupling in this solution is worse in comparison with the transformer with secondary turns distributed in between primary ones. Such solution will be presented in further part of the paper.

Optimization of the structure in respect of efficiency and energy density requires detailed analysis of power losses. Main sources of power losses are ohmic losses in copper and losses in magnetic core. The first source of losses is a square function of current density, so an important element of optimization is analysis of current density distribution. Such analysis can be carried out using current density distributions presented in Fig. 3. Presented distributions are obtained for rated conditions. In respect of power losses they are considered in qualitative way.



a) b)

Figure 3. Current density distribution in, a) coaxial transformer, b) planar transformer.

In Fig. 3a one can observe one part carrying load current (right side) and the second one which is in idle state (left side). The current in the primary is homogeneous because of litz wire. The secondary current is strongly inhomogeneous in the part of cooling channel – it increases power losses in the secondary. The current flowing in the idle state part is also a source of power losses. Additionally the load current induces reverse current in the idle state part located in the proximity of loaded part. More uniform current distribution can be observed in planar transformer. Because of small thickness of copper comparable to skin effect depth, the current flows at whole cross-section of wire. One can observe small inverse current in idle winding. It is much more small than current in idle part of coaxial transformer. Additionally, primary current in planar transformer does not exist in idle state. Such distribution produces considerably smaller power losses. Additionally, arrangement of windings in planar transformer suggest better coupling between windings. This feature has been confirmed in laboratory.

ISBN 978-84-617–9183–5

The quantitative analysis of power losses and efficiency has been carried out considering transformer as a two-port network. Transformers have been supplied by sinusoidal voltage source and loaded by full range of resistance loads (idle state to short circuit). The analysis has been carried out assuming linear lossless magnetic core. Characteristic of efficiency in planar transformer is shown in Fig. 4.

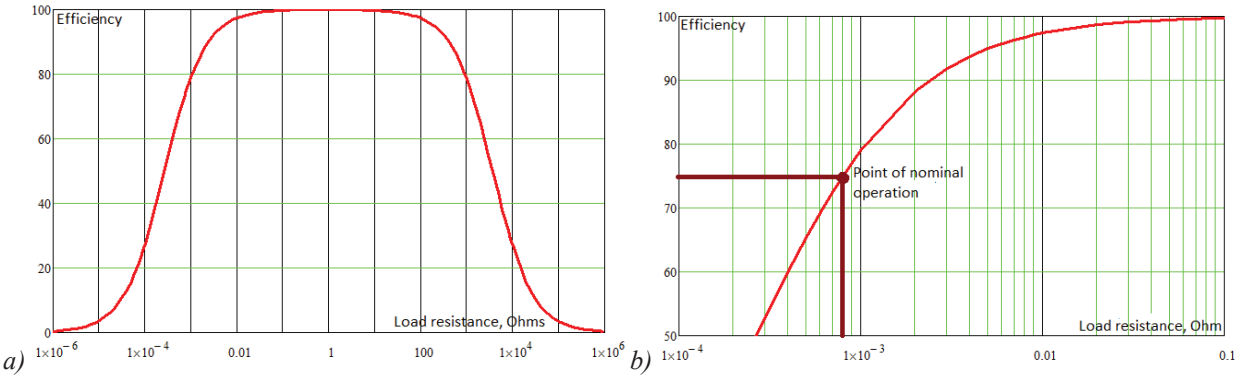


Figure 4. Efficiency of planar transformer, a) full range of loads, b) vicinity of operational point.

The efficiency of transformer is very high in broad range of loads (between 0.01 Ω and 100 Ω it is above 97%), but the operational point for spot welding process is located close to short-circuit state. Rated load resistance of considered system is about 0.8 mΩ. At this operational point the efficiency is about 75%. Operation in vicinity of short-circuit state means that power losses in magnetic core are negligible in comparison to power losses in copper. It confirms correctness of assumption neglecting of power losses in magnetic core. It is also an appointment for design of cooling – intensive cooling is required only for windings.

Presented here analysis concerns only to efficiency. Delivered power in transformer depends on the level of allowable power losses in the transformer. The input/output power is determined experimentally for constructed prototype transformer. Steady state operation of transformer refers to allowable power losses. Details of experiments as well as design of prototype transformer is described in the next section.

IV. THE PROTOTYPE TRANSFORMERS AND LABORATORY TESTS

Final properties of considered transformers have been confirmed by laboratory tests on constructed prototypes. Several prototypes have been constructed as a result of optimization and practical improvement. The prototype which relates to presented in previous sections numerical analysis is a planar transformer with a turn-to-turn ratio 18:1 and rated output current 3.3 kA. Photograph of this prototype transformer is shown in Fig. 5.



Figure 5. The prototype of planar transformer 16:1 turn-to-turn ratio connected to the rectifier block.

The transformer considered as a module of full transformer is connected to the rectifier block and loaded by a copper wire of parameters similar to spot welding process. The transformer is supplied by bridge inverter with

ISBN 978-84-617–9183–5

rectangular voltage waveform. The current in the transformer is controlled by pulse width of input voltage. Base waveforms recorded during tests are presented in Fig. 6. One can observe that rise/fall time of input current is about 60% of pulse width of input voltage. It results from leakage inductance of transformer and it reduces range of output current control.

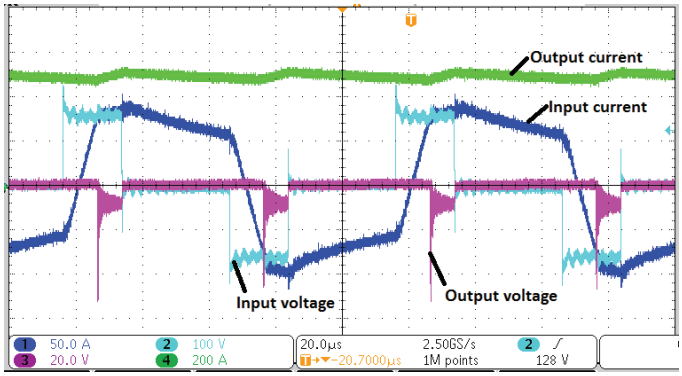


Figure 6. Waveforms of input and output voltages and currents in the module of planar transformer.

After some improvements, mainly focused on winding ends arrangement and current leads construction final prototype with turn to turn ratio of 50:1 has been constructed. The photograph of the prototype is shown in Fig. 7. After reducing leakage inductance from the level of 10 µH in the first prototype to the level of 4 µH in the final one, the maximum output current of the transformer was on the level of 15 kA, since rated output current is considered as 10 kA. Estimated average output power of the transformer at rated output current was about 35 kW, while instantaneous output power was about 100 kW (transformer operated with duty ratio about 35%). Characteristics of power, power losses and efficiency of transformer as a function of output current are presented in Fig. 8. Power losses in rectifier are estimated assuming voltage drop at each diode under carrying the current of 1 V.

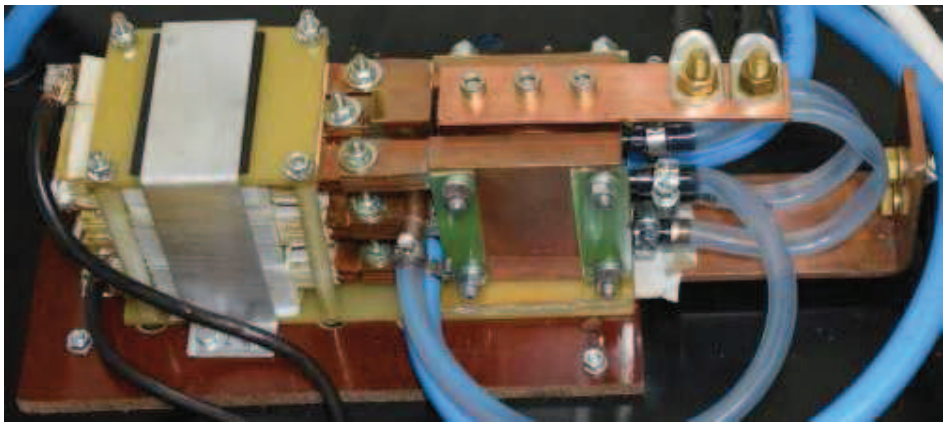


Figure 7. Final prototype of the transformer integrated with rectifier.

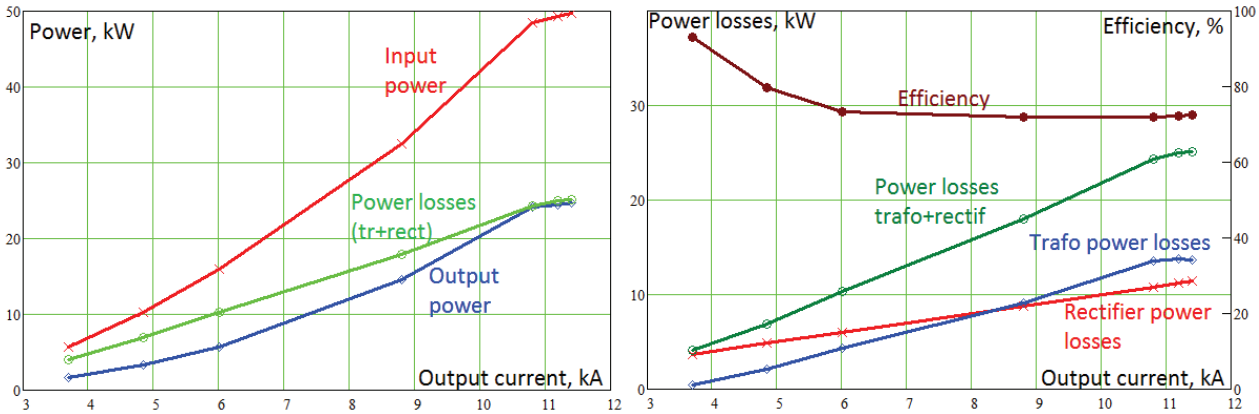


Figure 8. Power, power losses and efficiency measured at final prototype vs. output current.

ISBN 978-84-617–9183–5

One can observe that the power losses in the block of integrated transformer and rectifier is comparable to the output power (the efficiency of the bloc is about 50%). Taking into account nominal voltage drop at the diode in rectifier during carrying the current power losses in rectifier has been estimated. It is comparable to power losses in the transformer (at small output current power losses in rectifier are higher and at high output current they are slightly higher). Finally efficiency of the transformer has been determined. The efficiency of small currents is about 90% but it decreases with current and in the range of 6 to 11 kA of output current is near constant at the level of 75%. It very well confirms the efficiency calculated by FEM. Presented results shows that constructed transformer is a good candidate for application in DC spot welding machine.

V. CONCLUSIONS

Considered in the paper transformer is dedicated for DC spot welding machine and process. The results presented in the paper are based on numerical calculations and laboratory tests. Following conclusions can be drawn from the results of analysis:

1. Three different solutions of transformers have been proposed as a candidate for operation in welding system. Because of two diode rectifier connected to the output transformers have been designed as devices with two secondary windings
2. Planar transformer has been selected as a best candidate because of good coupling between windings and easy manufacturing process
3. Power and circuit properties of transformers have been calculated by FEM. 2D planar model has been used for calculations. The results shows better distribution of current density in planar transformer. The efficiency at operation point has been obtained at the level of 75%.
4. Laboratory tests on initial prototype confirmed importance of leakage inductance in the transformer. First prototype has the leakage inductance on the level of 10 H. It has been reduced more than twice in the final prototype.
5. Laboratory tests of final prototype confirmed possible operation with required level of output current. The maximum output current was about 15 kA. The efficiency determined under tests was about 75% and it very well fits to the efficiency calculated by FEM.

ACKNOWLEDGEMENT

Results presented in the paper have been obtained under work supported by the Polish National Centre for Research and Development (NCBR) with the project no. PBS3/B4/12/2015.

REFERENCES

[1] A. Ambroziak, M. Korzeniowski, *Using resistance spot welding for joining aluminum elements in automotive industry*, Archives of Civil and Mechanical Engineering, vol. X, no. 1, 2010, pp. 5-13.

[2] P. Shuai, J. Biela, *Design and Optimization of Medium Frequency, Medium Voltage Transformers*, European Conference on Power Electronics and Applications, EPE 2013, pp. 1-10.

[3] B. Grzesik, K. Bodzek, M. Stepien, *Modular transformer with any turn-to-turn ratio*, 13th International Symposium on Power Electronics, Novi Sad, Serbia&Montenegro, Nov. 2nd-4th, 2005.

[4] Z. Mikno, M. Stępień, B. Grzesik, *Optimising the operation of servomechanical force systems used in the joining of thin-walled metal elements in the automotive industry*, 2015 International Conference on Sustainable Mobility Applications, Renewables and Technology (SMART), Nov. 23-25, 2015, Kuwait.

[5] *Soft Ferrites and Accessories.* Data Handbook. Ferroxcube. July 2013.

[6] ANSYS User Manual, v. 15, 2014

ISBN 978-84-617–9183–5

Intelligent Transformers for Smart Grids

Goizeder PÁJARO, Oscar PICÓ, Miguel CUESTO

Regional Service Center for Transformers, ABB
Barrio Galindo s/n, 48510 Trapagaran, Vizcaya, Spain
e-mail: goizeder.pajaro@es.abb.com

Abstract— **Power transformers are one of the most important and expensive components of the electrical energy supply network. Future demands for increased power supply from a mix of generation sources will require Intelligent Transformers to support maintaining grid stability and to maximize reliability and availability.**

In this sense, recent development of solutions have aligned to the global concept of sustainability, providing more efficient transformers [1] with reduced environmental impact, and more reliable and transparent from an operational and maintenance point of view.

This paper presents the main technical challenges and the innovative solutions considered of interest for Intelligent Transformers, showing different approaches to address these requirements, including recent real cases of transformers with added-value solutions implemented. Challenges and advances in energy efficiency, use of ester dielectric fluids [2], intelligent monitoring [3] and asset management of power transformers and fleets will all be highlighted.

Finally an analysis of the current regulatory environment for each of the solutions mentioned above will be made, presenting recommendations for consideration in future revisions of international standards or working groups.

Keywords — **Power transformer, smart, intelligent transformers, energy-efficiency, environmental care, intelligent monitoring, transformer assessment.**

I. INTRODUCTION

Current environment in the power industry is partially due to the ageing of the infrastructures, with the following characteristics (among others):

- Majority of assets are > 30 years old
- Network short circuit power has changed (usually greater now)
- Knowledge of the assets may be reduced due to personnel turnover
- Limited maintenance being done and/or longer maintenance cycles with fewer outages
- Assets have varied loading
- Spare viability not always known
- More complex networks evolving due to renewable distributed generation

For all these reasons concepts like sensor technologies, monitoring and diagnostics, asset management solutions and expert services are continuously becoming more important. The main goal of this paper is to show the developments and state of the art regarding intelligent transformers, which cover the previously mentioned parts.

II. TRANSFORMER INTELLIGENCE

As explained in the introduction, the concept Transformer Intelligence® developed by ABB is structured in the way described in Fig. 1 on the following page:

ISBN 978-84-617–9183–5

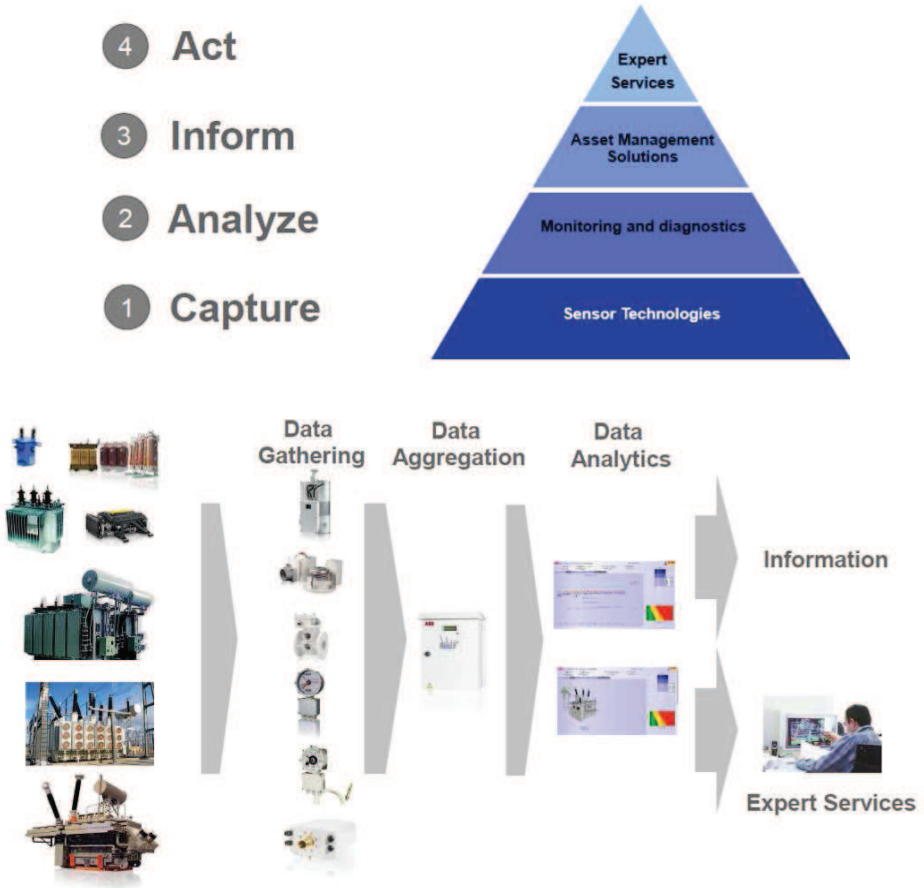


Figure 1. ABB Transformer Intelligence® conceptual definition.

This methodology has the following benefits:

- Optimize asset load, risk alerts and asset control online in real time, removing the analog lag time
- Drive condition based maintenance, ensuring money is only invested when and where it is needed
- Facilitate informed decision making about when to rehabilitate, repair or replace the transformer

In the following paragraphs each one of the levels contained in the concept will be explained in more detail.

III. SENSOR TECHNOLOGIES

The first step to enable intelligence to a transformer is to install a range of sensors that can detect symptoms of developing failures:

- Moisture and Hydrogen (see Fig. 2) or multi-gas monitor for online DGA.
- Oil level
- Oil and winding temperatures
- Bushing monitor
- Buchholz relay
- Load (current transformers)
- Air breather status
- On load tap changer parameters
- Cooling equipment operation: oil flow sensors, number of fans under operation, etc.

ISBN 978-84-617–9183–5



Figure 2. ABB Coresense™ device.

The compactness, reliability and low maintenance of these sensors together with a standardized connectivity (like Modbus RTU, Modbus IP, DNP3, IEC61850) are one of the main guidelines when developing new versions.

IV. MONITORING

The information recorded by the whole set of sensors previously described needs to be gathered by a monitoring system that will collect, store, organize, interpret and analyze data, and providing the following outputs:

- Early detection of malfunctions
- Overload assistance
- Real time data
- Remote access
- Stored data over long period
- Intelligent prognosis
- Advanced cooling control

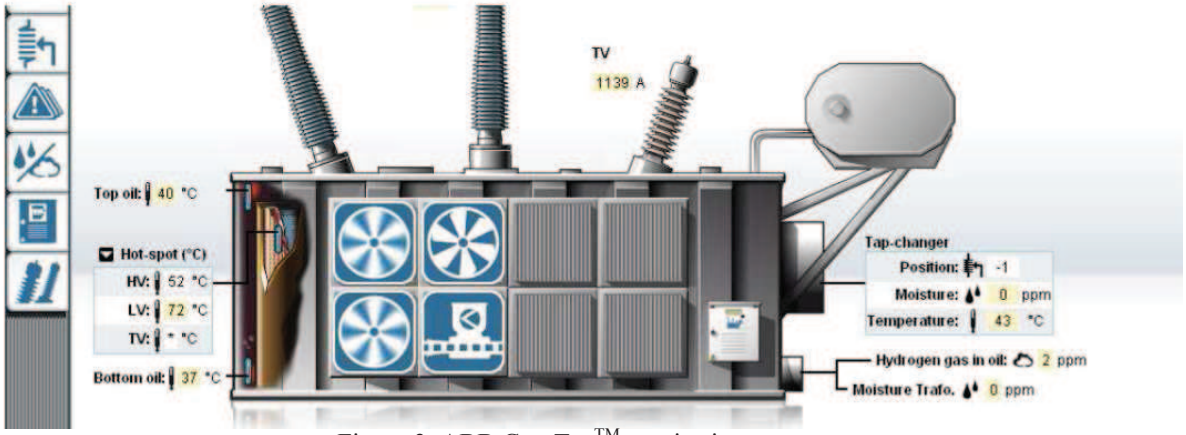


Figure 3. ABB CoreTec™ monitoring system.

V. ASSET MANAGEMENT SOLUTIONS AND EXPERT SERVICES

A method for assessment of large transformer fleets has been developed and successfully implemented in different cases. The main principles of this method are:

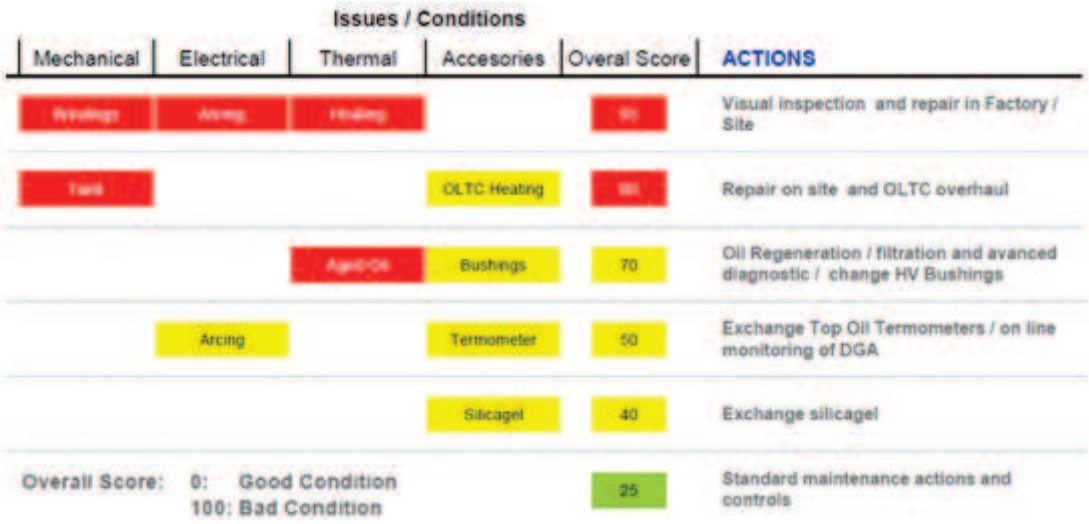
Analysis of transformer history. It consists of collecting the following information:

ISBN 978-84-617–9183–5

- Design data
- Information in the installed base system
- Results of the condition assessment
- Maintenance history

Condition and risk-assessment. From the combination of the analysis of transformer history and a basic diagnostic based on DGA the result will be a first fleet screening.

Taking into account all the transformer physical performance and the accessories a thorough condition evaluation could result as shown in the following example:



From the condition assessment the second step can provide for each evaluated transformer three different options:

- Normal condition: the transformer can be operated keeping the ordinary maintenance activities.
- Preventive: the condition of the transformer requires to take one or more actions.
- Urgent: in this case the operation of the transformer can be critical and an urgent action is needed.

Maintenance planning. Finally depending on the previous results a maintenance planning can be proposed like the following ones that summarize the life cycle of a transformer:

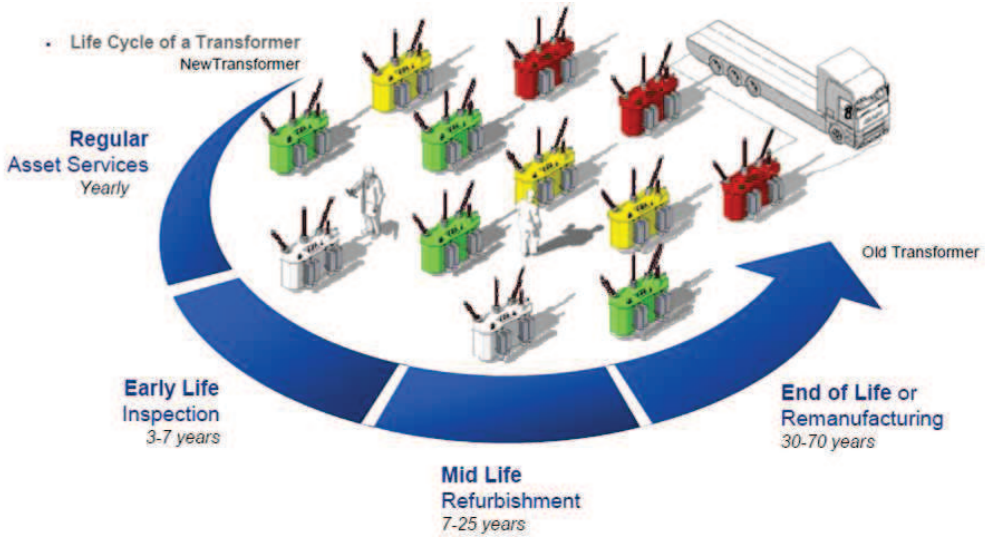


Figure 5. Example fleet assessment and maintenance planning.

ISBN 978-84-617–9183–5

The methodologies described above can also be included into fleet management software analysis tools which provide an overall view of your transformer fleet, highlighting those transformers at highest risk, and via an expert system recommending actions to mitigate risk. Fig. 6 below is an example of a typical system:



Figure 6. Example fleet assessment software showing DGA analysis of a transformer.

Expert services. On top of that and as a final complement for the concept of Transformer Intelligence®, the support of experts for activities such as design reviews, special testing and advanced diagnostics can be useful for certain cases.

VI. RETROFIT WITH ESTER FLUIDS

Finally and being a trend in transformers retrofit, it has been considered interesting to include a paragraph about retrofit of transformers with ester (biodegradable) oil.

Properties and pros/cons of ester fluids applied to transformers are well known and acceptance criteria are already properly addressed in the standards [2]. From technical point of view, there are several key aspects when considering the retrofit with this fluid of a transformer that was initially designed, manufactured and operated with mineral oil:

- Bushings
- Tap changer
- Cooling equipment
- Oil preservation system
- Materials compatibility
- Performance at very low temperatures

Regarding thermal evaluation and due to the higher viscosity of the ester fluids (especially at low temperatures) the result of the study may conclude in some recommendations about transformer power derating or alternatively upgrading the cooling equipment to keep the same power rating.

ISBN 978-84-617–9183–5

On the other hand it is important to remark than because of being the thermal class of ester oils higher than mineral oils, the combination of ester fluid with high temperature insulation can allow to increase the transformer rating keeping same weight and/or footprint. As an example please see below a real case:

- 26 year old, 15 MVA ONAF, 145 kV transformer
- Needed more power and overload capability but keeping same footprint to limit civil work
- Reduce risk of fire
- Solution developed: high temperature insulation combined with ester oil to replace mineral oil
- Result: upgrading tested up to 25 MVA, meaning 66% higher power rating

VII. CONCLUSIONS

Because of the current situation of ageing infrastructures and more complex networks, there is a real need of knowing the status of every transformer from performance and life expectancy point of views.

Taking advantage of the current technologies in both sensor and monitoring devices provides a more accurate and real time observation of the transformer performance.

These technologies, complemented with life expectancy that result from the condition assessment, are the basis to enable the presented Transformer Intelligence®, with the following main benefits:

- Ensure health and safety
- Reduce operating risks
- Optimize maintenance spend
- Secure longest life and best replacement strategy

The use of ester fluid in a transformers retrofit needs to be thoroughly evaluated before putting the transformer in service again. Depending on each case the final power rating of the transformer can be increased.

As a final remark it has been stablished a new Cigre working group about life extension (WG A2.55) to which maybe some of the methodologies and developments presented could contribute as a starting point. We will participate in this WG.

REFERENCES

[1] EU 548.2014 Implementing Directive 2009/125/EC of the European Parliament and of the Council with regard to small, medium and large power transformers. May 2014.

[2] IEEE C57.154-2012, IEEE Standard for the Design, Testing, and Application of Liquid-Immersed Distribution, Power, and Regulating Transformers Using High-Temperature Insulation Systems and Operating at Elevated Temperatures. Oct 2012.

IEEE C57.147. IEEE Guide for Acceptance and Maintenance of Natural Ester Fluids in Transformers. Jul 2008.

IEC 61099:2010, Specifications for unused synthetic organic esters for electrical purposes. Aug 2010.

IEC 62770:2013, Fluids for Electrotechnical Applications – Unused natural esters for transformers and similar electrical equipment. Nov 2013.

[3] IEC 61850-90-3, Communication networks and system for power utility automation. Part 90-3. Use of IEC 61850 for Condition Monitoring (Under release).

ISBN 978-84-617–9183–5

Measurements and Finite Element Model of Transformer Core Joints with DC and AC Excitation

Hilary K. CHISEPO[1], Leslie D. BORRILL[1, 2], C. Trevor GAUNT[1]

[1]Department of Electrical Engineering, University of Cape Town, South Africa, 7700
[2]Eskom Holdings, Cape Town, South Africa, 7441
e-mails: chshil001@myuct.ac.za; les.borrill@eskom.co.za; ct.gaunt@uct.ac.za

Abstract — **It is now well known known that geomagnetically induced currents (GICs) disturb the normal operation of power transformers. Half-cycle saturation of power transformers due to dc excitation causes stray flux to flow through structural parts, air space, and the tank - depending on the size of the GIC. This paper presents practical measurements and modelling of three industrially-made untanked single-phase four-limb transformers (1p-4L) resembling a real power transformer in terms of high quality grain oriented electrical core steel (GOES) and parallel winding assemblies. Ac testing was used to calibrate the FEM models before simulations with simultaneous dc and ac were run. Finite element models were useful for identifying areas of flux leakage under conditions of simultaneous dc and ac energization in the laboratory. The FEM and practical measurements were analyzed, and enable interpretation of the response of the test transformers' cores. This paper discusses why the core joint detail is an important consideration in FEM analysis with transformers exposed to GICs.**

Keywords — **geomagnetically induced currents, core joints, FEM, flux distribution**

I. INTRODUCTION

During a significant geomagnetic disturbance (GMD), geomagnetically induced currents (GICs) enter power transmission networks through grounded power transformer neutrals separated by long transmission lines [1]. GICs typically have a frequency in the order of milli-Hertz and are considered as quasi-dc currents in 50 or 60 Hz power systems [2]. Power transformers experience half-cycle saturation which gives rise to numerous unwanted conditions in power systems [1]-[3]. The transformer's active and non-active parts simultaneously experience excessive stray flux which may generate hot spots in the windings, tank and core, leading to insulation degradation and gassing [4]. In the same reference, GIC related failures in the Southern African network revealed that thermal damage can occur in three-phase power transformers even at low levels of GIC. As a result, South Africa's power utility, Eskom, now includes a dc withstand capability in transformer procurement specifications, and so do utilities in many other countries.

Three-phase three limb transformers have been widely perceived to be immune to GIC [5], [6]. However, more recently, the development of an enhanced transformer model led to the conclusion that GIC as low as 10 A/phase can saturate three-phase three limb power transformers due to the influence of the transformer tank, the air inside and structural parts [7], [8].

The main concern of the utilities is the overheating of power transformers and the draw of Mvar, but factory verification testing with dc is mostly impractical and is not widely applied. Design models that can positively impact transformer survival with predefined levels of GIC would be of great value to manufacturers to meet some of the specifications. Moreover, establishing a relationship between the level of GIC and the increased Mvar drawn by the transformer will assist utilities in power system analysis.

Some FEM studies have been reported, resulting in a good understanding of core saturation in different transformer types [5], [9]-[13]. Not all studies represent the transient characteristic of a real GIC, a transformer with simultaneous voltage driven ac-dc energization (i.e. GIC entering through the neutrals of three-phase transformer), validation with measurement results, or the effects of core joints. This paper presents the calibration of 2D FEM models based on laboratory measurement data taken from an adjacent study [14] on three single phase four limb (1p-4L) transformers. Results show that it is important to incorporate the concept of an equivalent air gap at the core joints in order to get a more realistic FEM model.

ISBN 978-84-617–9183–5

II. MODELLING APPROACH

A preliminary FEM simulation protocol was developed based on measurement data from three different bench-scale core structures of three single phase and two three phase transformers with three and five limbs (209/400 V, 300 VA, 3x1p-3L, 3p-3L, 3p-5L) [15]. GIC-like conditions were modelled with a dc voltage source injected in the neutrals of the transformers and all the experiments were performed in the transient domain to accommodate simultaneous ac and dc signals. Good correlation with the electrical measurement data was observed for reactive power (var) with varying dc, but the simulated no load magnetizing currents were consistently lower than measured for all the bench-scale physical transformers.

As part of a broad study of transformer response to GICs, practical measurements and various approaches to modelling transformers were then carried out on three industrially-made transformers without tanks. Conventional design calculations defined an 8.3 kVA, 209/390 V transformer. However, it was stacked with conventional butt joints and so the nominal rating was reduced to 110/206 V, 4.4 kVA after practical ac tests [14].

With nominal ac voltage applied, various levels of dc were injected to test the transformer response. In addition to numerous electrical measurements, search coils (SCs) were placed on the core as shown in Fig. 1, i.e. at the joints (SCs 60, 70, 80,100) and air spaces in the inner windows (SCs A-E). Analysis from some preliminary FEM flux density vector plots led to more air SC's being placed outside the transformer yoke at the T-joint with the wound limbs, namely Y1 and Y2, tightly against the core joints.

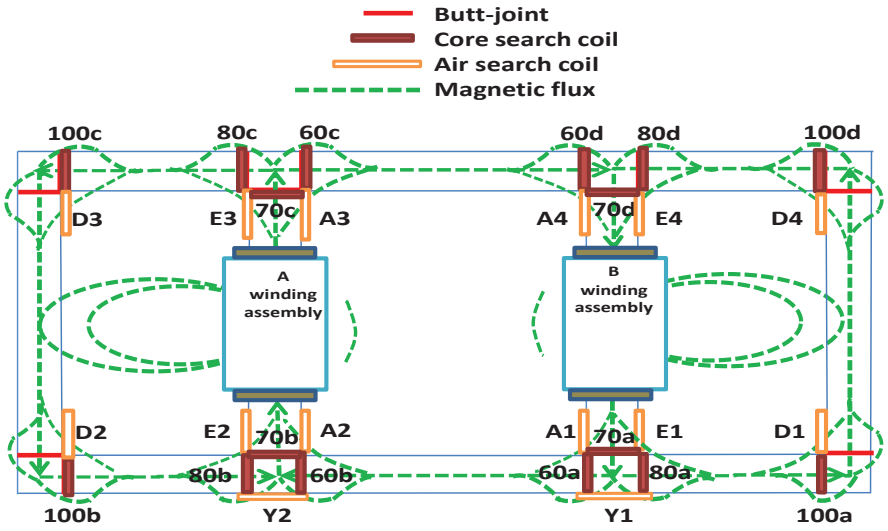


Figure 1. Placement of search coils on 1p-4L test transformers and determination of (leakage) flux in the laboratory.

The measured SC output voltages under conditions of ac excitation only, and ac and dc excitation were compared with the results from the FEM simulations of a core with fully modelled gaps at the joints. These measurements were used to adjust progressively the FEM model of the transformer until the same flux densities were obtained at all points in and around the core. Small differences between the measurements of the three 1p-4L transformers (TRFR 1, 2 and 3) provided data to vary the joint details to test the sensitivity of the FEM. It was clear that the joint details had a significant effect on the flux distribution.

Three cases of FEM models, shown in Table I, were constructed. The first is a core with solid joints without air gaps as represented in several publications. The second has air gap details based on that derived from the physical tests. The third case extends the gap model to a core with mitred joints typical of conventional power transformers. The purpose of the FEM analysis of the three cases was to determine whether the gap details make a significant difference in the flux distributions in an around a core.

Table I. Variations of Core Joint Detail Modelled in FEM

FEM study detail	ABBR.	Lab. Meas. for validation?	FEM Mesh Type
Solid core joints (No air gap)	FEM S	No	Refined Uniform
Butt joint with Equivalent Air Gap	FEM B-AG 1,2	Yes	Refined Uniform
Mitred joint with Equivalent Air Gap	FEM M-AG	No	Refined Uniform

ISBN 978-84-617–9183–5

The voltage at which saturation inception occurred at the joints of the three test transformers (V_{app}), TRFR 1, 2 and 3, was identified to occur at approximately 120/225V, based on air search coil measurements at the joints [14]. Various FEM models were tested with AC only at this inception voltage. FEM B-AG 1 is the model with a uniform equivalent air gap at the joints and FEM B-AG 2 is the model with the some air gaps at the joints adjusted to match, as closely as possible, the measured results due to unequal air gaps in the real transformers and it is arbitrarily based on TRFR 2.

III. RESULTS

A. AC results for calibration of FEM model

Fig. 2 shows the results of modelling the transformer with no air gap at the joint.

The FEM output in Fig. 3 illustrates the results when core joint detail is applied and is comparable with the measurements in Fig. 1. Comparison of the two plots indicates the solid joints produce significantly lower flux outside the transformer than when realistic airgaps are introduced. The extra leakage flux driven outside the core by air gaps at the joints is consistent with the measurements of the physical transformers.

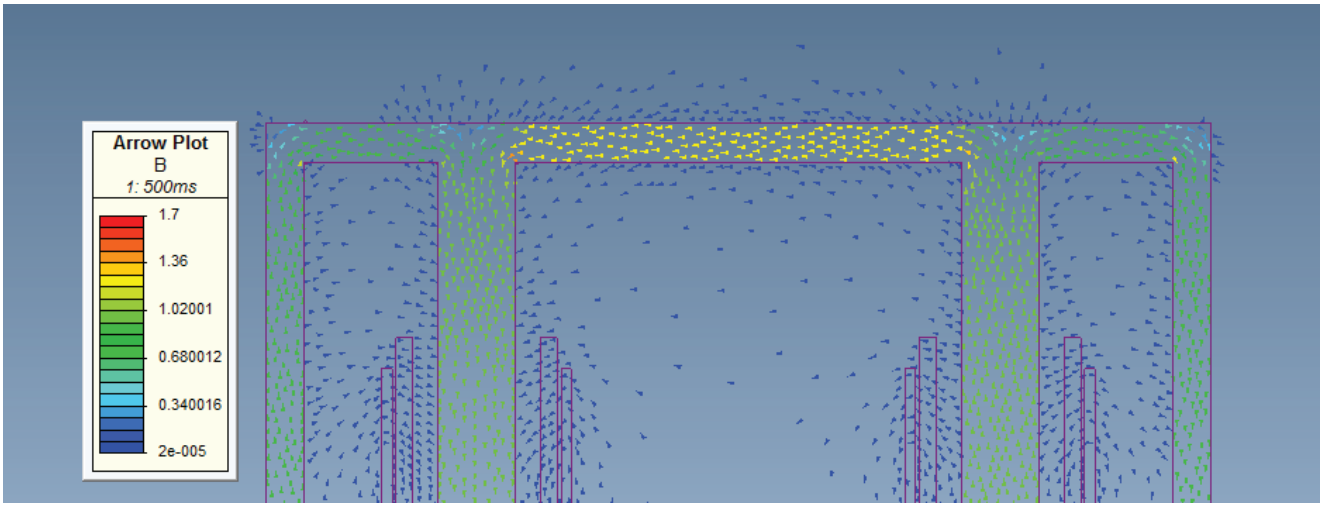


Figure 2. Flux distribution at V_{app} for FEM S without equivalent air gap at the core joints.

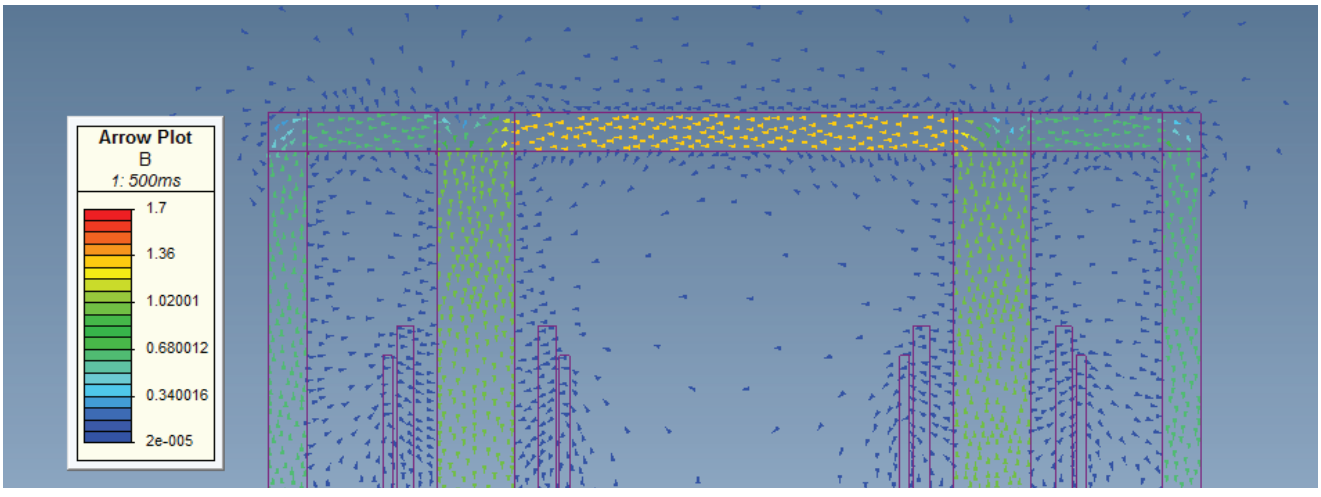


Figure 3. Flux distribution at V_{app} for FEM B-AG 1 with equivalent air gaps of equal dimensions.

Table II illustrates that a model with no air gap at the joints (FEM S) underestimates the magnetizing current I_{mag} at no load when compared with various measured results. The incorporation of an equivalent air gap (FEM B-AG 1, FEM B-AG 2) at the joints yields an I_{mag} comparable with the laboratory TRFRs.

When the same equivalent air gap is applied at the joints of the mitred model (FEM M-AG), there is a slight increase in the I_{mag} and the core losses are lower than with the butt joints, as expected.

ISBN 978-84-617–9183–5

Table III presents some search coil data with AC excitation only. The most important results here are that for FEM S, solved as an air tight butt joint core in the FEM domain, hardly any leakage flux is seen at SC A whereas there is a comparable leakage flux seen with the measured data for FEM B-AG 1 and FEM B-AG 2. FEM M-AG has a very small leakage flux when compared with the other joint configurations at this joint, as expected, but this shows that even mitred joints show a different response when an equivalent air gap applied.

Table II. Table Showing the AC Only Open Circuit Parameters of the Laboratory Transformers and Various FEM Models

Transformer	V_{in} RMS [V]	I_{mag} RMS [A]	P_{oc} [W]	Vout RMS [V]
TRFR 1	120	0.902	74	224
TRFR 2	120	0.836	70	224
TRFR 3	120	0.968	76	225
FEM S	120	0.334	75.8	225
FEM B-AG 1	120	0.909	76	225
FEM B-AG 2	120	0.891	76	225
FEM M-AG	120	0.528	68.4	225

Table III. Table Showing SC Coil RMS Voltage Measurements at V_{app}

Transformer	70 [V]	60 [V]	80 [V]	100 [V]	A [V]	E [V]	D [V]
TRFR 1	1.493	0.906	0.662	0.662	0.016	0	0
TRFR 2	1.498	0.914	0.642	0.642	0.014	0	0
TRFR 3	1.495	1.039	0.890	0.668	0.018	0.011	0
FEM S	1.466	0.955	0.515	0.515	0	0	0
FEM B-AG 1	1.460	1.039	0.424	0.424	0.011	0.007	0.006
FEM B-AG 2	1.460	1.004	0.458	0.458	0.011	0.007	0.006
FEM M-AG	1.462	1.036	0.437	0.437	0.004	0.004	0.002

A. Ac and dc results

The previous section showed that during ac excitation (at the commencement of symmetrical saturation) it is important to consider how the FEM core joints should be modelled in order to get a better representation of the actual transformer response. During severe GMDs stray flux cutting across the windings and, or leaking into the other parts of the transformer is one of the main factors affecting transformer survival or onset of degradation. This section presents results with ac and dc excitation whereby leakage flux measured results from TRFR 2 are compared with those of FEM S and FEM AG 1, 2 to investigate the effect of the core joint detail in conditions of half-cycle saturation. The mitred model is not considered here due to non-availability of test data for comparison.

Table IV. Table Showing Search Coil RMS Voltage Measurements with AC and DC Present

TRFR/FEM	DC (Amps)	SC A [V]	SC E [V]	SC D [V]
TRFR 2 actual	0	0	0	0
FEM S	0	0	0	0
FEM B-AG 1	0	0	0	0
FEM B-AG 2	0	0	0	0
TRFR 2 actual	1	0.174	0.136	0.064
FEM S	1	0.001	0.001	0.001
FEM B-AG1	1	0.100	0.070	0.025
FEM B-AG 2	1	0.110	0.075	0.026
TRFR 2 actual	7	0.326	0.276	0.167
FEM S	7	0.005	0.005	0.005
FEM B-AG1	7	0.227	0.180	0.110
FEM B-AG 2	7	0.230	0.183	0.111

ISBN 978-84-617–9183–5

It can be seen in Table IV that at nominal voltage (110 V RMS) without dc the search coil output voltages are all zero signifying that all the flux is contained in the core. When a dc component of 1 A is introduced the transformer starts to get saturated and when 7 A is injected the transformer is in deep saturation. By contrast, the FEM S simulation without any core joint detail does not show the leakage, with the SC outputs virtually zero for all dc levels.

FEM B-AG 1 with a uniform equivalent air gap at the joints and FEM B-AG 2 with equivalent air gaps calibrated according to ac tests on TRFR 2 show that there is significant flux leakage into the air space that is not represented by the FEM S model in the presence of ac and dc. Fig. 4 shows that though the FEM SC output voltages are consistently lower than the measured ones, they follow the same trend during half cycle saturation.

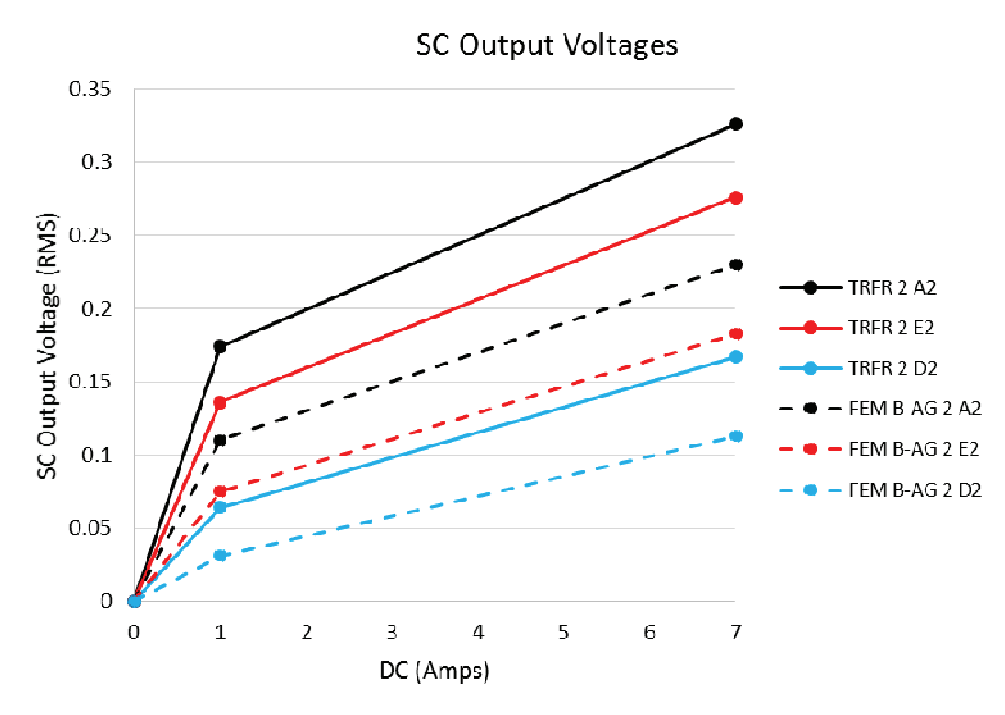


Figure 4. Measured and FEM air SC output voltages with simultaneous ac and dc excitation.

IV. DISCUSSION

The results showed that the incorporation of core joint detail and the inclusion of an equivalent air gap yield better results in 2D FEM simulation than modelling the transformer without that detail. Having gained confidence in the 2D models, simultaneous ac and dc energization was simulated in FEM with the same dc injection range as measured practically [14].

The 2D ac-dc FEM results do not completely correspond with the actual measurements, as illustrated by the differences in Fig. 4. It is expected that better correlation might be achieved with 3D FEM analysis incorporating equivalent air gaps.

The increase in flux outside the core has not taken into account the effects of tank walls and structural parts of the transformer. These are expected to add further to the influence of the core joints, and the importance of modelling them correctly, as demonstrated by this comparison of simulation and measurement.

V. CONCLUSIONS AND FUTURE WORK

Calibrating a 1p-4L FEM transformer model with ac measurement data resulted in a more realistic model that could be used to analyse transformer behaviour during ac-dc excitation. As a first approximation for the response, a 2D model was developed specifically to investigate the effect of the joints. Future work involves similar investigations in 3D with greater detail in the magnetic properties of the core material and lamination stacking. Results from these should contribute to better understanding of the actual conditions in power transformers during GMDs such as the effect of the tank and structural parts, orientation of the stray flux

ISBN 978-84-617–9183–5

through the windings (B_x, B_y, B_z), and the possible effects on the initiation of degradation in the presence of dc and GICs.

ACKNOWLEDGEMENTS

The test transformers, core and winding dimensions data and required material properties were provided by Royal Smit Transformers Netherlands. Infolytica Corporation supplied an academic license for FEM simulation and support. Eskom provided testing facilities at Brackenfell.

REFERENCES

[1] V. D. Albertson, B. Bozoki, W. E. Feero, J. G. Kappenman, E. V. Larsen, *et al., Geomagnetic Disturbance effects on power systems*, IEEE Trans. Power Delivery, vol. 8, no.3, pp. 1206-1216, July 1993.

[2] P. R. Price, *Geomagnetically induced current effect on transformers*, IEEE Trans. Power Del. vol. 17, no 4, pp. 1002-1008. October 2002.

[3] J. G. Kappenman and V. D. Albertson, *Bracing for the geomagnetic storms*, IEEE Spectr., vol. 27, no. 3, pp 27-33, March 1990.

[4] C. T. Gaunt and G. Coetzee. "Transformer failures in regions incorrectly considered to have low GIC-risk," in *Proc. 2007 IEEE PowerTech*. Lausanne, Switzerland, pp. 807-812.

[5] N. Takasu, T. Oshi, F. Miyawaki, S. Saito, and Y. Fujiwara, *An experimental analysis of dc excitation of transformers by geomagnetically induced currents*, IEEE Trans. Power Del., vol. 9, pp. 1173–1182, April 1994.

[6] M. A. S. Masoum and P.S. Moses, *"Impact of balanced and unbalanced direct current bias on harmonic distortion generated by asymmetric three-phase three-leg transformers,"* IET Elect. Power Appl., vol. 4, no. 7 pp. 507-515, 2010.

[7] A. Rezaei-Zare, *Enhanced transformer model for low- and mid-frequency transients - Part I: Model Development*, IEEE Trans. Power Del. vol. 30, no. 1, pp. 307-315, January 2015.

[8] A. Rezaei-Zare, *Enhanced transformer model for low- and mid-frequency transients - Part II: Validation and simulation results*, IEEE Trans. Power Del. vol. 30, no. 1, pp. 316 - 325, January 2015.

[9] N. Takasu, T. Oshi, F. Miyawaki, S. Saito, and Y. Fujiwara, *An experimental analysis of dc excitation of transformers by geomagnetically induced currents*, IEEE Trans. Power Del., vol. 9, pp. 1173–1182, April 1994.

[10] M. A. S. Masoum and P.S. Moses, *"Impact of balanced and unbalanced direct current bias on harmonic distortion generated by asymmetric three-phase three-leg transformers,"* IET Elect. Power Appl., vol. 4, no. 7 pp. 507-515, 2010.

[11] S. A. Mousavi, "Electromagnetic modelling of power transformers with dc magnetization," Licentiate thesis, Div. of Electromagnetic Eng., Royal Institute of Technology, Sweden. pp. 48-66, 2012.

[12] O. Bíró, G. Kockza, G. Leber, K. Preis, B. Wagner, *Finite Element Analysis of Three-Phase Three Limb Power Transformers under DC Bias,* IEEE Trans. Magnetics vol. 50, no. 2, February 2014.

[13] O. Bíró, G. Buchgraber, G. Leber and K. Preis, *Prediction of Magnetizing Current Wave-Forms in a Three-Phase Transformer Under DC Bias,* IEEE Trans. Magnetics vol. 44, no. 6, pp. 1554-1557, June 2014.

[14] L. D. Borrill, H. K. Chisepo and C.T. Gaunt, *Flux measurements with ac and dc components of current present show transformer equivalent circuit models need core joint details,* In Proc. IEEE POWERCON, Wollongong, Australia, September 2016.

[15] H. K. Chisepo, "*The response of transformers to geomagnetically induced currents*," M.Sc. dissertation, Dept. Elect. Eng., Univ. Cape Town, South Africa, 2014. Available at: https://open.uct.ac.za/handle/11427/111/browse?value=Chisepo%2C+Hilary+K&type=author [07 October 2015]

Use of the Hot-Spot Temperature in Determining Health Indices of Power Transformers

Félix ORTIZ, Fernando DELGADO, Agustín SANTISTEBAN, Cristina FERNÁNDEZ, Alfredo ORTIZ

Department of Electrical and Energy Engineering, University of Cantabria
Avenida Los Castros (ETSIIndustriales), 39005 Santander, Spain
Phone: (+34) 942201374, fax: (+34) 942201385, e-mail: ortizfa@unican.es

Abstract — **This paper proposes the modification of a health index that is applied to the status evaluation of fleets of transformers. Health indices usually consider the results of the tests performed on samples of dielectric oil that cools these machines. The most critical part of the transformer insulation is the dielectric paper covering the conductors forming part of the windings. Its life depends on the temperature that supports during operation. This temperature can be determined from studies based on the finite element method. The highest temperature suffered by the paper is located in the so-called hot spot of the windings. This paper proposes consideration of the hot-spot temperature in determining the health status of fleets of transformers.**

Keywords — **health index, hot spot temperature, degree of polymerization**

I. INTRODUCTION

Although transformers are very efficient devices, their rated performances being above 99%, the fact of being energized 24 hours a day throughout the year and that its operational life usually ranges from 20 to 40 years, means that these machines are the second component with higher losses in the grid. Their losses are estimated to account for 36% of all global losses in the transmission and distribution network. The impact of these losses is not confined exclusively to an economic cost, Harrison [1]. Globally, around 1056 million tons of CO2-equivalent greenhouse gas emissions can be associated with these losses, European Copper Institute [2].

In most of the developed countries, various agreements are nowadays requiring more rational use of energy. Diverse initiatives are being implemented to reduce the overall energy consumption. The European Union has promoted the Directive 2009/125/EC establishing a framework for setting ecodesign requirements applicable to energy-related products, European Parliament [3]. Considering power transformers, the European Union have published the Commission Regulation 548/2014, European Parliament [4]. This establishes the energy efficiency limits to be fulfilled by these machines. These limits are going to be applied in two steps. The first limits must be considered for machines bought from July 2015. In 2021 the limits will be updated towards more restrictive values.

The operation of power transformers is characterized by a certain efficiency. A low efficiency means a loss of power and a heat transfer process. Power transformers have a working point where the losses are minimal and the performance maximum. Thus, in any operating point where the load exceeds the optimum performance, the losses will increase, and accordingly, the working temperature inside the machine. This situation causes that windings and oil increase their temperature, and therefore their degradation. Specifically, it is the dielectric paper the material that suffers greater deterioration with increasing temperature. In this way, it seems necessary to predict, as accurately as possible, the value and location of the highest temperature (hot spot) of the paper that covers the windings, as it will be at that point where that paper suffers further degradation.

As it was stated in the previous para graph, the state of the insulation system is the major factor influencing the performance of the transformer. Most transformers have an electrical insulation system based on oil and paper. During service the dielectric materials within the transformer deteriorate, and small concentrations of impurities such as water, carbon monoxide, carbon dioxide and furan compounds accumulate in the oil. Since it is easy to obtain oil samples from power transformers, the information most commonly collected by transformer fleet managers relates to the physical and dielectric properties of the oil. These properties include dielectric strength, dissipation factor, colour and interfacial tension, and concentrations of dissolved gases, furans, acids and moisture.

ISBN 978-84-617–9183–5

Using these properties it is possible to determine whether a transformer has developed certain specific faults, e.g., partial discharges, arcing, sparking, overheating, etc. In this way, various health indexes have been proposed in order to characterize the general condition of a transformer, Haema [5], Jahromi [6] and Pradhan [7]. The factors taken into account in these indexes vary, and are given different statistical weightings depending on their influence on the general condition of the transformer.

None of the health indices published up to now have taken into account the temperature of the hot spot of the windings, which ultimately is the most unfavourable parameter regarding insulating paper degradation. This paper is intended to lay the groundwork for introducing this concept in health indices.

II. HEALTH INDEX

The health index that will be considered as the basis for this proposal is described below, Li [8]. It consists of four subindexes. The first subindex I(1) is concerned with the state of the insulating paper in the transformer, and consists of two factors. The first of these, HI(C,O), is concerned with the concentrations of CO and CO2 dissolved in the transformer oil, and the second, HI(fur), is concerned with the concentrations of furans in the oil.

$$I(1) = 0{,}3 \cdot HI(C,O) + 0{,}7 \cdot HI(fur) \tag{1}$$

The second subindex I(2) is concerned with the concentrations of five gases dissolved in the oil, namely H_2, CH_4, C_2H_6, C_2H_4, and C_2H_2, and is given by:

$$I(2) = \sum_{j=1}^{5} w_j \cdot F_{C,H\,(\mathrm{j})} \tag{2}$$

The third subindex I(3) is based on acid content of the oil (expressed as the mass of KOH required to neutralize 1g of oil), its dielectric strength, moisture content and dielectric loss, as given in:

$$I(3) = \sum_{j=1}^{4} w_j \cdot F_{oil\ (\mathrm{j})} \tag{3}$$

The fourth subindex I(4) is concerned with the age and loading of the transformer, and is given by:

$$I(4) = HI(0) \cdot e^{B \cdot (t_2 - t_1)} \tag{4}$$

where HI(0) is an initial factor, B is an aging coefficient, t_1 is the year in which HI(0) was evaluated, and t_2 is the year in which the state of the transformer is now being evaluated. HI(0) is related to the condition of the transformer when it entered service, and its value is usually 0.5, whereas it is about 6.5 when the transformer reaches the end of its service lifetime. With these values and the expected lifespan, t_{exp}, provided by the manufacturer, B can be determined using the following equation:

$$B = f_L \cdot \frac{\ln(6{,}5/0{,}5)}{t_{\exp}} \tag{5}$$

This expression depends on the load, f_L, at which the transformer operates. Finally, the overall health index I_2 is given by:

$$I = \sum_{i=1}^{4} k_i \cdot I(i) \tag{6}$$

where the weights k_1 (state of the insulating paper), k_2 (concentrations of five dissolved gases in the oil), k_3 (acid content of the oil) and k_4 (age and loading of the transformer) are 0.2661, 0.0946, 0.0699 and 0.5695 respectively. I lies in the range 0-10. The overall condition of the transformer, based on the value of I, is listed in Table I.

ISBN 978-84-617–9183–5

Table I. Transformer Condition as a Function of the Health Index

I	Condition
0 – 3.5	Very good
3.5 – 5.5	Good
5.5 – 7	Bad
7 – 10	Very bad

III. Methodology Proposed

The previous health index could be improved by considering the load index at which the machine is operating. Here, it is described the methodology followed by this study:

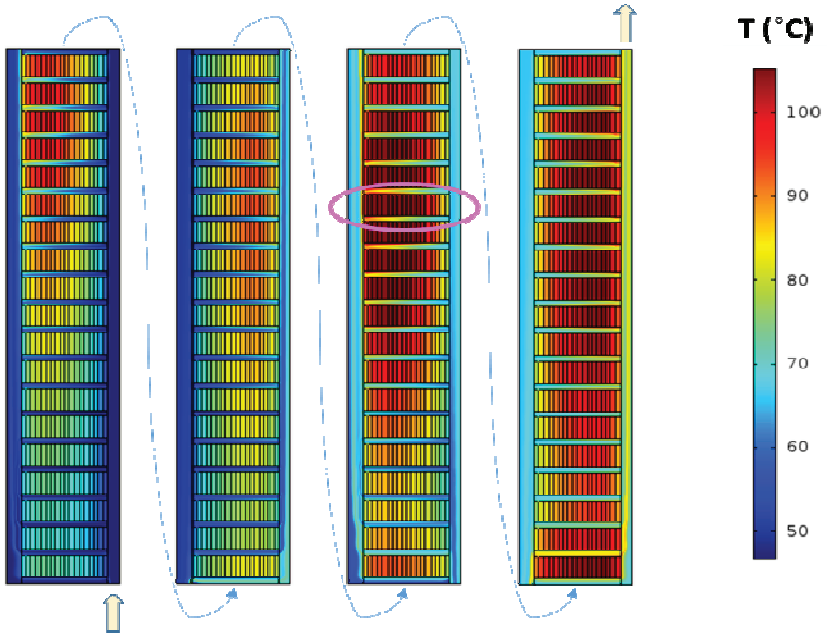


Figure 1. Determination of the hot spot temperature in the windings of a transformer.

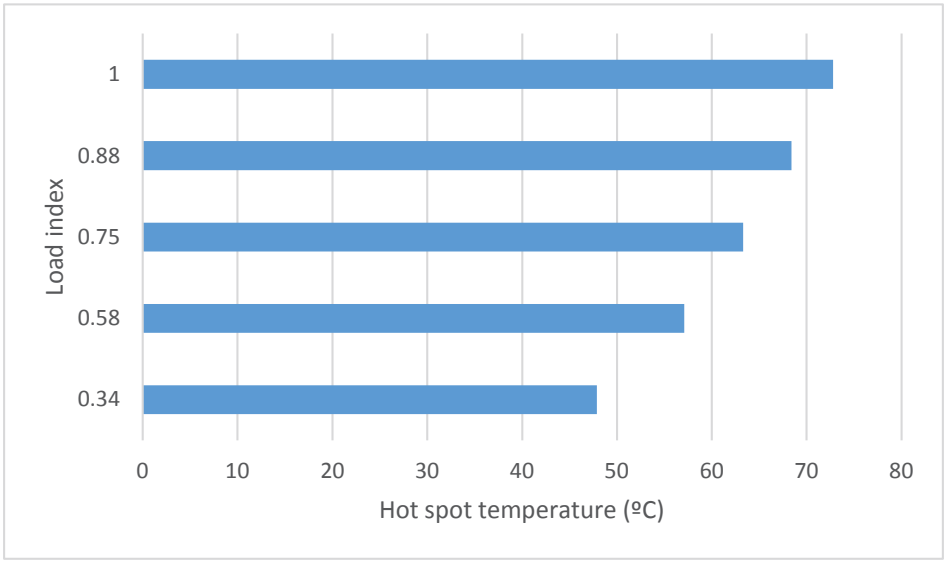


Figure 2. Evolution of the hot spot temperatures depending on the load index.

• The hot-spot temperature is determined by a software based on finite element method, in which the geometry of a transformer winding is inserted, a fluid-thermal model that considers the load level and the characteristics of the materials making up the winding, Fig. 1.

ISBN 978-84-617–9183–5

• Subsequently, the heat source is modified, ie the level of current flowing through the conductors of the winding. The heat produced by the windings is calculated, considering different values of current. These values are in a range from the optimal load up to full load.

• As a result of the previous step, an equation relating the load index with the hot spot temperature, and therefore, with the rate of aging of the insulation system of a transformer is obtained, Fig. 2.

• Using the above expression, the load factor f_L, corresponding to any value of current demanded, can be calculated more accurately. This will serve to obtain the aging coefficient defined by the health index proposed by Li [8].

IV. CONCLUSIONS

Health indices applied to transformer fleets tend to use the results of physicochemical analysis, dissolved gases and furan compounds. Some of these indices also consider the actual age of the machines, along with the load index. However, the load index is not related to any physical quantity directly involved in aging transformers. This work has presented a methodology which introduces the effect of the hot-spot temperature of windings in the calculation of the health index of transformers. To calculate this temperature is necessary knowledge of geometry and materials of the windings, for the subsequent application of finite element method.

REFERENCES

[1] Harrison, G.P., Maclean, E.J., Karamanlis, S., Ochoa, L.F. *Life cycle assessment of the transmission network in Great Britain.* Energy Policy 38, 3622-3631, 2010.

[2] European Copper Institute. *PROPHET II: The potential for global energy savings from high-efficiency distribution transformers,* 2014.

[3] European Parliament. Directive 2009/125/EC of the European Parliament establishing a framework for the setting of eco-design requirements for energy-related products, 2009.

[4] European Parliament. Commission Regulation (EU) No 548/2014 on implementing Directive 2009/125/EC of the European Parliament and of the Council with regard to small, medium and large power transformers, 2014.

[5] J. Haema, R. Phadungthin, *Development of Condition Evaluation for Power Transformer Maintenance,* Int. Conf. on Power Eng., Energy and Electr. Drives, pp. 620-623, 2013.

[6] A. N. Jahromi, R. Piercy, S. Cress, J. Service, W. Fan, *An Approach to Power Transformer Asset Management Using Health Index,* IEEE Electr. Insul. Mag., vol. 25, no. 2, pp. 20-34, 2009.

[7] [3] M.K. Pradhan, T.S. Ramu, *"On the Estimation of Elapsed Life of Oil-Immersed Power Transformers"*. IEEE Trans. Power Del. vol. 20, no. 3, pp. 1962-1969, 2005.

[8] Li, E., Song, B. *Transformer health status evaluation model based on multifeature factors.* International Conference on Power Systems Technology, pp. 1417-1422, 2014.

ISBN 978-84-617–9183–5

Determination of Three-Phase Three-Legged YNynd Transformer Zero-Sequence Impedance from Design Data

Elmer SORRENTINO

Universidad Simón Bolívar
Caracas, Venezuela
e-mail: elmersor@usb.ve

Juan Carlos BURGOS

Electrical Engineering Department
Universidad Carlos III de Madrid, Madrid, Spain
e-mail: jcburgos@ing.uc3m.es

Abstract — **Eight values of zero-sequence impedances of three-phase three-legged YNynd transformers are obtained from design data by using Finite Element Method (FEM). These values correspond to those obtained from standardized tests, by applying IEEE Std. C57.12.90 when tertiary delta winding is open (4 tests) or closed (4 tests). Two of these values are magnetizing impedances (Z_{0M}), and four values are short-circuit impedances (Z_{0SC}). The main problem in case of Z_{0M} is to consider properly the non-linearity of the tank steel. The main problem in case of Z_{0SC} is to obtain the currents in the short circuit windings. These impedances were computed by using approximate 2D FEM models. An exact 2D representation is not possible because the transformer is a 3D asymmetric apparatus. The results were validated by comparison with values obtained from zero-sequence tests in real transformers.**

Keywords — **Zero-sequence transformer impedances, three-phase three-legged transformers, FEM**

I. INTRODUCTION

Zero-sequence impedances (Z_0) of three-phase three-legged transformers can be classified as [1] magnetizing impedances (Z_{0M}) and short circuit impedances (Z_{0SC}). The standardized procedure to measure Z_0 is by feeding a wye winding with zero-sequence voltage [2-4]. In case of Z_{0M}, the current flows only by the winding connected to the source.In case of Z_{0SC}, there are zero-sequence induced currents in other windings. In YNynd transformers, Z_{0SC} can be measured with zero-sequence currents in only two windings, or in the three windings.

In three-phase three-legged units, Z_{0M} is non-linear and Z_{0M} values are different whether they are measured in outermost or innermost winding. Nonlinearity of Z_{0M} is mainly related to tank steel, and induced currents in tank can be very high because the sum of zero-sequence magnetic fluxes is not null inside the tank. Resistive component of Z_{0M} is not negligible, and it is strongly related to tank losses during the test for measuring Z_{0M}. In the literature, tank losses have been mainly computed for the case of positive-sequence impedances of transformers (Z_+), but there are important differences between tank losses for cases of Z_+ and Z_{0M} [5].

In three-phase three-legged transformers, nonlinearity of Z_{0SC} is seldom considered [6]. Only [7] shows that Z_{0SC} has a slight dependence on the current during the test. In general, nonlinearity of Z_0 is mainly related to tank steel. Resistive component of Z_{0SC} had not been considered in the literature. Power losses during Z_{0SC} tests mainly depend on currents in each winding, and on tank losses.

Different numerical methods have shown to be reliable as tools for design and analysis of transformers. However, specific literature about calculation of Z_0 is not abundant. Axial symmetry does not exist in 3D geometry of three-phase three-legged transformers. Therefore, 3D modeling should be applied, but it implies a huge size for the numerical problem because tank dimensions are much larger than skin depth for tank steel. For the sake of simplicity, some authors applied 2D simplified models for this problem but a systematic correlation between 2D and 3D geometries was not previously available.

In this paper, time-harmonic analysis was applied to 2D and 3D models, with the help of a FEM software [8]. This paper can be seen as a summary of findings from previous articles about for Z_{0M} [5] and Z_{0SC} [6]. The main differences between applying 2D models for Z_{0M} and Z_{0SC} are: a) the main problem for Z_{0M} is the nonlinearity, while the main problem for Z_{0SC} is the calculation of induced currents; b) the correlation between 2D and 3D geometries is much more important for Z_{0M} than for Z_{0SC}.

ISBN 978-84-617–9183–5

II. BASIC CONDITIONS FOR SIMULATIONS

II.1 ANALYSED GEOMETRIES

The analyzed 2D model is axis-symmetrical (Fig. 1a). On the other hand, a realistic simplified 3D model can be analyzed with the asymmetric geometry of Fig. 1b. Horizontal distances to the tank are different in real 3D cases; therefore, one "equivalent" horizontal distance (d) between tank and outermost winding must be considered in the 2D model. There are different options for an average value for d (d_{AVG}). Here, d_{AVG} is computed in order to obtain an area between outermost winding and tank (2D model) equals to one third of the real area between outermost windings and tank (Fig. 2).

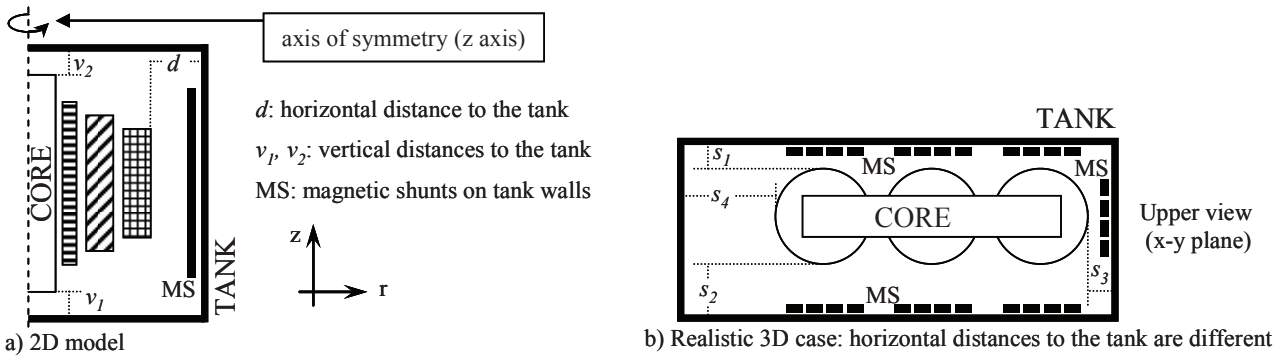


Figure 1. Details of 2D and 3D geometries.

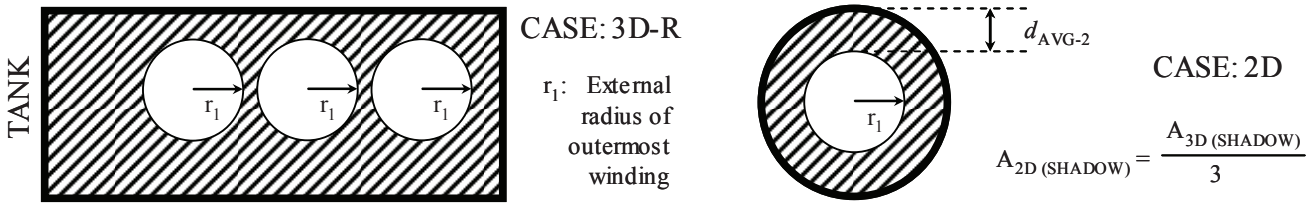


Figure 2. Auxiliary scheme to illustrate the definition of d_{AVG}.

II.2 MATERIAL PROPERTIES

Tank conductivity (σ_T) is assumed to be constant. An equivalent relative permeability for the tank (μ), constant in the tank thickness, is assumed. Transformer core and magnetic shunts on tank walls are simulated with a high magnetic permeability and a null value for the electrical conductivity, because they are made with sheets of high-permeability steel and the effect of eddy currents in them is negligible. Each transformer winding is simulated with a constant current density (in the rectangles illustrated in Fig. 1a) and a null value for the electrical conductivity, because each winding is formed by many subconductors, with practically the same current in each subconductor (i.e., eddy currents are avoided in the simulation of these rectangles, to obtain a constant current density).

II.3 COMPUTED VALUES FOR THE COMPARISONS

Values to be compared are reactances (X) and active power losses (P) during Z_0 tests. In case of Z_{0M}, P is related to tank losses added to winding losses and core losses. Winding losses are not included in models (they are independently estimated with the winding resistances), and core losses are considered negligible. Thus, only eddy losses in tank are considered in the models. In case of Z_{0SC}, tank losses (P_T) are obtained from the FEM software, and winding losses (P_W) during the tests are computed with the current of each winding and winding resistances. Thus, active power losses (P) during the Z_{0SC} tests are computed as P_T+P_W.

ISBN 978-84-617–9183–5

III. ZERO-SEQUENCE MAGNETIZING IMPEDANCES

III.1 INITIAL THEORETICAL COMPARISON BETWEEN 2D MODEL AND 3D MODEL

In this section, analyzed cases correspond to small transformers whose 3D simulation is feasible with reasonable computational resources. Four units were analyzed. They have the same active part for the transformer, and variations are in tank size, in position of active part within the tank, and in material properties.

By using $d=d_{AVG}$, X values from 2D model are greater than the corresponding values from 3D model. This fact implies that the "equivalent" value of d is lower than d_{AVG} (in order to obtain 3D results from 2D models). On the other hand, an "equivalent" value of d is also necessary to obtain the 3D results for P by using the 2D result for P multiplied by 3. For a given position of active part within the tank and material properties, Table I shows the equivalent distances for obtaining exactly the results of 3D models by using 2D models. Four equivalent distances were found (d_{X1}, d_{X2}, d_{P1}, d_{P2}); i.e., an equivalent distance for each variable: X_1 and X_2 are reactances, and P_1 and P_2 are tank losses (subscripts 1 and 2 are for outermost and innermost windings, respectively).

Table I. Equivalent Distances for Obtaining Exactly the Results of 3D Models by Using 2D Models

Tank size	VS	S	L	VL
d_{X1} (mm)	47	66	77	83
d_{X2} (mm)	80	102	116	124
d_{P1} (mm)	91	121	153	180
d_{P2} (mm)	84	114	148	176

The main importance of this result is the finding of the impossibility of using a single value of "equivalent distance" to obtain 3D results from 2D models. The physical meaning of this fact is that the size of the "equivalent tank" for this 2D model is dependent on the variable to be computed (X1, X2, P1 or P2).

Other interesting findings from the theoretical comparison between 2D model and 3D model are:

a) The effect of location of active part in x-y plane was analyzed by using 3D models. For analyzed cases, maximum variations are 5% for X, and 17% for P. These variations cannot be observed with 2D model because the position of active part in x-y plane does not have any influence on d_{AVG}.

b) 3D results and 2D results have the same qualitative behavior for variations in tank size: reactances increase and power losses decrease when tank size increases.

c) 3D results and 2D results have the same qualitative behavior for variations in active part position in z axis: results indicated that this effect can be neglected.

d) 3D results and 2D results have the same qualitative behavior for variations in material properties. Results indicated that these changes have an influence on "equivalent" distances. Thus, the application of a single value for constants (independent of steel properties) could give a reasonable accuracy. This key assumption is tested in the comparison of results of 2D model and measured impedances (Section III.3 of this paper).

III.2 DESCRIPTION OF THE APPROXIMATE METHOD

The approximate method uses an average distance in the 2D model, and seeks the proper constants (K_X and K_P), to calculate the required values. To calculate reactances, this method divides the magnetic energy of 2D model into two parts (Fig. 3): a) E_1, from symmetry axis until the radius that reaches the middle of the window; b) E_2, from the radius that reaches the middle of the window until the end of the space. Magnetic energy is mainly confined to the space until the tank due to shielding effect of tank. Fig. 3b shows that the region for computing E_1 is repeated three times in the 3D geometry, but some parts of the region for computing E_2 would be considered twice if E_2 were multiplied by 3. Therefore, a factor (K_X) is applied in order to consider that the region for computing E_2 is not repeated three times in the real 3D geometry. The magnetic energy of the 3D geometry (E_{MAG}), and the inductance (L_{3D}), are estimated as:

ISBN 978-84-617–9183–5

$$E_{MAG\text{-}3D} = 3\,E_1 + K_X\,E_2 \quad (1)$$

$$L_{3D} = 2\,E_{MAG\text{-}3D}/(3I^2) \quad (2)$$

Tank losses for the 2D model are directly obtained from the FEM software, and they are multiplied by a different coefficient (K_P) in order to estimate the tank losses for the 3D geometry (P_T).

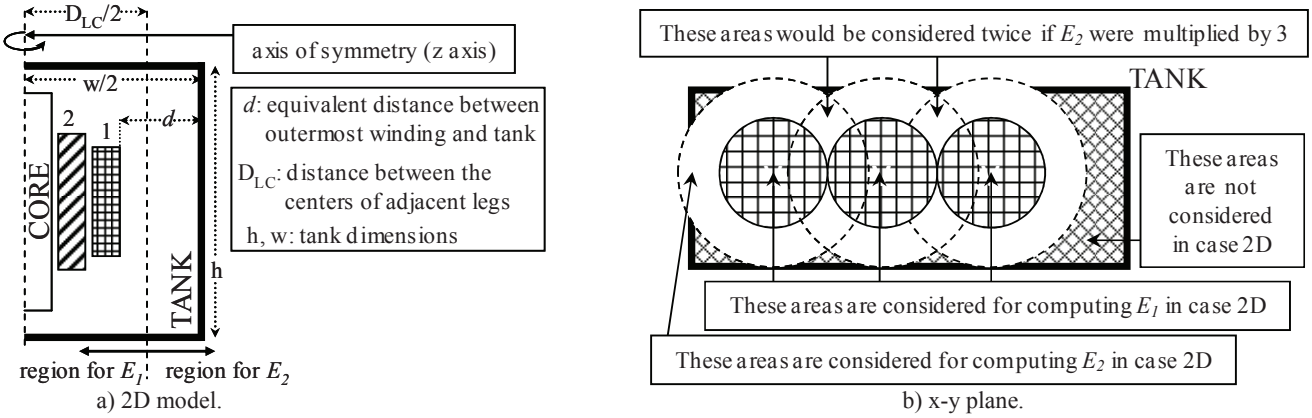


Figure 3. Auxiliary simplified schemes to illustrate the 2D approximation to the 3D geometry.

III.3 APPROXIMATION OF 2D RESULTS TO MEASURED VALUES

Tables II and III show the data from measurements, in two analyzed transformers, as a function of neutral current ($I_N=3I_0$; I_0: zero-sequence current). Tank conductivity (σ_T) is assumed to be known. Both options were tested: $5.85\cdot10^6$ Ω^{-1}/m (cases between AISI 1015 and 1025) and $7.04\cdot10^6$ Ω^{-1}/m (AISI 1008 or 1010). Results are similar with both values. Here, results are shown for $\sigma_T=7.04\cdot10^6$ Ω^{-1}/m. The equivalent permeability of tank is different for each test (μ_j; j=1,2,...,M; M: number of tests); thus, μ can be defined as a vector, whose components are the equivalent permeability of tank for each test: $\underline{\mu} = [\mu_1, \mu_2, ..., \mu_M]$.

Table II. Measured Data in Transformer 1 (25MVA, 45kV/16.05kV)

Test (j)	Side	I_N (pu) = 3 I_0	Z_{0M} (%)	X (%)	P (kW)
1	1	I_{N1} = 0.3077	75.05	69.89	71.32
2	1	I_{N1} = 0.3620	73.37	68.63	93.59
3	1	I_{N1} = 0.4171	71.97	67.55	118.93
4	1	I_{N1} = 0.4742	70.62	66.44	148.11
5	2	I_{N2} = 0.2669	87.34	82.66	52.48
6	2	I_{N2} = 0.3042	86.19	81.74	69.90
7	2	I_{N2} = 0.3576	84.19	79.99	92.78
8	2	I_{N2} = 0.3963	83.32	79.38	109.81

Table III. Measured Data in Transformer 2 (15MVA, 45kV/16.05kV)

Test (j)	Side	I_N (pu) = 3 I_0	Z_{0M} (%)	X (%)	P (kW)
1	1	I_{N1} = 0.2568	88.25	80.36	39.76
2	1	I_{N1} = 0.4060	82.25	75.61	88.04
3	1	I_{N1} = 0.4902	79.22	73.17	120.35
4	2	I_{N2} = 0.1236	104.60	96.12	10.45
5	2	I_{N2} = 0.1587	102.69	94.65	16.63
6	2	I_{N2} = 0.2028	100.27	92.78	25.92

Parameters to be computed are K_{X1}, K_{X2}, K_P, and $\underline{\mu}$. These parameters were computed by minimization of error between measured values and model results. Average of absolute percentage errors was used as objective Table IV shows the obtained optimal parameters. Permeability tends to follow a curve as a function of the per-unit value of I_N (Fig. 4), independently on which winding is connected to the power source during Z_{0M} test. The values of μ are slightly lower when outermost winding is connected to the power source during the test. A

ISBN 978-84-617–9183–5

procedure to estimate μ is suggested in [5], when measured values of Z_{0M} are unknown, and an average value can be applied for the approximation constants ($K_{X1} \approx K_{X2} \approx 2.13$, and $K_P \approx 3.95$).

Table IV. Obtained parameters

Unit 1	μ = [180.58, 157.27, 140.29, 127.68, 214.36, 197.73, 178.16, 161.92] K_{X1}=2.0879; K_{X2}=2.1042; K_P=3.4734
Unit 2	μ = [451.37, 314.50, 260.64, 725.86, 653.93, 569.03] K_{X1}=2.1142; K_{X2}=2.1676; K_P=4.4189

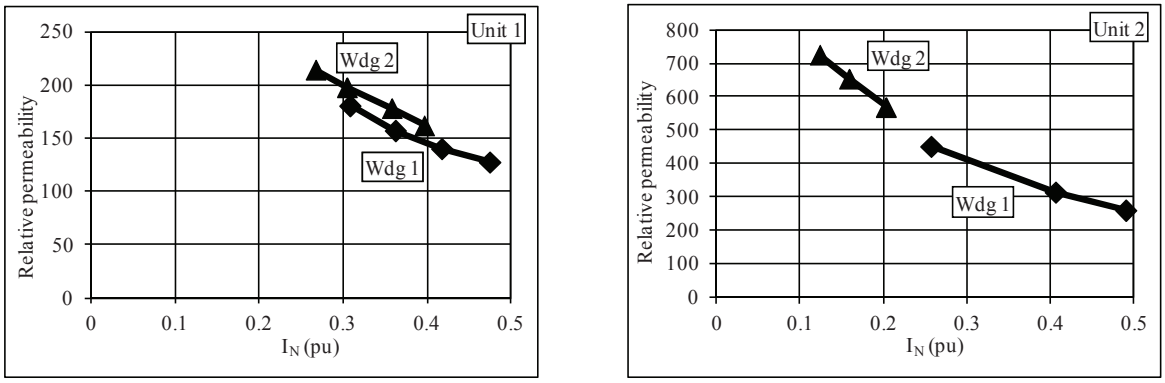


Figure 4. μ as a function of I_N. Wdg 1 and Wdg 2 are outermost and innermost windings, respectively.

IV. Zero-Sequence Short-Circuit Impedances

IV.1 Current in Each Winding and Current in the Tank

Current in winding connected to the power source is an input datum. Currents in short-circuited windings are found by an iterative process, to obtain a null value for the total induced voltage (V_W) in each short-circuited winding. V_W is computed by summing induced voltages at each turn (it is very important to note that the flux is different in each turn). For the turn *i*, the induced voltage (V_i) is related to the net flux inside this turn (Φ_i):

$$V_i = j\ \omega \Phi_i \qquad (3)$$

Only the axial component of magnetic flux density (B_Z) is necessary to compute Φ_i, as the numerical integral of B_Z in the area of the turn *i*:

$$\Phi_i = \int B_Z\ 2\ \pi r\ dr \qquad (4)$$

V_W, V_i, Φi, and B_Z are complex numbers. B_Z is computed by the FEM software for each point (*r*,z).

Current in the tank is directly computed by the FEM software, by including the proper condition for it. The application of this procedure to the windings would be incorrect because the result would be a non-uniform distribution of current density in the windings.

IV.2 Description of the Approximate Method for the 2D Model

The approximate method for the 2D model is similar to the afore-described method for Z_{0M}. K_X and K_P can be varied in a relatively wide range without an important loss of accuracy, as it is shown in section IV.3. Computed results of this paper are obtained with K_X=2.13 and K_P=3.95 (which were obtained for Z_{0M}, where the influence of these approximate constants is greater).

IV.3 Approximation of 2D Results to Measured Values

Table V shows the main characteristics of analyzed transformers. Power losses were not measured for units 3, 4 and 5; therefore, values of X were compared with measured values of Z in these cases (modules of Z are very near to values of X because the angle of these impedances is very close to 90º).

An exact determination of the value of μ for each Z_{0SC} test would require a set of specific tests for that purpose, and this procedure does not seem justifiable because the influence of μ on results is low (three values of μ were tested: 100, 400, 1000). Therefore, a practical solution is the use of an intermediate value of μ (μ=400).

ISBN 978-84-617–9183–5

Table V. Main Characteristics of Analyzed Transformers

Unit	MVA	kV	Case	MS	P_M	N_{Z0SC}
1	25/25/8.33	45/16.05/10	T21	No	Yes	6
2	15/15/5	45/16.05/10	T21	No	Yes	5
3	75/75/25	220/71/10	T21	Yes	No	6
4	30/30/10	132/16.05/10	T21	Yes	No	4
5	150/150/50	230/71/20	21T	No	No	4

MS: Magnetic shunts on tank walls. P_M: Availability of measured power. N_{Z0SC}: Number of available Z_{0SC} tests.

For cases with magnetic shunts on tank walls, computed values of Z_{0SC} have little variations as a function of μ. The maximum variation is in the order of 0.7% for these cases. For cases without magnetic shunts on tank walls: a) computed values of Z_{0SC} can vary as a function of μ, and the maximum variation is in the order of 10% for the analyzed cases; this fact is in concordance with an example found in [7], where 5% of variation in the measured values of Z_{0SC} is shown as a function of the current during the test; b) the effect of μ on the results is almost null when the main return path for the zero-sequence magnetic fluxex is not through the tank.

Fig. 5 shows the average of absolute value of percent errors for: a) the computed values of Z_{0SC} in comparison with measured values, as a function of K_X; b) the computed values of P during the Z_{0SC} tests, in comparison with measured values, as a function of K_P. In the first case, average error is practically the same for K_X between 2.0 and 2.7, and in the second case, average error is practically the same for K_P between 3.9 and 5.1.

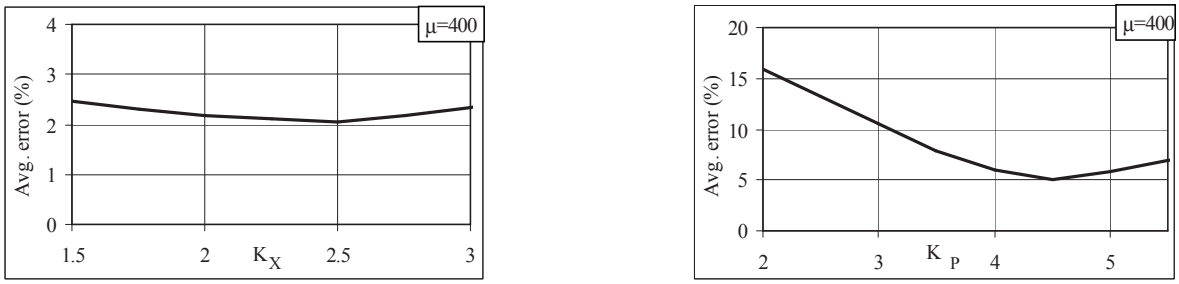


Figure 5. Average errors of computed Z_{0SC} as a function of K_X for the five analyzed units, and average errors of computed losses during Z_{0SC} tests as a function of K_P for units 1 and 2.

V. CONCLUSION

Zero-sequence impedances of three-phase three-legged YNynd transformers were obtained from design data by using Finite Element Method (FEM). 2D simplified models were applied for this problem and a systematic correlation between 2D and 3D geometries was developed. The results were validated by comparison with values obtained from zero-sequence tests in real transformers.

REFERENCES

[1] S. Kulkarni, S. Khaparde, *Transformer engineering: design and practice*, Marcel Dekker Inc., 2004.

[2] IEC Std. 60076-1, *Power transformers. Part 1: General*, 2011.

[3] IEC Std. 60076-8, *Power transformers. Part 8: Application guide*, 1997.

[4] IEEE Std. C57.12.90, *IEEE Standard test code for liquid-immersed distribution, power, and regulating transformers*, 2010.

[5] E. Sorrentino, J.C. Burgos, *Application of 2D linear models for computing zero-sequence magnetizing impedances of 3-phase core-type transformers*, Electric Power Systems Research, Vol. 117, p. 123-133, Dec. 2014.

[6] E. Sorrentino, J.C. Burgos, *Application of 2D linear modeling for computing zero-sequence short-circuit impedances of 3-phase core-type YNynd transformers*, Electric Power Systems Research, Vol. 122, p. 1-9, May 2015.

[7] A. Carlson, J. Fuhr, G. Schemel, F. Wegscheider, *Testing of power transformers*, ABB AG, 2003.

[8] Comsol Inc., *Comsol Multiphysics (software)*, version 3.5a, 2008.

ISBN 978-84-617–9183–5

Experience on Short Circuit Design Conception and Validation of a 570 MVA, single-phase GSU-Transformer by SC-Withstand Tests on a Mock-Up

Miguel CUESTO[1], Jose PORRERO[1], Marta MUÑOZ[1], Jorge CAMARA[1], Patrice HURLET[2], Alain TANGUY[3], *Mohammed RYADI*[3]
[1]ABB s.a, Cordoba, Spain
[2]EDF – CNEPE, France
[3]EDF – R&D, France
e-mail: miguel.cuesto@es.abb.com

Abstract— **One of the most demanding and destructive situations that a power transformer can experience during its lifetime is a short circuit. The design of a transformer's short circuit withstand capability is a key feature to be validated during the procurement process. As part of a contract between EDF Nuclear and ABB to supply 570 MVA, 420 kV single-phase GSUs for use in nuclear power plants distributed in France, and in order to validate the short circuit withstand capacity of the design proposed prior to manufacturing the units, a mock-up was developed that would represent the electrodynamic forces within the full-scale unit, mainly because the full-scale unit cannot be tested in laboratories due to its high rating.**

This paper focuses on the work between the utility and transformer manufacturer presenting the design conception of a mock-up in order to represent short circuit stresses, winding types, etc. that are comparable to those in a full-scale unit. Graphs showing calculated stresses along windings are included. The paper describes short circuit tests performed on the mock-up at the end of 2014. Two special transparent windows were installed in the tank wall in order to record potential movement of the windings during each shot.

Compared to previous publications, an added value of this paper is the consideration of clamping forces monitored on each winding by gauges installed in the insulation, as well as conclusions about the measurements performed.

Finally, the paper concludes with some considerations and recommendations for defining similar criteria when using a mock-up to create short circuit validation of a full-size transformer. This may help to avoid misunderstandings between the end-user and manufacturer, and contribute to ongoing revision of IEC 60076-5.

Keywords — **Power transformer – mock-up – short circuit testing – short circuit calculations**

I. INTRODUCTION

Historical EDF's policy is to check the mechanical strength of its fleet of power transformers by testing. In order of priority, the four preferred approaches by this customer are:

- Calculation based on minor evolution of design/manufacturing of units, already fully tested.
- Test at full power.
- Test on a wound leg in case where the unit consists of several identical coils in parallel.
- Test on a mock-up when faced to test facilities limitations.

Qualification on mock-up led to introduce a specific requirement in the customer's specifications, already presented in [3]. The feedback of qualifications conducted in 2009 and 2010 led to point out the importance of a mock-up with the following features:

- Representation of about 1/3 to 1/4 of a wound leg, strictly according to the same diameters of the coils and by using the same cables.
- Presence of a magnetic core, oil and a realistic clamping system more representative of the unbalances by the end leakage flux.
- Investigating the beginning of failure process due to spiralling or buckling.

ISBN 978-84-617–9183–5

Despite these efforts the degree of similarity between a mock-up and a real transformer is always a cause of discussion between the transformer user and the manufacturer, as more representative mock-ups are possible. The customer and manufacturer agreed to build a mock-up to validate the short circuit resilience of a 570 MVA 420 kV 1-phase GSU transformer.

II. MOCK-UP DEFINITION

Requirements for mock-up conception

The main data for the transformers are:

Rated voltages

High Voltage (HV) winding	$405/\sqrt{3} \pm 2.47$ % kV
Low Voltage (LV) winding	20 kV

Calculated short circuit impedance on 570 MVA base

Ratio 415/20 kV	14.86 %
Ratio 405/20 kV	14.90 %
Ratio 395/20 kV	14.98 %

The agreement was to perform tests on a mock-up simulating the most critical stresses in a full-scale transformer when a short circuit occurs:

- Radial buckling and spiralling in an LV winding subjected to compressive forces.
- Tensile deformation in an HV winding subjected to tensile forces.
- The mock-up should have a 20% margin between the radial stresses appearing during short circuit and the critical stresses when the failure starts.
- Axial stresses in line with nominal short circuit values.

The electrical design of the mock-up should have the same short circuit stresses as the real transformer. The mechanical design should ensure the mock-up has the same ability to withstand short circuit forces as the real transformer. By complying with both of these requirements, the real transformer's ability to withstand short circuits is validated by the test of the mock-up.

Electrical design

As the transformer is provided with taps in the HV winding, the number of turns in the mock-up HV winding was selected to represent the highest stresses appearing in the real transformer at the most onerous tap position. Comparison between the transformer and the mock-up is provided in the following Table I:

Table I. Comparison of Main Parameters Between Transformer and Mock-Up

Parameter	Mock-up	570 MVA Transformer
Number of phases	1	1
Core-form configuration	2 return limbs + 1 wounded limb	2 return limbs + 2 wounded limbs
Winding arrangement	Core - LV - HV	Core- LV-HV
Number of wound legs	1	2
Number of windings per leg	2	2
Type of HV winding	Disc winding with center entry	Disc winding with center entry
Interleaved discs in HV winding	Yes	Yes
Type of LV winding	Two layer Helical in axial split	Two layer helical in axial split
HV winding conductor	CTCE / TEE	CTCE / TEE
HV conductor covering	Thermally upgraded crepe paper	Thermally upgraded crepe paper
LV winding conductor	CTCE	CTCE
LV conductor covering	Netting tape	Netting tape
Clamping system	Flitch plates, core clamps, yoke bolts and winding support feet	Flitch plates, core clamps, yoke bolts and winding support feet
LV exit support	Yes	Yes
Type of joint between LV terminals and busbars	Bolted	Bolted

ISBN 978-84-617–9183–5

Mechanical design

The mock-up mechanical design went through different stages as manufacturer and customer defined the similarity between the mock-up and the real transformer.

In an initial approach, as the main goal is to reproduce the transformer radial forces (compressive and tensile stresses as well as spiralling), the mock-up was designed as a portion of the windings with a core steel frame forcing the magnetic flux to be axial, as shown in the picture below. The mock-up was therefore not provided with a real core:

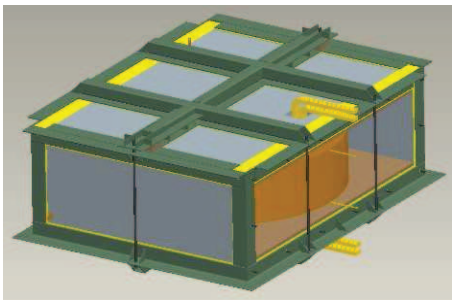


Figure 1. Mock-up initial mechanical design. Magnetic frame around the windings.

The fact was raised that the mechanical design of the mock-up should be representative of the real transformer in terms of spiralling in the LV winding. The ability to withstand spiralling in LV windings is highly dependent upon the winding clamping, and the system used to support the winding exits. The customer and manufacturer then agreed that one of the most important aspects to be considered in the comparison was the clamping system used for both the transformer and the mock-up. Well-pressed windings greatly contribute to the capacity to withstand the effect of spiralling in LV windings.

To ensure the real transformer would be able to withstand spiralling forces, the mock-up was designed with a real transformer core and the same clamping system as a real transformer, as a means of assuring the equivalence of both the real and mock-up transformer. After some intermediate stages, the result can be observed in Fig. 5.

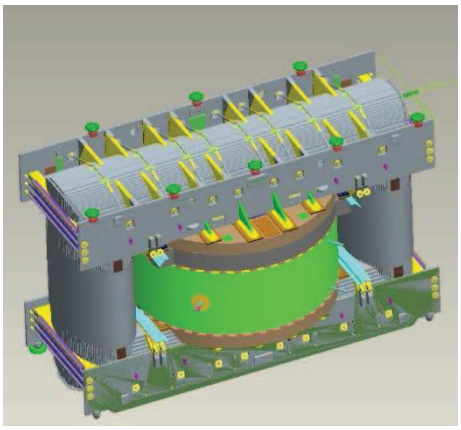


Figure 2. Final mock-up mechanical design including a real core with same clamping system as a real transformer.

As mentioned in [3] when dealing with a model dedicated to the short circuit test, the general design is driven by the mechanical design which is achieved reproducing the mechanical constraints on the conductors and the insulation structure (spacers, pressboard blocks, clamping platforms…). The dielectric insulating structure in the mock-up does not correspond at all to the structure of the real transformer, what is completely normal. Additional information can be obtained if the dielectric performance of the mock-up is compared before and after the short circuit test as some variation in winding dimensions, including connections, could result in a dielectric defect.

Short circuit current calculation

The transformer nominal short circuit currents were calculated for all fault types and tap changer positions. It was shown that the three-phase fault in LV terminals was the most demanding. The axial and radial forces

ISBN 978-84-617–9183–5

resulting from those currents circulating through the transformer were calculated by performing a fieldplot of both cases.

Stresses in the mock-up were also calculated by considering the same short circuit currents circulating through the windings. Because of the difference in the geometry, the field and consequently the stresses were shown to be different in the mock-up and in the real transformer. For this reason, in order to get the same maximum radial stress in the LV winding outer layer for both the transformer and the mock-up, the short circuit current was increased up to 105.4%. It was concluded that in order to achieve similarity between the transformer and the mock-up it should be tested at 105.4% of the transformer short circuit currents.

Radial stresses calculation

The radial stresses appearing in the transformer along the winding height were calculated for both tap positions:

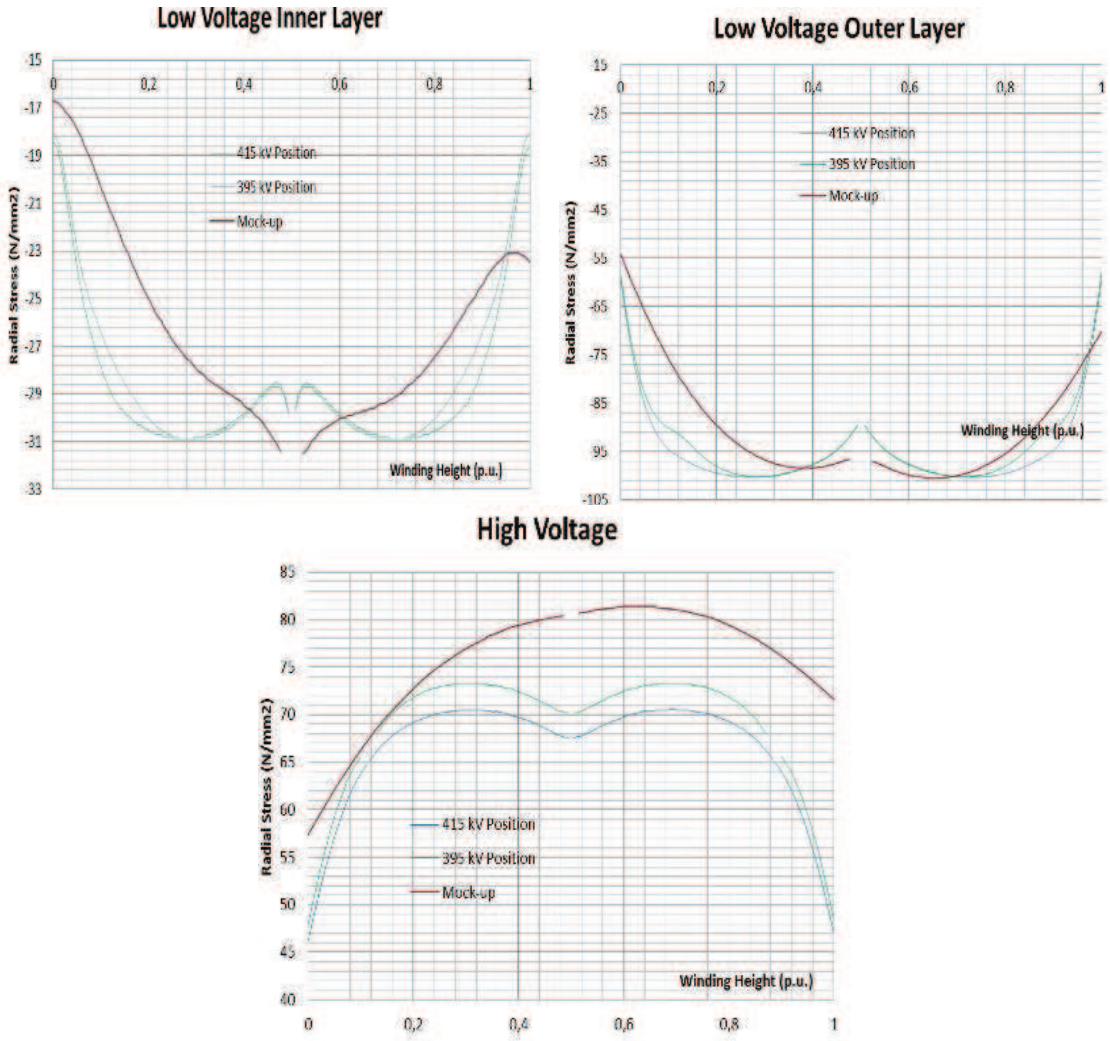


Figure 3. Radial stresses in the mock-up.

A summary of maximum tangential stress along the winding is shown in Table II:

Table II. Summary of Maximum Tangential Stress: 570 MVA Transformer @ 100% Rated Short Circuit Current and Mock-Up at 105.4% Rated Short Circuit Current

SUMMARY OF RADIAL TANGENTIAL STRESSES:						
Winding	LV inner layer		LV outer layer		HV	
	Trafo	Mock-up	Trafo	Mock-up	Trafo	Mock-up
Tangential stress [N/mm2]	-30.9	-31.5	-100.3	-100.5	73.3	81.4
Tangential stress type	Compressive		Compressive		Tensile	

ISBN 978-84-617–9183–5

Axial stresses calculation

The electromagnetic accumulative axial forces along the winding were calculated by means of a magnetic fieldplot by considering the maximum unbalance of winding magnetic centers due to manufacturing tolerances.

The manufacturer has developed a dynamic winding model to evaluate the dynamic axial forces that the windings have to withstand in case of short circuit. The stresses in the transformer spacers due to those dynamic axial forces along the winding have been calculated also for both highest and lowest tap position. In this case the dynamic model showed higher stresses than taking into account only the static values.

At this stage, it is important to note that even if the mock-up is not fully representing the real transformer behavior, it is an appropriate way to demonstrate the specific know-how of the transformer manufacturer.

The stresses in the transformer spacers due to those electrodynamic axial forces along the winding have also been calculated for both highest and lowest tap positions. The axial stresses in the mock-up at 105.4% rated short circuit current were also calculated through the dynamic model:

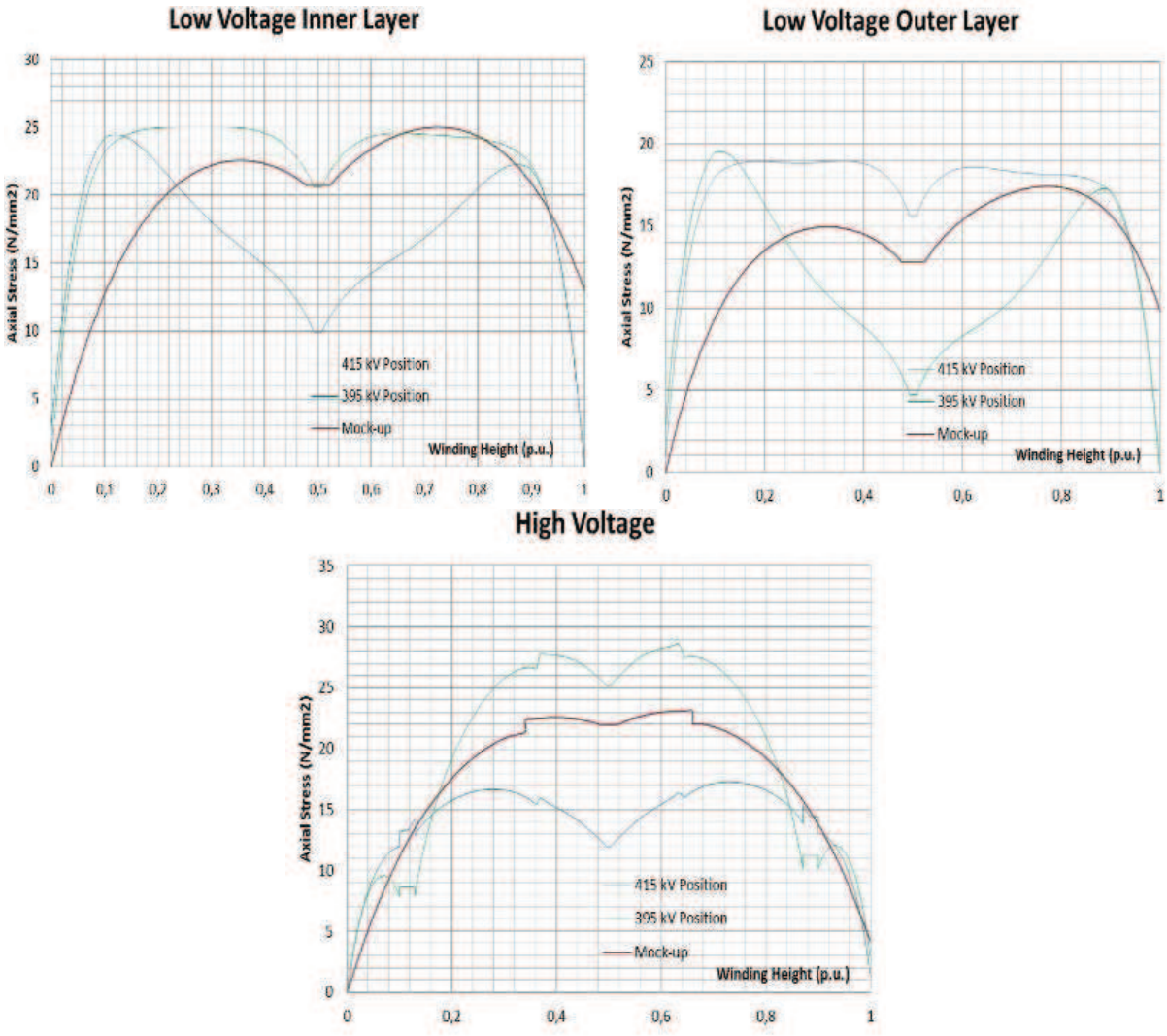


Figure 4. Axial stresses in the mock-up.

Table III. Summary of Maximum Axial Stress: 570 MVA Transformer at 100% Rated Short Circuit Current and Mock-Up at 105.4% Rated Short Circuit Current

	Maximum axial stress along the winding (N/mm2)	
	Trafo	Mock-up
LV inner layer	25.0	25.0
LV outer layer	19.6	17.4
HV winding	28.6	23.1

ISBN 978-84-617–9183–5

Spiralling
Spiralling of helical coils subjected to compressive stress refers to the tendency of the winding to tighten up on the cylinder or on the coil underneath by twisting itself towards a smaller diameter on a high pitch winding. Spiralling depends on the tangential stress produced during a short circuit, and the cross section area of the turn cables.

The ability of a winding to withstand spiralling depends on the friction surface in the winding, and the system used to lock the exit. The friction surface is the spacer area between the winding turns. The mock-up was designed to have a 108% higher spiralling stress than the real transformer when 105.4% of short circuit current circulates through the winding.

Short circuit forces during the test
As the customer requested performing the test at a short circuit current leading to 120% of the nominal short circuit stresses in the transformer, the final short circuit current during the test should be 1.054 x √1.2 =1.153, which is 115.3% of the nominal short circuit current.

The final stresses on the mock-up and the transformer at 115.3% and 109.5% rated current respectively are summarized in Tables IV and V:

Table IV. Summary of Maximum Tangential Stress: 570 MVA Transformer @ 109.5% Rated Short Circuit Current and Mock-Up at 115.3% Rated Short Circuit Current

SUMMARY OF RADIAL TANGENTIAL STRESSES						
Winding	LV inner layer		LV outer layer		High voltage	
	Trafo	Mock-up	Trafo	Mock-up	Trafo	Mock-up
Tangential stress [N/mm2]	-37.1	-37.8	-120.4	-120.6	88.0	97.7
Tangential stress type	Compressive		Compressive		Tensile	

LV inner layer in the mock-up is tested at 122% of standard tangential stress in the transformer, LV outer layer in the mock-up is tested at 120% of standard tangential stress in the transformer, and HV winding in the mock-up is tested at 133% of standard tangential stress in the transformer. Those figures are higher or in line with the 120% margin between the nominal short circuit stresses in the transformers and those to be tested in the mock-up.

Table V. Summary of Maximum Axial Stress: 570 MVA Transformer @ 109.5% Rated Short Circuit Current and Mock-Up at 115.3% Rated Short Circuit Current

	Maximum axial stress along the winding (N/mm2)	
	Trafo	Mock-up
LV inner layer	30.0	30.0
LV outer layer	23.5	20.9
HV winding	34.3	27.7

The LV inner layer in the mock-up is tested at 120% of standard maximum axial stress in the transformer, LV outer layer in the mock-up is tested at 107% of standard maximum axial stress in the transformer, and HV winding in the mock-up is tested at 97% of standard maximum axial stress in the transformer.

Spiralling stress at 115.3% rated short circuit current was 108% higher than spiralling stress on the transformer at 109.5% rated short circuit current.

To sum up, radial stresses in the mock-up are tested up to a minimum of 120% of the transformer radial stresses as requested by the customer. Axial stresses in the mock-up are tested up to a minimum of 97% of the transformer axial stresses being therefore in line with the rated values. Spiralling stress is tested up to 129% of the spiralling stress in the transformer exceeding the requirement of 120% specified by the customer.

ISBN 978-84-617–9183–5

III. SHORT CIRCUIT WITHSTAND TEST

Prior to the short circuit test at the test laboratory, a range of IEC FAT routine tests were carried out in the manufacturer's factory. Dielectric tests performed before and after the short circuit test are an additional tool in order to detect any displacement that could have weakened the insulation of the transformer

Additionally, marks on busbars, leads connections and pressboard supports were performed during manufacture, before and after vapor-phase treatment, on those parts which tend to show clear deformations and displacements in the event of a failure due to short circuit forces, and several photos of these sections were taken for the comparative analysis.

As previously mentioned, the procedure for the short circuit test in the laboratory facilities was the result of an agreement between the purchaser and manufacturer, based on the IEC 60076-5 standard and the customer's own specifications. The mock-up transformer (Fig. 10) was submitted to three main successive tests at a current level equivalent to 120% of required stresses and a $1.9x\sqrt{2}$ peak factor. It is worth mentioning the previous configuration and calibration tests agreed upon by both parties involved as well as based on test laboratory common practice and experience, in order to check the configuration of the set-up as well as to prove the short circuit withstand capacity of the mock-up at 100% of stresses.

The maximum reactance deviation was about 0.1 %, which falls within the uncertainty of the measurements. This almost negligible deviation in short circuit impedance, in addition to the absence of gas generation, abnormalities in the FRA measurements and visible disturbances after the tests, led to the short circuit test being considered a success.

Besides the design and manufacture of a mock-up to validate the short circuit strength of the GSU transformer, for investigation purposes the mock-up was equipped with two windows (Fig. 11 and 12) on the low-voltage panel to record slow-motion videos of the displacement of the upper LV exit and the central discs of the HV winding, as well as a special set-up and procedure to measure and monitor the evolution of the clamping forces of the windings before, after and during short circuit tests.

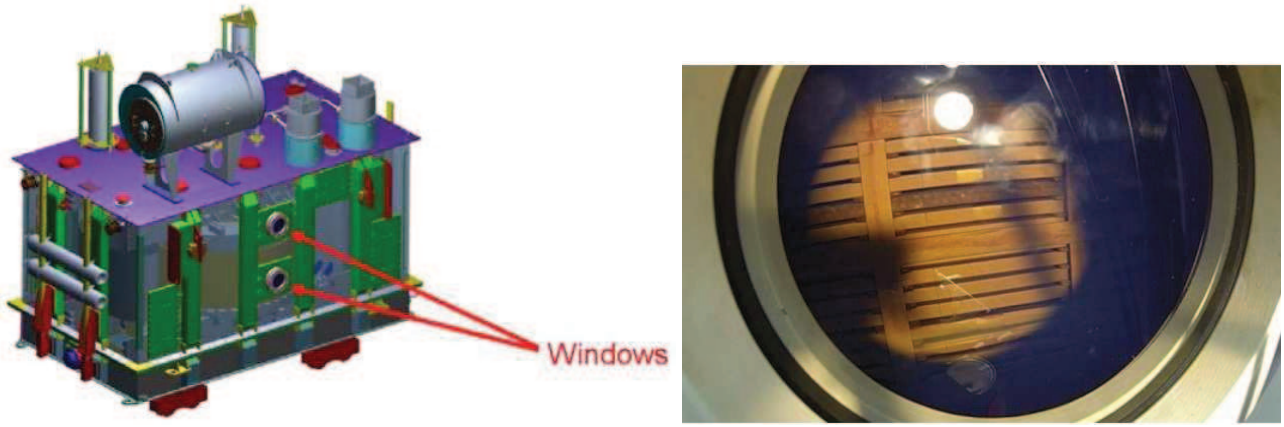


Figure 5. Mock-up with the location of the windows

IV. CLAMPING MONITORING

The design, manufacture and test of the mock-up includes an innovative procedure and set-up to measure and monitor clamping forces and their evolution after each short circuit test. In contrast to previous solutions to measure the clamping force of the whole winding assembly, this set-up could monitor the clamping of each winding separately, which meant a better and more accurate analysis of different winding behaviors.

ISBN 978-84-617–9183–5

A deep analysis of the measurements registered by the sensors after each short circuit test and at steady state showed a general behavior and evolution of the remaining clamping forces for both windings as expected, with a decrease in the pressure measured. Nevertheless, it is worth pointing out the different evolution of this pressure at each winding, which shows a lower decrease in terms of percentage of initial clamping force which remains in HV windings, compared to LV windings.

Therefore, in light of the results, it is concluded that short circuit cases lead to an expected limited or acceptable decrease of the axial pressure of every winding, but at a different rate mainly depending on elemental geometrical differences and distribution of axial short circuit forces at each coil. These geometrical characteristics, such as the winding type, cross section of the cable, diameter or the quantity of insulation material, define the elastic properties of the winding, and have a direct impact on the evolution of its clamping force.

V. CONCLUSIONS

A mock-up transformer was short circuit tested to verify the mechanical resistance of a large 570 MVA GSU transformer that due to its large size could not be tested at full scale. It was observed how the degree of representativeness of the mock-up with respect to the real transformer can be increased in steps, from similarity of the windings to including more details such as insulation structure, including a full core section identical to the real transformer, replicating the clamping system design principle as similar as possible and providing representative cleats and leads and additional details that increase complexity. Enhanced representativeness is key to ensuring the similarity between the mock-up and the real transformer.

Slow-motion video recordings as well as a detailed mapping and marking of all the pieces subjected to movement supported an exhaustive analysis of potential displacements during the short circuit test. These results not only showed no significant displacement, but also that the impedance variation during the test was extremely low, confirming the strength of the mock-up and the large 570 MVA GSU transformer it represented.

It was shown how important it is to perform measurements of the clamping effort during the different steps of the short circuit test separately in each of the windings, instead of the complete set as a whole, because the behavior of each coil is different due to different constructive characteristics.

Deep technical discussions are needed between the end user and the manufacturer during an initial design stage, highlighting the importance of a clear definition of the similarity criteria in advance in order not to leave it open to interpretation. The complexity and the cost of the mock-up are directly related to this similarity criteria.

Beyond the design qualification of the 570MVA transformer represented, these results allow each party to make progress in terms of consolidation of specifications or design rules. Several lessons should contribute to support the future revision of 60076-5 publication.

REFERENCES

[1] G. Bertagnolli: *The ABB Approach to Short-circuit Duty of Power Transformers* (1st Edition 1996).

[2] IEC 60076-5 Edition 3.0 2006-2. *Power transformers-Part 5-Ability to withstand short circuit*.

[3] CIGRE SC A2A3B3 Colloquium 2015. *Specifications and testing of very large power transformers concerning qualification of short-circuit capability of new designs and new materials*.

ISBN 978-84-617–9183–5

ISBN 978 - 84 - 617 – 9183 – 5

The institutions involved with ARWtr 2016

* Universidade de Vigo, Spain
* Technical University of Lodz, Poland
* FEUGA - Fundación Empresa-Universidad Gallega, Spain
* CIGRE, Spanish National Committee
* CIGRE, Portuguese National Committee
* A2 CIGRE Transformers Working Group
* IEEE PES Spanish Chapter
* IEEE Transformers Working Group, USA
* IBERDROLA, Group of Energetic Spanish Companies, Spain
* GAS NATURAL FENOSA, Spain
* REE,Red Eléctrica de España, Spain
* REN, Redes Energéticas Nacionais, Portugal
* ARTECHE,Instrument Transformers,Bilbao, Spain
* ABB Brown Boveri S.A., Córdoba Spain
* ABB Technology Center for Transformers, Zaragoza, Spain
* ABB Centro Regional de Servicios de Bilbao, Spain
* ABB, Transfo Development Center, Lugano, Switzerland
* ABB Inc., Releigh, NC, USA
* ABB Corporate Research Center, Baden, Switzerland
* ABB, Transformer, Zürich, Switzerland
* EDF-CNEPE, France
* EDF-R&D, France
* MR Reinhausen Luxembourg S.A., Luxembourg
* MR Maschinenfabrik Reinhausen GmbH, Germany
* MVA Luxembourg SA, Luxembourg
* NYNAS AB, UK – Nynas Petróleo S.A., Spain & Portugal
* NYNAS Naphthencs, Sweden
* OMICRON Tecnologias España S.L., Spain
* DUPONT Energy Solutions, USA
* GE Grid Solutions, Spain
* GE Grid Solutions, Germany
* GE Grid Solutions, France
* University of Stuttgard, Germany
* EFACEC Transformers R&D, Portugal
* Indian Institute of Technology - Mumbai,India
* Universidad Carlos III, Madrid, Spain
* Institute of Mechatronics and Inf.Systems, Lodz, Poland
* CEIS, Madrid, Spain
* Power Transformers Institute of Lodz, Poland
* Chalmers University of Technology, Sweden
* Megger Instruments S.L., Spain
* Megger Sweden AB, Sweden
* Universidad Pontificia Comillas, Spain

ISBN 978 - 84 - 617 – 9183 – 5

* ORMAZABAL Corporate, Spain
* ORMAZABAL COTRADIS, Spain
* Universidad del Valle, Colombia
* Technical University of Athens, Greece
* Middle East Technical University, Ankara, Turkey
* Polytechnic Institute of New York University,US
* University of Delf, Netherlands
* M&I Materials Ltd, UK
* University of Pavia, Italy
* University of Southampton, UK
* OMICRON Energy Solutions GmbH, Berlin, Germany
* TEKNIKER Fundation, Gipuzkoa, Spain
* EDF R&D THEMIS, France
* Universidad de Cantabria, Spain
* Christian-Albrechts University, Kiel, Germany
* Aalborg University, Denmark
* The Silesian University of Technology, Poland
* Universidad Politécnica de Madrid, Spain
* Krilinex Power Solutions, Spain
* RADICE, Brazil
* TREETECH, Brazil
* Sea Marconi S.a.s, Italy
* Católica de Santa Catarina, Brazil
* Universidade Regional de Blumenau, Brazil
* WEG Energía, Brazil
* ALTAIR, France
* Instituto de Investigación Tecnológica (IIT), Spain
* LCOE-FFII, Madrid, Spain
* DIAEL S.L., Spain
* Instituto Nacional y Energías Limpias (INEL), Mexico
* IEH, University of Stuttgard, Germany
* BSS Hochspannungstechik GmbH, Germany
* Institute of Welding, Blogloslawienego Czeslawa, Poland
* University of Cape Town, South Africa
* Eskom Holdings, Cape Town, South Africa
* Universidad Simón Bolivar, Caracas, Venezuela
* TPV Diagnostics and Research Ltd, Budapest, Hungary
* TERMISET, Spain
* OMEXOM, Spain
* TRANSFORMADORES GEDELSA S.A., Spain
* TJH2b, Spain
* Universidad Politécnica de Madrid, Spain
* Gas Natural Fenosa Engineering, S.L.U., Spain
* GAS NATURAL SDG S.A., Spain
* Trafoexperts, Transformer Services, Switzerland
* Spanish Association for Innovation in Transformers

ISBN 978 - 84 - 617 – 9183 – 5

ISBN 978 - 84 - 617 – 9183 – 5

Address for Correspondence

ARWtr 2016 Secretariat
ETSII – Dep. of Electrical Engineering
Campus Lagoas, 9 – 36310 Vigo, Spain

Tel.: 00 34 86 813478 – Fax: 00 34 986 814014
E-mail: arwtr2016@uvigo.es - ARWtr 2016 Website: http://webs.uvigo.es/arwtr2016

ISBN 978 - 84 - 617 – 9183 – 5

e-ARWtr 2016

Advanced Research Workshop on transformers

The collected material in this book was provided thank to the contribution of the participants of the Advanced Research Workshop on Transformers 2016 (ARWtr 2016) held in La Toja Island, Spain.

ARWtr 2016 establishes a meeting place for specialists from industrial, academic and research world to share practical knowledge and establish links of collaboration on new trends and issues in modern power, instrument and high frequency transformers.

An international group of outstanding transformer experts, the key speakers, as well as participants presented and stimulated the discussion by means of contributions within ARWtr 2016 in oral and poster sessions respectively.

The key topics of the ARWtr 2016 were concerned with: Design & New Technology; Special applications; Materials; Diagnostic; Maintenance; Economics; and Performance.

An important task was developed for ARWtr 2016 committee members. An especially mention have to be done to section chairmen for their invaluable effort by reviewing the proposals and organising of the programme.

The decisive support was given by the sponsors and institutions involved with the ARWtr 2016.

ARWtr Directors

ISBN 978 - 84- 617 - 9183- 5

Published & Edited by
Xose M. López-Fernández